Brunel
UNIVERSITY
WEST LONDON

CHARACTERISATION OF COLLAGEN-DERIVED BIOMATERIALS

A thesis submitted for the degree of Doctor of Philosophy

By

Lisandra Eunice de Castro Brás

School of Health Sciences and Social Care – Biosciences

Brunel University

May 2009

ABSTRACT

One of the main problems in healthcare is the loss or failure of organs or tissues resulting from diseases, post-surgery complications, trauma or organ failure. As a result of tissue and organ shortage, there is a need for biomaterials designed to promote tissue regeneration resulting in good quality repair of tissues or organs, to maintain or repair biological function. Collagen, as one of the main proteins in the human body, has been extensively used in the development of biomaterials which can be used as tissue substitutes or can assist in tissue regeneration.

Before commercialisation is allowed all biomaterials must prove to be functional and suitable for clinical use. Therefore, the evaluation of biomaterials requires rigorous and relevant testing. Biomaterials must be able to perform with an appropriate host response in a specific application. Tests must provide information to understand the host response, long-term outcome and issues pertaining to these.

In the research reported in this thesis, an acellular porcine derived cross-linked collagen-based biomaterial (Permacol® surgical implant) was analysed with a wide range of evaluation and compared to acellular noncross-linked and cellular, naturally cross-linked, equivalents. These matrices were characterized relating to their structure, composition and mechanical and biochemical properties. In addition, biological characterisation was performed through several studies designed to evaluate and compare biological responses *in vitro*, as well as *in situ* assessment of biocompatibility and effectiveness as a repair material and as bulking tissue.

Permacol® surgical implant was shown to be biocompatible, effective and efficient when used as bulking tissue and for soft tissue repair; furthermore, this biomaterial was resistant to enzymatic digestion and tolerant to bacterial presence suggesting that it could be used in some complicated clinical situations.

"The important thing is not to stop questioning. Curiosity has its own reason for existing."

Albert Einstein

ACKNOWLEDGMENTS

First and above all I would like to thank my principal supervisor, Dr Paul Sibbons, for the help, encouragement and unequivocal support throughout these three years, not to mention his advice and friendship. His support has been invaluable both on an academic and personal levels, for which I am tremendously grateful.

My warmest thanks to Professor Colin Green for his personal support and generosity. I also thank him for reading my thesis and giving me many valuable suggestions.

I would like to acknowledge my principal supervisor, Dr Ian Kill, for his support and help thoughout my PhD, especially for taking care of all paperwork and making everything go smoothly!

I would like to acknowledge all members of the Theatres and Histology teams for providing such a good work environment and for helping me with all the animal work.

I am most grateful to Dr Roberto Motterlini and his group for their advice and for allowing me to use their facilities and equipment.

I would like to extend my thanks to my friends for all the support and patience shown throughout, especially in the last few months when I was living in my own little world. I thank in particular Abi and Neelam for being always present when I needed.

Um obrigado muito especial para a GiPi e para a Márcinha, as melhores irmãs do Mundo, que sempre me apoiaram a 200%, e que vieram visitar-me no primeiro ano, e no segundo e terceiro anos juntámo-nos outra vez, assim nunca me senti sozinha!
Para o Pai Braz e a Mãe Alice um muitíssimo obrigado pela educação que me deram, pelo amor e apoio sempre demonstrados e que fizeram de mim a pessoa que sou hoje. Muito obrigada queridos pais!

TABLE OF CONTENTS

Page

LIST OF FIGURES

Page

LIST OF TABLES

Page

GLOSSARY OF ABBREVIATIONS

Ø – Diameter

2-D – Two-dimensional

3-D – Three-dimensional

ABC – Avidin biotin complex

Abs – Absorbance

ANOVA – Analysis of variance

APMA – 4-Aminophenylmercuric acetate

APTS – 3-Aminopropyl)triethoxysilane

BSA – Bovine serum albumin

BSAC – British Society for Antimicrobial Chemotherapy

BSE- Backscattered electrons

CAB – Columbia agar with horse blood

CEN – European Committee for Standardisation

CFU – Colony-forming units

CLED – Cysteine lactose electrolyte deficient

DAB – 3, 3'-Diaminobenzidine

DMEM – Dulbecco's modified Eagle's medium

DMSO – Dimethylsulfoxide

DNA – Deoxyribonucleic acid

DPX – Di-(n-butyl) phthalate in xylene mounting medium

EB – Evans blue dye

EBA – Evans blue-albumin conjugate

ECs – Endothelial cells

ECM – Extracellular matrix

ECN – European Chemical News

E. coli – *Escherichia coli*

EDC – 1-Ethyl-3-(3-dimethylaminopropyl) carbodiimide hydrochloride

EDTA – Ethylenediaminetetraacetic acid

ELISA – Enzyme-linked immunosorbent assay

FBS – Foetal bovine serum

FDA – United States Food and Drug Administration

FM – Fibroblast medium

GAGs – Glycosaminoglycans

GC – Germinal centres

HBSS – Hank's balanced salt solution

H&E – Haematoxylin and eosin

HMDI – Hexamethylene diisocyanate

HPLC – High performance liquid chromatography

IgG – Immunoglobulin G

IHC – Immunohistochemistry

IL – Interleukin

i.m. - Intramuscular

IMS – Industrial methylated spirit

i.p. - Intraperitoneal

LSD – Least significant difference

MMPs – Matrix metalloproteinases

m.o. – Microorganism

MT-MMP – Membrane-type matrix metalloproteinases

MTT – 3 - (4, 5 – Methylthiazolyl - 2) - 2, 5 - diphenyltetrazolium bromide

NACWO – Named animal care and welfare office

NBF – Neutral buffered formalin

NCTC – National Collection of Type Cultures

NHU – Normal human urothelial cells

NonXL – Noncross-linked acellular dermal porcine collagen

NPI – Nanocrystalline silver particles

NPIMR – Northwick Park Institute for Medical Research

OD – Optical density

OECD – Organisation for Economic Co-operation and Development

PBS – Phosphate buffered saline

PCL – Polycraptolactone

PGA – Polyglycolic acid

PLA – Polylactic acid

PM – Post mortem

PET – Polyethylene terepthalate

PPL – Personal licence holder

PT-FM – Samples pre-treated in fibroblast medium

PT-PBS – Samples pre-treated in PBS

PVA – Polyvinyl acetate

Raw – Cellular dermal porcine collagen

SD – Standard deviation

SDAC – Sabouraud dextrose agar with chloramphenicol

SDW – Sterile distilled water

SEM – Scanning electron microscopy

SIS – Small intestinal submucosa

SM – Smooth muscle cells

SSD – Silver sulphadiazine

Staph. aureus – *Staphylococcus aureus*

TBS –Tris buffered saline

TBS-T – Tris buffered saline with 0.1% Tween

TIMP – Tissue inhibitor of metalloproteinases

TNBS – Trinitrobenzene-sulphonic acid

TSL – Tissue Science Laboratories plc.

U.K. – United Kingdom

USA – United States of America

VEGF – Vascular endothelial growth factor

vWF – von Willebrand factor

XL – Permacol® surgical implant

1.0 INTRODUCTION

A recurrent problem faced in healthcare is the loss or failure of organs or tissues. The clinical need for tissue and organ substitutes originates from diseases (age-related, inherited and infectious), congenital defects, tumour resection, post-surgery complications, trauma or organ failure. The healthcare costs for patients with tissue loss or organ failure exceeds billions annually (Bottano and Heidaran, 2001) and the number of deaths resulting from inadequate supply of suitable tissue or organ substitutes indicates the extent of the problem and the need for efficient, long-term, cost-effective solutions.

The quest for the ideal tissue or organ substitute started over a century ago, scientists and surgeons have been pursuing biomaterials to promote tissue regeneration in replacement or repair of lost or damaged tissue to achieve biological function. Recent literature is replete with the investigation of such biomaterials. Tissue engineering is an emerging multidisciplinary field involving biology, medicine and engineering with the purpose of improving health and quality of life by restoring, maintaining or enhancing tissue and organ function (Metcalfe and Ferguson, 2007). The current gold standard for tissue replacement or repair is autografts, where a tissue is transplanted from one site to another on the same patient. Autologous grafts are not without disadvantages, including added surgical complexity, donor site morbidity, limited amounts of material for grafting procedures and, occasionally, absorption or partial absorption of the graft (Cillo *et al.*, 2007).

When autologous tissue is not available or suitable, allografts become the most common choice. The ideal tissue for transplantation would be sourced from a genetically identical donor (isograft) but, if this is not available and urgently needed, a non-identical but as close a match as possible member of the same species is used. Unfortunately, autografts and allografts are not easily available and are difficult to preserve, which makes xenografts (transplant from a different species) a valuable putative tissue replacement alternative.

Xenotransplantation into humans offers a potential treatment for end-stage organ failure but it also raises many contentious medical, legal and ethical issues. A

continuing concern is disease transmission; other causes of concern are tissue/organ rejection and the fact that animals have different lifespan than humans and their tissues age at a different rate (Lavery, 2000). Because there is a worldwide shortage of tissue and organs for human clinical implantation, a high percentage of patients awaiting replacement tissue and organs die on the waiting list. Recent advances in understanding the mechanisms of transplanted tissue and organ rejection have brought science to a stage where it is reasonable to consider that tissue and organs from other species may be engineered to minimize the risk of rejection and could therefore be used as an alternative to human tissues, possibly reducing organ shortages.

Techniques to replace or repair tissue/organs have historically relied solely on pure tissue grafting but developments in tissue engineering are beginning to provide alternative treatments. In addition to engineered organs, synthetic and natural biomaterials continue to be developed and many are nowadays in clinical use. There are two main approaches to tissue engineering for generating tissues or organs. One involves cell-free materials and the other relates to delivering cells in combination with synthetic or natural matrices to contribute to the regeneration process (Glowacki and Mizuno, 2008). In this thesis, only cell-free biomaterials will be considered.

Tissue engineered biomaterials may originate from a wide range of sources both synthetic and natural. Materials frequently used as scaffolds include natural polymeric materials, synthetic polymers or ceramics, biodegradable polymers or polymers with adsorbed proteins or immobilized functional groups (Chung and Park, 2007). Examples of natural materials include hydroxyapatites, hyaluronan, polypeptides, glycosaminoglycans (GAGs), fibronectin and collagen (Metcalfe and Ferguson, 2007). Common synthetic materials used in tissue engineering are polylactic acid (PLA), polyglycolic acid (PGA) and polycraptolactone (PCL) (Chung and Park, 2007). A major disadvantage of synthetic materials is the lack of cell-recognition signals which influences cell-matrix interaction. Natural materials also have the advantage of inducing lower inflammatory reactions and, for many, being of low toxicity.

An appropriate and effective scaffold needs to fulfill physical, mechanical and biological requirements (Hin, 2004), which can be grouped in four broad categories:

1. Biocompatibility: be non-toxic, non-antigenic, induce low inflammatory and low immune reactions;

2. Sterilization: biomaterials must be able to withstand sterilization and retain their original structure and function;
3. Function: biomaterials are designed dependent on the clinical application. To perform accordingly the material must either be non-degradable or undergo controlled degradation or remodelling whilst allowing enough time for adequate host tissue ingrowth and should integrate with the immediately surrounding host tissue and encourage neo-vascularisation;
4. Manufacture: be cost effective and off-the-shelf.

The extracellular matrix (ECM) comprises many of the required features for an ideal biomaterial; it is designed and manufactured by the resident cells of each tissue and organ and is in dynamic equilibrium with its surrounding microenvironment, which makes it the ideal biologic scaffold material (Badylak, 2007). The structural and functional properties of the ECM molecules provide cell-cell interaction and cell-matrix interaction, as well as providing a dynamic, mobile and flexible substratum or conduit for blood vessels and for the diffusion of nutrients (Cen *et al.*, 2008). The complex three-dimensional (3-D) structure of ECM has not been fully characterised, therefore, mimicking it in the laboratory has proved to be difficult. As an alternative, biologically intact ECM or ECM components have been used as biological scaffolds both *in vivo* and *in vitro* to facilitate appropriate cell growth and differentiation.

Usual ECM constituents of connective tissue are collagen, hyaluran, elastin and GAGs. Collagen has a dominant role in maintaining the biologic and structural integrity of ECM. Collagen is the main constituent of skin, cartilage and tendons, as well as the organic component of teeth, cornea and bone. It constitutes approximately 25 to 33% of the total protein in mammals (Harrington, 1996). Therefore, any procedure resulting in degradation, damage or loss of integrity of this protein has significant health implications (Watanabe, 2004).

In the 1970s and the 1980s, because of the expansion of medical applications of biomaterials, research scientists focused their studies on collagen as a biomedical implant because of its excellent biocompatibility and weak antigenicity (Friess, 1998; Lee *et al.*, 2001a). However, although it presents many benefits in tissue engineering there are limitations to its use, particularly, when in its native form, due to its biodegradability, lack of mechanical strength and ineffectiveness in the management of infected sites (Friess, 1998). Therefore, methods to eliminate or decrease these

deficiencies have been extensively studied through the course of tissue engineering history by improvement of physical, chemical and biological properties to develop the potential for collagen based applications.

It is important to have knowledge of the native structure and chemical properties of collagen to understand the characteristics of isolated collagen materials and the effects resulting from treatments and modifications to improve its potential range of tissue restoration use.

1.1 COLLAGEN

The first widespread use of collagen in the surgical field was as suture material most commonly referred to as catgut (Lynn *et al.*, 2004). Catgut is derived from intestinal tissue, from cattle or sheep, which was treated to eliminate all non-collagenous molecules and cross-linked to promote strength. Due to the extended historic use of collagen materials produced from different sources by an assortment of methods and because of the structural complexity of the protein, the term collagen is usually applied generically and may describe individual molecules, a native fibril *in situ* or *in vitro*, fibril aggregates or denatured gelatine (Friess, 1998).

1.1.1 Collagen Molecule

The collagens are a family of proteins that are the major components of vertebrate tissues. A collagen molecule is constituted by a unique triple-helix configuration of three chains of polypeptides subunits, known as α–chains, ending in non-helical carboxyl and amino terminals (telopeptides), one at each extremity (Figure 1.1). Each chain is a left-handed helix and the three helices are wound into a right-handed triple helix (Harrington, 1996). The triplet sequence Gly-X-Y is common within the triple helical domain, where Gly stands for glycine, X and Y are often proline and hydroxyproline (Cen *et al.*, 2008). Glycine has the smallest side group and its repetition at every third position allows close package of the chains into a helix. The

amino acids in collagen molecules contain amine groups (-NH2), acids (-COOH) and hydroxyls (-OH). These groups, in conjugation with the amide bond of the polymer, are locations for possible chemical reactions on collagen.

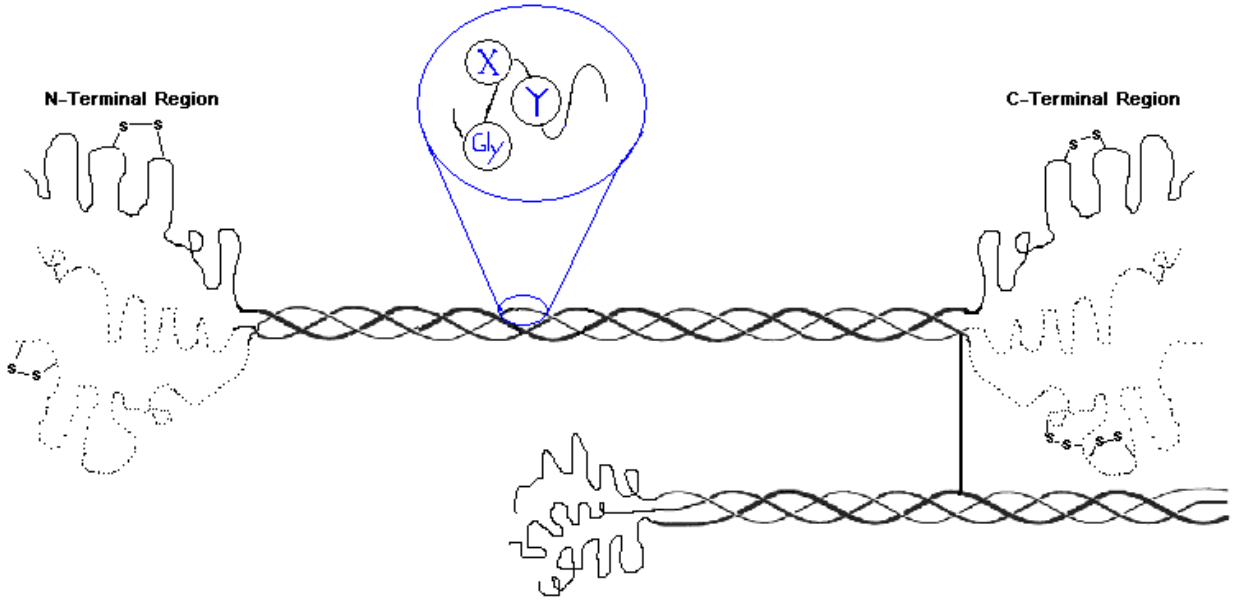

Figure 1.1 – Diagram of a collagen molecule.

Collagen molecules assemble to form microfibrils, consisting of four to eight collagen molecules, which in turn form fibrils which have a variable diameter depending on tissue type and stage of development. Fibrils organize into collagen fibres, which can form even larger fibre bundles (Kavitha and Thampan, 2008). In their natural state, the collagen triple helices are stabilized by intra- and intermolecular cross-links and by interchain hydrogen bonds. When a collagen molecule is denatured these bonds are disrupted and results in gelatin formation. True collagenases cleave the collagen helix in fibrillar forms under physiological conditions of pH and temperature. Other enzymes can only degrade the soluble form of collagen (gelatin) and non helical regions (Varani *et al.*, 2000).

1.1.2 Collagen Types

There are at least 20 genetically different vertebrate collagen types, which are generally associated with particular tissues (Metcalfe and Ferguson, 2007). Collagen

types vary in the length of the helix (from 600 to 3000 amino acids) and the nature and size of the non helical portions (Friess, 1998). Collagens have been classified into fibrillar, nonfibrillar and novel collagens. The fibrillar collagens include types I, II, III, V and XI. Of these, the first four are the main types, being present in dermis, tendon, bone, vessels, cornea and cartilage (Cen *et al.*, 2008).

Herein, only collagen type I will be discussed since it is undoubtedly the most abundant collagen type in nature and the majority of collagen derived biomaterials, for biomedical applications, are based on this type.

Collagen type I is predominant in higher order animals especially in tendon, dermis, bone, dentin, fibrocartilage, cornea, intestine, large vessels and uterus (Friess, 1998). Collagen type I molecule contains three polypeptide α-chains, each consisting of more than 1000 amino acids. There are only minor differences between this collagen type from different vertebrate species (Friess, 1998), which partially explains its low antigenicity.

The tertiary structure refers to the fundamental unit also known as tropocollagen: three polypeptide chains intertwine to form a right-handed triple-helix with an average molecular weight of 300kDa, a length of 300nm with a diameter of 1.5nm. Additionally, the regions at the amino and carboxyl terminal chain ends of the molecule are not incorporated into the helical structure and are denoted as telopeptides. The terminal regions are believed to contribute to most of the antigenic properties of collagen (Khor, 1997).

1.1.3 Natural Cross-links

The primary reason for the usefulness of collagen in biomedical application is that collagen can form fibres with considerable strength and stability through its self-aggregation and intra- and intermolecular cross-linking (Lee *et al.*, 2001a). Initially, the formation of cross-links is mediated by lysyl oxidase during fibril formation which is limited to the telopeptide regions. Intramolecular cross-links occur between two α–chains in the non-helical section of the same molecule by condensation of two aldehydes. Intermolecular cross-links form between the telopeptide region of one molecule and the helical region of an adjacent molecule (Friess, 1998). Natural cross-

linking gives high tensile strength and proteolytic resistance to collagen, evidenced by its function as the primary structural protein in the body. Nevertheless, it is still liable to collagenolytic degradation by enzymes such as collagenase and telopeptide-cleaving enzymes. Hence, it is often necessary to confer structural stability and collagenase resistance to implant materials by introduction of exogenous cross-linking into the molecular structure.

1.1.4 Collagen Antigenicity

Until 1954, collagen was mainly considered to be non-immunogenic. Although the clinical incidence of immune reactions to acellular collagen implants is not frequent, they do occasionally occur, and thus an understanding of their cause is essential for the design and application of new biomaterials (Lynn *et al.*, 2004).

Macromolecular features on an antigen molecule which interact with antibodies are referred to as antigenic determinants; these elicit different levels of interactions. Antigenic determinants of collagen can be divided into three categories (Lynn *et al.*, 2004):

- Helical – antibodies depend on 3-D conformation to recognise the antigen (A-determinants);
- Central – recognition is based on amino acid sequences and the antigen determinant is located within the triple helix;
- Terminal – when antigenic determinants are located in the non-helical telopeptide terminal regions (P-determinants).

Collagen has shown a high degree of evolutionary stability in the triple helical region and variation in the amino acids sequence does not exceed more than a few percent between mammalian species. Because telopeptides show a greater degree of variability, many biomaterials are pre-treated to remove the non-helical telopeptides (Glowacki and Mizuno, 2008).

The immune response to an antigen involves a wide range of molecules and cell types, in which the cascade of events from recognition to elimination of antigen is complex and comprises both humoral (antibody-mediated) and cell-mediated responses. It is

important to understand that certain antigenic determinants are often hidden epitopes, only interacting with antibodies when the triple helix has unwound.

1.2 STRUCTURE AND PROPERTIES OF BIOMATERIALS

The physical and mechanical properties of biomaterials must match as closely as possible the properties of the tissues to be substituted and those of the surrounding tissues. Although collagen, proteoglycans, water and cells constitute the bulk of the human body, it is the arrangement of these components that differentiates tissue types (Silver and Christiansen, 1999). When designing a biomaterial the clinical application needs to be considered with regard to characteristics and properties of the biomaterial(s) which include chemical, toxicological, electrical, morphological, physical and mechanical properties.

Matrix components and structure will mostly define the interactions between host cells and biological scaffold. The behaviour of the collagen macromolecules constituting the biomaterial and their packing arrangement will ultimately dictate how the biomaterial will perform *in situ*. The orientation of collagen fibres within a tissue will change drastically the mechanical properties of the tissue. In addition to molecule orientation and matrix 3-D architecture, the surface properties of the matrix used as a biomaterial have a major role in determining host response and biocompatibility.

After implantation, body fluids interact with the scaffold matrix, this interaction is dependent on surface signals and morphology, and eventually fluid-implant interaction will affect protein conditioning and cell adhesion to the matrix (Black, 2006).

In recognition of the importance of interfacial chemistry, considerable efforts have been made to design biomaterials with specific surface properties to optimize *in vivo* and *in vitro* performances, while retaining the desired bulk features.

Cell attachment, migration, proliferation and differentiation are phenomena related to development and wound healing. Although much is known in this area, the mechanisms regulating these processes are not fully understood.

Many studies have confirmed the importance of substrate topography in cell behaviour (Brown *et al.*, 1998; Garcia *et al.*, 2006; Ng and Swartz, 2003; Rhee and

Grinnell, 2007). Cells become oriented in response to the underlying surface, usually referred to as contact guidance. When developing a biomaterial one constant concern is designing it in a way to improve the ability of cells and tissue to attach, integrate, migrate and interact normally with the implant. There are several factors which will influence cell adherence to the substrate, including surface charge, composition, energy, oxidation level and morphology relevant to cell-matrix interactions (Silver and Christiansen, 1999).

Adhesion of cells to a substrate involves several steps: attachment to the surface, reorganization of cytoskeletal components, formation of adhesion plates and deposition of an organized ECM (Grinnell and Lamke, 1984). Cells adhere to ECM collagen by one or more cell attachment factors that have specific receptors for ECM molecules such as collagen and fibrinogen (Friedl and Bröcker, 2000). Integrins are a family of cell surface adhesion proteins that mediate cell-to-ECM adhesion and cell-to-cell adhesion. Proteins of the ECM, including collagen, bind to integrins in the extracellular region of a plasma membrane receptor (Batchelor and Chandrasekaran, 2004). Adhesion proteins not only promote cell attachment but also induce cell migration and differentiation. Cell migration is thought to occur as a response to cell-surface stimulation by ECM molecules (Silver and Christiansen, 1999).

Cell-cell and cell-matrix interaction are essential in several biological processes, including successful transplantation and implantation. Cellular interactions are also fundamental for angiogenesis or neo-vascularisation of the biomaterial to occur. The scaffold ECM provides critical support for vascular endothelium, primarily through adhesive interactions mediated by integrins positioned on the endothelial cells (ECs) surfaces (Davis and Senger, 2005). These interactions together with focal adhesions and cells ability to stimulate multiple downstream signalling pathways regulate cell adhesion, proliferation and survival within the matrix (Metcalfe and Ferguson, 2007), culminating in vascularisation of the matrix.

1.3 BIOCOMPATIBILITY OF BIOMATERIALS

As medicine advances and the application of novel materials receives increasing interest, the market for biocompatible materials increases continuously. The ability of

potential materials to fulfill their purpose is dependent upon several features including biocompatibility, non-toxicity, sterility, integration with host tissue, local tissue reactions, structure/dimension retention, provide adequate correction without migration, easily manipulated by the surgeon, provide tissue bulk where required, be long lasting yet able to be removed if necessary, allow host tissue ingrowth with good aesthetic results, offer a rapid recovery time, be accessible and non-expensive.

The evaluation of materials ability to perform, with an appropriate host response in a specific application, requires suitable testing, that is, tests must provide solutions to understand the host response, long-term outcome and issues pertaining to these.

Biomaterials in clinical use must be approved by the US Food Drug Administration (FDA) and/or by the European Committee for Standardisation (CEN), which implies performing to certain standards by complying to the requirements of ISO 10993 (EN 30993), which refers to biological evaluation of medical devices as shown in Table 1.1 (Braybrook, 1997). However, host responses are complex and may be unique; it is this complexity which restricts the accuracy and reliability of existing tests. It is becoming all the more evident that severe limitation in the function and/or biocompatibility of a number of commercially available biomaterials may still exist.

Table 1.1 – Contents of ISO 10933 (EN 30993): Biological evaluation of medical devices.

Part 1	Guidance on selection of tests
Part 2	Animal welfare requirements
Part 3	Tests for genotoxicity, carcinogenicity and reproductive toxicity
Part 4	Selection of tests for interaction with blood
Part 5	Tests for cytotoxicity: *in vitro* methods
Part 6	Tests for local effects after implantation
Part 7	Ethylene oxide sterilisation residues
Part 8	Clinical investigation (not part of EN 30993)
Part 9	Degradation of materials related to biological testing
Part 10	Tests for irritation and sensitisation
Part 11	Tests for systemic toxicity
Part 12	Sample preparation and reference materials

Many of the adverse responses to implants are associated with interactions between the surface of the biomaterial and host components of biological pathways and/or inflammatory mediators; in addition, residues or secondary products resulting from the implant remodelling or degradation may also induce an adverse response from the host. Adverse effects include complement depletion after activation of the complement system, resulting in an increased predisposition to infection, local inflammation and foreign body response to implant materials (Silver and Christiansen, 1999). Clinical reports describing epidemiological studies are sparse, since the number of complications associated with the use of implants is low and usually are related to isolated cases. Published studies are mainly retrospective reviews after the appearance of a number of clinical reports on unfavourable outcomes associated with major health concerns.

1.4 HOST RESPONSE: BIOLOGICAL EFFECTS OF BIOMATERIALS

The host response continuum is a cascade of responses that begin with the implantation procedure and with the presence of the foreign biomaterial. It includes inflammatory and wound healing responses, foreign body reactions and occasionally biodegradation and fibrous encapsulation. Assessment of biological responses is a measure of the magnitude and duration of the adverse effects in homeostatic mechanisms that determine the host response (Anderson, 2001).

When a biomaterial is implanted it will cause a cellular and tissue response. The nature and level of the response must be considered when assessing the relative safety of the biomaterial. Cellular responses include:

- Cell adaption, such as changes in the type and quantity of proteins synthesised;
- Cell size and number;
- Cell shape;
- Cellular injury.

Contact with foreign cells and/or implants may lead to host cellular changes and ultimately to cell death. In the presence of a stimulus, cells will try to adapt to the new

environment; cell degeneration is sometimes reversible and does not always culminates in cell death, although continuous exposure to the insult may lead to eventual death.

When cell size increases without an increase in the number of cells in the tissue (hypertrophy) when in contact with an implant, it is usually as result of excessive synthesis of proteins (Silver and Christiansen, 1999), as hypertrophy usually results from a chemical change or stress. Hyperplasia, or increase in cell number, can occur in normal or pathological situations, a known example is the proliferation of fibroblasts in granulation tissue during wound healing. Hyperplasia may be due to any number of causes including chronic inflammatory response, hormonal dysfunctions, increased demand or compensation for damage or disease.

In the presence of a new substratum cells may change in shape dependent on cell-matrix interactions and cell adhesion to the substrate. Cell injury resulting from the presence of a biomaterial may originate from physical, chemical or immune factors, or combination of any or all of these.

1.4.1 Biodegradation

Most biomaterials are biodegradable, these are frequently used in applications requiring temporary presence in the body. Biodegradation occurs at different rates depending on matrix components and cross-linking level. Some implants will degrade within a short period of time, while others are slowly remodelled and degraded by the host cells. Biomaterial biodegradation is an important factor that should be considered during design of a material and that choice should relate to the intended clinical application.

In situ biodegradation can not be neglected since it will affect the material's physical and chemical properties leading to loss of integrity and ultimately to functional failure. Furthermore, the degradation of the matrix *in situ* may result in release of bioproducts with different properties from the bulk material in terms of biological response and may show some level of toxicity towards host cells and surrounding tissue. A well-known example in recent medical history is the *in vivo* degradation of silicone gel breast implants (Braybrook, 1997).

Degradation products may remain at the site of implantation or may be transported by cells or fluid to other parts of the body, including blood stream. The level of their biological acceptance depends on their nature and concentration. Even though toxicity tests are one of the requirements of ISO 10933, the effects of degradation products on the body can only be truly accessed on a case-by-case basis.

When evaluating biodegradation the amount of degradation during a given period of time, the nature of the degradation products and the origin of the degradation products must be taken into account. Furthermore, it is also important to analyse degradation products in adjacent tissues and in distant organs.

Biomaterial degradation is mostly accomplished by phagocytic activity. Macrophages may coalesce to form multinucleated foreign body giant cells; giant cells and macrophages are often the more prevalent cells in the process of implant material degradation.

1.4.2 Wound Healing

Wounds naturally heal by themselves and usually the only long-term effect is a scar which will become less noticeable with time. During development, the embryo shapes and remodels its tissues converting a single fertilized egg cell into a minute model of the adult organism. Surprisingly, wounds made early in gestation, in embryos of many species including humans, heal quickly and do not leave a scar (Wadman, 2005). As a result of these findings, researchers have been analysing embryogenesis in the hope of improving adult wound healing. Ideally wounds would heal without scarring and delayed or non-healing wounds would be provided with the necessary stimulus to progress towards a healing wound. While the means to provide perfect healing are not achieved and since clinicians are presented daily with numerous wounds, which will differ in type and level of severity, novel treatments to assist and improve wound healing are being developed and many of these treatments use biomaterials as support tissue for host tissue regeneration.

1.4.2.1 Acute Wounds

Since a biomaterial is needed for repair, regeneration or replacement of a tissue, implantation results in tissue injury. It is this injury and the subsequent perturbation of homeostatic mechanisms that lead to the cellular cascades of wound healing.

Wound repair is a complex process that does not occur in a haphazard manner but rather in a carefully regulated and systematic cascade that correlates with the appearance of different cell types in the wound during various stages of the healing process. The healing procedure requires temporal and spatial coordination of different processes, including haemostasis and inflammation, formation of new tissue, angiogenesis and matrix remodelling (Jackson *et al.*, 2005; Krampert *et al.*, 2005).

Acute wounds are those without an underlying healing defect that usually occur secondarily to surgery or trauma in a healthy individual, healing quickly and completely.

Repair of wounded tissue is a complex biological occurrence in which numerous cells, cytokines, growth factors, proteases and ECM components act together to restore the integrity of injured tissue (Kuhn *et al.*, 2000). These events are also regulated by cell-cell interaction and cell-matrix interaction. Cells that participate in wound healing include resident cells, such as epithelial cells, fibroblasts, dendritic cells and endothelial cells. In addition, newly recruited cells, including platelets, neutrophils, T cells, natural killer cells and macrophages from the circulation converge to the area and become involved (Lingen, 2001).

Inflammation

Contrary to an immune response, inflammation resulting from a host response to the presence of a biomaterial is a non specific defence mechanism.

Tissue injury causes the disruption of blood vessels and plasma extravasates. A clot forms and platelets degranulate at the site of injury re-establishing haemostasis and providing a provisional ECM for cell migration (Ehrlich and Krummel, 1996). Platelets not only facilitate the formation of a clot but also secrete several mediators of wound healing that attract and activate macrophages and fibroblasts (Broughton *et al.*, 2006; Singer and Clark, 1999). Inflammation results in vasodilatation and

increased vascular permeability. Interstitial flow is present in soft tissues as an important component of the microcirculation between blood and lymphatic vessels, and interstitial flow is increased during events such as inflammation and wound healing where an influx of inflammatory cells and active angiogenesis factors both contribute to increased fluid flux into the surrounding tissues (Ng *et al.*, 2005).

The predominant cell type present during inflammation varies with time of injury. In general, neutrophils predominate in the early stages (days to weeks) and eventually are replaced by monocytes as the predominant cell type (Stevens *et al.*, 2002). Three factors account for this change in cell type: (*a*) neutrophils are short-lived and disintegrate after 24 to 48 hours post activation (Anderson, 2001); (*b*) following emigration from blood vessels, monocytes differentiate into macrophages, which are long-lived cells (up to months) (Stevens *et al.*, 2002); (*c*) monocyte emigration may continue for days to weeks, depending on the injury and implanted biomaterial (Jackson *et al.*, 2005).

Macrophages are the major source of angiogenic activity in a healing wound; they make and secrete a vast array of enzymes and growth factors, and are central to both debridement and regulation of wound metabolism (Arnold and West, 1991). Macrophage angiogenic activity is switched on in a wound when oxygen tension is low and lactate is high from anaerobic metabolism (Folkman and Shing, 1992). At the same time, the extracellular environment is being modified by phagocytosis and secretion by inflammatory cells (Arnold and West, 1991). The degradation of the ECM, which is required so that ECs can migrate between the collagenous dermis, depends on the production of collagenase (Singer and Clark, 1999). Proteolysis is required to allow inflammatory cells to enter the wound site and to degrade the provisional fibrin clot. Proteinases are involved in cell migration, in wound contraction and in scar remodelling (Krampert *et al.*, 2005).

Proliferation

The final phases of inflammation coincide with the migration of fibroblasts and ECs and the formation of granulation tissue. Angiogenesis and fibroplasia then take place, with fibroblasts being the predominant cell type producing collagen and ECM (Metcalfe and Ferguson, 2007). In the initial phase of capillary sprouting, the basement membrane of ECs in the parent blood vessel is degraded; most degradation

is mediated by EC proteinases and a variety of matrix metalloproteinases (MMPs) (Benbow *et al.*, 1999; Carmeliet, 2004; Folkman, J., 1997). As angiogenesis proceeds ECM serves essential functions in supporting key signalling events involved in regulating EC migration, invasion, proliferation, morphogenesis, survival and ultimately blood vessel stabilization, all of which are critical for neo-vascularisation. During vessel sprouting ECM is degraded by proteinases, such that proteolytic remodelling of the ECM occurs in a balanced manner; insufficient breakdown prevents vascular cells from leaving their original position, but conversely excessive degradation removes critical support and guidance cues for migrating EC and, in fact, inhibits angiogenesis (Carmeliet, 2004).

During angiogenesis ECs change their morphology from tubular to flat and elongated (growth of sprout) and back to tubular (established capillary blood vessels) (Folkman and Shing, 1992). Coincident with this spindle-shape transition, EC precursors align and connect into solid, multicellular, precapillary cord-like structures that form an integrated polygonal network (Davis and Senger, 2005). Differentiation and maturation of the ECs, lumen formation, recruitment of pericytes and coalescence of tubes into loops completes the process of new blood vessel formation (Rundhaug, 2005). In the early stages of wound healing, a large number of immature vessels form (Carmeliet, 2003). Later, some are pruned and the remaining vessels mature. A number of clinical and experimental observations support the concept that the association between the vascular tube and the mural cells mediates vessel stabilization or maturation. Vessels are dependent upon exogenous survival factors for a critical period of time during their development. In the absence of associated pericytes or smooth muscle cells, the nascent endothelial tube requires vascular endothelial growth factor (VEGF) for survival (Darland and D'Amore, 1999). The sources of VEGF in wounds are quite abundant. A number of cell types, including macrophages, fibroblasts and endothelial cells are known to produce VEGF (Brown *et al.*, 1998; Lingen, 2001).

Early granulation tissue is composed largely of type III collagen, an isoform which provides the elasticity required for the increased cellularity in the healing wound. In a mature scar or normal skin, type I and III collagen are the majority of collagen present, and type I predominates (Epstein and Munderloh, 1978). Fibroblast is the most important cell synthesising collagen. Rough endoplasmic reticulum in the

fibroblast is the site of collagen synthesis (Deodhar and Rana, 1997; Sempowski *et al.*, 1995).

Maturation and Remodelling

Granulation tissue is a contractible tissue that responds to agonists which stimulate smooth muscle. Wound contraction orientates an initial random collagen matrix. Fibroblasts are involved in ECM deposition as well as wound contraction. The gradual increase in ECM stiffness by fibroblast tractional forces is mandatory for their further evolution into myofibroblasts, which actively close the wound by contraction. Once epithelium has covered the wound, myofibroblasts normally disappear by apoptosis and the granulation tissue eventually evolves into a scar (Ng *et al.*, 2005) .
Remodelling and contraction of the granulation tissue result in an organized network of collagen and elastin fibres leading to the formation of scar tissue (Jackson *et al.*, 2005). Most critical to remodelling is conversion of the type III collagen matrix to a type I collagen, the predominant collagen isoform in normal tissue (Deodhar and Rana, 1997; Sempowski *et al.*, 1995).
As wounds mature, more collagen is deposited, cross-linked and organized. Over time most of the cellular components - vessels, fibroblasts, in particular myofibroblasts and inflammatory cells - slowly disappear leaving a relatively acellular scar (Arnold and West, 1991; Brown *et al.*, 2002).

1.4.2.2 Chronic Wounds and Infection

Chronic skin wounds affect approximately 3% of individuals over 60 years of age and are a cause of disease and disability in the elderly population (Davies *et al.*, 2007). A chronic wound is defined as one in which the normal process of healing is disrupted at one or more points in the phases of haemostasis, inflammation, proliferation and remodelling. In most chronic wounds, however, the healing process is thought to have stopped in the inflammatory or proliferative phases.
Non-healing wounds are an important source of morbidity with high treatment costs; as a result, research for treatments and devices that would decrease the rate of

occurrence of chronic wounds is a priority for many scientists and clinicians. Research in chronic wound healing is closely connected with advances in tissue engineering. Biomaterials are being developed to assist in the repair of the damaged tissue by providing a new matrix to support cell proliferation and structure for new tissue deposition.

Many factors can impair healing; local factors include the presence of foreign bodies, tissue maceration, ischaemia and infection. The majority of chronic wounds are colonized with bacteria but not all chronic wounds are infected. Wounds are considered to be infected when bacterial growth overwhelms the host immune system and compromises wound healing (Edwards and Harding, 2004). Therefore, biomaterials used on chronic wounds not only need to assist in the wound repair process but should also show some resistance to bacterial degradation and should not induce bacterial proliferation. Systemic factors that can delay healing include patients' overall health condition and can be as diverse as advanced age, malnutrition, diabetes and renal disease, to name but a few. In addition to local and systemic factors, growth factors, cytokines, proteases, cellular and extracellular elements all play important roles in different stages of the healing process. Alterations in one or more of these components can account for the impaired healing observed in chronic wounds.

Chronic inflammation is characterized by the presence of macrophages, monocytes, lymphocytes and plasma cells, with proliferation of blood vessels and connective tissue. Although the chemical and physical properties of a biomaterial may lead to chronic inflammation, movement in the implant site caused by migration of the biomaterial may also produce a chronic inflammatory response (Anderson, 2001). Lymphocytes and plasma cells are involved primarily in immune reactions and are key mediators of antibody production and delayed hypersensitive responses.

A critical factor in the pathogenesis of many chronic wounds is a combination of the presence of bacteria, inflammatory cells and the resulting elevated amounts of proteolytic enzymes (Cavallini, 2007; Mustoe, 2004). Wound fluid harvested from chronic wounds has been shown to inhibit fibroblast proliferation (Falanga, 1993) and to degrade specific MMPs substrates (Trengove *et al.*, 1999).

MMPs form a multigene family, containing at least 16 members in humans, which share a structurally similar domain structure, in particular the zinc dependent catalytic domain and the activation peptide (Konttinen *et al.*, 1999). These enzymes are secreted in their latent form, except membrane-type matrix metalloproteinases (MT-

MMPs) and stromelysin 3 and are activated by proteolytic cleavage of a propeptide domain at the N terminus of the molecule (Benbow *et al.*, 1999; Konttinen *et al.*, 1999). MMPs are responsible for controlled degradation of the extracellular matrix in several biological systems, as for example in embryogenesis, angiogenesis and wound healing. MMPs are produced by many different cells including fibroblasts, macrophage, neutrophils and eosinophils (Brandner *et al.*, 2007). High levels of MMPs and low levels of their endogenous tissue inhibitors (TIMPs) have been found in chronic wound fluid and can add to the excessive proteolysis of tissue (Brandner *et al.*, 2007). MMPs can cleave different native collagen types (collagenases), including dermal ECM collagen and denatured collagen (gelatinases); other MMPs can cleave other substrates as elastin, fibronectin, proteoglycans and laminin (Falanga, 2002).
When choosing a biomaterial for implantation into chronic wound sites or into infected fields, it is critical to select a biomaterial with some resistance to proteolytic digestion. If implant infection or degradation occurs, the surgeon will have to remove the scaffold which will result in increased costs and patient morbidity.

1.4.3 Immune Response

Upon injury a biochemical cascade is activated which will lead to the process of wound healing and if appropriate to the activation of a specific mechanism of defence, an immune response. The immune system involves several cells, such as lymphocytes and plasma cells, as well as mediating factors so that immune responses involve a complex process. A constituent of the immune system is the complement system, an important element of the host's defence mechanisms against foreign bodies (e.g. implants) and mediates an immunological response to injury. When blood contacts the surface of an implanted biomaterial, the complement system is activated, if the surface signals indicate a foreign-body, complements will induce a specific immune response and help recruit inflammatory cells (Batchelor and Chandrasekaran, 2004).
Specific responses will depend on the exact features of the chemical composition and conformation or structure of the foreign material. The immune response will follow two mechanisms, cellular and humoral. In each case, the foreign body is referred to as an antigen and the host will produce antibodies against it.

The humoral responses involve production of antibodies by B-cells, which will move freely in the blood stream. The antibodies will attach to the antigen forming a complex; the antibody-antigen complex may then accumulate at the site, be transported to the lymph nodes by phagocytes or be catabolised by other cells (Black, 2006).

Cell-mediated responses entail another class of lymphocytes, T-cells. They produce and store different classes of antibodies, mainly bound to the cell surface membrane. These antibodies are highly specific and must be directly presented to the antigen.

1.5 BIOMATERIAL DESIGN (COLLAGEN DERIVED)

During the history of tissue engineering, various collagen-based biomaterials have been developed for the repair of skin wounds and soft tissue injuries. These biomaterials are available in several forms including dispersions, solutions, gels and sponges (Friess, 1998). The collagen used for the construction of such materials usually has an animal source and is often prepared by proteolytic enzymatic digestion under acidic conditions (Abraham *et al.*, 2000). The resulting solubilised collagen can then be reconstituted as a solid, gel or sponge by increasing the pH of the solution and stabilising the collagen molecules by cross-linking (Oliver *et al.*, 1980). A disadvantage of that process is the loss of the natural structure of the collagen by cleavage of intra- and intermolecular bonds, resulting in materials with low tensile strength with an amorphous structure and susceptible to reabsorption.

A novel group of collagenous biomaterials are those in which the natural collagen keeps its 3-D architecture. The structure and matrix composition of a biomaterial will define host response, cell-cell and cell-matrix interactions. Host cell infiltration, cell proliferation, angiogenesis and deposition and organization of new host ECM are common events during the remodelling of biological scaffolds.

It is important for a biomaterial to interact with the surrounding tissue in a beneficial way without delaying the healing process. An acellular scaffold should be biocompatible and should not induce tissue-specific reactivity. If structural proteins do evoke an antigenic reaction this should induce only a marginal inflammatory reaction, and should not result in immunological rejection of the material.

There are many factors which will affect the performance of a biomaterial *in vivo*; therefore, the design and manufacture of a biological prosthesis should be a careful exercise. The major factors to consider are functional purpose and host response.

The following is a brief description of the main procedures used in the manufacture of collagen derived biomaterials.

After harvest of collagenous tissues it is of the utmost importance to preserve the tissue before protein degradation occurs. The objective is to prolong the tissues structure and mechanical integrity and remove the cellular constituents. Methods usually include cell extraction and cross-linking. By creating new chemical bonds between the collagen molecules the tissue is reinforced and at the same time maintains its original configuration. Biological materials to be used as implants should be mechanically strong enough to maintain structural integrity during early implantation, especially if an inflammatory response occurs and the biomaterial is exposed to the proteolytic action of products from inflammatory cells. It is also thought that by cross-linking proteins some of their antigenic epitopes will be masked, so that cross-linking decreases tissue reactivity.

1.5.1 Cell Extraction

In 1972 Oliver and co-workers showed that it was feasible to use a basic solution of trypsin-purified allogenic skin collagen for the repair of skin defects subcutaneously in animals (Oliver *et al.*, 1972). The success of those experiments led to the study of acellular xenografs.

Cell extraction methods vary with type of enzyme(s), extraction reagents, incubation period and washing buffers.

Some enzymes used in cell extraction such as trypsin, pepsin or pronase, remove the terminal telopeptides of collagen molecules, the resulting material is called atelocollagen and benefits from the removal of the antigenic P-determinant located on the non-helical section of the molecule resulting in a decrease in antigenicity and lower immune responses (Friess, 1998). Telopeptide cleavage results in collagen whose triple helix is intact, in which both the amino (N)- and carboxyl (C)-

telopeptides hold important roles in cross-linking and fibril formation. In addition, telopeptide removal increases significantly collagen solubility (Lynn *et al.*, 2004).
Later, Courtman and colleagues reported a cell extraction process which provided acellular bovine pericardia (Courtman *et al.*, 1994). The cell extraction process removes lipid membranes and membrane-associated antigens as well as soluble proteins, with the main objective of decreasing the antigenic response to these xenograft materials. However, even with complete extraction of cellular proteins, a cross-species response directed toward the structural proteins could still be expected if acellular tissues were used as a xenograft (Liang *et al.*, 2004). This cross-species response can be further reduced by modifying acellular tissues with a cross-linking reagent (Courtman *et al.*, 2001).

1.5.2 Cross-linking

Oliver and colleagues found that in contrast to allografts, xenografts were absorbed and were associated with a prominent mononuclear reaction (Oliver *et al.*, 1975). In a second experiment, they tested human derived implants treated with different concentrations of glutaraldehyde or formaldehyde and found that when implanted subcutaneously in rats, these implants resisted degradation and showed no evidence of a persisting cellular immune response (Oliver *et al.*, 1980).
Protein cross-linking may be achieved by physical, chemical and enzymatic processes. Physical methods include freeze-drying, heating and/or exposure to ultraviolet or gamma radiation (Khor, 1997). Enzymatic processes are initiated by the enzyme lysyl oxidase, in collagen and elastin and are further mediated by specific enzymes (Reiser *et al.*, 1992). Chemical cross-linking typically uses bifunctional reagents that interact with collagen at two different sites. In the studies reported in this thesis, the focus will only be on chemical methods of cross-linking.
For years glutaraldehyde was the cross-linking reagent of choice and was widely used for the treatment of collagenous tissue for bioprostheses. Bioprosthetic heart valves were for several decades cross-linked with glutaraldehyde, although around 50% of implanted valves failed after 10 years of implantation because of tissue degeneration and calcification (Isenburg *et al.*, 2005). In tissue, collagen is commonly found

associated with elastin, as in blood vessels where elastin is abundant (Khor, 1997); another example is in dermis where the complex of these proteins protects the body against mechanical injury by conferring elasticity to the skin. It was found that although glutaraldehyde could efficiently stabilize collagen it was unable to do the same to elastin, which leaves this protein highly susceptible to enzymatic degradation. Elastin is characterised by its lysine-derived cross-links – isodesmosine and desmosine (Lee *et al.*, 2001a). These two compounds are tetra-functional, meaning that the elastin matrix must be cleaved at four distinct sites before these compounds can be solubilised. Extracellular elastin is naturally highly cross-linked (Tyagi and Simon, 1993), but in the presence of infection or inflammation elastin is susceptible to degradation.

Although cross-linking with glutaraldehyde brought many advantages this reagent is known to markedly alter tissue stiffness and promote tissue calcification (Sung *et al.*, 1997). Toxicity and calcification *in situ* are the two major problems encountered with glutaraldehyde cross-linked bioprostheses (Glowacki and Mizuno, 2008). Calcification is caused by several factors such as the presence of phospholipids that can attract calcium ions, or voids and cavities in the tissue created by the removal of proteoglycans during processing or cellular degradation (Lee *et al.*, 2001b). *Glutaraldehyde-fixed tissues are predisposed to trap foreign particles that may lead to nucleation centres for calcium. Increased calcium uptake leads to a build-up of calcium phosphate, which in time mineralizes into calcium hydroxyapatite* (Khor, 1997).

An alternative to aldehyde cross-linking is the use of hexamethylene diisocyanate (HMDI), a bifunctional molecule where the terminal isocyanate can react with amines of lysine on collagen to form the urea bond. This cross-linking reagent yields tissues which slowly degrade to non-toxic products (Friess, 1998). The cytotoxic effects and mechanical properties of collagen and tissue treated with HMDI have been investigated and appear to be well tolerated, being much less toxic than glutaraldehyde (Oliver and Grant, 1995).

1.6 CLINICAL APPLICATIONS

With the purpose of finding efficient, novel, therapeutic agents for the constantly increasing number of patients with tissue/organs defects or loss, tissue engineering is being used as a research tool. Currently, natural biological materials are commercially marketed for tissue regeneration, repair or replacement (Table 1.2). On the basis of sales reports, it is estimated that thousands of ECM scaffolds are used annually (Derwin *et al.*, 2006). Although there are several synthetic and biological biomaterials, originated from different primary sources, the focus in this thesis will only be on mammalian collagen derived biomaterials.

Table 1.2 – Partial list of commercially available biomaterials composed of ECM.

Product	Company	Tissue type	Cross-linked	Form	Application
Acellular Oasis®	Healthpoint	Porcine small intestinal submucosa (SIS)	No	Dry sheet	Partial and full thickness wounds, burns
AlloDerm	LifeCell	Human dermis	No	Dry sheet	Tissue reconstruction
Axis™ dermis	Mentor	Human dermis	No	Dry sheet	
CollaMend	Davol	Porcine dermis	Yes	Dry sheet	Hernia repair
CuffPatch™	Arthrotek	Porcine, collagen type I	Yes	Hydrated sheet	Reinforcement of soft tissues
Dura-Guard®	Synovis Surgical	Bovine pericardium		Hydrated sheet	Spinal and cranial repair
Graft Jacket®	Wright Medical Tech	Human dermis	No	Dry sheet	Repair of integument tissue
OrthADAPT™	Pegasus Biologicals	Horse pericardium	Yes	Hydrated	Tendon and ligament repair
Permacol®	Tissue Science Laboratories	Porcine dermis	Yes	Hydrated sheet	Soft connective tissue repair
Restore™	DePuy	Porcine SIS	No	Sheet	Reinforcement of soft tissue
Stratasis®	Cook SIS	Porcine SIS	No	Dry sheet	Urinary incontinence
SurgiMend™	TEI Biosciences	Foetal bovine skin	No	Dry sheet	Soft tissue reconstruction
Surgisis®	Cook SIS	Porcine SIS	No	Dry sheet	Soft tissue repair
TissueMend®	TEI Biosciences	Foetal bovine skin	No	Dry sheet	Surgical repair, rotator cuff reinforcement
Veritas®	Synovis Surgical	Bovine pericardium	No	Hydrated sheet	Soft tissue repair
Xenform™	TEI Biosciences	Foetal bovine skin		Dry sheet	Soft tissue repair

1.7 PERMACOL® SURGICAL IMPLANT

Permacol® surgical implant (Tissue Science Laboratories, Aldershot, UK) is a sterile, moist, and tough but flexible sheet of acellular cross-linked porcine dermal collagen (Saray, 2003). After the initial mechanical process to remove the hair and epidermis, acetone is used to saponify the dermal material removing any lipids and fat deposits (Coons and Barber, 2006), after which the dermis is thoroughly washed with saline solution to remove the acetone. The cell extraction process is done by digestion with trypsin solution pH 7.0 to 9.0 to remove antigenic proteins and cellular elements such as hair follicles and sweat glands at a temperature lower than 23^{o}C. The material is stabilised by cross-linking with a diisocyanate (HMDI) in an electroneutral environment and breaks down to urea. The cross-linking confers stability against attack by endogenous proteolytic enzymes such that they do not break down and become reabsorbed following implantation (MacLeod *et al.*, 2004b). Ultimately, Permacol® is stored immersed in sterile 0.1M phosphate buffer, pH 7.2 containing sodium azide, and sterilised by gamma radiation. The sheets are double vacuum packed and heat sealed in sachets of aluminium foil (inner) and polyester/polythene (outer) sachets and stored at room temperature.

Unlike other medical collagen products in either injectable or dressing form, the original architecture of the collagenous fibrous material is preserved and Permacol® is claimed to comprise 1 to 5% of elastin, present as fibres (US Patent no. 5,397,353).

Permacol® surgical implant is commercialized for soft tissue reconstruction and repair. It has been used in a variety of surgical fields since 1998 (Harper, 2001; Liyanage *et al.*, 2006; Smith *et al.*, 2007) and it has been used successfully for the reconstruction of human soft tissue and as a supporting tissue in numerous gynecologic, urologic and general surgical procedures (Figure 1.2) involving the treatment of abdominal wall defects (Chaudhry *et al.*, 2008; Liyanage *et al.*, 2006; Parker *et al.*, 2006; Pentlow *et al.*, 2008; Richards *et al.*, 2005), hernia repair (Abhinav *et al.*, 2008; Inan *et al.*, 2007; Saettele *et al.*, 2007), soft tissue reconstruction (Benito-Ruiz *et al.*, 2006; Cillo *et al.*, 2007), stress incontinence and vaginal and rectal prolapse (Dench *et al.*, 2006).

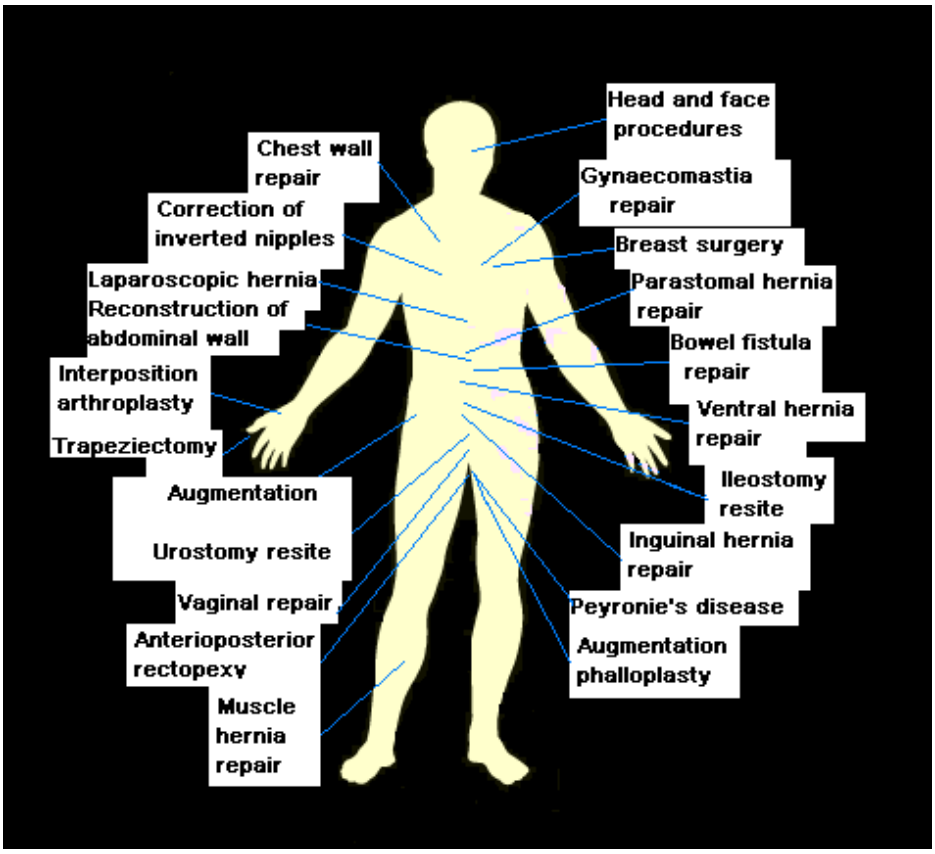

Figure 1.2 – Partial list of sites of Permacol® implantation in the body.

In studies reported in this thesis, the properties and performance of collagen derived biomaterials in several *in vitro* and *in vivo* settings were investigated. The majority of the work performed focused on a specific acellular cross-linked dermal collagen scaffold (Permacol® surgical implant). Permacol®'s mechanical, biochemical and biological characteristics were compared to acellular noncross-linked equivalents and to natural, cellular, porcine dermal collagen.

Although Permacol® surgical implant has been licensed for permanent implantation into humans since 1998, published basic-research studies are limited. Permacol® surgical implant clinical use has increased steadily in the last few years. In 2005, literature research using the parameters Permacol or Pelvicol (Permacol® surgical implant trade name used in the USA) resulted only in 29 published papers related to scientific research and clinical reports on Permacol® surgical implant. Three years later, using the same parameters in a literature research, 85 articles were found published, both in clinical and research fields.

Even though basic knowledge concerning this biomaterial has increased, there are still contradictory reports in the literature. A better understanding of the implant matrix and cell-matrix interactions is surely indispensable to accurately predict clinical outcomes.

2.0 COMMON MATERIALS AND METHODS

2.1 *IN VITRO* STUDIES

2.1.1 Reagents and Solutions

Hydrex®, Videne® antiseptic solution and 70% Industrial Methylated Spirit (IMS) were purchased from NHS Logistics (Cotes Park Industrial Estate, Alfreton, Derbyshire DE55 4QJ, U.K.). 0.9% sodium chloride sterile solution was purchased from Baxter Health Care Ltd. (Newbury, Berks RG20 7QW, U.K.). Liquid paraffin BP was purchased from NHS pharmacy (Northwick Park Hospital, Harrow HA1 3UJ, U.K.). Hank's Balanced Salt Solution (HBSS), 0.25% trypsin - ethylenediaminetetraacetic acid (EDTA) solution, Dulbecco's Modified Eagle's Medium **(**DMEM), Fetal Bovine Serum (FBS), Methylthiazolyldiphenyl-tetrazolium bromide (MTT), trypan blue solution (0.4% v/v), double processed tissue culture water and dimethylsulfoxide (DMSO) were purchased from Sigma-Aldrich Company Ltd. (Gillingham, Dorset SP8 4XT, U.K.). Penicillin-Streptomycin solution (5000:5000), dispase from *Bacillus polymyxa* and (10X) Dulbecco's Phosphate Buffered Saline-without calcium, magnesium (PBS) were purchased from Invitrogen (Inchinnan Business Park, Paisley PA4 9RF, U.K.). MTT solution was prepared in PBS and dispase solution was prepared in HBSS with 200U/mL penicillin and 200μg/mL streptomycin.

All solutions were warmed in a water bath at 37^{o}C before use, unless otherwise stated.

2.1.2 Primary Culture of Porcine Fibroblasts

All cell culture procedures were aseptically undertaken in a biological safety cabinet class II (Microflow, Bioquell U.K. Limited, Hants SP10 5AA, U.K.).

Using sterile techniques a split thickness skin biopsy was performed on the dorso-lateral surface of Large White/Landrace crossbreed pigs. Skin was shaved and brush washed with Hydrex®; soaked with Videne® antiseptic solution for 5 minutes; thoroughly washed with 70% IMS and a layer of liquid paraffin spread to cover the area to be harvested. A compressed air powered dermatome (Zimmer® Ltd., Swindon, Wiltshire SN2 6XY, U.K.) was used with a 5cm width plate and 0.612mm thickness to cut the biopsy. Skin biopsies were stored at 4°C in 0.9% sodium chloride sterile solution until used.

Skin samples were washed twice in HBSS with 200U/mL penicillin and 200µg/mL streptomycin. The biopsy area was measured and placed in 20mL of dispase solution at 2mg/mL overnight at 4°C. Dispase is a neutral protease that provides an effective and gentle cleavage of the basement membrane zone region and does not damage cell membranes. The following day the preparation was allowed a few minutes at room temperature before being incubated at 37°C for 2 hours. The skin sample was again washed in HBSS with 200U/mL penicillin and 200µg/mL streptomycin and the dermis stripped from the epidermis. The dermis was cut into small pieces and 10mL of 0.25% trypsin-EDTA solution with 200U/mL penicillin and 200µg/mL streptomycin added, followed by incubation at 37°C for 2 hours. The dermis was scraped and 10mL of fibroblast medium (DMEM with 10% FBS, 200U/mL penicillin and 200µg/mL streptomycin) added. A centrifugation was performed at room temperature (400xg) for 4 minutes in a bench-top centrifuge (MSE Harrier 15/80, Sanyo Gallenkamp Plc., Leicestershire, U.K.). The supernatant was rejected and the pellet resuspended in 10mL of fresh fibroblast medium. This solution was carefully transferred to a 75cm^2 culture flask (Sarstedt, 68 Boston Road, Leicester LE4 1AW, U.K.) and incubated at 37°C in a Galaxy R incubator (RS Biotech Laboratory Equipment Ltd., Riverside Business Park, Ayrshire, KA11 5AN, Scotland, U.K.) with 95% O_2, 5% CO_2 and 100% humidity. Cells were cultured, with medium changes every two days, until the desired confluence was reached.

2.1.3 Sub-culture of Fibroblasts

In order to maintain cell lines, fibroblasts were sub-cultured when approximately 80% confluence was reached to prevent the cells from entering the G_0 phase of mitosis. If cells are allowed to grow to a confluent state they can sometimes stay in the G_0 phase for a long period of time and some may never recover after sub-culture.

The old medium was rejected and the flasks thoroughly washed with 5mL of PBS to eliminate any possible toxins and residues from the old medium. Cells were trypsinised with 4mL of trypsin-EDTA solution at 37^{o}C with regular monitoring until all cells have detached from the base of the flasks and from each other. The contents of the flasks were carefully transferred to individual 15mL tubes containing 7mL of fresh fibroblast medium and slowly mixed to allow enzyme inactivation. A sample was taken for cell counting. Tubes were centrifuged at room temperature and the resulting pellet resuspended in sufficient fibroblast medium to prepare a new set of flasks, with a final volume of 10mL, in a 1 to 3 ratio. Subsequent media changes took place every 2 days and cells were not used after passage number 4 for any experiments (P = 4).

2.1.4 Cell Counting

Trypan blue is a vital stain used for assessment of cell viability; dead cells stain blue (trypan blue positive), while live cells exclude the dye. Trypan blue solution (0.4% v/v) was added in a 1:1 ratio to each cell culture sample and cells were counted within 30 minutes to avoid a possible increase in the dead cell population due to the trypan toxicity. Cells were counted using disposable counting 10-chambers slides (Fast-Read 102^{TM}, Immune Systems Ltd., Paignton TQ4 7XD, U.K.). Each slide has a standardised depth providing accuracy and precision for the quantification of particulate material in a known volume of fluid.

2.1.5 Cell Preservation

Preservation of cell cultures at low temperature is a technique widely used to maintain backups or reserves of cells without the associated effort and expense of feeding and caring for them. The success of the freezing process depends on four critical areas: proper handling and careful harvesting of the cultures, the use of the appropriate cryoprotectant agent, a controlled rate of freezing and storage under proper conditions.

A wide variety of chemicals provide adequate cryoprotection, however, DMSO and glycerol are the most convenient and widely used. Some cell lines are adversely affected by prolonged contact with DMSO, but this can be reduced or eliminated by adding the DMSO to the cell suspension at 4^{o}C and removing it immediately upon thawing. Although less toxic to cells than DMSO, glycerol can cause osmotic problems, especially after thawing.

The cooling rate used to freeze cultures must be just slow enough to allow the cells time to dehydrate but, fast enough to prevent excessive dehydration damage. A cooling rate of -1^{o}C to -3^{o}C per minute is satisfactory for most animal cell cultures. The best way to control cooling rates is by using electronic programmable freezing units.

Two vials of each primary culture were frozen. After harvesting a culture, 1mL of cold FBS was added and gently mixed with cells, this solution was divided into 2 cryotubes. Concurrently a FBS with 20% DMSO solution was prepared on ice. 500μL of the latter were carefully added drop by drop to the cryotubes, resulting in a final concentration of 10% DMSO (v/v). Because an electronic programmable freezing unit was not available cells were immediately frozen at -70^{o}C.

When thawing of cells was necessary, the frozen vials were quickly thawed at 37^{o}C; the medium containing the cryoprotectant discarded and replaced with fresh fibroblast medium and all contents removed to a 75cm^{2} culture flask which was placed in the incubator at 37^{o}C.

2.1.6 MTT Cell Proliferation Assay

Measurement of cell viability and proliferation forms the basis for numerous *in vitro* assays of a cell population's response to external factors. The reduction of tetrazolium salts is now widely accepted as a reliable way to examine cell proliferation. The yellow tetrazolium MTT (3 - (4, 5 – dimethylthiazolyl - 2) - 2, 5 - diphenyltetrazolium bromide) is reduced by metabolically active cells by the action of mitochondrial dehydrogenase enzymes, to generate reducing equivalents such as NADH and NADPH. The resulting intracellular purple formazan can be solubilised and quantified by spectrophotometric means. The MTT Cell Proliferation Assay measures the cell proliferation rate and conversely, when metabolic events lead to apoptosis or necrosis, the reduction in cell viability. The MTT reagent yields low background absorbance values in the absence of cells. For each cell type the linear relationship between cell number and signal produced is established, thus allowing an accurate quantification of changes in the rate of cell proliferation.

The MTT test was performed in 96-well-plates (Nunc, Sarstedt Ltd., Leicester, LE4 1AW, U.K.); 100μL of each sample was placed in each well with 1/10 of tetrazolium MTT in a 5mg/mL concentration. Fibroblast medium was used as blank. Plates were left overnight at 37^{o}C. Media was removed and 100μL of isopropanol added to dissolve the formed formazan crystals. The absorbance was read at 570nm in a Versa$_{max}$ plate reader (Molecular Devices Ltd., Wokingham, Berkshire, RG41 5TS, U.K.), using 630nm as the reference absorbance.

2.2 *IN VIVO* STUDIES

All *in vivo* assays were performed according to the regulatory guidelines of the U.K. Home Office which controls scientific procedures on animals in the U.K. and does so by the issue of licences under the Animal (Scientific Procedures) Act 1986. The regulations complied with in the studies conformed to the European Convention for the protection of Vertebrate Animals Used for Experimental and Other Scientific

Purposes (Strasbourg, Council of Europe) and achieved the standard of care required by the US Department of Health and Human Services Guide for the Care and the Use of Laboratory Animals. The Home Office Licence governing the studies directly specified the limits of severity of effects on the animals.

2.2.1 Animals

All animals were obtained from an established supplier at minimal disease status, accredited by the Home Office, transported in an air-conditioned van in boxes with moisturized food and bedding material. Male rats Wistar-Han^{TM} and Sprague Dawley, 250g – 300g, were purchased from Harlan U.K. Ltd. Shaws Farm, Blackthorn, Bicester, Oxon, OX25 1TP, U.K. They were examined for disease or injury on arrival into the test facility by the senior animal technician and during the acclimatisation period by the Named Animal Care and Welfare Officer (NACWO) and the person in day to day charge of animal husbandry before being admitted to the study. The animals were allowed to acclimatise for at least one week prior to use.

2.2.2 Accommodation

Animals were housed in groups, 4 rats per cage, until the day of surgery and were housed singly thereafter. Rats were individually identified by cage label. Lillico gold chips (Wm. Lillico & Son (Wonham Mill) Ltd., Surrey RH3 7YF, U.K.) were used as bedding. Cardboard tubes and wood sticks were given to each animal as environmental enrichment. At all times animals were allowed water and food *ad libitum*. A standard, RM1 (E), rat pellet-chow diet was provided (Special Diet Services, Witham, Essex CM8 3AD, U.K.). No known substances were expected to be present in the diet at levels which might adversely affect the results of the studies.

2.2.3 Environmental Monitoring

The temperature 20^{o}C (± 3^{o}C) and humidity 55% (±15%) were monitored and light cycles were automatically controlled for 12 hours light/dark periods.

2.2.4 Drugs

Hypnorm (fentanyl/fluanisone) was purchased from Vetapharma Ltd. (Sherburn in Elmet, Leeds, LS25 6 NB, U.K.); Diazepam (5mg/mL) was acquired from Hameln Pharmaceuticals Ltd. (Gloucester Business Park, Gloucester, GL3 4AG, U.K.). Temgesic (buprenorphine 0.3mg/mL) was obtained from Schering-Plough Ltd. (Shire Park, Hertfordshire, AL7 1TW, U.K.). Lethobarb (Sodium pentobarbitone 200mg/mL) was purchased from Fort Dodge Animal Health (Southampton, SO30 4QH, U.K.). 0.9% (w/v) sodium chloride intravenous infusion was purchased from Baxter Health Care Ltd. (Newbury, Berks RG20 7QW, U.K.)

2.2.5 Anaesthesia

Anaesthesia was given to provide humane restraint, a reasonable degree of muscle relaxation to facilitate procedures and sufficient analgesia to prevent the animal experiencing pain. The small body size of the rat makes intravenous injection difficult and drugs are usually administered by the intraperitoneal (i.p.) or intramuscular (i.m.) routes. Since there is a wide variation in drug response between different strains of rat, gender and individuals, a drug combination that provides a wide margin of safety was used. Before any surgical procedure animals were weighed and general anaesthesia given according to animal weight. Animals were given an i.m. injection of Hypnorm (0.6ml/kg) (Flecknell, 1996), followed with an i.p. injection of diazepam (2.5mg/kg) (Green, 1982). Before surgical procedure the surgery site was clipped of hair and sterilised with Hydrex®. Surgical drapes were used to isolate the operative

field and to keep the animal warm. Anaesthesia was maintained over the surgical procedure with i.m. injections of Hypnorm at the operator's discretion.

2.2.6 Recovery

Following surgical procedures animals were subcutaneously injected with 3μg of buprenorphine analgesic (diluted 1/10 in 0.9% sodium chloride sterile solution). When the surgical procedure was longer than 30 minutes, 10mL of warm 0.9% (w/v) sodium chloride were given subcutaneously to prevent dehydration. Animals were kept warm and watched closely for the next 6 hours. The day of surgery was considered as day 0. During the following day (day 1) another dose of analgesic was given and each animal was carefully examined and records maintained on individual animal forms. Animals were returned to the animal accommodation. Post operatively, animals were observed daily for food and water intake, general wellbeing, appearance of incision site and any signs of undue stress or pain. Any abnormal behaviour was reported to the on duty NACWO.

2.2.7 Humane End Points

It is often possible to reduce the severity of the procedures by the use of appropriate end points. There are three possible end points to every experiment: experimental end point, error end point and humane end point. The first refers to an experiment that runs its course and allows adequate experimental data to be collected; the second "error end point" occurs when unforeseen events happen, invalidating the experiment thus leading to a premature termination of the experiment; thirdly a "humane end point" is undertaken when the animal is killed to limit its suffering.

2.2.8 Necropsy

Animals were sacrificed by an overdose of an anaesthetic using a route and an anaesthetic agent appropriate for the size and species of the animal. At each termination animals were weighed and sodium pentobarbitone was injected i.p. When necessary a second injection of lethal anaesthetic agent was directly injected into the heart.

After euthanasia an external examination was performed and any comments recorded on a post mortem (PM) form. The operative sites were identified and exposed and the complete operative site together with adjacent tissue removed. Depending on the aim of the study, all tissue removed was fixed for at least 5 days in 10% neutral buffered formalin (NBF) solution or divided into at least two pieces; in the latter only one piece was fixed and the remaining tissue was used for tensiometry and/or frozen in liquid nitrogen and kept at -80°C.

2.2.9 Histology

Tissue was fixed in 10% NBF to preserve cells and tissue constituents and to inhibit post-mortem changes by preventing autolysis and bacterial decomposition and putrefaction. Fixation also safeguards the tissue against the deleterious effects of the various stages of tissue processing and preparation of sections. Once tissue was fixed, blocks of tissue were taken from the fixed samples to include the material under test and adjacent tissue. These tissue blocks were processed to paraffin wax embedding by routine automated procedures (see Section 2.2.9.2). The latter involves the inclusion of each tissue block in a paraffin wax mass to enable thin sections to be cut. The observation of tissues with the microscope requires a section thin enough to allow transmission of light through it; for that reason two 5μm sections were cut from each block in a transverse orientation using a microtome (Anglia Scientific, Cambridge CB4 4SW, U.K.). One section was stained with haematoxylin and eosin (H&E) and the other with picro sirius red F3B (see Sections 2.2.9.3 and 2.2.9.4, respectively). Sections were visualised using an Olympus BX40 microscope (Olympus Optical Co., Ltd., London EC1Y 0TX, U.K.) with a CCD colour Olympus DP70 digital camera.

Sections were examined for general healing, cellular penetration and cellular density, vascularisation, tissue integration, implant structure retention and collagen degradation.

When tissue mineralisation was observed specific stains were used to identify the mineral or minerals present. For calcium identification, von Kossa's method and Alizarin Red S method were followed, as described respectively in Sections 2.2.9.5 and 2.2.9.6.

2.2.9.1 Reagents

10% NBF, xylene and industrial methylated spirit 99% were purchased from Genta Medical (Marston Business Park, York YO26 7QF, U.K.). Toluene and paraffin wax were acquired from Bios Europe Ltd. (Lancashire WN8 9PS, U.K.). Di-(n-butyl) phthalate in xylene mounting medium (DPX) was acquired from Raymond A. Lamb Limited (Eastbourne BN23 6QE, U.K.). Haematoxylin Gill III was acquired from Surgipath® Europe Ltd. (Peterborough PE3 8YD, U.K.). Hydrochloric acid, ammonium hydroxide and sulphuric acid were purchased from Fisher Scientific UK (Leicestershire LE11 5RG, U.K.). Eosin and sirius red F3B were purchased from BDH Laboratory Supplies (Poole BH15 1TD, U.K.). Silver nitrate, sodium thiosulphate and alizarin red S were purchased from Sigma-Aldrich Company Ltd. (Gillingham, Dorset SP8 4XT, U.K.).. 0.1% nuclear fast red in 5% aluminium sulphate was acquired from Pioneer Research Chemicals (Colchester, Essex, CO2 8HX, U.K.). Acetone was purchased from Chemix (U.K.) Ltd. (Bolton, Lancashire, BL7 9EP, U.K.).

2.2.9.2 Tissue Processing and Embedding

Before tissue can be embedded in paraffin wax, dehydration is an essential step as paraffin wax will not penetrate tissues in the presence of water. This is achieved by immersing the tissue in increasing alcohol concentrations. Since paraffin wax is

almost insoluble in alcohol it is necessary to replace the latter with a reagent that is soluble with both substances (alcohol and paraffin wax) and which may be eliminated before proceeding with the wax impregnation of the tissues. Toluene was used as clearing agent because of its rapid action, its ability to raise the refractive index of tissue rendering it slightly transparent and its volatility to allow easy elimination during paraffin wax impregnation. Tissue was processed in a Tissue-Tek® VIP 3000 processor (Miles Scientific, Naperville IL60566, U.S.A.) using an overnight schedule as follows.

Solution	Time	Temp.	Pressure/Vacuum
1. Buffered formal saline	2.0 h	RT	Y
2. 70% IMS	1.0 h	RT	Y
3. 95% IMS	1.0 h	RT	Y
4. 100% IMS	1.0 h	RT	Y
5. 100% IMS	1.0 h	RT	Y
6. 100% IMS	1.0 h	RT	Y
7. 50% Absolute IMS/Toluene	1.0 h	RT	Y
8. Toluene	0.5 h	RT	Y
9. Toluene	1.0 h	RT	Y
10. Toluene	0.5 h	RT	Y
11. 56^{o}C paraffin wax	0.5 h	60^{o}C	Y
12. 56^{o}C paraffin wax	1.5 h	60^{o}C	Y
13. 56^{o}C paraffin wax	1.5 h	60^{o}C	Y

All tissue blocks were handled and paraffin wax embedded using electrically heated forceps in the embedding centre to prevent paraffin wax and tissues from adhering to the forceps. For each tissue block a suitable sized embedding mould was chosen, filled with wax from the dispenser and any air bubbles removed; the tissue block was placed in the centre of the mould and gently pressed against the mould base ensuring all tissues areas were at the same level throughout the block. Moulds were placed in a cryo-console until the wax had solidified. Paraffin wax blocks were removed from the embedding moulds and cleaned free of excess wax; at this point blocks were ready to be sectioned.

2.2.9.3 Haematoxylin and Eosin Stain

Haematoxylin and eosin (H&E) stain is the most widely used stain in histology for cellular morphology visualization. The staining technique comprises the application of the haematoxylin basic dye which stains the basophilic structures in a blue-purple colour and the acidic eosin stains eosinophilic structures pink. The basophilic structures contain nucleic acids, therefore chromatin-rich nucleus and ribosome will be stained by haematoxylin. Eosin stains connective tissue and generally intracellular or extracellular proteins, so most of the cytoplasm will stain pink.

Sections were dewaxed for removal of all traces of wax, hydrated in decreasing concentrations of alcohol, to eliminate the clearing reagent, and stained in a Gill's III haematoxylin solution, differentiated in acid-alcohol and counterstained with a 0.5% aqueous eosin solution. Before sections were cleared, all traces of water were removed by dehydration in ascending grades of alcohol. Xylene was used as clearing agent and slides were mounted in DPX mounting medium for permanent preservation. All slides were manually stained using the schedule described in Table 2.1.

Table 2.1 – Routine H&E staining.

REAGENT	TIME
Xylene 1	5 minutes
Xylene 2	2 minutes
*Absolute IMS	2 minutes
95% IMS	2 minutes
70% IMS	2 minutes
*Running tap water	2 minutes
Gill's III Haematoxylin	1.5 minutes
Running tap water	Up to 5 minutes
*1% acid-alcohol (HCl in 70% IMS)	3 seconds
Running tap water	4 minutes
0.5% aqueous eosin	5 minutes
*Running tap water	20 seconds
*70% IMS	30 seconds
*95% IMS	30 seconds
Absolute IMS	2 minutes
*Xylene 1	2 minutes
Xylene 2	Until ready to mount
DPX	-

* Slides were agitated during immersion.

2.2.9.4 Picro Sirius Red Stain

When sirius red, a strong acidic dye, reacts with collagen its normal birefringence is enhanced because the dye molecules attach to the collagen fibrils in such a way that their long axes are parallel. Well conserved and physiologically normal collagen shows bright birefringence using a polarised light microscope whereas denatured or degraded collagen appears black and non-birefringent. The staining method is schematized in Table 2.2.

Table 2.2– Routine picro sirius red staining.

REAGENT	TIME
Xylene 1	5 minutes
Xylene 2	2 minutes
*Absolute IMS	2 minutes
95% IMS	2 minutes
70% IMS	2 minutes
*Running tap water	2 minutes
Picro sirius red	1 hour
Running tap water	2 minutes
Gill's III Haematoxylin	1.5 minutes
Running tap water	Up to 5 minutes
1% acid-alcohol (HCl in 70% IMS)	3 seconds
*Running tap water	4 minutes
*70% IMS	30 seconds
*95% IMS	30 seconds
Absolute IMS	2 minutes
*Xylene 1	2 minutes
Xylene 2	Until ready to mount
DPX	-

* Slides were agitated during immersion.

2.2.9.5 Von Kossa's Stain

Von Kossa's technique is commonly used to demonstrate deposits of calcium or calcium salts, it stains the anions (usually carbonate or phosphate) so it is not specific for the calcium ion itself. In this method, tissue sections are treated with a silver nitrate solution and the silver is deposited by replacing the calcium, reduced by a strong light and thereby visualized as metallic silver.

Tissue containing known positive calcium deposits or un-decalcified bone should be used as positive control.

This method stains calcium salts black or dark brown, the nuclei will stain red and cytoplasm pink. The staining protocol is schematized in the following table.

Table 2.3 - Von Kossa's method.

REAGENT	TIME
Xylene 1	5 minutes
Xylene 2	2 minutes
Absolute IMS	2 minutes
95% IMS	2 minutes
70% IMS	2 minutes
Running tap water	1 minutes
Deionised water	2 minutes
5% silver solution	1 hour Placed in bright sunlight, or in front of a 60-watt lamp, with foil (or mirror) behind the jar to reflect the light
Deionised water	30 seconds Repeat step 3 times
5% Hypo-sodium thiosulfate	5 minutes
Running tap water	30 seconds
Deionised water	1 minute
Nuclear Fast Red	5 minutes
Running tap water	1 minute
70% IMS	30 seconds
95% IMS	30 seconds
Absolute IMS	2 minutes
Xylene 1	2 minutes
Xylene 2	Until ready to mount
DPX	-

2.2.9.6 Alizarin Red S

Alizarin Red S, an anthraquinone derivative, may be used to identify calcium in tissue sections. The reaction is not strictly specific for calcium, since magnesium, manganese, barium, strontium and iron may interfere, but these elements usually do not occur in sufficient concentration to interfere with the staining. Calcium forms an Alizarin Red S-calcium complex in a chelation process. The end product stains orange-red and is birefringent under polarised light.
Tissue containing known positive calcium deposits or un-decalcified bone can be used as positive control. The protocol is schematized in Table 2.4.

Table 2.4 - Alizarin Red S method.

REAGENT	TIME
Xylene 1	5 minutes
Xylene 2	2 minutes
Absolute IMS	2 minutes
95% IMS	2 minutes
70% IMS	2 minutes
Deionised water	30 seconds
Alizarin Red S solution	30 seconds to 5 minutes until an orange-red colour shows
Shake off excess dye and blot sections	
Acetone	20 seconds
Acetone – Xylene (1:1)	20 seconds
Xylene	Until ready to mount
DPX	-

2.2.10 Tensiometry

In studies where the implant integration with surrounding tissue was mechanically tested, an In-Spec 2200 portable tensiometer (Instron®, Coronation Road, Bucks

HP12 3SY, U.K.) was used. Part of the tissue outside of the treatment area was attached to the movable end of the tensiometer and the test material attached to the fixed end of the tensiometer (Figure 2.1). The movable section of the tensiometer moved away from the fixed end at a constant speed of 0.167mm/sec until dissociation occurred either at the test material/tissue junction or in the associated tissues or within the test material.

Figure 2.1– Tensiometer In-Spec 2200.

3.0 BIOPHYSICAL AND BIOCHEMICAL CHARACTERISTICS OF COLLAGEN DERIVED MATRICES

There are many commercially available collagen derived biomaterials and more are being engineered with the purpose of developing the ideal tissue repair material. Collagenous biomaterials differ with respect to primary source, methods of preparation, type of cross-linking, structure, content and prescription of use.

After implantation, a biomaterial is expected to, with time, perform and develop the same functions as the tissue it has substituted and to interact appropriately with the surrounding tissues. This may include maintaining initial shape or remodelling to the required shape, which ideally should be similar to the implanted architecture; transmit and absorb loads, sustain cells and act as a scaffold that supports tissue architecture. For a scaffold to perform appropriately it should fulfil several requirements, including being biocompatible and functional. Biocompatibility and functionality are dependent on the scaffold physical, mechanical, biochemical and biological properties, which includes low antigenic components, similar topography to the tissue to be replaced, cell adhesion surface signals, firmness and resistance to biodegradatation.

Oliver and co-workers reported a cell extraction process which used a crystalline solution of trypsin to yield acellular dermal collagen, it was hypothesized that by eliminating cellular components cellular antigens were removed (Oliver *et al.*, 1972). They also reported the use of aldehyde cross-linking to promote resistance to collagenase. With both processes – cell extraction and protein cross-linking – they aimed to produce a xenograft (porcine dermis implanted in rats) feasible to be used for repair of soft body tissue by increasing collagen stability and reducing or suppressing tissue antigenicity. Cross-linking agents have been reported to alter tissue antigenicity and provide resistance to enzymatic digestion (Courtman *et al.*, 2001). By cross-linking the residual proteins it is expected to further reduce any cross-species reaction. Collagen low antigenicity makes it one of the proteins of choice for xenografts (Lynn *et al.*, 2004).

3.1 STRUCTURE AND PROPERTIES OF COLLAGENOUS BIOMATERIALS

3.1.1 Introduction

Biomaterials derived from natural tissue normally consist of a tri-dimensional architecture, which keeps the original extracellular matrix structure but lacks cellular components. Acellular biological tissues can provide a natural micro-environment for host cell migration to accelerate tissue regeneration.

Acellular xenografts will have species-specific differences in the primary structure of the residual proteins when compared to host proteins, which may evoke a significant immune response and eventually lead to implant rejection. However, it is likely that some xenogenic proteins elicit a stronger immune response than do others (Liang *et al.*, 2004).

When biological materials are chosen as biomaterials, these are expected to perform well due to the morphology of the ECM and surface signals which can improve cell-matrix and tissue-matrix interactions. However, most biomaterials are pre-treated before implantation and these procedures may alter the structure and properties of the biomaterials.

The mechanical properties of collagenous biomaterials are dependent on the properties of the collagen fibrils, including size and orientation, but also of the content of collagen within the material and of the presence of other components. Other factors such as cross-linking level, matrix porosity, extent of tissue hydration and cell presence will also influence materials properties.

In this study some of the collagen matrices tested were treated with trypsin to remove cellular constituents and thus reduce the antigenic load within the biomaterial and by this minimize the immunologic degradation of the materials *in situ*. In addition, collagen matrices were cross-linked with HMDI not only to minimize cross-species reaction but also to increase resistance to proteolytic digestion.

Porcine collagen matrices were characterised through a series of tests related to their physical, mechanical and biochemical properties.

3.1.2 Aims and Objectives

- Characterize collagenous biomaterials related to their physical, mechanical and biochemical properties.
- Compare cross-linked materials to analogous noncross-linked materials.

3.1.3 Hypothesis

Cell extraction and cross-linking of porcine dermal collagen alter its characteristics, specifically physical and structural properties.

3.1.4 Materials and Reagents

Sodium bicarbonate, potassium permanganate ($KMnO_4$), 5% picrylsulfonic acid solution (TNBS), sodium acetate trihydrate, ninhydrin, hydrindantin, dimethylsulfoxide (DMSO), chloramine-T, citric acid, Evans blue, Trizma base, sodium chloride, calcium chloride dihydrate, phosphate buffered saline tablets (PBS), 37% hydrochloric acid, phenylmethanesulfonyl fluoride (Ph-$MeSO_4F$), oxalic acid, 4-aminophenylmercuric acetate (APMA), sulphuric acid and hog pancreatic elastase were purchased from Sigma-Aldrich Company Ltd. (Gillingham, Dorset SP8 4XT, U.K.). Glacial acetic acid, sodium hydroxide, absolute ethanol and n-propanol were acquired from Fisher Scientific UK (Leicestershire LE11 5RG, U.K.). Collagenase type I, human neutrophil elastase, MMP-8 and Methoxysuccinyl-Ala-Ala-Pro-Val-ρ-nitroanilide were purchased from Calbiochem (Merck Chemicals Ltd, Nottingham, NG9 2JR, U.K.). 390 MMP FRET Substrate I was purchased from Cambridge

BioScience Ltd (Cambridge CB5 8LA, U.K.). Nitrogen was purchased from BOC gases (Manchester, M28 2UT, U.K.). Miller Elastin Stain was acquired from Surgipath® Europe Ltd. (Peterborough PE3 8YD, U.K.). Weigert's Haematoxylin solutions A and B were purchased from Pioneer Research Chemicals (Colchester, Essex, CO2 8HX, U.K.).

Permacol® surgical implant (Permacol®), noncross-linked acellular dermal porcine collagen (NonXL), and dermal porcine collagen (Raw) were supplied by TSL plc.

3.1.5 Methods

3.1.5.1 Tensile Strength

The mechanical properties of biomaterials depend on a number of factors. The force per unit required to deform a tissue to a fixed extension varies depending on how fast the deformation is applied. Therefore it is important to standardise conditions before testing for mechanical properties. When a force is placed on a material, there is an immediate elastic response and a time-dependant response. If a material does not present a time-dependant response it is considered to exhibit purely elastic behaviour, with a time-dependant response it exhibits visco-elasticity (Silver and Christiansen, 1999).

Tensile strength of Permacol®, NonXL and Raw collagen samples was determined as described in Section 2.2.10. The tensile strength of each material was characterised by measuring the load required to stretch the material until it failed or until the limit of extension of the tensiometer was exceeded. Six samples from different batches were used per type of matrix.

3.1.5.2 Water Uptake

The water absorbency of a biomaterial is greatly influenced by its composition, molecular weight, degree of cross-linking and also by the properties of liquids to be absorbed. Swelling properties of biomaterials may be characterized by water absorption. The swelling behaviours of dried collagen matrices (Permacol®, NonXL and Raw) were carried out by immersion in deionised water at 25°C ± 1°C in a water bath. The water absorbed was determined by weighing the samples, after blotting to remove surface water, at various pre-determined time intervals. Swollen matrices were weighed with an analytical balance.

The water absorbed by collagen matrices was quantitatively represented by the equilibrium water content (EWC):

$$EWC = \frac{W_{eq} - W_0}{W_0}$$

Here, W_{eq} is the weight of the swollen matrix at time of equilibrium or maximum water uptake, and W_0 is the initial dry weight of the matrix.

The degree of swelling at each time point was calculated in percentage according to the following formula:

$$Degree\ of\ swelling\ (\%) = \frac{W_t - W_0}{W_0} \times 100\%$$

Where W_t is the sample weight at time t and W_0 the initial dry weight.

3.1.5.3 Cross-linking Quantification

The *in vivo* degradation rate of a biological prosthesis may be controlled by its cross-linking degree.

Two methods were used to quantify levels of cross-linking in collagen matrices.

3.1.5.3.1 Trinitrobenzene-sulfonic Acid Method

Okuyama and Satake proposed, in 1960, the use of trinitrobenzene-sulphonic acid (TNBS) as a reagent specific for primary amino groups, since then several methods were described using this reagent for free amino group quantification (Okuyama and Satake, 1960). TNBS method is a spectrophotometric assay of the chromophore formed by the chemical reaction of TNBS with free primary amino groups (Figure 3.1). The intensity of the colour formed, measured in terms of absorbance, is linearly related to the concentration of the free amino groups present in the tested sample.

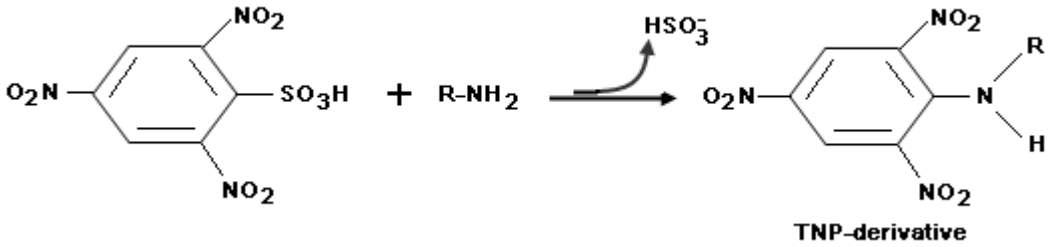

Figure 3.1 – Reaction of TNBS with primary amines, originating TNP-protein derivatives.

Samples were dehydrated in desiccators for 72 hours or until completely dry. Dry weights were measured from 6 samples of each collagen matrix (Permacol®, NonXL and Raw collagen).

Samples were put individually in screw-capped tubes and 400µL of deionised water added to each; 4 extra tubes per matrix were prepared as negative controls to these only water was added. Tubes were left overnight at room temperature.

To each tube 400µL of a 4% sodium bicarbonate solution, pH 8.0, and 400µL of aqueous 0.1% TNBS solution were added. Tubes were kept in the dark since TNBS solution is photosensitive. Tubes were heated at 40^{o}C for 2 hours and then left to cool down to room temperature. Reaction was terminated by hydrolysis with 1.2mL of 6N HCl at 60^{o}C for 90 minutes. After allowing tubes to cool down to room temperature, the resulting solution was mixed just prior to absorbance measurement at 420nm, which gives the content of the TNP-amine complex. Values were normalised by subtracting the absorbance of the negative controls.

3.1.5.3.2 Ninhydrin Method

The ninhydrin method was introduced in 1948 by Moore and Stein for quantitative determination of amino acids (Moore and Stein, 1954). Ninhydrin reacts with amino groups (Figure 3.2) producing a chromophore named Ruhemann's purple (RP) with a maximum absorbance at 570nm and a coefficient of extinction of 22000L.mol^{-1}.cm^{-1} (Friedman, 2004).

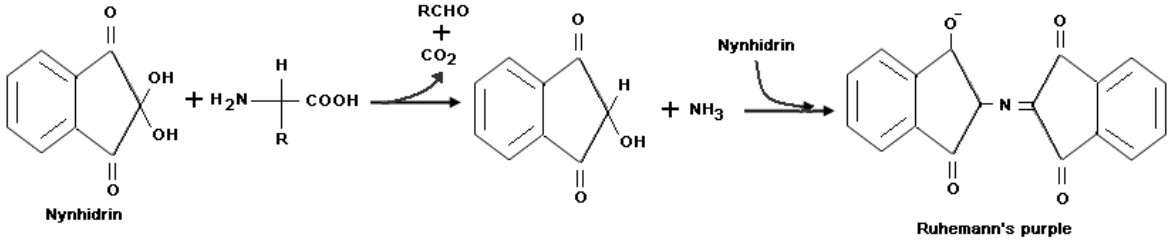

Figure 3.2 – Reaction of ninhydrin with amino acids.

Before performing the ninhydrin assay, samples were hydrolysed overnight in 6M HCl. Samples were dehydrated in desiccators for 72 hours or until completely dry. Dry weights were measured from 6 samples of each collagen matrix (Permacol®, NonXL and Raw collagen). Each sample was placed in 15mL glass containers with screw-caps, to each sample 1.5mL of the acid solution was added, the solution should not use more than 10% of the total volume of the container. Container lids were left slightly unscrewed to avoid excessive pressure. Tubes were placed in an oven (Weiss Gallenkamp, Loughborough LE11 3GE, U.K.) at 100^{o}C overnight.

For every experimental day a ninhydrin solution was prepared fresh. Table 3.1 shows the working solutions used for this method.

Table 3.1 – Buffer and solutions used in the ninhydrin assay. The final concentrations are represented in brackets.

	Sodium Acetate Buffer	Ninhydrin Solution
Solute	sodium acetate trihydrate (4M)	ninhydrin (112mM) + hydrindantin (9.3mM)
Solvent 1	deionised water	DMSO (dissolve under a stream of nitrogen) (75%)
Solvent 2	glacial acetic acid (10%)	sodium acetate buffer (25%) (bubbled with nitrogen for 2min, sealed and stored)
pH	5.5	-
Storage	4^{o}C	4^{o}C

One ml of the hydrolysate was placed in a screw-cap tube with 1mL of ninhydrin solution, 4 negative controls per matrix were prepared with ninhydrin solution and water instead of hydrolysate. Tubes were placed in a boiling water bath for 10 minutes, after which they were cooled on an ice bath. To each tube 5mL of 50% n-propanol was added to inactivate the reaction. Tubes were briefly mixed and immediately after, sample absorbances were read at 570nm. Absorbance was normalised using the negative controls values.

3.1.5.4 Matrix Components and Structure

Matrix components and surface properties are a significant determinant of the capacity of host cells to adhere and migrate into the matrix.
Collagen matrices were observed using histological analysis via light microscopy and scanning electron microscopy.

3.1.5.4.1 Histology

Strips of each collagen matrix were cut (out of the package) and fixed in 10% NBF for histological analysis as described in Section 2.2.9. From each wax block 2 sections of 5µm thickness each were cut and put onto glass slides in a hot plate at 60^{o}C for at least 4 hours. Slides were allowed to cool down before any staining process.

One section was stained with H&E following the protocol as in Table 2.1. The other slide was stained with a modified picro/Miller stain (Table 3.2).

Haematoxylin stains basophilic structures such as nucleic acids, with a blue-purple colour and the alcohol-based acidic eosin colours eosinophilic components bright pink; eosinophilic structures are usually intra- and extracellular proteins.

Miller's stain is composed of three dyes: Victoria blue 4R, new fuchsin (an iron resorcin lake) and crystal violet. The complex formed from the basic fuchsin, binds to the elastic fibres, resulting in a blue-black staining. Picro sirius red stains collagen fibres red and collagen is birefringent under polarised light.

Table 3.2 – Modified picro/Miller stain.

REAGENT	TIME
Xylene 1	5 minutes
Xylene 2	2 minutes
Absolute IMS	2 minutes
95% IMS	2 minutes
70% IMS	2 minutes
Running tap water	2 minutes
Acid potassium permanganate*	5 minutes
Deionised water	1 minute (rinse until clear)
1% Oxalic acid	2 minutes
Deionised water 1	1 minute (rinse until clear)
Deionised water 2	4 minutes
70% IMS	1 minute
95% IMS	1 minute
Miller's stain	1 hour
95% IMS	1 minute
Running tap water	2 minutes
Weigert's Haematoxylin**	10 minutes
Running tap water	1 minute (wash)
1% acid-alcohol (HCl in 70% IMS)	5 seconds
Running tap water	5 minutes (wash)
Deionised water	30 seconds
Picro sirius red	45 minutes
Deionised water	10 seconds (blot dry)
70% IMS	10 seconds
95% IMS	10 seconds
Absolute IMS	10 seconds
Xylene	2 minutes
DPX	-

*Acid potassium permanganate (0.5% $KMnO_4$ in 3% H_2SO_4).

**Weigert's Haematoxylin (1:1 (v/v) Weigert'A:Weigtert's B).

3.1.5.4.2 Pore Size

Pore size has been shown to be a major determinant for the type of ingrowth that can occur within a biological prosthesis. Biologic prostheses should have microstructure with high porosity for cell migration and ingrowing, pore size between 20 to 200μm are considered appropriate for cellular penetration (Wang and Hon, 2003). In addition, pores must be interconnected to allow ingrowth of cells, diffusion of nutrients, removal of waste products and vascularisation. Pore size was measured with DPController software (Olympus Optical Co., Ltd.), at an objective magnification of forty times.

3.1.5.4.3 Scanning Electron Microscopy

Scanning electron microscopy (SEM) is a method for high-resolution imaging of surfaces. An incident electron beam is raster-scanned across the sample's surface, and the resulting electrons emitted from the sample are collected to form an image of the surface. The electrons interact with the atoms that make up the sample producing signals that contain information about the sample's surface topography together with composition and other properties such as electrical conductivity.

Imaging is typically obtained using secondary electrons for the best resolution of fine surface topographical features. Secondary electrons are electrons generated as ionization products. Alternatively, imaging with backscattered electrons gives contrast based on atomic number to resolve microscopic composition variations as well as topographical information. Backscattered electrons (BSE) consist of high-energy electrons originating in the electron beam that are reflected or back-scattered out of the specimen interaction volume. Heavy elements (high atomic number) backscatter electrons more strongly than light elements (low atomic number), and thus appear brighter in the image. BSE are used to detect contrast between areas with different chemical compositions.

The advantages of SEM over light microscopy include greater magnification (up to 100,000X) and much greater depth of field.

For conventional imaging, the SEM requires that specimens be conductive for the electron beam to scan the surface and that the electrons have a path to ground. Therefore, samples need to be pre-treated before SEM analysis:

1. Slides with fixed tissue sections (5µm) were dewaxed in xylene and allowed to dry.
2. Each slide was mounted on an aluminium stub and introduced into the chamber of a sputter coater (2000V, 20mA, 5nm/min) to provide a very thin film of gold and increase conductivity before SEM examination.
3. Samples were inserted in the electron microscope (Zeiss Supra™ 35VP Gemini, Oxford Instruments) and each sample analysed for secondary electron imaging and back scattered electron imaging.

3.1.6 Statistical Analysis

One-way analysis of variance (ANOVA) was used to compare tensile strength parameters, degree of swelling, cross-linking level and pore size between types of matrices; results were presented as average ± standard deviations. For all statistical analysis a P value less than 0.05 was considered statistically significant, when $P<0.05$ a Bonferroni post-hoc test was performed for comparison within groups. Statistical analysis was performed using SPSS Statistics 16.0 (SPSS Inc. Chicago, USA). Graphical representation of data was performed using Graphpad Prism statistics software, version 4 (GraphPad Software, Inc., USA).

3.1.7 Results

3.1.7.1 Tensile Strength

Tensile strength was analysed for Permacol®, NonXL and Raw collagen. Sutures snapped in all samples, therefore, matrix failure was not observed in any sample.

Results are displayed in the following tables, average and standard deviations were calculated per type of matrix.

Table 3.3 – Tensiometry results for Permacol® surgical implant.

Matrix	Maximum Load (kg)	Extension at Maximum Load (mm)	Total Extension (mm)
Permacol® 1	3.899	41.690	41.910
Permacol® 2	3.745	43.620	44.390
Permacol® 3	3.001	39.340	39.900
Permacol® 4	2.796	47.040	50.100
Permacol® 5	1.305	24.630	28.450
Permacol® 6	3.575	35.640	35.870
Mean	**3.054**	**38.660**	**40.103**
SD	**0.958**	**7.879**	**7.421**

Noncross-linked samples presented higher maximum loads compared to Permacol® and Raw collagen, but lower extensions.

Table 3.4 – Tensiometry results for NonXL implants.

Matrix	Maximum Load (kg)	Extension at Maximum Load (mm)	Total Extension (mm)
NonXL 1	3.645	41.040	43.330
NonXL 2	3.100	38.370	39.000
NonXL 3	2.366	36.050	37.860
NonXL 4	3.522	33.630	34.120
NonXL 5	3.550	44.150	44.730
NonXL 6	3.594	36.850	37.310
Mean	**3.296**	**38.348**	**39.392**
SD	**0.496**	**3.760**	**3.966**

Table 3.5 – Tensiometry results for Raw collagen.

Matrix	Maximum Load (kg)	Extension at Maximum Load (mm)	Total Extension (mm)
Raw 1	3.506	37.640	37.770
Raw 2	2.161	35.610	39.520
Raw 3	1.320	60.410	61.730
Raw 4	3.361	33.500	33.850
Raw 5	2.881	31.920	32.100
Raw 6	3.627	39.440	39.630
Mean	**2.809**	**39.753**	**40.767**
SD	**0.906**	**10.478**	**10.717**

There were no significant differences between the types of matrix for all parameters analysed.

Figure 3.3 shows the mean values for the stress-strain curves for each matrix. At the beginning of the curve a flat region is observed [A-B] where the matrix has not fully responded to the load applied. Once the matrix starts responding it stretches originating a nearly linear region [B-C], the curve transits to a non-linear behaviour [C-D] that leads to the curve peak (maximum load). Complete failure is observed when neither load or extension increase [E].

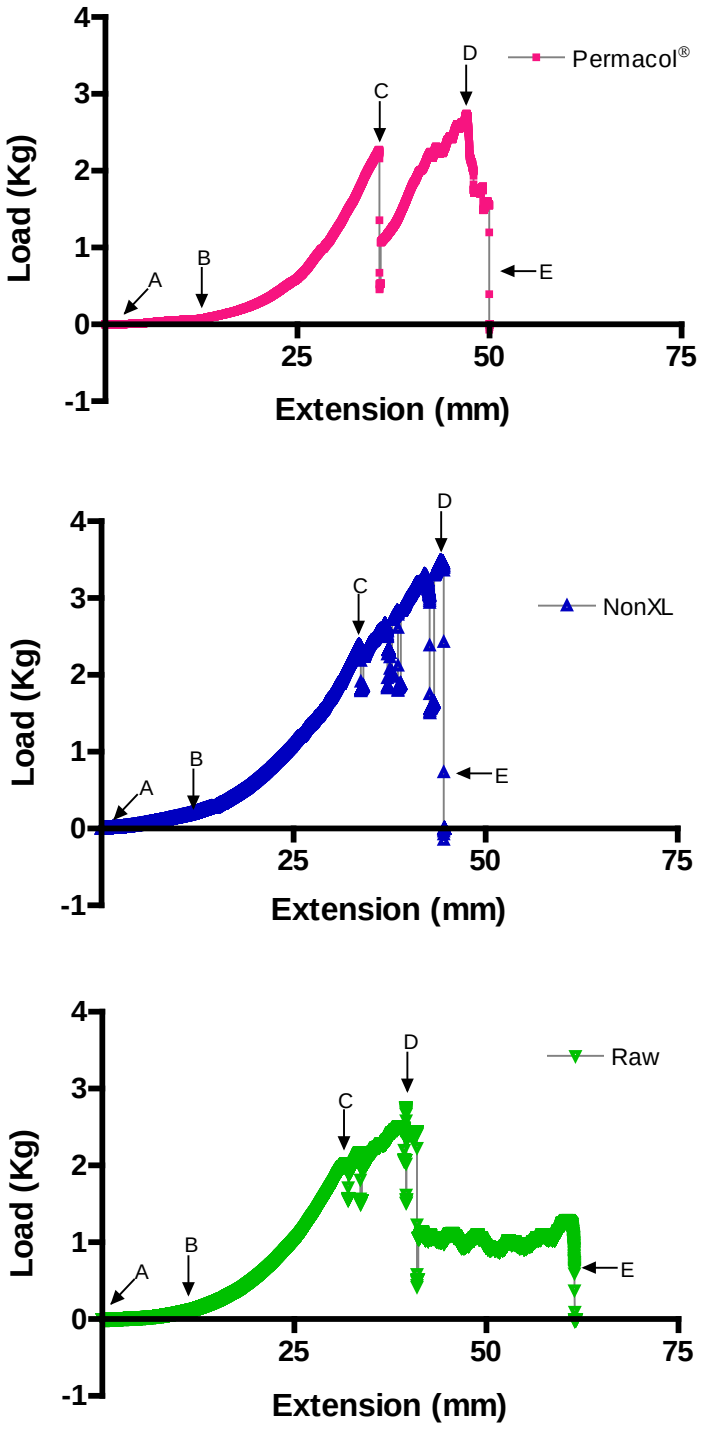

Figure 3.3 – Graphical representation of stress-strain curves per type of matrix. Mean values were used per each matrix, resulting in slightly irregular curves. D represents the maximum load, the extension from B to D is the extension at maximum load and from B to E total extension.

3.1.7.2 Water Uptake

Water uptake was assessed through degree of swelling of each matrix and equilibrium water content. ECW was higher for the NonXL matrix (1.18 ± 0.03), followed by Raw collagen (1.11 ± 0.03) and finally Permacol® (1.10 ± 0.01) (Figure 3.4).

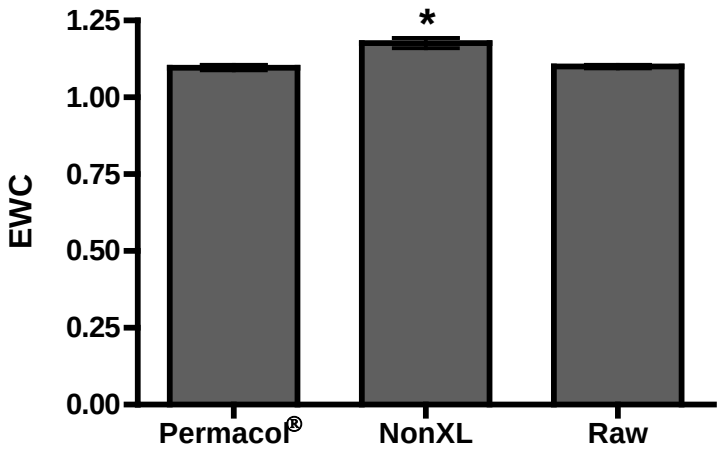

Figure 3.4 – Equilibrium water content per collagen type, mean values and standard deviations were calculated. * P<0.05.

Permacol® and Raw samples showed a similar profile of water uptake, although Permacol® matrix reached equilibrium quicker, there was no statistical difference between these matrices. NonXL collagen water uptake rate was slower and it took longer for this matrix to reach equilibrium, although it presented the highest degree of swelling at equilibrium. NonXL degree of swelling over time was statistically different from Permacol® (P<0.01) and Raw collagen (P<0.05) samples. The degree of swelling was plotted against time (Figure 3.5).

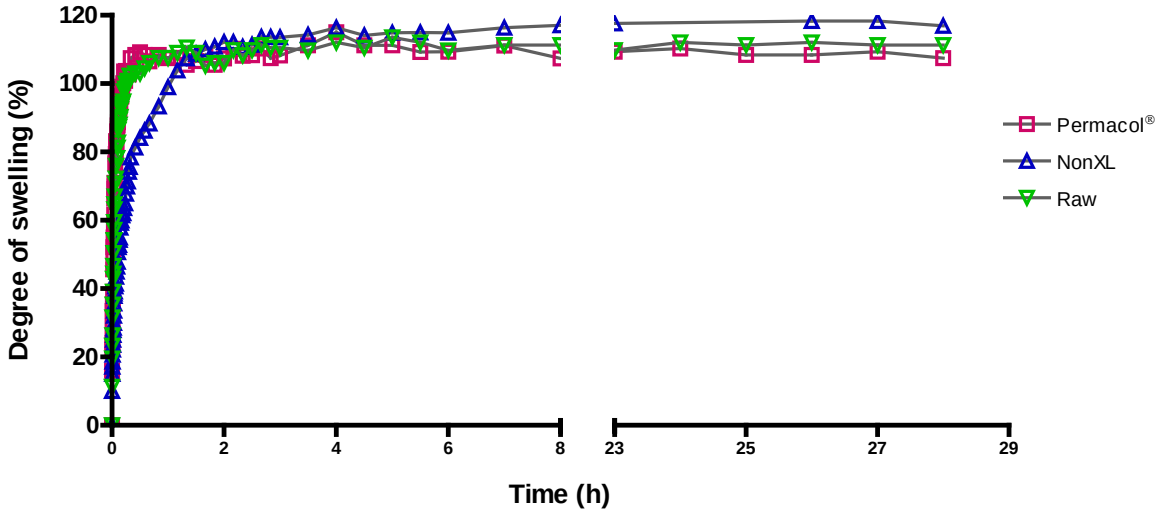

Figure 3.5 – Percentage of degree of swelling of collagen matrices.

3.1.7.3 Quantification of Cross-linking in Collagen Samples

3.1.7.3.1 TNBS Method

After addition of the aqueous TNBS solution samples developed an orange colour, this was visible throughout the reaction. When the reaction was terminated, by lowering the pH using acid and heating the samples for 90 minutes, Permacol® and NonXL samples were completely solubilised after the incubation period; Raw samples were still visible although with less volume. Just before absorbance measurement samples were mixed in a vortex, after this step Raw samples solubilised, although not completely; since Raw solutions were turbid, these were quickly centrifuged before absorbance measurement.

The next table shows results after values had been normalised. Mean and standard deviations (SD) were calculated.

Table 3.6 – Absorbance was measured at 420nm to quantify the content of free amino groups present in the collagen matrices. Values were normalized by subtraction of the negative controls.

Absorbance/mg tissue					
Permacol® 1	0.011	**NonXL 1**	0.020	**Raw 1**	0.021
Permacol ®2	0.014	**NonXL 2**	0.019	**Raw 2**	0.022
Permacol® 3	0.011	**NonXL 3**	0.020	**Raw 3**	0.019
Permacol® 4	0.015	**NonXL 4**	0.020	**Raw 4**	0.023
Permacol® 5	0.013	**NonXL 5**	0.017	**Raw 5**	0.021
Permacol® 6	0.014	**NonXL 6**	0.022	**Raw 6**	0.021
Mean	**0.013**	**Mean**	**0.019**	**Mean**	**0.021**
SD	**0.002**	**SD**	**0.002**	**SD**	**0.001**

Permacol® showed the lowest values for free amino groups in the matrix, which is not surprising since this collagen biomaterial is cross-linked, free amino group values were statistically significant ($P<0.001$) when compared to NonXL and Raw matrices. Raw collagen presented the highest number of free amino groups, implying that of the 3 types of collagen matrices tested this is the one with the lowest level of cross-linking. Although the NonXL samples are not cross-linked they were trypsinized to remove any cellular components, the enzyme treatment probably affects the collagen structure eliminating some amino groups. The following figure shows the mean values with standard deviations for all collagen matrices.

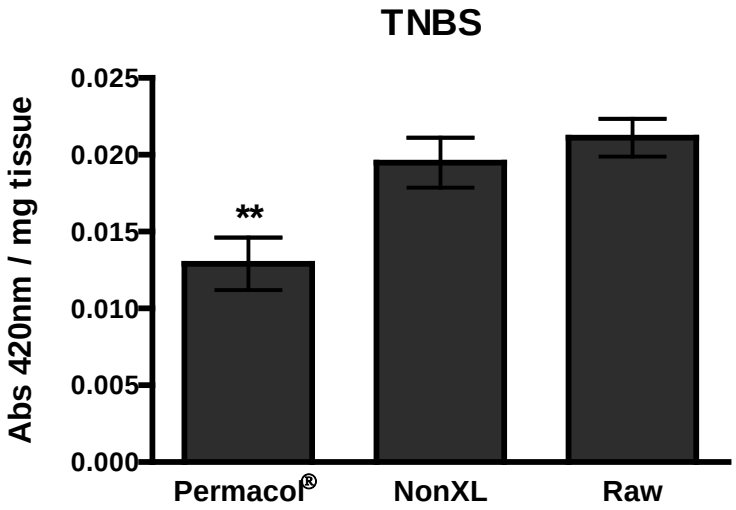

Figure 3.6 – Free amino group content in the collagen matrices, quantified by the TNBS assay.

3.1.7.3.2 Ninhydrin Method

After addition of the ninhydrin solution to the samples a purple coloration was observed confirming the production of the chromophore Ruhemann's purple. Ninhydrin assay showed a significant difference in the free amino group content of the NonXL collagen when compared to the other 2 matrices tested. The differences observed with this assay were not as significant as observed with TNBS, furthermore, the ninhydrin method quantified more free amino groups in the NonXL samples while with TNBS assay the absorbance readings showed higher amino content in the Raw matrix. Values were plotted in a graph; absorbance was calculated per mg of sample dry weight (Figure 3.7).

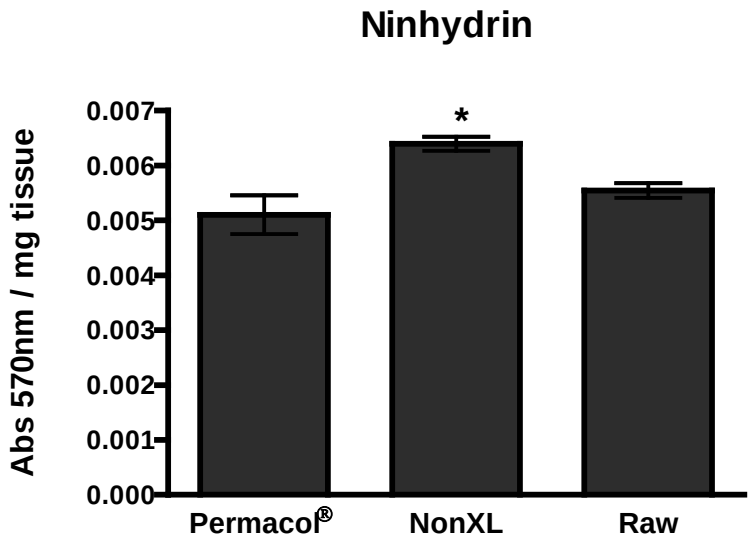

Figure 3.7 – Ninhydrin assay: absorbance readings per mg of dry weight of tissue.

3.1.7.4 Matrix Components and Structure

3.1.7.4.1 Histology

The collagen samples tested were composed mostly of thick fibres and were not very porous, which indicates that samples were harvested probably from the reticular dermis.

Histological analysis of the collagen matrices revealed considerable differences between their structures. In Raw collagen, although the fibres are compact except for hair follicles, there is not much space visible between collagen fibres, the overall structure does not show specific fibre orientation or pattern. In these samples cellular material is visible especially surrounding the hair follicles (Figure 3.8).

All matrices tested were very similar in composition, being almost entirely constituted by collagen alone. Raw samples showed elastin residues, although at very low concentrations.

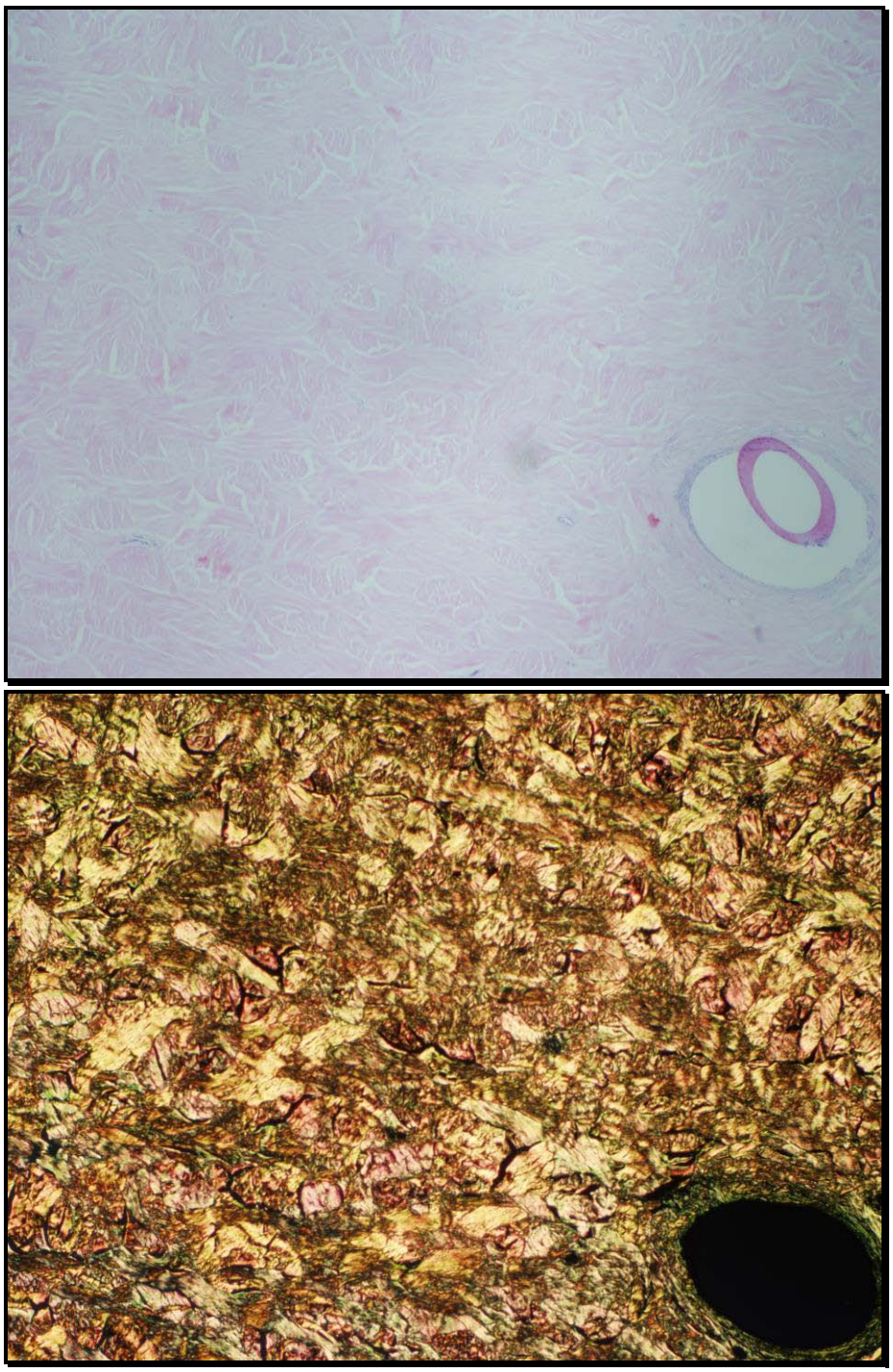

Figure 3.8 – Pictures represent sections from Raw collagen. The top figure was stained with H&E and the bottom figure with picro sirius red (40X).

In the noncross-linked collagen there is no evidence of cellular material; collagen fibres are more visible probably because of the increase in fissures since the interstitial tissue has been removed (Figure 3.9).

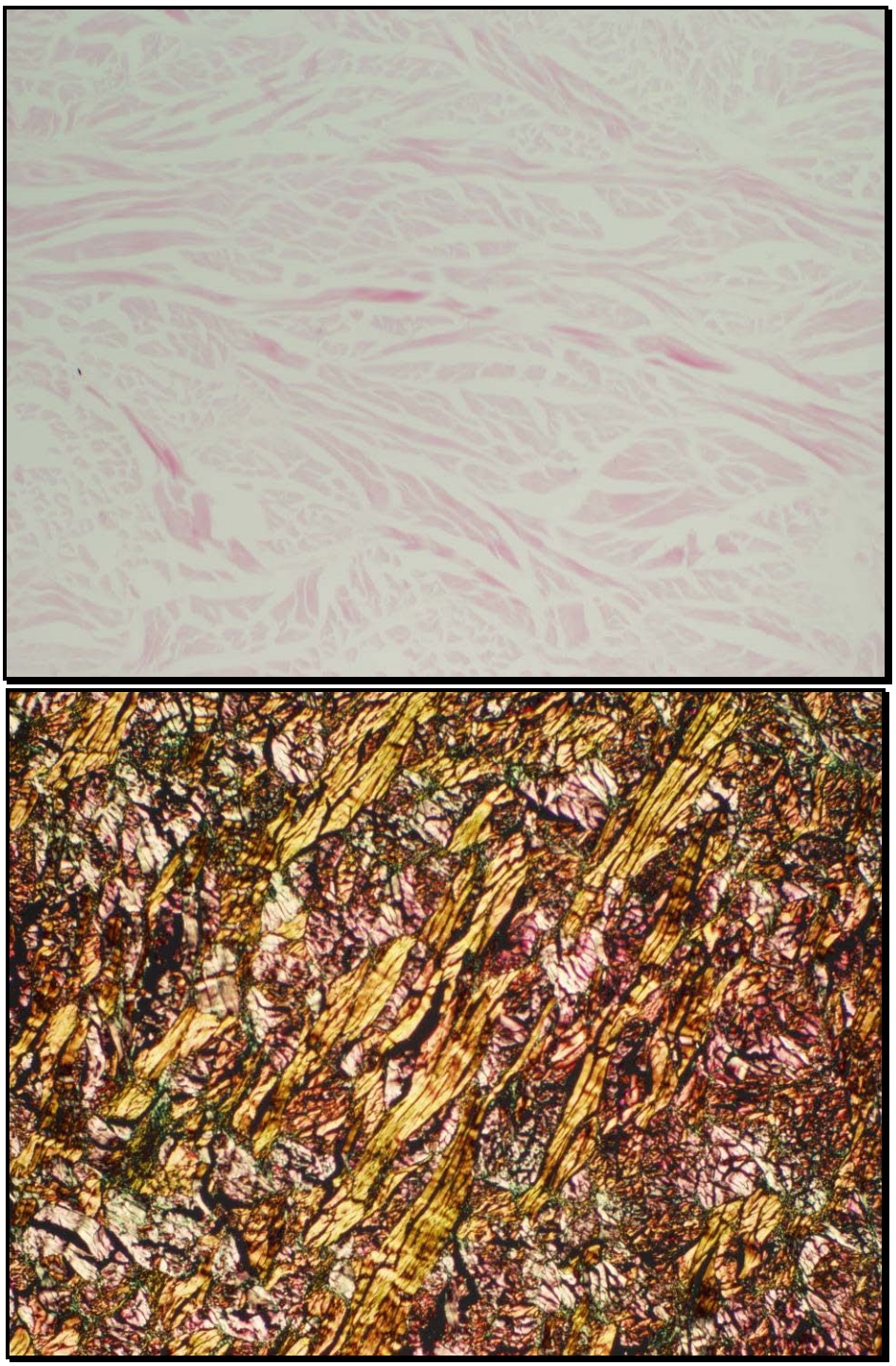

Figure 3.9 – Noncross-linked porcine collagen sample stained with H&E (top) and picro sirius red (bottom) (40X).

The process of cross-linking induces ligation between the proteins present in the sample; this makes samples more compact and well structured. Collagen fibres in Permacol® are well defined, with spatial orientation and with a better resolution (Figure 3.10).

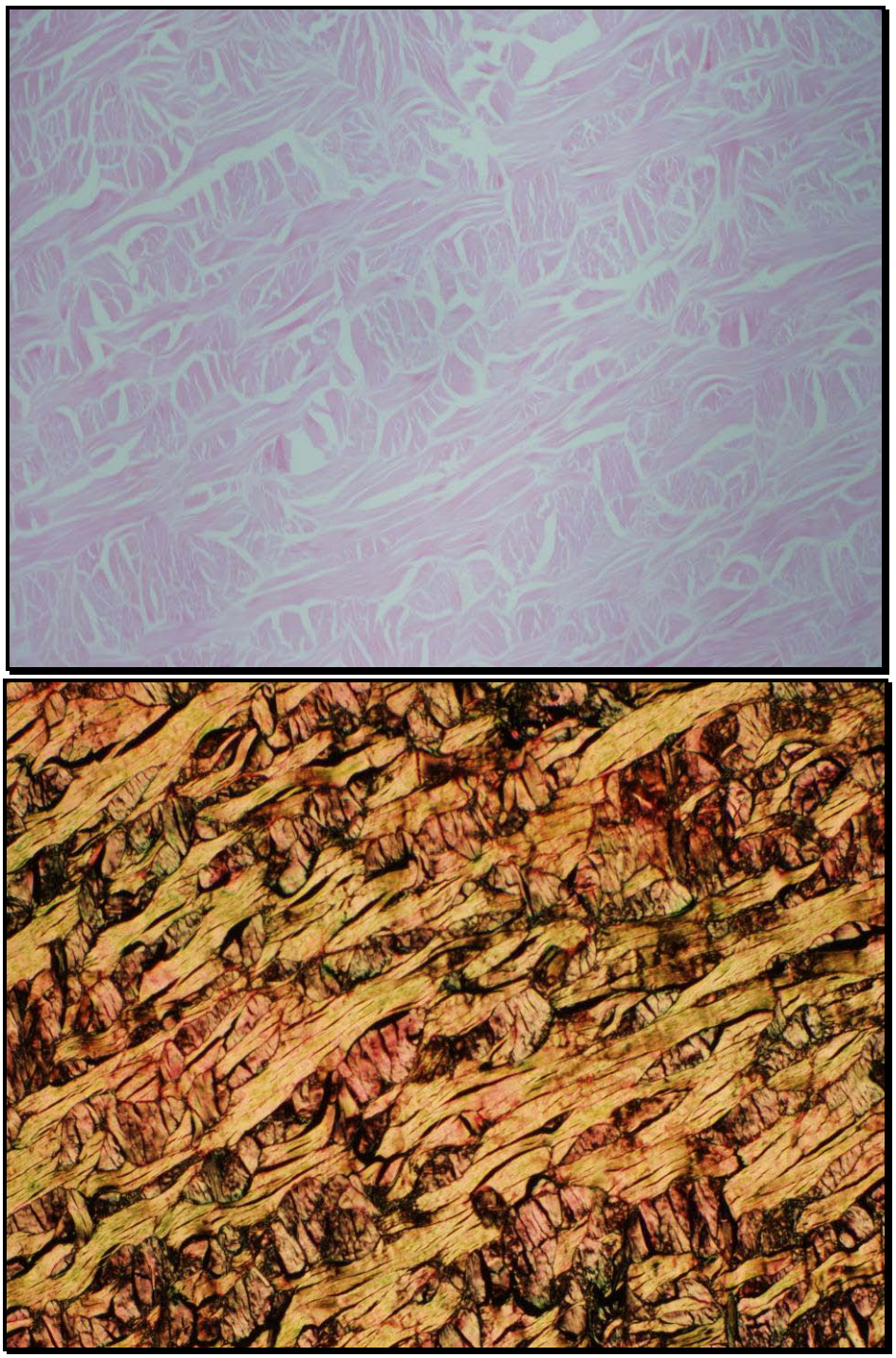

Figure 3.10 – Permacol® samples stained with H&E (top) and picro sirius red (bottom) (40X).

All collagen matrices showed birefringent collagen, which is indicative of good quality, non-denatured, collagen as observed with picro sirius red staining.

3.1.7.4.2 Pore Size

Pore size varied within each type of collagen matrix and between collagen matrices. NonXL showed increased pore size as expected, as a consequence of the cell extraction method. Permacol® had the lowest mean pore size which might be a result of the cross-linking method. Mean and standard deviations were calculated (Table 3.7).

Table 3.7 – Pore size (μm) of each collagen matrix.

	Mean ± SD	**Range**
Permacol®	15.2 ± 3.53	[11.0 – 21.0]
NonXL	20.3 ± 1.79	[18.0 – 23.1]
Raw	17.2 ± 5.26	[10.0 – 21.3]

3.1.7.4.3 SEM

Differences in collagen matrix structure and molecule orientation were confirmed by SEM. Raw collagen showed an amorphous structure and fibres were not as well defined as observed in the other two matrix types. Permacol® and NonXL collagen fibres were well defined and a pattern was visible at lower magnification (Figure 3.11). At higher magnification NonXL collagen fibres looked damaged and were less defined compared to the Permacol® matrix.

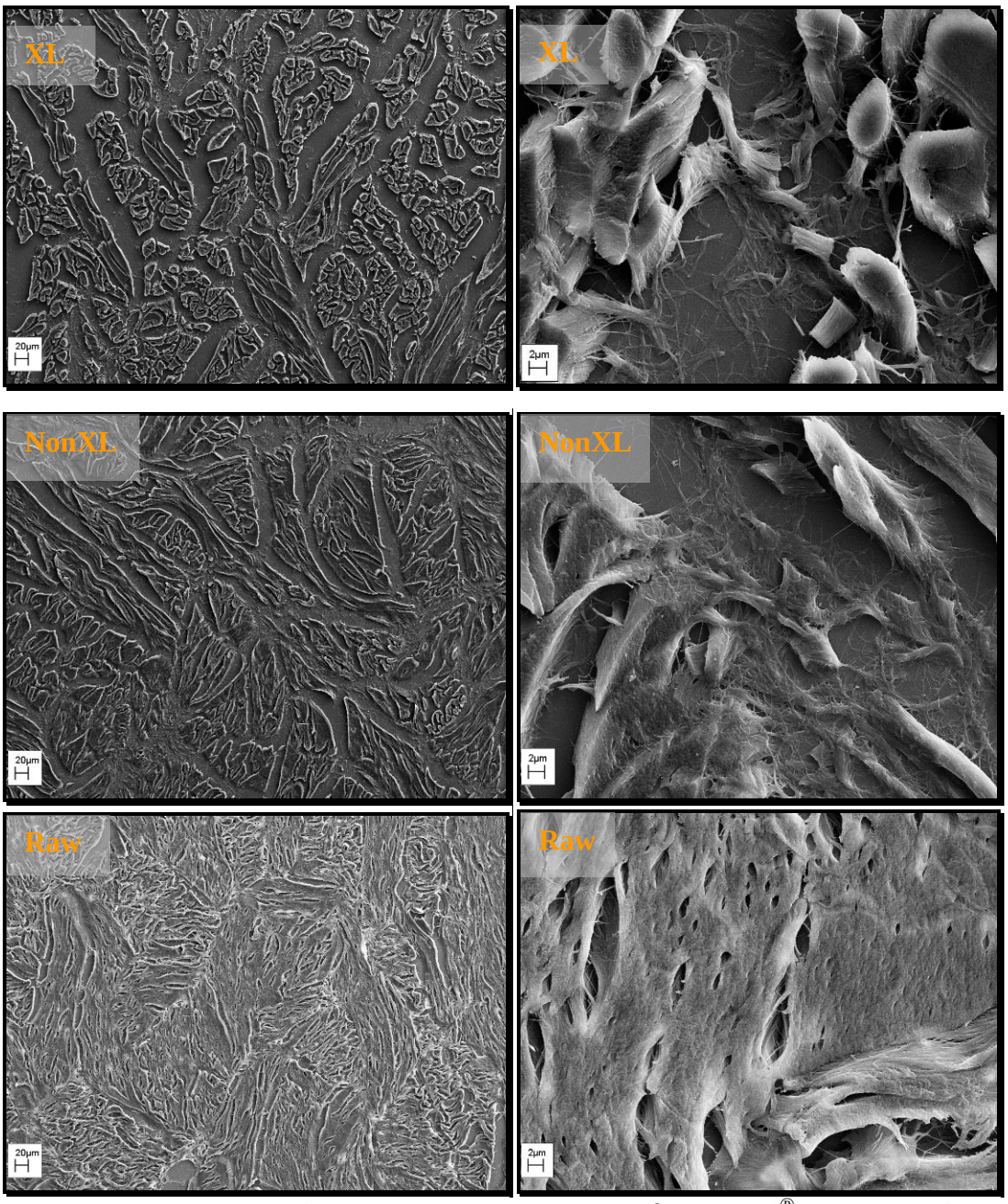

Figure 3.11 – Scanning electron microscopy images of Permacol®, NonXL and Raw collagen matrices. Left column: 500X; Right column: 6000X.

3.1.8 Discussion

Currently there is a wide range of biomaterials available for tissue repair or tissue substitution. Surgeons can choose from synthetic and natural biomaterials and these prostheses are further categorised depending on source, manufacturing process,

components and clinical applications. Before a decision is made on which prosthesis is more suitable for a particular patient, surgeons must be well informed regarding properties, prescription and probable outcomes of a specific biomaterial. Therefore, it is of most importance for a biomaterial to be well characterized.

Tensile strength showed some variation between matrices although differences were not significant. Samples were resistant to the force applied and there was no matrix failure, in all samples tested sutures snapped with the tension applied.

When assessing water uptake in the different collagen matrices, NonXL showed a slightly higher value compared to the other 2 biomaterials indicative of a higher absorbance capacity. The swelling ratios for the NonXL samples were initially lower and equilibrium was reached later for this matrix; this may be explained by the low cross-linking density in these samples caused by the cell extraction process, which may result in difficulty to initially retain the absorbed water within the matrix but with time NonXL matrices absorbed more water at equilibrium than Permacol® and Raw samples. Permacol® and Raw collagen samples showed similar profiles and similar ECWs, which implies that the cross-linking level of Permacol® is probably similar to Raw porcine collagen.

During cross-linking quantification by TNBS assay, where the content of free amino groups in the collagen matrices is determined, Permacol® samples showed a significant lower amount of free amino groups, which is related to a higher level of cross-linking. Ninhydrin assay was also used for cross-linking quantification but results were different from the TNBS assay. With this method there was no significant difference between Permacol® and Raw collagen samples, suggesting that in this case the ninhydrin method is not sensitive enough to detect differences in the cross-linking levels between these two types of collagen matrices.

TNBS assay showed a higher content of free amino groups (indicative of a lower cross-link level) in the Raw collagen samples, followed by NonXL collagen and finally Permacol®. NonXL samples are enzymatically digested, which affects the collagenous material not only by eliminating the cellular fraction but also by breaking some of the intra- and intermolecular cross-links of the collagen molecules. Following this line of thought one would expect NonXL samples to show to lowest level of cross-link but the enzymatic digestion may affect the amino groups since trypsin is

responsible for cleaving peptide bonds following a positively-charged amino acid residue, which releases the N-terminus of the peptide. The N-terminus is required for the TNBS reaction; if during trypsinization some of the N-terminii were cleaved from the collagen molecules, the amount of TNP-derivatives will be lower. Ninhydrin assay showed contrary results, NonXL samples presented the lowest level of cross-linking. Furthermore, results obtained with the ninhydrin assay were much lower than the values obtained with the TNBS assay. Permacol® showed the lowest number of free amino groups, which relates to a higher level of cross-linking, in both methodologies. This discrepancy between TNBS and ninhydrin assays has been reported before by Panasiuk and colleagues (Panasiuk *et al.*, 1998), they found that these methods were not correlated and considered results obtained with the TNBS method more accurate than those from ninhydrin assay.

In accordance with the cross-linking quantification assays, pore size was also lower in Permacol® samples. The cross-linking of collagen molecules increases the physical proximity between fibres and as a consequence pore size and the space between natural septae diminishes. Except for NonXL samples, the average pore size of matrices was bellow 20µm. Although the literature recommends scaffolds with pore size between 20 and 200µm (to facilitate cell migration), raw collagen samples showed an average pore size of 17.2 ± 5.26µm; porcine dermal collagen is natively cell populated, this implies that scaffold pore size can have a wide range and high pore size is not essential for cellular penetration, other factors such as cell type and matrix composition and structure will also influence cell migration.

Histological and SEM analyses showed differences in the matrix structures and fibre orientation. Raw collagen contained a compact structure compared to the noncross-linked collagen and Permacol®, this was expected given that the two latter matrices undergo enzymatic treatment which could result in more fissures where the interstitial tissue was previously, because of the compact and slightly amorphous structure of Raw matrix, fibres were not well defined and were difficult to discern. Cross-linking imparts a superior resolution of fibres and the matrix structure is more organized as observed in the Permacol® surgical implant samples.

3.1.9 Conclusion

The physical, mechanical and structural properties of the collagen matrices tested in this study varied depending of the treatment(s) used in the processes performed to create the biomaterials. Structurally, Raw collagen was very different from the other two matrices, the cell extraction process is quite aggressive, depleting the matrix of all non-collagenous tissues. Despite the differences in structure and collagen fibre orientation, water uptake profile was not statistically different between Permacol® surgical implant and Raw porcine collagen. There was a significant difference between the free amino group content of Permacol® and the other matrices, independent of the method used (TNBS or ninhydrin); however, it is important to note that average values were not very different between matrices, e.g. Permacol® = 0.013 ± 0.002, Raw = 0.021 ± 0.001; Permacol® = 0.0051 ± 0.0004, Raw = 0.0055 ± 0.0001 using the TNBS and ninhydin assays respectively. This suggests that Permacol® surgical implant is not highly cross-linked and it is possible that the cross-linking process mainly establishes the intra- and intermolecular bonds that were cleaved during cellular extraction, adding only a few more cross-links between molecules. Nevertheless, the pore size decreased after cross-linking which is a typical effect of cross-linking.

3.2 PROTEOLYTIC DIGESTION OF COLLAGEN BASED BIOMATRICES

3.2.1 Introduction

The growing demand for natural products with applications in the clinical field has directed interest to the study of biomaterials with multiple functions, such as collagen. Mature native collagens are insoluble in water and therefore they can only be degraded by a few specific enzymes. Collagen degradation occurs in various physiological and pathological conditions, such as embryonic development, tumour invasion and wound healing. Wounds heal by a complex cascade of events including coagulation, inflammation, granulation tissue formation and tissue remodelling. During the inflammatory phase neutrophils and macrophages accumulate in the surrounding tissue and secrete and activate a range of proteases including matrix metalloproteinases (MMPs) and serine proteases (Jackson *et al.*, 2005).

MMPs are a homologous group of zinc-dependent extracellular endopeptidases, responsible for the breakdown of the major protein components of the ECM (Netzel-Arnett *et al.*, 1991) and are produced by several cell types, including leukocytes. Neutrophils provide host defence against foreign bodies including bacterial and fungal infection, but they can also cause pathological tissue destruction mediated by the release of proteolytic enzymes, which are stored in intracellular granules. These granules are divided into primary and secondary depending on the type of enzymes they store; primary granules contain high quantities of serine proteases, including neutrophil elastase, the secondary granules store neutrophil collagenase, also named MMP-8 (Kafienah *et al.*, 1998; Siedle *et al.*, 2002). These enzymes are present in increased amounts when a chronic wound is formed. MMP-8 has been reported to hydrolyse collagen type I and collagen type III, although it shows higher substrate specificity towards collagen type I (Mallya *et al.*, 1990b). Neutrophil elastase has been associated with a variety of inflammatory diseases and has been implicated in non-healing wounds. Though all wounds require elastase for proper healing, the

presence of high levels of this enzyme in non-healing wounds has been associated with the degradation of proteoglycans, collagen, growth factors and fibronectin.
Excessive accumulation of these enzymes interferes with the remodelling of the ECM, cell migration and impairs healing. Consequently, when using biomaterials in problematic areas, especially within a chronic wound, it is useful to predict their performance and to choose a material which would present some resistance to proteolytic digestion.
A substantial amount of literature has covered the progress of cross-linking treatments to modify the mechanical and degradation properties of collagen implants in order to improve the resistance against enzymatic degradation. Physical, enzymatic, chemical and combination treatments have been extensively developed, characterised and applied in both *in vitro* and *in vivo* studies. The biomaterials tested in this study were cross-linked with HMDI and 1-ethyl-3-(3-dimethylaminopropyl) carbodiimide hydrochloride (EDC), to increase resistance to proteolytic digestion.

3.2.2 Aims and Objectives

- Assess the resistance of collagen derived matrices to proteolytic enzymes.
- Compare cross-linked to noncross-linked materials.
- Compare two cross-link reagents.

3.2.3 Hypothesis

Cross-linking of collagen derived biomaterials increases matrix resistance to proteolytic activity.

3.2.4 Materials and Reagents

DMSO, Trizma base, sodium chloride, calcium chloride dihydrate, phenylmethanesulfonyl fluoride (Ph-$MeSO_4F$), 4-aminophenylmercuric acetate (APMA) and hog pancreatic elastase were purchased from Sigma-Aldrich Company Ltd. (Gillingham, Dorset SP8 4XT, U.K.). Sodium hydroxide and EDTA were acquired from Fisher Scientific UK (Leicestershire LE11 5RG, U.K.). Collagenase type I, human neutrophil elastase, MMP-8 and Methoxysuccinyl-Ala-Ala-Pro-Val-ρ-nitroanilide were purchased from Calbiochem (Merck Chemicals Ltd, Nottingham, NG9 2JR, U.K.).

Permacol®, noncross-linked acellular porcine collagen (NonXL), dermal porcine collagen (Raw) and EDC cross-linked acellular dermal porcine collagen (EDC-XL) were supplied by TSL plc.

3.2.5 Methods

3.2.5.1 Collagenase Digestion

The degradation of native collagen is initiated by the action of collagenases. Therefore, collagenase digestion of cross-linked matrices is usually the method of choice to predict the rate of collagen fibre degradation *in vivo* (Speer *et al.*, 2006).

Lyophilised collagen matrices (Permacol®, NonXL, Raw and EDC-XL collagen) were weighed and added to a 2mL bacterial collagenase solution (21U/mL) in assay buffer (50mM Tris, 10mM $CaCl_2$, pH 7.4). Experiments were carried out in triplicate and the same number of samples were used as negative controls (matrix and assay buffer only). Samples were incubated at 37°C for 3h, 8h and 24h. Inactivation of reaction was performed by adding 0.2mL of 10mM EDTA pH 8.0. Samples were washed in deionised water and lyophilised. New dry weights were recorded and percentage of weight loss (digested tissue) calculated by the following equation:

$$\%\ Weight\ Loss = \frac{Wi - Wf}{Wi} \times 100\%$$

Here W_i represents the initial dry weight and W_f the final dry weight.

3.2.5.2 Porcine Pancreatic Elastase Assay

Elastase is a serine protease that has been associated with a variety of inflammatory diseases and has been implicated in a destructive proteolysis in non-healing wounds. Though all wounds require a certain level of elastase for proper healing, the presence of high levels of elastase in non-healing wounds has been associated with the degradation of elastin, proteoglycans, collagen, growh factors and fibronectin necessary for wound healing (Trengove *et al.*, 1999). Following the same principle as in the collagenase assay, elastase was used to assess elastin stability. Permacol® is HMDI cross-linked to provide resistance to enzyme degradation. Permacol®, process intermediates and EDC cross-linked collagen were tested for resistance to elastase.

Several enzyme concentrations and incubation times were tested before appropriate standard conditions were protocolled.

Permacol®, NonXL, Raw and EDC-XL collagen were lyophilised and dry weights measured. At least 8 samples were used per collagen matrix (4 samples to be tested and 4 to act as negative controls) per time point. Porcine aorta was used as positive control since this tissue contains high amounts of elastin.

Samples weighing 50 ± 0.5mg were placed in amber-eppendorf tubes with 1mL of 0.2M Tris buffer, pH 8.0. To half the tubes (tested samples) 0.14U of elastase were added per mg of tissue.

Tubes were incubated in a water bath at 37^{o}C for 24, 48, 72 and 96 hours. After incubation reactions were terminated by adding elastase inhibitor – Ph-$MeSO_4F$ – in a concentration three times superior to the elastase. Tubes were left in the dark at room temperature for 15 minutes

Samples were rinsed 3 times in deionised water and lyophilised. The new dry weights were measured and percentage of weight loss calculated as described before. Samples were hydrated in deionised water overnight and fixed in 10% NBF for histological analysis. A picro/Miller stain was performed to visualise collagen and elastin within the matrix.

3.2.5.3 Human Neutrophil Elastase Assay

Human neutrophil elastase (HNE) is a strong basic glycoprotein with specificity for small hydrophobic amino acids; therefore, HNE has broad substrate specificity and can degrade a wide range of extracellular proteins including elastin, proteoglycans, immunoglobulines, denatured collagens, fibronectin and laminin (Siedle *et al.*, 2002). It has also been shown to cleave native collagen types I and III in the helix (Mallya *et al.*, 1990b) and telopeptides of collagen types I, II and III (Kafienah *et al.*, 1998).

Before test samples were used human neutrophil elastase (HNE) assay was performed with Elastase Substrate I (MeOSuc-Ala-Ala-Pro-Val-ρNA) to confirm enzyme activity.
Human neutrophil elastase was reconstituted in 100mM Tris pH 5.5 with 500mM NaCl, divided into aliquots and stored at -20^{o}C. A 50mM MeOSu- stock solution was prepared by dissolving the substrate in DMSO and stored at -20^{o}C.
Immediately before the assay, the substrate stock solution was dissolved in an equal volume of 200mM Tris, pH 8.0. Six concentrations of enzyme were used (100ng, 250ng, 500ng, 1µg, 2.5µg and 5µg) and two controls were prepared, one with MeOSu- only and the other with 1µg of HNE only.
A 96-well plate was prepared with 430µL of the reaction buffer (100mM Tris, pH 7.5 with 500mM NaCl) in each well. To rows 1 to 6, 20µL of the diluted substrate solution was added. Each row was incubated with a different enzyme concentration. To the 7th row 20µL of the diluted substrate solution was added and to the 8th row no substrate was added, instead 1µg of HNE was placed in each well.
The well-plate was incubated at 25^{o}C and the change in absorbance monitored at 405nm for a period of 2 hours to observe the hydrolysis of nitroanilide.

The dry weights of lyophilised test samples (Permacol®, NonXL and Raw) were measured and recorded. Porcine aorta was used as positive tissue. Negative controls were prepared from each type of collagen matrix and from porcine aorta. Control matrices were incubated in the respective enzyme-free buffer solution under the same conditions as in the digestion studies. Enzyme concentration and incubation times

were manipulated until elastin digestion was observed in the positive control; at that point the experimental conditions were used as test conditions for all samples.
Before digestion samples were hydrated in deionised water for 1 hour following which samples were placed in individual tubes and 550µL of reaction buffer added. To test samples and positive control 50µg of HNE (21U/mg) was added (Trengove *et al.*, 1999). Samples were incubated at 25^{o}C ± 2^{o}C for 48 hours. Each sample was rinsed in deionised water and lyophilised, new dry weights were measured and percentage of weight loss calculated. Samples were once again hydrated overnight and fixed in 10% NBF for histological analysis after picro/Miller stain.

3.2.5.4 MMP-8

MMP-8 or human neutrophil collagenase is one of the few proteolytic enzymes that catalyses extracellular fibrillar collagen (Kafienah *et al.*, 1998). MMP-8 is mainly produced by neutrophils, where it is concentrated in secretory granules that are degranulated on neutrophil activation. This enzyme was also identified at low levels in monocytes and in alveolar macrophages (Tyagi and Simon, 1993). MMP-8 has been reported to degrade type I collagen at a higher rate than type III collagen (Hasty *et al.*, 1987; Mallya *et al.*, 1990a; Nwomeh *et al.*, 1999).
MMP-8 is observed as soon as 24 hours after a wound healing process is activated and it is present in the wound area up to 7 days after injury. At its highest levels MMP-8 concentration varies between 500 and 2500ng per millilitre of wound fluid (Aiba-Kojima *et al.*, 2007).

MMP-8 was acquired in its inactive form; therefore, organomercurial activation was necessary just prior to use. A 0.02M solution of APMA was prepared in 0.1M NaOH and pH adjusted to 11.0. MMP-8 was activated in this solution in a ratio of 1:10 (APMA:MMP-8) for 2 hours at 37^{o}C.
Lyophilised porcine collagen samples (Permacol®, NonXL and Raw) were weighted (approximately 6mg) and incubated in 100mM Tris buffer pH 7.5 (assay buffer) with MMP-8 at various concentrations (0.5 – 3µg) for different periods of time at 37^{o}C, negative controls were prepared from each matrix type. After rinsing samples with

deionised water, samples were once again lyophilised and new dry weights measured. Percentage of digested tissue was calculated.

3.2.6 Statistical Analysis

Two-way analysis of variance (ANOVA) was used to compare percentage of digested tissue between type of matrix and incubation period. Levene's test of equality of error variances was used to test the assumption that variances are equal; if Levene's $P<0.05$ and variances statistically different one-way ANOVA analysis was used to compare matrices per incubation time and Tamhane's post-hoc test performed to compare groups. For all statistical analysis a P value less than 0.05 was considered statistically significant. Statistical analysis was performed using SPSS Statistics 16.0 (SPSS Inc. Chicago, USA). Graphical representation of data was performed using Graphpad Prism statistics software, version 4 (GraphPad Software, Inc., USA).

3.2.7 Results

3.2.7.1 Collagenase Digestion

Dry weight loss increased with time of incubation for all collagen types tested. Permacol® and Raw collagen samples showed similar results at all time points. NonXL samples lost higher amounts of collagen at 8h and 24h compared to the other 3 matrices. EDC-XL matrices showed the lowest weight loss at all time points; after 3h incubation samples did not show weight loss and after 8h and 24h of collagenase digestion EDC-XL samples showed only marginal weight loss. Percentage of weight loss was calculated per incubation time and values were normalised with values obtained from control samples (Figure 3.12).

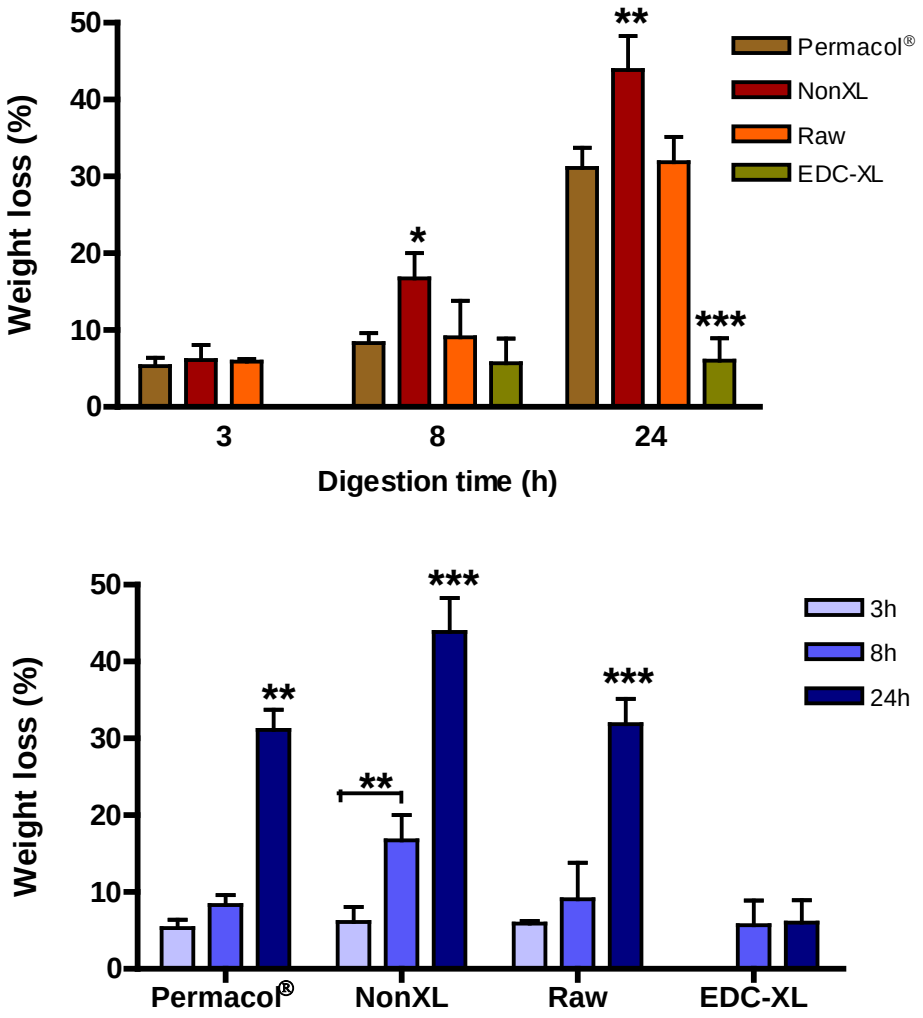

Figure 3.12 – Percentage of weight loss for collagen matrices after collagenase digestion. Mean and standard deviations were calculated and used for graphical representation. *P<0.05, **P<0.005, ***P<0.001.

When comparing matrix weight loss at each incubation time, the amount of collagen digested from NonXL samples was statistically different from the other matrices at 8h (P<0.05) and 24h (P<0.01). The difference between EDC-XL samples and the other collagen matrices at 24h was also significant (P<0.001). Each matrix was individually analysed and incubation times compared. Except for the EDC-XL samples all matrices showed a significant increase of collagen digestion after 24h incubation. The increase in weight loss of NonXL samples from 3 to 8h was also significant. Incubation time is a significant factor for matrix digestion when other variables are constant, such as enzyme concentration.

3.2.7.2 Porcine Pancreatic Elastase

Percentage of dry weight loss increased with the incubation time in all collagen matrices tested. The noncross-linked samples had the highest values of weight loss at all incubation times, followed by the untreated, raw collagen samples. Permacol® and EDC-XL showed higher resistance to elastase digestion and the percentage of weight loss was lower compared to the other matrices.

The weight of control samples also changed; at 24 and 48h the control Raw collagen samples increased weight. Permacol® control samples increased weight at all incubation times. Noncross-linked collagen control samples increased weight at 24, 48 and 72h. EDC-XL control samples did not increase weight, contrarily these samples lost weight. Due to this change in the control samples, values were normalised for the tested collagen matrices.

Figure 3.13 shows results for elastase digestion, normalised values were used, error bars represent standard deviations.

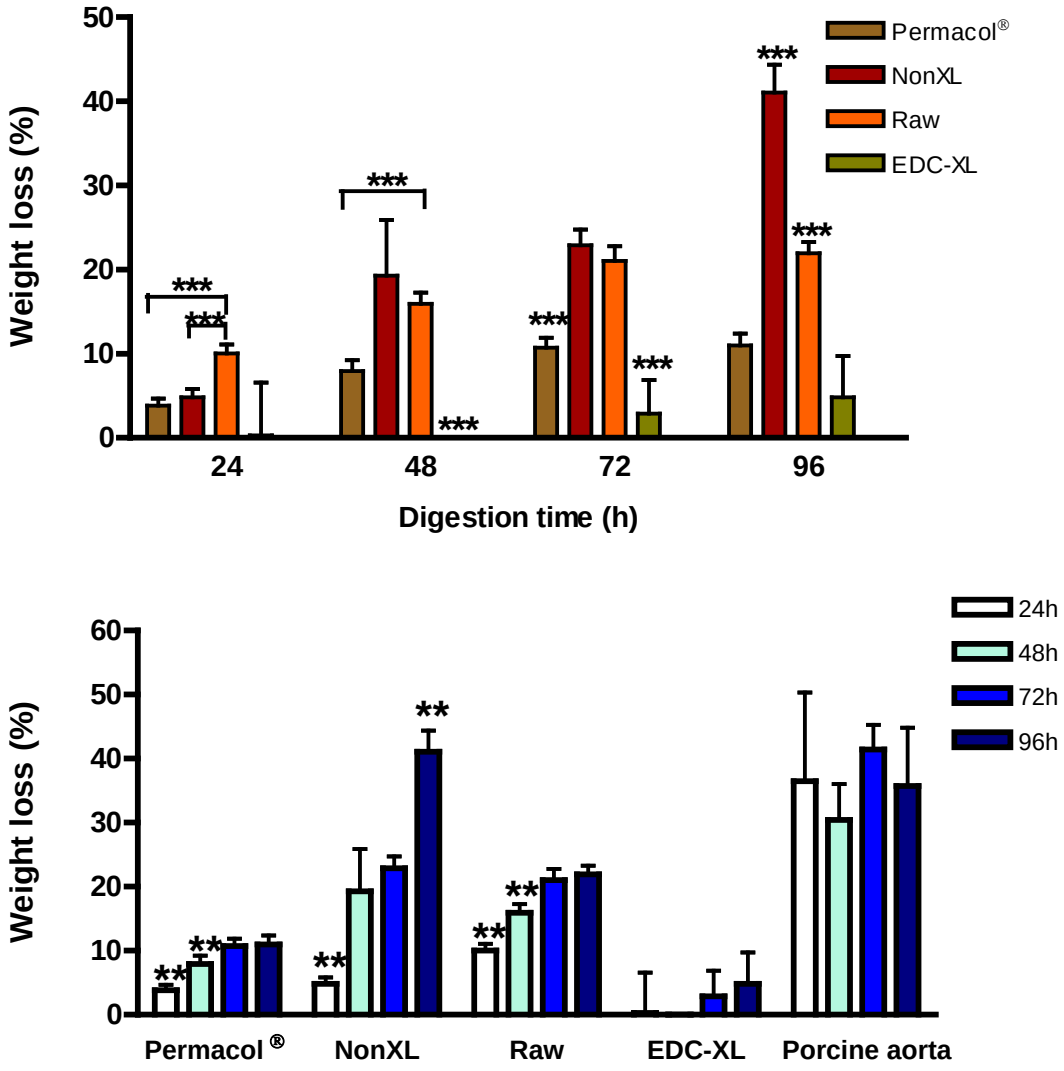

Figure 3.13 – Normalised percentage of weight loss, after elastase digestion, for all collagen matrices at different incubation periods. Mean and standard deviations were calculated and used for graphical representation. **P<0.005, ***P<0.001.

There was a statistical difference between groups when analysing each incubation time point. A significant difference was observed between matrices at all time points, except at 24h and 48h where Permacol® weight loss was not significantly different from NonXL and EDC-XL weight losses. NonXL and Raw collagen weight losses were not significantly different at 48h and 72h.

When analysing type of matrix a significant difference was observed with incubation time. With Permacol® and Raw collagen matrices there was evidence of significant differences between incubation times except between 72 and 96 hours. NonXL

samples did not show a significant difference in weight loss between 48h and 72h incubation but all other groups within this matrix showed significant differences. EDC-XL samples did not show significant differences independent of incubation time.

Histological analysis did not show elastin in the control samples of Permacol®, NonXL and EDC-XL collagen, and only very marginal amounts of elastin were present in the control samples of Raw collagen (Figure 3.14). With time, a slight variation in the fibres structure was observed, interstitial space seemed to increase, this was observed in all matrices.

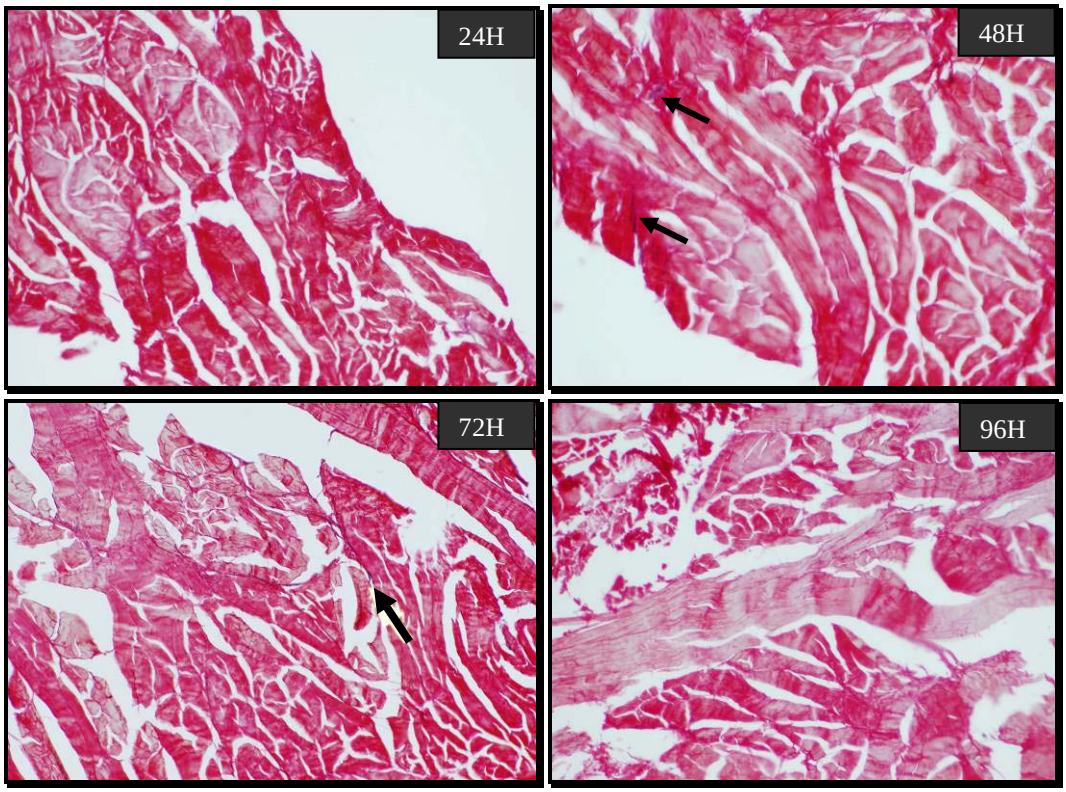

Figure 3.14 – Raw collagen control samples at different incubation times; arrows show elastin in blue (picro/Miller stain, 200X).

To test elastase activity and substrate specificity porcine aorta was used as positive control (Figure 3.15).

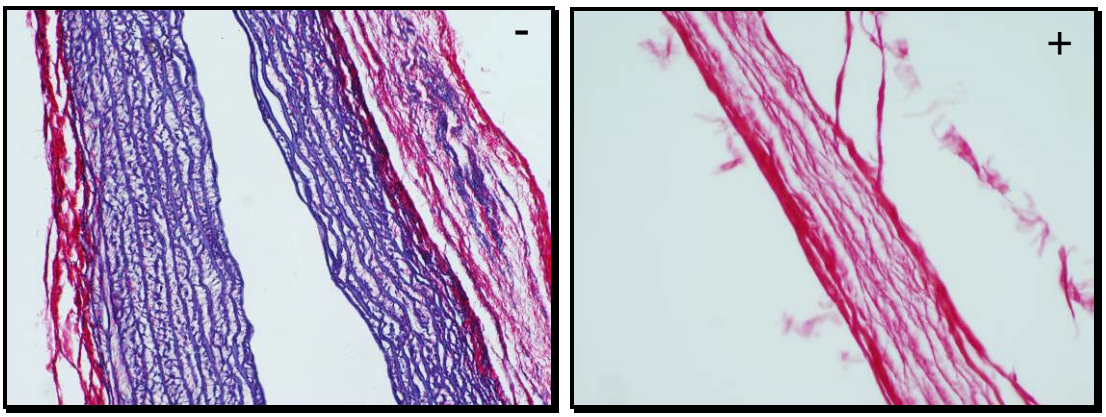

Figure 3.15 – Porcine aorta used as positive control for elastase digestion after 48 hours incubation. Left: control sample, incubated with buffer only, blue=elastin, pink=collagen, 200X. Right: reaction with 1mg/mL elastase, 400X. Picro/Miller stain.

Elastin was not visible in any of the collagen matrices after elastase digestion, independent of incubation time.

In all controls and samples tested collagen was naturally birefringent and non-degraded (Figure 3.16).

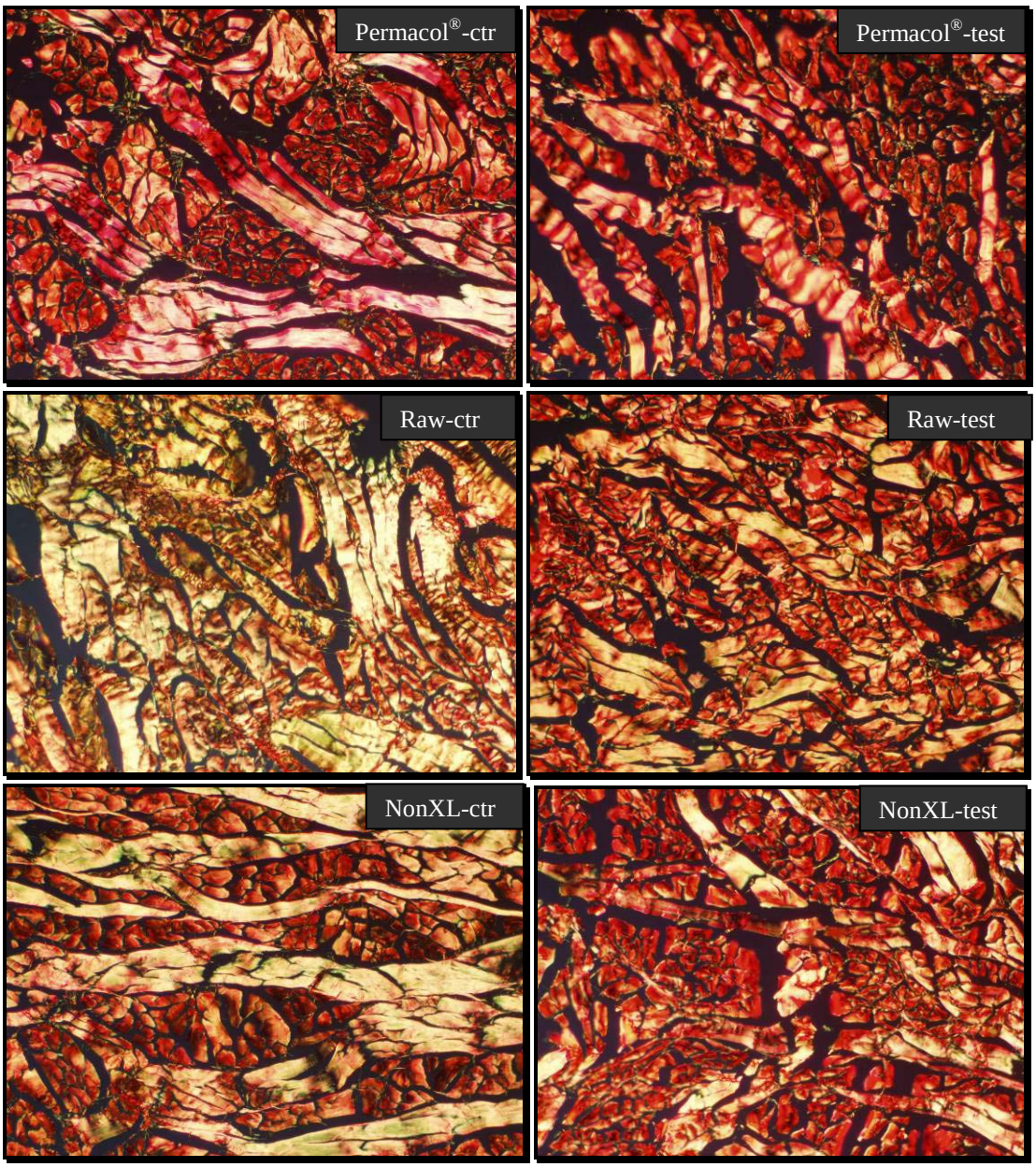

Figure 3.16 – Collagen matrices after 96h elastase assay, picro/Miller stain under polarised light, 200X.

3.2.7.3 Human Neutrophil Elastase

HNE-substrate assay showed increased hydrolysis of nitroanilide over time and hydrolysis rate was dependent on enzyme concentration. The reaction was very fast for 2.5µg and 5µg of enzyme and since the first absorbance reading was taken after 10 minutes of incubation, the substrate had been exhausted by then. For 100ng, 250ng

and 500ng the reaction was still active going after 2 hours incubation. When testing 1µg of HNE it was possible to observe substrate consumption until approximately 1 hour. The absorbance values were converted into concentration using the nitroanilide coefficient of extinction (ε=8800$M^{-1}cm^{-1}$) at 410nm (Trengove *et al.*, 1999). Concentrations were plotted against time, mean ± SD values were used (Figure 3.17).

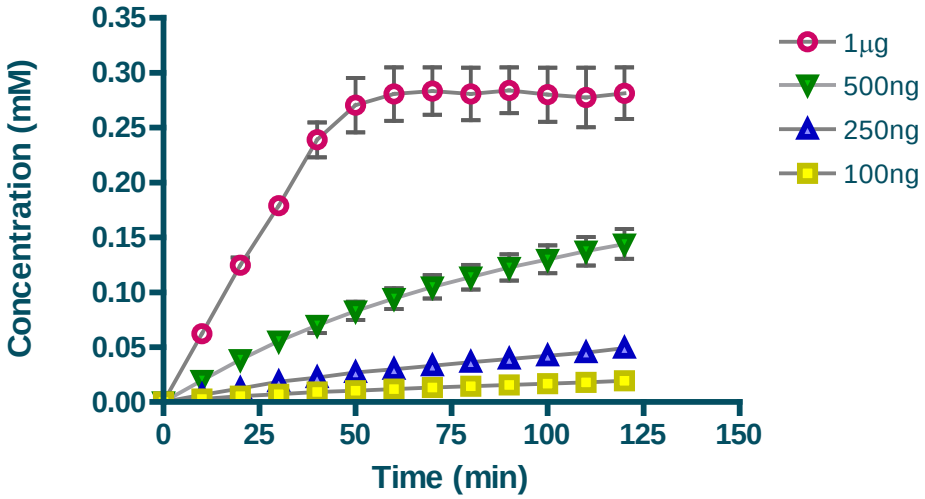

Figure 3.17 – Hydrolysis of nitroanilide over time with different concentrations of enzyme.

Several enzyme concentrations (1µg to 50µg) were tested but elastin digestion was only observed in the positive tissue with 50µg of HNE. Lower concentrations had no effect on porcine elastin; 50µg was the minimal enzyme concentration with which elastin digestion was observed.

Control tissue, porcine aorta, showed approximately 17% of weight loss after digestion with human neutrophil elastase. Noncross-linked samples lost 10% of their dry weight after digestion. Permacol® and Raw collagen not only did not show any weight loss but had an increase in weight (Figure 3.18).

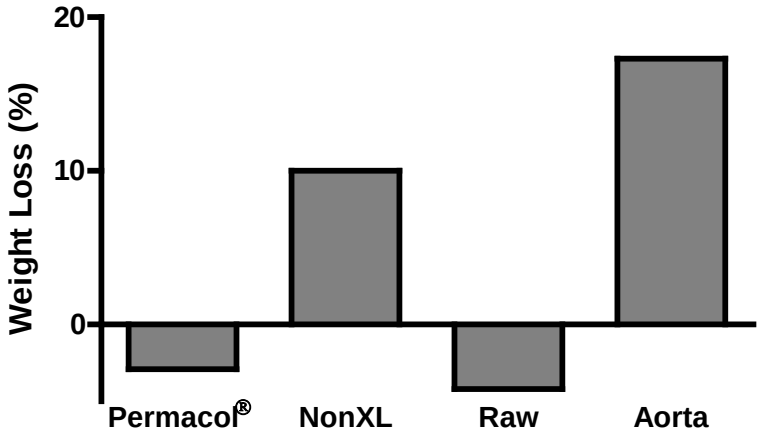

Figure 3.18 – Graphical representation of the variation of dry weight of collagen samples after digestion with human neutrophil elastase for a period of 48h.

Histology showed elastin degradation in the control tissue, collagen from both adventitia and intima showed some level of degradation, but degradation was more evident in the latter (Figure 3.19 and Figure 3.20).

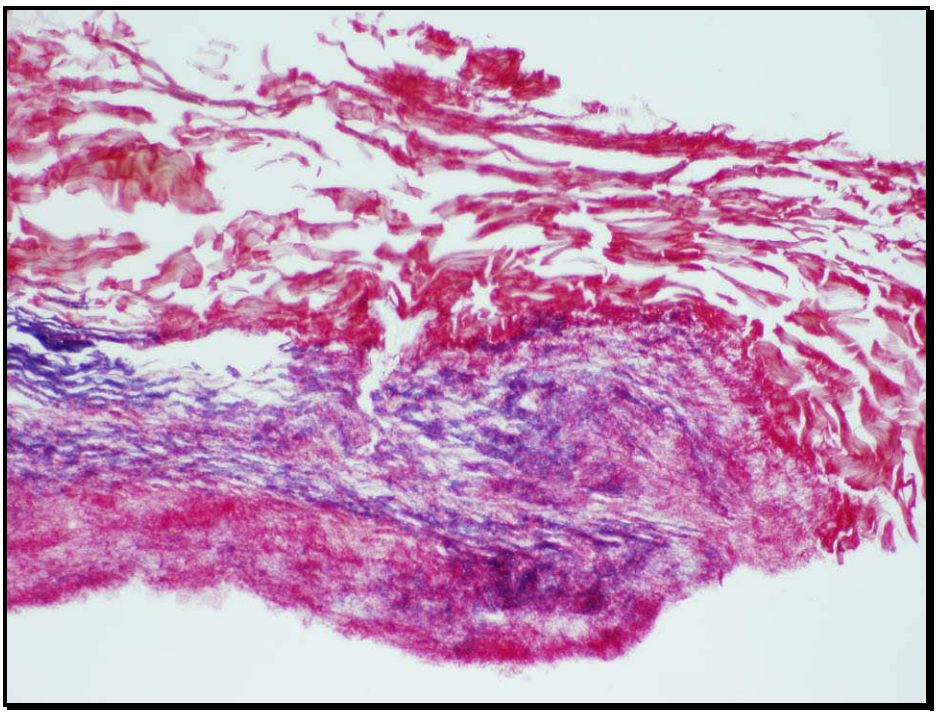

Figure 3.19 – Porcine aorta digested with human neutrophil elastase, showing elastin degradation (picro/Miller, 100X).

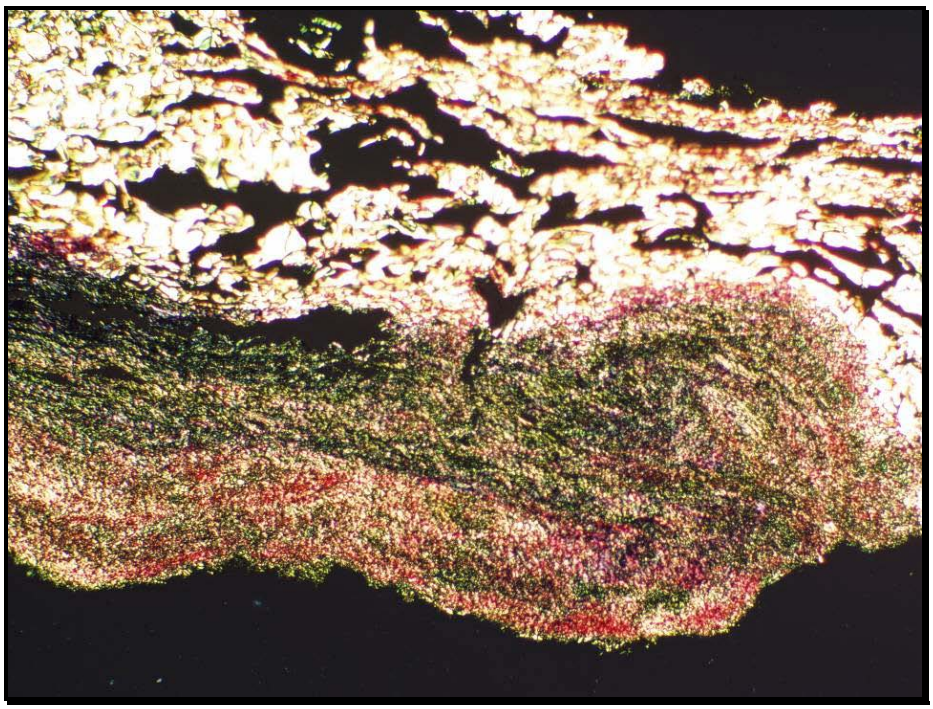

Figure 3.20 – Porcine aorta digested with human neutrophil elastase under polarised light, showing some collagen degradation (picro/Miller, 100X).

Negative control aorta showed high levels of elastin in the media layer and the elastica interna is still visible (Figure 3.21).

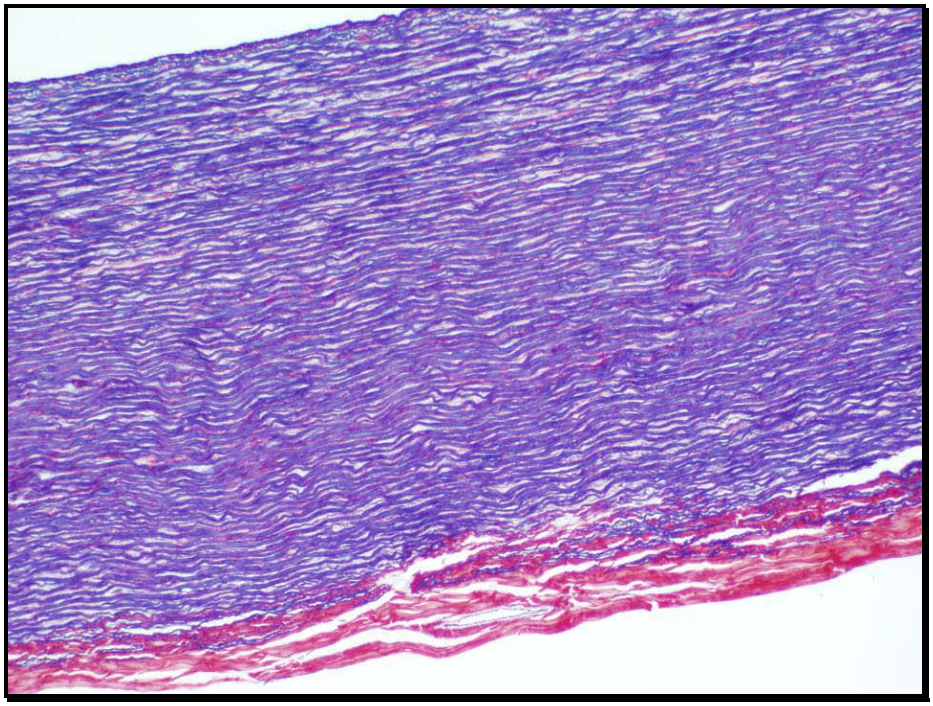

Figure 3.21 – Negative control of porcine aorta during human neutrophil elastase assay (picro/Miller, 100X).

Collagen matrices did not show any histological evidence of elastin and collagen degradation.

3.2.7.4 MMP-8

No tissue digestion was observed in the collagen samples, independent of enzyme concentration and incubation time used.

3.2.8 Discussion

During implantation some tissue damage will occur including rupture of blood vessels, this will lead to a wound healing process. The presence of an implant and the process of tissue regeneration attract inflammatory cells to the implantation site which will accumulate in the surrounding tissues and may penetrate into the implant. Theses cells secrete and activate a range of proteases including MMPs and serine proteases with proteolytic activity that may affect the structural integrity of implants. This chapter studied enzymatic digestion of dermal collagen matrices and evaluated matrix resistance to enzymatic degradation.

Permacol® and Raw samples showed similar results for collagenase digestion, once again suggesting that Permacol® has similar level of cross-link to un-processed porcine dermal collagen. NonXL matrices showed statistical differences in percentage of digested tissue compared to the other collagen matrices. EDC-XL collagen was slightly digested after 8h incubation with collagenase, but tissue digestion did not increase with increasing incubation periods.

When analysing matrices resistance to porcine elastase, the weight gain observed in the control samples was unforeseen. Although a volume increase was expected after incubation, after an overnight lyophilisation samples should return to their original weight or even lose some. This increase in weight may be caused by accumulation of salts from the buffer or from the inhibitor reagent within the matrix; over time this

effect is diminished. Histology did not show any structural difference in the control samples over incubation time.

The positive control tissue confirmed that the elastase was active and digested all the elastin present in porcine aorta and probably some of the collagen.

Permacol®, Raw collagen and NonXL collagen tested showed some difference in the structure and configuration of fibres over the incubation time; the space between fibres increased and fibre thickness seemed to have decreased over time.

Since elastin was not found in the control samples, except for the Raw collagen, the weight loss (in some cases 40% of the original weight) suggests that elastase is digesting the collagen. Porcine pancreatic elastase has a strong specificity for alanine, leucine and valine hydrolyzation, but this enzyme has also been reported to hydrolyze peptide bonds near glycine residues (Lee, 2001). Consequently, since every third residue in collagen molecules is glycine, it is possible that elastase is damaging the collagen. Contrary to what was observed with collagenase EDC-XL tissue digestion increased with time of incubation; although, the weight loss observed was marginal.

A more specific elastase assay was performed using human neutrophil elastase. Once more, except for Raw collagen, elastin was not observed in the collagen matrices tested. This may be result of chance but it also suggests that Permacol® surgical implant and its noncross-linked equivalent do not have elastin or have marginal amounts of elastin. Raw collagen is trypsinized to extract cellular content and originates NonXL collagen samples. Although trypsin is suppose to leave elastin and native collagen unaffected (Lee *et al.*, 2001a), the absence of elastin in Permacol® and NonXL samples suggests some loss of elastin during the manufacturers process.

Human neutrophil elastase did not digest Permacol® and Raw collagen samples, these samples increased weight during the HNE assay but tissue digestion was recorded in NonXL samples. HNE has been reported to cleave rat type I collagen fibrils at 0.01U/mL, although at a slower rate than neutrophil collagenases (Kafienah *et al.*, 1998). In this study 1.75U/mL of HNE were used, which suggests that the weight loss present in NonXL samples is derived from breakdown of the helices of collagen type I. This can be explained by the treatments performed in this matrix; contrary to Permacol® this matrix was not cross-linked, therefore, resistance to enzymatic digestion has not been conferred. In addition, NonXL samples were subjected to

trypsin digestion as a decellularisation process leaving them more susceptible to degradation by proteolytic enzymes.

MMP-8 did not digest the collagen samples under the conditions tested. MMP-8 is known to cleave collagen type I (Aiba-Kojima *et al.*, 2007; Mallya *et al.*, 1990b; Netzel-Arnett *et al.*, 1991; Nwomeh *et al.*, 1999), which is the main collagen type in dermis. MMP-8 levels in chronic wound fluids have be found to have a high variation from 100ng to 2500ng per mL of wound fluid (Aiba-Kojima *et al.*, 2007), in this study 500ng of enzyme were used per mg of tissue, which might not be enough for digestion of fibrillar collagen without the presence of other enzymes. MMPs are present not only in non-healing wounds but also during normal wound healing (Nwomeh *et al.*, 1999), in both cases collagen degradation is dependent on the activation of several enzymes, usually activation is temporal and more than one MMP are present at the same time (Nwomeh *et al.*, 1999; Rayment *et al.*, 2008; Siedle *et al.*, 2002; Welgus *et al.*, 1990). Although MMP-8 is observed at high levels at wound sites, its enzymatic specificity may depend on other enzymes.

3.2.9 Conclusion

Tripsinisation of collagen samples results in increased susceptibility to collagenase digestion. NonXL samples are acellular but not cross-linked, after incubation in a bacterial collagenase solution these samples showed tissue degradation. Chemical and natural cross-linked samples, Permacol® and Raw collagen respectively, had similar profiles and, after the enzymatic assay, percentage of weight loss due to collagenase digestion was lower in Permacol® than for NonXL matrices. EDC-XL samples showed more resistance to collagenase and elastase digestion, suggesting that this cross-linking agent confers higher resistance to enzymatic digestion.

In the assay presented here, hog pancreatic elastase seems to be elastin-specific although the weigh loss observed in the tested samples suggests that after all elastin has been digested the elastase digests collagen. Noncross-linked matrices were more vulnerable to the elastase digestion (both porcine and human); therefore, these data suggest that cross-linking of porcine collagen materials confers resistance to elastase.

The pancreatic elastase assay gives further evidence to this hypothesis, since Permacol® samples showed increased resistance to elastase degradation when compared to NonXL and Raw collagen.

Collagenase-2 (MMP-8), under the conditions tested, did not degrade collagen type I matrices - Permacol®, NonXL and Raw collagen matrices.

3.3 ASSESSMENT OF FLUID FLOW PATTERNS IN COLLAGEN MATRICES

3.3.1 Introduction

Physiological interstitial flow is the movement of fluid through the extracellular matrix of a tissue, often between blood vessels and lymphatic capillaries; it includes interstitial fluid and transcellular fluid. It provides convection necessary for the transport of large proteins through the interstitial space and constitutes an important component of the microcirculation. In addition to its role in transport, interstitial flow also provides a specific mechanical environment to cells in the ECM, by playing an important role in determining interstitial organization and architecture (Ng *et al.*, 2005). Many cell types, including fibroblasts and smooth muscle cells, reside within a 3-D environment and are exposed to interstitial fluid forces, therefore, if a biomaterial does not encourage and maintain interstitial flow this may affect cell adhesion and infiltration into the material matrix.

Aside from its role in tissue architecture, enhanced fluid percolation in a biomaterial is essential for nutrient exchange, toxin removal and vascularisation.

Evans blue dye (EB) has been used for many years as an indicator of vascular macromolecular transport due to its unique binding properties. EB is widely used to study blood vessel and cellular membrane permeability as it is non-toxic, it can be administered as an intra-vital dye and has a high affinity to serum albumin – using this protein as its transporter molecule (Fry, 1977). The EB–albumin conjugate (EBA) can be: (i) identified macroscopically by the blue colour within tissue (Matsuda *et al.*, 1995); (ii) observed by red auto-fluorescence in tissue sections examined by fluorescence microscopy (Brussee *et al.*, 1997); and (iii) assessed and quantified by spectrophotometry (Hamer *et al.*, 2002; Hawkins and Egleton, 2006). Evans blue dye is not only easy to use but it can also be removed from the vascular system by diffusion into the extra vascular tissues while still bound to albumin.

In this study, a flow chamber assay was developed to examine the effects of a solution particularly rich in calcium in two types of collagen matrices. A second procedure was performed where Evans blue dye was used to observe interstitial flow through collagen matrices in a rat model.

3.3.2 Hypotheses

Fluid flow pattern is different between cross-linked collagen matrices and noncross-linked collagen matrices. Cross-linked collagen offers resistance to fluid flow and can act as a membrane, retaining calcium salts when in contact with calcium solutions.

3.3.3 Aims and Objectives

- Compare Permacol® and noncross-linked matrices related to interstitial fluid flow in a rat model.
- Determine fluid flow pattern in cross-linked collagen.

3.3.4 Materials and Methods

Permacol® surgical implant (thickness 1.0mm) and noncross-linked collagen (NonXL) (thickness 1.5mm) were supplied by TSL plc. Collagen matrices were used from the same batch to eliminate possible variations.
Evans blue dye, calcium chloride and Trizma® base were purchased from Sigma-Aldrich Company Ltd. (Gillingham, Dorset SP8 4XT, U.K.); 0.9% sodium chloride was acquired from Baxter Health Care Ltd. (Newbury, Berks RG20 7QW, U.K.) and sterile Millex®-SV 5.0µm filter units were purchased from Millipore (UK) Ltd (Watford, Herts. WD18 8YH); collagenase type I was acquired from Calbiochem (Merck Chemicals Ltd., Nottingham, NG9 2JR, U.K.).

3.3.4.1 Studies Design

Ussing Chamber

An Ussing Chamber was modified and used to test fluid flow through Permacol® and NonXL collagen. Ussing Chambers are well established perfusion chambers, made from solid acrylic with eight entry ports for fluid lines, electrodes or agar bridges. The fluid compartments in each side of the chamber are separated by the membrane being studied. Four sharp stainless steel pins on one side of the chamber hold the membrane in position and mate with holes in the opposite chamber interface. Six entry ports were sealed with several layers of parafilm and two entry ports left open, one in each side of the chamber. One entry port was used for fluid entry and the other for fluid drainage. The entry port was connected by a tube to a Gilson Minipuls II peristaltic pump with a head speed of 5rpm (Anachem, LU1 3JJ, U.K.), which allowed constant fluid flow from a reservoir. The reservoir was kept at 37^{o}C and was filled with a 2.7mM $CaCl_2$, pH 7.0 solution, since this calcium molarity has been reported as the calcium concentration found in intertistial fluid (Diem and Lentner, 1970).

Collagen matrices were cut into 1cm x 1cm pieces and (one at each time) placed in the chamber, immobilization of matrix was obtained by perforation with the stainless steel pins. After placement of the collagen matrix, the chamber was quickly closed to avert matrix dehydration. The pump was turned on at a speed of 9.1mL/min and the chamber was checked for any liquid leak, if outflow was not observed the time was recorded as t_0 and the pump/chamber apparatus left working for 3 and 6 hours. The speed of fluid flow at the exit was measured.

At the end of each experiment matrices were fixed in 10% NBF and processed for routine histology.

Evans Blue Dye

Female Sprague-Dawley rats (inbred) were used with weights between 270 – 370g. The study comprised 48 animals distributed into four experimental groups, as in Table 3.8.

Table 3.8 – Experimental groups and time points design.

End time-point	1 hour	3 hours	24 hours	72 hours
Permacol®	2	4	8	8
Noncross-linked collagen	2	4	8	8
control	1	1	1	1

A 0.5% solution of Evans blue dye was prepared in 0.9% saline solution and sterilized by filtration through a 5.0µm filter.
All matrices were trimmed to 1.5cm x 2.0cm sizes just prior implantation.

3.3.4.2 Surgical Procedure

Animals were anaesthetised according to the procedure described in Section 2.2.5.
All surgery was done using sterile techniques. The following surgical procedure was followed for all animals:

1. A ventral midline incision was made from just below the level of the rib cage extending approximately 1.5cm distally.
2. Skin was elevated and retracted to create one subcutaneous "pocket" on one side of the midline.
3. Haemostasis was maintained by careful dissection – no electrocautery was used.
4. The collagen matrices (Permacol® or NonXL collagen) were placed in the pocket.
5. The ventral midline incision was closed with interrupted sutures.
6. 0.5% Evans blue solution was injected intra-dermally in two opposite sites, just touching the side of the collagen matrices, 0.1% (volume) of Evans blue solution was injected per body mass, e.g. an animal weighting 300g would receive in total 0.3mL of 0.5% Evans blue solution.
7. Once recovered from anaesthetic, animals were returned to the animal accommodation, singly housed.

3.3.4.3 Necropsy

Animals were euthanased (as described in Section 2.2.8) and implants removed. Implants were macroscopically observed and areas showing Evans blue infiltration measured by ImageJ software (U. S. National Institutes of Health, Bethesda, Maryland, USA). Implants from 1 hour and 3 hours groups were divided in two, one half was fixed in 10% NBF for histological analysis and the other half immediately frozen in liquid nitrogen and kept at -80^{o}C for cryostat sectioning. Implants from 24 hours and 72 hours groups were stored in a sterile vial with 2mL of 0.2M Tris pH 8.0.

3.3.4.4 Histology

Tissue kept for histological analysis was processed and embedded according to Section 2.2.9.2 and 5µm sections made from each wax block. All sections were pre-treated as described in Table 3.9 before microscopical analysis. Sections were observed using a light microscope for Evans blue dye infiltration.

Table 3.9 – Treatment of sections with Evans blue dye.

Reagent	Time
Xylene 1	5 minutes
Xylene 2	2 minutes
Absolute IMS	2 minutes
95% IMS	2 minutes
70% IMS	2 minutes
Running tap water	2 minutes
70% IMS	30 seconds
95% IMS	30 seconds
Absolute IMS	2 minutes
Xylene 1	2 minutes
Xylene 2	2 minutes
DPX	Mount

To perform cryo-sectioning, frozen tissues (previously stored at -80^{o}C) were removed from the freezer and immersed in liquid nitrogen, samples were kept submerged until just immediately after cryo-sectioning. Frozen tissue was quickly removed from the liquid nitrogen and cut into 0.5cm x 0.5cm blocks with appropriate plane faces for sectioning. Each block of tissue was mounted in specimen holders, which were standing vertically in dry ice. To attach the block of tissue to the specimen holder water was added, drop by drop, to the interface of tissue/holder; in this way the tissue is envolved by an ice coating which keeps it secure. Specimen holders (with tissue) were then placed inside the cryostat. A cryostat (JUNG CM3000, Leica) was used to obtain 8µm sections in glass slides which were dipped into acetone and allowed to dry while inside the cryostat. Slides were stored at -20^{o}C until observed under the microscope.

3.3.4.5 Evans Blue Dye Measurement

Implants stored in Tris buffer were denatured at 70^{o}C for 30 minutes and allowed to cool down to room temperature. Once cool 18mg of collagenase type I was added to each sample and solutions were incubated at 37^{o}C for 24 hours.
All samples were centrifuged at 400xg for 5 minutes and supernatant removed to a new tube. Evans blue labelled albumin (EBA) amounts were quantified by absorbance readings of the supernatants at 620nm, 0.2M Tris pH 8.0 was used as blank (Abraham *et al.*, 1996; Hamer *et al.*, 2002; Harada *et al.*, 2005; Hawkins and Egleton, 2006).

3.3.5 Statistical Analysis

Absorbance readings were compared between groups using an unpaired t-test, a P value less than 0.05 was considered significant.

3.3.6 Results

Samples used in the Ussing chamber assay did not show any deposits of calcium after 3h and 6h of a calcium solution flowing through matrices.

Although the fluid exited the chamber at a slightly lower speed than its entrance, there was no significant difference between both matrices tested.

One animal from group NonXL 72 hours died post operatively due to anaesthetic problems.

One hour post intradermal injection of Evans blue both type of implants showed some dye absorption which extended through the total thickness of the implants (Figure 3.22). There was no statistical difference between the dyed areas of Permacol® and NonXL implants.

Figure 3.22 – Permacol® implant one hour post implantation.

After 3 hours dye absorption was higher both in colour and areas affected. NonXL implant showed more dye absorption compared to Permacol® implants (Figure 3.23 and Figure 3.24), but differences were not significant.

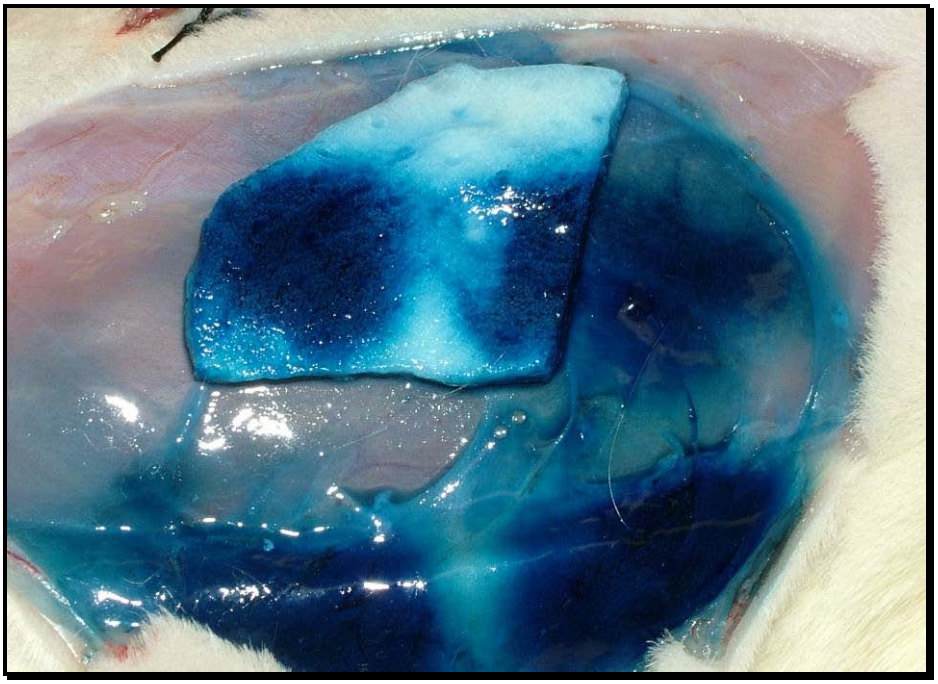

Figure 3.23 – NonXL implant after 3 hours of implantation.

Figure 3.24 – Permacol® implant 3 hours post implantation.

After 1 day and 3 days implantation all implants had absorbed Evans blue dye which was visible throughout the total area and thickness of implants, no difference was observed in the absorption level between implant type (Figure 3.25 and Figure 3.26).

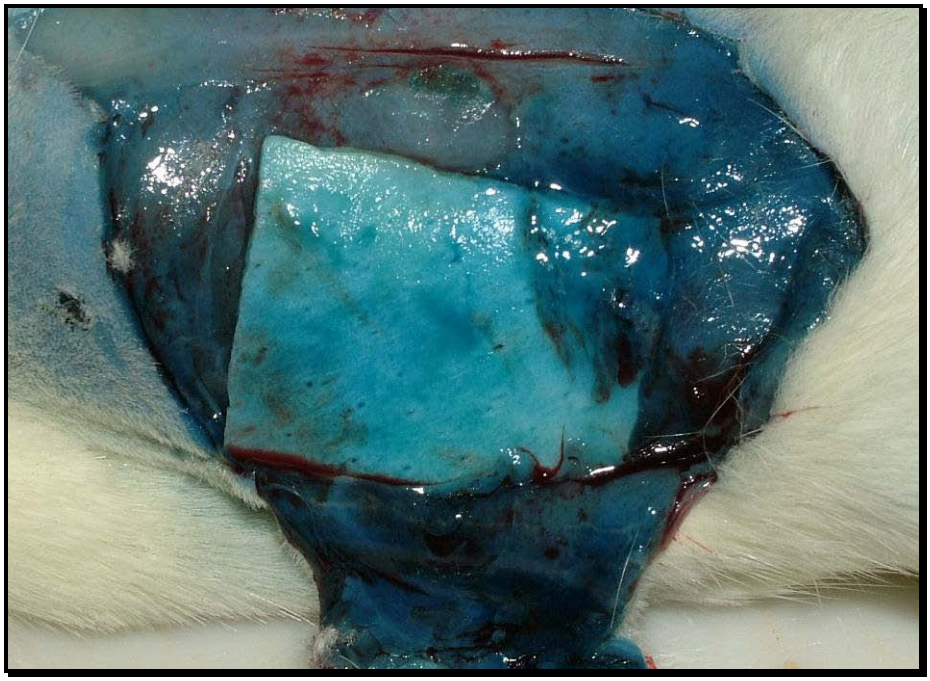

Figure 3.25 – NonXL implant 72 hours post implantation.

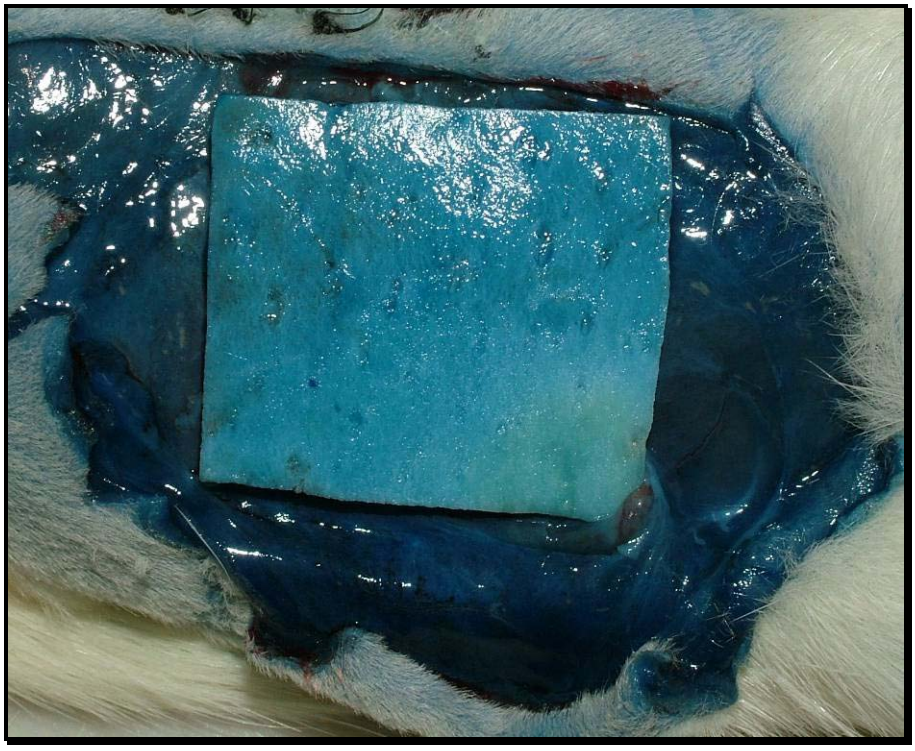

Figure 3.26 – Permacol® surgical implant 72 hours post implantation.

Control animals showed, at all time points, Evans blue dye uniformly spread through the area of injection, after 72 hours animals showed a light blue colour underneath the skin over the whole body (Figure 3.27).

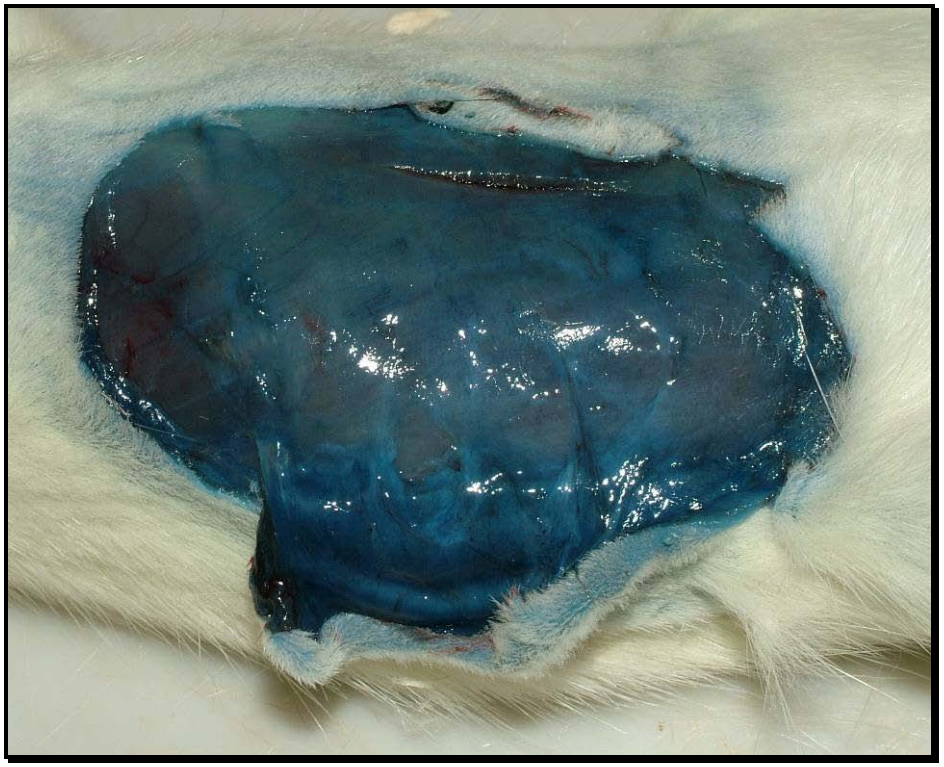

Figure 3.27 – Control animal 72 hours after being injected intradermally with Evans blue dye.

Paraffin wax embedded and cryo-sections were observed with a light microscope. In the first, the blue dye was too light and differentiation between stained and non stained areas was difficult. In the cryo-sections Evans blue dye was observed extending through all depth of implants, the blue colour was not intense enough to produce good quality pictures.

After collagenase digestion Evans blue labelled albumin was measured as described in Section 3.3.4.5. Results are represented in Table 3.10. Since collagen matrices had different thicknesses, results were calculated per volume (mL). Mean ($\overline{X}$) and standard deviations (SD) were calculated for all groups.

Table 3.10 – EBA quantification at 620nm.

	24 Hours				72 Hours			
	Permacol®		NonXL		Permacol®		NonXL	
	OD_{620nm}	OD/mL	OD_{620nm}	OD/mL	OD_{620nm}	OD/mL	OD_{620nm}	OD/mL
	0.480	1.60	0.350	0.78	0.150	0.50	0.186	0.41
	0.143	0.48	0.253	0.56	0.146	0.49	0.213	0.47
	0.176	0.59	0.236	0.52	0.094	0.31	0.359	0.80
	0.417	1.39	0.388	0.86	0.260	0.87	0.321	0.71
	0.321	1.07	0.413	0.92	0.269	0.90	0.353	0.78
	0.418	1.39	0.423	0.94	0.328	1.09	-	-
$\overline{X}$=	**0.326**	**1.086**	**0.344**	**0.764**	**0.208**	**0.693**	**0.286**	**0.636**
SD=	**0.139**	**0.463**	**0.081**	**0.180**	**0.091**	**0.302**	**0.081**	**0.180**

Figure 3.28 shows the graphical representation for EBA readings per volume of matrix.

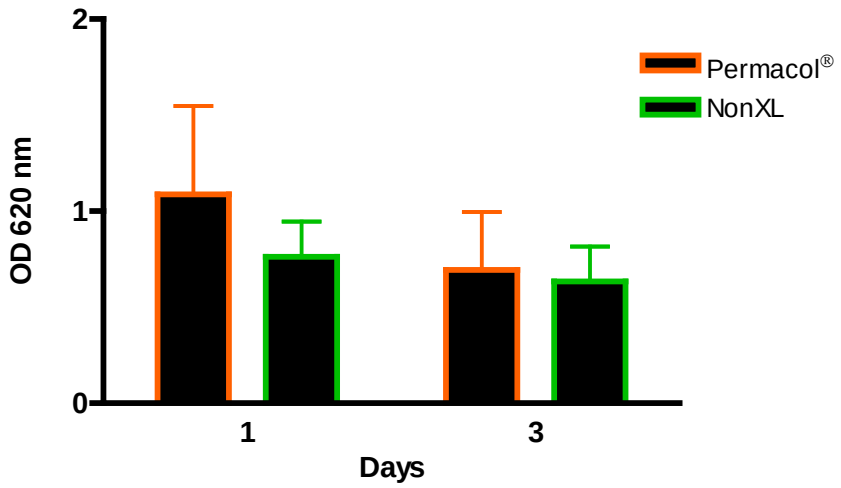

Figure 3.28 – Results for EBA absorbance at 620nm, error bars represent standard deviations.

3.3.7 Discussion

Due to matrix composition some materials may produce some resistance to flow of a fluid, this resistance is created by the matrix and its interactions with fluids attempting to flow through it. In the study reported here a cross-linked matrix was tested against its non-cross-linked equivalent. Matrices were tested in a modified Ussing chamber under the same conditions; the speed of the fluid leaving the chamber was compared between both matrices to predict if one matrix was producing more resistance to flow than the other. This was not observed at any stage; although fluid was leaving the chamber at a slightly lower speed than the entrance speed, this decrease was observed for both matrices.

Because calcification was occasionally observed in Permacol® surgical implants after implantation in rats, and calcification was not observed in NonXL implants, it was suggested that the cross-linked structure of Permacol® was acting as a filter and, with time, calcium deposits were accumulating within the collagen. To test this theory calcium solution, at the same concentration as encountered in interstitial fluid (Diem and Lentner, 1970), was used in this study. Both matrices types were capable of liquid absorption and fluid moved through the entire depth of matrix. Although both matrices were in contact with the calcium solution for 6 hours, calcium deposits were not visible within the collagen. This suggests that for matrix calcification, Permacol® needs to be in contact with calcium for long periods of time or calcification only occurs *in situ*. Permacol® calcification will be further discussed in detail in Chapter 5.2 and Chapter 5.3.

In a different experiment, interstitial fluid flow through Permacol® was observed by using Evans blue dye, a dye that combines strongly with albumin, NonXL implants were used as controls. There was no difference in areas infiltrated with EBA between implant types; moreover, after digestion of collagen matrices there was no evidence of significant differences between the amounts of EBA absorbed by the collagen matrices.

3.3.8 Conclusion

This study showed that Permacol® surgical implant and NonXL collagen offer similar resistance to calcium chloride solution, under the conditions tested. Calcium deposits were not observed within the collagen matrices in the Ussing chamber assay. *In vivo*, both matrix types showed equal permeability to interstitial fluid. Both hypotheses tested in this study were disproved since there was no apparent difference between cross-linked and noncross-linked collagen matrices.

4.0 CELL PROLIFERANTION AND INFILTRATION IN COLLAGEN MATRICES

Biomaterials must be thoroughly tested before permission is granted for human use therefore, biological prostheses biocompatibility is evaluated to provide assurance that the final biomaterial will be safe for human use and will perform appropriately.

Biological performance has two aspects, material response and host response (biocompatibility). During the last 40 years this evaluation has been primarily carried in animal models (Braybrook, 1997). However, such tests are time consuming, expensive and many times limited for ethical reasons. The ISO 10993-2 recommends that *animal experiments shall not be performed before appropriate tests, if available, are carried out*. For these reasons *in vitro* models have been established to evaluate material cytotoxicity, matrix degradation, apoptosis induction, cell-cell interaction, cell-matrix interaction, cell adhesion, migration and proliferation in the matrix of potentially implantable scaffolds.

Cell culture refers to the growth of initially matrix-free, disassociated cells. Exposure to biomaterials may be through direct contact, diffusional contact or by inclusion of particles or extracts from materials in the culture media (indirect contact) (Black, 2006). Tissue culture uses portions of living tissue, maintained in a viable state *in vitro*, this method usually requires a substrate instead of a suspension solution. Exposure to the biomaterial is similar to that for cell culture.

For cell culture or tissue culture results to be relevant and useful while analysing material or host response of a biomaterial, care is needed while designing an experiment. There are factors that cannot be overemphasized such as replication, sterilization, controlled conditions, selection of the appropriate cell type and consideration of the dosage and time of exposure of cells to biomaterial. The latter is important because cells may tolerate materials at low levels or for short periods of time, but they may be adversely affected if dosage and exposure are increased.

4.1 AN *IN VITRO* ASSESSMENT OF FIBROBLAST INTERACTION WITH DIFFERENT PORCINE COLLAGEN SUBSTRATES

4.1.1 Introduction

Several biocompatible materials have been studied for their suitability as matrices for tissue engineering. These include natural polymers and their synthetic analogues. Collagen is regarded as one of the most useful biomaterials. The excellent biocompatibility and safety due to its biological characteristics, such as biodegradability and weak antigenicity have made collagen a primary resource in medical applications (Friess, 1998; Lee *et al.*, 2001a). *In vivo*, collagen promotes natural cell interactions such as cell migration and proliferation, it is biocompatible and it can be remodelled. *In addition to the low cross species immunogenicity, the use of collagen is perpetuated by the possession of lesser known bioactive influences not observed when using synthetic material which can influence adhesion, spreading and morphology* (Jarman-Smith *et al.*, 2004). Collagen represents the chief structural protein accounting for approximately 30% of all vertebrate body protein; it is the major constituent of the extracellular matrix (Friess, 1998). *In vivo*, the ECM of the connective tissue is remodelled continuously, allowing modification and infiltration of cells. ECM degradation and remodelling results from the action of proteolytic enzymes, which are secreted primarily by fibroblasts (Jarman-Smith *et al.*, 2004).

Fibroblasts synthesize, organize and maintain connective tissues during development and in response to injury and fibrotic disease (Grinnell, 2003). The performance of these activities depends on the capability of cells to exert mechanical force and to remodel the ECM. When fibroblasts are cultured within an ECM such as collagen or fibrin, cells experience a more intricate physical environment and a different topography from cells on two-dimensional (2-D) surfaces (glass or plastic tissue culture substrata). Fibroblasts exhibit unique features when they interact with 3-D collagen matrices and the interaction between cells and the matrix leads not only to changes in cell shape but also to matrix remodelling and contraction (Brown *et al.*,

1998; Grinnell *et al.*, 1999; Tomasek *et al.*, 1992; Xu *et al.*, 1998). Hence, culturing fibroblasts within a 3-D environment has proven to be a valuable tool in studying numerous cellular functions under conditions that resemble the *in vivo* situation more closely than fibroblast monolayer cultures (Bell *et al.*, 1979).

In a 3-D matrix, attached fibroblasts do not have a flat shape and lamellar extensions, as occurs on 2-D surfaces, but range in shape from dendritic (lower mechanical load) to stellate to bipolar (greater mechanical load), depending on matrix stiffness and tension (Eckes *et al.*, 2000; Grinnell, 1994; Jiang and Grinnell, 2005). Similar morphological features have been described for cells in tissues.

Fibroblasts in 3-D matrices initially spread without forming stress fibres and have few focal adhesions. Over time fibroblasts interact with the matrices and cells penetrate into the substance of the matrix and become entangled with matrix fibrils (Rhee and Grinnell, 2007). Harries and co-workers showed that matrix contraction occurs as a consequence of motile activity by cells trying to migrate through the matrix (Harris *et al.*, 1981). Depending on the surgical purpose, contraction is not always desirable in an implanted material; in certain situations the implant structure should be preserved intact for a prolonged period of time while it provides support and strength, for instance when used as a bulking material. Therefore, in such a case, it is vital to prolong the materials' original structural and mechanical integrity. Methods to achieve this typically focus on creating new additional chemical bonds between the material molecules so that these supplementary links reinforce the tissue robustness. Ideally, the treatment should maintain the original character of the tissue, such as its flexible mechanical properties, whilst preventing significant shrinkage (Khor, 1997). The methods used to achieve this principle have the generic label of 'cross-linking processes'. Cross-linking may be effected by chemical, physical or enzymatic techniques. All contribute to increase the mechanical stability of biomaterials.

Permacol® surgical implant has shown variability in cellular penetration and density and subsequent vascularisation after *in vivo* implantation. Since it is not known if the cross-linking process compromises cell adherence, the current study now described was designed to assess the ability of this cross-linked collagen matrix to support cell adhesion, infiltration and proliferation over time, whilst retaining its original structure. Moreover, fibroblast-matrix interactions were assessed using cross-linked

and noncross-linked collagen matrices. Comparison of Permacol® with manufacture process intermediates (varying in strength of cross-linking) should elucidate the effect of the cross-linking process in cellular ability to attach and penetrate collagen matrices or even to survive on the surface.

4.1.2 Hypothesis

The variability observed in cellular density and cellular penetration of Permacol® surgical implants is due to the cross-linking process used in their preparation.

4.1.3 Aims and Objectives

- Compare fibroblast attachment, infiltration and penetration into three dermal collagen matrices – normal porcine collagen, acellular porcine collagen and cross-linked acellular porcine collagen (Permacol® surgical implant).
- Evaluate pre-treatment of collagen matrices as a factor influencing cellular proliferation.

4.1.4 Materials and Methods

All collagen matrices were supplied by TSL plc. Samples were supplied moist in sterile saline in double vacuum packed aluminium foil/polyethylene sachets which are impermeable to oxygen and are sterilised by gamma irradiation. All samples were kept at 4°C until needed.

In this study three biomaterials were tested: (i) Permacol® surgical implant (hereafter referred as XL); (ii) the manufacturer's product preceding the cross-linking process – noncross-linked acellular collagen (NonXL); and (iii) dermal porcine collagen (Raw). Each collagen matrix was derived from the same batch to eliminate variations.

Eight discs of 1.6cm in diameter (2.01cm^2 area) were cut from each of the collagen matrices; of these, 4 discs were left soaking overnight in PBS (PT-PBS) and the remaining 4 in fibroblast medium (PT-FM) supplemented with antibiotics (as described in Section 2.1.2). The next day 4 more discs with the same dimensions were prepared from each collagen matrix and since they were not pre-treated with any solution, were labelled as "Non-soaked".

Two 24-well plates were used (Nunc, Fisher Scientific UK Ltd., Leicestershire LE11 5RG, U.K.) for this experiment. Each well (∅=1.6cm) received a collagen disc. The first plate was prepared with the XL and NonXL samples as in Figure 4.1 and the second plate had in the first 3 columns the Raw samples, one empty column and the last 2 columns were incubated with fibroblasts only, as control wells.

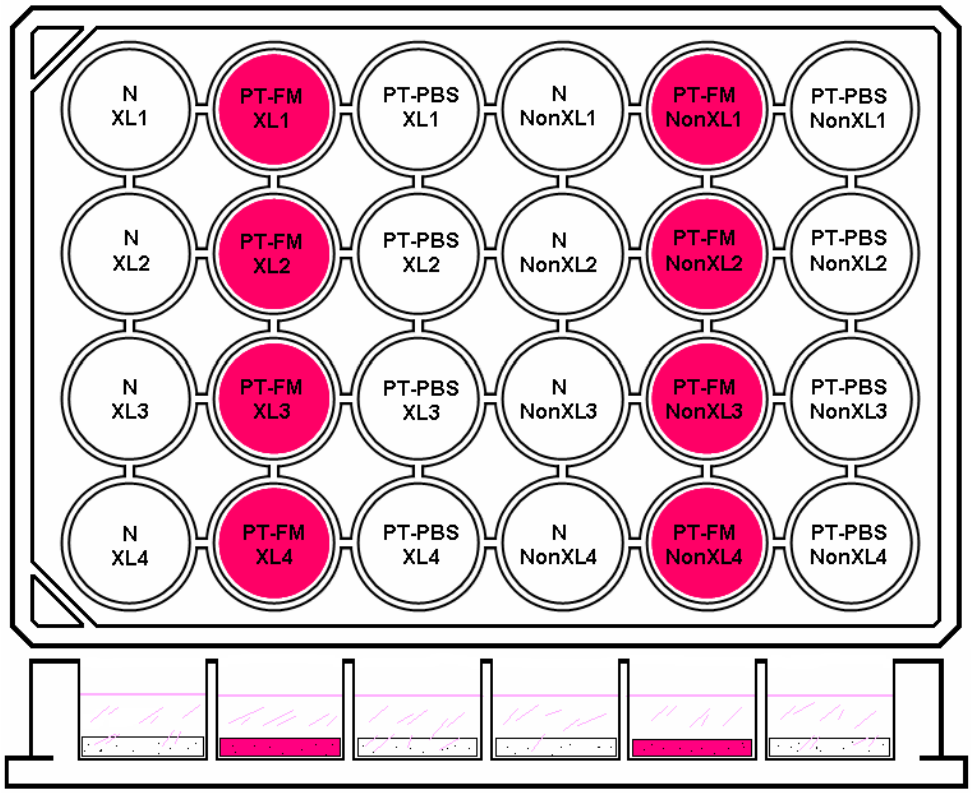

Figure 4.1– 24-well plate with collagen matrices fitted in the bottom of each well. PT-FM matrices showed a pink coloration. N = non-soaked matrix.

Primary cultures of porcine fibroblasts were used (see Section 2.1.2) in all *in vitro* experiments. All experiments were repeated at least twice. A sample of the porcine

skin used for cell extraction was fixed in 10% NBF as control tissue. Routine histological analysis was performed as described in Section 2.2.9.

Early passage porcine fibroblasts (P≤4) were seeded on the top of each disc, at a density of $1x10^6$ cells/well (*i.e.*, $5x10^5$ cells/cm^2 in a volume of 0.5mL). The volume in each well was made up to 2mL with fibroblast medium (FM). Plates were incubated at 37°C with 5% CO_2 and 100% humidity. Cells were cultured for 28 days with medium changes every 2 days. At each medium change the old medium was stained with trypan blue (1:1) for dead cell counting (Section 2.1.4) and viable cells were quantified by the means of a MTT test (Section 2.1.6).
At the end of the study all samples were fixed in 10% NBF for histological analysis and the empty plates were observed in an inverted reflected-light microscope (Axiovert 25 CA, Carl Zeiss) to look for fibroblast attachment to the plastic surface.
A porcine skin biopsy was fixed in 10% NBF and processed for histological analysis to assess porcine dermal collagen structure and collagen/cells interaction.

4.1.5 Results

At the end of the study, plates were observed for fibroblast attachment to the base of each well. All control wells showed 100% fibroblast attachment and confluence. The wells with the PT-PBS matrices showed the lowest numbers of attached fibroblasts: only one well of the XL samples showed marginal numbers of fibroblasts in monolayer; the NonXL wells were cell free; and wells with Raw matrices had marginal amounts of attached fibroblasts, predominantly at the edges of the well.
Non soaked matrices showed moderate quantities of cells at the edges of all XL wells, the same was observed in the NonXL and Raw wells with the exception that, in these, fibroblasts were also visible at the centre of the wells.
Wells holding PT-FM samples contained the highest number of fibroblasts attached to the plastic surface and cells were observed in monolayer both at the edges and centre of all PT-FM wells.
The next illustration represents the cell attachment to the base of the wells.

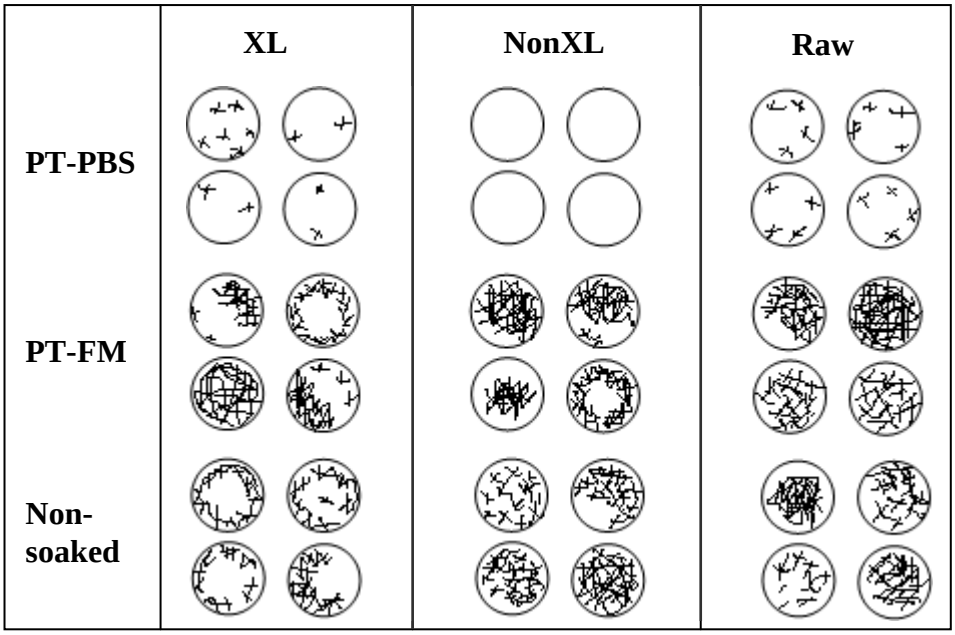

Figure 4.2 – Schematic representation of cell attachment to the base of each well.

At each medium change old medium was kept for cell counting and cell viability tests. Manual cell counting was performed with trypan blue for differentiation between dead and viable cells.

The number of cells microscopically observed in the medium was not high, suggesting that cells were preferably attached. Also, viable fibroblasts were more frequently detected than dead cells. In all samples pre-treated with PBS the number of viable cells in the medium was very low. Non-soaked XL matrices showed initially some viable cells in the medium but those numbers decreased rapidly after the first week. XL matrices pre-treated with fibroblast medium contained the highest quantity of viable cells in suspension. NonXL samples showed mostly low numbers of viable fibroblasts with the exception of the PT-FM samples at 21 days. Raw matrices showed the lowest number of viable cells in suspension. These results are schematised in Table 4.1.

Table 4.1 – Viable cells present in the medium suspension (fibroblasts/mL medium) over the time course of the study.

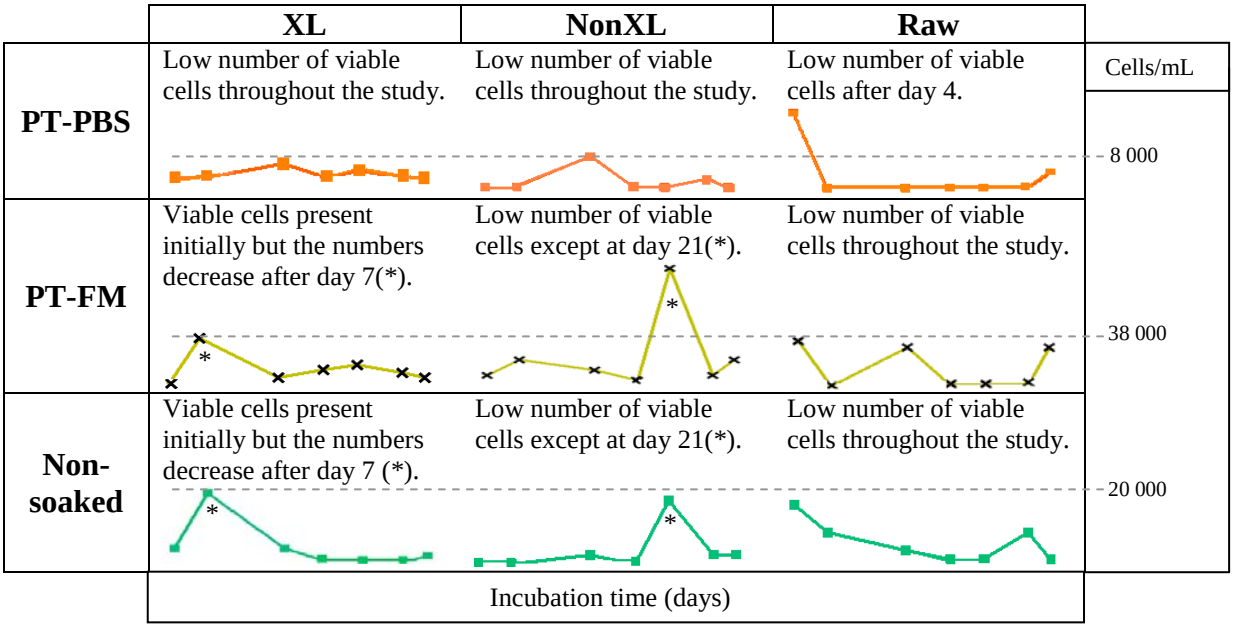

Cells that stained blue with trypan blue were counted as dead cells. XL samples pre-treated with FM had a high number of dead fibroblasts at 7 days but dead cells were minimal thereafter. Non-soaked XL matrices showed low numbers of dead cells, except at 21 days. All 3 types of collagen matrices pre-treated with PBS showed very low quantities of dead cells in the medium. Independent of the treatment, all NonXL samples had low numbers of dead fibroblasts in suspension; the same was observed for the Raw samples with the exception of the non-soaked samples at 21 days.

An MTT proliferation assay was used to assess cell viability in the medium. To obtain a true sample absorbance a baseline wavelength of 630nm was used as a reference absorbance; after this first step a second beam of light having a wavelength of 570nm was directed through the sample to obtain a measured sample absorbance; by analysing the reference absorbance and the measured sample absorbance we obtained a true sample absorbance.

In the XL samples, cell viability remained fairly constant throughout the experiment, independently of the pre-treatment used. NonXL and Raw samples did not show cell proliferation in the medium during this study when pre-treated with FM or when untreated matrices were used. NonXL samples pre-treated with PBS demonstrated a constant cell proliferation rate until day 14, after which there was an increase in cell

proliferation. In the Raw collagen matrices pre-treated with PBS the amount of viable cells in suspension increased over the time course of the study. Figure 4.3 to Figure 4.5 show the MTT test results; values were normalized by subtraction of the mean cell proliferation value obtained from the controls, mean and standard deviation values were calculated per each matrix per parameter tested.

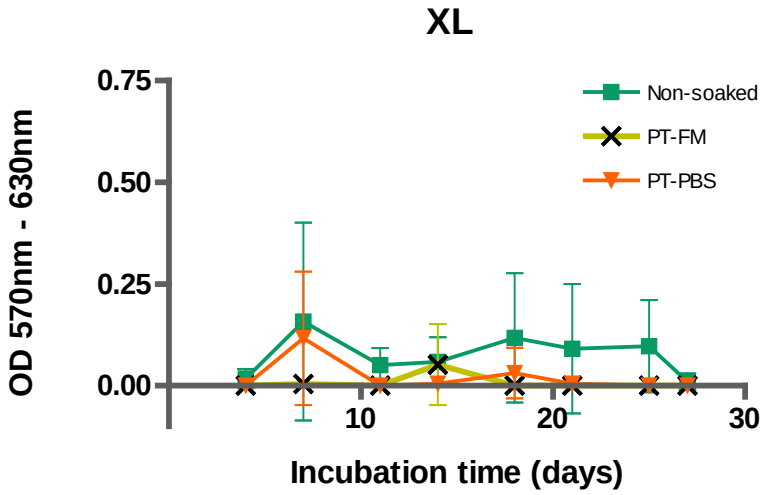

Figure 4.3 – MTT test results for fibroblasts when incubated with XL samples for a period of 28 days.

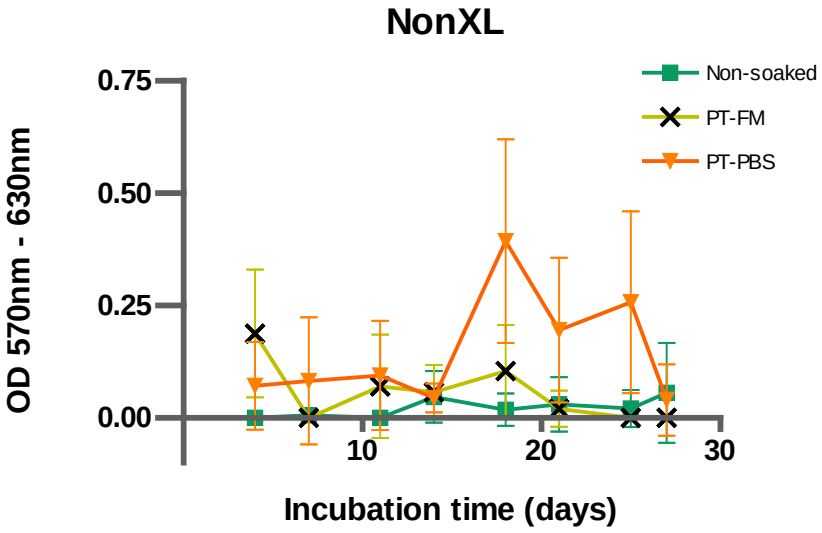

Figure 4.4 – MTT test results for fibroblasts when incubated NonXL samples with for a period of 28 days.

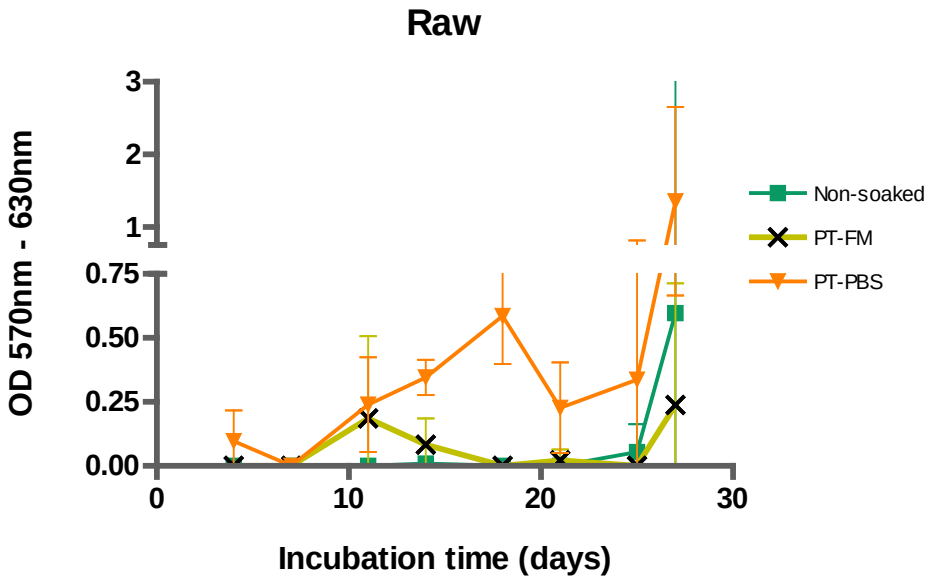

Figure 4.5 – MTT test results for fibroblasts when incubated with Raw samples for a period of 28 days.

Sections of porcine dermal collagen used as histological control tissue showed collagen populated with high numbers of fibroblasts (Figure 4.6).

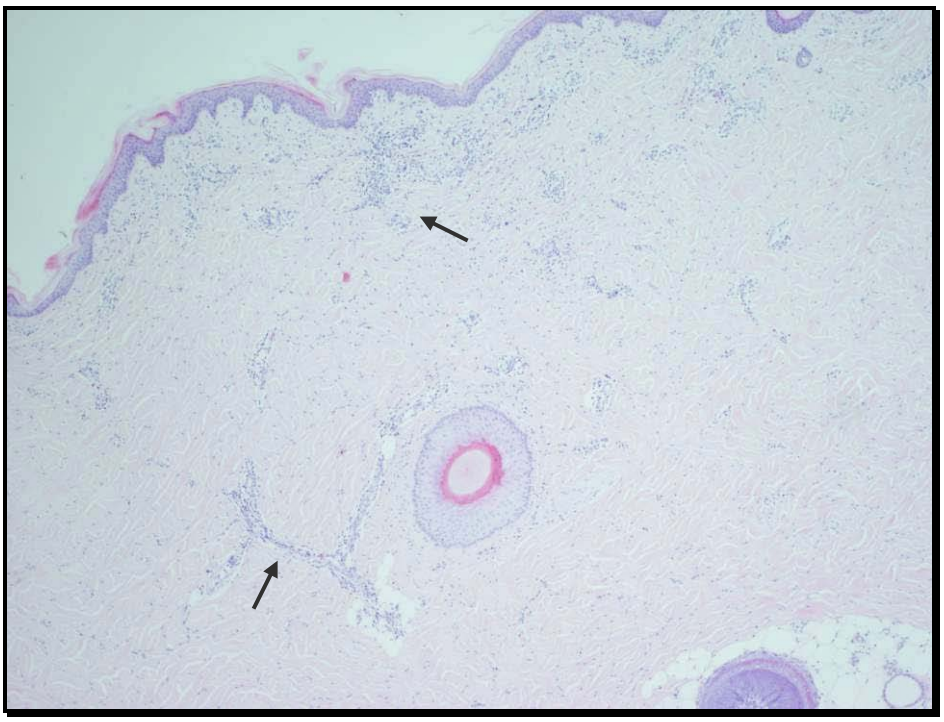

Figure 4.6 – Porcine skin used as control tissue. Collagen is populated with high numbers of fibroblasts (H&E, 40X).

The histopathological analysis of the collagen substrates showed absence of fibroblasts in both XL and NonXL samples pre-treated with PBS. The PT-PBS Raw collagen samples had variable results: 2 samples did not show cells at the surface or within the matrix, in 1 sample a low number of fibroblasts were visible at the matrix surface and the 4th sample presented a layer of fibroblasts covering the top of the matrix (Figure 4.7).

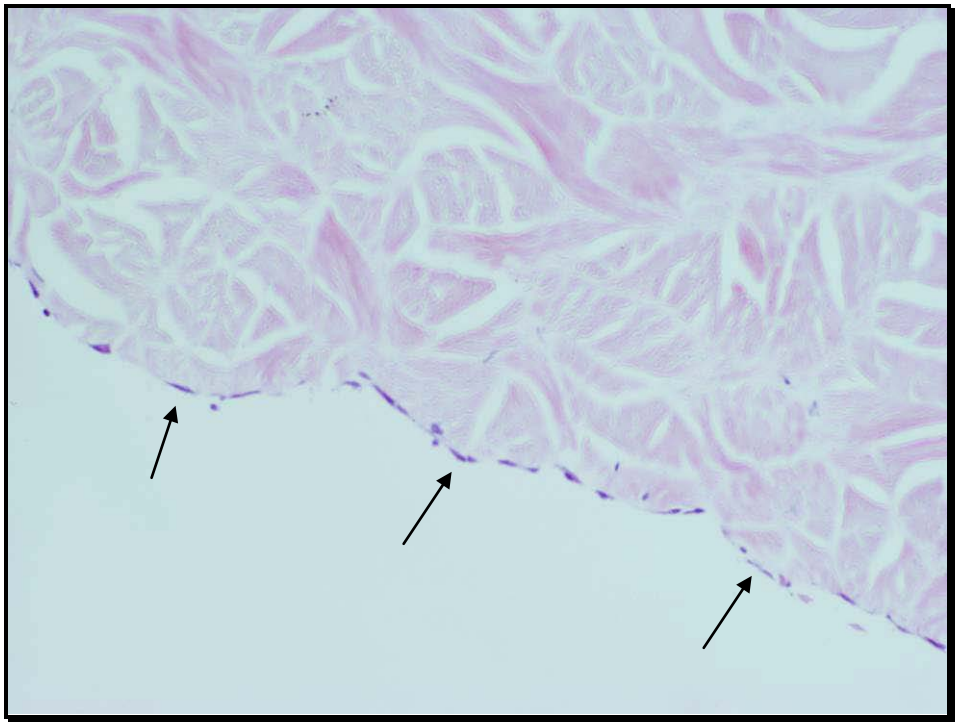

Figure 4.7 – Fibroblasts covering the surface of a PT-PBS Raw matrix, 28 days post incubation (H&E, 100X).

Samples pre-treated with FM showed a higher affinity to fibroblast infiltration and attachment; XL and NonXL samples had fibroblasts attached to their surface while Raw samples showed cells at the surface as well as some level of cellular penetration (Figure 4.8 to Figure 4.10).

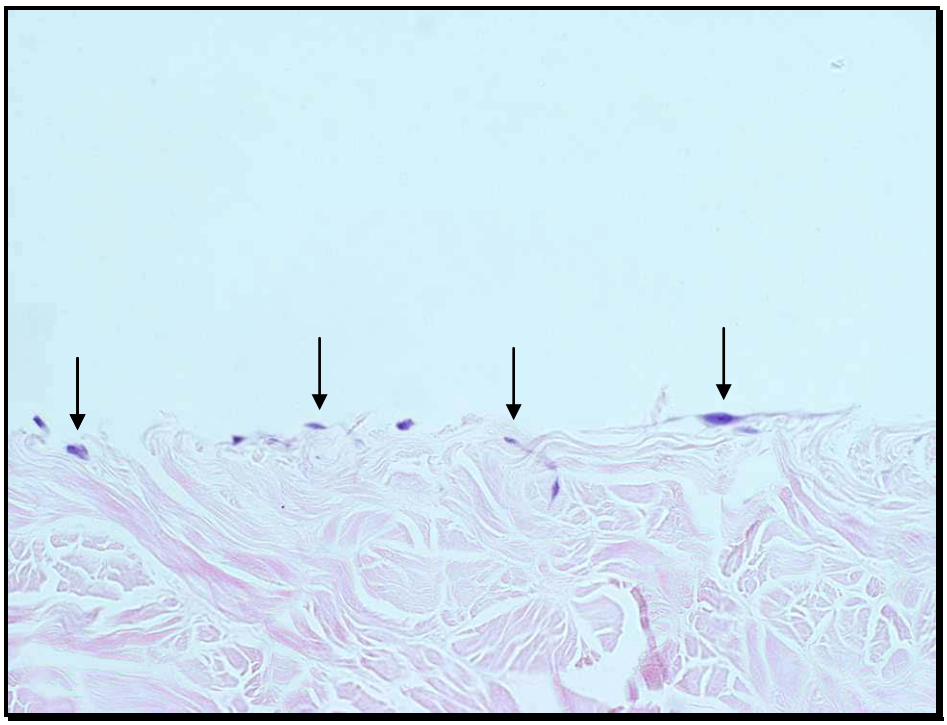

Figure 4.8 – Fibroblasts at the surface of XL samples pre-treated with fibroblast medium (H&E, 200X).

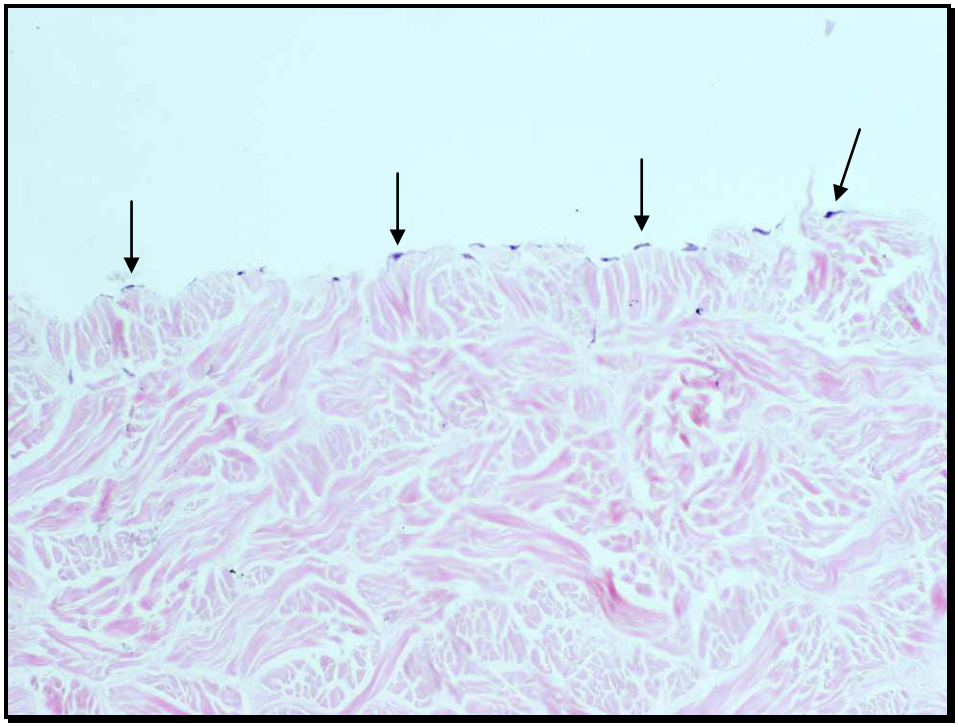

Figure 4.9 – Fibroblasts at the surface of NonXL samples pre-treated with fibroblast medium (H&E, 100X).

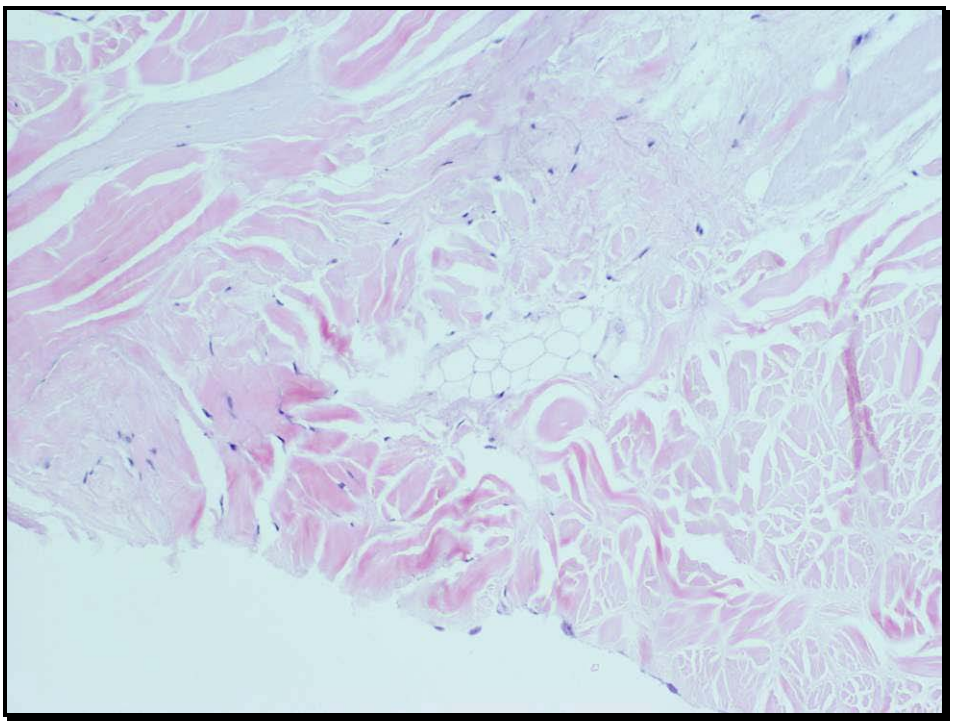

Figure 4.10 – Fibroblasts at the surface and infiltrating a Raw collagen sample pre-treated with fibroblast medium (H&E, 100X).

Non-soaked matrices showed the highest numbers of cell attachment and cell penetration for all collagen matrices tested. XL samples and Raw samples both allowed fibroblast proliferation at the surface with some fibroblast infiltration (Figure 4.11 and Figure 4.12, respectively).

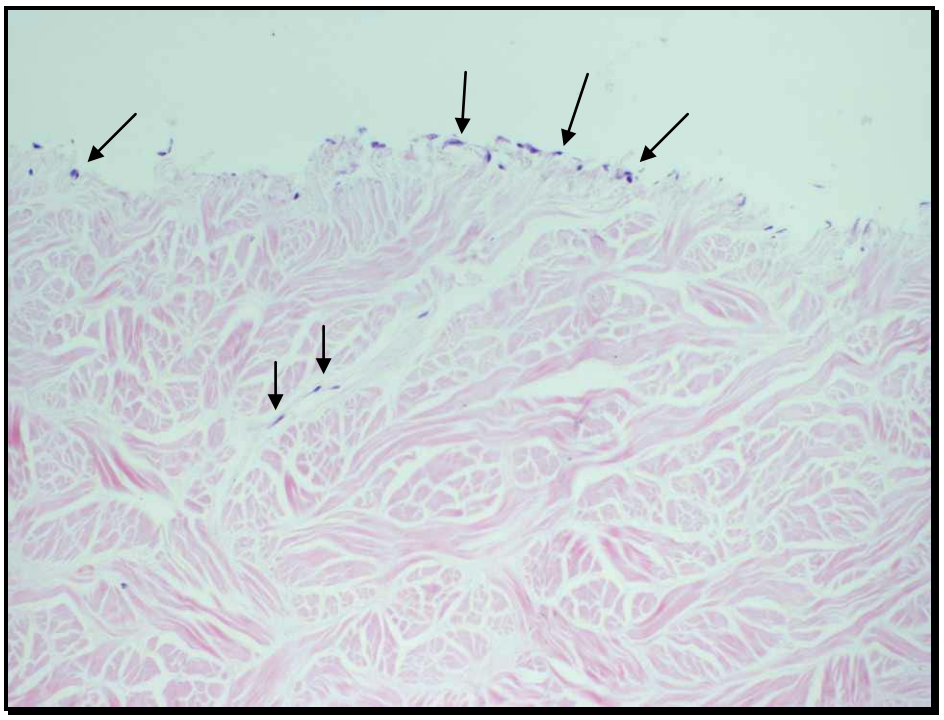

Figure 4.11 – Non-soaked XL sample with fibroblasts at the surface and penetrating through natural fissures (H&E, 100X).

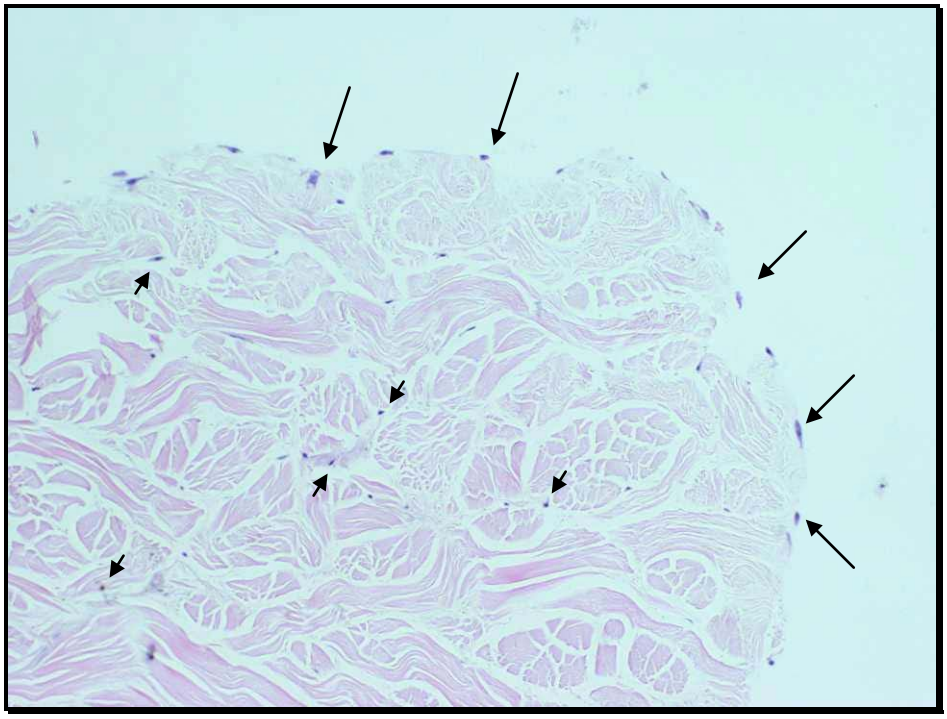

Figure 4.12 – Non-soaked Raw sample with fibroblasts at the surface and penetrating through natural fissures (H&E, 100X).

Non-soaked NonXL matrices did not show cellular penetration but had fibroblasts attached to the surface (Figure 4.13).

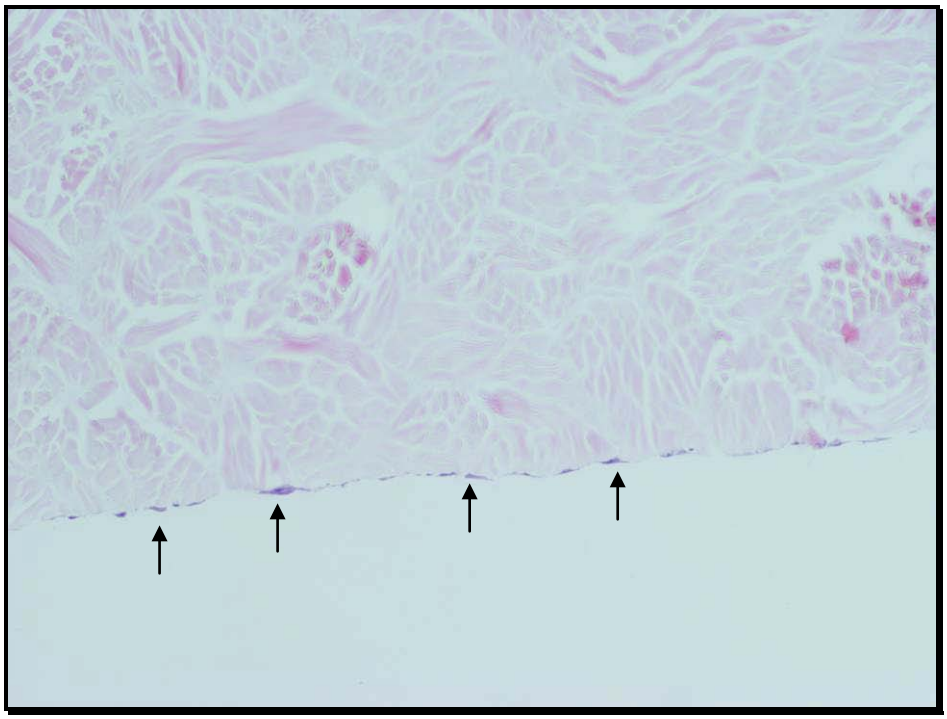

Figure 4.13 – Non-soaked NonXL matrix showing fibroblasts at the surface without cell penetration (H&E, 100X).

Independent of pre-treatment and type of collagen matrix, 28 days post incubation collagen was of good quality and showed no degradation or remodelling of the matrix; furthermore, collagen structure was not altered throughout the experiment (Figure 4.14).

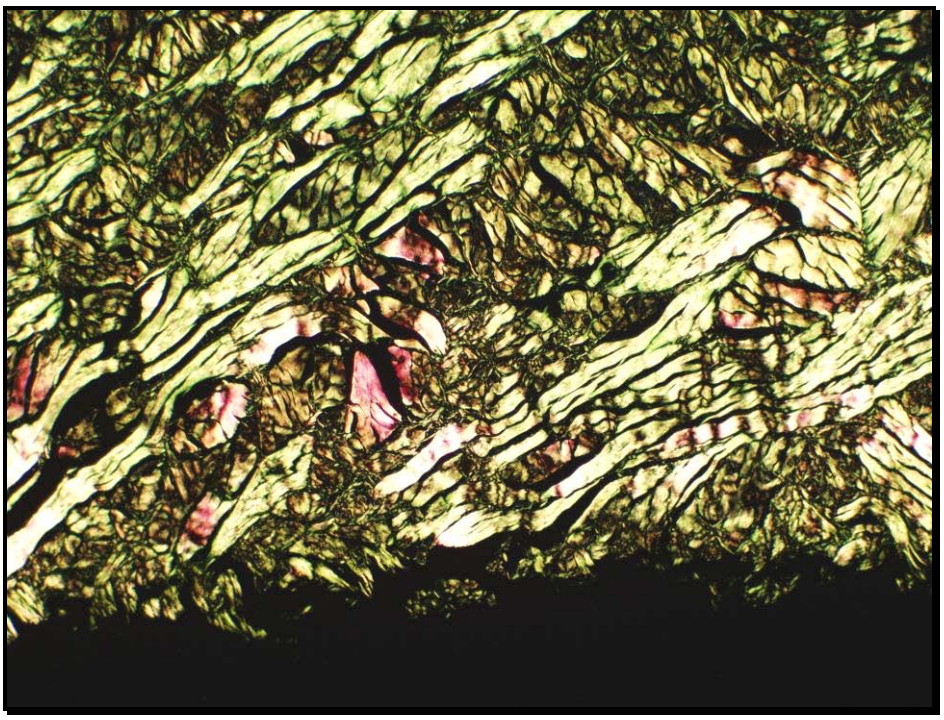

Figure 4.14 – Highly birefringent collagen under polarized light showing a non-denatured XL collagen matrix, 28 days post incubation (picro sirius red, 100X).

4.1.6 Discussion

Fibroblasts are commonly present in dermis; hence, one would expect fibroblasts to easily infiltrate dermal collagen derived biomaterials. This was not observed during this study.

Plate-wells where PT-PBS collagen samples were placed showed the lowest number of fibroblasts. Since there were no cells attached to the plastic surface at the end of the experiment it was reasonable to expect fibroblasts to be in suspension or attached to the collagen matrices but none of these outcomes were observed. Samples pre-treated with PBS showed low numbers of viable cells throughout the study despite the number of dead fibroblasts counted being low during the incubation period. PT-PBS Raw collagen was the only matrix that showed fibroblast attachment to its surface but this was observed only in 2 samples. These results suggest that: *i)* the fibroblast population used as inoculum in the PT-PBS wells died in the early stages of the study and the remaining fibroblasts proliferated at a slow rate; or *ii)* pre-soaking the

collagen matrices with PBS impaired cell attachment, cells remained in suspension and were removed at the first medium change.

Fibroblast death or inability of attachment resulting from pre-treating a matrix with PBS was intriguing and unexpected. PBS is extensively used as a washing buffer during cell culture. While sub-culturing the primary cultures of porcine fibroblasts the old medium was rejected and PBS was used to thoroughly wash the flasks to eliminate any possible toxins and residues from the old medium. It is known that attached cells can not be left in PBS for long periods of time without any medium, otherwise cells will start floating and lose their ability to attach to the surface. Since cells need Ca^{2+} to attach to a substratum, in the presence of PBS only, cell-receptors will dislodge from the specific ligands. In this study, cells were not left in PBS for more than a few seconds and cells were seeded in fibroblast medium.

It is well known that the extracellular environment influences cell behaviour with respect to morphology, cytoskeletal structures and functionality. Surface charge, surface energy and surface oxidation are physicochemical properties that affect cell response (den Braber *et al.*, 1996). One possible explanation for lack of cellular attachment to or penetration into the matrices is that the pre-treatment of the tested collagen matrices with PBS changed the chemical surface properties of the matrices interfering with protein attachment. Cells do not attach easily in a direct way to the surface of a substratum; instead the proteins from the serum that supplements the medium are rapidly adsorbed by the substratum translating its structure and composition into biological language. Later, cell-receptors attach to the protein ligands. Thus, the capacity of materials to adsorb such proteins from serum, in an active state, determines their ability to support cell adhesion and proliferation. Protein adsorption may be promoted or impaired by enthalpic and entropic changes within the surface-water-protein system (Wilson *et al.*, 2005). Changes may result from partial dehydration of protein and sorbent surfaces, redistribution of charged groups in the interface and conformational changes in the protein molecule (Haynes and Norde, 1994). The salt concentration in PBS may have altered the osmolarity of the collagen matrices and/or the surface charge, decreasing serum protein attachment and therefore, fibroblast adhesion.

These results may also be connected to the matrices structure. As observed in Section 3.2 these collagen matrices have a tendency to accumulate salts from the buffers. PBS salts may have been retained within the matrices and were later solubilised by the

fibroblast medium, causing an increase in the salts concentration of the medium and making the medium a hypertonic solution which would cause osmotic stress leading to cell shrinking as result of an osmotic adaptation.

Raw collagen samples have not been exposed to chemical treatments; this may explain the fibroblast attachment in the PT-PBS samples. Raw collagen ECM contains other components besides collagen, including glycosaminoglycans (GAGs) which are thought to support fibroblast attachment, migration and proliferation *in vitro* (Ojeh *et al.*, 2001).

Neither the decellularization process nor the cross-linking processes seem to compromise cell adherence, since XL and NonXL matrices had very similar results.
Pre-treatment of samples with FM did not impair cell attachment as fibroblasts were observed forming a monolayer at the surface of all 3 matrices; in the Raw samples a low level of cellular migration was observed through the natural fissures of collagen.
When no pre-treatment was used all matrices behaved similarly, each providing a surface for cell attachment. Both XL and Raw samples showed localized cell penetration.
The results reported here are partially in agreement with a study performed by Jarman-Smith and colleagues where the ability of Permacol® to support human primary fibroblast outgrowth from explant was compared to tissue culture plastic and PET (polyethylene terepthalate). The authors reported that the collagen matrix showed the least amount of cell retention compared to the other two matrices; however, the general trends were similar for all three scaffolds (Jarman-Smith *et al.*, 2004). They found that fibroblasts remained preferably at the surface of the matrices and did not penetrate, which is in agreement with our results. They pre-treated all matrices with FM, PBS and cysteine and used non pre-treated matrices as controls. They found the highest viable cell activity in the PT-FM samples, and PT-PBS and PT-cysteine samples gave better results than the non pre-treated matrices. This last result is not in accordance to the findings reported here, where normal, non pre-treated, Permacol® sustained fibroblast attachment and proliferation on the surface while PT-PBS samples did not.

It was observed that fibroblasts cultured on cross-linked and noncross-linked collagen matrices for a period of 28 days, remained mainly on the surface of the matrices and did not penetrate easily into the matrix. Their growth and attachment was supported by all three types of collagen matrices analysed. Under constant *in vitro* conditions fibroblasts may not produce collagenases necessary for the remodelling of the matrix and subsequent infiltration of cells; this may explain why cellular penetration was rarely observed. However, an *in vivo* environment is rather different, especially at a wound site where collagenolytic proteases can be produced not only by fibroblasts but also by immune cells migrating into the area - increasing the rate of collagen degradation and matrix remodelling. Kimuli and co-workers assessed the potential of Permacol® as a matrix for urological tissue engineering; they cultured normal human urothelial (NHU) and smooth muscle (SM) cells individually and in co-culture (Kimuli *et al.*, 2004). NHU attached and formed a monolayer on the surface of Permacol®, but SM cells only colonized the surface of Permacol® when co-cultured with NHU cells. To further investigate this they used the highly invasive EJ bladder cancer cell line, which formed a monolayer of cells on the surface by day 1, penetrated the matrix by day 7 and further penetration was observed until 14 days when the matrix degenerated. They hypothesized that SM cells failed to infiltrate Permacol® because of its level of cross-linking and that EJ cells were able to do it due to their proteolytic activity, to test this hypothesis they digested Permacol® with collagenase prior to cell seeding. Collagenase digestion failed to facilitate Permacol® penetration by SM cells, although it led to a rapid and widespread invasion by EJ cells. These results and the results obtained in this study, where Permacol® and NonXL collagen had similar results, suggest that cross-linking is not the major factor in preventing cells from penetrating the matrix.

It is important for a biomaterial to provide physical, chemical and biological features for cellular attachment, proliferation and infiltration. These features are associated with nutrient supply, waste product removal and neo-vascularisation; if a biomaterial does not allow nutrient access to its interior there will be no point in cells populating those areas. Geometrical surface properties such as shape, size and topography of a surface, can also influence cellular interactions (den Braber *et al.*, 1996; Desai, 2000; Vidaurre *et al.*, 2007). The macro- and micro-structural properties of biomaterials are of high importance. They affect not only cell survival, growth, reorganization,

intracellular signalling and migration, but also cell morphology and gene expression that relate to cell growth and preservation of native phenotypes (Figallo *et al.*, 2007; Leong *et al.*, 2003). It was thought that the cross-linking process of Permacol® surgical implant might affect the collagen structure, fibre alignment and orientation, and decrease pore size but, as discussed in Chapter 3.0, the cross-linked collagen shows natural fissures, with enough pore diameter for cell migration.

In the next chapter the ability of some cells to penetrate Permacol® surgical implant in localized areas will be discussed, especially where natural septae are present, but seem incapable of consistently achieving an even spread or regular pattern.

4.1.7 Conclusion

In the study presented here fibroblasts were cultured using three different types of dermal collagen matrices as a 3-D substratum. Cells remained mainly on the surface of the matrices and did not penetrate easily into the matrix, independent of the type of matrix or pre-treatment performed. Fibroblasts growth and attachment was supported by all three types of collagen matrices analysed.

Permacol® surgical implant has been designed for permanence when implanted *in vivo* and since fibroblasts did not remodel or change in any way Permacol® matrix, the present results suggest that this biomaterial can be used as a bulking material without fear of the material shrinking or contracting. In addition, Permacol® surgical implant's apparent resistance to contraction is likely to be of importance for the reduction of scarring when used in wound healing. Nevertheless, *in vivo* studies are required to corroborate these hypotheses.

4.2 ASSESSMENT OF SKIN EXPLANT OUTGROWTH INTO COLLAGEN SUBSTRATES

4.2.1 Introduction

Explant culture is a common method utilized to establish primary cell cultures. This technique isolates cells from one or more pieces of tissue. In brief, the tissue is harvested in a sterile manner (explant), often minced, and pieces placed in a cell culture dish containing growth media especially selected to facilitate cellular migration of the cells of interest from the explant. Over time, progenitor cells migrate out of the tissue onto the surface of the dish. These primary cells can then be further expanded and transferred into new culture flasks/plates.
Explant culture is commonly performed in plastic Petri dishes or well-plates; these can be supplemented with spacers for mesh supports and media or the explant can be placed on stainless steel mesh or grids, or supporting substrates. These substrates facilitate the attachment of the explant to the culture vessel as well as promoting the maintenance of the differentiated phenotype.

In contrast to cell culture which implies the relatively homogeneous isolation and culture of specific types of cells in defined media and under controlled conditions, explant culture utilizes slices or small segments of organs or tissues which contain multiple cell types. Explant culture offers several significant advantages for studies of cellular biology. These include preservation of the histiotypic relationships among cells of an organ without any disturbance of the cellular or tissue architecture which is caused by enzymatic, chemical or mechanical separation (Resau *et al.*, 1991). During explant outgrowth, the cell phenotype remains intact and the effect of the adjacent basement membranes and cells on each other helps to maintain typical cell-cell interaction.

We have studied earlier how fibroblasts behave when seeded on Permacol® surgical implant, acellular noncross-linked collagen and dermal porcine collagen. In a similar experiment, porcine skin biopsies were used to evaluate explant outgrowth in the same three porcine collagen matrices. In the first experiment fibroblasts remained mainly at the surface of the matrices and cellular penetration was rarely observed. It is not known if those results were related to cell isolation techniques, which may affect cell phenotype and therefore histiotypical features. This study will assess explant cell migration into the collagen matrices, the type of cells migrating and cell-matrix interaction.

4.2.2 Hypothesis

Permacol® surgical implant, acellular noncross-linked collagen and dermal porcine collagen are capable of supporting porcine skin explant outgrowth.

4.2.3 Aims and Objectives

- Compare the effect of enzymatic cell isolation versus explant culture techniques, relative to cell attachment, proliferation and penetration into collagen matrices.
- Assess the ability of cross-linked and noncross-linked collagen matrices to support skin explant outgrowth over time.

4.2.4 Materials and Methods

Experimental procedures were similar to the protocol followed in Chapter 4.1. As before, all collagen matrices were supplied by TSL plc.

Permacol® surgical implant (XL), noncross-linked acellular collagen (NonXL) and dermal porcine collagen (Raw) were tested. Each collagen matrix was derived from the same batch to eliminate variations.

Four discs, 2cm in diameter (3.14cm^2 area) were cut from each of the collagen matrices; discs were left soaking overnight in fibroblast medium (PT-FM) supplemented with antibiotics. The next day 4 more discs with the same dimensions were prepared from each collagen matrix and since they were not pre-treated with any solution, were labelled as "Non-soaked".

Two 12-well plates were used (Nunc, Fisher Scientific UK Ltd., Leicestershire LE11 5RG, U.K.) for this experiment. Each well (∅=2.0cm) received a collagen disc. The first plate was prepared with the PT-FM samples and the second plate with the non-soaked samples.

A skin biopsy was isolated as in Section 2.1.2 and skin explant containing both epidermis and dermis were cut into 0.5cm x 0.5cm pieces. Three pieces of skin explant were placed on top of each matrix disc; collagen matrices and skin were soaked with fibroblast medium and moved to an incubator, at 37°C with 5% CO_2 and 100% humidity, for 6 hours to allow skin attachment to the matrices. Three skin pieces were placed in a plastic Petri dish, to act as control, and treated in the same manner as the test matrices. Part of the skin biopsy was fixed in 10% NBF and processed for histological analysis to be used as control for tissue morphology and cell-type location and density.

The volume in each well was made up to 1mL with fibroblast medium (FM) and plates returned to the incubator. Skin in the control dish was submerged in FM. Explant cultures were kept for 21 days with medium changes every 2 days.

The control plate was microscopically observed for cell outgrowth at various times throughout the study.

At the end of the study all samples were fixed in 10% NBF for histological analysis and the empty plates were observed using an inverted reflected-light microscope to look for cell attachment to the plastic surface.

4.2.5 Results

At day 2 a bacterial contamination occurred but a decision was made to continue the experiment for 20 days and observe the interaction of bacteria with the collagen matrices tested. The experiment was repeated and the explant outgrowth observed. Results from the explant outgrowth experiment will be described first followed by the results obtained when the bacterial contamination occurred.

4.2.5.1 Skin Explant Outgrowth

After day 3 cells outgrowth was observed from the skin explants placed in the control plate and cells continued to proliferate until the end of the study.
Histology from the skin biopsy showed dermal collagen easily populated by cells (Figure 4.15).

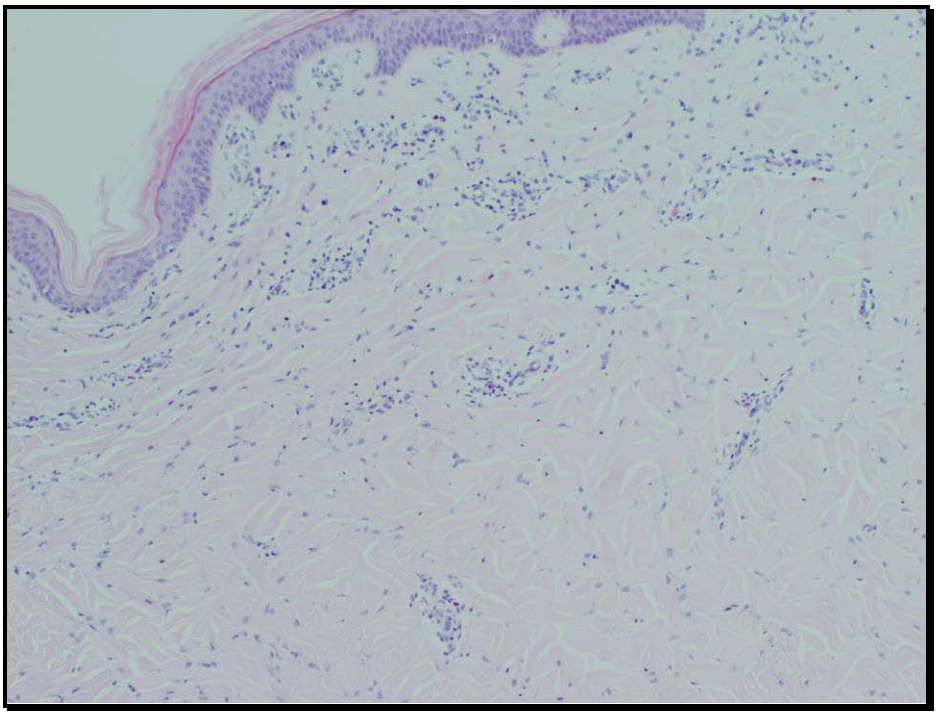

Figure 4.15 – Porcine skin biopsy (H&E, 20X).

At the end of the experiment plates were observed for cell attachment to the plastic surface. Wells where non-soaked matrices were placed had low numbers of cells attached to the plastic surface. The same was observed for PT-FM Raw samples. XL and NonXL samples pre-treated with fibroblast medium had minimal amounts of cells attached to the plastic surface of the wells.

The histopathological analysis of the collagen matrices showed cells only at the surface of the collagen matrices, but cellular penetration was not observed. Non-soaked samples had low numbers of cells attached to the surface. Non-soaked XL samples showed cells at the surface but these did not form an even monolayer (Figure 4.16).

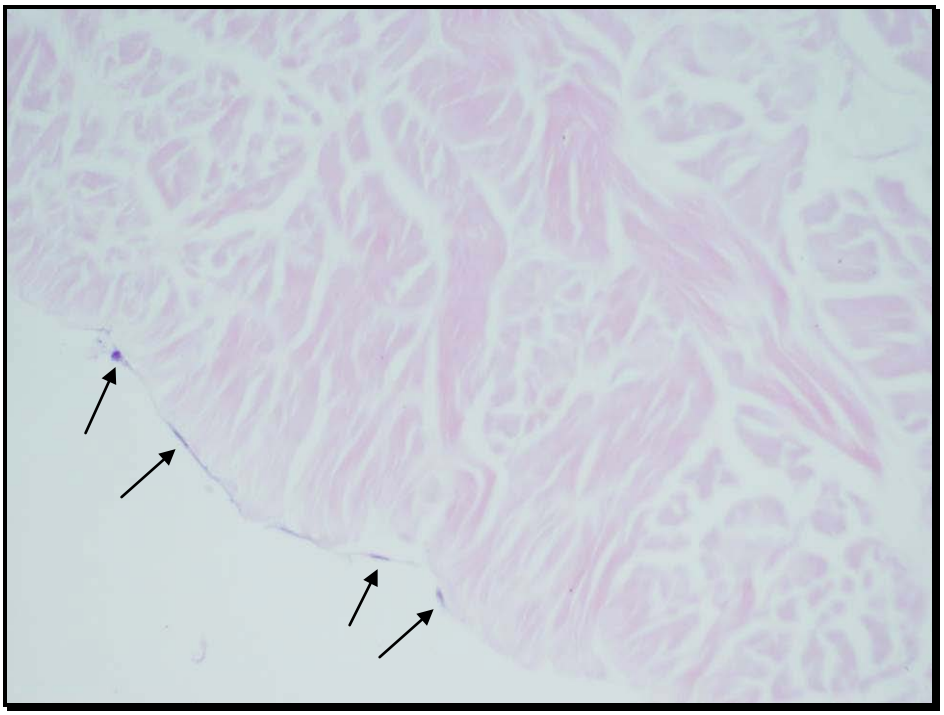

Figure 4.16 – Non-soaked XL collagen matrix with low number of cells in monolayer at the surface of the matrix (H&E, 200X).

Non-soaked NonXL did not show cell attachment or penetration and non-soaked Raw collagen matrices showed only a few cells attached to the surface (Figure 4.17).

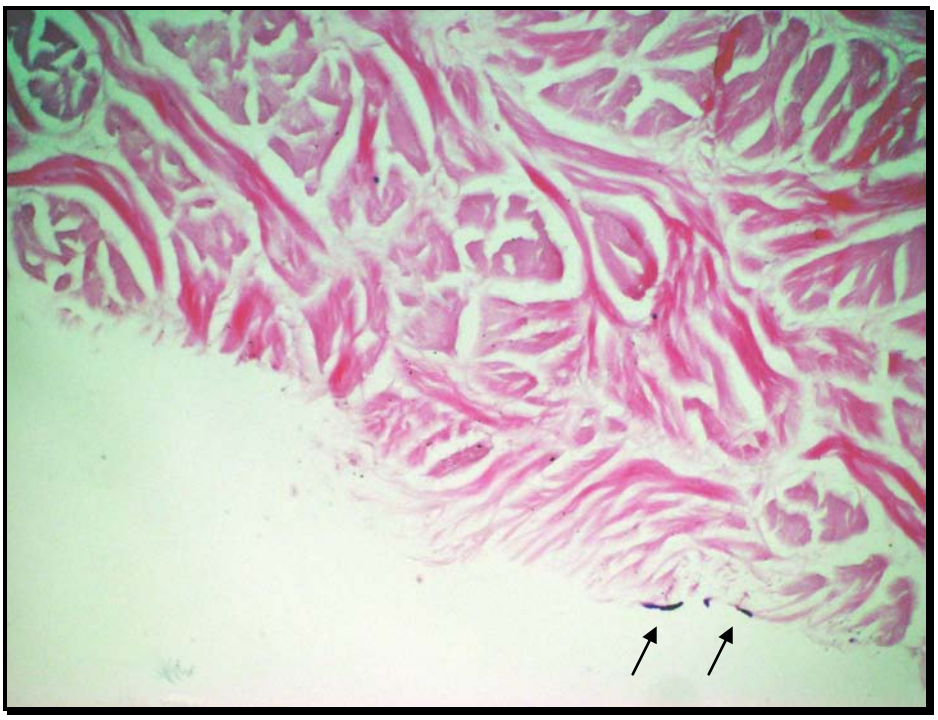

Figure 4.17 – Non-soaked Raw sample with very low cell attachment (H&E, 200X).

All PT-FM collagen matrices had cells attached to their surface, although at marginal numbers (Figure 4.18 to Figure 4.20).

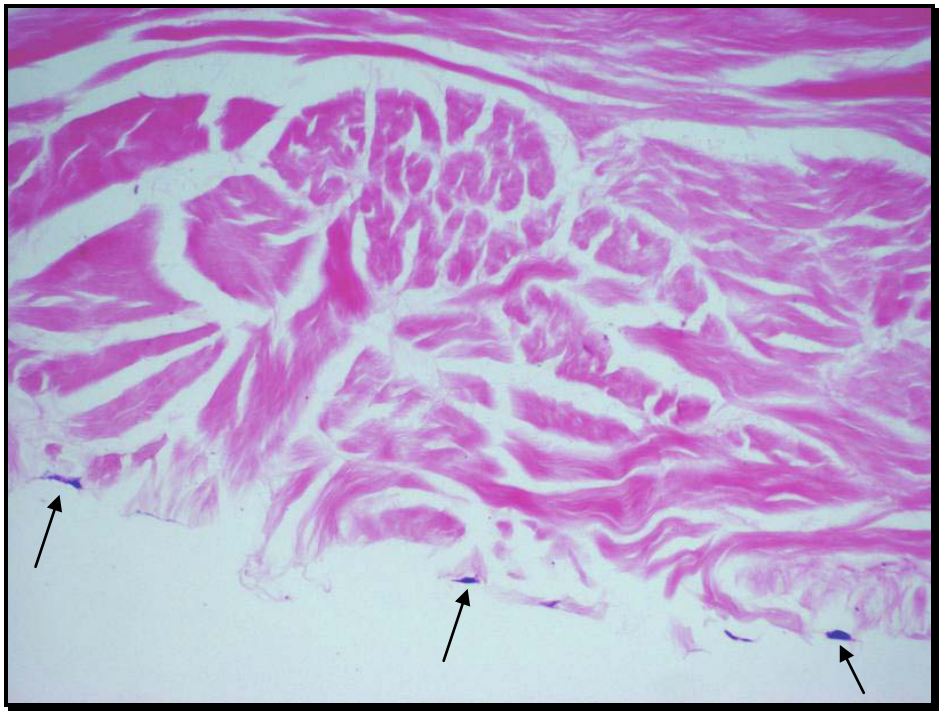

Figure 4.18 – PT-FM XL collagen with cells derived from explant outgrowth at the surface, 21 days post implantation (H&E, 200X).

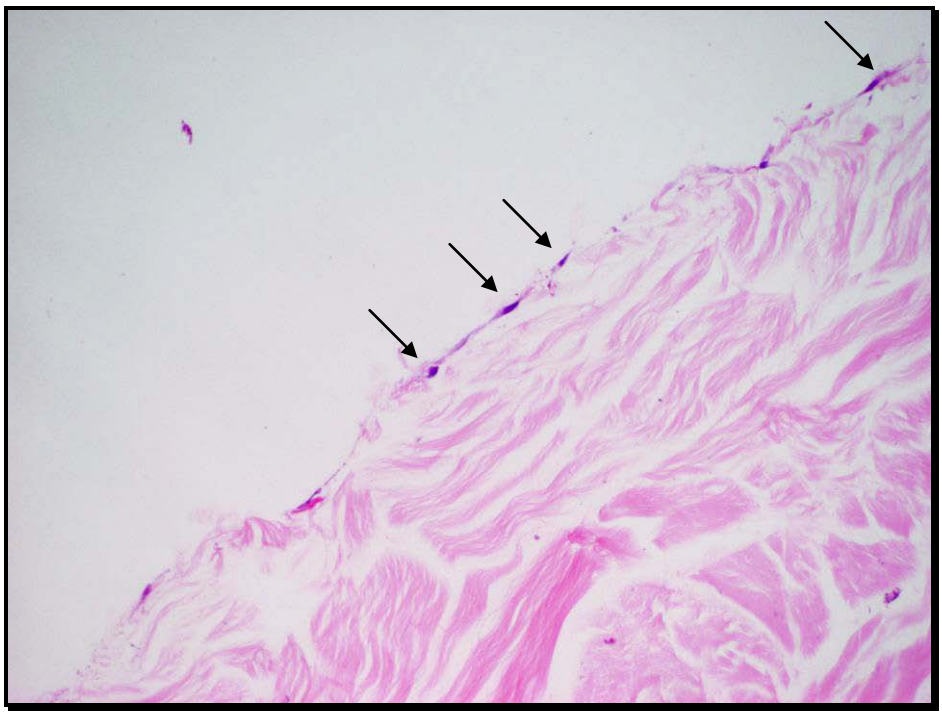

Figure 4.19 – PT-FM NonXL collagen with cells derived from explant outgrowth at the surface, 21 days post incubation (H&E, 200X).

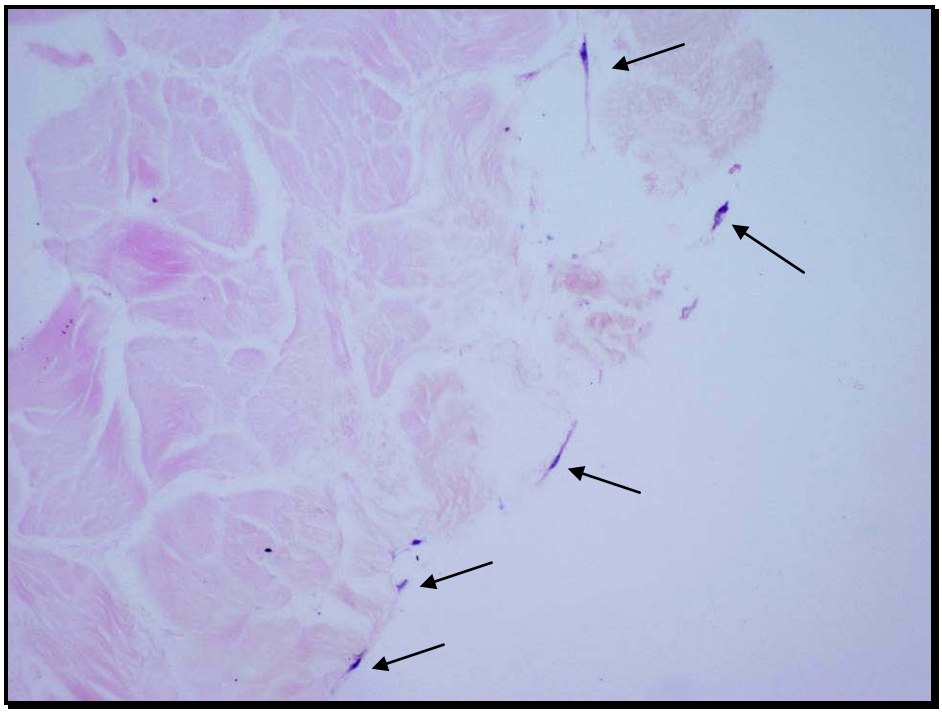

Figure 4.20 – PT-FM Raw collagen with fcells derived from explant outgrowth at the surface, 21 days post incubation (H&E, 200X).

Skin explants were also processed for routine histology. The majority of the skin explants showed cells within the extracellular matrix, although cell numbers were not as high as found normally in skin (Figure 4.21). Half of the explants from the non-soaked XL group had only a few cells within the extracellular matrix but cells were visible forming a monolayer at the surface of the explant (Figure 4.22).

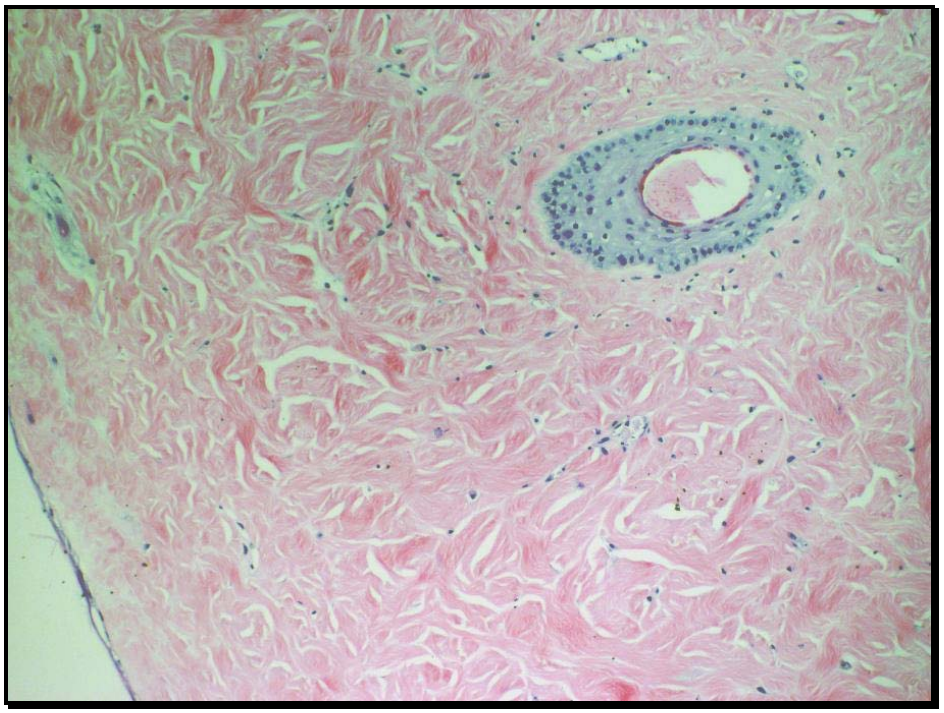

Figure 4.21 – Skin explant showing cells within the matrix (H&E, 100X).

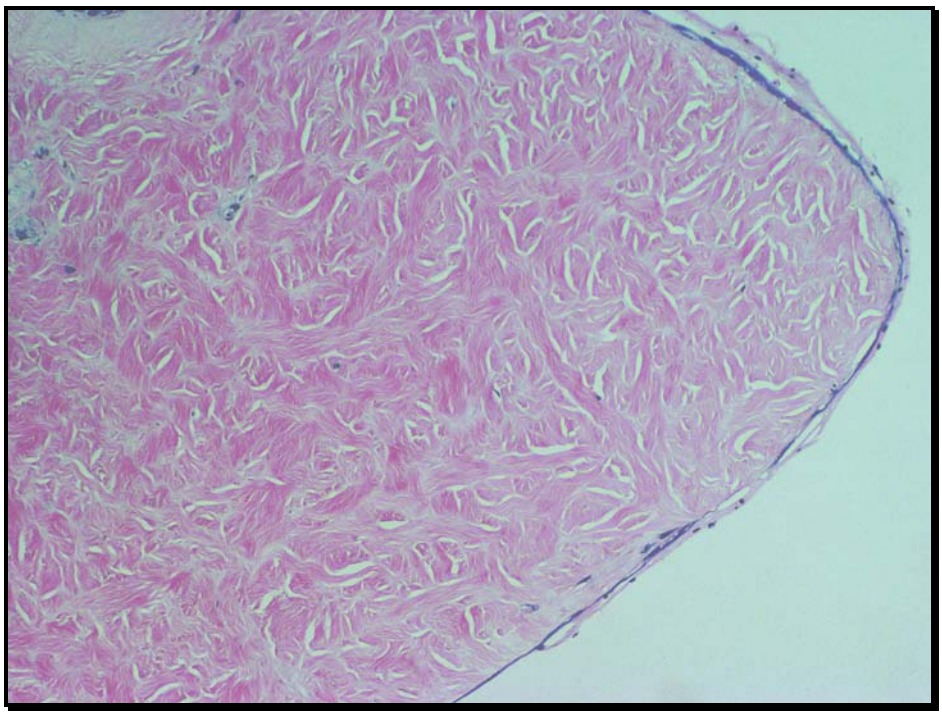

Figure 4.22 – Skin explant with a low number of cells within the matrix but with cells at the surface (H&E, 40X).

All collagen matrices showed good, non-denatured, collagen after 3 weeks incubation with skin explants.

4.2.5.2 Skin Explant and Bacteria

At day 2 a bacterial contamination occurred most likely due to poor skin sterilization, resulting in contaminated explant. Plates were visibly contaminated with some of the explants floating in the medium.

When using Raw collagen as a substrate, bacteria were able to attach to both sides of the matrix, producing a biofilm at the surface, but not easily penetrating the matrix. This surface layer degraded the collagen in contact with it, and it was possible to see a first wide (compared to the other matrices) layer formed by degraded collagen and bacteria (Figure 4.23).

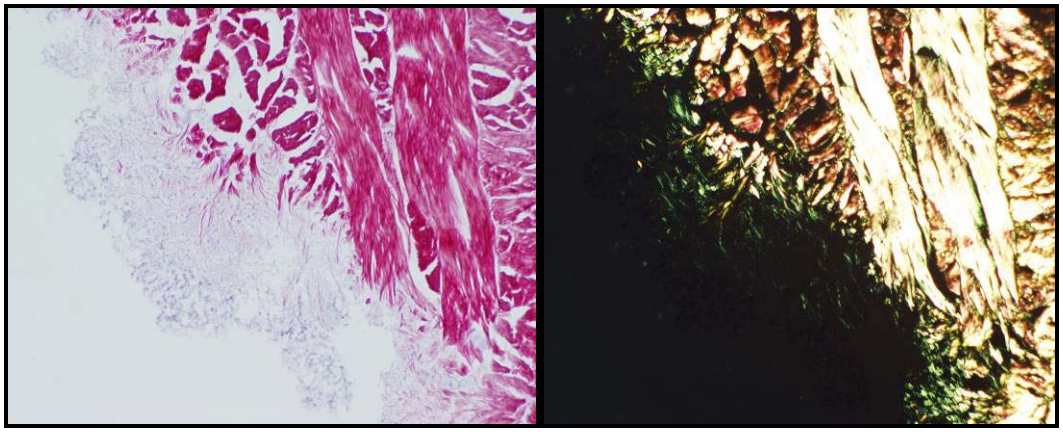

Figure 4.23 – Surface layer of bacteria in raw collagen. There is some level of penetration of bacteria into the matrix and the collagen at the surface was degraded (picro sirius red stain, right image: polarized light, 200X).

Although there was a small degree of bacterial penetration, bacteria mainly stayed at the surface of Raw collagen samples (Figure 4.24).

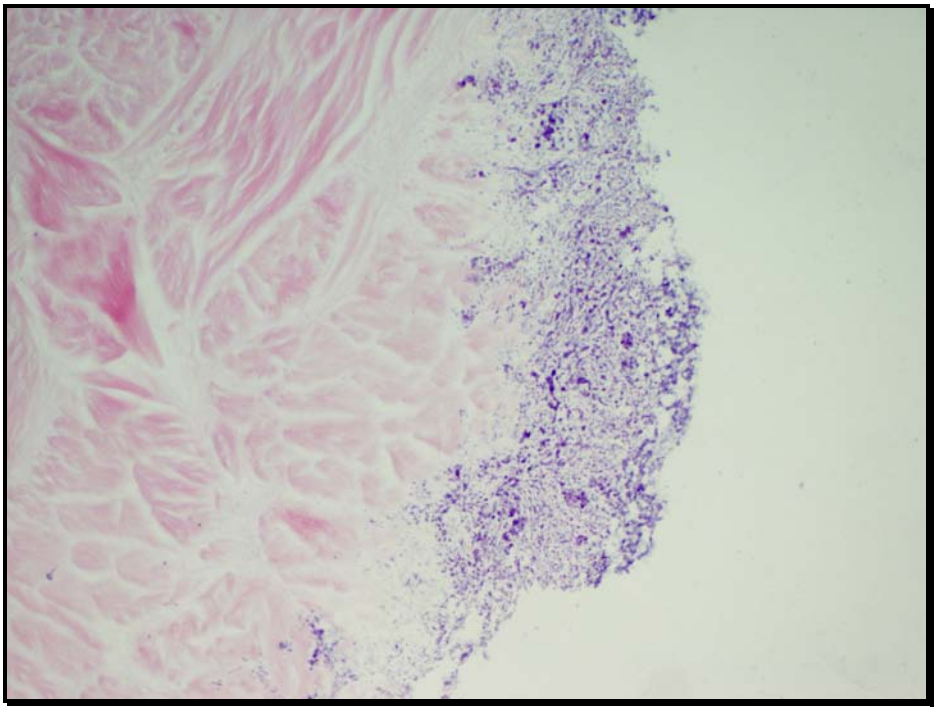

Figure 4.24 – A layer of bacteria at the surface of Raw collagen, not penetrating into the matrix (H&E, 200X).

NonXL samples showed some bacterial penetration with a low level of collagen degradation but mostly bacteria were seen on the surface of the collagen. There were a few extraordinary situations where bacteria were found in clusters inside the matrix, but it is not possible to see how they reached such a level of penetration (Figure 4.25).

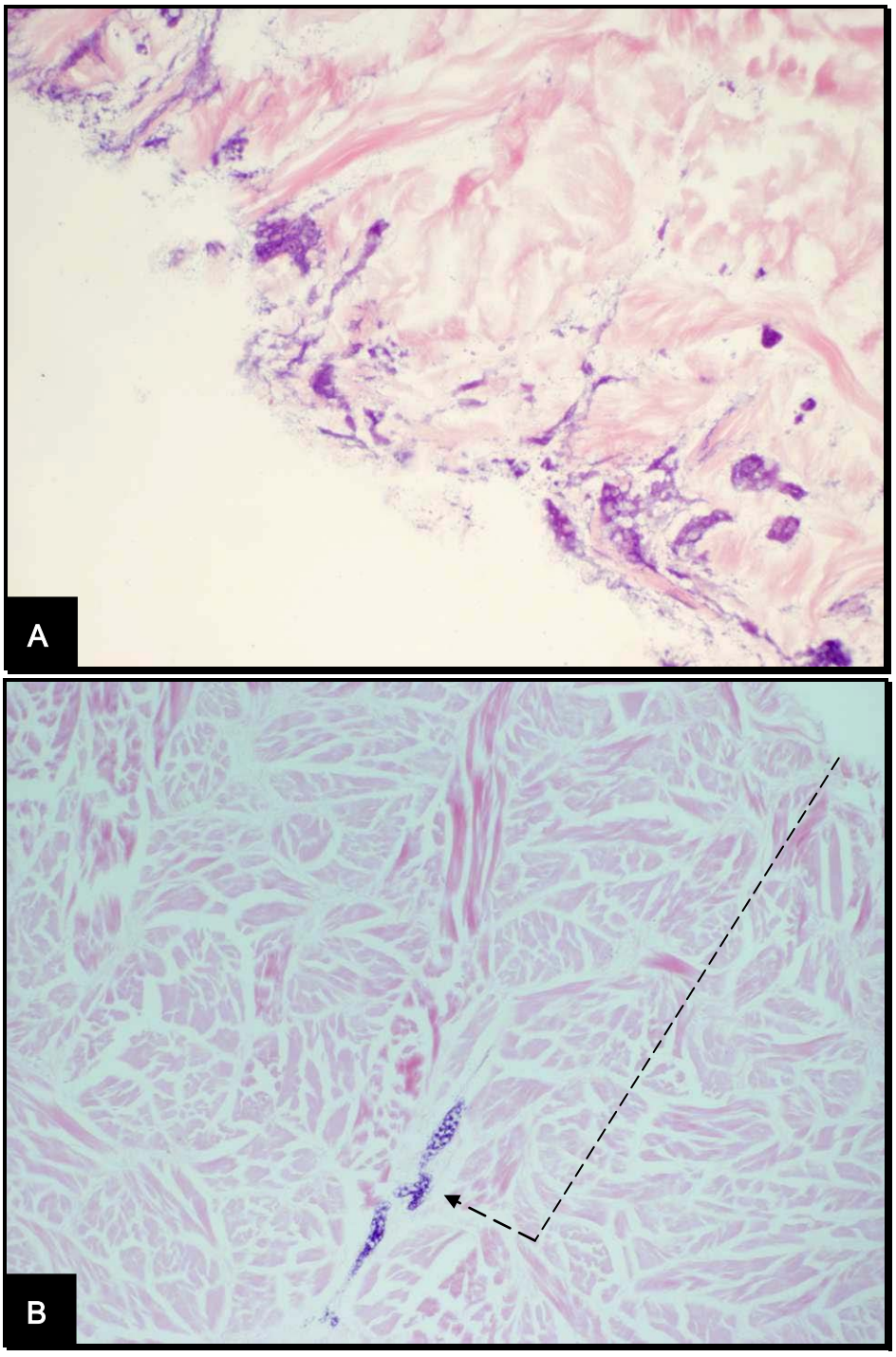

Figure 4.25 – NonXL collagen matrices after 21 days incubation. Figure A shows high amounts of bacteria on the surface of the collagen matrix, with little penetration

(H&E, 200X). Figure B shows bacteria in the centre of a NonXL implant, although the surface of the matrix is cell free (H&E, 100X).

Permacol® samples showed high concentrations of bacteria on the surface of the matrix; when the bacterial load was high bacteria were observed penetrating through the natural septae of collagen (Figure 4.26).

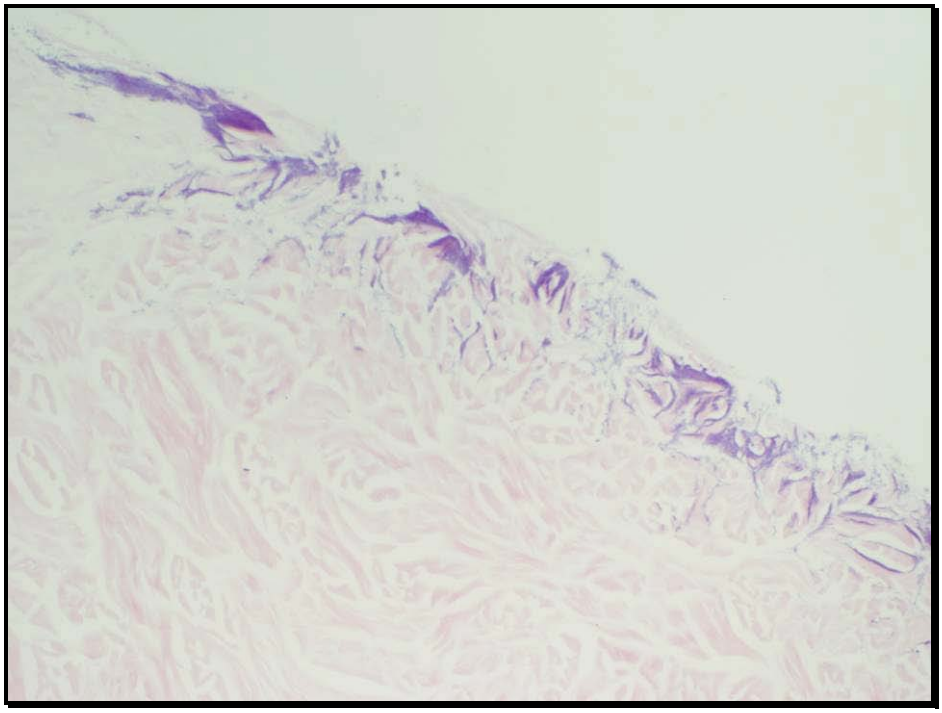

Figure 4.26 – Permacol® samples showing bacterial penetration after 3 weeks incubation (H&E, 100X).

Although both noncross-linked and Permacol® samples showed high numbers of bacteria on the surface, with some level of penetration, picro sirius red stain under polarized light showed good quality collagen in all Permacol® samples and degradation in the noncross-linked samples was very low (Figure 4.27 and Figure 4.28).

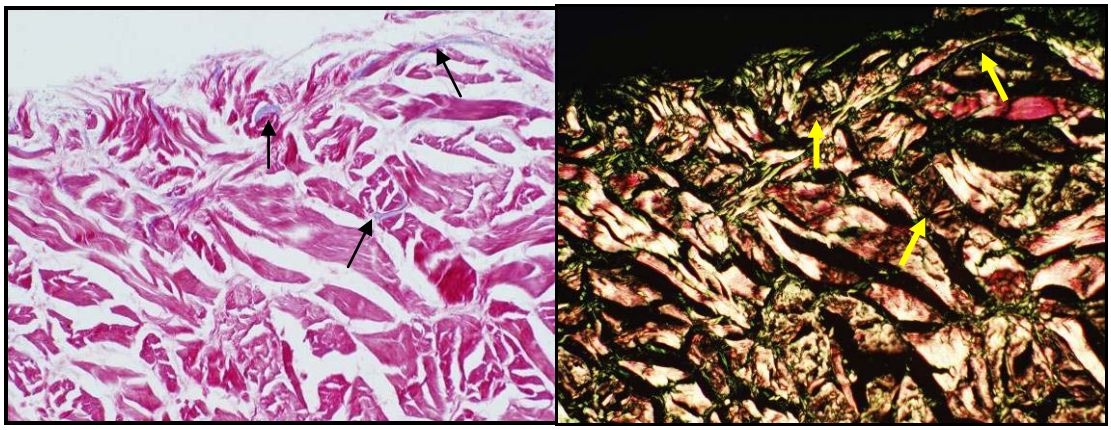

Figure 4.27 – Permacol® implant with some bacterial penetration but non degraded collagen (picro sirius red, 100X).

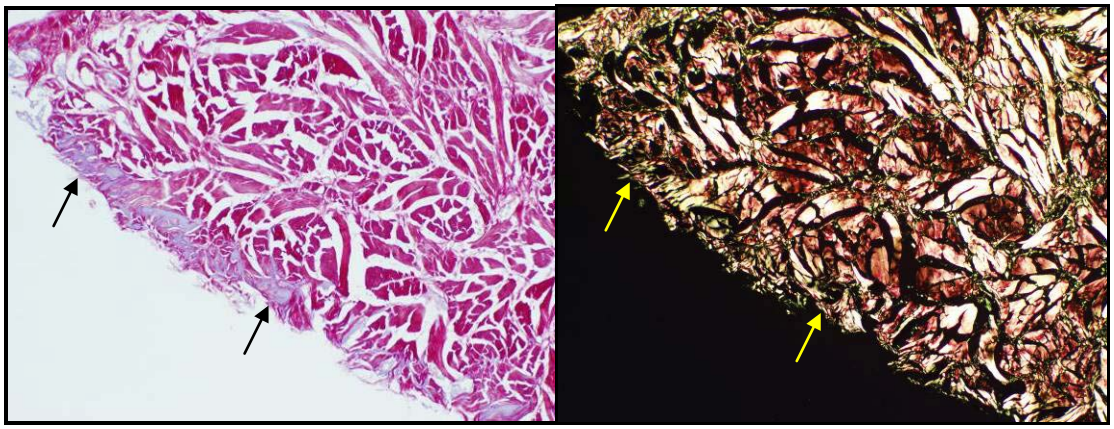

Figure 4.28 – Noncross-linked implant surface with a high bacterial load but no collagen degradation (picro sirius red, 100X).

4.2.6 Discussion

The cells observed outgrowing from the porcine skin explants showed a fibroblast-like morphology. Morphologically there was no difference between the cells obtained by enzymatic extraction and the cells from the explants. Nevertheless, explant outgrowth produced less cells than cell seeding after enzymatic digestion.

Non-soaked matrices had low efficiency as support for explant outgrowth. Permacol® was the only non pre-treated matrix that supported cell outgrowth. Noncross-linked matrices did not sustain cell outgrowth and non-soaked Raw samples showed only a few cells on the surface.

In this study only one soaking regime was chosen – fibroblast medium – taking into consideration the results obtained in Chapter 4.1 it was decided to exclude pre-treatment with PBS. When the collagen matrices were pre-treated with fibroblast medium, the proliferation of cells from skin explant demonstrated that all samples were capable of supporting the outgrowth of cells.

As observed previously, cells failed to infiltrate the biomaterials and remained as a monolayer on the surface. For uses in tissue engineering it is important for cells to be able to penetrate into the matrix. It can not be concluded that the decellularization process or the cross-linking procedure influence cell attachment, proliferation and infiltration, since raw collagen behaved similarly to Permacol® and noncross-linked collagen.

It is important to consider that an *in vitro* experiment is a controlled environment and very different from an *in vivo* situation, which will always be influenced by multiple variables in a complex system. Therefore, *in vivo* studies are necessary to elucidate why cells do not infiltrate these collagen matrices as readily as expected.

When bacterial contamination occurred, it was decided to isolate those plates in an empty incubator and allow the bacteria to interact with the collagen matrices during 20 days. The medium was changed every two days and occasionally every day since bacterial proliferation rate was very high.

Although the experiments were carried out over almost 3 weeks there was only slight penetration of bacteria into the matrices. Regardless of some sporadic penetration of cells into the matrices, in general bacteria remained at the surface or in the medium and this was independent of the soaking regime.

When follicular pores were present bacteria would infiltrate through these but translocation from pores into adjacent tissue was not observed. Occasionally, bacteria appeared isolated in the centre of a matrix; this outcome was intriguing since there were no pores connecting that location to the surface. One explanation is that the transverse section cut the bottom of a follicular pore which had been invaded by bacteria.

The cross-linking process seems to confer a higher level of resistance to bacterial degradation, since all cross-linked samples were not degraded by bacteria. The

processed but noncross-linked matrix was more resistant to bacteria when compared to the raw, non-processed collagen, possibly because of the absence of interstitial tissue.

Despite the small level of penetration and some degradation, it is obvious that bacteria do not easily invade collagen matrices, independent of the treatment used in each matrix.

Raw collagen samples used in this study showed low numbers of cells. This is not in agreement with what was observed in normal skin, which had numerous cells, indicating that collagen in normal situations is well vascularised. The difference between normal skin and raw collagen is a sign that the storage process is by itself partially decellularising the samples; this may signify that the trypsinization step adopted by the manufacturers may be excessive where this storage regime is used.

4.2.7 Conclusion

Dermal porcine collagen (Raw) and acellular dermal collagen (NonXL) require matrices pre-treatment with fibroblast medium before being able to support cell outgrowth from skin explants. Under the same conditions, Permacol® supported cell attachment and proliferation with and without matrix pre-treatment.

When in presence of bacteria, collagen dermal matrices were only marginally infiltrated by the micro-organisms, bacteria usually kept to the surface or where in suspension. A low level of collagen degradation was observed in the NonXL and Raw collagen matrices, but not in the Permacol®.

The apparent resistance of Permacol® to bacterial digestion suggests that this biomaterial may perform well in infected areas, and this could have many surgical benefits.

4.3 AN *IN VITRO* MODEL FOR ASSESSMENT OF PERMACOL® SURGICAL IMPLANT PERFORMANCE IN A CONTAMINATED FIELD

4.3.1 Introduction

In the light of observations made from Chapter 4.2, where skin explant unintentionally infected collagen matrices in culture, it was decided to examine the interaction of Permacol® surgical implant with bacteria.

Chronic wounds are an important source of morbidity, affecting more than 1% of the U.K. population and with treatment costs above £1 billion per year (Davies *et al.*, 2001; Edwards and Harding, 2004; Hill *et al.*, 2003; Thomas and Harding, 2002). Chronic wounds do not occur in laboratory animals; therefore, pre-clinical experimental study of this condition has been difficult. There are two factors that may explain the absence of chronic wounds in laboratory animals; first it is not common to find truly aged animals and second, the majority of animals are loose skinned and their open wounds heal almost completely by wound contraction (Mustoe, 2004). In humans, chronic skin wounds are common in the elderly population, occurring in the setting of some degree of local tissue ischemia but can also result from traumatic tissue loss and surgical procedures (Falanga, 1993).

Non-healing wounds are biologically characterized by prolonged inflammation, defective re-epithelialization and impaired matrix remodelling (Davies *et al.*, 2001; Young *et al.*, 2006). The hallmark feature of chronic inflammation is ongoing tissue damage often caused by the inflammatory cells present – mainly neutrophils, macrophages and lymphocytes – and the microbiological bioburden (Di Vita *et al.*, 2006; Kingsley, 2003). The wound healing course can be divided into three phases: inflammation, proliferation and maturation; a high bioburden can disrupt the orderly healing sequence, producing a chronic inflammatory and therefore a non-healing wound (Kingsley, 2003).

A critical factor in the pathogenesis of most chronic wounds is the combination of the presence of bacteria, the leukocytes attracted by the latter and the high proteolytic environment that will result from that situation. The high level of leukocytes at the wound surface produces proteases and oxidants that degrade the extracellular matrix and cytokines, inhibiting cell migration and impairing cellular closure (Mustoe, 2004; Xu *et al.*, 2007). Furthermore, in all chronic wounds there is an interaction between patient and the bacteria present in the wound. This interaction varies from contamination through colonization on to local infection (critical colonization) and finally to spreading infection. The concept of critical colonization is relatively recent and defines a transition state between bacterial surface colonization that does not impair the healing process and invasion of the bacteria into viable tissue (Edwards and Harding, 2004; Kingsley, 2003).

A contaminated wound refers to a wound with a bacterial bioburden that is not harmful to the host and where micro-organisms are not replicating and pose no threat to healing (Bergin and Wraight, 2007; Edwards and Harding, 2004). Colonized wounds display replicating micro-organisms adherent to the wound that impede wound healing but there is no further tissue damage (Edwards and Harding, 2004). Wound infection can be characterized by the presence of replicating organisms within a wound with subsequent host injury (Edwards and Harding, 2004; Kingsley, 2003).

The exact level of bacterial bioburden necessary for a contaminated wound become an infected wound is not known; but will depend on a multitude of microbial and host factors, including the type of bacteria present and the patient general health and immune condition (Bowler *et al.*, 2001). However, the 10^5 rule has been long established and states that a level of bacteria equal to or greater than 10^5 CFU per gram of wound tissue is sufficient to confirm clinical infection (Bergin and Wraight, 2007; Edwards and Harding, 2004; Kingsley, 2003). The clinical relevance of this theory has been questioned, since the required density of a given organism to became infectious varies with the type of organism, as well as being influenced by the organism's interactions with surrounding microflora (Bowler *et al.*, 2001; Bowler, 2003).

Analysis of microflora associated with chronic wounds has revealed a large number of aerobic and anaerobic species from a range of genera. Typical pathogens of infected wounds are methicillin-sensitive *Staphylococcus aureus, Pseudomonas aeruginosa* and *Escherichia coli* (Bergin and Wraight, 2007; Brook and Frazier, 1998; Daeschlein

et al., 2007; Davies *et al.*, 2007; Edwards and Harding, 2004; Kingsley, 2003; Valencia *et al.*, 2004). In addition to bacteria, yeasts can occasionally be isolated from chronic wounds, *Candida* spp. being most commonly isolated from deep tissue (Hill *et al.*, 2003; Sapico *et al.*, 1980).

Research in chronic wound healing is intricately linked with developments in tissue engineering. Until recently surgical procedures to replace soft tissue loss would exclusively rely on grafting. Currently novel materials from natural or synthetic sources used as skin substitutes have the potential to provide alternative treatments.

Implantation of synthetic materials into contaminated fields has lead to high rates of infection (Alaedeen *et al.*, 2007; Gaertner *et al.*, 2007). Biologic meshes seem to be a better alternative; the possible benefits of biomaterials include more appropriate host tissue ingrowth, vascularisation and infection tolerance/resistance. If a patient shows clinical signs of mesh infection, the surgeon is often required to remove the mesh, resulting in added procedures and potential morbidity for the patient (Albo *et al.*, 2006; Carbonell *et al.*, 2005). The ability of a biomaterial to resist or tolerate infection is of extreme clinical significance. The performance of a biological mesh in an infected field depends on the level of bacterial attachment, the composition and durability of the biomaterial and the interaction with the host's tissue and local responses.

A variety of modern wound dressings have been developed that claim to restore the bacterial burden to an acceptable level promoting healing (Bergin and Wraight, 2007). Permacol® surgical implant has been used in the treatment of infected diabetic leg ulcers (data not published) but hitherto Permacol® performance in the presence of specific bacterial overload has not been tested.

Studies in poly-microbial chronic infections suggest that the specificity of micro-organisms is more important than bacterial bioburden. Based on this assumption, Permacol® surgical implants were cultured, in the present experiment, with each of the following clinically relevant pathogens individually: methicillin-sensitive *Staphylococcus aureus, Pseudomonas aeruginosa, Escherichia coli* and *Candida albicans*. Some authors support the idea that rather than the presence of a particular bacterium, it is the number of different bacterial species that correlates positively with delay of healing (Bowler *et al.*, 2001; Edwards and Harding, 2004; Hill *et al.*, 2003); therefore, Permacol® was also incubated with a poly-microbial culture containing the

4 micro-organisms mentioned above, thus presenting a worse case scenario and potentially greatest challenge.

4.3.2 Hypothesis

Permacol® surgical implant will perform well, and maintain their structure and composition, in the presence of micro-organisms commonly present in infected chronic wounds.

4.3.3 Aims and Objectives

- To assess Permacol® surgical implant performance when cultured with chronic wound pathogens, with regard to collagen degradation, cellular penetration and matrix remodelling.
- Analyse Permacol® surgical implant for bactericidal or bacteriostatic properties.

4.3.4 Materials

Hycolin was purchased from Solmedia Ltd. (Colchester Rd, Romford RM3 0AQ, U.K.). Nutrient broth medium, purified water, 90 mm ∅ CAB (Columbia Agar with horse Blood) plates, 90 mm ∅ SDAC (Sabouraud Dextrose Agar with Chloramphenicol) plates and 90 mm ∅ CLED (Cysteine Lactose Electrolyte Deficient) plates were purchased from OXOID (Oxoid Limited, Wade Road, Hampshire, RG24 8PW, U.K.).

All micro-organisms used were obtained as reference bacterial culture purchased from the National Collection of Type Cultures (NCTC) (Colindale Avenue, London NW9 5EQ, U.K.): *Staphylococcus aureus* (NCTC #6571), *Pseudomonas aeruginosa*

(NCTC #10662), *Escherichia coli* (NCTC #10418) and *Candida albicans* (NCTC #3179).

4.3.5 Methods

This study was performed in the laboratories of the Department of Microbiology of Northwick Park Hospital.
Experiments were carried out with one micro-organism (m.o.) at each time, for the individual culture experiments and on different days to avoid cross-contamination.
Before each experiment all surfaces and instruments were disinfected with a 2% solution of Hycolin, a phenolic disinfectant.

Permacol® was cultured with each of the following micro-organisms separately *Staphylococcus aureus, Pseudomonas aeruginosa, Escherichia coli* and *Candida albicans* as well as in a poly-microbial culture containing all 4 micro-organisms.

A confluent growth suspension was obtained for each m.o. in an overnight culture. In summary, an inoculating loop was held inside a flame for a few seconds to bring it to redness and then cooled (flame sterilization technique by a Bunsen burner); once cooled, the loop was used to isolate a colony-forming unit (CFU) of the required m.o. from an agar plate (plates were previously prepared by the Department of Microbiology staff upon reception of the NCTC strains). The CFU was inoculated into 10mL of nutrient broth medium and this suspension was left to grow overnight at 37°C with 100% air in a LEEC incubator (LEEC Ltd. Colwick Industrial Estate, Nottingham NG4 2AJ, U.K.). *Candida albicans* has a slower growth rate, compared to the other tested micro-organisms and consequently, was incubated for 36 hours.
On the following day the micro-organism growth (test suspension) was determined by measurement of the optical density (OD). Nutrient broth medium was used as blank. A spectrophotometer (CECIL CE1011, 1000 series) was used at a wavelength of 500nm to quantify the amount of turbidity of the culture. The amount of light scattered from the solution is proportional to the cell number, the instrument measures the light that it is not scattered by the sample – the optical density of the sample.

A sensitivity test was performed according to the British Society for Antimicrobial Chemotherapy (BSAC). It was necessary to standardize the method used since the density of the inoculum is an important factor determining the inhibition of microbial growth. Therefore, the standardised BSAC method requires the use of a consistent density of inoculum. A semi-confluent growth was chosen because an incorrect inoculum is easily detected by eye.

The OD of the test suspension was measured followed by dilution to an appropriate density (Table 4.2).

Table 4.2 – The inoculum was diluted by transferring the appropriate volume of the test suspension (μL) to 5mL of sterile distilled water (SDW), within 15min of measuring the optical density.

Optical Density	**Coliform Enterococci Staphylococci *Moraxella spp.***	***Pseudomonas spp.***	***Haemophilus spp.* Haemolytic streptococci *Strep. pneumoniae***
0.01 – 0.05	250*	125	Neat
0.06 – 0.15	125	80	250
0.16 – 0.35	40	20	125
0.36 – 0.60	20	10	80
0.60 – 1.00	10	10 (in 10mL SDW)	40

*This dilution was also chosen for *Candida albicans*.

After performing the appropriate dilution the new test suspension was mixed and left at room temperature for a few minutes. In the meantime, 5 sterile flasks were prepared by the flame sterilisation technique with 5 pieces of Permacol® (1 x 1 x 0.15cm) in each flask and 10mL of nutrient broth medium. Four of the flasks were inoculated with 125μL of the new test suspension (T_1 to T_4) and the other flask was kept as negative control. Positive controls were obtained by culturing 125μL of the new test suspension of the relative m.o. in 10mL of nutrient broth medium. Positive controls were made in triplicate (C^+_1 to C^+_3) (Figure 4.29).

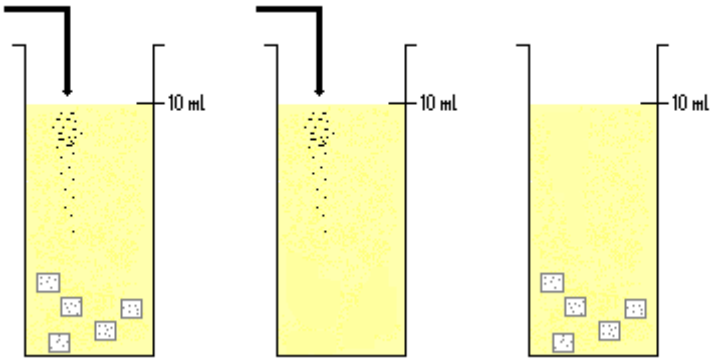

Figure 4.29 – Schematic design of each experiment. The left picture represents the test flasks with 5 pieces of Permacol® and the m.o. inoculum, in the centre the positive control with m.o. only and the picture at the right shows the negative control without m.o. and with Permacol®.

All flasks were incubated at 37°C with 100% air. At 1, 2, 4, 6 and 8 hours one piece of Permacol® from each flask was removed and fixed in 10% NBF for histological analysis, H&E and picro sirius red stains were performed. To count the number of CFU present on the piece of Permacol® at each time point a sample of each microbial suspension was used according to the Miles and Misra technique. Serial dilutions were prepared and agar plates divided into numbered sections.

CAB plates contain a multiple-purpose medium suitable for the cultivation of fastidious organisms and as such were used to culture *Staphylococcus aureus*, a β–hemolytic gram-positive coccus, and *Pseudomonas aeruginosa* a gram-negative pathogen. CLED medium is recommended for diagnosis of urinary bacteriology and gives clear colonial differentiation of all urinary pathogens; therefore, CLED plates were used for *Escherichia coli* growth, a facultative anaerobic gram-negative bacterium which can be found in urinary tract infections. SDAC plates were chosen to grow *Candida albicans* since this is a medium used for isolation of fungi and yeasts. When Permacol® was incubated with the poly-microbial culture CAB plates were used for CFU growth.

The inoculum used from each dilution in the respective section of the plate was exactly 20μL. After inoculation, plates were allowed to dry and were incubated for 18 hours at 37°C with 100% air. Sections where more than 20CFU were present without any confluence were utilised to make the viable counts. Viable counts per m.o. per

time point were obtained by taking the average of counts for the same dilution in the test (T_1 to T_4) and control (C^+_1 to C^+_3) flasks.

The number of CFU per mL of medium was calculated through the following equation:

$$CFU / mL = \frac{number\ CFU\ counted \times dilution\ factor}{20\ \mu L} \times 10^3\ \frac{\mu L}{mL}$$

Growth curves were obtained for each m.o to determine which growth phase was taking place at the time of Permacol® inoculation. Fresh medium was inoculated with a CFU and the population growth was monitored over 24 hours. It was important to ensure that the inoculum used in the sensitivity test contained micro-organisms that were dividing regularly and were at the beginning or halfway through the exponential phase. This guaranteed that Permacol® was cultured with micro-organisms that were growing exponentially.

During each experiment an extra plate was used to inoculate the medium from the negative control (Permacol® only). This plate was divided in 5 sections (1, 2, 4, 6 and 8 hours) and 20 μL of the medium was inoculated at each time point.

4.3.6 Statistical Analysis

Bacterial counts were normalized using a $\log_{10}$ transformation. Data are expressed as mean ± standard deviation (SD). A two-tail paired t-test was used to compare each test to the respective control; a $P<0.05$ was taken as statistically significant.

4.3.7 Results

Permacol® had no significant influence on the growth of any of the micro-organisms assessed. A two-tail t-test was employed to compare the test sample at a given time point to the control sample at the same time point (two paired groups). This test calculates the difference between each set of pairs and if pairing is effective both

measurements should vary together. There was no significant difference in bacterial growths when cultured in the presence of Permacol® or when the m.o. was cultured by itself, pairing was significantly effective for the 4 groups analysed.

Figure 4.30 to Figure 4.33 show the microbial growth for each m.o. tested. Average values were used per time point and standard deviations calculated.

When a poly-microbial culture was used it was not possible to count the CFU since clear colonial differentiation was not obtained, colonies from the different organisms grew co-localised with each other (Figure 4.34).

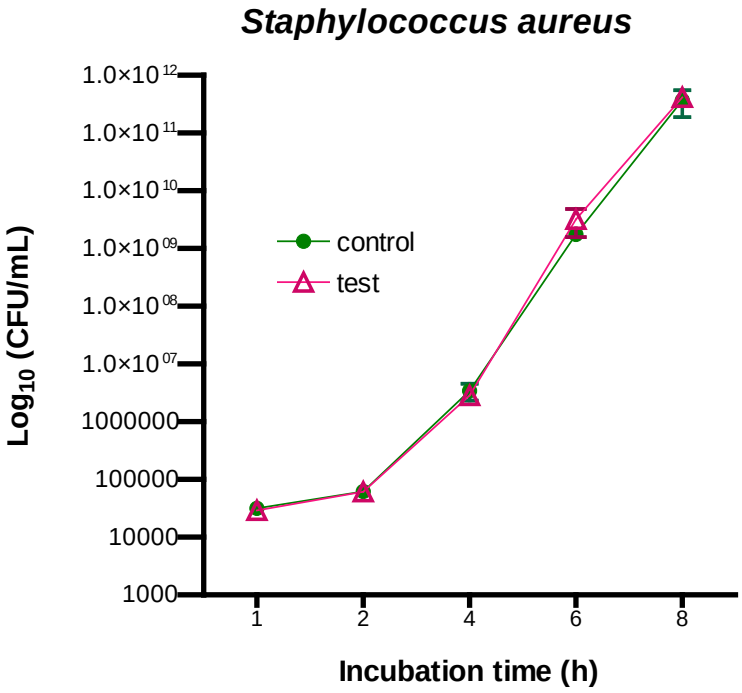

Figure 4.30 – Growth of *Staphylococcus aureus* when cultured with and without Permacol® for a period of 8 hours.

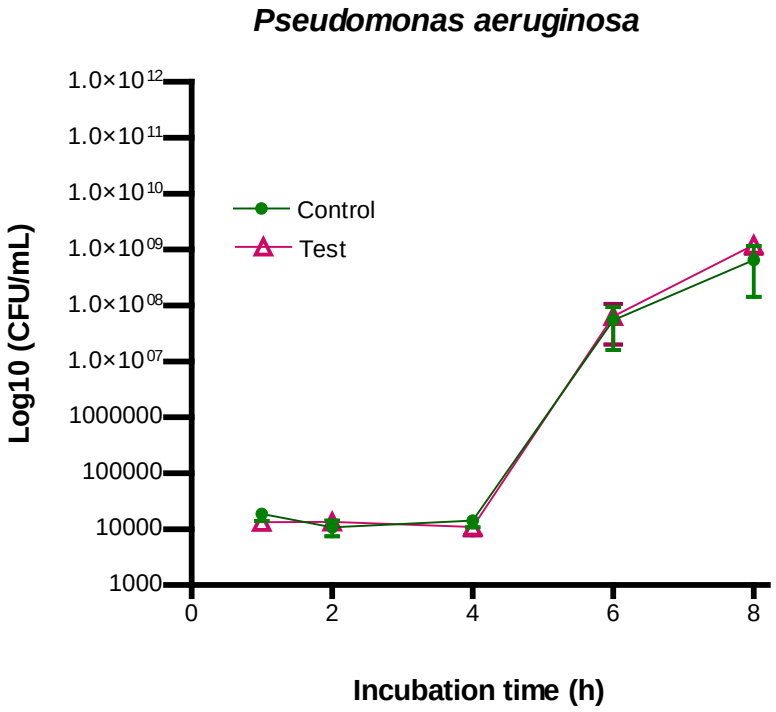

Figure 4.31 – Growth of *Pseudomonas aeruginosa* when cultured with and without Permacol® for a period of 8 hours.

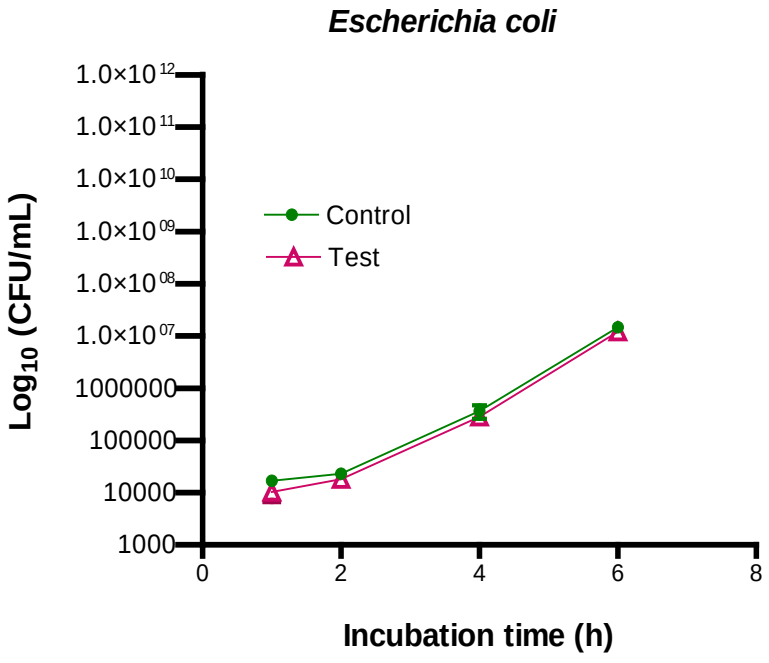

Figure 4.32 – Growth of *Escherichia coli* when cultured with and without Permacol® for a period of 8 hours.

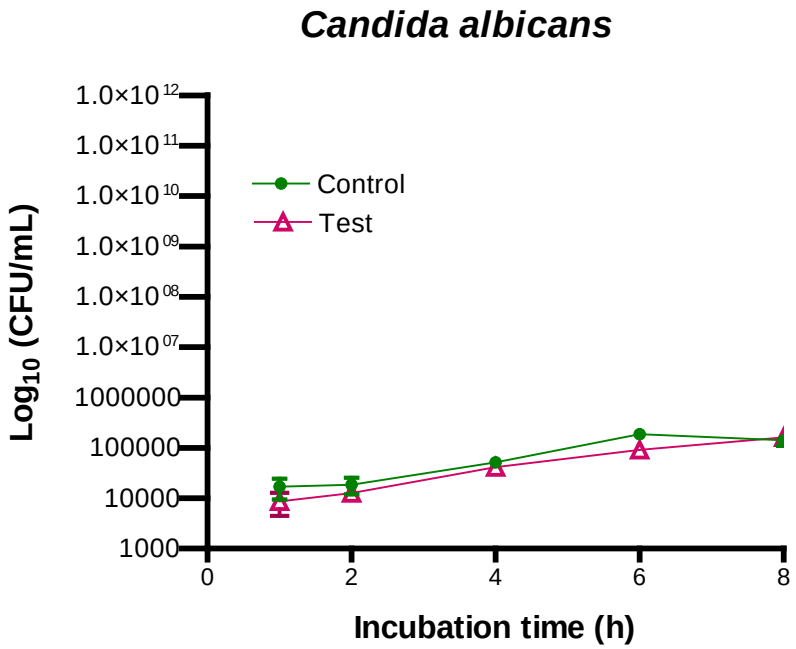

Figure 4.33 – Growth of *Candida albicans* when cultured with and without Permacol® for a period of 8 hours.

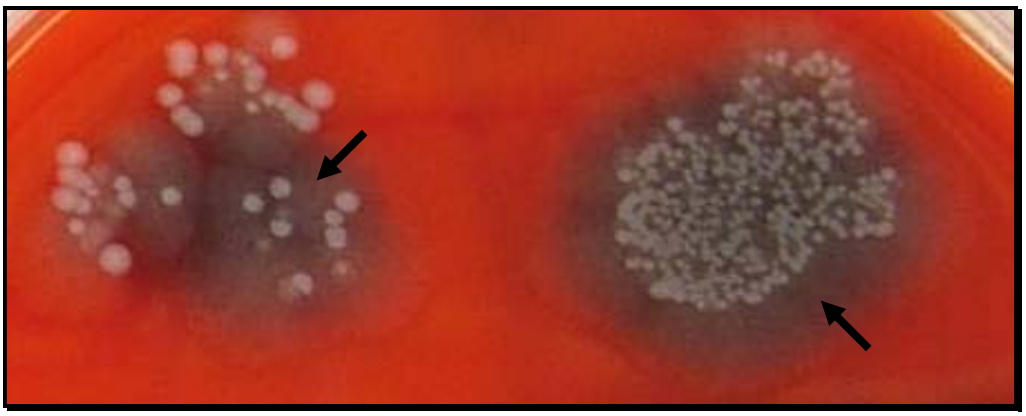

Figure 4.34 – CAB plate cultured with the poly-microbial suspension. *Pseudomonas aeruginosa* colonies (arrows) are visible underneath the other species colonies.

The histological analysis revealed similar results to those obtained previously with the skin explant study (section 4.2). Micro-organisms were visible on the surface of the collagen matrix at increasing concentrations during the incubation time.

Staphylococcus aureus reached the highest concentrations at all time points, but bacteria were mainly at the edges of the implant (Figure 4.35) and cellular penetration was marginal reaching on average only 5% of the depth of the matrix (Figure 4.36).

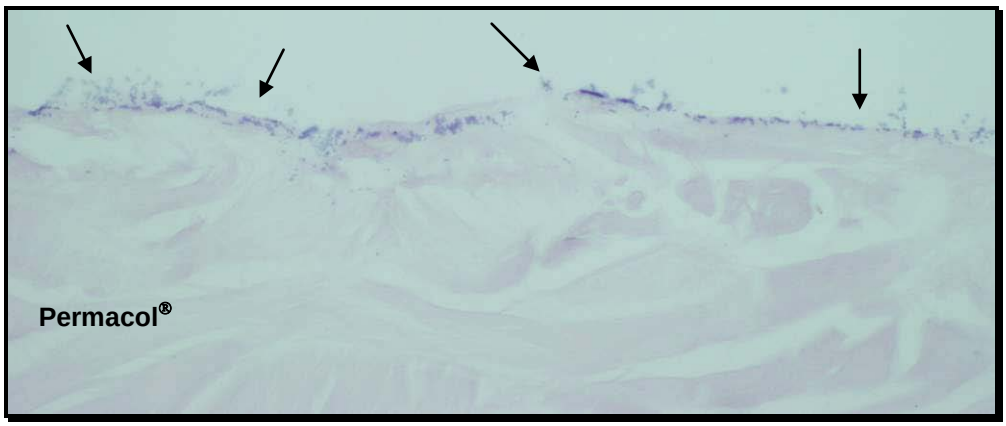

Figure 4.35 – *Staphylococcus aureus* (arrows) at the edges of the collagen matrix after 8 hours incubation (H&E, 400X).

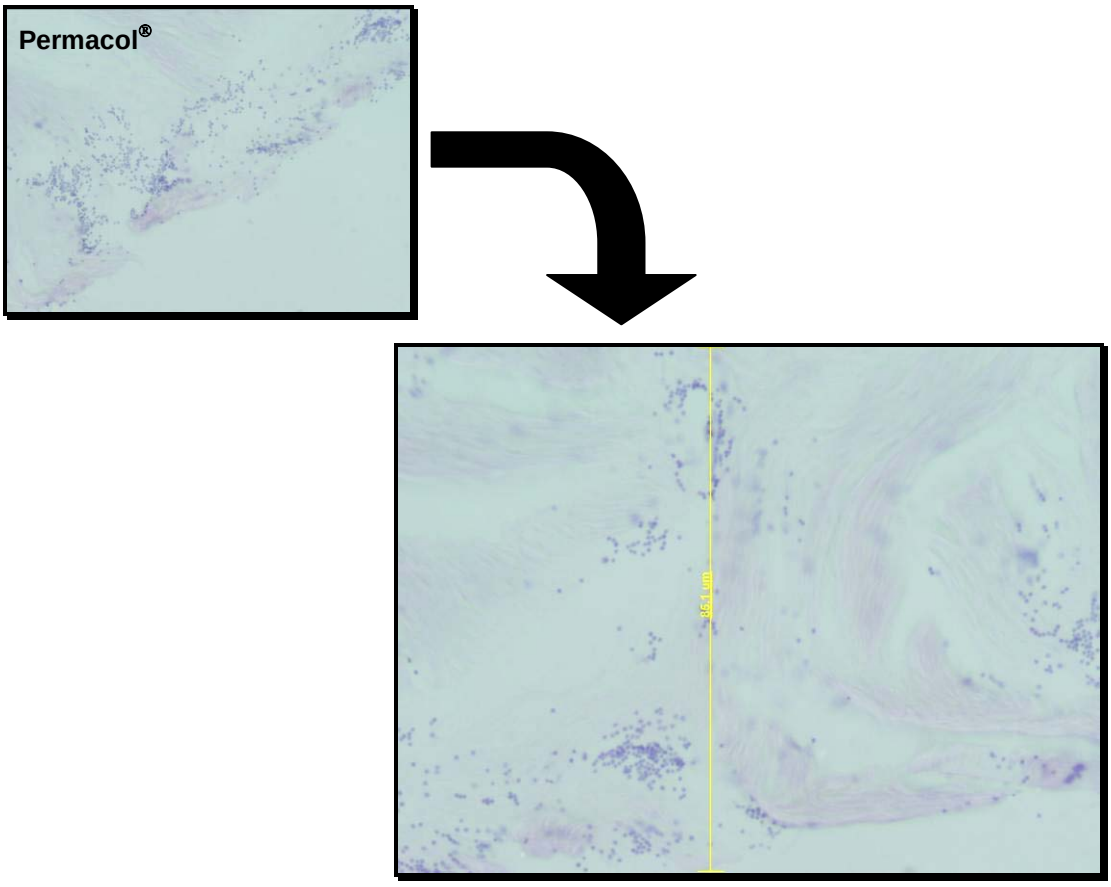

Figure 4.36 – *Staphylococcus aureus* infiltrating the collagen matrix 8 hours post inoculation. Bacteria penetration reached a maximum of 85.1μm; this represents 5% of Permacol® cellular penetration (H&E, 1000X).

Pseudomonas aeruginosa and *Escherichia coli* did not penetrate the collagen matrix and were observed mainly in clusters at the surface of Permacol® (Figure 4.37 and Figure 4.38 respectively).

Figure 4.37 – *Pseudomonas aeruginosa* (arrows) at the edges of Permacol®, 8 hours post inoculation. Dash line outlining Permacol® edge (H&E, 1000X).

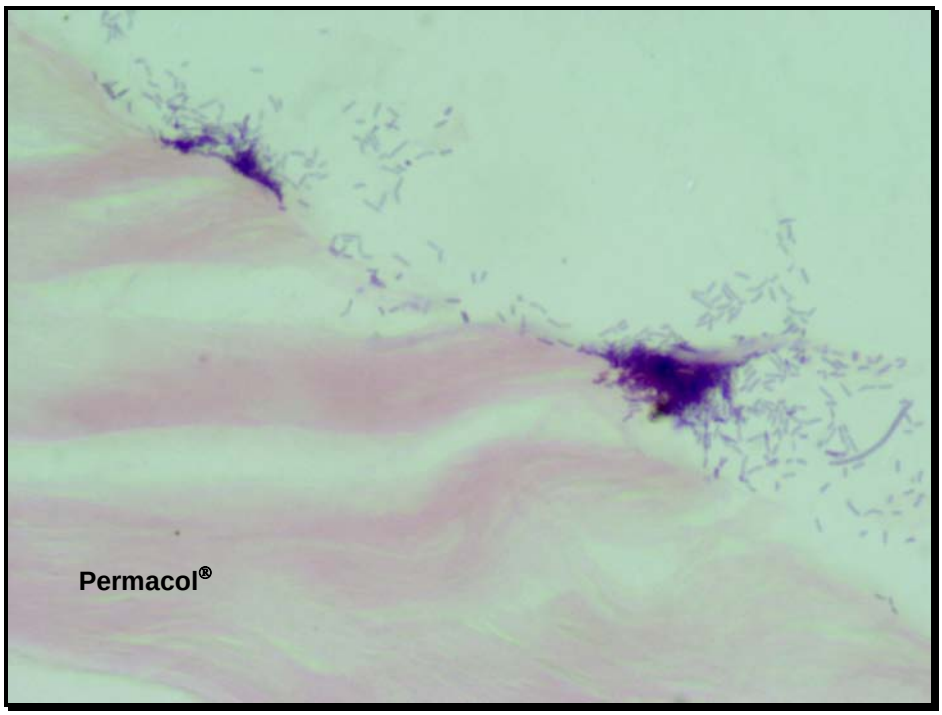

Figure 4.38 – High density of *Escherichia coli* at the surface of Permacol®, 8 hours post inoculation (H&E, 1000X).

Candida albicans did penetrate Permacol®, even at low concentrations, although penetration levels were minimal (Figure 4.39).

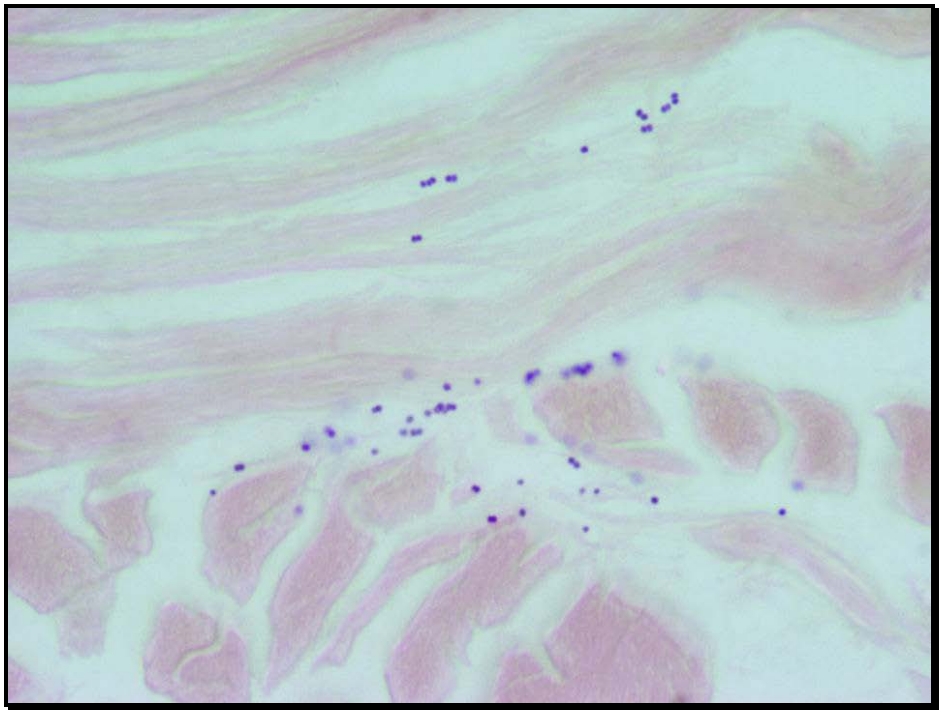

Figure 4.39 – *Candida albicans* within the collagen fibres of Permacol®, 8 hours post inoculation (H&E, 1000X).

When the 4 micro-organisms were inoculated together growth was not inhibited and the micro-organisms coexisted easily. After 8 hours of incubation in the poly-microbial suspension Permacol® surface was extensively covered with micro-organisms but microbial penetration was still marginal (Figure 4.40).

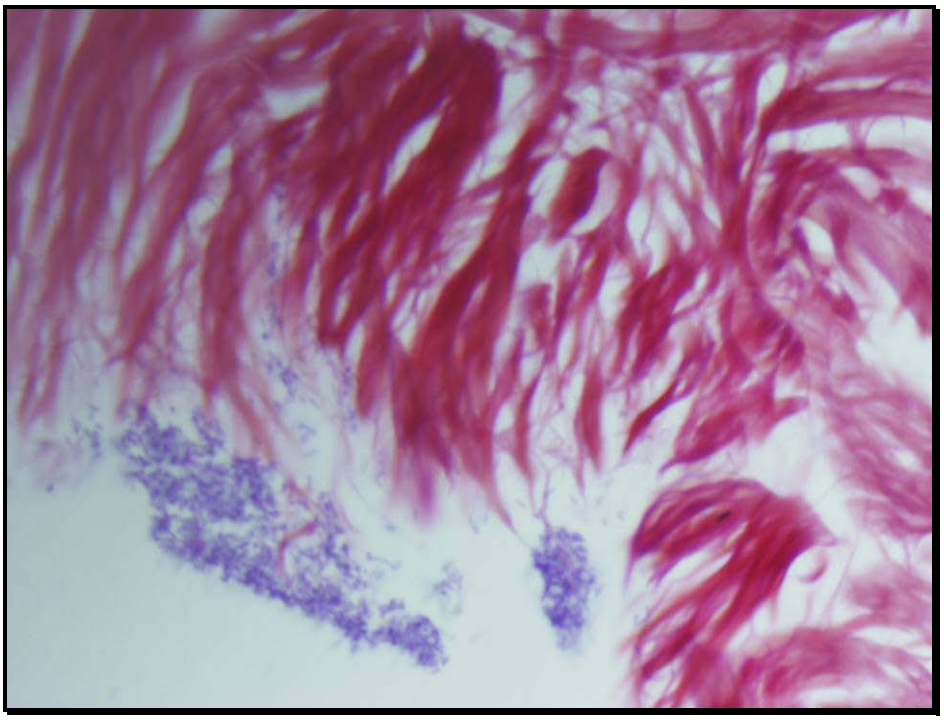

Figure 4.40– Permacol® 8 hours post inoculation with the poly-microbial culture. Microbial penetration is marginal (picro sirius red, 1000X).

Independent of the level of microbial penetration, collagen was not degraded at any time throughout this experiment (Figure 4.41). Collagen was highly birefringent, an indication of good quality, non-degraded, collagen.
There was no CFU growth in the negative control plates.

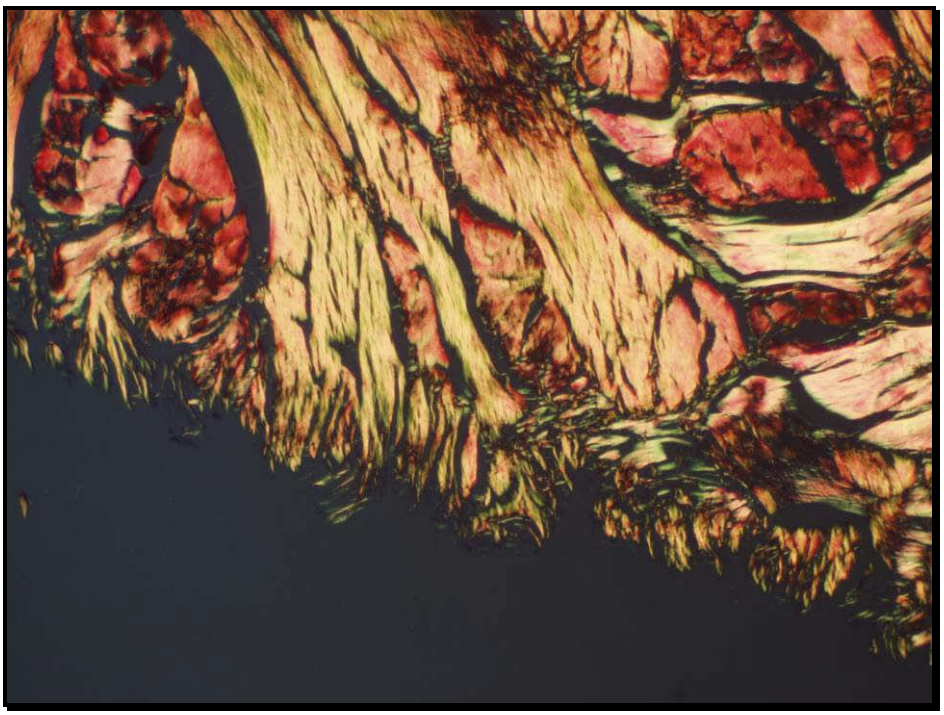

Figure 4.41– Permacol® after 8 hours incubation with the 4 micro-organisms tested. There was no collagen degradation or matrix remodelling (picro sirius red, 400X).

4.3.8 Discussion

A number of putative human pathogenic micro-organisms, including *Pseudomonas aeruginosa*, *Staphylococcus aureus*, *Candida albicans* and *Escherichia coli*, have been reported to produce enzymes which can degrade collagen, (Harrington, 1996; Pichova *et al.*, 2001; Waldvogel and Swartz, 1969). Therefore, collagen derived biomaterials should be tested against potential pathogens before being surgically used in an infected field.

Staphylococcus aureus and *Escherichia coli* individually had an exponential growth throughout the experiments. *Pseudomonas aeruginosa* took 4 hours to acclimatise to the new culture conditions but after adaptation there was an exponential growth. *Candida albicans* showed a slower growth rate compared to the other micro-organisms; nevertheless, its cellular density consistently increased.

The negative control plates were used to guarantee that: *i)* each batch of medium used was sterile; *ii)* nutrient broth medium did not degrade or change the configuration of Permacol® surgical implant; *iii)* Permacol® surgical implant was sterile and *iv)* the technique used for removal of each piece of Permacol® surgical implant, at each time point, was not promoting cross-contamination. Since all negative control plates were clean after 8 hours of incubation it is reasonable to assume that none of the variables mentioned above influenced the results.
The Miles and Misra technique was chosen in preference to OD measurements in order to calculate the viable CFU and test Permacol® for bactericidal or bacteriostatic effects. Bactericidal refers to a substance (or a condition) capable of killing bacteria while a bacteriostatic agent will only inhibit the growth of bacteria and not necessarily kill them.

There was no significant difference in the growth rates of any of the micro-organisms when cultured alone or with Permacol® surgical implant. Permacol® did not show a bactericidal or bacteriostatic effect and microbial growth was not influenced by its presence.
Permacol® structure and microbial presence were established by H&E staining. Permacol® morphology was unaffected by the microbial load during the experiments. Furthermore, the major constituent of Permacol® – collagen – was tested for degradation by picro sirius red staining and showed highly birefringent collagen, which is an indication of good quality, non degraded collagen. Therefore, none of the organisms tested here alone or in combination were capable of degrading or denaturing the Permacol® matrix under the test conditions used.

The results from this study show that the micro-organisms as tested here do not have enough collagenolytic action to degrade Permacol® surgical implant. There are two possible explanations for these results: the strains tested do not produce collagenases or they do produce collagenases but the cross-link of Permacol® protects it from microbial digestion (from the particular strains tested).
Other bacterial models could be designed to confirm the potential resistance of Permacol® to microbial proteases, for example, normal porcine collagen could be used, in a similar study, to analyse whether the cross-linking process is accountable

for the observed Permacol® resistance to bacterial collagenolysis. It was decided not to proceed with this line of research, since, from a clinical point of view, it is not feasible to isolate and identify all strains of microbes present in a wound. That would be extremely time-consuming and laborious, factors that would hinder a clinician when dealing with infected, non-healing wounds. Moreover, infected wounds can have a diverse microflora, making it difficult to predict each pathogen. Therefore, for any constructs or matrix to be used in the treatment of such wound, it is essential to have a biomaterial that can tolerate the presence of bacteria and that will not be easily degraded or contribute, as a nutritious matrix, to bacterial spread and increased density.

4.3.9 Conclusion

In the *in vitro* study presented here, Permacol® surgical implant showed tolerance to the presence of *Pseudomonas aeruginosa, Staphylococcus aureus, Candida albicans* and *Escherichia coli* and was not degraded by any of the extracellular proteases of these micro-organisms. In addition, Permacol® surgical implant did not increase the microbes' growth rate.

5.0 BIOCOMPATIBILITY AND PERFORMANCE OF COLLAGEN DERIVED BIOMATERIALS IN A RODENT MODEL

After detailed analysis of biomaterials by physical and biological *in vitro* testing, on occasion the data collected is not sufficient to satisfy all questions and more tests are required to provide further information related to host and material responses and a more complex environment than provided by *in vitro* techniques is required. Although the use of species other than human involves many limitations and concessions, it is the common judgement that such tests, where materials are in direct contact to systemic physiological processes, are a necessary practical and ethical precedent to human clinical testing.

Biomaterials have a history of generally safe and satisfactory use. Regardless of tissue engineering improvement and advance on biomaterials durability, they are not perfect and many have a lifespan of only a few years. Biomaterials related complications continue to occur either soon after implantation or later on; therefore, it is essential to have detailed information on their performance *in vivo* and when possible, human explanted materials (or autopsy) should be carefully examined to evaluate performance of the implanted material. The purpose of biological testing is to provide preliminary data for biomaterials, prior to their use in humans.

Reactions to biomaterials may occasionally differ from animal to animal and from human to human; nevertheless, biomaterials will produce responses *in vivo* which are more or less typical of the materials employed to manufacture them, in the same way treatments used in the manufacture process should also lead to a characteristic response (Braybrook, 1997).

The same biomaterials may produce different outcomes depending on the implantation site; different locations in the body will be subject to diverse mechanical loads and stress, such as those induced by constant body or fluid movements in contrast to sites normally at rest.

Usually the clinical site chosen for initial non-functional testing is soft tissue; this assessment is based on the supposition that cytotoxic effects have a general action and because soft tissues are easy to approach surgically in animals (Black, 2006). Non-

functional tests focus on the direct interaction between the biomaterial and its components and the chemical and biological properties of the surrounding environment. If the biomaterial is intended for use in high load locations and/or if it will have an active function rather than a non-active bulking purpose, then a functional test is needed. Several animal species are used depending on the material to be tested and on the clinical application.

5.1 ASSESSMENT OF THE *IN VIVO* BIOCOMPATIBILITY AND GENERAL PERFORMANCE OF A SILVER COATED – DRESSING IN A RAT MODEL

5.1.1 Introduction

The human body is protected from the external environment by an outer layer of skin and subcutaneous tissue. When skin is wounded due to injuries or disease, a set of complex biochemical events takes place to repair the damage and the body attempts to cover the wound to prevent infection by the growth and migration of epithelial cells. This natural method is slow and depends on the health condition of each individual and explains why infection of the wound can occur. Infected wounds are a major clinical problem and are implicated in delay in rate of wound healing. Wound management by clinicians helps wound healing by the cleansing and removal of dead tissue from the wound and by the application of appropriate local dressings onto the wound to create a moist environment.

Even though topical antimicrobial agents have been utilised in wound care for thousands of years, during the 20th century the discovery and development of antibiotics provided potent antimicrobial agents with high specificity, revolutionising clinical therapy. However, emergence of antibiotic-resistant strains of pathogens has led to the need to find alternative treatments.

Modern wound dressings are constantly being developed to restore infection to an acceptable level and with this promote healing. Silver containing matrices are one such new group of dressings and are available in a variety of forms, all having free silver ions as the active ingredient.

Silver has been used in clinical settings as an antimicrobial for over a century, and silver sulphadiazine (SSD) is still a common antimicrobial used in the treatment of chronic wounds (Klasen, 2000b; Klasen, 2000a). Silver exerts its antimicrobial effects by binding to negatively charged components in proteins and nucleic acids, thereby implementing structural changes in bacterial cell walls, membranes and nucleic acids,

which affects viability (Cooper, 2004; Klasen, 2000b; Klasen, 2000a). Hence, silver ions that bind to the DNA of bacteria and bacterial spores block transcription, and those that bind to cell surface components interfere with the respiratory chain at the cytochrome level; as a result, silver ions reduce the ability of bacteria to replicate (Bergin and Wraight, 2007). Silver can be delivered as metallic, nanocrystalline or ionic form and is effective against a broad range of anaerobic, aerobic, $Gram^-$ and $Gram^+$ bacteria, yeasts, filamentous fungi and viruses.

The results from the *in vitro* assessment of Permacol® surgical implant performance in a contaminated field were promising, showing Permacol® surgical implant tolerance to typical wound pathogens. Conversely, this biomaterial did not exert a bactericidal or bacteriostatic effect and microbial growth was not influenced by its presence. Since Permacol® surgical implant does not seem to have an effect on the pathogens tested or be affected by them, it comes as a prospective dressing to be used in contaminated fields.

TSL plc. are developing a second generation of Permacol® surgical implant that is protected from the effect of bacterial infection in the first ten to fourteen days post-implantation, by treatment with a silver coating. It is important to assess if the silver coating does not detrimentally affect the standard *in vivo* characteristics and biocompatibility of Permacol® surgical implant. Additionally, it is imperative that the dressing sustains release of low concentrations of silver ions over time. Different concentrations of nanocrystaline silver (NPI) coated Permacol® were tested for biocompatibility and *in vivo* characteristics when implanted subcutaneously in a rat model. Non-coated Permacol® surgical implant was also included as control.

5.1.2 Hypotheses

Silver coated-Permacol® and Permacol® surgical implant *in vivo* performances will be comparable, related to host tissue and cellular response when implanted subcutaneously in a rat model.

Silver is not detrimental to Permacol® *in vivo* performance.

5.1.3 Aims and Objectives

- Study silver coated-Permacol® implant biocompatibility and general *in vivo* performance when implanted subcutaneously in a rat model.
- Analyse and compare different concentrations of silver coated-Permacol®.
- Evaluate silver coated-Permacol® as a future asset for implantation in infected areas.

5.1.4 Materials and Methods

The study was performed in compliance with the Good Laboratory Practice Regulations 1999 (S.I. No 3106), as amended by 2004 regulations (SI 994) which are based on the principles of good laboratory practice as adopted by the Organisation for Economic Co-operation and Development, ENV/MC/CHEM (98) 17. They are in conformity with, and implement the requirements of Directives 2004/09/EC and 2004/10/EC.
Various stages of the study, including the protocol, critical animal phases and the final report were audited by the NPIMR Quality Assurance Unit in compliance with facility quality assurance standard operating procedures.

Permacol® surgical implant, nanocrystaline silver coated-Permacol® (0.03% NPI-Permacol® and 0.05% NPI-Permacol®) and 0.05% PVA-Permacol® were supplied by TSL plc. in sterile sealed packages. PVA (polyvinyl acetate) was used as the delivery agent for nanocrystaline silver; therefore, it was added to the experiment as control.

5.1.4.1 Study Design

The rat was chosen as the species for this study because of published and in-house knowledge of dermal pathogeneses in this species. Additionally, the rat is the lowest evolutionary animal in which this work could reasonably be carried out.
Twenty-four male Wistar-Han™ rats were randomly distributed between 4 experimental groups and divided in 2 experimental end-points (Table 5.1).

Table 5.1 – Study groups and time point design.

Test material	2 weeks	4 weeks
0.03% NPI-Permacol®	3 rats	3 rats
0.05% NPI-Permacol®	3 rats	3 rats
0.05% PVA-Permacol®	3 rats	3 rats
Permacol®	3 rats	3 rats

All test materials were cut into 2.5cm x 2.5cm pieces and left in sterile saline solution until implantation. Pieces of all biomaterials were kept and fixed with 10% NBF for histological analysis and to act as controls.

5.1.4.2 Surgical Procedure

Animals were anaesthetised according to the procedure described in Section 2.2.5.
All surgery was done using sterile techniques. The following surgical procedure was followed for all animals:

1. A ventral midline incision was made from just below the level of the rib cage extending approximately 1.5cm distally.
2. Skin was elevated and retracted to create one subcutaneous “pocket” on each side of the midline.
3. Haemostasis was maintained by careful dissection – no electrocautery was used.

4. The collagen matrices were placed one in each pocket, such that each animal received 2 pieces of the same type of test material.
5. The ventral midline incision was closed with interrupted sutures.
6. Once recovered from anaesthetic, animals were returned to the animal accommodation, singly housed.

The day of surgery for each rat was considered as Day 0.

5.1.4.3 Necropsy

Animals were euthanased and a composite of skin, subcutaneous tissue, implant and underlying muscle was harvested en bloc and fixed in 10% NBF for routine histology.

5.1.5 Statistical Analysis

Because of the low number of samples per group (N=3) a non-parametric test would have little power, therefore, a one-way analysis of variance (ANOVA) was chosen to compare statistically significant mean differences between all groups, followed by a Bonferroni post test to compare pairs of group means. Statistical analysis was performed using SPSS Statistics 16.0 (SPSS Inc., Chicago, USA). Graphical representation of data was performed using Graphpad Prism statistics software, version 4 (GraphPad Software, Inc., USA).

5.1.6 Results

Non implanted matrices were histologically analysed to check for structural differences among them and to be kept as controls for comparison of matrices before and after implantation. All collagen materials tested showed the same structural matrix, the only difference being a brown granular coat (silver coating) in the NPI-

coated samples, 0.05% NPI-Permacol® presented a thicker and darker layer of coating material (Figure 5.1 and Figure 5.2).

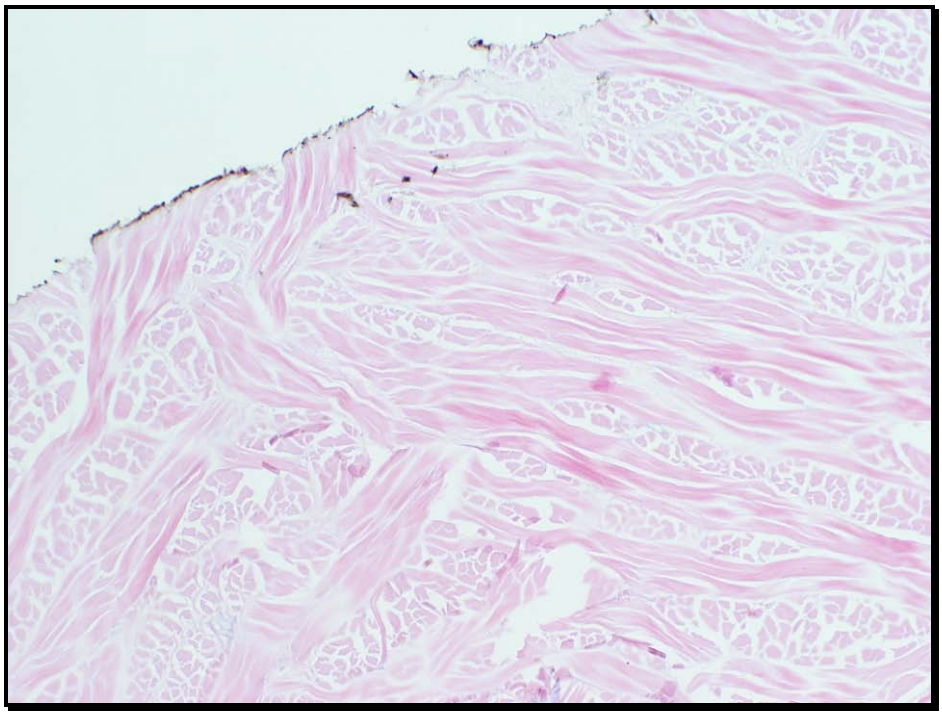

Figure 5.1 – 0.03% NPI-Permacol® matrix before implantation (H&E, 100X).

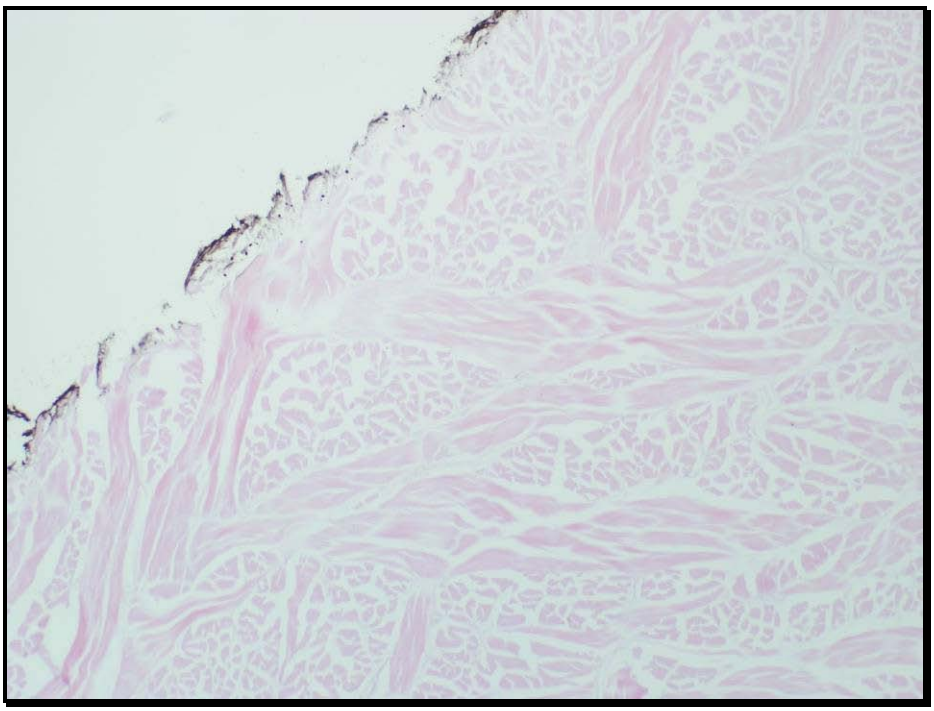

Figure 5.2 – 0.05% NPI-Permacol matrix before implantation (H&E, 100X).

All samples examined comprised 5μm histological sections stained either with haematoxylin and eosin (H&E) or with picro sirius red F3B.

Sections were examined, using a light microscope with polarising ability, for the following features: acute inflammation, chronic inflammation, seroma, cellular density, integration with surrounding tissue, cellular penetration, macrophages and giant cell presence.

Semi-quantitative analysis included quantification of inflammatory cells, neo-vascularisation and cellular density (fibroblasts). A minimal of seven fields per slide were counted at an objective magnification of forty times. Fields were randomly selected within the collagen implant itself and at the interface between the implant and surrounding host tissue. The extent of cellular penetration was quantified (in percentage of the depth of the entire test sample) by measuring minimal and maximal cell penetration per implant thickness (in the same area). A minimum of six randomly selected fields per slide were measured with DPController software (Olympus Optical Co., Ltd.), at an objective magnification of ten times. For descriptive purposes, a semi-quantitative histological scoring criterion was generated (Table 5.2).

Table 5.2 – Scoring criteria used for the semi-quantitative histological analysis, units are described per field view.

Level → / Criterion ↓	Absent	Marginal	Minimal	Moderate	Complete/ Severe
	0	1	2	3	4
Cellular density	No cells	[1 – 30] cells	[31 – 60] cells	[61 – 90] cells	More than 90 cells
Cellular penetration	No cells	1% – 25% penetration	26% – 50% penetration	51% - 75% penetration	More than 75% penetration
Neo-vascularisation	No vessels	[1 – 5] vessels	[6 – 10] vessels	[11 – 15] vessels	More than 15 vessels
Macrophages and giant cells	No cells	[1 – 2] cells	[3-4] cells	[4 – 5] cells	More than 5 cells

Tissue integration was scored with regard to the amount of actual tissue micro-interdigitation (fibroblasts, fibrin, collagen) seen between the edges of the implant and the immediately adjacent host tissue.

In the text the term mild is used and this is a classification between minimal and moderate.

There was no evidence of extrusion of the implants or implant migration within the implantation site, despite the absence of any anchoring suture.

The control implants (Permacol®) after 14 days of implantation showed marginal acute inflammatory response and marginal macrophage-rich chronic response at the edges of the implants. There was evidence of cell penetration into the implants in some areas, but the majority of the implant was cell free (Figure 5.3). One of the animals had a sub-clinical seroma. Integration with the surrounding tissue was good for this time with the fibroblastic layer emanating from the host tissue integrated with the edge of the Permacol®. Cellular density and cellular penetration were poor, except in natural pores. At the edges of the implants a few fully formed vessels were visible. There was no adverse reactivity in any of the host tissues adjacent to the implant.

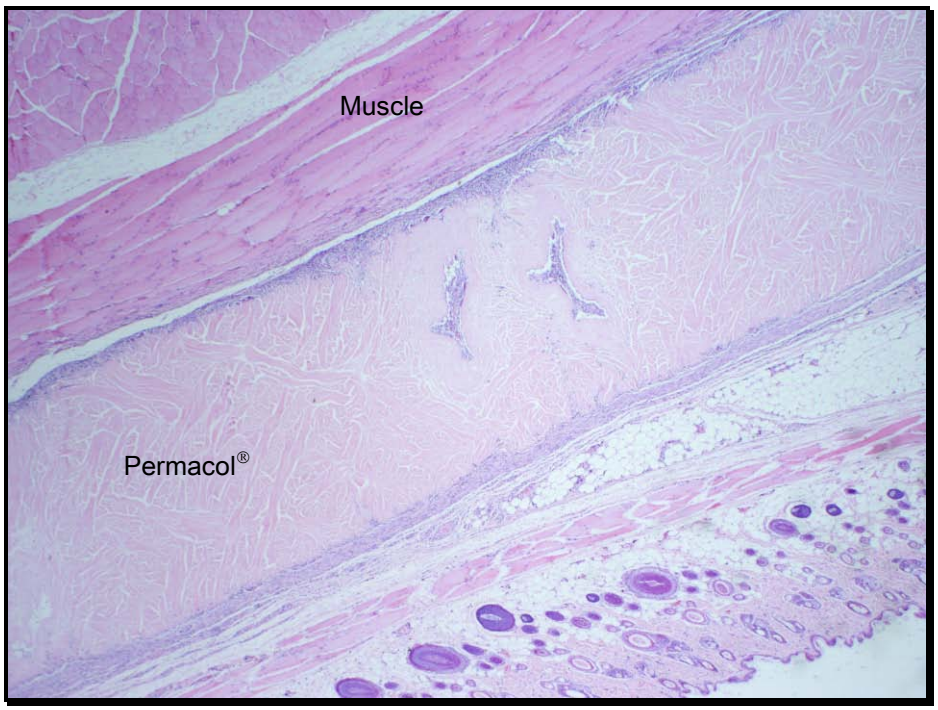

Figure 5.3 – Permacol® implant between panniculus layer of the skin and the underlying rectus abdominus muscle layer, two weeks post implantation (H&E, 20X).

0.05% PVA-Permacol® implants at 14 days showed marginal acute inflammatory response around the implant and a low cellular penetration, except in pores. Integration was marginal with the surrounding tissue and the cellular density was slightly higher than in the Permacol® implants. Neo-vascularisation was present within the edges of the implant (Figure 5.4).

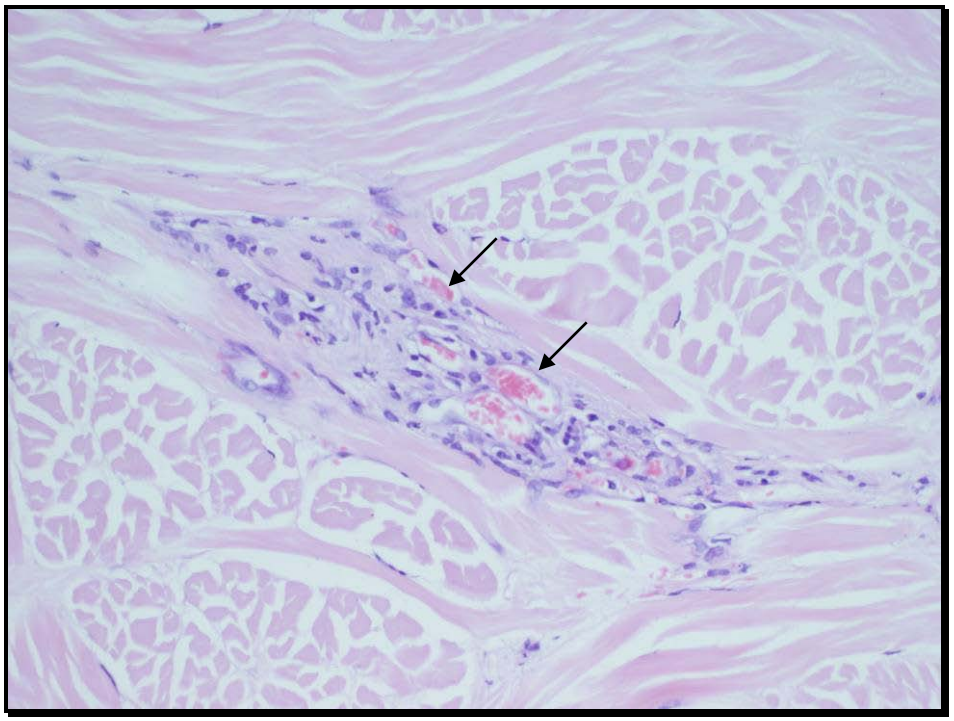

Figure 5.4 – 0.05% PVA-Permacol® implant with fully formed vessels (arrows) after 14 days of implantation (H&E, 100X).

Fourteen days post implantation integration with the adjacent tissue was marginal in the 0.03% NPI-Permacol® implants; and there was no reactivity in the host tissue. Cellular penetration was moderate, although cellular density was low; vessel sprouts and fully formed vessels were present (Figure 5.5). High numbers of macrophages were current where silver granules were present, in these areas integration with the surrounding tissue increased. Macrophages were visible ingesting the silver particles (Figure 5.6).

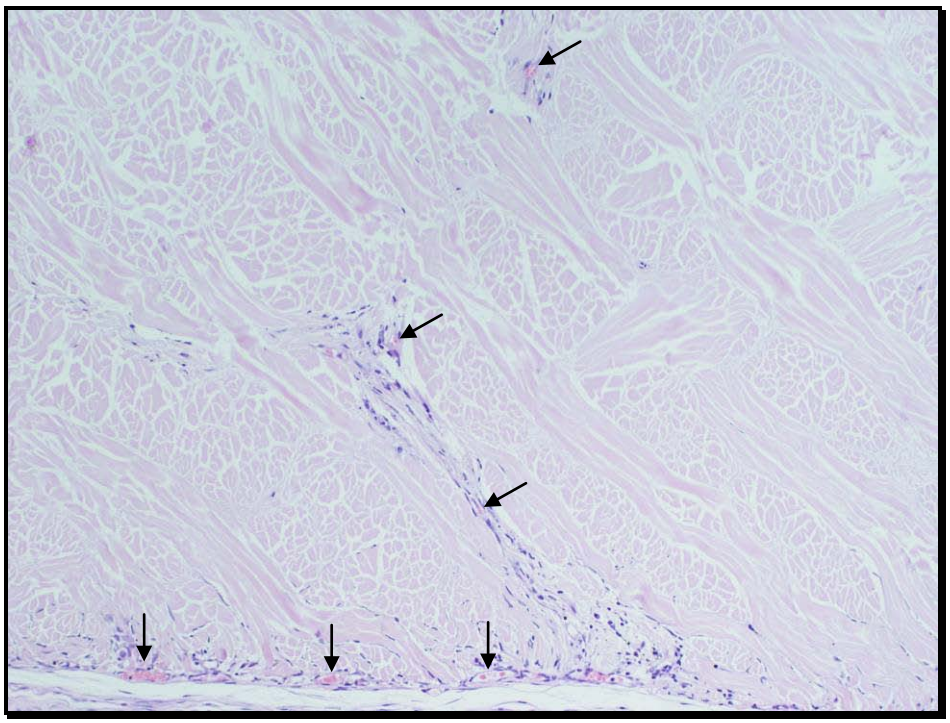

Figure 5.5 – Mild cellular penetration in 0.03% NPI-Permacol® implants after 14 days of implantation, black arrows show fully formed vessels (H&E, 100X).

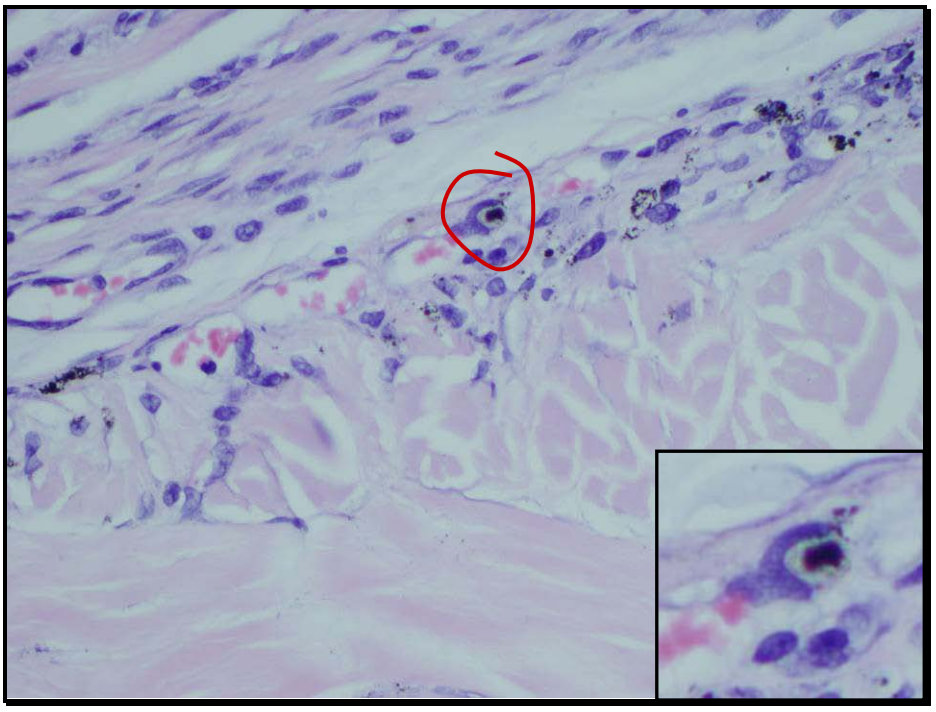

Figure 5.6 – Silver granules at the edge of a 0.03% NPI-Permacol® implant. Macrophages ingesting nanocrystaline particles of silver in detail (H&E, 400X).

One animal from the 0.05% NPI-Permacol®-14 days' group had to be resutured on day 3 of the study and did not recovered from the anaesthesia. The implant and surrounding tissue were removed and processed for histological analysis. On day 3 cells penetrated the implant further than observed in the 14 days implants. Cellular density was mild, especially on the periphery of the implant (Figure 5.7). No vessels were observed.

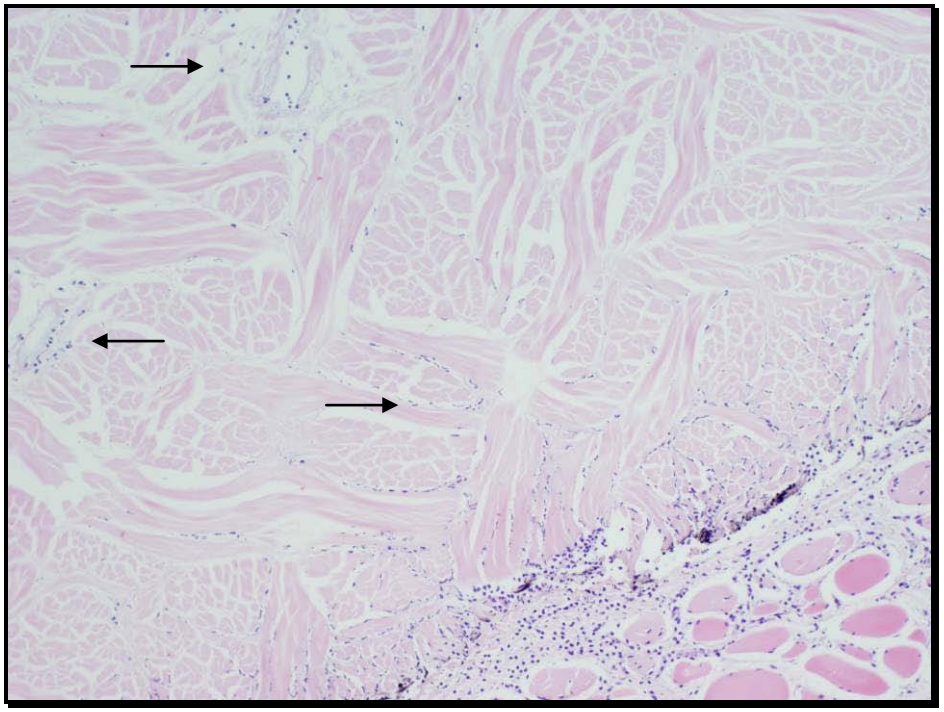

Figure 5.7 – Cells penetrating a 0.05% NPI-Permacol® implant after 3 days of implantation (H&E, 100X).

In this implant silver granules were especially visible and in some zones they seemed to be diffusing to the interior of the matrix (Figure 5.8).

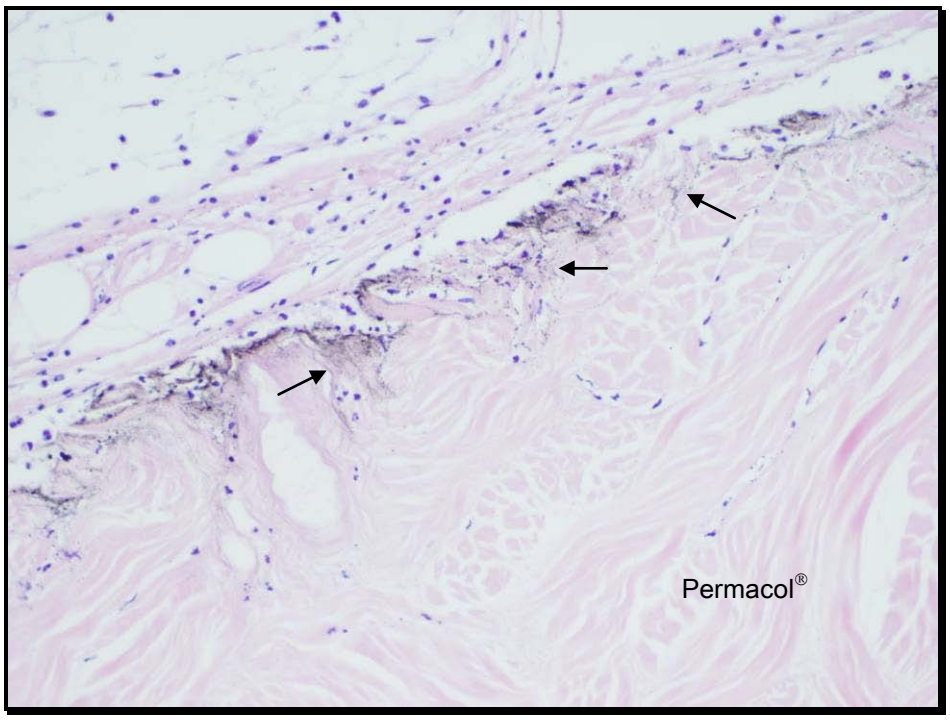

Figure 5.8 – Silver granules (arrows) in the edge of a 0.05% NPI-Permacol® implant after 3 days of implantation (H&E, 200X).

Both remaining animals implanted with 0.05% NPI-Permacol® showed poor cellular penetration and low cellular density 14 days post implantation (Figure 5.9). Integration with the surrounding tissue was good. Natural pores were well populated with cells and showed mature vessels. One of the implants showed a marginal acute inflammatory response. Both implants presented vessel sprouts and formed vessels in their margins.

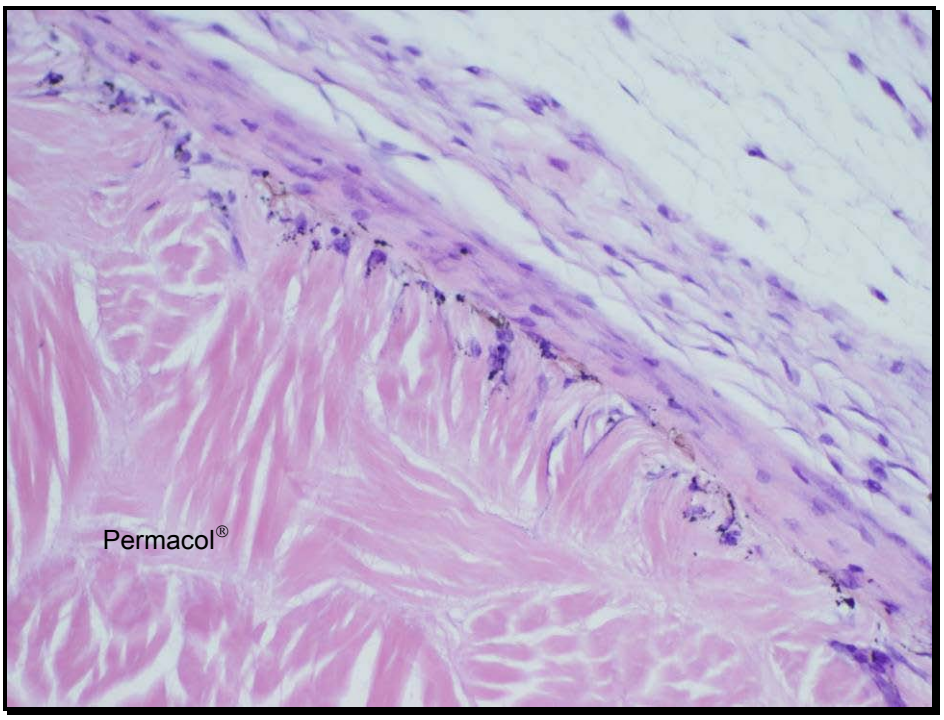

Figure 5.9 – Poor cellular penetration in a 14 day 0.05% NPI-Permacol® implant (H&E, 200X).

Figure 5.10 and Figure 5.11 show comparison, for each of the parameters assessed, between Permacol®, 0.05% PVA-Permacol®, 0.03% NPI-Permacol® and 0.05% NPI-Permacol® implants at 14 days post implantation. Minimal and maximal values of cellular penetration were used to create the graph. Mean and standard deviations were calculated.

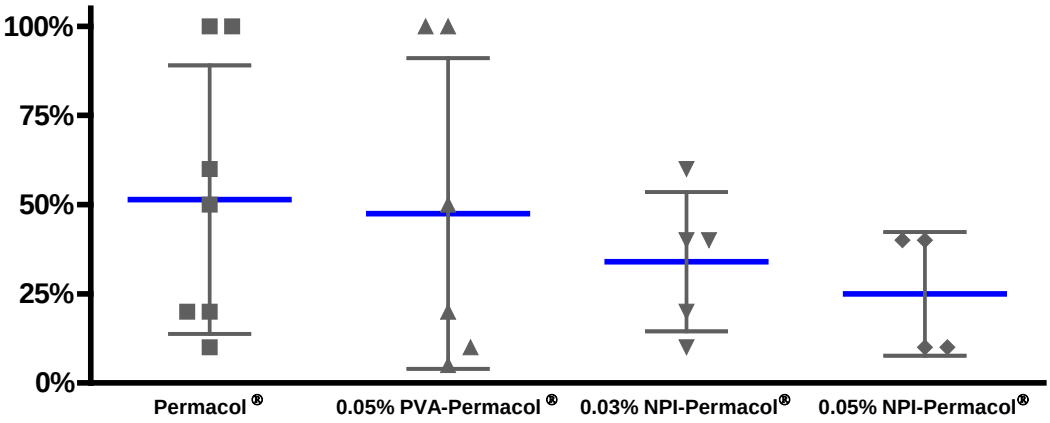

Figure 5.10 – Cellular penetration levels 14 days post implantation. Mean values, for both minimal and maximal levels of cellular penetration, were used per animal.

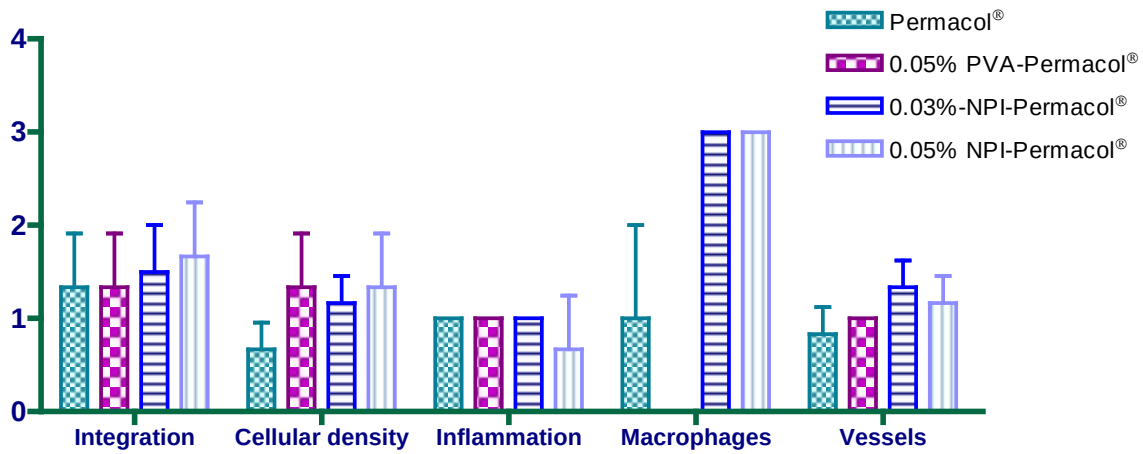

Figure 5.11 – Schematic representation of parameters analysed at 14 days post implantation, according to the scoring criteria described in Table 5.2.

The parameters analysed showed no significant difference between all groups and between pairs of groups.

Integration with surrounding tissue increased in Permacol® implants at 28 days post implantation. Cellular penetration was 100% through the natural fissures of the material, but much lower in the remaining implant. Cellular density was mild (Figure 5.12) and many vessel sprouts and formed vessels were visible in the edges of the implants. One Permacol® implant showed marginal acute and chronic inflammatory response and a few giant cells were present (Figure 5.13).

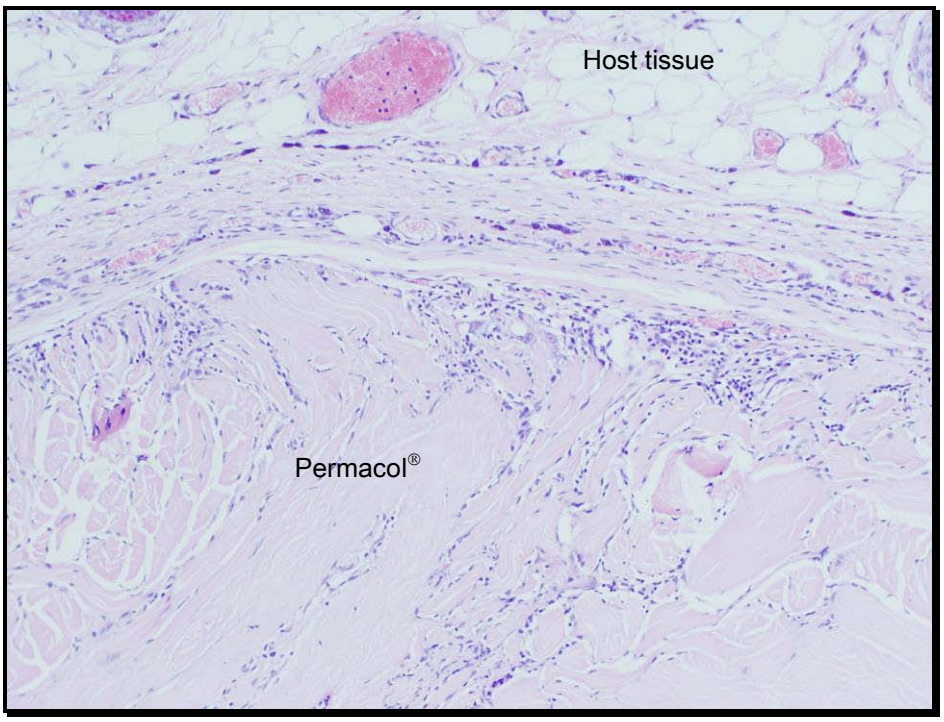

Figure 5.12 – Permacol® implant after 28 days of implantation (H&E, 100X).

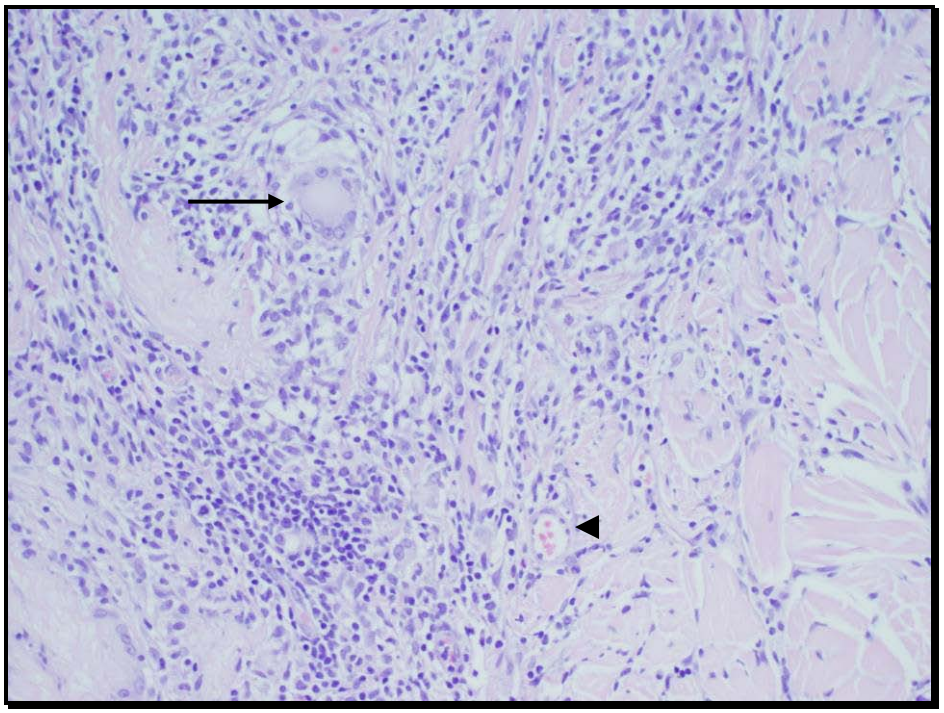

Figure 5.13 – Giant cell (arrow) and mature vessel (arrow head) in a Permacol® implant after 28 days of implantation (H&E, 200X).

One animal from the 0.05% PVA-Permacol® group (28 days) was sacrificed one week earlier than protocol due to continuous chewing of the abdominal zone. Since the implant was exposed several times, some parts of it were dry and with a yellow coloration. Probably because of the open wound an acute and chronic inflammatory response was visible between the implant and the skin.

All other implants from this group showed good integration with adjacent tissues, poor cellular density and marginal cellular penetration. Despite the reduced number of cells present, there were many fully formed vessels in the edges of the implants (Figure 5.14).

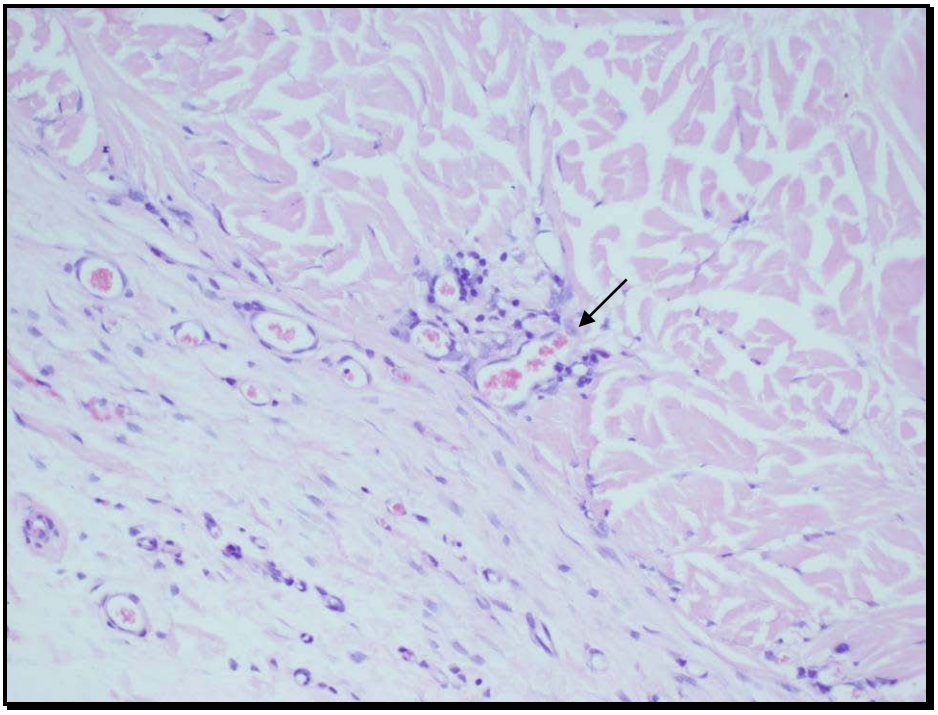

Figure 5.14 – 0.05% PVA-Permacol® implant 28 days post-implantation with mature vessels in its edge (H&E, 200X).

28 days after implantation a few silver granules were visible only at the edges of the 0.03% NPI-Permacol® implants (Figure 5.15). Integration was moderate, cellular density and cellular penetration were marginal, neo-vascularisation was mild with the majority of the vessels present in the borders whereas the implant centre was mostly acellular, except where natural pores were present.

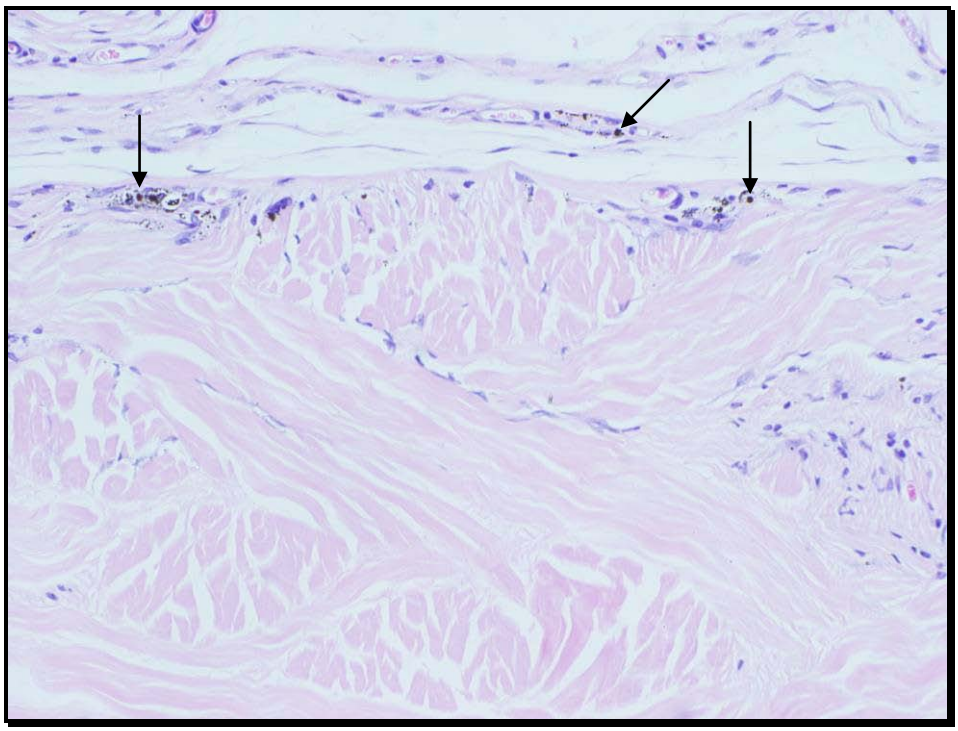

Figure 5.15 – 0.03% NPI-Permacol® implant after 28 days of implantation, arrows are indicating silver granules (H&E, 200X).

As in the 0.03% NPI-Permacol® implants, the silver granules in the 0.05% NPI-Permacol® implants at 28 days post implantation were present in small quantities in the implant edges and completely absent from the centre of the implants (Figure 5.16). 0.05% NPI-Permacol® implants after 28 days implantation showed moderate levels of integration with the surrounding tissue. Cellular density was marginal as well as cellular penetration. Vessel sprouts and mature vessels were visible in the implant borders.

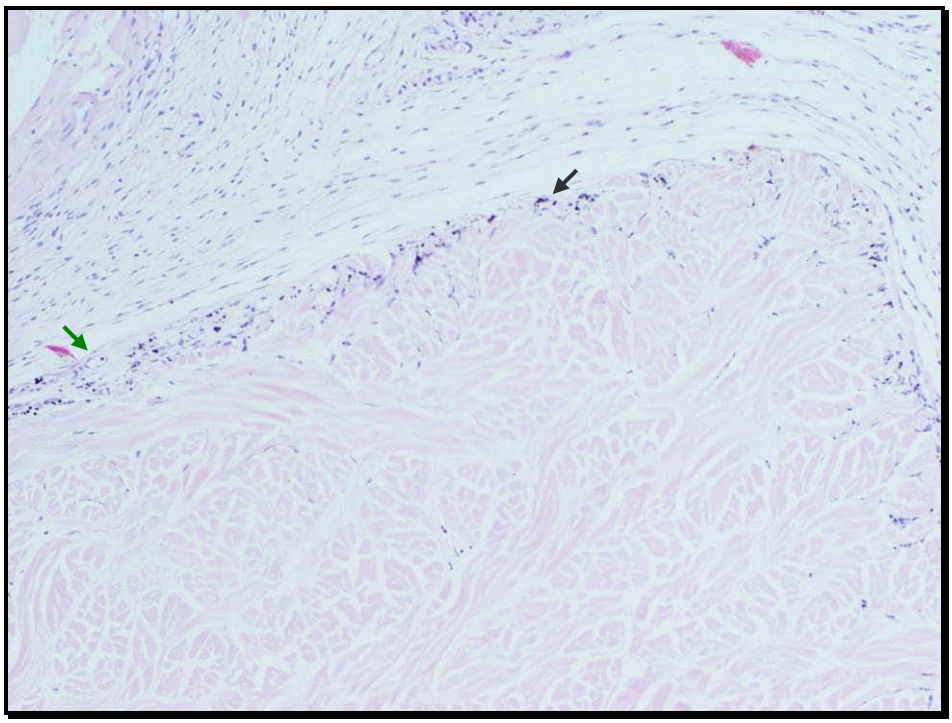

Figure 5.16 – Poor cellular density in a 0.05% NPI-Permacol® implant after 28 days of implantation. Black arrow indicates silver granules; green arrow shows vessel sprouts (H&E, 100X).

On examination under polarised light, normal, non-denatured collagen patterning was demonstrated in all 4 materials at both time points (Figure 5.17).

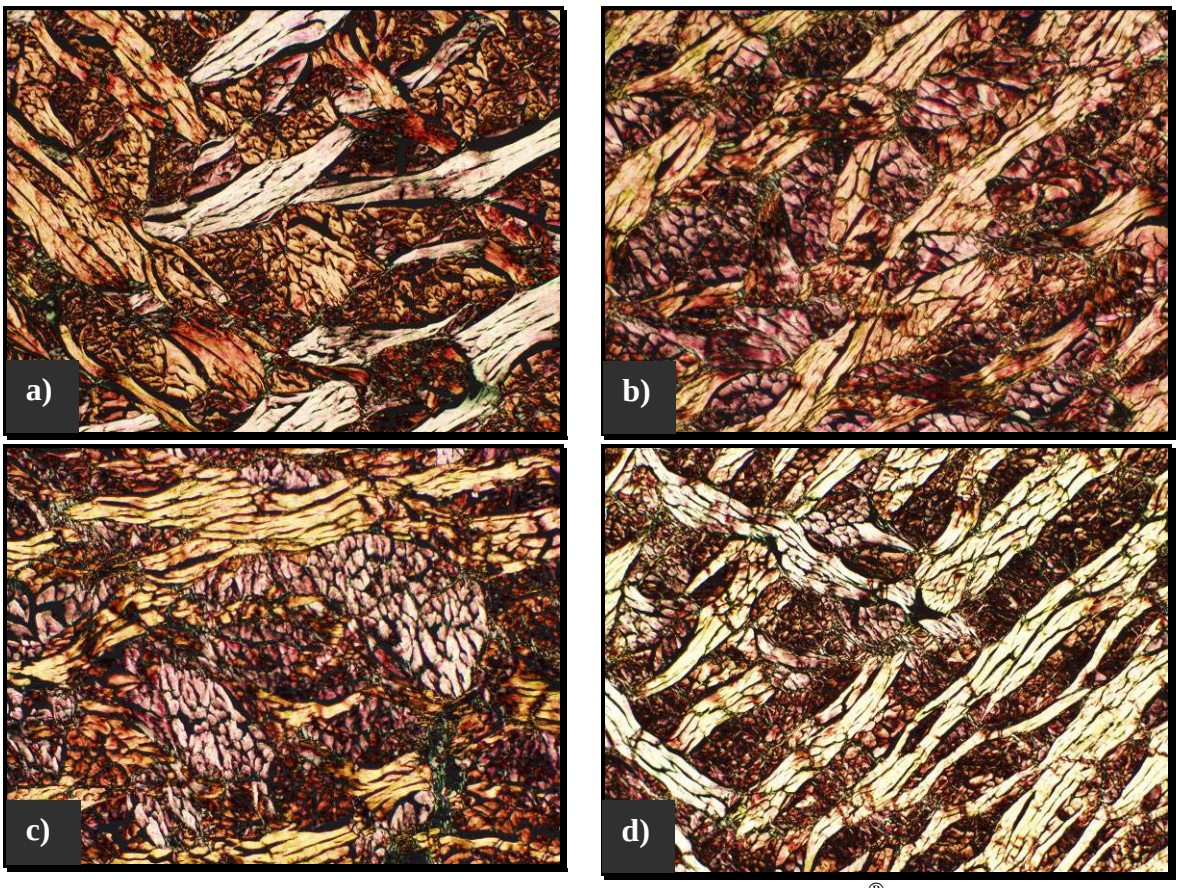

Figure 5.17 – Implants stained with picro sirius red: a) Permacol® implant 14 days post implantation (100X); b) 0.05% PVA-Permacol® implant 14 days after implantation (100X); c) 0.03% NPI-Permacol® implant 28 days post implantation (100X); d) 0.05% NPI-Permacol® implant 28 days post implantation (100X).

Figure 5.18 and Figure 5.19 show the histological results 28 days post implantation. Minimal and maximal values of cellular penetration were used to create the graph. Mean and standard deviations were calculated.

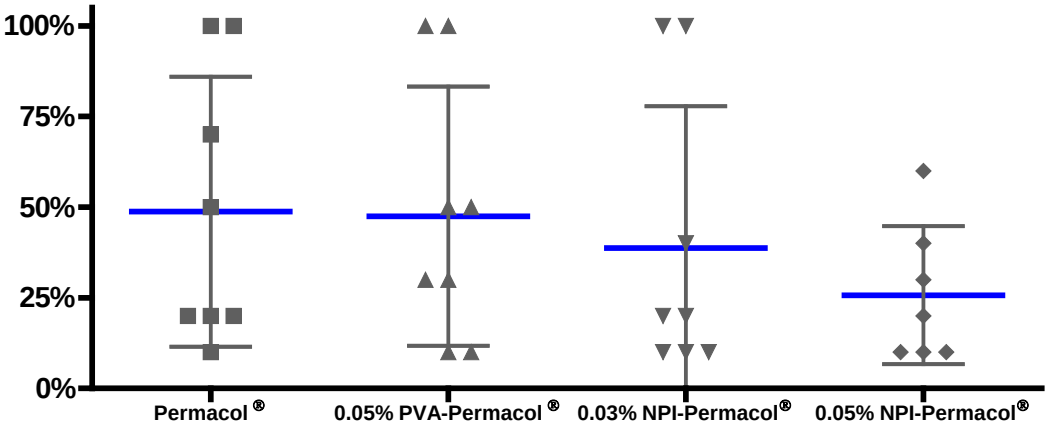

Figure 5.18 – Cellular penetration 28 days post implantation. Mean values, for both minimal and maximal levels of cellular penetration, were used per animal.

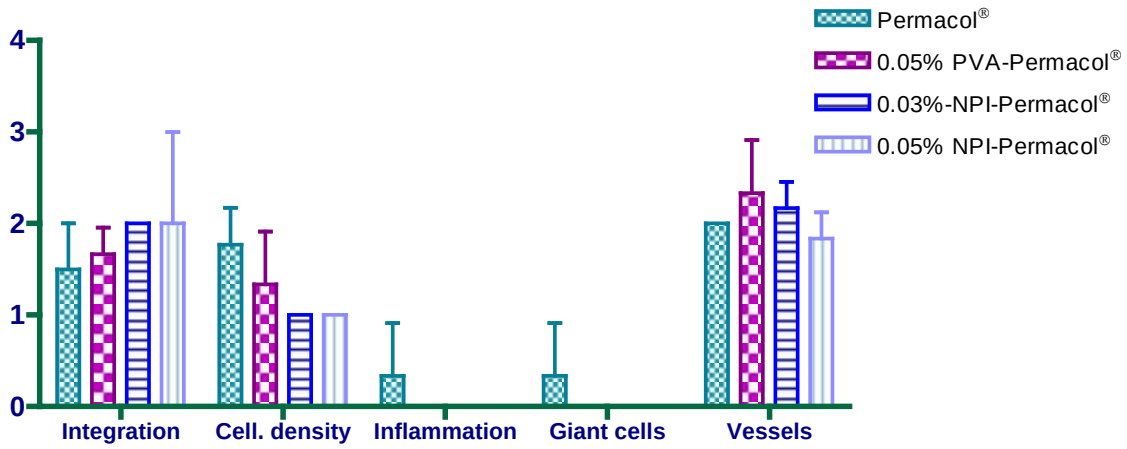

Figure 5.19 – Schematic representation of parameters analysed at 28 days post implantation, according to the scoring criteria described in Table 5.2.

The parameters analysed showed no significant difference between all groups and between pairs of groups.

The following figures show comparison of each histometric parameter between both time-points for all variants of Permacol® tested.

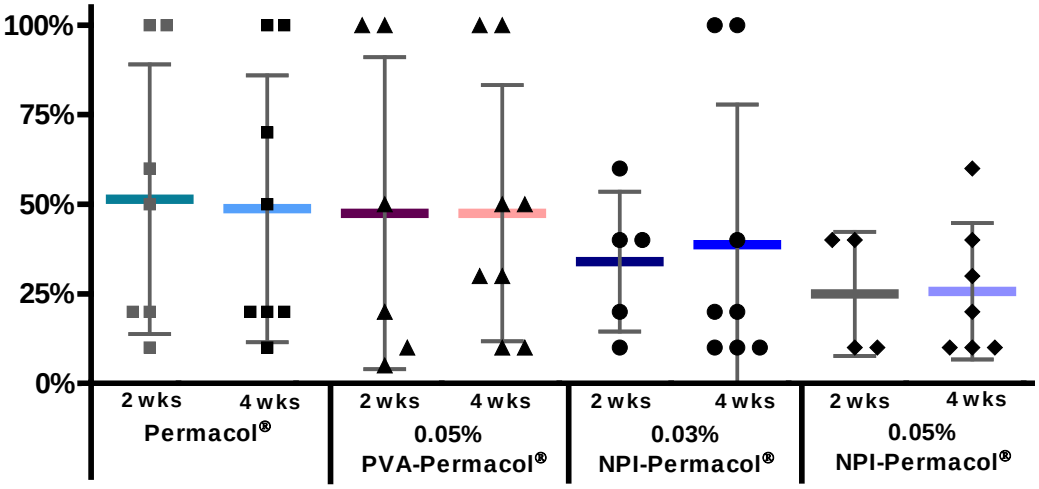

Figure 5.20 – Results for cellular penetration through the study. Mean values, for both minimal and maximal cellular penetration, were used per animal.

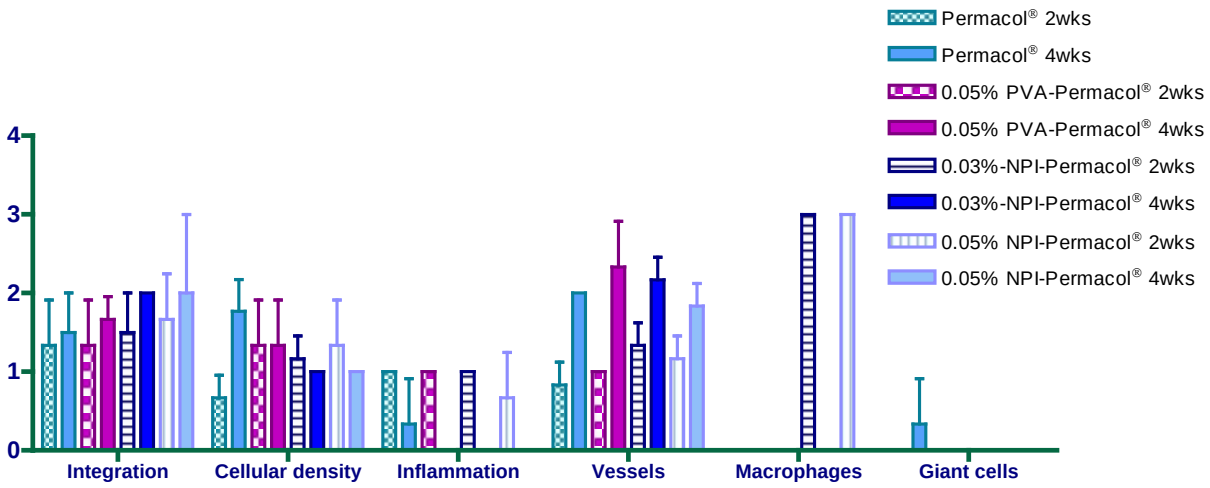

Figure 5.21 – Graphic representation of the histometric parameters analysed along the study, according to the scoring criteria described in Table 5.2.

There was no significant difference between groups and within groups.

5.1.7 Discussion

Silver is a broad-spectrum antimicrobial agent that has been used topically for centuries (Bergin and Wraight, 2007; Burd *et al.*, 2007). The metal interferes with microbial respiratory cytochromes, electron transport and DNA replication (Cooper, 2004; Klasen, 2000b; Klasen, 2000a). Silver's mechanism of action enables it to be effective against gram-positive and gram-negative aerobic and anaerobic bacteria, yeast, fungi and viruses (Lu *et al.*, 2008; Smetana *et al.*, 2008; Vlachou *et al.*, 2007). Therefore, implants coated with nanocrystalline silver particles may reduce bacteria colonization when applied into infected sites.

This study was designed with several aims; first to define any effects silver coating would have on Permacol® structure; second to see if silver coating would influence Permacol® standard performance *in vivo*; and third, decide whether Permacol® is a suitable dressing for sustained silver release in a contaminated field.

All modified collagen matrices retained the same structure and configuration as Permacol® surgical implant sheet. Therefore, the coating process had no effect on Permacol® structure. The pre-implantation silver coated matrices showed an interrupted coat of silver granules at the implant margins, and these were also seen around the walls of the natural pores within the matrix. The silver granules seemed darker and the coat layer slightly thicker in the 0.05% PVA-Permacol® matrix, which may be a result of silver concentration.

The implant recovered from the animal that died 3 days post implantation showed a higher level of cellular density compared to all the other implants. Cells were visible penetrating the matrix and reaching 40% of the implant in thickness. This indicates that the silver coating does not impede cellular penetration of Permacol® in the early stages of implantation. Silver granules were observed spreading to the inside of the matrix, but it was impossible to determine whether they were carried by cells or by interstitial fluid. At 14 and 28 days post implantation silver granules present in the implants were approximately 10% and 5% respectively, of the initial quantity. If silver coating is to be maintained for longer periods of time during implantation, the coating process should be revised.

Although 2 weeks post implantation macrophages were visible ingesting the nanocrystaline silver particles, at 4 weeks collagen matrices were not degraded which

suggests that the earlier presence of macrophages was caused by the presence of the silver particles and not by the collagen implants. Four weeks post implantation macrophages were absent although there were silver particles present, especially at the edges of the implants. Silver was observed at low levels, which may explain the absence of macrophages.

At 14 days post implantation Permacol® implants were associated with marginal acute inflammatory response, while at 28 days marginal acute and chronic inflammation was evident in only one of the implants. However, while integration with the surrounding tissue increased, there were giant cells present. The decrease of the inflammatory response over time is in keeping with the normal wound healing process and was also observed by Macleod and colleagues in a study where Permacol® was implanted subcutaneously in a rat model (MacLeod *et al.*, 2005). Giant cells were present only in the Permacol® implants at 4 weeks, thus their presence is not related to the silver coating.

In all matrices, implant/tissue integration and neo-vascularisation were higher after 28 days of implantation; these results suggest that these two parameters may be correlated.

Cellular penetration mean values were similar at both end time points for all matrices tested. This did not happen for cellular density, which increased over time in the Permacol® samples, was constant in the 0.05% PVA- Permacol® implants and decreased in both dressings treated with silver. Cellular penetration does not seem dependent on cellular density since implants with marginal cellular density were occasionally penetrated 100% in depth.

0.03% NPI-Permacol® and 0.05% NPI-Permacol® implants showed similar characteristics throughout the study reported here. Both silver concentrations appeared non-toxic and although in the earlier stages of implantation marginal levels of inflammation were observed, these subsided over time.

Silver-dressings are designed to have controlled and prolonged release of silver during the treatment time. Many factors will influence the clinical performance of this approach: the concentration of silver, type of silver, silver distribution, mode and strength of silver binding to the material and dressing affinity to moisture.

Silver-delivery dressings can be categorised in two major groups: those that have silver content on the surface (silver coating) or impregnated into the dressing such that

those particles are delivered to the wound rapidly from the dressing; and those that have high absorptive capacities and keep the silver content until the dressing absorbs wound exudate or moisture (Burd *et al.*, 2007). The first group deliver silver to the wound site after direct contact while the second group releases silver according to the amount of moisture absorbed. Silver coated-Permacol® belongs to the first group and, as observed in this experiment, 3 days post implantation nanocrystalline silver was rapidly being removed from the surface of the material. Moreover, 14 days post implantation high numbers of macrophages were present and ingesting the silver particles. In an infected wound macrophages may be too "busy" digesting bacteria to respond to the nanocrystalline silver particles, allowing it enough time to reduce bacteria levels. To confirm that silver-coated Permacol® is of significant value as an anti-microbial dressing an *in vivo* model of infected wound would have to be used.

5.1.8 Conclusion

In the rodent model reported here 0.03%-NPI Permacol® and 0.05%-NPI Permacol® showed similar results in all parameters assessed. Integration with the surrounding tissue was marginally higher in these materials compared to Permacol® and 0.05% PVA-Permacol®.

All collagen matrices assessed in this study did not show affinity with host cells; cellular density and cellular penetration were at low levels after 2 and 4 weeks implantation. Nevertheless, the inflammatory response was marginal and subsided with time.

The *in vivo* performance of Permacol® does not seem to be affected when coated with 0.03% and 0.05% nanocrystalline silver. However, if silver coating is to be maintained for longer periods of time during implantation, the coating process should be revised since sustained release of silver ions was not observed. Furthermore, macrophages were activated by the presence of the nanocrystalline silver.

Nanocrystalline silver has been shown to have antimicrobial properties and anti-inflammatory activity, augmenting the induction of apoptosis of inflammatory cells (Bhol and Schechter, 2005). Nanocrystalline silver has therefore been promoted as a potential therapeutic agent for treating inflammatory diseases but it may not be

beneficial when bacterial infection and severe inflammation are present, since inflammatory cells are vital to eliminate pathogens and induction of apoptosis in these cells has to be a timely controlled process.

5.2 ASSESSMENT OF THE BIOCOMPATIBILITY OF PERMACOL® SURGICAL IMPLANT AND A NONCROSS-LINKED EQUIVALENT IN A RODENT MODEL

5.2.1 Introduction

The use of artificial and natural tissue substitute matrices for repair and replacement of tissue defects, both trauma associated and post elective surgery is a common treatment for many conditions. Surgeons need repair materials which are biocompatible, non-toxic, permanent, integrate into host tissue, maintain volume and are non degradable when a bulking material is required, are easily manipulated and are "off-the-shelf". Autologous fat comprises many of the features of the ideal soft-tissue substitute, but a variable degree of resorption makes it difficult to predict the necessary transfer volume, this process increases theatre time, autologous tissue has limited availability and the retrieval of sufficient material may also increase morbidity. Intrinsic drawbacks of autologous materials have motivated research to synthesize new biomaterials – artificial and natural. Many artificial materials do not fulfil enough of the required parameters to the level necessary to be effective. Newer, mostly natural, biologic materials are now available and in increasing use. Many of these off-the-shelf biomaterials are composed of extracellular matrix, which purport advantages due to their natural 3-D structure and diverse protein content.

Permacol® surgical implant is an acellular dermal porcine biomaterial and its use is steadily increasing both in numbers and types of clinical applications. Acellular tissue matrices have the benefit of containing intact structural proteins which promote cell ingrowth with reduced inflammatory response; in addition, to reduce antigenicity and improve stability, Permacol® surgical implant is chemically cross-linked. Porcine and human dermis show differences with respect to microvascular architecture, degree of density and dermal-epidermal integration; however, porcine dermis is to a large extent structurally and immunologically similar to human dermis (MacLeod *et al.*, 2004a). One of the main criteria in determining the success of a biomaterial is tissue

biocompatibility. Tissue reaction to an implant may vary from complete integration with native tissue to severe inflammatory and immune responses culminating in rejection of implant. Collagen is well known for its low antigenicity and this makes it an ideal material for tissue engineering.

Although previous studies showed Permacol® surgical implant as biocompatible and being mostly accepted by the host tissue with marginal inflammatory response (Harper, 2001), there was limited cellular infiltration. Furthermore there is a temporal change in cellular density/penetration and subsequent vascularisation of Permacol® surgical implant.

It was hypothesized that the apparent resistance to cellular penetration in Permacol® surgical implant was a result of cross-linking. Permacol® surgical implant and a noncross-linked equivalent were compared for biocompatibility, cellular response and implant structure/resilience, in a rat model.

5.2.2 Hypothesis

Permacol® surgical implant and noncross-linked acellular collagen do not have similar biocompatibility and tissue integration when implanted subcutaneously in a rodent model.

5.2.3 Aims and Objectives

- To study the effect of cross-linking in Permacol® implant, by comparing the end-product with the product before the cross-linking process (noncross-linked acellular collagen); by evaluation of strength of implant/host tissue integration, tissue reaction, cellular penetration, vascularisation and general healing, in a rodent model.
- Establish whether there is good early vascularisation in the 3 months implants, if there are mature vessels present in the 6 and 12 months implants and if an increase in the vascularity is related to apoptotic stimuli.

- Assess Permacol® surgical implant suitability as a subcutaneous implant for soft tissue repair and as a bulking material.
- Assess Permacol® surgical implant performance for the first time in a long term *in vivo* study, in a rat model.

5.2.4 Materials and Methods

The study was performed in compliance with the Good Laboratory Practice Regulations 1999 (S.I. No 3106), as described in Section 5.1.4.
Permacol® surgical implant and noncross-linked acellular collagen (NonXL) were supplied by TSL plc. as 5cm x 5cm sheets, Permacol® surgical implant had a thickness of 1.536 ± 0.072mm and NonXL thickness was 1.51 ± 0.105mm. Collagen matrices were derived from the same batch to eliminate variations.

5.2.4.1 Study Design

The rat was chosen as the species for this study because of published and in-house knowledge of dermal pathogeneses in this species. Additionally, the rat is the lowest evolutionary animal in which this work could reasonably be carried out.

Three experimental end-points were chosen – 3, 6 and 12 months post implantation, groups G1, G2 and G3 respectively. One experimental group (6 animals) and one control group (2 animals) were designed for each time point, resulting in a total of 24 male Wistar – Han™ rats. For direct comparison between collagen matrices each animal was implanted with both Permacol® and NonXL collagen; implant location was performed randomly, i.e., one type of implant was not specifically placed on the animal's left or right side subcutaneous pocket. Animals were randomised, identified with numbers and distributed within the 6 groups.
Since animals from group G3 had to be kept in cages for 12 months it was decided to allow them 30 minutes of exercise twice a week, to improve their quality of life and

make sure that the sedentary environment would not induce health problems and interfere with the study. A "playground" area was designed with various toys and 3 animals were placed together in the common area, at each time, to interact and exercise.

5.2.4.2 Surgical Procedure

Permacol® surgical implant and NonXL collagen were cut into 3.5cm x 1.5cm pieces and left in sterile saline solution until implantation. Pieces of both biomaterials were kept and fixed with 10% NBF for histological analysis as a pre-implantation control.

Animals were anaesthetised according to the procedure described in Section 2.2.5. All surgery was done using sterile techniques. The following surgical procedure was followed for all animals:

1. A ventral midline incision was made from just below the level of the rib cage extending approximately 1.5 cm distally.
2. Skin was elevated and retracted to create one subcutaneous "pocket" on each side of the midline.
3. Haemostasis was maintained by careful dissection – no electrocautery was used.
4. The collagen matrices were placed one in each pocket and implant-type location recorded.
5. The previous step was not performed on the control animals.
6. The ventral midline incision was closed with interrupted sutures.

The day of surgery for each rat was considered as Day 0.

5.2.4.3 Necropsy

Animals were euthanased and a composite of skin, subcutaneous tissue, implant and underlying muscle was harvested en bloc (as described in Section 2.2.8). From the block of tissue recovered one third (longitudinally) was used fresh for integration strength testing by way of a tensiometer, another third was frozen in liquid nitrogen and kept at -80 ^{o}C and the remainder was fixed in 10% NBF for routine histology and immunohistochemistry (see Section 2.2.9 and Section 2.2.10 respectively).

5.2.4.4 Tensiometry

Peritoneal wall outside of the treatment area was sutured to the mobile end of the tensiometer and the treatment material was sutured to the static end of the tensiometer. Tension was applied at a constant load until dissociation occurred either at the treatment/peritoneal wall junction or in the associated tissues.

5.2.5 Scanning Electron Microscopy

To further pursue some of the results obtained, a few samples were observed with the use of a scanning electron microscope. SEM was performed as previously described in Section 3.1.5.4.3.

5.2.6 Statistical Analysis

Histometric scores (integration, cellular density, cellular penetration, inflammatory cells and neo-vascularisation) were analysed per matrix type and per end-point using a two-way ANOVA with repeated measurements to look for interaction between factors. These tests were performed in conjugation with Levene's test to check for

homogeneity of variances; when variances were significantly different two separate one-way variance analysis were performed instead. A one-way ANOVA was used to compare implant thickness in all groups per time point, followed by a post hoc test to compare results between groups and to compare each group to pre-implanted Permacol®. One-way ANOVA was also used to analyse mineralisation occurrence and tensiometry results over time. When the ANOVA (one-way and two-way) results were significant, least significant difference (LSD) and Bonferroni post hoc tests were used to identify differences within groups; when the variances were unequal Tamhanes's T2 post hoc test was used. $P<0.05$ was considered as statistically significant for all tests applied. Statistical analysis was performed using SPSS Statistics 16.0 (SPSS Inc. Chicago, USA). Graphical representation of data was performed using Graphpad Prism statistics software, version 4 (GraphPad Software, Inc., USA).

5.2.7 Results

One animal from group G3 had to be re-sutured 2 days post surgical procedure and did not recovered from the anaesthesia. At the end of each time point all animals were healthy with body weight values as expected. There were no situations which the NACWO or the PPL License Holder were unable to deal with and therefore nothing was referred to the named Veterinary Physician.

5.2.7.1 Tensiometry

Tensiometry results are displayed in Table 5.3 to Table 5.8. Tensiometry studied the resistance of the complex between implant and tissue to a constant force applying a separation moment measured as the maximum tension the material can withstand without integration failure. The individual materials within the complex may also fail. Separation means separation between the implant and the surrounding tissue. The graft tension orientation was always the same; each matrix was sutured to the static

end of the tensiometer. Maximum load refers to the maximum force, applied to the complex between implant and tissue, sustained during the test. Extension at maximum load is the amount of stretch or elongation the complex undergoes until the maximum load point is reached. Total extension is the stretch or elongation the complex undertakes until separation or failure.

At 3 months post implantation the maximum load mean of Permacol® was 0.551 ± 0.208kg, this value was lower for the noncross-linked collagen implants which had a maximum load mean of 0.378 ± 0.128kg. The mean extension at maximum load was slightly higher in the Permacol® implants (23.12 ± 7.449mm) when compared to the noncross-linked samples (16.41 ± 5.214mm). A greater maximum load indicates greater integration between the implant and the adjacent tissue and/or a greater tensile strength of the materials. All Permacol® implants and 4 of the noncross-linked implants failed by separating from the surrounding tissue. One noncross-linked implant did not fail and the travel limit of the tensiometer was exceeded. In another noncross-linked implant the sutures connecting the implant/tissue complex to the movable end of the tensiometer snapped before any form of failure had been registered.

Table 5.3 – Tensiometry results for Permacol® samples, 3 months post implantation.

Animal number	Max Load (kg)	Ext at Max Load (mm)	Total Extension (mm)	Separation
2	0.616	24.41	51.10	Yes
4	0.153	8.125	23.37	Yes
6	0.585	26.73	43.92	Yes
11	0.771	24.93	43.56	Yes
12	0.568	27.59	59.36	Yes
16	0.611	26.95	46.30	Yes
Mean	**0.551**	**23.12**	**44.60**	
SD	**0.208**	**7.449**	**11.960**	

Table 5.4 – Tensiometry results for noncross-linked acellular collagen, 3 months post implantation.

Animal number	Max Load (kg)	Ext at Max Load (mm)	Total Extension (mm)	Separation	Comments
2	0.537	19.68	53.70	Yes	
4	0.242	14.38	-	Yes	Unable to record total extension
6	0.245	11.29	30.08	No	Suture snapped
11	0.470	22.60	74.49	No	Travel limit exceeded
12	0.307	10.05	34.42	Yes	
16	0.465	20.43	38.70	Yes	
Mean	**0.378**	**16.41**	**46.28**		
SD	**0.128**	**5.214**	**18.107**		

At 6 months post implantation Permacol® implants showed slightly lower maximum load values (0.592 ± 0.353kg) and lower total extension (48.57 ± 17.871mm) compared with noncross-linked collagen implants (0.823 ± 0.474kg and 59.1 ± 10.043mm, respectively), the extension at maximum load was similar for both implant types. In this group, 3 Permacol® implants failed by separation and the other 3 did not reached failure point, one because the muscle split and sutures snapped in the other 2. Four of the noncross-linked collagen implants failed by separation at 6 months post implantation, in 1 implant the muscle split and sutures snapped in the other.

Table 5.5 – Tensiometry results for Permacol® implants, 6 months post implantation.

Animal number	Max Load (kg)	Ext at Max Load (mm)	Total Extension (mm)	Separation	Comments
1	0.445	14.19	30.98	Yes	
7	0.335	48.67	66.84	No	Muscle split
8	0.146	27.63	34.96	No	Suture snapped
9	0.817	51.15	68.55	Yes	
10	0.691	35.01	-	Yes	Unable to record total extension
13	1.119	32.64	41.51	No	Suture snapped
Mean	**0.592**	**34.88**	**48.57**		
SD	**0.353**	**13.715**	**17.871**		

Table 5.6 – Tensiometry results for noncross-linked collagen implants, 6 months post implantation.

Animal number	Max Load (kg)	Ext at Max Load (mm)	Total Extension (mm)	Separation	Comments
1	0.634	33.19	69.74	Yes	
7	1.083	27.50	53.93	No	Muscle split
8	1.653	34.12	61.52	Yes	
9	0.534	46.72	70.02	Yes	
10	0.691	35.01	44.12	No	Suture snapped
13	0.341	19.10	55.24	Yes	
Mean	**0.823**	**32.61**	**59.10**		
SD	**0.474**	**9.123**	**10.043**		

Twelve months post implantation there was a pronounced increase in the mean of the maximum load values (0.946 ± 0.198kg) of Permacol® surgical implants, suggesting an increase of tissue integration. Extension at maximum load diminished in these implants and total extension increased moderately (Table 5.7). The noncross-linked implants mean values decreased for all parameters analysed (Table 5.8). In group G3 4 Permacol® implant separated from the surrounding tissue; one Permacol® implant

and one noncross-linked implant failed because sutures tore through the implant; the muscle ripped in one Permacol® implant and in 3 noncross-linked implants.

Analysis of results did not show any statistical difference between the tensiometry parameters analysed per time point and per implant type.

Table 5.7 – Tensiometry results for Permacol® surgical implants, 12 months post implantation.

Animal	Max Load (kg)	Ext at Max Load (mm)	Total Extension (mm)	Separation	Comments
26	1.240	44.27	56.31	Yes	
28	1.041	37.59	77.71	Yes	
29	0.826	15.95	56.94	Yes	
30	0.740	17.43	25.37	No	Sutures teared implant
31	0.883	36.31	63.20	No	Muscle split
Mean	**0.946**	**30.31**	**55.91**		
SD	**0.198**	**12.81**	**19.12**		

Table 5.8 – Tensiometry results for noncross-linked collagen implants, 12 months post implantation.

Animal	Max Load (kg)	Ext at Max Load (mm)	Total Extension (mm)	Separation	Comments
26	0.574	19.51	28.74	No	Sutures tear implant
28	0.548	20.01	78.96	Yes	Muscle split, travel limit exceeded
29	0.587	26.39	63.31	No	Muscle split
30	0.553	57.8	78.95	No	Few muscle fibres attached, travel limit exceeded
31	0.746	19.8	50.52	No	Muscle split
Mean	**0.602**	**28.70**	**60.10**		
SD	**0.082**	**16.52**	**21.19**		

5.2.7.2 Histopathology

Samples from the control animals showed no reactivity in the tissue or any problem that could have resulted from the surgical procedure.

Autopsy showed no evidence of inflammation around the implants. From each sample two transverse sections were made, one stained with haematoxylin and eosin and the other stained with picro sirius red. Sections were examined, using a light microscope with polarising ability, for the following features: general healing, cellular density, neo-vascularisation, integration with surrounding tissue, cellular penetration, implant structure retention, inflammatory response and collagen degradation.
The semi-quantitative histometric grading system used was as described in Section 5.1.6.

All animals were healthy with body weights as expected at the respective end-time point.

Group G1 – 3 months:

No evidence of an acute inflammatory response was seen in the tissues surrounding any of the implants or within the implants.
At 3 months post implantation integration with the surrounding tissue was low to moderate in the Permacol® implants (Figure 5.22 and Figure 5.23) and low to minimum in the noncross-linked collagen implants (Figure 5.24). When comparing the values of tissue integration of both matrices there was no significant difference between Permacol® and noncross-linked collagen, although Permacol® reached moderate levels of integration in 2 implants. Two of the noncross-linked collagen implants showed a fibrous layer surrounding the implant which was not an obstacle for cellular penetration (Figure 5.25), suggesting that it may be part of the integration process rather than encapsulation.

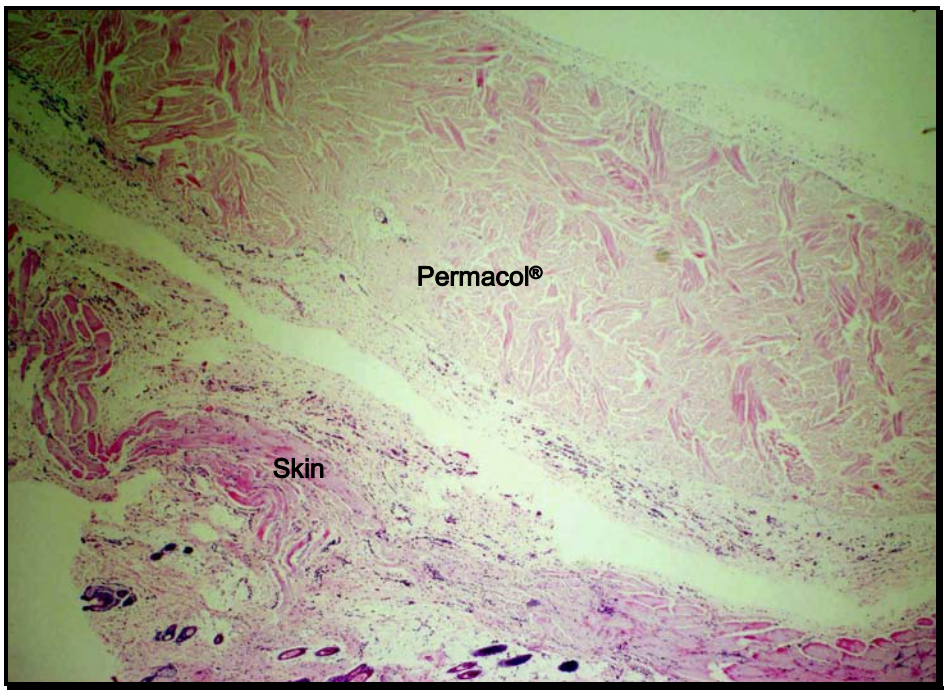

Figure 5.22 – Permacol® implant poorly integrated with the host tissue after 3 months implantation (H&E, 20X).

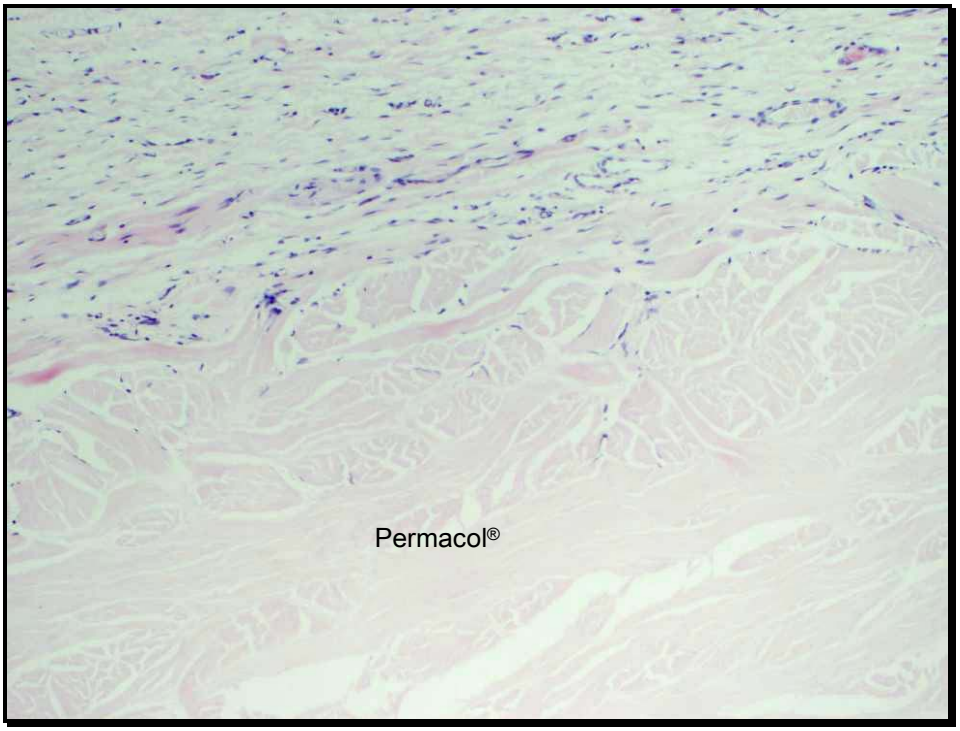

Figure 5.23 – Permacol® implant moderately integrated with cells emanating from the surrounding tissue, 3 months post implantation (H&E, 100X).

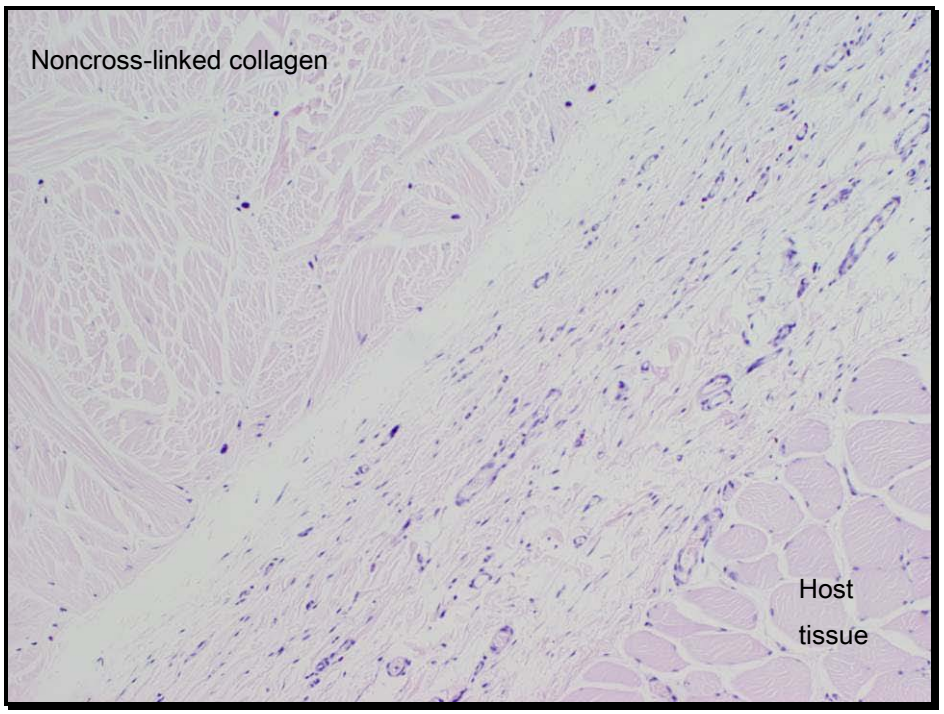

Figure 5.24 – Noncross-linked collagen implant 3 months post implantation showing low integration with the surrounding tissue (H&E, 100X).

Figure 5.25 – Fibrous layer surrounding a NonXL implant, 3 months post implantation (picro sirius red, 40X).

After 3 months post implantation, Permacol® implants showed mostly ≤20% cellular penetration in 4 implants. Cellular penetration was scored with regard to depth of cellular infiltration into the implant. In the other 2 Permacol® implants cellular penetration varied between levels 30% and 50% and in a few zones reached 100% (Figure 5.26).

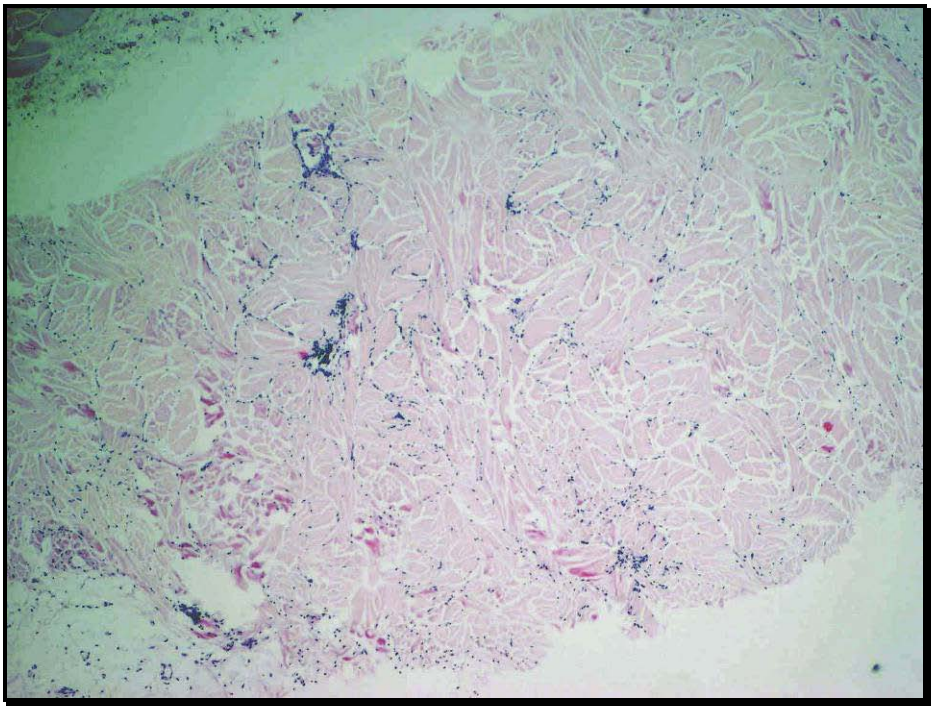

Figure 5.26 – Permacol® implant 3 months post implantation with 100% cellular penetration (H&E, 40X).

The noncross-linked implants after 3 months of implantation showed moderate cellular penetration, reaching occasionally, in all implants, 100% of cellular penetration (Figure 5.27). Implants with a higher number of cells achieved a superior level of penetration, but complete cellular penetration was still possible in implants with a low cellular density.

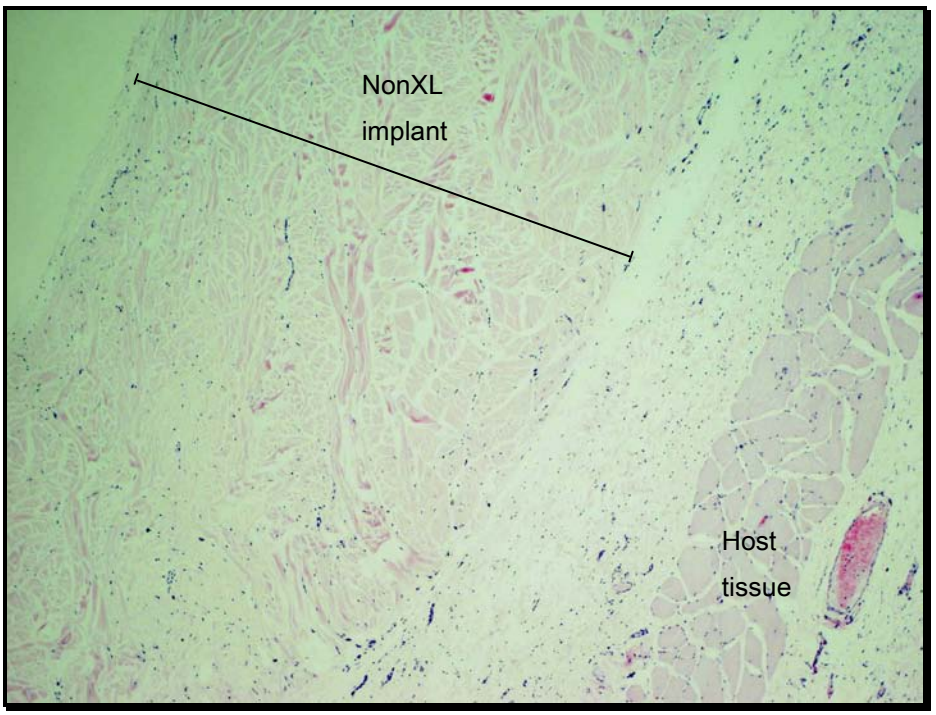

Figure 5.27 – NonXL implant, 3 months post implantation, with 100% cellular penetration and a minimum cellular density (H&E, 40X).

Cellular density was generally low in both collagen matrices, except in two implants from each matrix where a minimum cellular density was accomplished (Figure 5.28 and Figure 5.29); these implants also showed higher levels of cellular penetration.

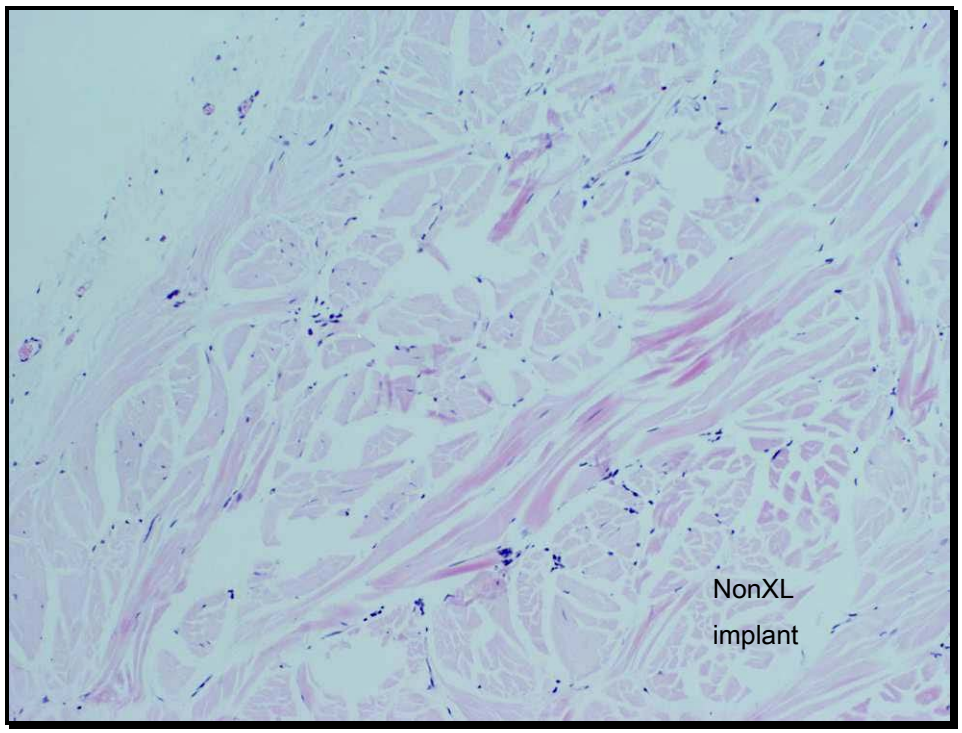

Figure 5.28 – Minimal cellular density in a NonXL implant, 3 months post implantation (H&E, 100X).

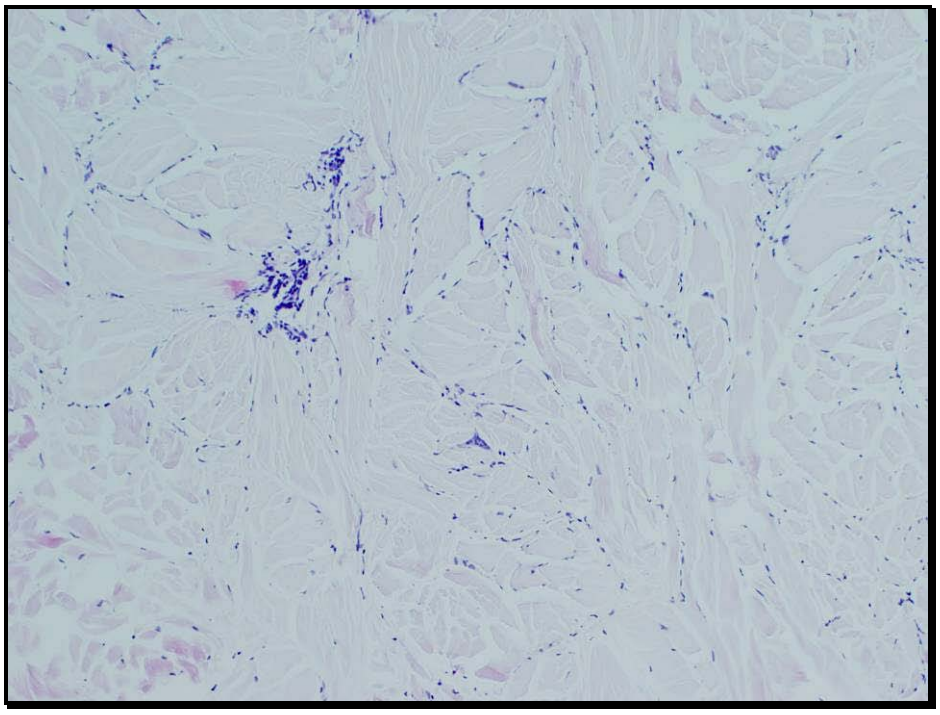

Figure 5.29– Feature of a Permacol® implant with a level of 2.5 cellular density, 3 months post implantation (H&E, 100X).

For both Permacol® (Figure 5.30) and noncross-linked variant neo-vascularisation was observed both in the edges and centre of implants, although vessel sprouts and fully formed vessels were more commonly present in the edges of the implants. The number of fully formed vessels was superior to the number of vessel sprouts.

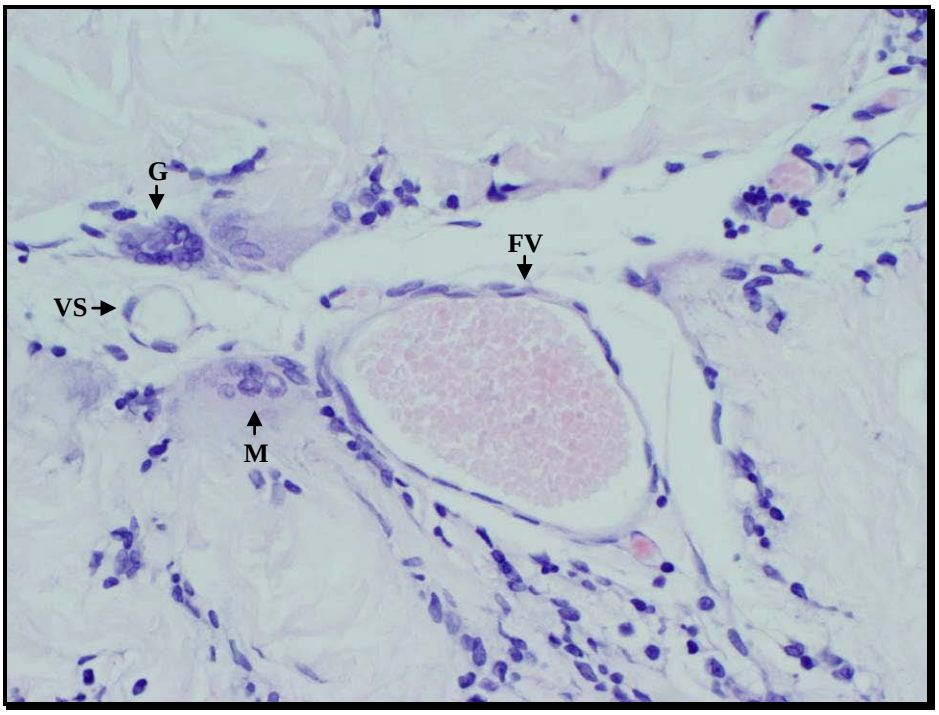

Figure 5.30 – Fully formed vessel (FV) with blood cells in the lumen and vessel sprouts (VS) in a Permacol® implant, 3 months post implantation. Giant cell (G) and macrophages (M) are also present (H&E, 400X).

Vessels were particularly localized in the borders of the noncross-linked implants, but all noncross-linked implants showed vessel sprouts and mature vessels in the centre (Figure 5.31).

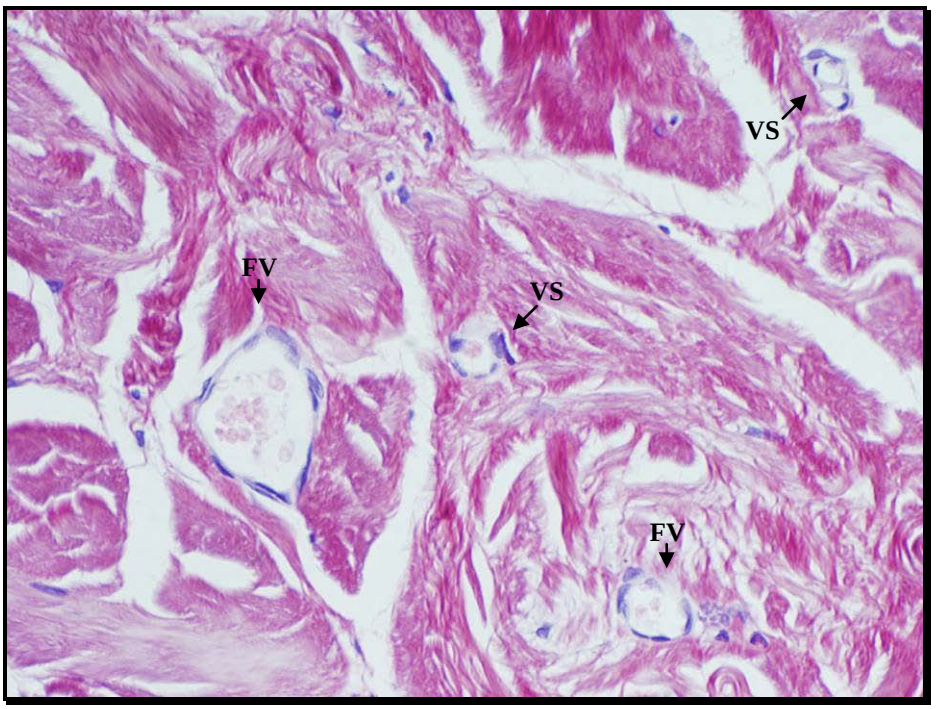

Figure 5.31 – Fully formed vessels (FV) and vessels sprouts (VS) in a NonXL implant, 3 months post implantation (picro sirius red, 400X).

Macrophages and giant cells were present in five of the six Permacol® implants, at 3 months post implantation (Figure 5.32). Giant cells form around fragments of tissue, which could be fragments from the implant or fragments resulting from tissue damaged during the surgical procedure. The occurrence of these cells suggest the presence of unwanted fragments of tissue/material but it is not clear which tissue/material they are engulfing or its origin – host or implant. Macrophages and giant cells are normally associated with an inflammatory response, although, in this case, no other inflammatory cells are present suggesting that their presence may be related to a different source rather than an inflammation. Giant cells can result from a foreign body type reaction.

Noncross-linked implants had lower numbers of macrophages and giant cells were not present.

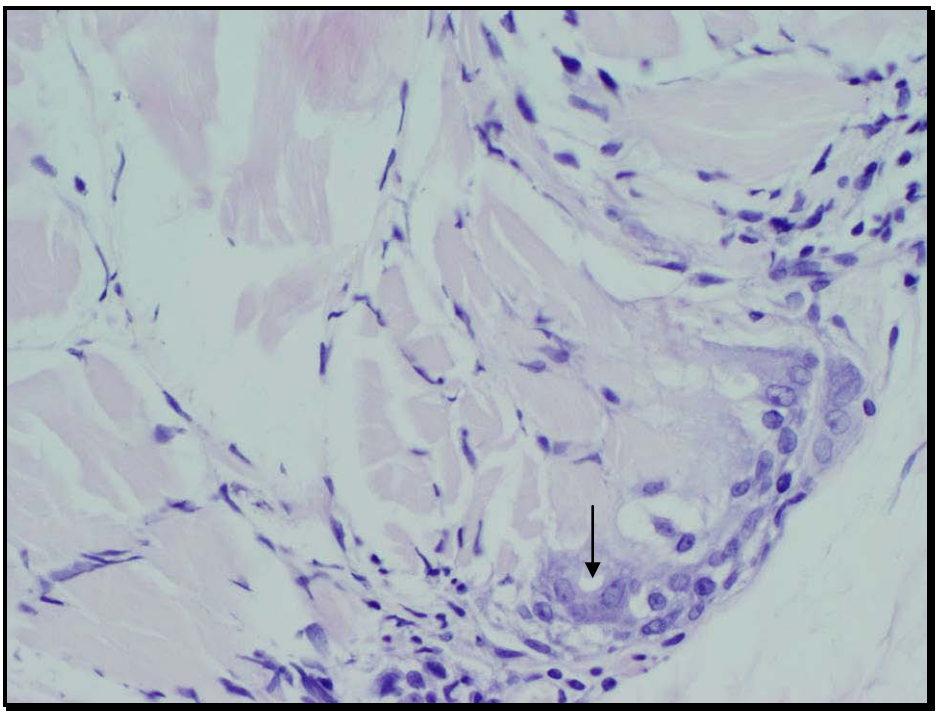

Figure 5.32 – Macrophages and formation of a giant cell (arrow) in a Permacol® implant after 3 months implantation (H&E, 400X).

On examination under polarized light, normal, non-denatured collagen patterning was present in both collagen matrices (Figure 5.33).

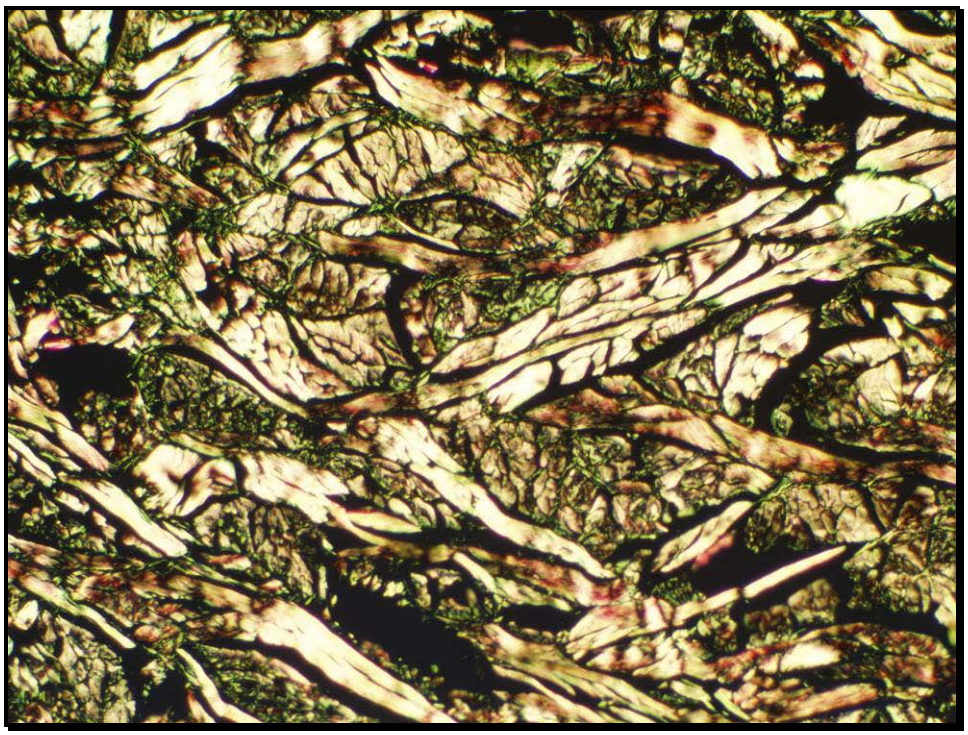

a)

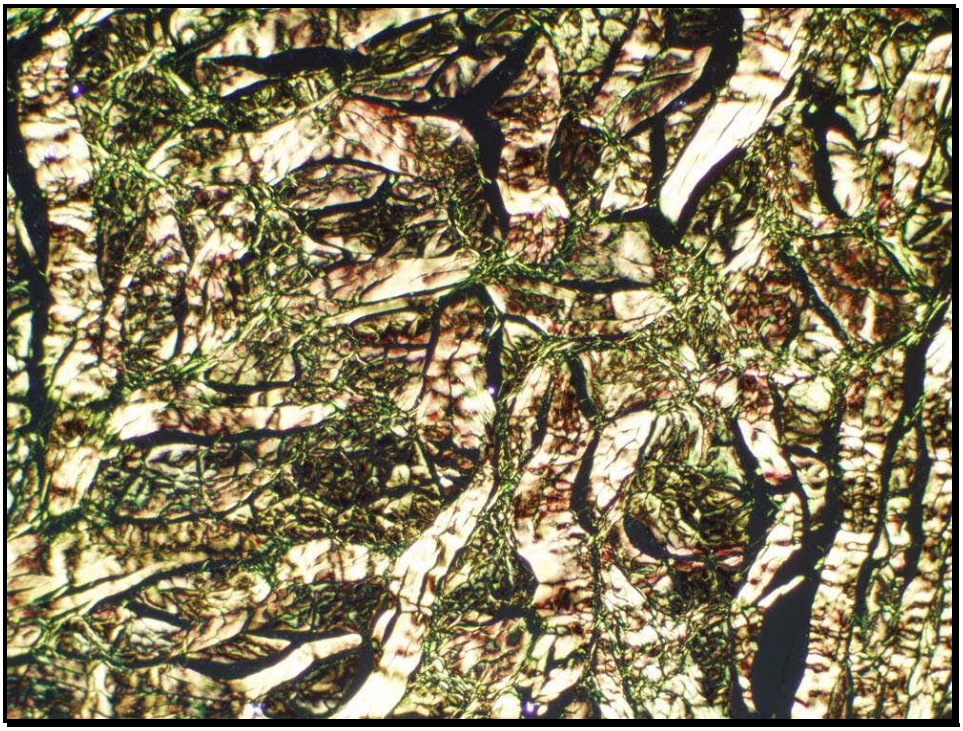

b)

Figure 5.33 – Implants stained with picro sirius red under polarized light, after 3 months of implantation. a) Noncross-linked collagen, 100X. b) Permacol®, 100X.

The next graph shows the results for the 3 months group. Means and standard deviations were calculated.

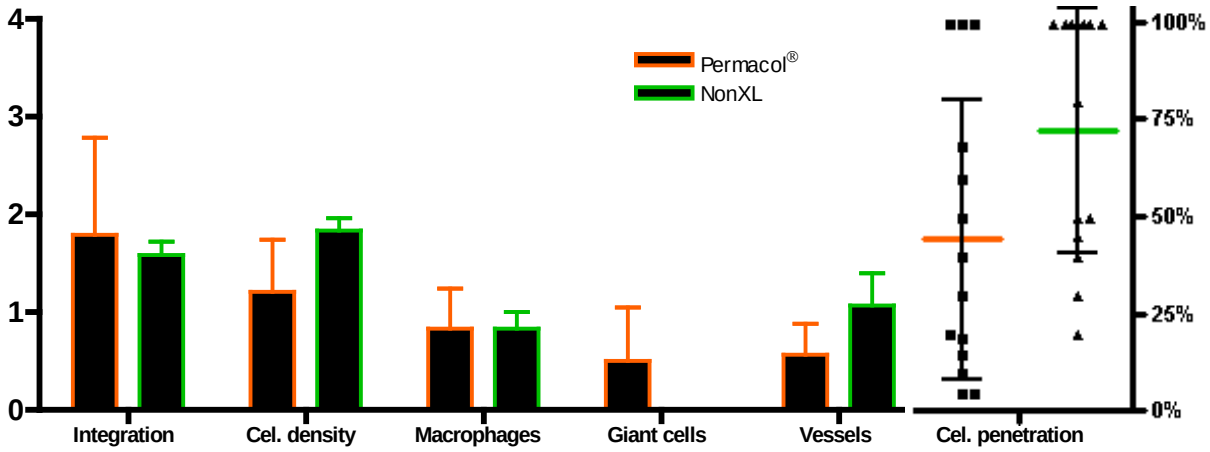

Figure 5.34 – Histometric scores for the 3 months group, according to the scoring criteria as described in Table 5.2.

Group G2 – 6 months:

Acute inflammatory response was not observed in any of the implants and in the surrounding tissues.

At 6 months post implantation noncross-linked implants showed low to minimum integration with surrounding tissue, while tissue integration in Permacol® implants was low to moderate (Figure 5.35 and Figure 5.36).

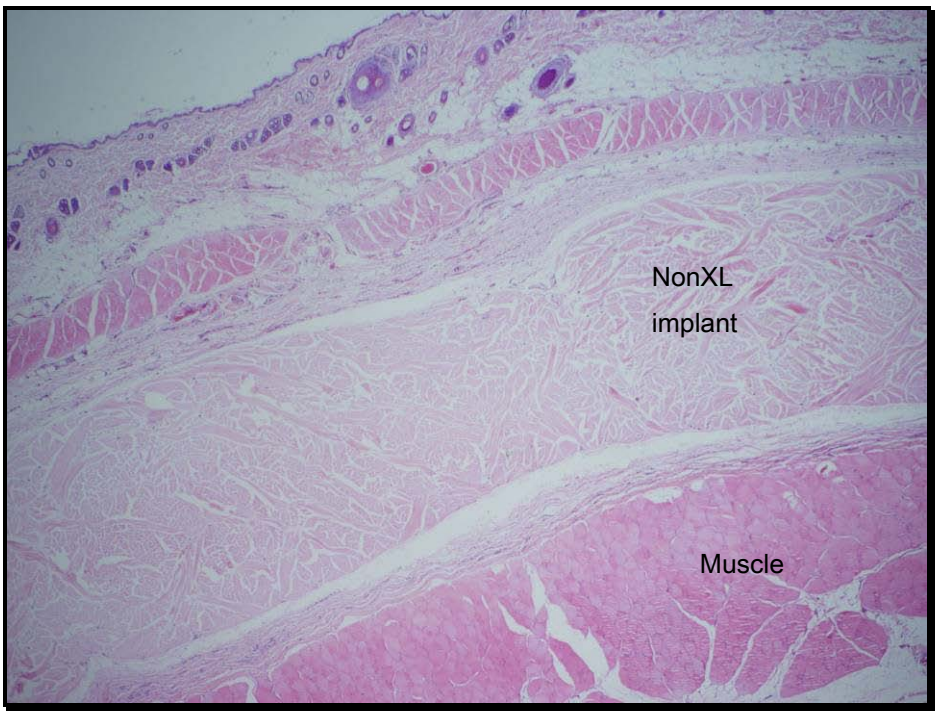

Figure 5.35 – NonXL implant with a low level of integration at 6 months post implantation (H&E, 20X).

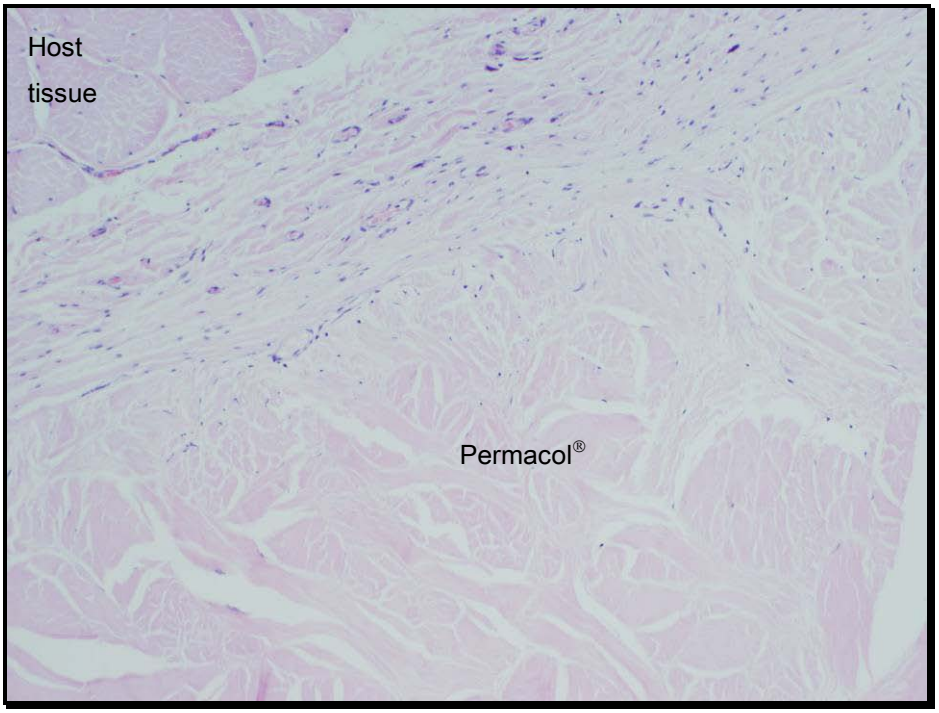

Figure 5.36 – Permacol® implant, 6 months post implantation, showing a moderate level of integration with the surrounding tissue (H&E, 100X).

Five of six of the noncross-linked implants reached 100% cellular penetration at 6 months post implantation (Figure 5.37), the minimum level of cellular penetration achieved in these implants was 30%. Permacol® implants showed lower levels of cellular penetration compared to the noncross-linked samples (Figure 5.38).

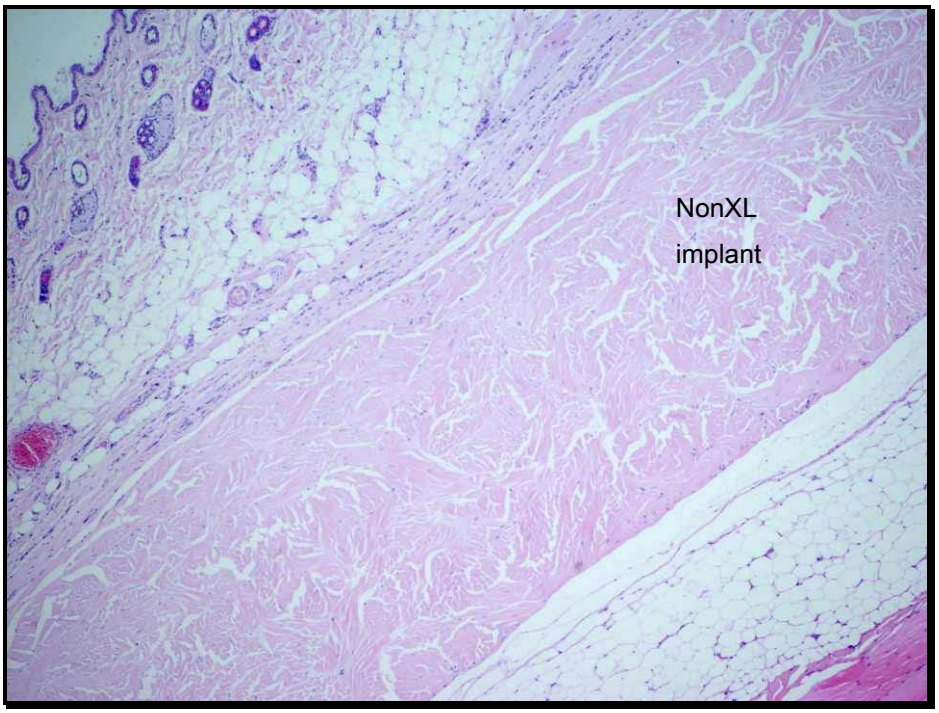

Figure 5.37 – NonXL implant, 6 months post implantation, with 100% cellular penetration regardless of the number of cells present (H&E, 40X).

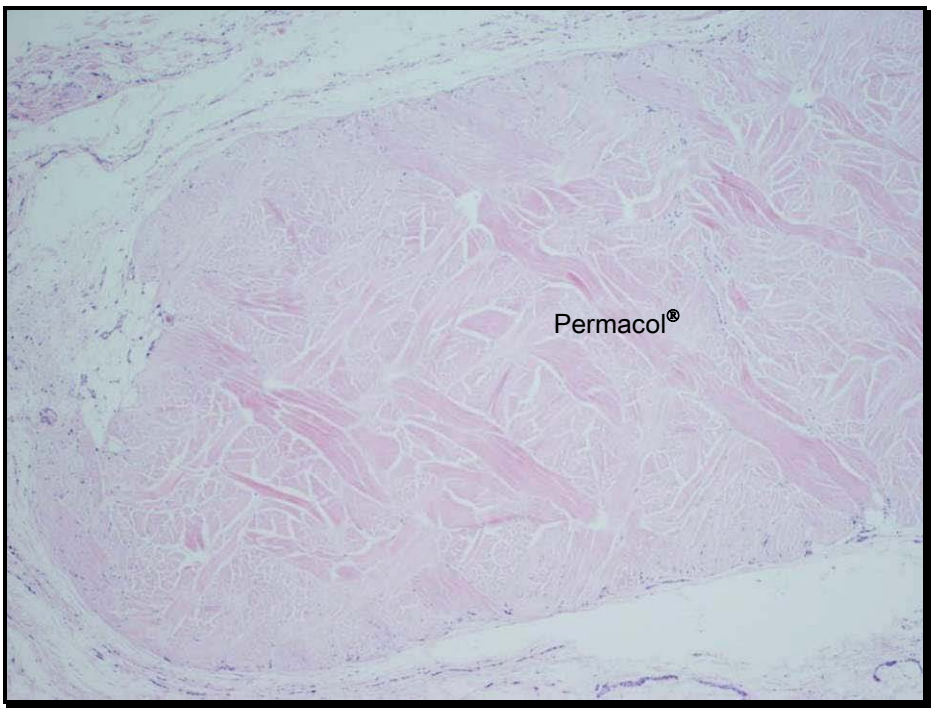

Figure 5.38 – Permacol® implant after 6 months implantation with low cellular density and low cellular penetration (H&E, 40X).

Cellular density for Permacol® was low in 5 of the 6 implants of this group (Figure 5.39). As observed at 3 months the noncross-linked implants were slightly more cellular than the cross-linked implants (Figure 5.40).

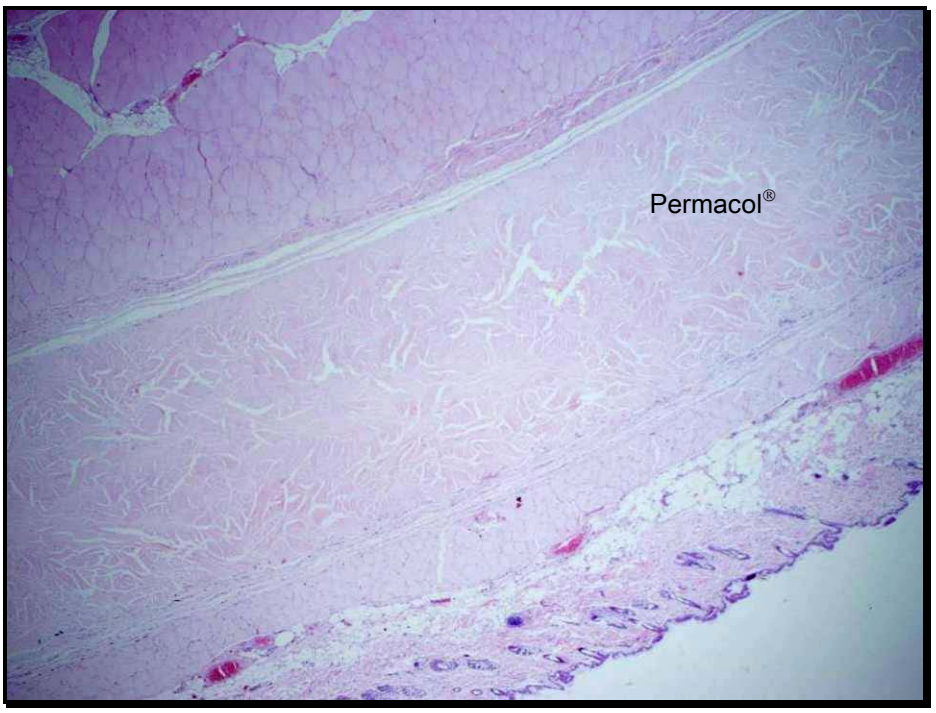

Figure 5.39 – Low cellular density in a Permacol® implant, 6 months post implantation (H&E, 20X).

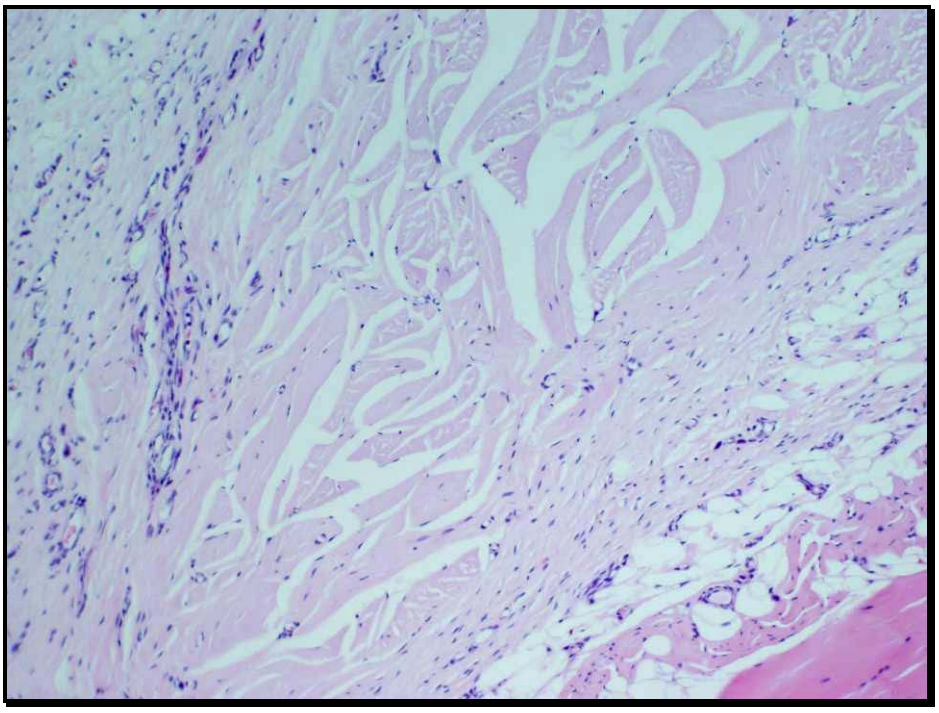

Figure 5.40 – Moderate cellular density in a NonXL implant, 6 months post implantation (H&E, 100X).

Vessel sprouts and formed vessels were observed in the edges and centre of the implants, although more frequently in the edges. At 6 months post implantation the number of mature vessels present in both matrices was undoubtedly superior to the number of vessel sprouts observed (Figure 5.41 and Figure 5.42). Permacol® implants had more vessels present than noncross-linked implants.

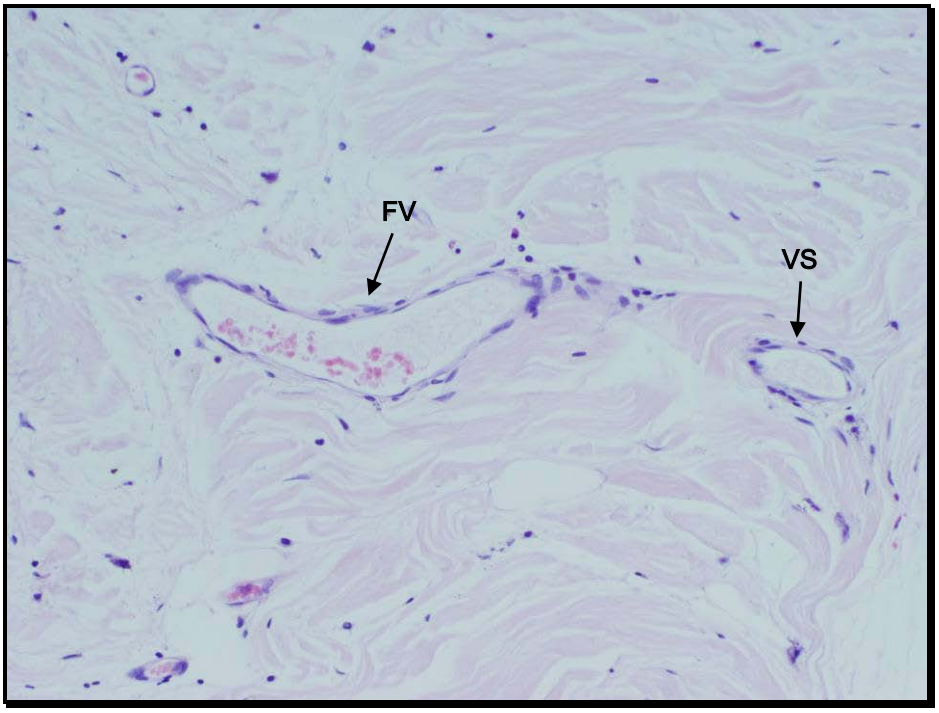

Figure 5.41 – Formed vessel (FV) and vessel sprout (VS) in a NonXL implant, 6 months post implantation (H&E, 200X).

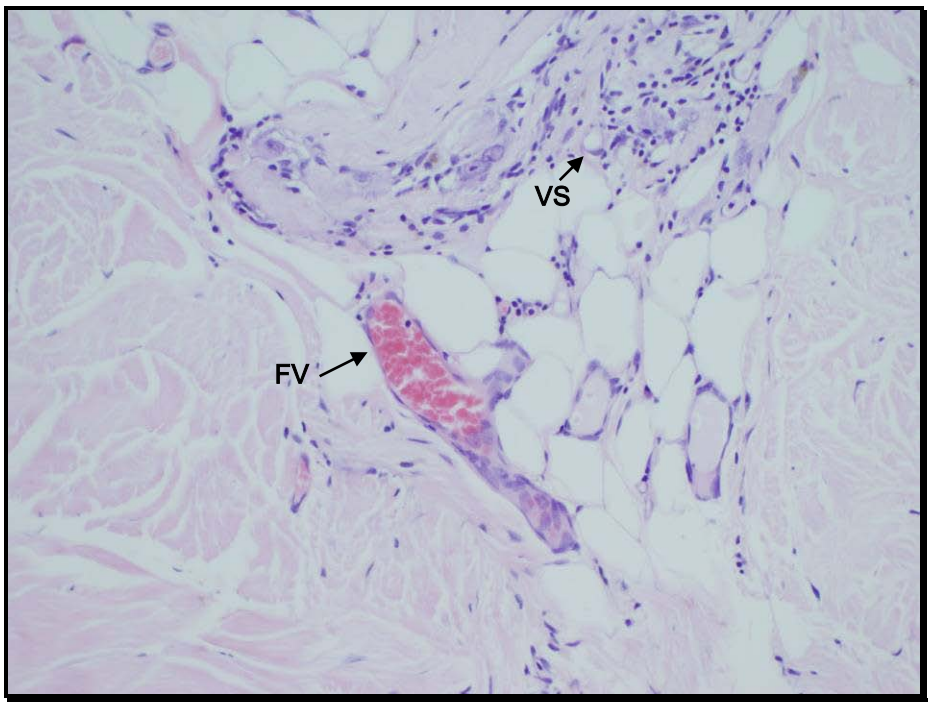

Figure 5.42 – Formed vessel (FV) and vessel sprouts (VS) in a Permacol® implant, 6 months post implantation (H&E, 200X).

One implant of the noncross-linked collagen matrix showed slight collagen degradation; despite this fact cells were still present in this area of the implant (Figure 5.43); the other 5 noncross-linked implants had naturally birefringent, non-denatured collagen. Normal, non-denatured collagen was observed in all Permacol® implants 6 months post implantation.

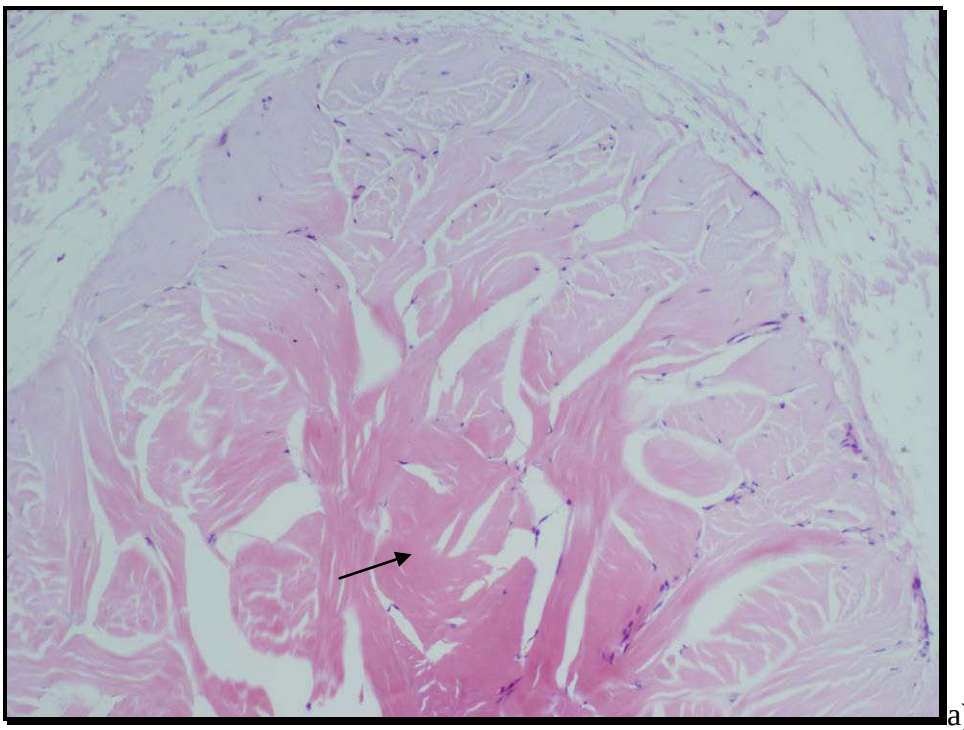

a)

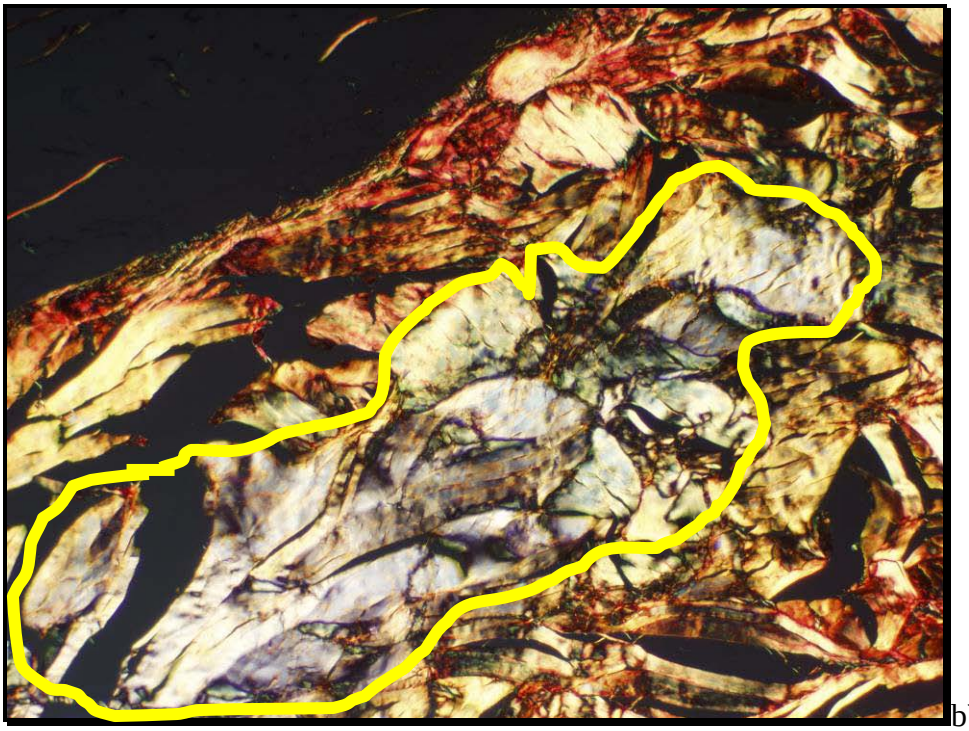

b)

Figure 5.43 – Degraded collagen in a NonXL implant, 6 months post implantation. a) Degraded collagen stained darker pink (H&E, 100X). b) Degraded collagen delimited by yellow line (Picro sirius red, 100X).

Noncross-linked and Permacol® implants showed low numbers of mast cells and one Permacol® implant had giant cells and macrophages at one aspect. Permacol® implants (4 of 6 implants) at 6 months post implantation showed mineralisation or early stages of mineralisation mainly in the centre of the implants (Figure 5.44).

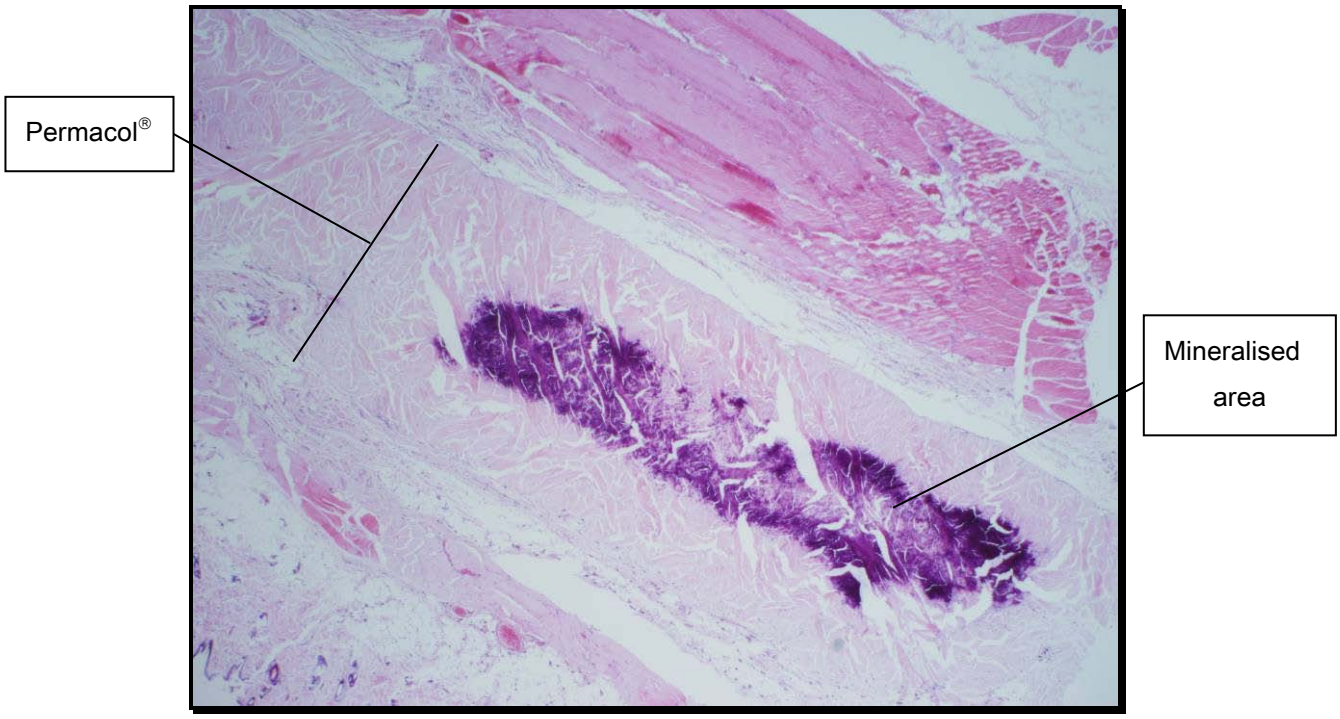

Figure 5.44 – Mineralisation in the centre of a Permacol® implant after 6 months implantation (H&E, 20X).

Interestingly there was not a cellular response to the mineralised area; no cells were visible surrounding the mineralised tissue, even in implants where the mineralisation was quite prominent (Figure 5.45).

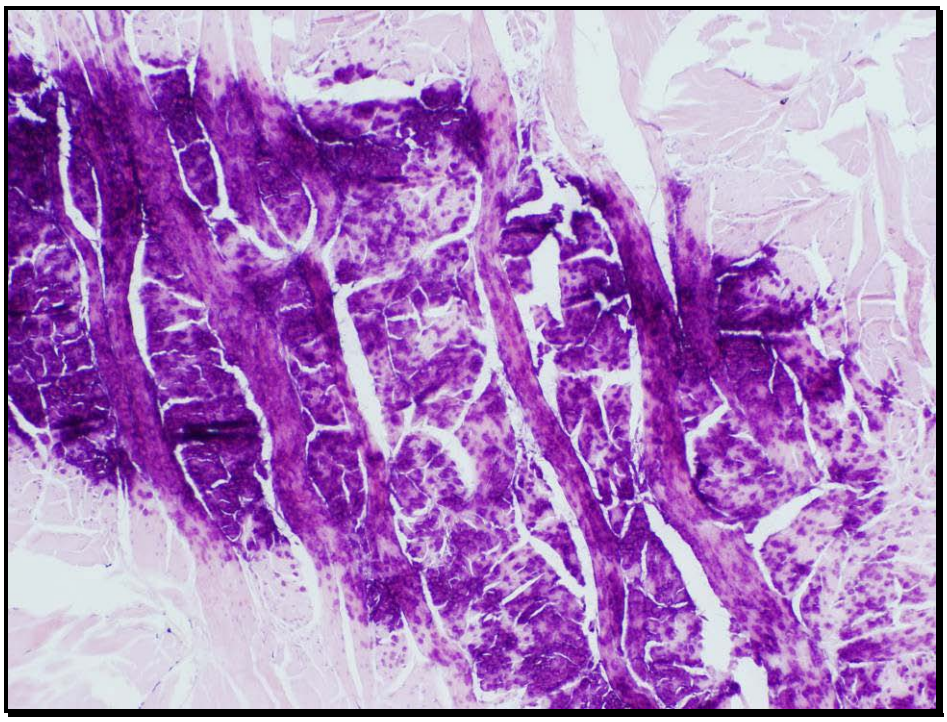

Figure 5.45 – Mineralised tissue in the centre of a Permacol® implant, 6 months post implantation, without a cellular response (H&E, 100X).

To identify the mineral deposits von Kossa's and Alizarin Red stains were performed. Connective tissue known to have calcium was used as positive control (Figure 5.46). Calcium deposits stain black with Von Kossa and when stained with Alizarin red calcium shows enhanced birefringence.

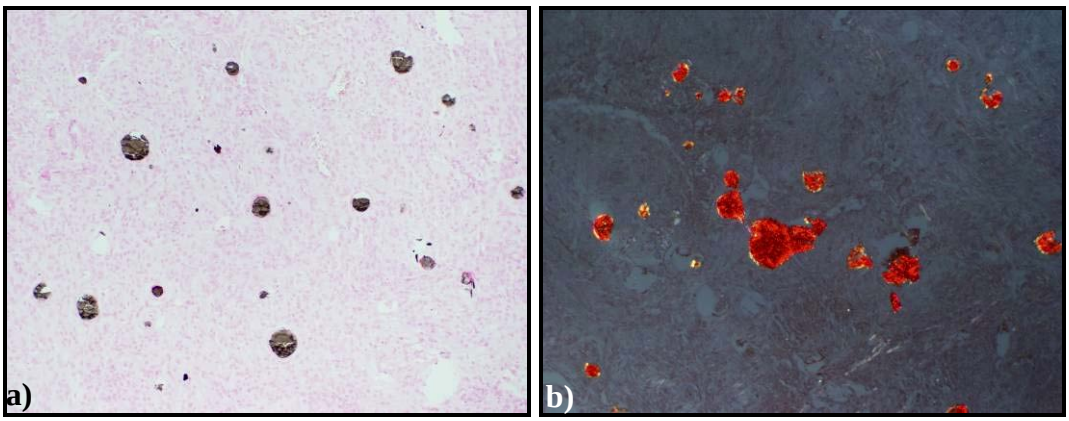

Figure 5.46 – Connective tissue with calcium deposits. a) von Kossa, 100X. b) Alizarin red S, 100X.

The unknown mineral present in the Permacol® implants was identified as calcium salts (Figure 5.47 and Figure 5.48).

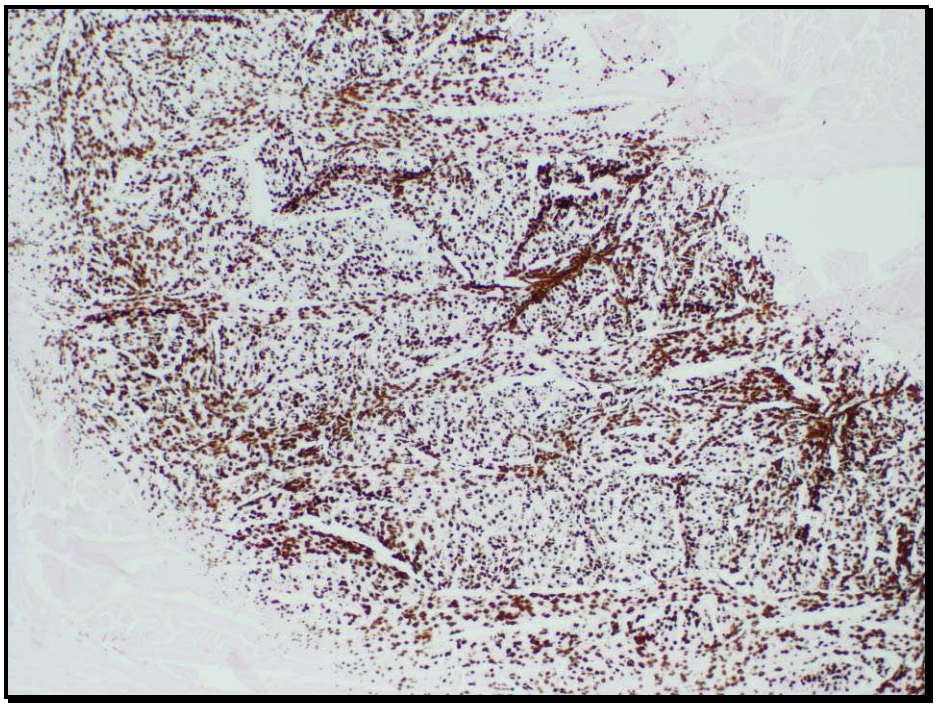

Figure 5.47 – Permacol® implants with calcium deposits (Von Kossa's, 100X).

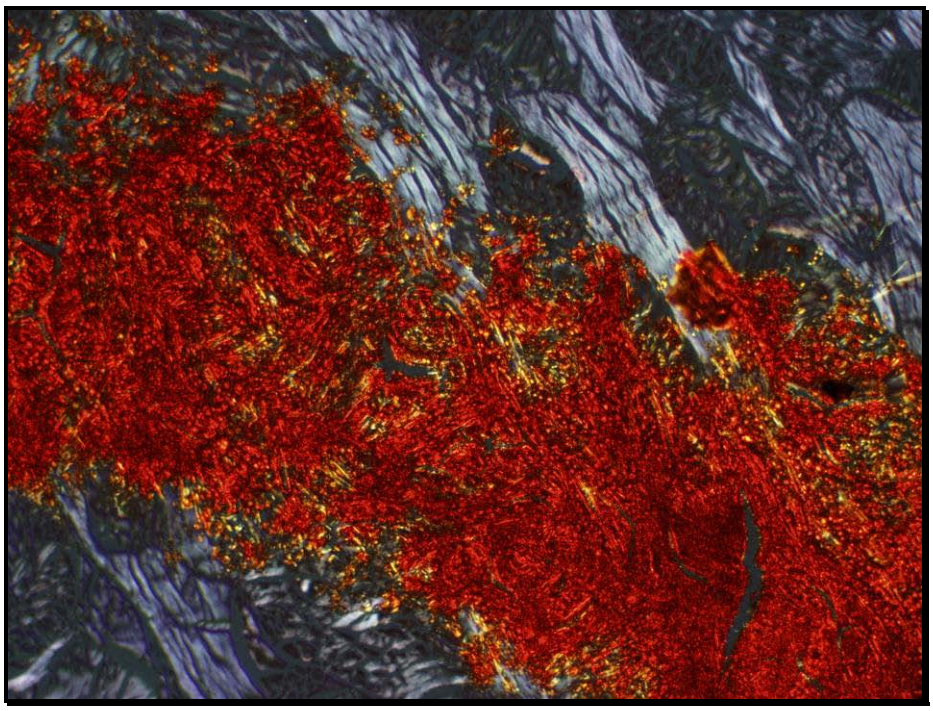

Figure 5.48 – Permacol® implants with calcium deposits (Alizarin Red S, 100X).

Figure 5.49 shows the results for the 6 months group. Mean and standard deviations were calculated for all parameters analysed.

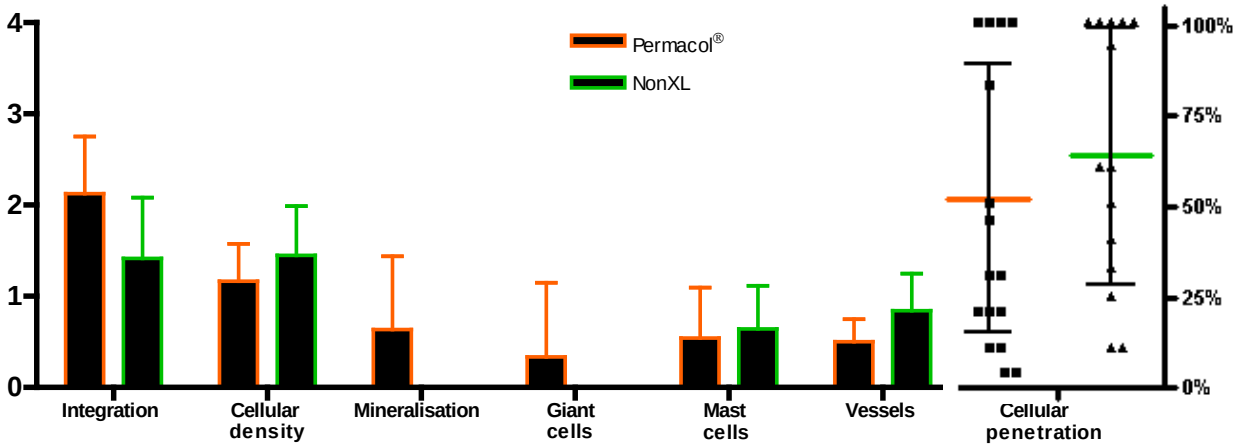

Figure 5.49 – Histometric scores for the 6 months group, according to the scoring criteria described in Table 5.2.

Group G3: 12 months

Implants were easily identified 12 months post implantation. Control group showed no sign of the surgical procedure, samples taken for histology showed perfectly healthy skin and abdominal wall.

No evidence of an inflammatory response was observed at this time point.

Permacol® surgical implants showed moderate integration with the surrounding tissue, fibrin micro-interdigitations were observed connecting the implant to the immediately adjacent host tissue (Figure 5.50). Noncross-linked collagen had minimal integration with the surrounding tissue (Figure 5.51).

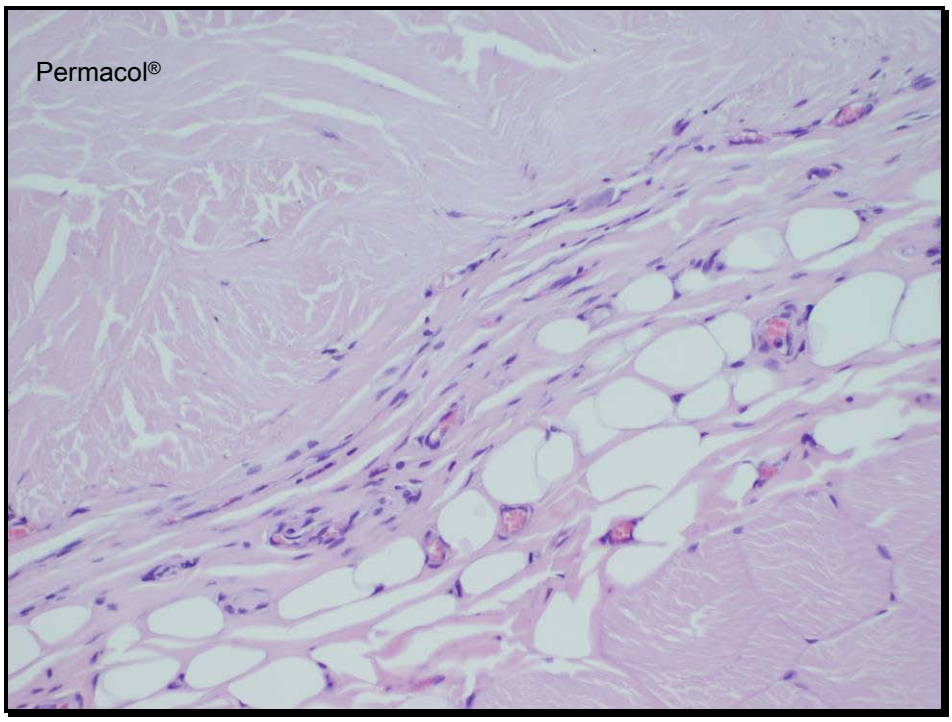

Figure 5.50 – Integration with surrounding tissue in a Permacol® implant, 12 months post implantation (H&E, 200X).

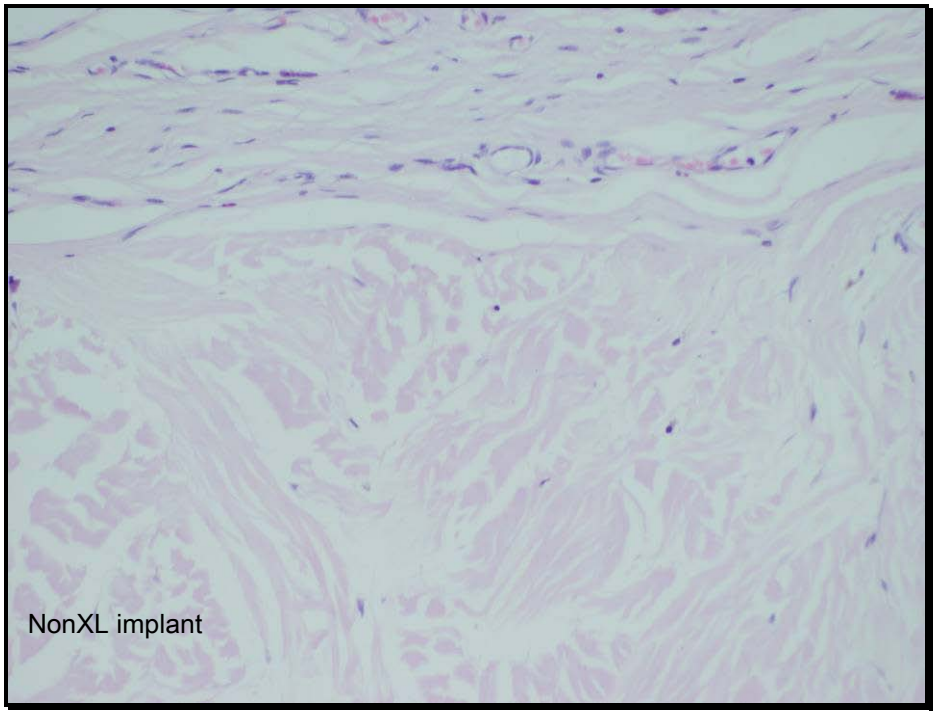

Figure 5.51 – Integration with surrounding tissue in a noncross-linked implant, 12 months post implantation (H&E, 200X).

Cellular density was minimal in Permacol® implants and cells penetrated 100% in depth all implants (Figure 5.52). Although cellular penetration reached 100% in the noncross-linked implants, cellular density was marginal in 3 implants and minimal in the other 2 (Figure 5.53).

Cells were seen more often within the matrix than in the natural fissures between the collagen fibres.

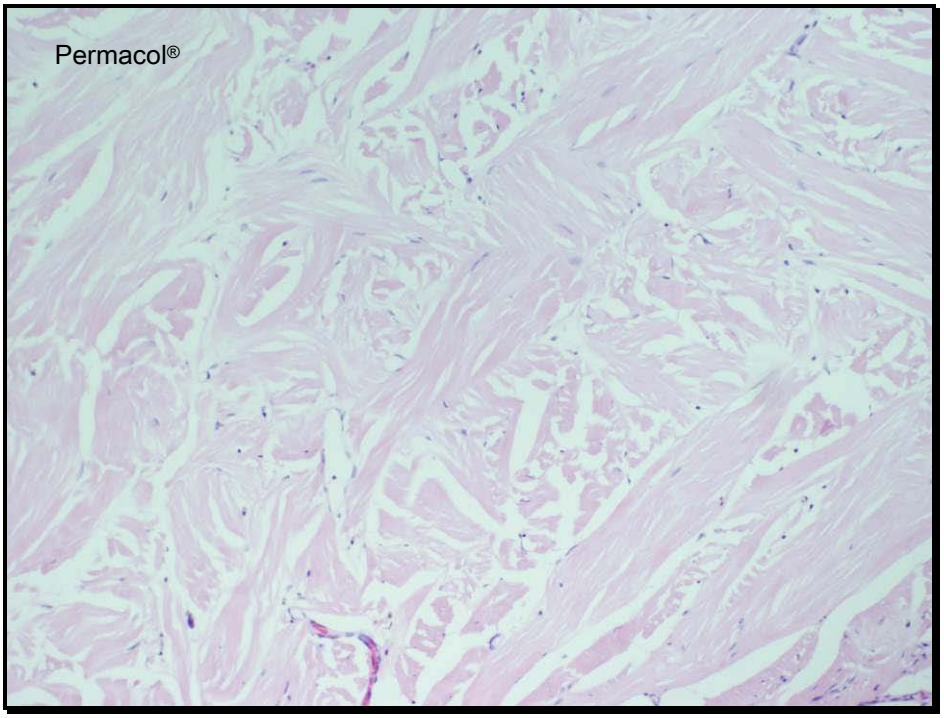

Figure 5.52 – Minimal cellular density in a Permacol® implant, 12 months post implantation (H&E, 100X).

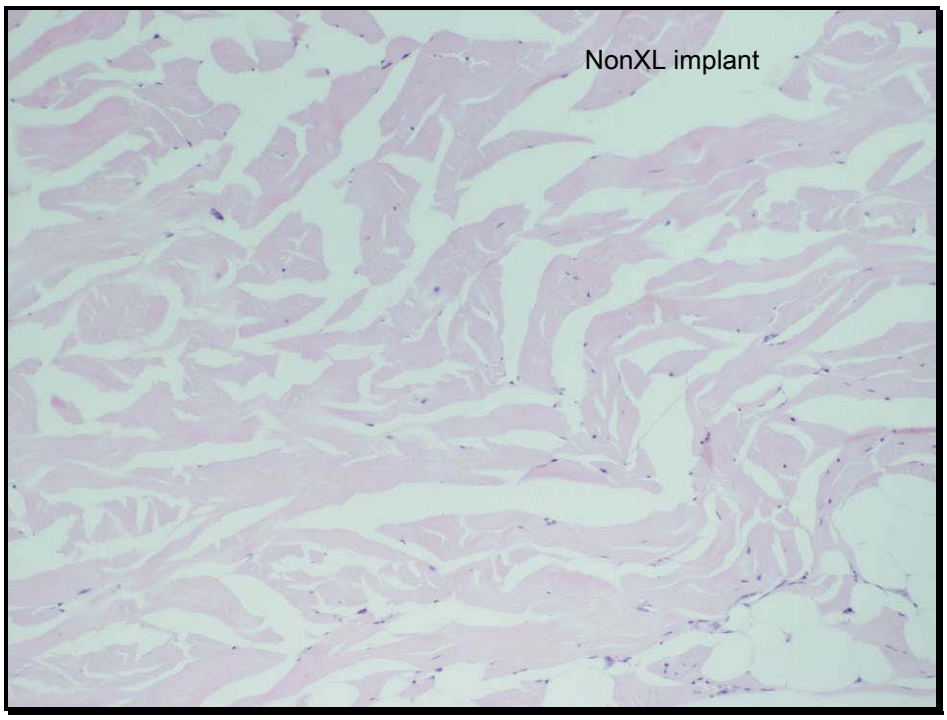

Figure 5.53 – Marginal cellular density in a noncross-linked implant, 12 months post implantation (H&E, 100X).

One Permacol® implant showed lymphocytes and giant cells surrounding an artefact (Figure 5.54); under polarized light (image in the corner) it was possible to confirm that the artefact did not belong to the implant and was probably remains of a swab.

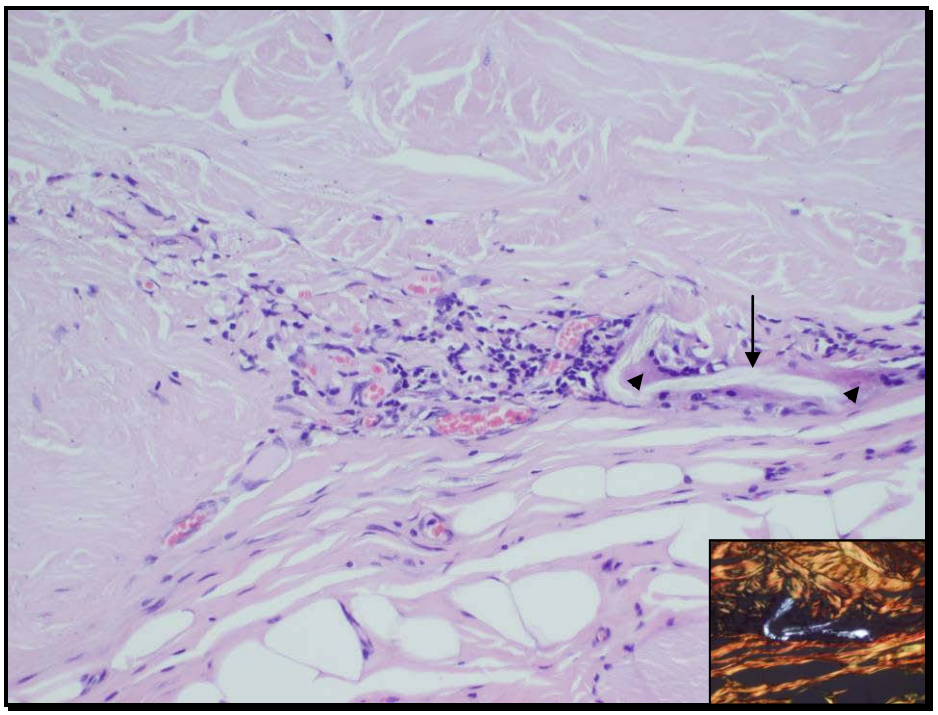

Figure 5.54 – Lymphocytes in one aspect of a Permacol® implant, in their proximity an artefact (arrow) is being ingested by giant cells (arrow heads) (H&E, 200X).

Mast cells were observed at low numbers in 3 Permacol® implants and in 2 non-cross-linked collagen implants (Figure 5.55); these findings suggest a foreign body response, although leukocytes numbers were low.

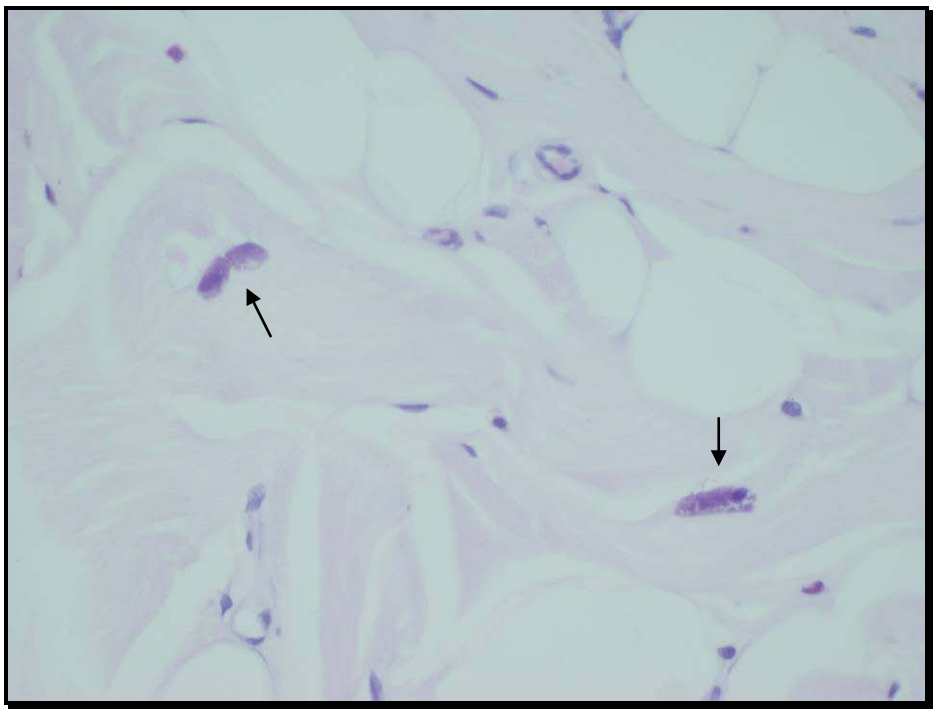

Figure 5.55 – Mast cells in a noncross-linked implant (H&E, 400X).

Mature vessels and vessel sprouts were observed at marginal values in the centre of Permacol® implants to support cellular density and in minimal values at the edges (Figure 5.56). Noncross-linked implants showed less vascularisation and vessels were observed mainly at the edges of implant.

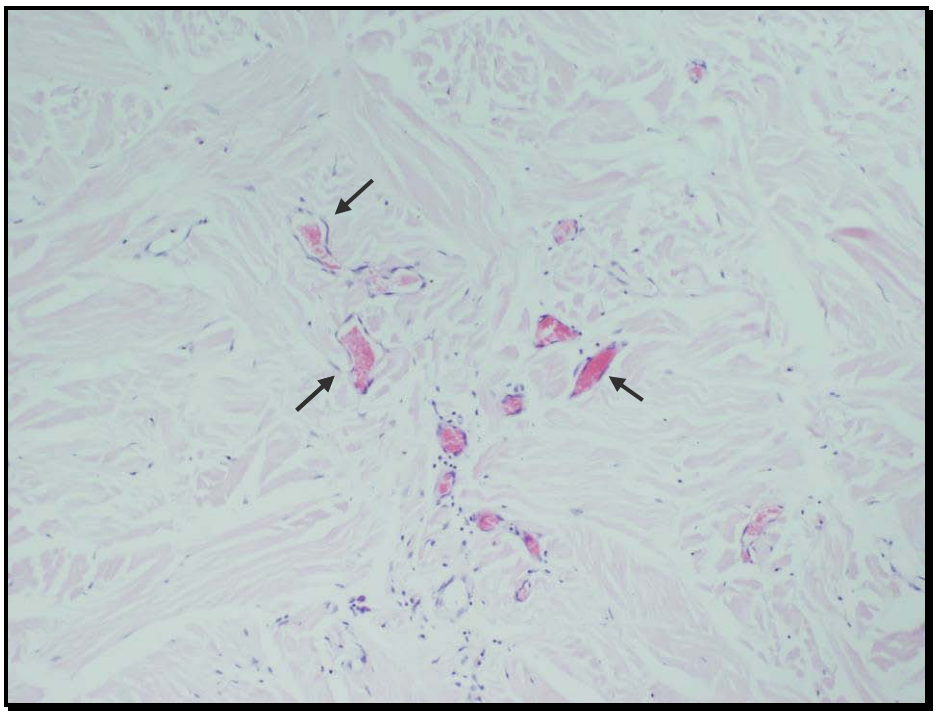

Figure 5.56 – Vessels in the centre of a Permacol® implant, 12 months post implantation (H&E, 100X).

One Permacol® implant showed an interesting feature of integration at one extremity; fragments of collagen were separated (not digested or remodelled) from the main matrix and were integrated within the surrounding tissue (Figure 5.57). Nearby, macrophages and a giant cell were present.

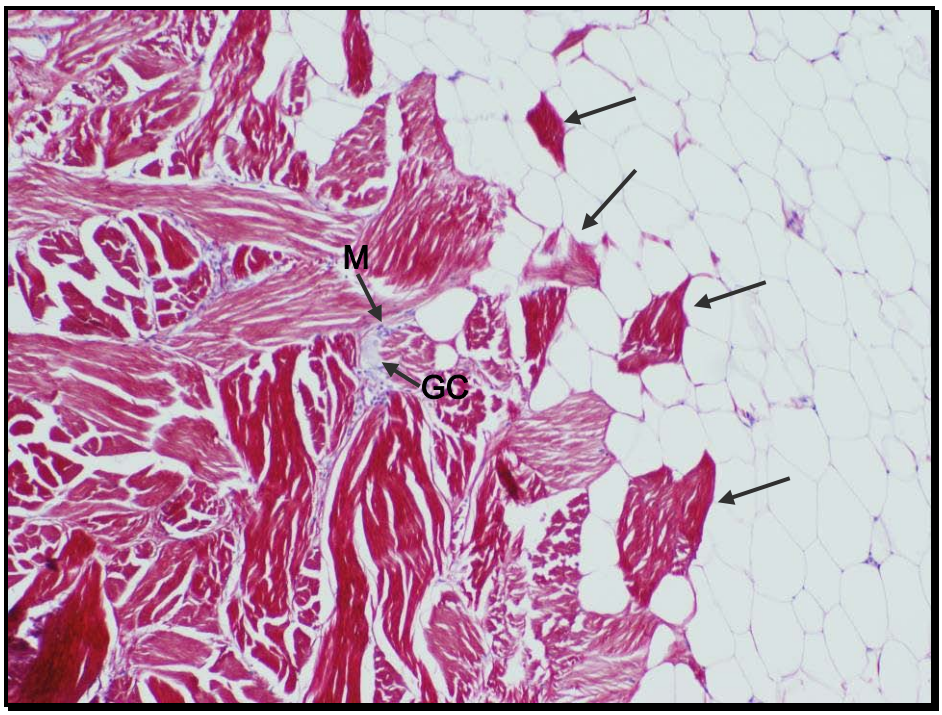

Figure 5.57 – Fragments of a Permacol® implant separated from the matrix and integrated within surrounding tissue (picro sirius red, 100X). Macrophages (M) and a giant cell (GC) were observed within the matrix.

In the same Permacol® implant mineralisation was present distributed through 3 main focuses (Figure 5.58), mineral deposits were concentrated in the centre of the matrix and covered approximately 10% of the implant. This was the only implant showing mineral deposition 12 months post implantation.

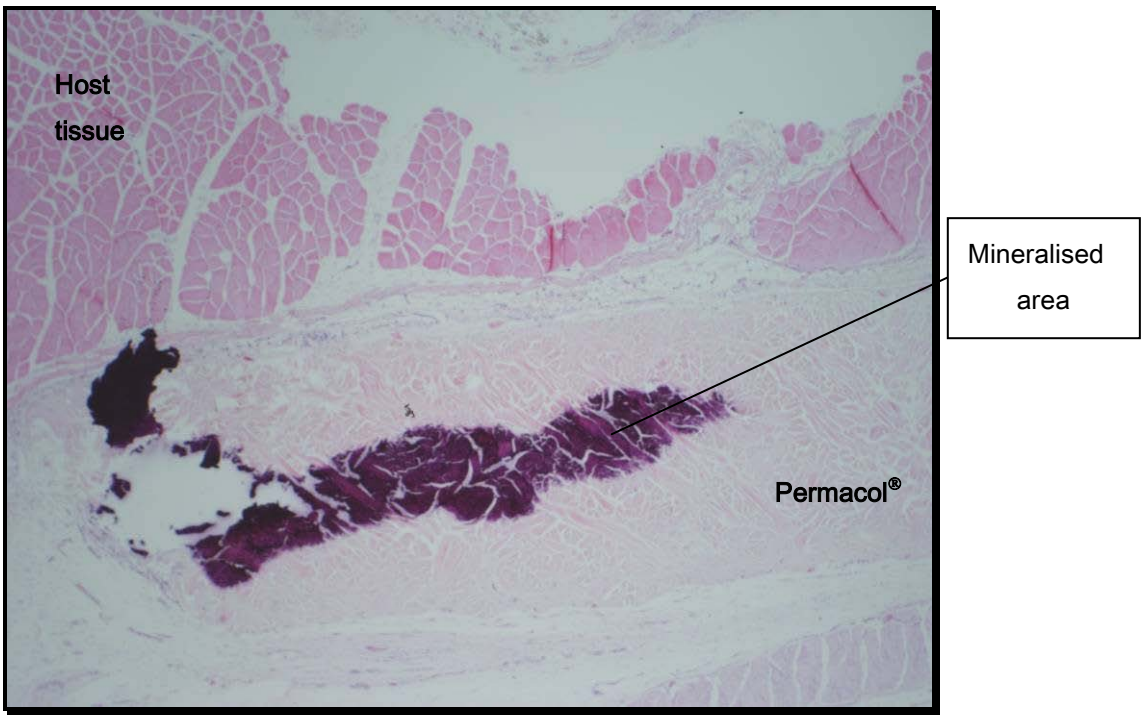

Figure 5.58 – Mineralisation in a cross-linked implant, 12 months post implantation (H&E, 20X).

As observed before mineralisation was not detrimental to cellular density and did not caused an immune or inflammatory response. In addition, collagen was not degraded under the mineral deposits (Figure 5.59).

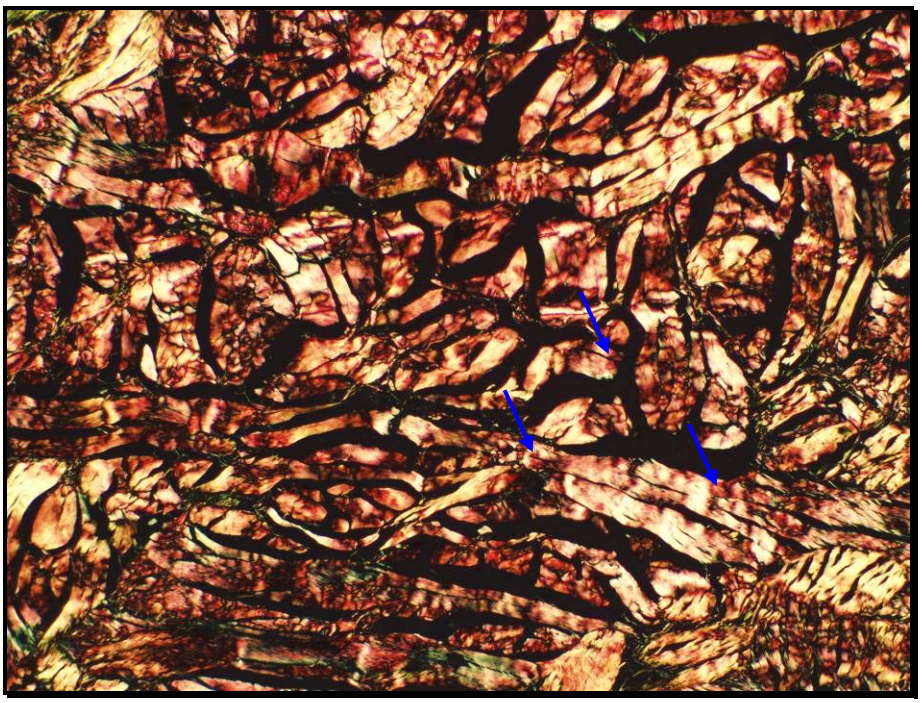

Figure 5.59 – Good quality collagen in a cross-linked implant despite of calcium deposits in the matrix (blue arrows) (picro sirius red, 100X).

Implants did not show evidence of collagen degradation in group G3, independent of the type of matrix. Although, NonXL implants showed a decrease in implant thickness and the edges of the implants were rounder when compared to Permacol® implants, suggesting some absorption of the collagen.

Figure 5.60 shows the results for the 12 months group. Mean and standard deviations were calculated.

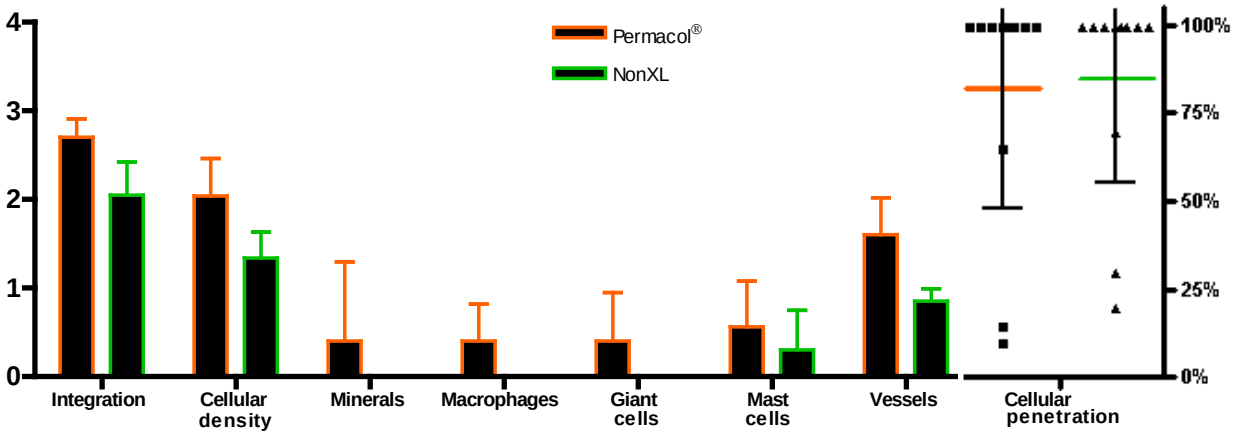

Figure 5.60 – Histometric scores for the 12 months group, according to the scoring system described in Table 5.2.

The next table shows the results from the statistical analysis; NS stands for a non significant difference. Integration was statistically significant for both factors – implant type and implantation time – but the interaction between factors was not significant, *i.e.*, the biomaterials did not respond differently through time.

Table 5.9 – Statistical results for both implant types throughout the study.

	Integration	**Cellular density**	**Cellular penetration**	**Macrophages**	**Vessels**
Type of matrix	P<0.05	NS	NS	NS	NS
Time	P<0.05	NS	P<0.05	P<0.001	P<0.05
Implantation site * Time	NS	P<0.01	NS	NS	P<0.01

The factors tested showed a significant interaction for cellular density, meaning that matrices types were populated in a different way along the study, this trend is graphically represented in the next figure , while cellular density increased over time in Permacol® implants, the opposite was observable in the NonXL implants.

Cellular penetration was not significantly different between implants variants along the study, but the 12 months group was significantly different when compared to the other groups.

Macrophage presence and neo-vascularisation were statistically different between time points, in specific groups 3 months and 12 months respectively. Vessels presence showed interaction between implant type and time points.

Figure 5.61 to Figure 5.63 show comparison between the 3, 6 and 12 months results. The mean and standard deviation were calculated for each parameter analysed.

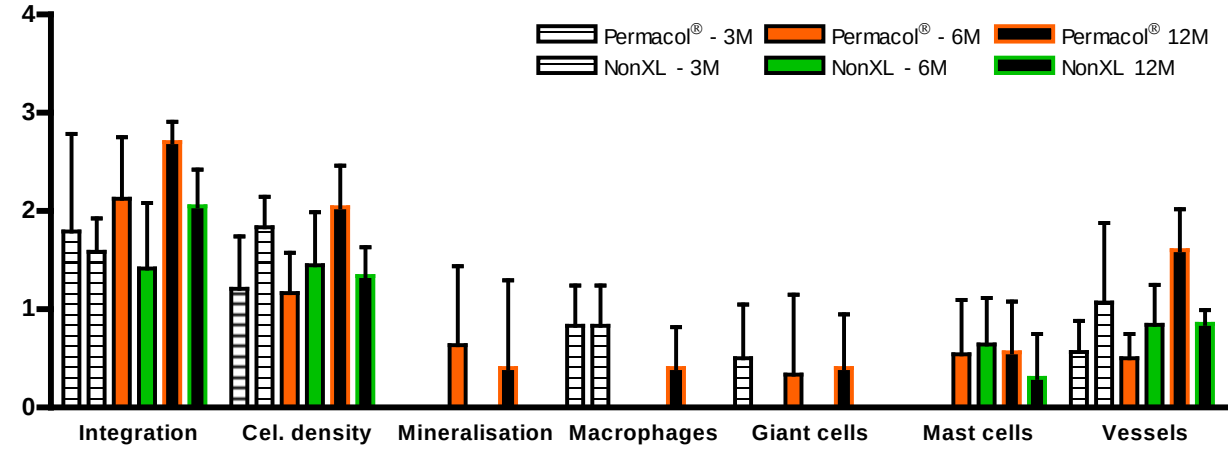

Figure 5.61 – Comparison between results of all groups. Scoring system used as described in Table 5.2.

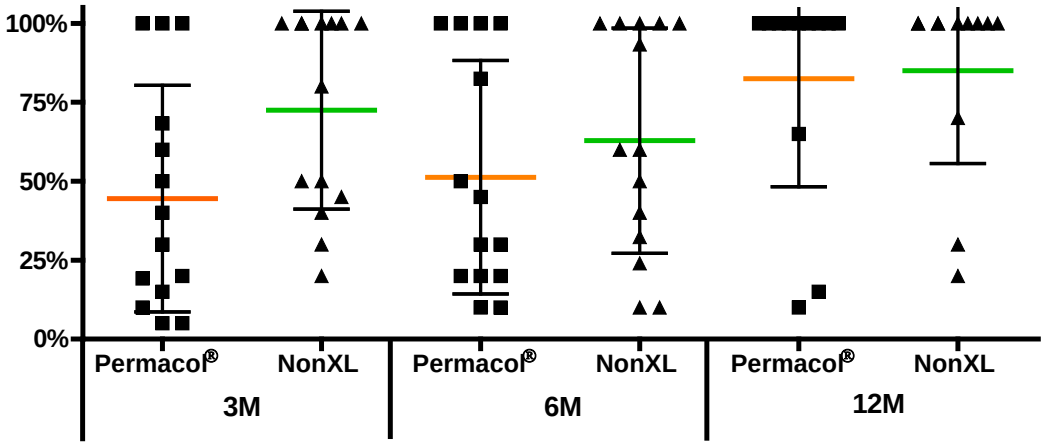

Figure 5.62 – Cellular penetration throughout the course of the study. Mean values, for both minimal and maximal cellular penetration, were used per animal.

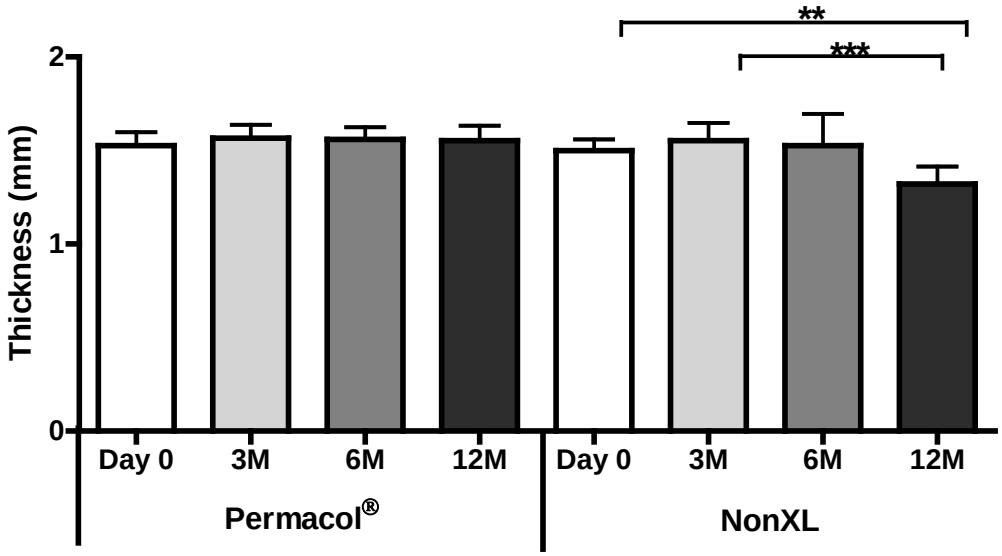

Figure 5.63 – Implants thickness along the study. ** P<0.005, *** P<0.001.

5.2.7.3 Scanning Electron Microscopy

Since it was difficult to visualize if the calcium salts, found in the mineralised implants, were deposited on top of the collagen fibres or if they were integrated with the fibres, scanning electron microscopy (SEM) was performed on those samples.
Secondary electron imaging showed mineral deposits on the collagen fibres (Figure 5.64), non-implanted Permacol® was used as control. INCA program was used to identify the composition of the mineralised samples (Figure 5.65).

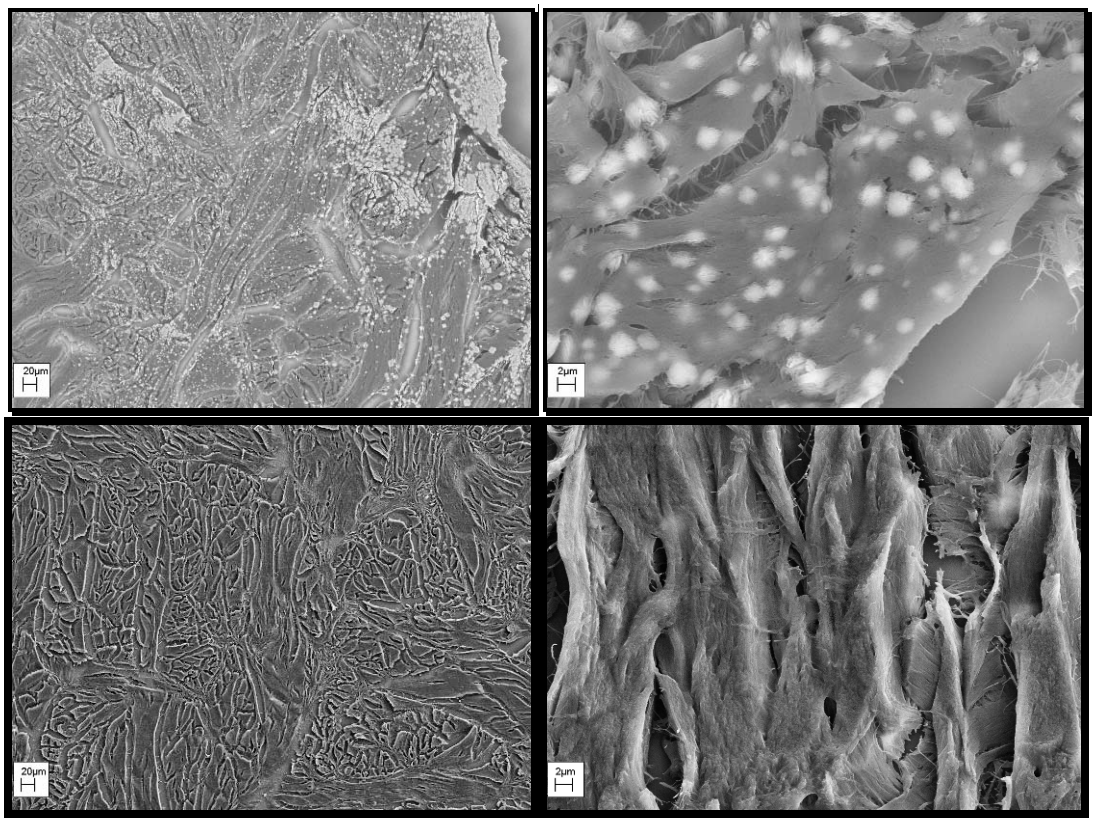

Figure 5.64 – Secondary imaging analysis of Permacol® surgical implant. Top row shows a mineralised implant 6 months post implantation, in a rat model, and the bottom row shows control, non-implanted, Permacol® (SEM, left column: 500X, right column: 6000X).

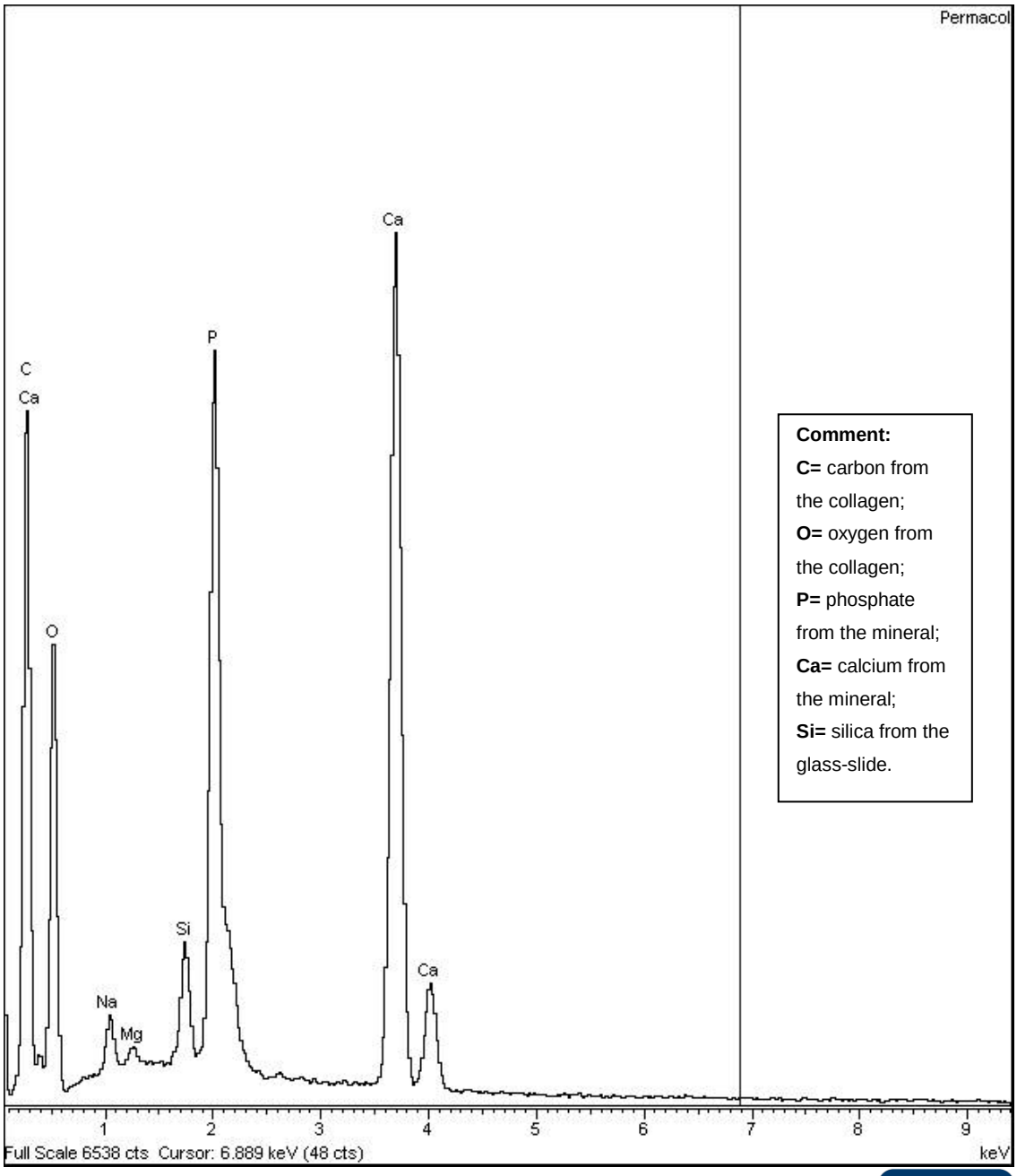

Figure 5.65 – Components analysis of the mineralised samples.

Backscattered electron imaging was performed to localize each of the elements found during the composition analysis (Figure 5.66).

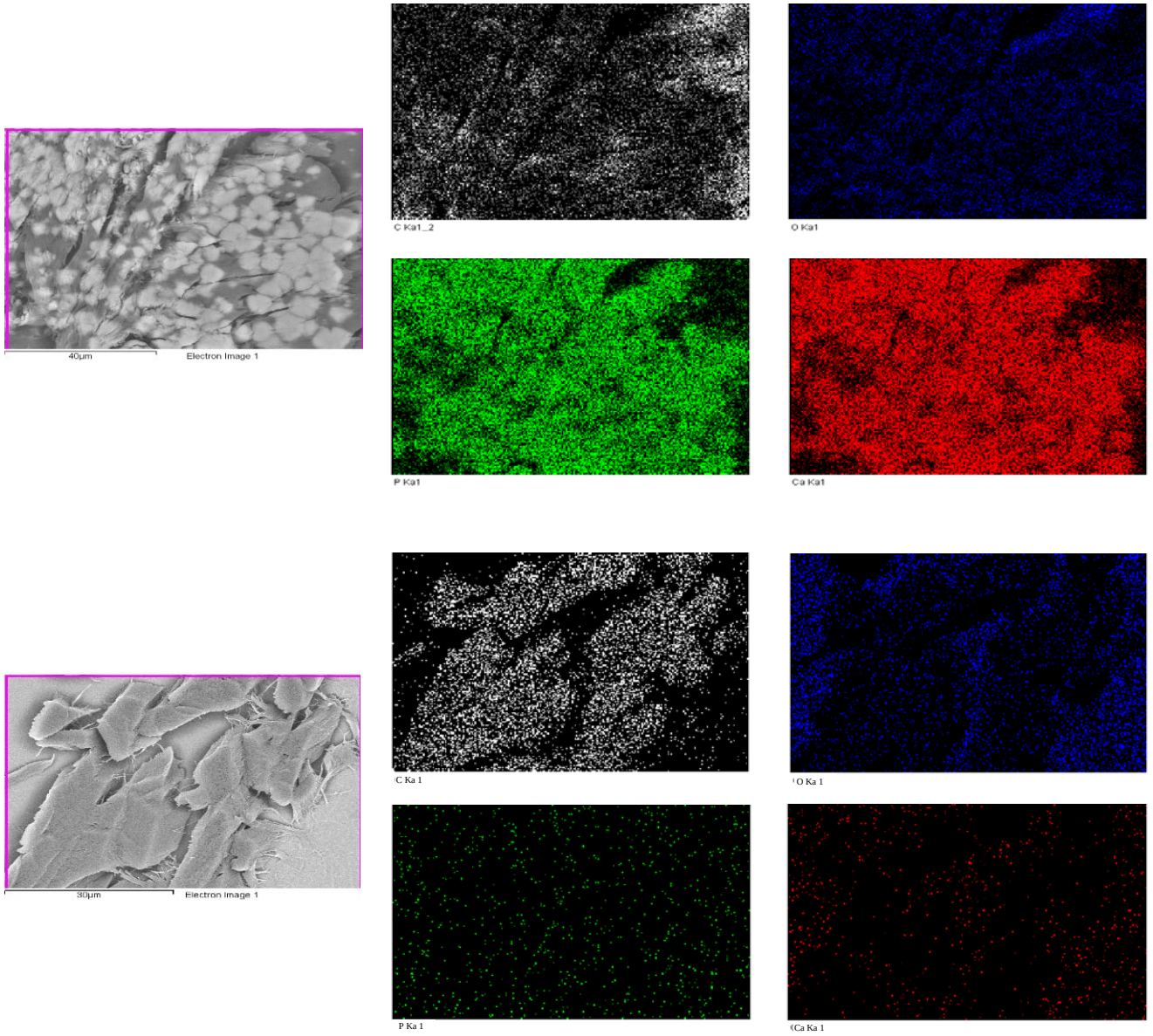

Figure 5.66 – Backscattered electron image analysis of Permacol® surgical implant. Top five images refer to a mineralised implant 6 months post implantation; the bottom five images are the control tissue – Permacol® not implanted.

Legend:

White C= carbon from the collagen

Blue O= oxygen from the collagen

Green P= phosphate from the mineral

Red Ca= calcium from the mineral

The elements present in the mineralised areas were calcium and phosphate, confirming that this mineral is hydroxyapatite.

5.2.8 Discussion

The range of biomaterials commercially available for treatment, augmentation and replacement of lost or damaged tissues markedly increased in the past decade. An ideal biomaterial should be biocompatible, non-toxic, allow formation of strong new host tissue in the defect with good aesthetic results, offer a rapid recovery time, be easily manipulated and adjustable to body surfaces, provide adequate correction without migration, provide tissue bulk where required and be long lasting yet able to be removed if necessary.

This study evaluated Permacol® surgical implant suitability as a subcutaneous implant for soft tissue repair and as a bulking material. Additionally, the effect of cross-linking in Permacol® was assessed by comparing the end-product with the product before the cross-linking process (noncross-linked acellular collagen).

The apparent reduction in cellular presence between 3 months and 6 months post implantation was intriguing. Although at 6 months post-implantation both matrices showed a slight decrease in cellular presence, the maximum tensiometer loads at failure were higher than those of 3 months post-implantation demonstrating good strength of integration. Statistically there was not a significant difference for the tensiometry results between both matrices tested. Histopathology showed that integration with the surrounding tissue increased slightly at 6 months post implantation in the Permacol® implants but this trend was not observable for the noncross-linked samples. Cellular density decreased again at 12 months post implantation for noncross-linked implants but cellular penetration increased. Permacol® showed an increase both in cellular density and penetration at 12 months post implantation.

Cellular ingrowth failure in Permacol® implants has been reported by other authors (MacLeod *et al.*, 2005; Valentin *et al.*, 2006) and the cross-linking process was suggested as one of the causes for the paucity of cellular penetration and cellular

density. If this was true, we would expect noncross-linked implants to show a higher extent of cell penetration since the trypsinisation process used to decellularize the matrix should leave the implant more permeable to cellular infiltrates.

Integration with surrounding tissue increased for both matrices in group G3, suggesting that at long term implants are incorporated by the host although remodelling of collagen was not observed. There was no significant variation in Permacol® implants thickness throughout the study, suggesting that implants maintained their volume when implanted subcutaneously. This result is consistent with those of Kelley and colleagues; they implanted Permacol® subcutaneously in a mouse model and reported that volume and weight of implants remained unchanged for 12 months (Kelley *et al.*, 2005). Noncross-linked implants had significant difference in thickness at 12 months post implantation (compared to the other time points), so it is likely that with time these implants are absorbed since they lack cross-linking.

Cellular penetration was greater in the noncross-linked implants, even in the implant where a fibrous layer was visible between the implant and host tissue. Fibrous encapsulation was described by Valentin and co-workers as a host response to Permacol® surgical implant over a 112-day study (Valentin *et al.*, 2006); however, in the study reported here this feature was not observed over a period of 12 months.

Macrophages and giant cells were observed at 3 months post implantation in 5 and 3 of the 6 Permacol® implants, respectively; these values decreased at 6 months but macrophage presence increased once more 12 months post implantation. The presence of macrophages and giant cells are usually related to non-immunological foreign body reactions, although their presence can also be activated by immunological factors such as low toxicity organisms, infection and in hypersensitivity reactions. Macrophages are the main cell present in a chronic inflammatory reaction and are usually accompanied by lymphocytes and plasma cells, the last two cell types were not present in numbers that would indicate a chronic inflammatory reaction.

Mast cells were observed at 6 and 12 months post implantation in both matrices. These cells are a tissue-based inflammatory cell of bone marrow origin that is associated with innate and acquired immunity with immediate and delayed release of inflammatory mediators (Prussin and Metcalfe, 2003). In the skin, mast cells appear in higher number near blood vessels, hair follicles, sebaceous glands and sweat

glands. Human skin contains approximately 10,000 mast cells per cubic millimetre (Metcalfe *et al.*, 1997).

The presence of macrophages and mast cells suggest a cellular reaction, but their low numbers do not seem to be related to an inflammatory response.

Collagen degradation and implant remodelling were not observed in either type of collagen matrices at the time points investigated, except for a small degree of collagen degradation in one noncross-linked implant. Noncross-linked implants showed a decrease in thickness after 12 months implantation, which may be related to implant absorption, although there was no cellular evidence of that. Macleod and co-workers reported some evidence of absorption over a 20 week period study where Permacol® was subcutaneously implanted in a rat model; they have also described poor vascularisation of the implants after 2 weeks implantation (MacLeod *et al.*, 2005). In the study reported here, absorption of the implants was not observed and both matrices tested showed minimal vascularisation both at the edges and centre of the implants, inclusive at 12 months post implantation.

Mineralisation (calcium deposits) was observed in 4 of 6 Permacol® implants at 6 months post implantation and in 1 implant at 12 months. This phenomena has been observed before in another in-house study and was also reported by Kelley and colleagues (Kelley *et al.*, 2005). Since mineral deposition was not observed in any of the noncross-linked implants the results suggest that mineralisation may be associated with the cross-linking process. Although some cross-linking agents are known to cause mineralisation (eg. glutaraldehyde), currently available literature supports hexamethylene diisocyanate (HMDI), the cross-linking agent used in Permacol®, as not causing mineralisation (Friess, 1998; Oliver and Grant, 1995).

HMDI may not be the direct source of mineralisation but may cause it in the course of the structural changes induced by cross-linking. Since cross-linking increases the number of chemical bonds between the collagen fibres, the protein fibres lose some of their ability to move as individual chains; mineralisation may occur as a result of this new configuration, which may somehow impede the flow of the minerals/salts present in the interstitial fluid thus causing retention of these elements within the implants. Or, if the interstitial fluid does not easily flow through the implant, the implant may eventually dry in the centre, although the tests performed in Section 3.3 showed that

interstitial fluid was able to go through Permacol®, including at the centre. Nevertheless, that experiment was carried out only for 3 days.

SEM studies showed that non implanted Permacol® did not have calcium or phosphate deposits, which refutes the hypothesis that mineralisation occurs due to the cross-linking process itself. The SEM results support the hypothesis of mineral deposition *in situ* over time, especially since the mineral was found to be hydroxyapatite, a common mineral in bone ECM. ECM mineralisation is a physiological process in growth plate cartilage, teeth and bone; when present in any other body parts it is considered a pathological process. Hydroxyapatite contains calcium (Ca) and inorganic phosphate (Pi) ions and is deposited both within and between collagen fibrils. When studying ectopic mineralisation Murshed and co-workers discovered that the extracellular concentration of Pi and the concentration of ECM mineralisation inhibitors are prime factors for ECM mineralisation (Murshed *et al.*, 2005). If Permacol® calcification was a consequence of a cellular response, Pi extracellular concentrations would increase in the body and ECM mineralisation should be seen in both implant types as well as in other body parts, which has not been observed here. This suggests that tissue/cellular response to the implant was not the cause for the presence of calcification.

When mineralisation was observed at 6 months it was thought that it would increase long term but this was not the case in the study reported here. At 12 months only one of five Permacol® implants showed mineralisation; it is not known if mineral deposition decreases over time or if the other four implants belonging to group G3 had ever been mineralised.

Interestingly, mineralisation did not cause any immune or inflammatory response from the host. Despite the cellular paucity in samples with calcium deposits, there was no adverse effect in any of the surrounding tissue and the implant/host complex was retained without detriment. This suggests that Permacol® mineralisation is not detrimental to its performance *in vivo*. Implant mineralisation increases matrix rigidity which, depending on the site of implantation, may not be desirable for aesthetic purposes. Apart from this study, to the author's best knowledge, the only known long-term *in vivo* study with Permacol® (published to date) was performed with mice for 12 months by Kelley and co-workers (Kelley *et al.*, 2005). They reported dystrophic calcification and bone formation at 12 months. The implantation site may be a pre-

requisite for mineralisation occurrence; in the study presented here and in Kelley and colleagues reported study, Permacol® was implanted subcutaneously in a considerable stable and stationary position, this factor may be a cause for mineralisation. If implants were under regular motion or pressure, the results might be entirely different.

5.2.9 Conclusion

In the rat model reported here, Permacol® and noncross-linked acellular collagen showed similar results for integration with surrounding tissue and cellular population. Even after 12 months implantation, matrices did not show degradation, breakdown or remodelling of the collagen, except for 1 noncross-linked implant that presented some collagen degradation at 6 months. The noncross-linked matrix also showed some loss of implant thickness at 12 months post implantation which may be related to collagen absorption.

Results imply that the number of cells in the implant does not influence the level of penetration since there were several implants with a low cellular density but with cells penetrating 100% in depth of the implant.

The majority of the neo-vascularisation was found in the borders of the implants, all implants showed vessel sprout presence and fully formed vessels were observed in twenty two of the twenty three implants.

This study has demonstrated that cross-linking is not detrimental to the general *in vivo* performance of Permacol® with respect to tissue integration, biocompatibility, cellular penetration, cellular density, neo-vascularisation and cellular apoptosis. In general, cellular response was similar in both matrices, disproving the hypothesis tested in this study.

5.3 IMPLANTATION SITE INFLUENCE IN IMPLANT CELLULAR RESPONSE IN A RODENT MODEL

5.3.1 Introduction

During the last decade, tissue engineering has been increasingly discussed as a promising option to circumvent the limitations of existing techniques for tissue reconstruction. To improve wound healing, skin substitutes and biomaterials have been systematically investigated.

Permacol® surgical implant has been used in most of the major surgical specialities and since 1998 has been used in over 100 different types of procedures (Harper, 2001; Liyanage *et al.*, 2006). However, some *in vivo* studies have shown that there can be significant variability in cellular density and cellular penetration and subsequent vascularisation of Permacol®. Some authors believe that the pore size of a biomaterial is critical to its performance, Macleod and colleagues used the diamond CO_2 laser to treat Permacol® surgical implant and assess if by increasing the porosity of the matrix the rate and degree of vascularisation of Permacol® would be enhanced (MacLeod *et al.*, 2004c). They found that while laser treatment encouraged fibrovascular ingrowth into the new pores (made by laser), the surrounding untreated matrix remained poorly vascularised. Since matrix cellular density was not altered by laser treatment it was hypothesized that cellular response to Permacol® may depend on the site of implantation and the relative vascularity of surrounding host tissue.

Adult muscle is highly vascularised, with copious blood vessels being essential for adequate oxygenation of the tissue and for supporting increased metabolic demands. The vascular system is structured to optimize tissue support through the processes of convection and diffusion. Simply described, the large vessels of the systemic circuit allow bulk flow delivery to the small vessels within a muscle, at high pressure. The small vessels modulate flow distribution to the capillary network bathing the cells. The capillary network, in turn, allows diffusive exchange between the vascular vessels and the intracellular area of the muscle fibres. Blood flow can change nearly 100-fold

from rest to maximal aerobic exercise (Prior *et al.*, 2004). The contractile activity of skeletal muscle fibres increases capillary perfusion, which enables dilation of the terminal arterioles increasing the capillary surface area for diffusion and consequently promotes the extraction of available oxygen (Segal, 2005).

The function and high vascularity of skeletal muscle makes it an ideal candidate for Permacol® implantation when testing for cellular response dependent on surrounding tissue vascularisation.

Another highly vascularised organ is the liver. The liver receives its blood supply from the hepatic artery and the portal vein before these vessels narrow into many small branches with close association to the biliary tree. The association of these vessels, hepatic artery, portal vein and bile duct, is named the portal tract. Each intra-hepatic bile duct is accompanied by a branch of the hepatic artery and is surrounded by a well-developed vascular network, *i.e.*, the peribiliary vascular plexus (Masyuk *et al.*, 2003). Terminal branches of the hepatic portal vein and hepatic artery drain together and combine as they enter sinusoids in the liver. Sinusoids are distensible vascular channels lined with highly fenestrated or "holey" endothelial cells and bounded circumferentially by hepatocytes (Young *et al.*, 2006). Liver architecture allows blood to flow through the sinusoids and empty into the central vein of each lobule; therefore, blood flows constantly from the portal tract to the hepatic venules, making this organ a highly vascularised tissue.

This study was designed to further understand Permacol® and host tissue interaction by Permacol® implantation into two highly vascular sites, liver and muscle.

5.3.2 Hypothesis

Implantation site has an effect on the cellular response and general performance of Permacol® surgical implant.

5.3.3 Aims and Objectives

- Study the biocompatibility and *in vivo* performance of Permacol® surgical implant in two significantly vascular sites, in a rodent model.
- Compare Permacol® surgical implant performance in sites with high vascularity to its performance in subcutaneous location in the rat.

5.3.4 Materials and Methods

Permacol® surgical implant was supplied by TSL plc. as 5cm x 5cm sheets with 1.536 ± 0.072mm thickness. Permacol® surgical implant, for all implantations, was derived from the same batch to eliminate variations.

5.3.4.1 Study Design

Male Sprague-Dawley™ rats were used with weights between 300 and 400g. Two treatment groups were constructed and divided between 3 time points. This resulted in a total of 16 animals for the complete study as in Table 5.10.

Table 5.10 – Study groups and time point design.

Termination time point						
Months	**3**		**6**		**12**	
Group	**M1**	**L1**	**M2**	**L2**	**M3**	**L3**
Animals	**3**	**3**	**3**	**3**	**2**	**2**

Permacol® surgical implant was implanted in the scalenus posterior muscle in groups M1, M2 and M3 and into the liver in groups L1, L2 and L3.

5.3.4.2 Surgical Procedure 1

1. Rats from group M were induced to and maintained under general anaesthesia.
2. A dorsal cranio-caudal skin incision was made just lateral to the spine from a point 1cm distal to the edge of the scapula extending approximately 1.5cm distally.
3. The scalenus posterior muscle was identified.
4. The scalenus posterior muscle was divided longitudinally to provide an intramuscular "pocket". This procedure was performed on each side of the spine.
5. Haemostasis was maintained by careful dissection – no electrocautery was used.
6. Permacol® surgical implant (approximately 1.0cm x 1.0cm) was implanted into both scalenus posterior muscle pockets (2 implants per animal).
7. The muscle pockets were closed with vicryl absorbable sutures.
8. The skin incision was closed with interrupted sutures.

5.3.4.3 Surgical Procedure 2

1. Rats from group L were induced to and maintained under general anaesthesia.
2. A ventral midline incision was made from just below the level of the rib cage extending approximately 1.5cm distally.
3. Another midline incision was made through the peritoneal wall.
4. A lateral liver lobe was identified and carefully exposed.
5. A small incision was made in the liver and an internal pocket opened with microsurgical blunt-ended scissors. The exposed organ was kept moist with saline sterile solution at all times.
6. Permacol® surgical implant (approximately 0.8cm x 0.8cm) was implanted into the liver pocket.
7. The pocket was carefully closed with microsurgical absorbable sutures.
8. The peritoneal wall was closed with vicryl absorbable sutures.
9. The ventral incision was closed with interrupted sutures.
10. To replace any loss of fluids, 5mL of 0.45% NaCl and 5% glucose solution was injected subcutaneously.

The day of surgery was considered as Day 0. As described in the previous chapter animals from the 12 months group were allowed 30 minutes of exercise twice a week.

5.3.4.4 Necropsy

At the relevant times animals were euthanized and implants identified. In groups M the implant and the surrounding muscle were harvested en bloc. Scalenus posterior muscle not in contact with the implants was harvested to be used as control. In groups L the liver lobe with the implant was harvested and another lobe harvested to be used as control. All samples were fixed in 10% NBF and processed for routine histological analysis.

5.3.5 Statistical Analysis

Histometric scores (integration, cellular density, cellular penetration, inflammatory cells and neo-vascularisation) were analysed per implantation site and over time using a two-way ANOVA to look for interaction between factors. These tests were performed in conjugation with Levene's test to check for homogeneity of variances, when $P<0.05$ and variances were significantly different two separate one-way variance analysis were performed instead and Tamhane's T2 post-hoc test used. A one-way ANOVA was used to compare implant thickness in all groups per time point, followed by Bonferroni's test to compare results between groups and to compare each group to pre-implanted Permacol®. One-way ANOVA was also used to investigate adhesion formation and mineralisation occurrence over time. When the ANOVA (one-way and two-way) results were significant a Bonferroni post hoc test was used to identify differences within groups. Statistical analysis was performed using SPSS Statistics 16.0 (SPSS Inc. Chicago, USA). Graphical representation of data was performed using Graphpad Prism statistics software, version 4 (GraphPad Software, Inc., USA).

5.3.6 Results

During the surgical procedure one animal died from the anaesthesia and another had to be sacrificed because of liver damage as a result of the surgical procedure. Both animals were replaced. All other animals recovered well from surgery.

At the end of each time point animals were healthy with body weight values as expected.

From each sample taken for histological analysis two transverse sections were made, one stained with haematoxylin and eosin and the other stained with picro sirius red. Sections were examined, using a light microscope with polarising ability, for the following features: general healing, cellular density, vascularisation, integration with surrounding tissue, cellular penetration, implant structure retention, giant cell presence and collagen degradation.

The grading system used was as described in Table 5.2.

Group M1

After retracting the skin surrounding the operative site, one of the Permacol® implants was found at the surface of the spinotrapezius muscle associated with fascia and a layer of cutaneous maximus muscle; the other 5 implants were not visible.

At 3 months post implantation no inflammatory reaction was present. Integration with the surrounding tissue was minimal (Figure 5.67).

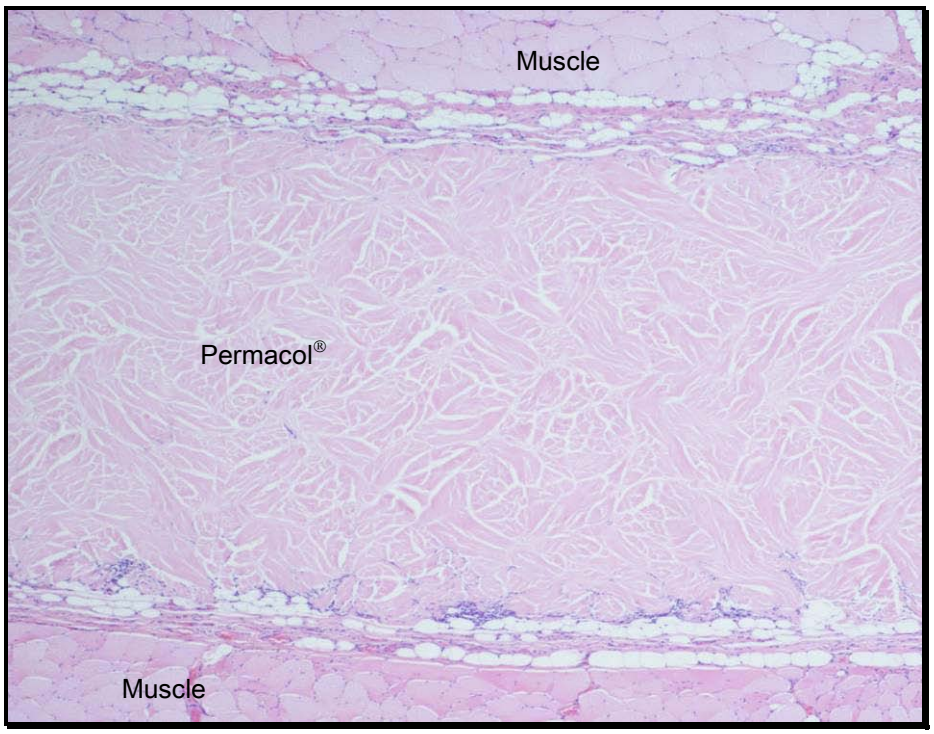

Figure 5.67 – Minimal Permacol® integration with the surrounding tissue after 3 months implantation (H&E, 40X).

Cellular density was low and cellular penetration varied from 10% to 40% (Figure 5.68).

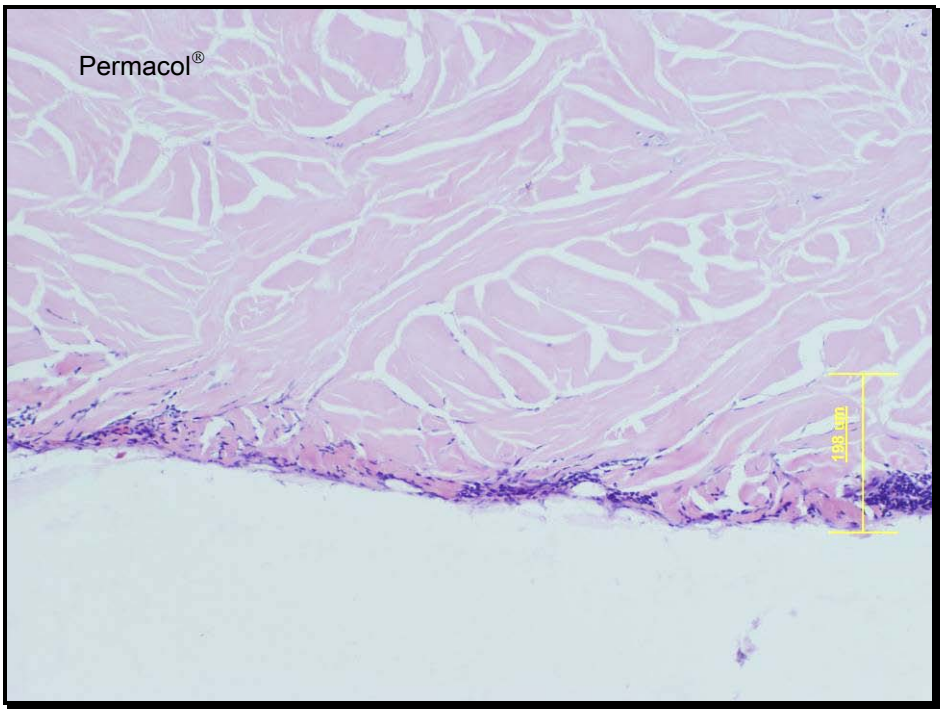

Figure 5.68 – Approximately 10% of cellular penetration in a Permacol® implant, 3 months post implantation (H&E, 100X).

From the 6 pieces of Permacol® implanted in group M1 (2 per animal) 2 showed accumulation of minerals, both in the edges and centre of the implant. Interestingly, these 2 pieces were implanted in different animals. A Von Kossa's stain was performed to confirm the mineralised areas as being calcium deposits (Figure 5.69). ImageJ software (Rasband, W.S., ImageJ, U. S. National Institutes of Health, Bethesda, Maryland, USA) was used to calculate the calcified area per implant. One implant showed calcium deposits in 30% of its area, while in the other 40% of the area was calcified.

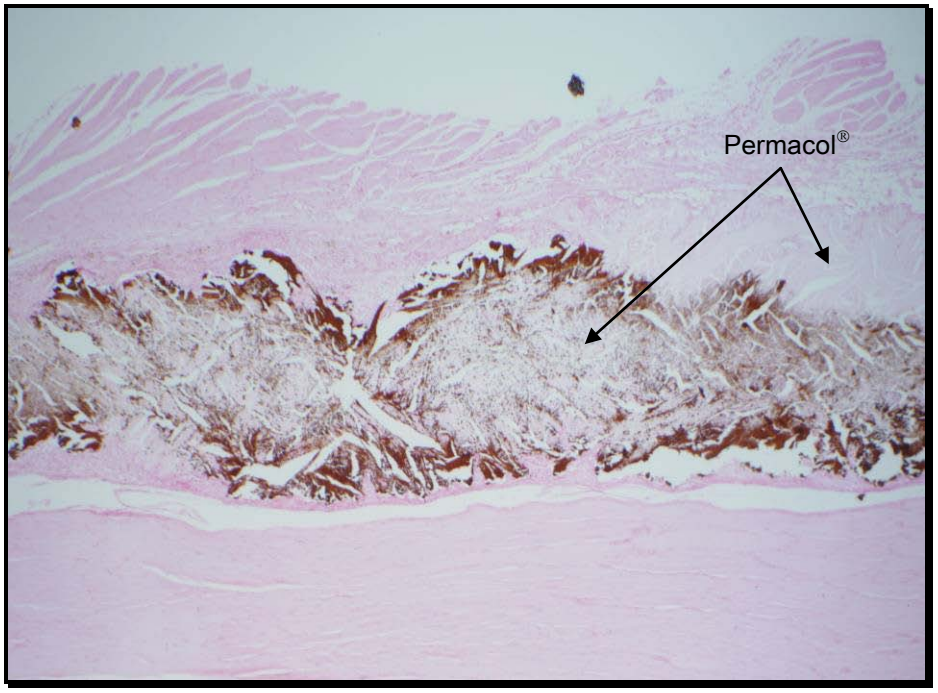

Figure 5.69 – Beginning of mineralisation in a Permacol® implant 3 months post implantation (Von Kossa's, 20X).

Cellular density, for group M1, was low reaching a 1.5 level. A few vessel sprouts were observed at the edges of the implants, in these areas integration with surrounding tissue was moderate (Figure 5.70). Macrophages were visible in 2 implants. All implants of group M1 showed good quality collagen, including the implants with mineralised areas (Figure 5.71).

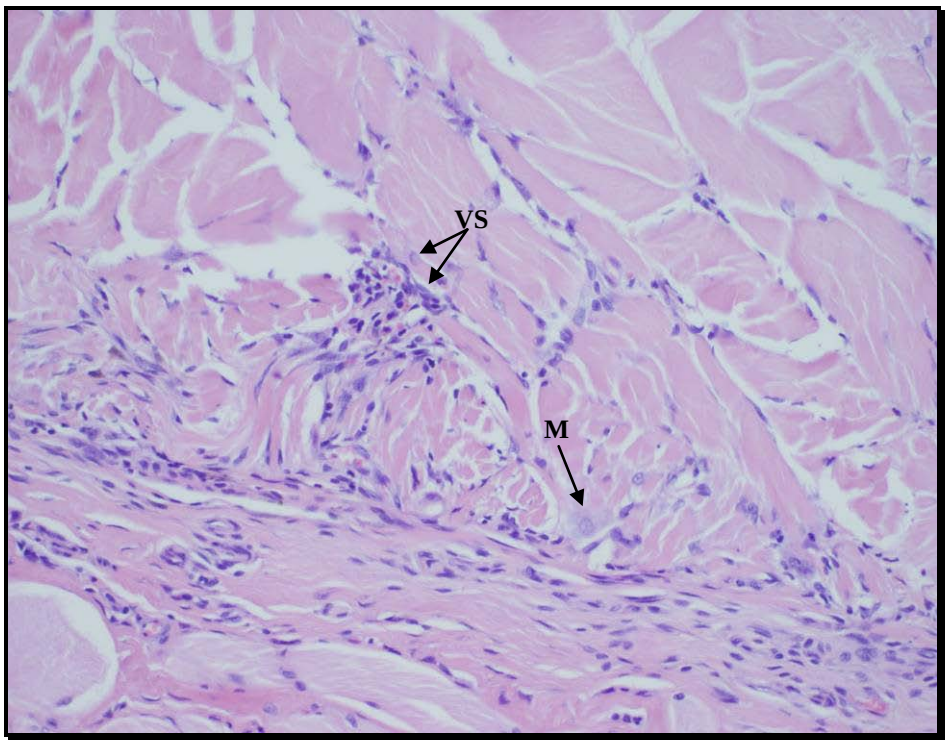

Figure 5.70 – Vessel sprouts (VS) and macrophage (M) present in an implant, 3 months post implantation (H&E, 200X).

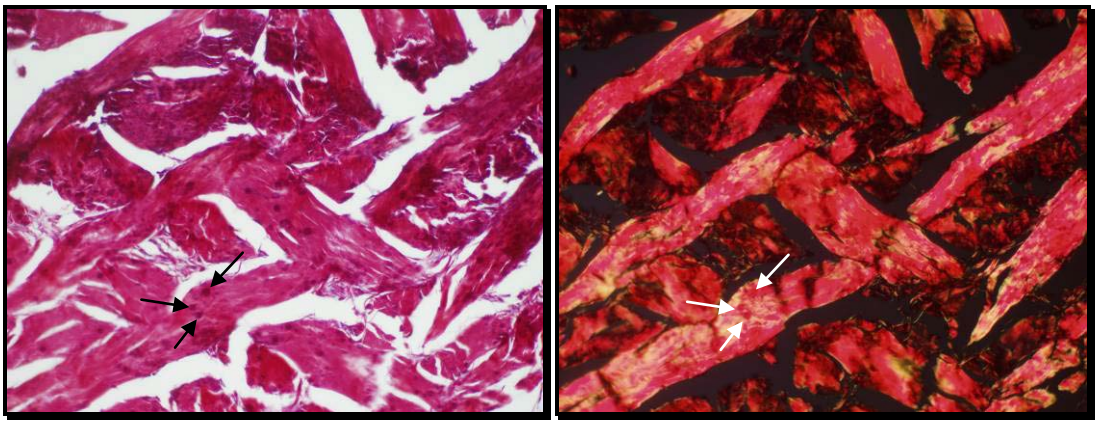

Figure 5.71 – Permacol® surgical implant 3 months post implantation. The left image shows the mineral deposits in dark pink, the same section under polarised light is visible in the right image, collagen is still birefringent in the mineralised areas (picro sirius red, 200X).

The muscle used as control tissue showed no tissue reactivity.

Non-implanted Permacol® had an average thickness of 1.536 ± 0.072mm. After 3 months intramuscular implantation the implant thickness decreased slightly reaching a mean value of 1.2 ± 0.23mm.

The figure below shows the results for group M1 (mean values from all 6 implants).

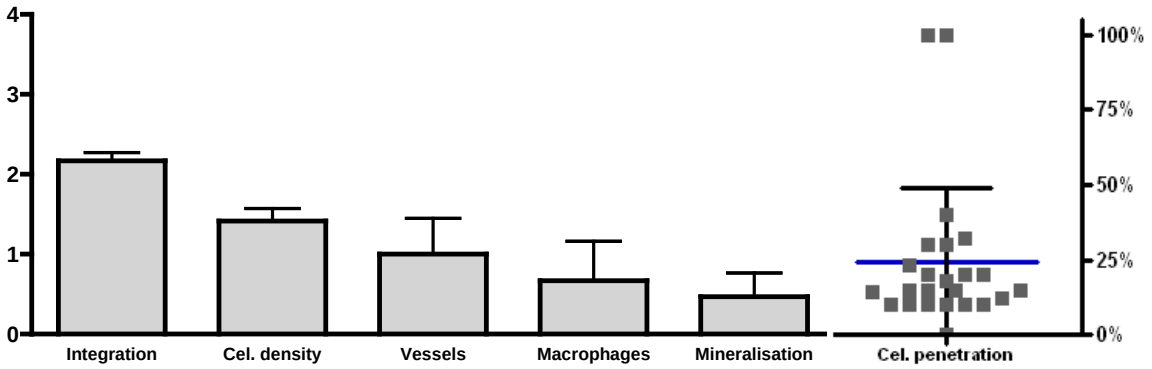

Figure 5.72 – Results for group M1, error bars show standard deviation. Graph was plotted according to the scoring system described in Table 5.2.

Group M2

Six months post implantation Permacol® implants were deep into the muscle layers and were difficult to locate (Figure 5.73).

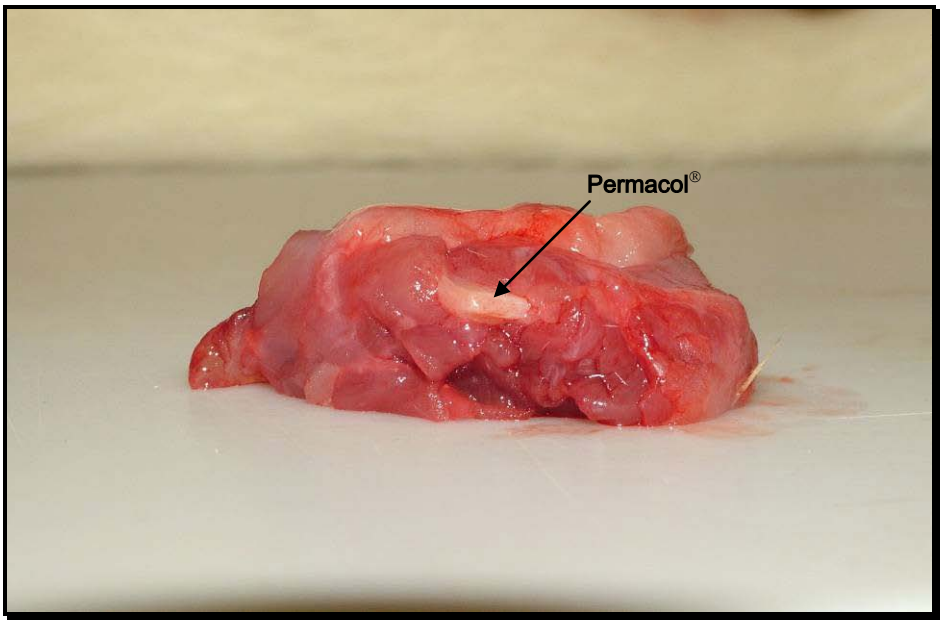

Figure 5.73 – Permacol® surgical implant intramuscularly, 6 months post implantation.

Integration with surrounding tissue was mostly moderate (Figure 5.74).

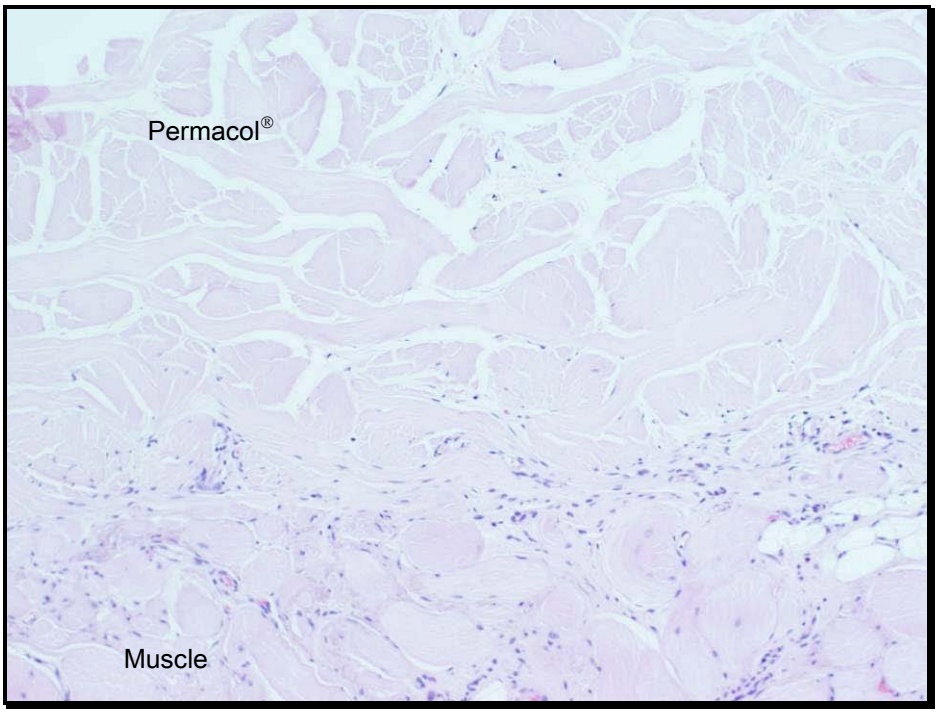

Figure 5.74 – Moderate integration of Permacol® with the surrounding tissue (H&E, 100X).

Cellular density decreased to a marginal level (level 1) when compared to group M1; in general cells were populating the edge of the implant except when natural pores were present in the centre, which enable cells to penetrate further into the implant (Figure 5.75).

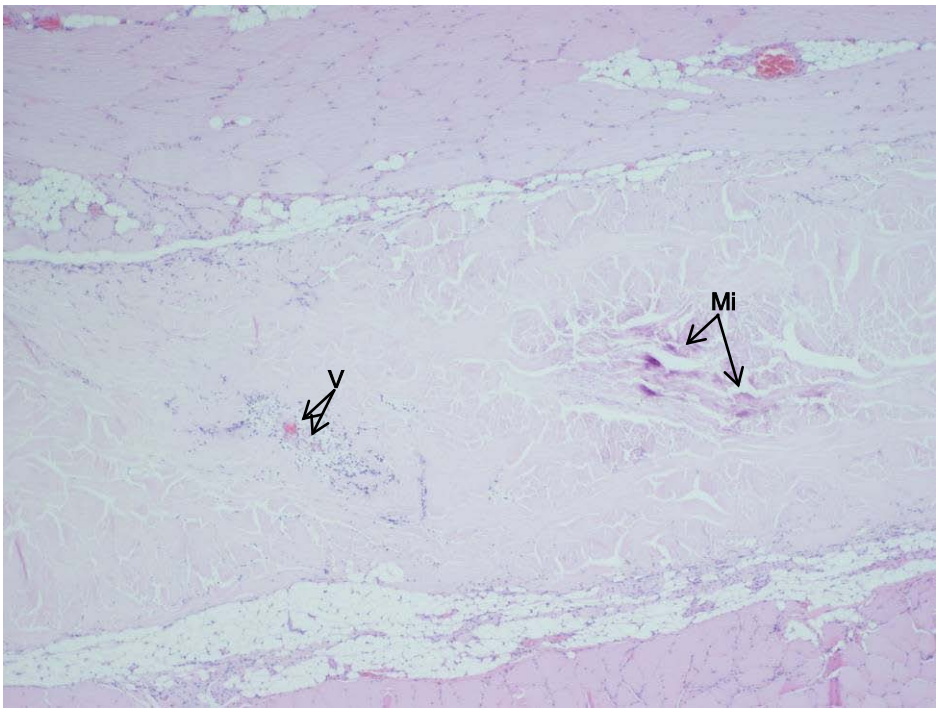

Figure 5.75 – Cells easily populated the natural pores of the implant even when these were located in the centre of the implant. Fully formed vessels were present (V) and deposition of minerals (Mi) was visible in one aspect of the implant (H&E, 40X).

Cellular penetration was predominantly low and varied from 0% to 33%, except when natural pores were present. At 6 months post implantation Permacol® implants showed a mean thickness of 1.2 ± 0.189mm.

All implants showed vessel sprouts and fully formed vessels at the edges of the implant (Figure 5.76) and occasionally in the centre, as seen in Figure 5.75, when cellular population increased.

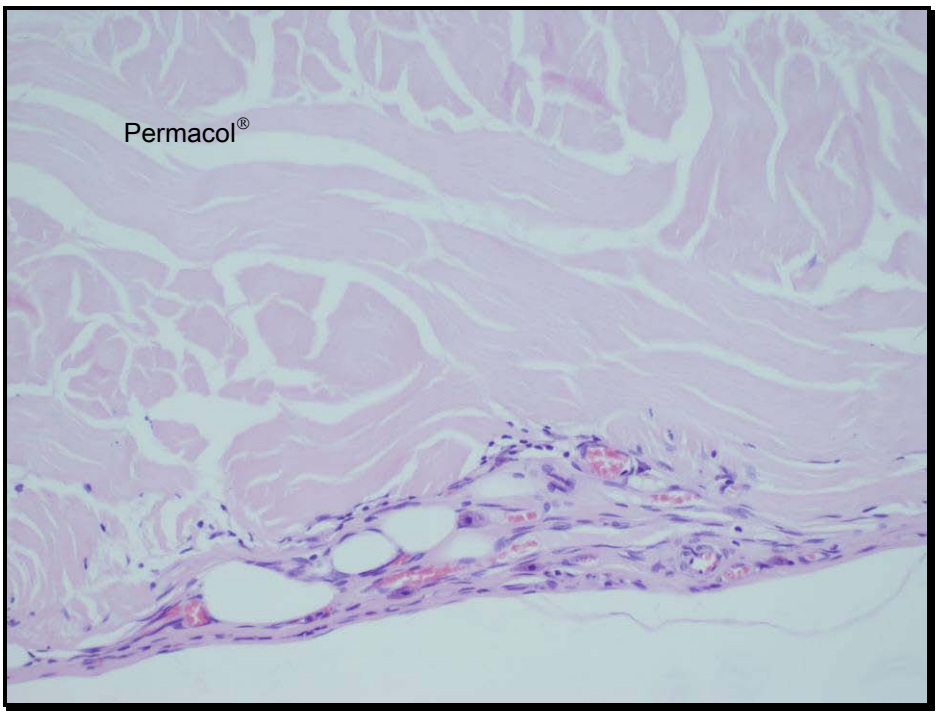

Figure 5.76 – Vessel sprouts and fully formed vessels at the edge of a Permacol® implant, 6 months post implantation (H&E, 200X).

Four of the 6 Permacol® implants showed calcium accumulation at different levels (5%, 20%, 40% and 40%) at 6 months. Calcium deposition was not restricted to the centre of the implant, 3 of the implants showed minerals both in the edges and centre (Figure 5.77 and Figure 5.78).

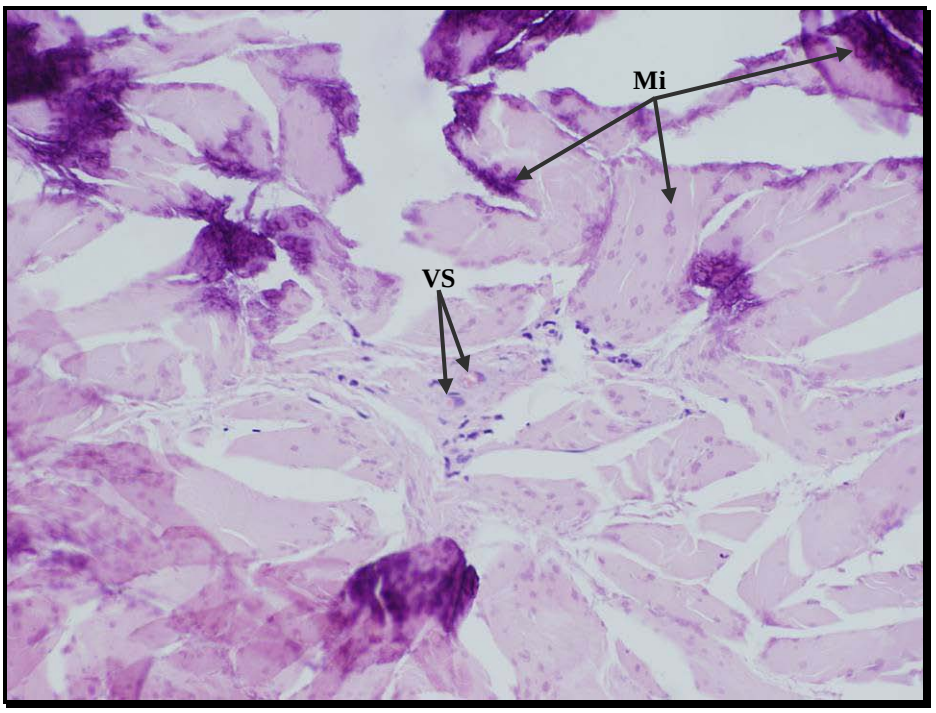

Figure 5.77 – Beginning of mineralisation (Mi) in the centre of a Permacol® implant, 6 months post implantation. Cells and vessel sprouts (VS) are visible in the mineralised area (H&E, 200X).

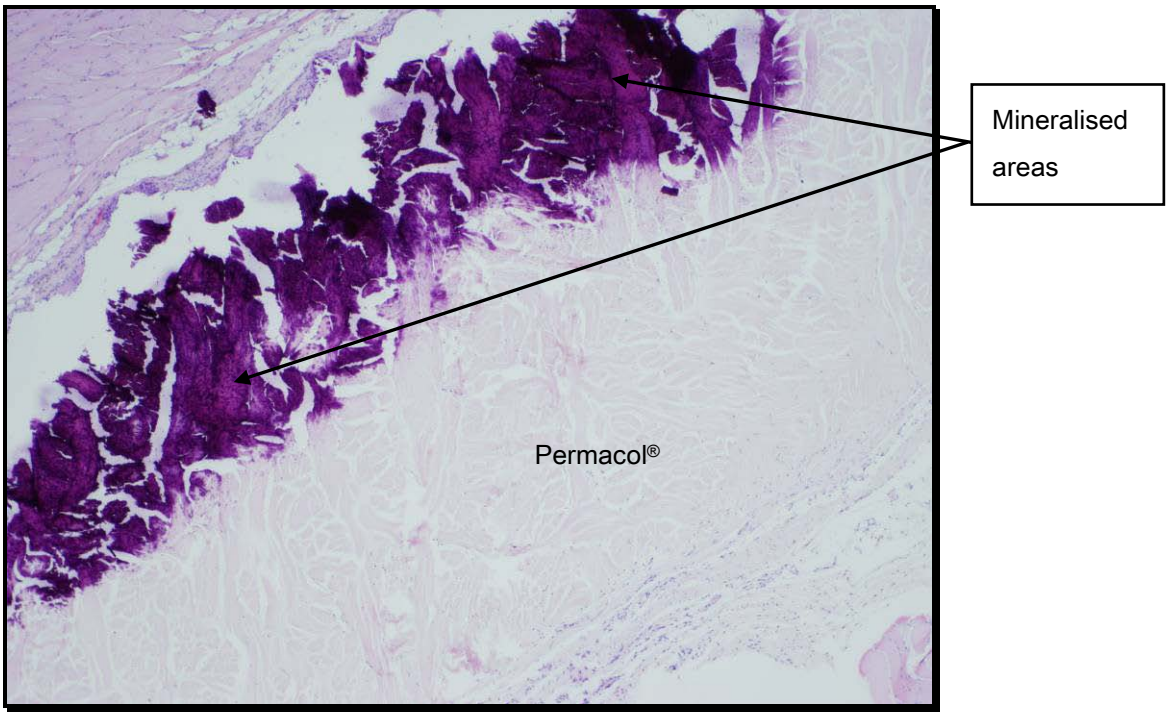

Figure 5.78 – Mineralisation at the edge of a Permacol® implant, 6 months post implantation (H&E, 40X).

No tissue reactivity was observed in the control tissue or in the implantation site. All implants showed good quality collagen under polarised light. Fibres with minerals showed no collagen degradation, minerals were bright-pink under polarised light (Figure 5.79).

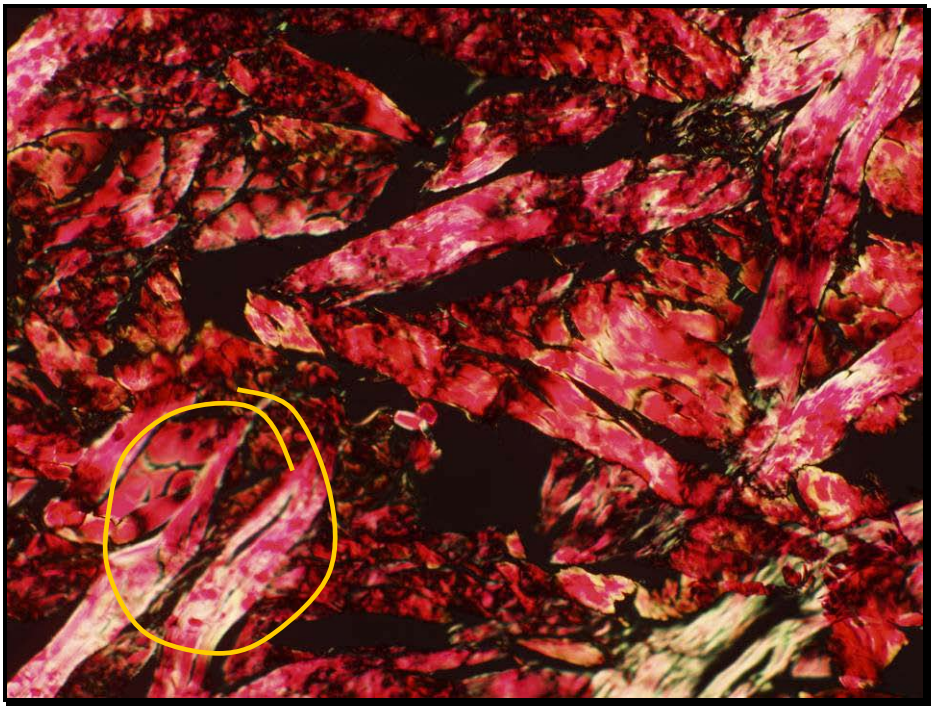

Figure 5.79 – Non-denatured collagen. Minerals are bright-pink under polarised light (picro sirius red, 200X).

Figure 5.80 shows the results for the group M2 (mean values from all 6 implants).

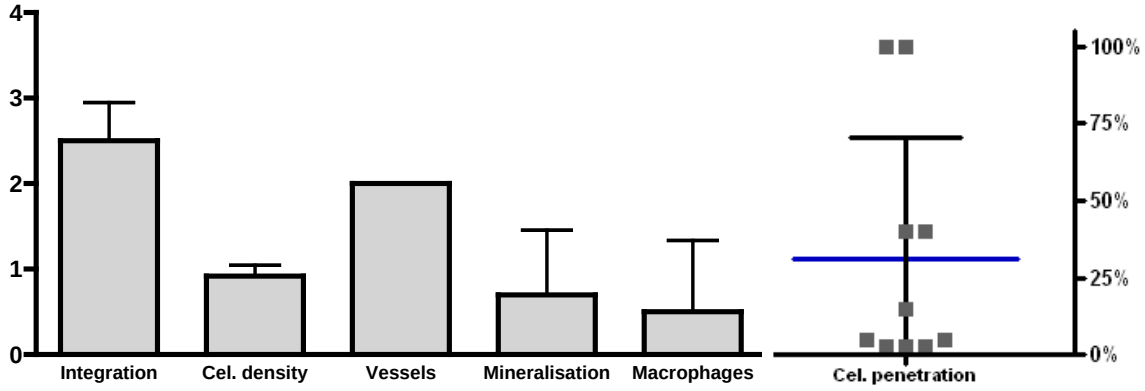

Figure 5.80 – Results for group M2, error bars show standard deviation. Scoring system used as described in Table 5.2.

Group M3

Twelve months post implantation one of the animals had one implant at the surface of the spinotrapezius muscle associated with fascia and a layer of cutaneous maximus muscle, the other 3 implants were deep into the muscle layers and were difficult to localize.
One animal developed a pressure wound in the tail and was found one morning without the extremity of the tail, the wound healed and the animal was fine until termination day.

Histological analysis of the implants showed mineralised tissue in all 4 implants, mineralised areas were approximately 30%, 55%, 60% and 70% of the area of implant. When mineralisation was observed at the edges of the implant integration with surrounding tissue was minimal, otherwise integration was mostly moderate (Figure 5.81).

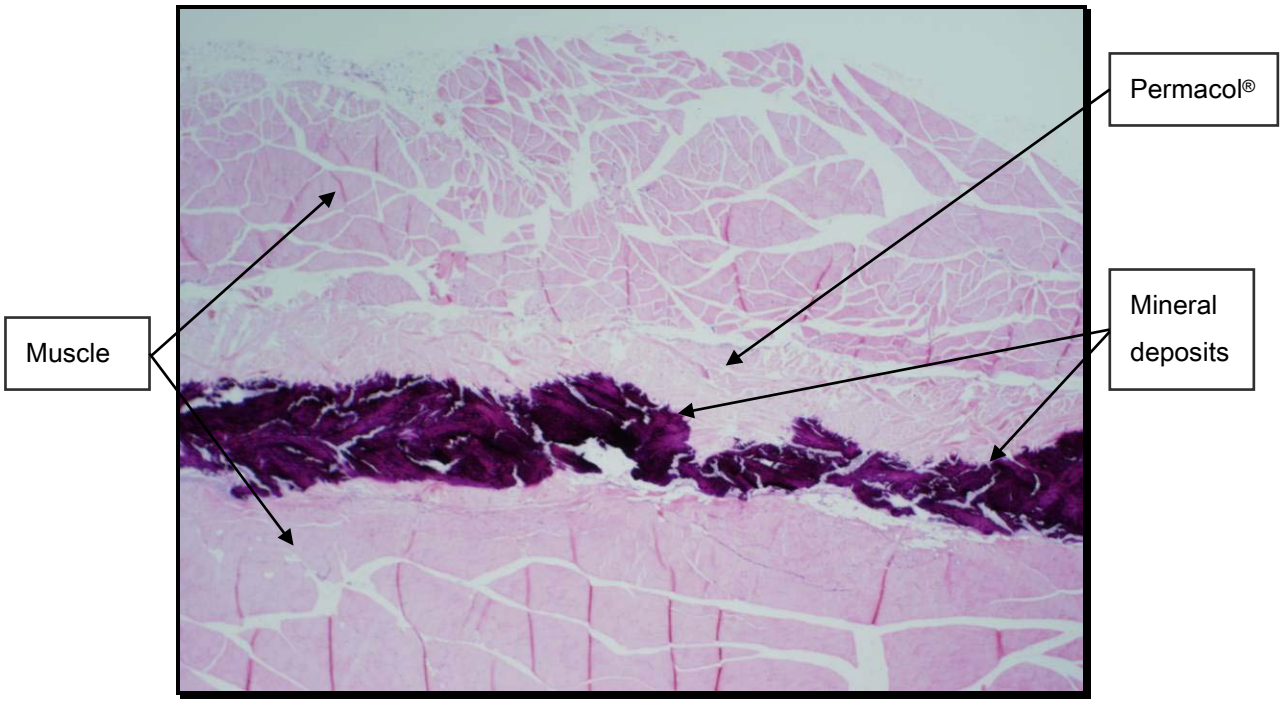

Figure 5.81 – Mineralisation in a Permacol® implant after 12 months intramuscular implantation (H&E, 20X).

Muscle adjacent to the implants was healthy and well cellularised, there was no tissue inflammation and calcium deposition was not observed in the surrounding tissues.

Good quality, non degraded collagen was observed under polarised light in all implants, inclusive of areas where mineral deposition was present.

Mature vessels and vessel sprouts were present at the edges of the implants, including in the proximity of mineralised matrix (Figure 5.82). It was difficult to identify vessels in the centre of the implants since most central areas were calcified.

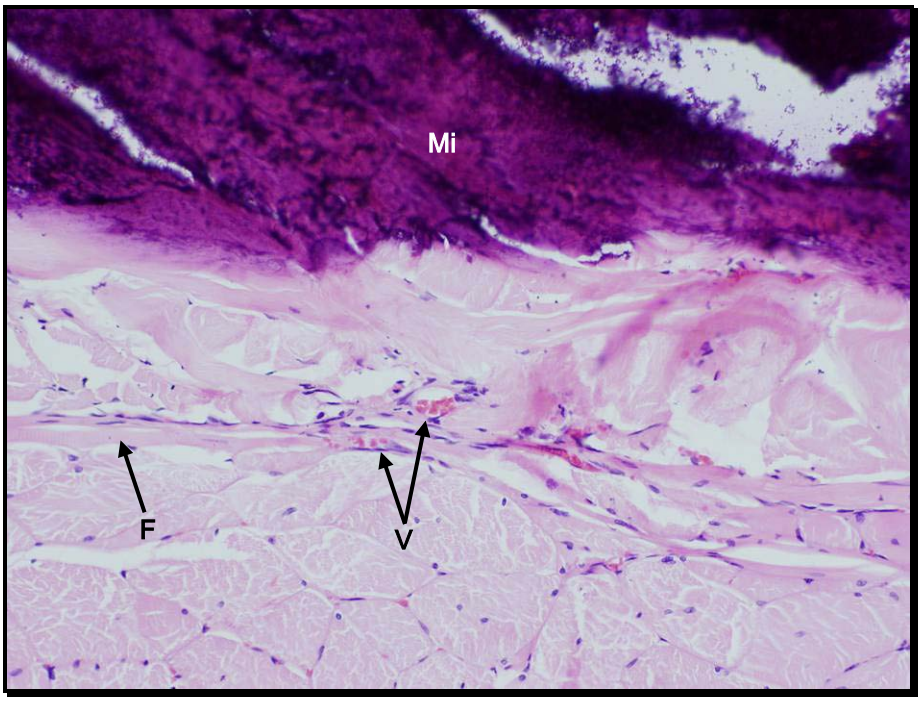

Figure 5.82 – Vessels (V) were present in the edges of implants, although cellular density was not high and mineralised tissue (Mi) was in the proximities. Fibrin (F) fibres were present between the implant and the muscle, probably as part of the integration process (H&E, 200X).

In one animal implants had minimal cellular density and cellular penetration varied from 10% to 60%. Both implants from the other animal showed minimal cellular density and cellular penetration reached, in a few localised areas, 100%, but it was mostly 50%.

Macrophages were observed in one aspect of an implant, near mineral deposits (Figure 5.83).

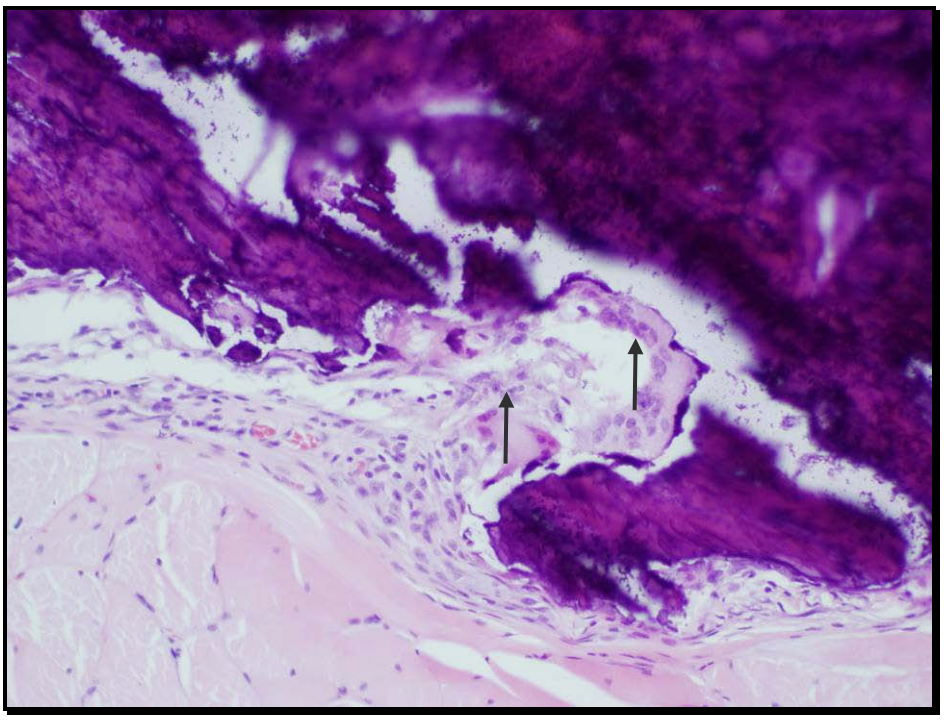

Figure 5.83 – Arrows show macrophages in one aspect of a Permacol® implant, 12 months post implantation (H&E, 200X).

None of the implants showed inflammatory or immune responses. Despite the mineralised areas, implants kept their configuration and the mean thickness of implants was 1.275 ± 0.159mm.

The figure below represents graphically the histometric results for group M3.

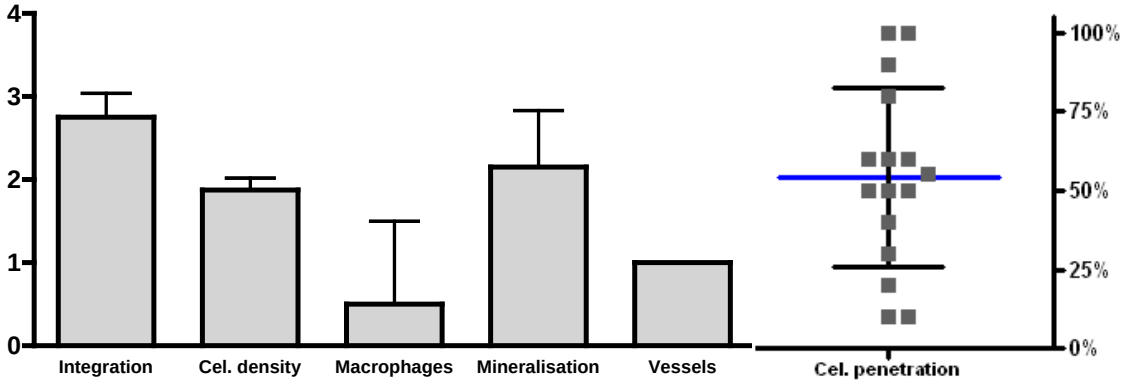

Figure 5.84 – Results for Permacol® implanted intramuscularly for a period of 12 months. Scoring system used as described in Table 5.2.

Group L1

In this group each animal received one piece of Permacol® surgical implant, placed in a pocket made in a lobe of the liver. After 3 months, animals were sacrificed and the operative site identified and exposed. In all animals the liver looked healthy and the implant was visible at the surface of the liver lobe covered entirely by the peritoneum. In 2 animals a second liver lobe was attached to part of the implant (Figure 5.85). In the third animal omentum fat adhesions were visible macroscopically (Figure 5.86). Although the liver lobe was kept moist at all times the surgical procedure caused damage to the peritoneum and the liver lobe was sutured as a result of the procedure. It is likely that adhesions formed between the liver lobe and the omentum as a result of the surgical procedure. Corroborating this theory is the fact that there was no adhesion observed in the other surfaces of the lobe used to create the pocket.

Figure 5.85 – Permacol® implant (arrow) 3 months post implantation. The implant was at the surface of the lobe and a second lobe was present attached to the implant.

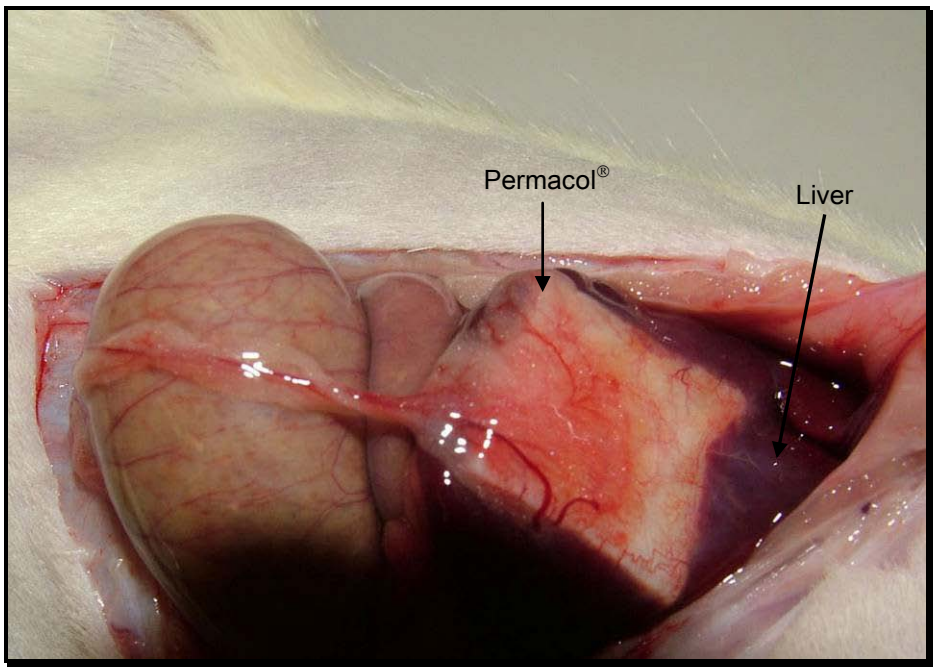

Figure 5.86 – Permacol® implanted into the liver, 3 months post implantation. Adhesions are visible between the implant and the bowel.

The adhesion observed was not directly connected to the Permacol® surface; which adds to the hypothesis that the adhesion was caused by the surgical procedure and not by the implant. Permacol® was covered by a layer of collagenous tissue termed Glisson's capsule - this capsule is the normal outer surface of the liver. The adhesion observed formed between the Glisson's capsule and the omentum. The vessels observed in the border of the omentum are a typical feature of an adhesion (Figure 5.87).

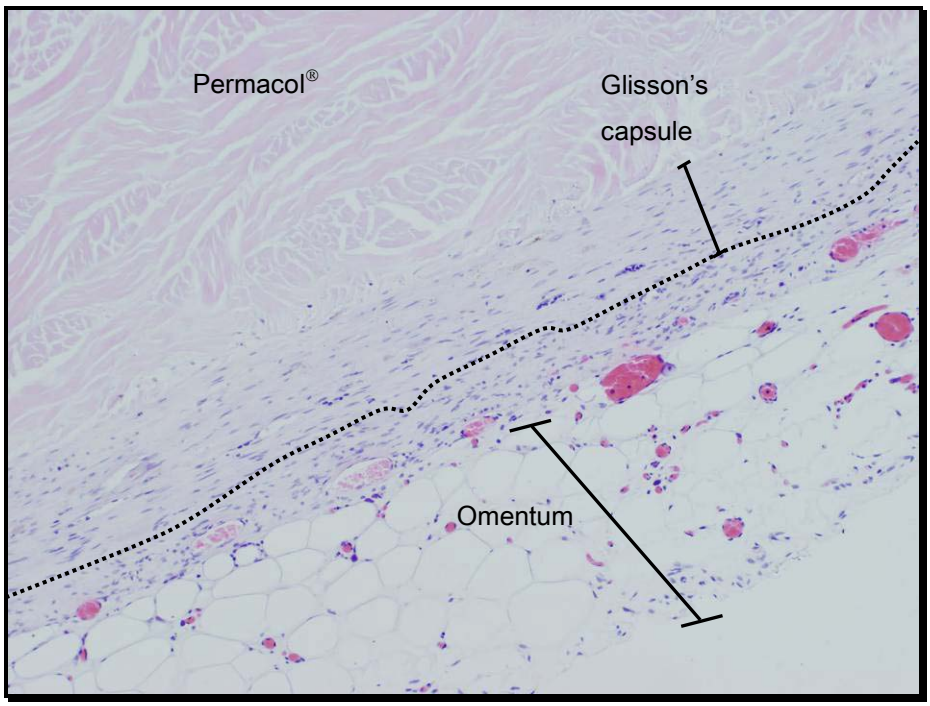

Figure 5.87 – Permacol® implant 3 months post implantation. The dotted line shows the division between the collagenous capsule – with arranged fibres – and the fibrous tissue constituting the adhesion between the liver and the omentum (H&E, 100X).

There was no inflammatory response present in the surrounding tissue or implants and Permacol® was well tolerated by the liver.

Figure 5.88 shows the control tissue. The liver is a solid organ composed of tightly packed (pink-stained) plates of epithelial cells termed hepatocytes, separated by fine vascular sinusoids (pale-stained) through which blood flows.

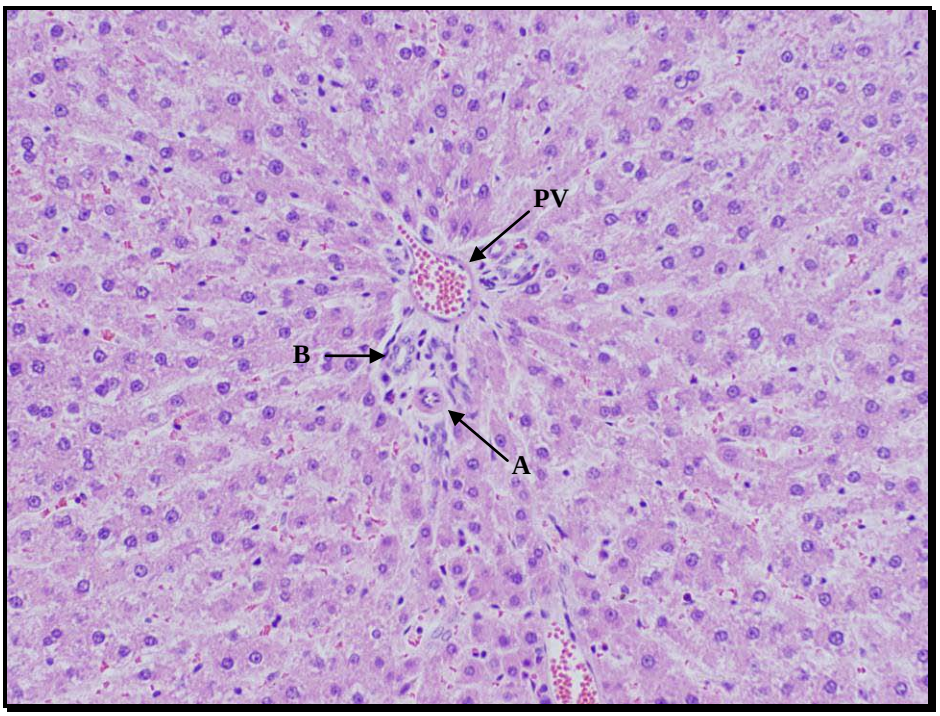

Figure 5.88 – Control tissue. Detail of liver showing a portal tract containing 3 main structures: hepatic portal vein (PV), hepatic artery (A) and bile duct (B) (H&E, 200X).

Cellular density was low (level 1) and cellular penetration varied between 5 and 15% (Figure 5.89). There was no presence of mineralisation or inflammatory response.

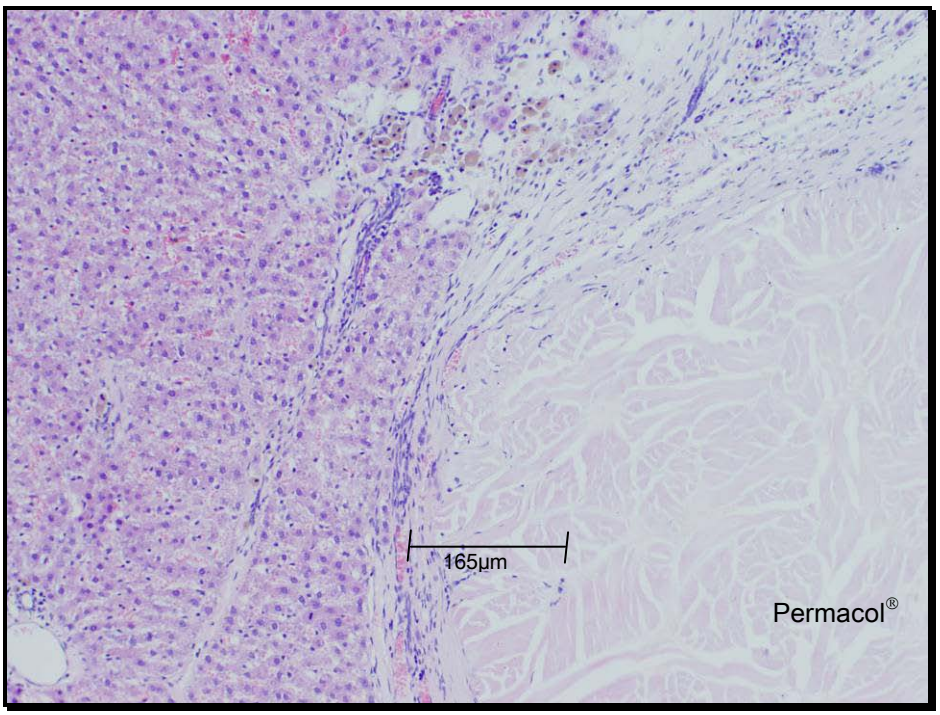

Figure 5.89 – Marginal cellular penetration in a Permacol® implant, 3 months post implantation (H&E, 100X).

None of the implants was completely at the surface of the liver; each implant had at least one side still inserted in the liver. The Permacol® visible at the surface was the implant region closest to the opening of the pocket. Implants had minimal to moderate integration with the surrounding tissue (Figure 5.90).

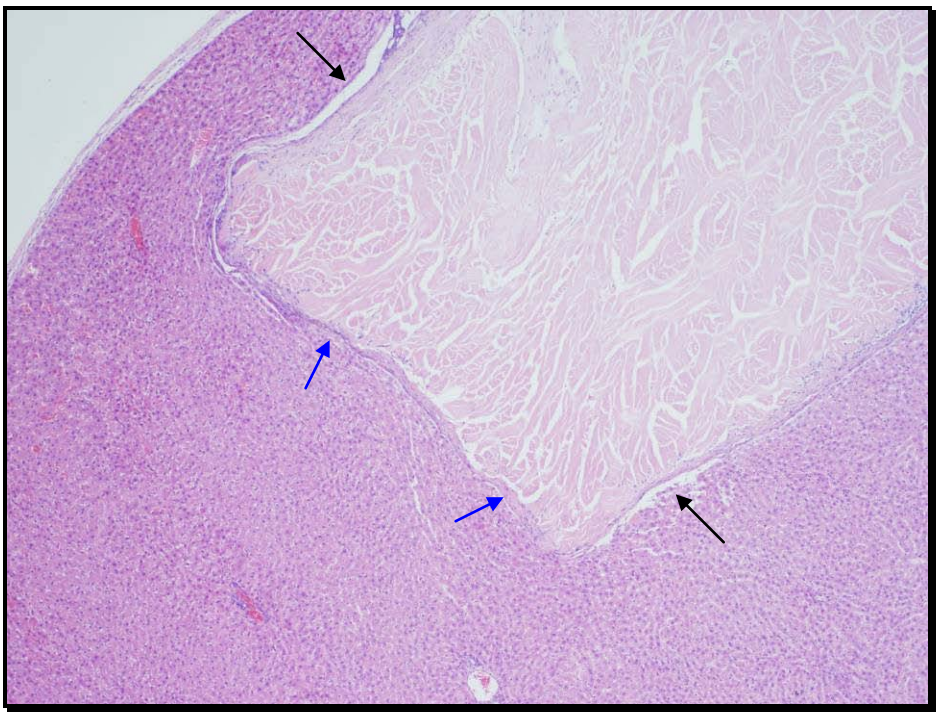

Figure 5.90 – Permacol® implant partially inserted into the liver with minimal (black arrows) and moderate (blue arrows) integration (H&E, 40X).

Macrophages were present in one aspect of an implant (Figure 5.91).

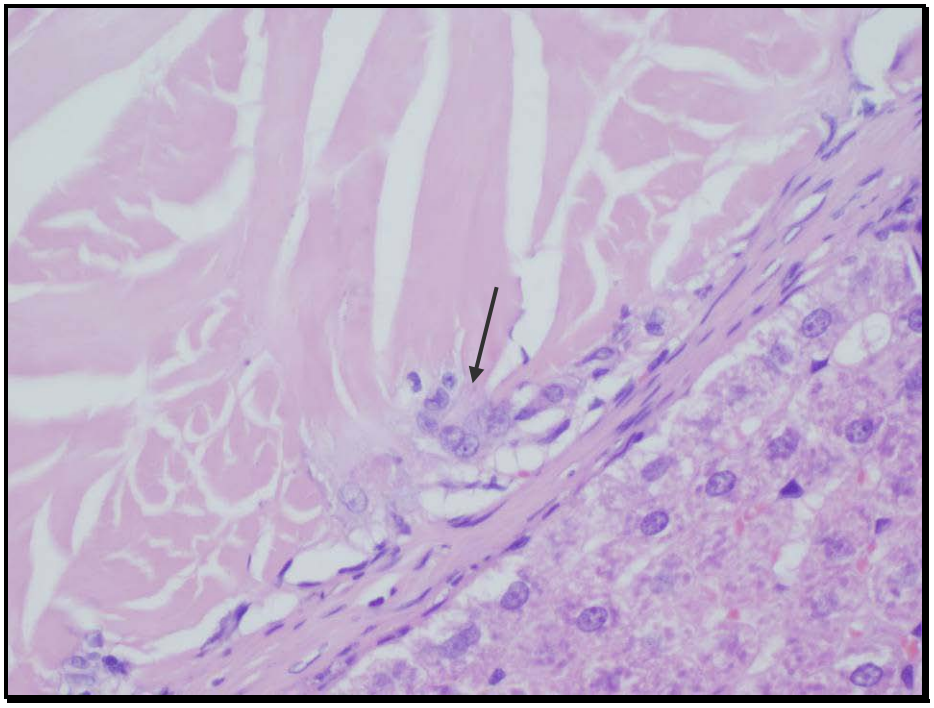

Figure 5.91 – Group of macrophages in an implant, 3 months post implantation (H&E, 400X).

All implants showed natural birefringence under polarised light, an indicator of good quality collagen; there was no degradation of the implants (Figure 5.92). Implants showed an average thickness of 1.59 ± 0.083mm.

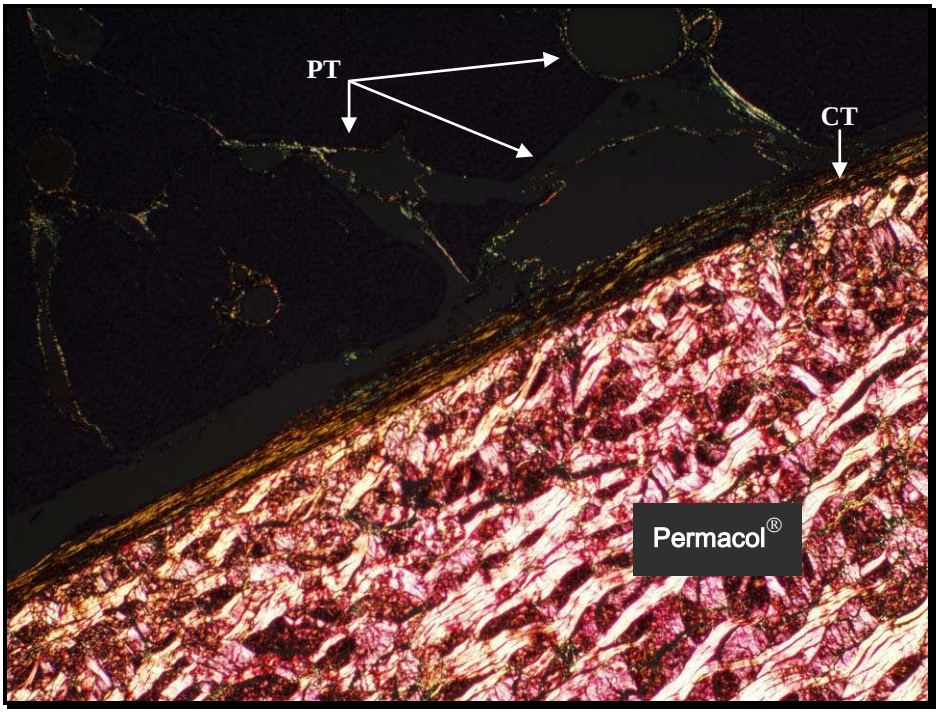

Figure 5.92 – Liver portal tracts (PT), collagenous tissue (CT) and Permacol® implant after 3 months implantation in the liver (picro sirius red, 40X).

The figure below shows the results for group L1 (mean values for all 3 implants).

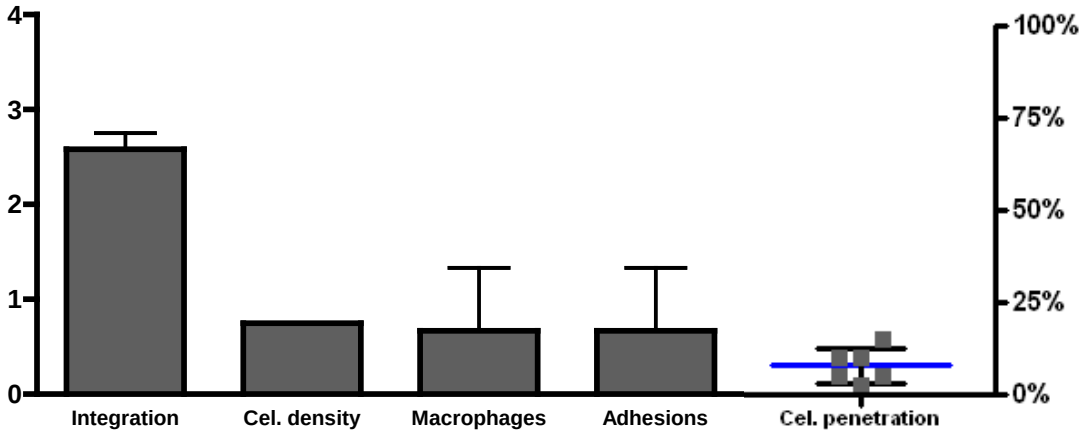

Figure 5.93 – Results for group L1, error bars show standard deviations. Scoring system used as described in Table 5.2.

Group L2

Permacol® implants were visible at the surface of liver 6 months post implantation; a second lobe was attached to the implants (Figure 5.94).

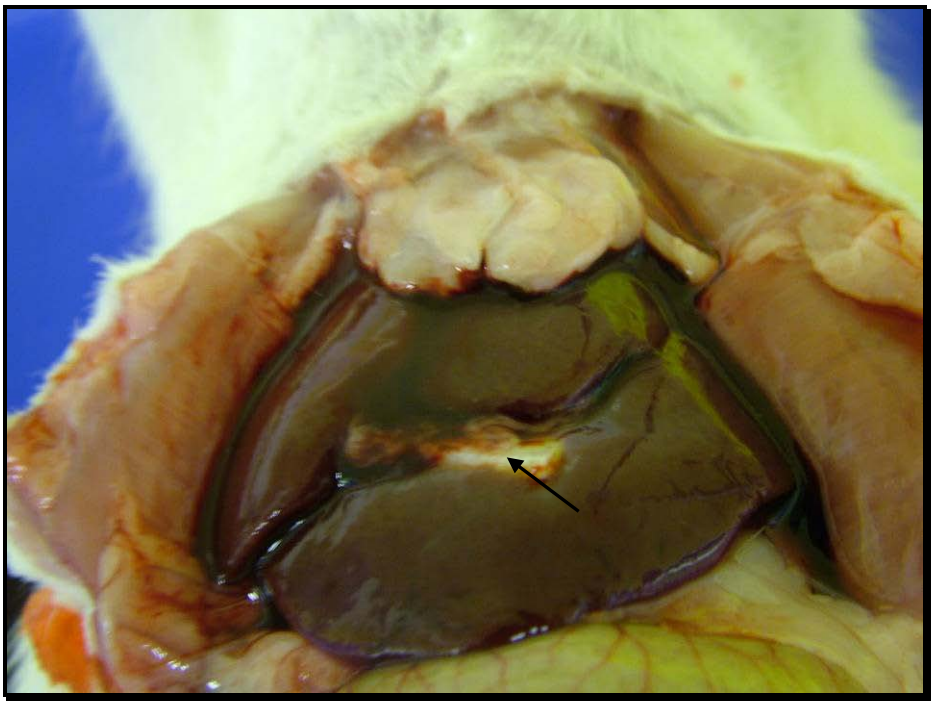

Figure 5.94 - Permacol® implant 6 months post implantation in liver.

There was no tissue reactivity or inflammatory response in the control tissue or in the implantation site. Once more, probably as a result of the surgical procedure, adhesions between omentum and the liver were macroscopically observed in 2 of the implants; one of these implants also had a second lobe attached and in this animal the adhesion was much smaller when compared to the other animal.

Although cellular density was very low, integration with the hepatic tissue was moderate. Cells were mostly present in a fibrous layer surrounding the implants; a small fraction of these cells infiltrated the implant and in a few aspects reached approximately 30% of cellular penetration (Figure 5.95).

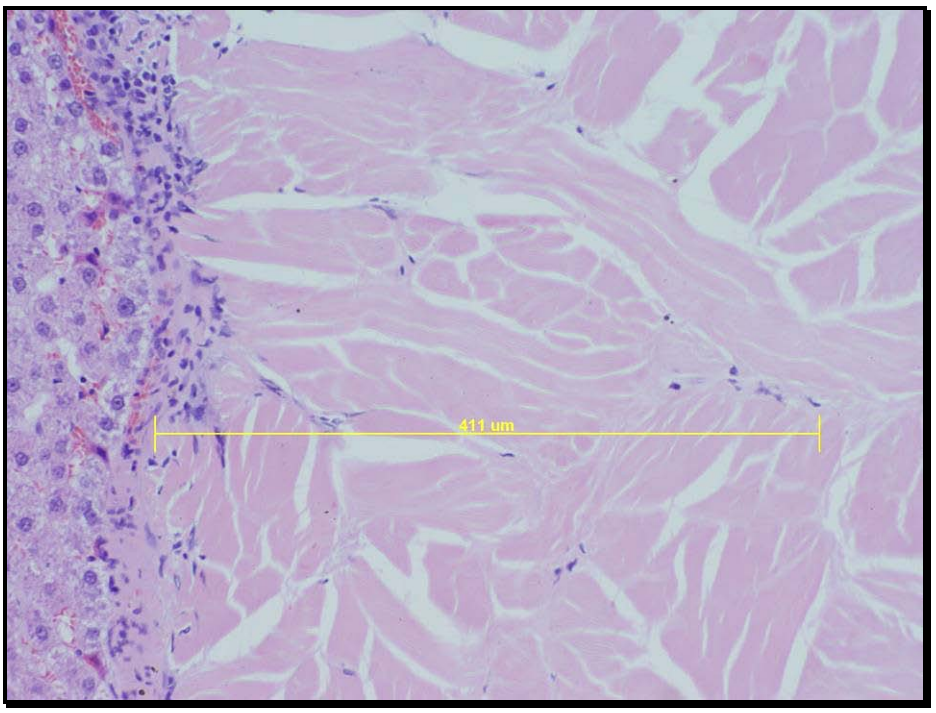

Figure 5.95 – Moderate cellular integration of a Permacol® implant with hepatic tissue, with approximately 30% of cellular infiltration (H&E, 200X).

Macrophages and giant cells were observed at the edge of one implant but there was no degradation or remodelling of the implant (Figure 5.96).

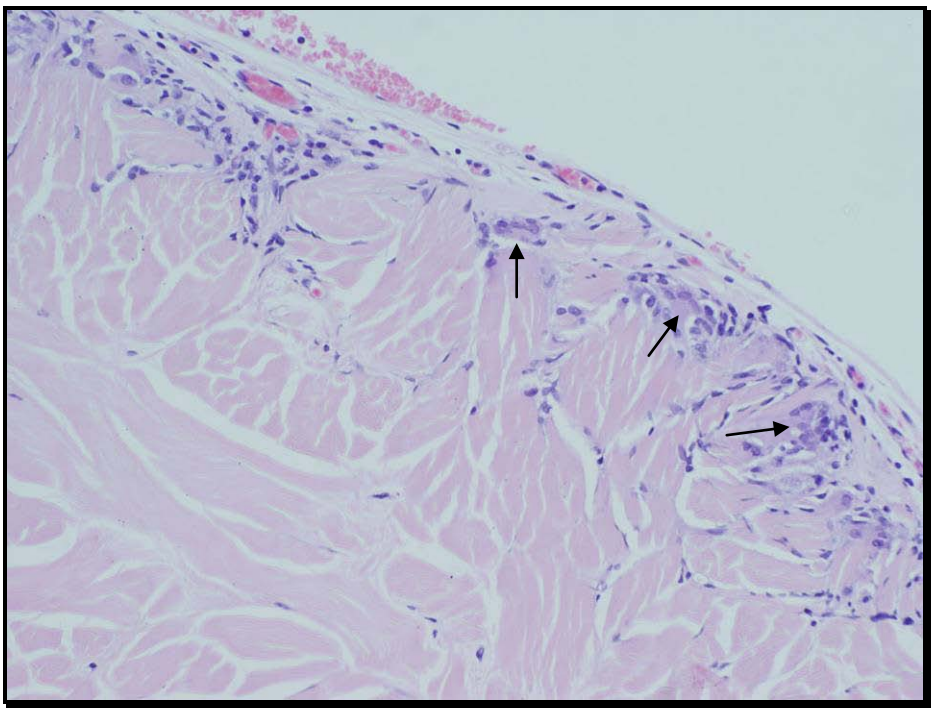

Figure 5.96 – Macrophages and giant cells observed at the edge of an implant, 6 months post implantation (H&E, 200X).

Vessels were observed at the edges of the implant to sustain cellular population (see Figure 5.95). Good quality collagen was present in all implants; there was no degradation of the implants, although the mean thickness of the implant decreased slightly to 1.56 ± 0.043mm.

Figure 5.97 shows the results for group L2 (mean values for all 3 implants).

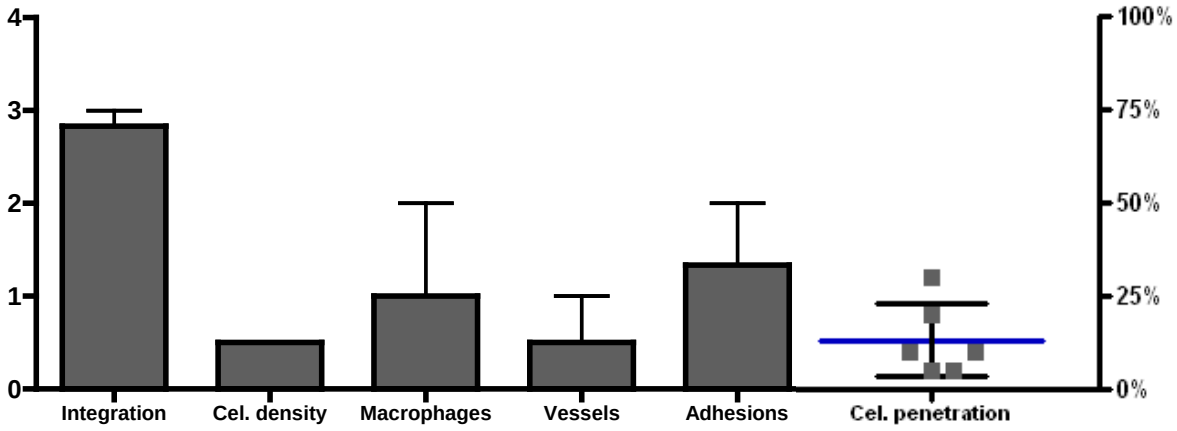

Figure 5.97 – Results for group L2 (error bars show standard deviation). Scoring system used as described in Table 5.2.

Group L3

Animals were healthy 12 months post implantation with body weights as expected. During necropsy Permacol® was easily identifiable at the surface of the liver lobe, another liver lobe was attached to Permacol® and both implants showed a small omentum adhesion.

Inflammatory or immune responses were not observed in the implants or in the surrounding hepatic tissue (Figure 5.98).

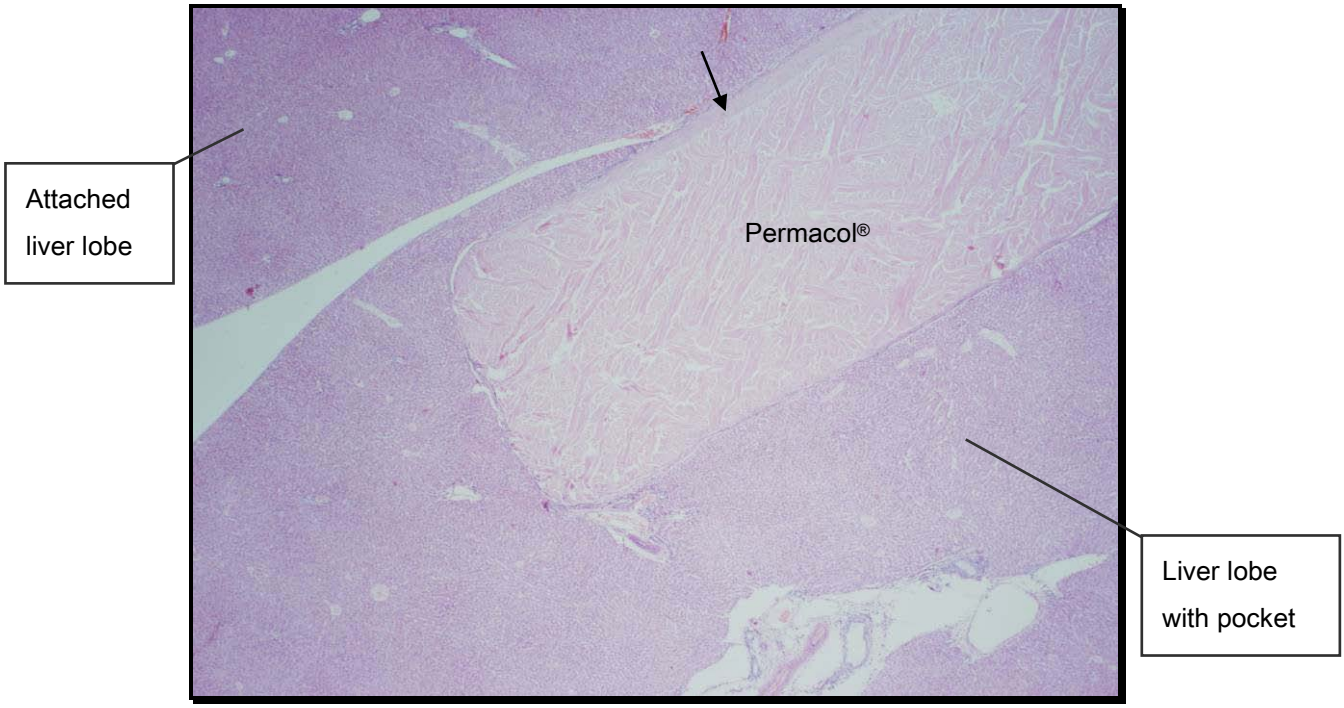

Figure 5.98 – Permacol® implant semi-inserted in the liver pocket, another liver lobe is attached to the surface of the implant. Arrow shows the fibrin capsule observed only between the adherent liver lobe and Permacol® (H&E, 20X).

Both implants showed moderate integration with the immediately adjacent hepatic tissue, cellular density was very low and cellular penetration reached a maximum of 10% (Figure 5.99). Vessels were observed only in one implant at the edges.

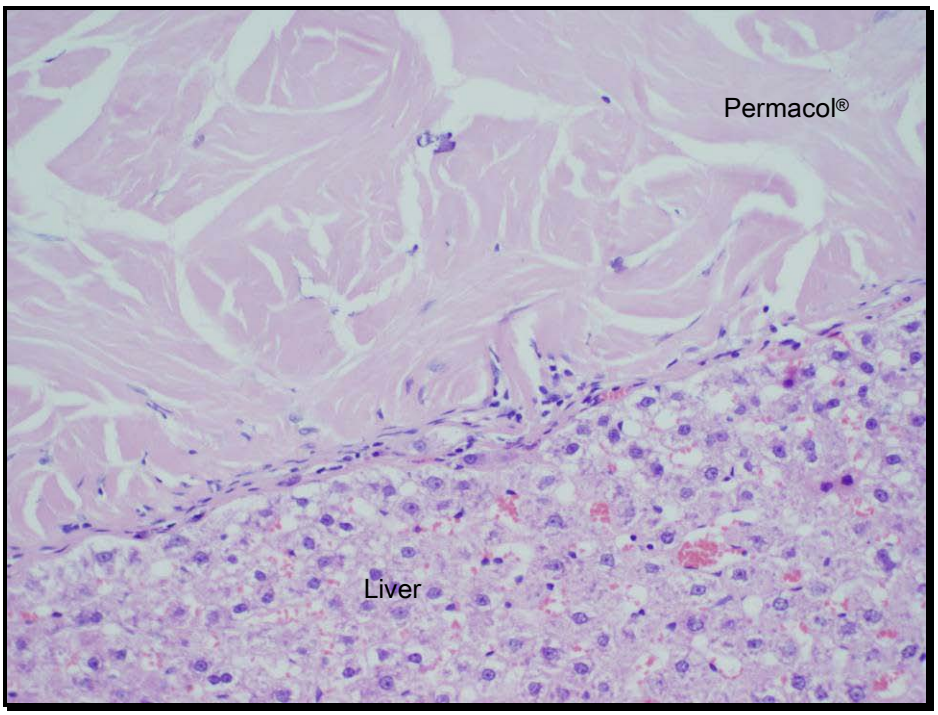

Figure 5.99 – Moderate integration of Permacol® with hepatic tissue, cellular density and cellular penetration are low (H&E, 200X).

There was no evidence of mineralisation in both implants, at 12 months post implantation.

Fibrin was observed between implants and hepatic tissue and it is not clear if it is part of the Glisson's capsule. In this small layer of fibrin large numbers of what seem to be bile ducts were present (Figure 5.100).

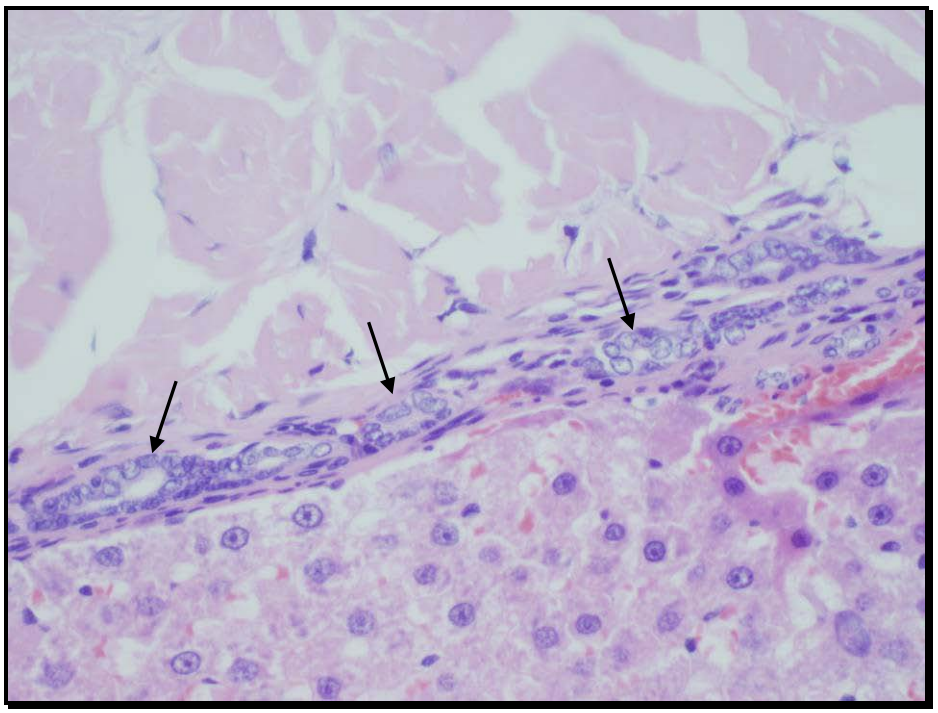

Figure 5.100 – Small layer of fibrin between hepatic tissue and Permacol®, numerous ducts (arrows) are visible along this layer (H&E, 400X).

There was no collagen degradation and implants kept their configuration with a thickness of 1.664 ± 0.084mm.

Figure 5.101 shows the results for Permacol® implanted in the liver after a period of 12 months.

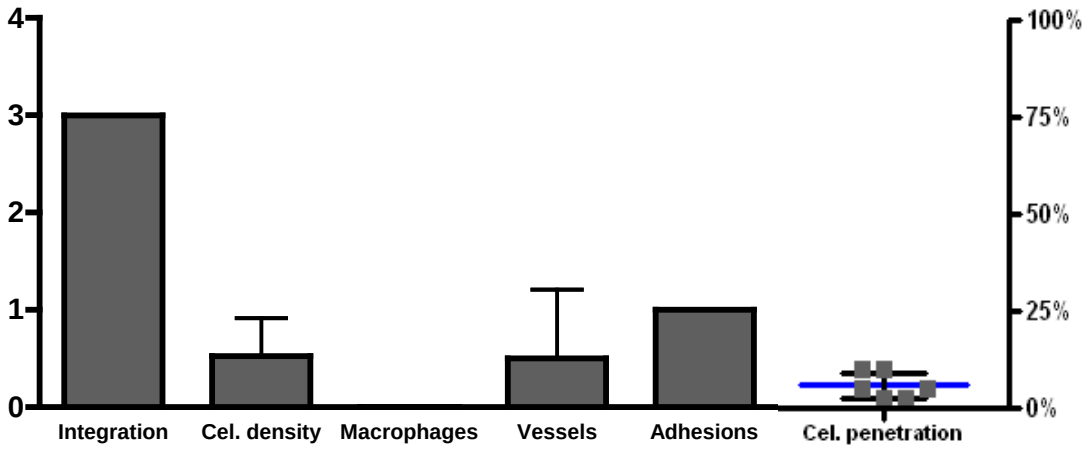

Figure 5.101 – Histometric results for Permacol® implanted into liver, 12 months post implantation, according to the scoring system described in Table 5.2.

Table 5.11 shows the statistical results for this study. Integration was statistically significant for both factors – implantation site and time – but the interaction between factors was not significant, *i.e.*, Permacol® integration in both implantation sites did not respond differently to time. This can be easily verified in Figure 5.104 where the level of integration increased similarly over time in both implantation sites.

Table 5.11 – Statistical significance for each factor analysed and for the interaction between factors.

	Integration	**Cellular density**	**Cellular penetration**	**Macrophages**	**Vessels**
Implant site	P<0.05	P<0.001	P<0.001	NS	P<0.05
Time	P<0.05	P<0.05	NS	NS	NS
Implantion site * Time	NS	P<0.05	NS	NS	NS

Cellular density was significantly different for both factors and for the interaction between these, meaning that the implantation sites tested influenced Permacol® cellular density over time. Results were not significantly different for cellular penetration, macrophage presence and neo-vascularisation for the time points used in this study; in addition, there was no evidence of an interaction between implantation site and time for these parameters. However, cellular penetration was significantly influenced per implantation site and implant location also had a significant effect in neo-vascularisation.

Figure 5.102 and Figure 5.103 show the results per site of implantation.

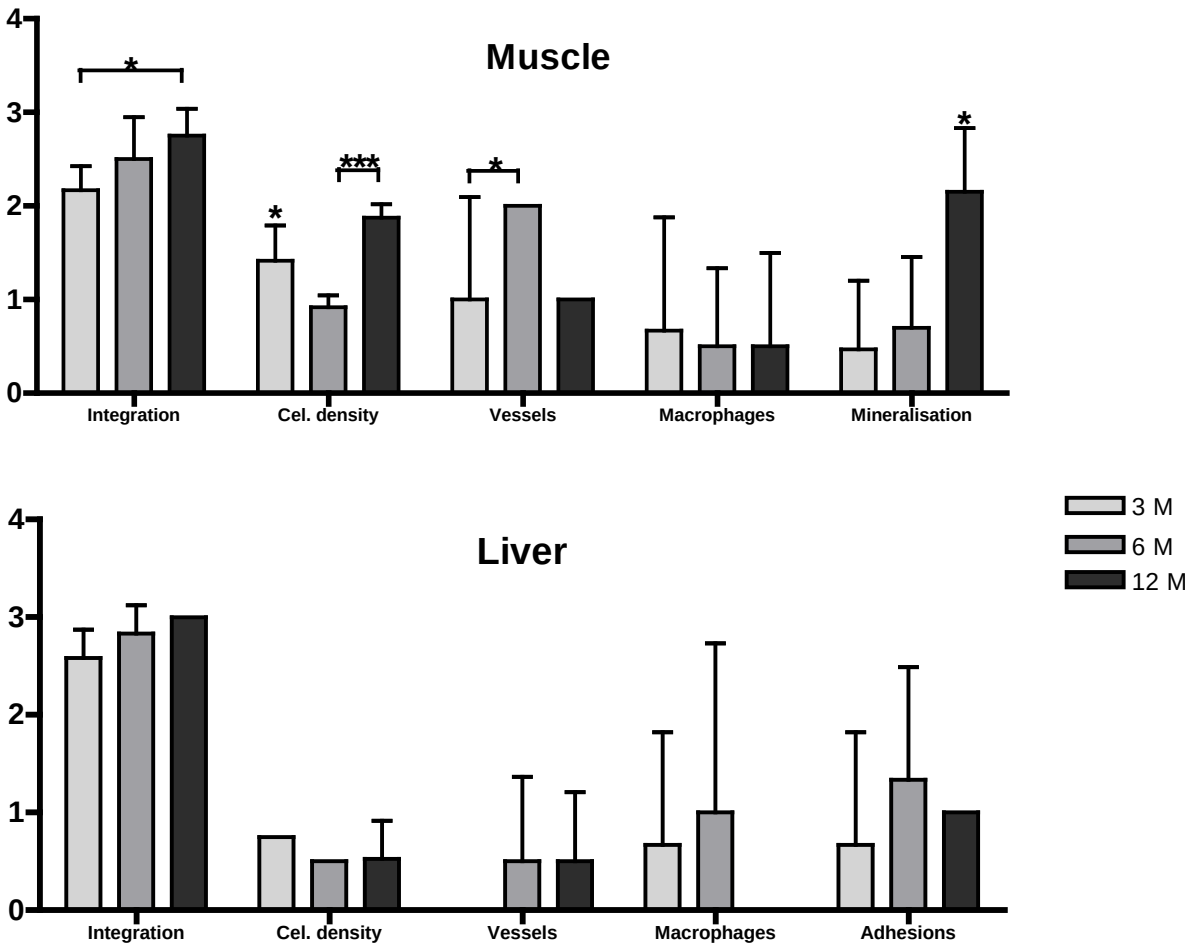

Figure 5.102 – Histopathology results per site of implantation, statistical significance was compared between groups (error bars show standard deviations, * = P<0.05 and *** = P<0.001). Scoring system used as described in Table 5.2.

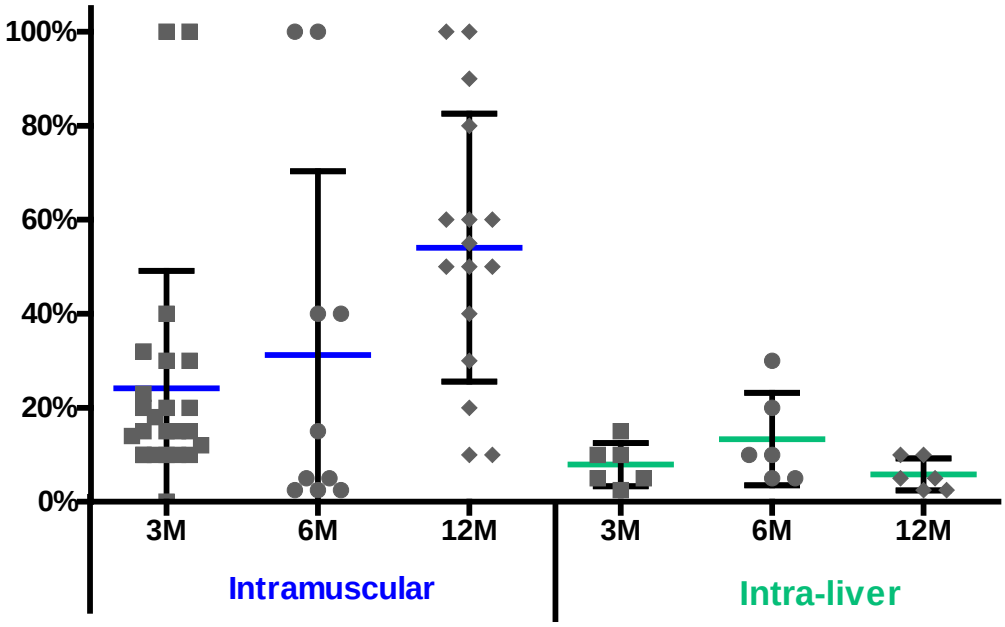

Figure 5.103 – Cellular penetration per site of implantation. Mean values, both for minimal and maximal cellular penetration, were used per animal.

Implant thickness was measured along the course of this study to evaluate implant contraction, shrinking or absorption. The figure below shows the results for the variation of thickness of Permacol® surgical implant in both implantation sites. Results were compared to pre-implanted (out of the package) Permacol® and to Permacol® implanted subcutaneously.

There was no significant difference between pre-implanted Permacol® and Permacol® implanted subcutaneously, at all time-points. A significant difference was observed at 12 months post implantation between pre-implanted and intra-liver Permacol® and between subcutaneously and intra-liver implanted Permacol®. Permacol® implanted intramuscularly showed significant differences when compared to the other 3 Permacol® groups, at all time-points.

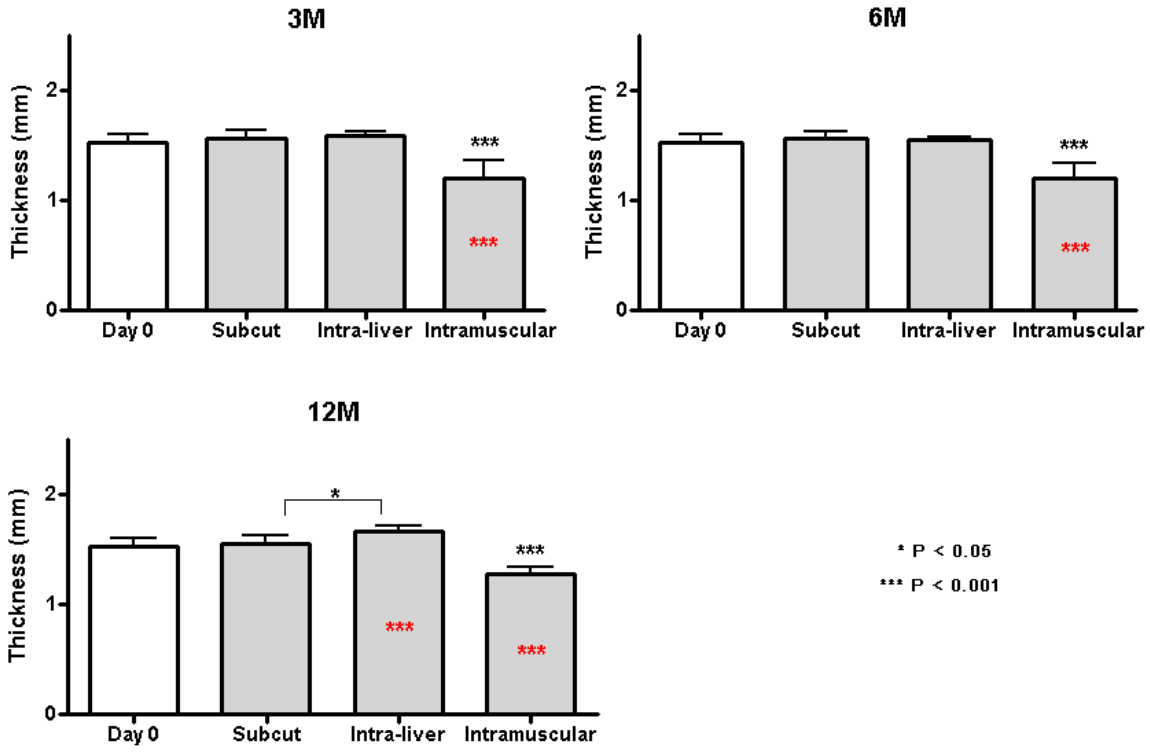

Figure 5.104 – Permacol® surgical implant thickness measurements in 3 test groups (according to site of implantation) per time-point. All groups were compared to pre-implanted Permacol® (in red).

5.3.7 Discussion

It was hypothesized that cellular response to Permacol® may depend on the site of implantation and the relative vascularity of surrounding host tissue. Adult muscle and liver comprise highly vascularised tissues and, therefore, were chosen as test implantation sites.

In surgical procedure 1 a parasagittal section was made to avoid the spinal cord, Permacol® was implanted distal and inferior to the scapula to avoid dislocation from body movements. One implant was later found at the surface of the spinotrapezius muscle, which suggests that during surgery this implant was not positioned deep enough and the animal movements displaced it.

For muscle, three months post implantation no inflammatory response was observed in the implants or surrounding tissue and, except for a few macrophages present in 2 implants, inflammatory cells were absent. This was also observed at 6 and 12 months

time points. These results were similar to Permacol® subcutaneous implantation, except at 12 months where macrophage levels were minimal.

Even though cellular density was marginal at 3 months post implantation and decreased to lower levels at 6 months in the muscle groups, cellular penetration reached, in some places, 40% and increased over time. Both cellular density and cellular penetration reached higher levels after 12 months implantation. Again there was significant difference between the implantation sites in these parameters. As observed when Permacol® was implanted subcutaneously, the extension of cellular penetration does not seem related to the level of cellular density.

While in Section 5.2 neo-vascularisation seemed related to cellular density, a reasonable assumption since an acellular tissue has no need for a vascular network, in the muscle groups vessel sprouts and mature vessels were present at higher numbers when cellular density was at its lowest level. Nevertheless, this fact may be explained by the increase in cellular penetration, as a consequence of which the number of vessels observed at the centre of implants increased.

Integration associated with the fibroblastic layer emanating from the host tissue to the edge of the implant was minimal to moderate in the 6 groups tested; furthermore, integration levels were significantly different both over time and between implantation sites.

Once more, while integration increased the population of cells decreased in all implants from 3 to 6 months, suggesting that tissue integration is not related to cell presence, a finding consistent with the previous study (Section 5.2).

Implant contraction and shrinking were analysed by implant thickness measurements along the study. Permacol® implanted intramuscularly showed significant differences when compared to all Permacol® groups, at all time-points. It is not clear if this difference is related to the mineralisation observed in this group. In the liver groups, a significant difference was observed only at 12 months post implantation between pre-implanted and intra-liver Permacol®.

There are technical factors that can influence this result, such as the embedding and sectioning techniques. In the first case, if the implant is not embedded perpendicular to the surface of the mould subsequent sections will not be in a transverse plane as expected. During sectioning the position of the blade in relation to the block will have great influence, if these are not perfectly parallel the thickness of each tissue layer

may be incorrect. These factors may increase or reduce the observed thickness of the implant but since the decrease in the thickness was present in all implants of the intramuscular groups and sometimes in an accentuated way, results suggest a contraction of the collagen. This contraction may be a result of the implant calcification or a consequence of a cellular response.

It is known that fibroblasts have a natural ability to contract collagen, as in wound healing during wound contraction. In response to injury, many interstitial fibroblasts acquire morphological and biochemical features of contractile cells, named myofibroblasts, synthesizing and depositing type I collagen into the wound provisional matrix. They subsequently contract the type I collagen matrix, facilitating wound closure (Nho *et al.*, 2006). An increase in matrix density results in a corresponding decrease in matrix volume. This theory – cell contraction – is one of two existing theories to explain the mechanism of wound contraction. It is unlikely, though, that Permacol® contraction resulted from fibroblastic activity, since deposition of new collagen and remodelling of the biomaterial matrix was not observed.

The second theory is referred to as cell locomotion and proposes the process of cell translocation through ECM as the origin of tension on the matrix which will bring the wound edges together (Roy *et al.*, 1999; Sethi *et al.*, 2002). It is presumed that the centripetal tractional forces exerted by extending pseudopodia at the leading edge of migrating fibroblasts bring the wound edges closer (Tomasek *et al.*, 2002). If the matrix is restrained, in response to force exerted by the cells, collagen fibrils become oriented in the same plane as the underlying restraint; under these conditions mechanical loading develops within the matrix (Grinnell, 2003). When the matrix becomes sufficiently rigid to resist the force exerted by the cells, equilibrium is achieved and a subpopulation of the cells enters apoptosis or becomes quiescent (Desmouliere *et al.*, 1995; Grinnell, 2000).

During the surgical procedure a pocket was made in the posterior scalenus muscle, damaging its structure and a natural wound healing process was activated. It is possible that, during the proliferation phase, fibroblasts exerting traction forces aligned collagen fibrils contracting Permacol® while contracting the surrounding matrix. Although the precise mechanisms involved in the Permacol® implant contraction are unknown, the cell locomotion theories could explain the matrix contraction and partially the low cellular density observed. Intra-liver Permacol®

implants showed lower cellular density at all time points, which may explain why there was no implant contraction in those groups.

Calcium deposition increased over time in intramuscular implants, 2 of the 6 implants showed mineralisation 3 months post implantation and at 6 months mineralisation was evident in 4 of the 6 implants and in the final time point all implants had mineral deposits. These occurrences are difficult to explain since there was no cellular response or pathology associated with the mineralised collagen and some animals had both a mineralised implant and a non-mineralised implant. Calcification of implants was observed in the previous study (Section 5.2). In the discussion it was suggested that the implantation site may be a pre-requisite for mineralisation occurrence. These results give further evidence in favour of that hypothesis. Skeletal muscle fibre cells are activated through the calcium release channel, which induces the sliding interaction between actin and myosin fibres, contained within the muscle cell, so that they move towards each other, thereby shortening (contracting) the muscle cell. Permacol® surgical implant shows a tendency to store calcium deposits, which was increased when placed in a site where calcium is more abundant. Muscle cells store high amounts of calcium in the sarcoplasmic reticulum, which releases calcium when the muscle fibres are activated; therefore, intramuscularly implantation may promote implant calcification. This could explain the temporal change in implant mineralisation when comparing subcutaneous to intramuscular implantation. In the first, mineralisation was observed only at 6 months while in the latter study mineralisation occurred as early as 3 months post implantation. These results support the hypothesis of calcium deposition *in situ* over time and add to the idea that mineralisation is related to the interstitial fluid and that Permacol® acts as a membrane, retaining minerals in places where its structure is more compact and dense, probably as a result of cross-linking.

In surgical procedure 2, Permacol® was implanted into a pocket made in the liver. At all end-time points implants were partially at the surface of the liver lobe where they had been implanted and some had another lobe attached to the Permacol®. Omentum fat adhesions were visible in 1, 2 and 2 implants respectively at 3 months, 6 months and 12 months post implantation.

Liver consists of a continuous parenchymal mass and is entirely covered by Glisson's capsule, an adherent membranous sheet of collagenous and elastic fibres. The main blood vessels and ducts were observed through the liver within a branched collagenous framework - portal tracts – showing a good structure of the liver with no lasting damage from the surgical procedure. Mammals maintain a constant liver-to-body mass ratio and in response to injury the liver is capable of natural regeneration (Khan and Mudan, 2007). In a normal adult liver, mature differentiated hepatocytes are quiescent; however, upon receiving a regenerative stimulus 95% of hepatocytes undergo cell division while maintaining their metabolic function (Hata *et al.*, 2007; Khan and Mudan, 2007). A resected rat or mouse liver undergoes compensatory hyperplasia in which the initial liver mass (and its functions) is restored within approximately 1 week after surgery (Hata *et al.*, 2007). The most commonly used model is the 70% partial hepatectomy model in rodents, which was originally described by Higgins & Anderson in 1931 (Higgins and Anderson, 1931).

Based upon the literature it is possible that the surgical procedure undertaken in the liver groups induced a natural tissue regeneration process in the liver and as a result of that process implants were pushed through the pockets towards the surface.

Implants were still partially enclosed in the hepatic tissue, including when adhesions were observed. These results suggest that (i) the liver regeneration was not complete, since not all areas of the implants were at the border of the liver, or (ii) the liver accepted the implant presence and Permacol® would remain between the collagenous membrane (Glisson's capsule) and the hepatic tissue.

There was no inflammatory response present within the surrounding tissue and implants; the only inflammatory cells observed were Kupffer cells (hepatic macrophages) but at low numbers. Permacol® surgical implant was well tolerated by the liver tissue.

Cellular density within the implant was low and decreased over time. Regardless of this, integration with surrounding tissue was mild to moderate attesting again to the notion that regular cellular presence is not essential for tissue integration to occur. Cells are present in higher numbers in the early stages of implantation but it is not known if this immediate increase in cellular density is enough to establish future good integration, or if implant/tissue integration origins from the regular but lower number of fibroblasts observed throughout the study in the interface of implant and adjacent

host tissue. There is a substantial gap between the time-points in this study, so it is not known the level of cellular density between the observations time. New blood vessels were observed at 6 and 12 months post implantation at the periphery of the implants; neo-vascularisation was not present in the centre of the implants but these areas were cell free, which explains vessel absence.

Mineralisation was not observed in any of these implants in liver, giving further evidence of the hypothesis that the implantation site influences mineral deposition. All implants showed natural birefringence under polarised light, an indicator of good quality, non-denatured collagen; implants maintained their structure and were not remodelled. In this study there was no tissue reactivity in the control tissues or implantation sites.

5.3.8 Conclusion

In the rodent model reported here the collagen matrix does not support high cellular population; cellular density and cellular penetration were at low levels in the implants when implanted in both tissue types. Nevertheless, there was no inflammation and there was no evidence of immune response; this demonstrates that Permacol® does not cause a foreign body type reaction. Permacol® is recognised as being a purified, generic dermal collagen matrix. Consequently progenitor cells from the liver and muscle are not stimulated by physical/topographical signals from the matrix to differentiate into specialist cell types. Despite the levels of cellular density and cellular penetration being marginal to minimal, integration with the surrounding tissue increased over time and reached moderate levels, suggesting that the presence of cells within the matrix, at all times, is not necessary for good integration to occur. Even in the mineralised areas implants showed no collagen degradation, collagen was highly birefringent under polarised light and implants were not remodelled or degraded.

It has previously been hypothesised that cellular response to Permacol® could be influenced by the implantation site. In this study two different highly vascular sites were chosen, muscle and liver, and the cellular response was low in both models, which is in accord with the results obtained in the subcutaneous study reported in Section 5.2. These results suggest that, as a non specialized tissue, Permacol® does

not necessarily promote movement or differentiation of cells within the matrix, independent of the surrounding tissue.

5.4 EXPERIMENTAL EVALUATION OF TWO BIOLOGIC PROSTHESES FOR ABDOMINAL HERNIA REPAIR IN A RAT MODEL

5.4.1 Introduction

Abdominal wall defects caused by trauma, incisional hernias and tumour resection are a common and challenging problem for surgeons. Surgical repair of these types of defects can be further problematic if the wound extends through a large area and in the presence of contamination. The best operative approach for repair of these defects is still controversial, but the rising number of published papers in this area has increased the amount of information regarding commercially available prosthetic materials, and by doing so gives surgeons a very useful tool to help them choose the most suitable material for a particular patient and the best operative approach.

There are several methods available for abdominal wall defects repair. Primary closure is widely used but in cases of large defects adequate tissue for direct closure is generally not available and most surgeons agree that in such a case the defect should be repaired in a tension-free manner using a prosthetic mesh material (Saettele *et al.*, 2007). The use of prosthetic biomaterials significantly reduces tension and has considerably decreased recurrence rates after repair of abdominal wall defects. These biomaterials have also provided support for the closure of difficult abdominal hernias.

Several synthetic and biologically derived materials have been used clinically to repair abdominal hernias. The ideal hernia repair material should have an adequate strength for the intended surgical application, be easily manipulated (surgeon friendly), non-toxic, biocompatible, allow fibroblast ingrowth and neo-vascularisation and withstand sterilization.

Non-absorbable synthetic materials are commonly employed, polypropylene mesh being the most used (Catena *et al.*, 2007; Hammond *et al.*, 2008). Although these meshes increase abdominal wall strength by mechanical tension, it usually results in mesh contraction, which potentially causes serious complications such as adhesions, fistula formation, skin erosion and increased susceptibility to infection. In addition,

mesh extraction can be difficult due to dense tissue incorporation. Therefore, the use of non-absorbable synthetic meshes in contaminated fields has been strongly discouraged on the basis of high rates of morbidity (Liyanage *et al.*, 2006; Parker *et al.*, 2006).

Absorbable meshes have also been used for abdominal hernias repair, including synthetic and natural materials. Biological prostheses are derived from bovine, porcine and human sources. Normally, these are collagen based and treated to remove cellular elements; additionally some biomaterials are cross-linked to delay the degradation of the collagen by blocking collagenase-binding sites (Gaertner *et al.*, 2007).

An ideal material for abdominal hernia repair would provide strength, flexibility, host tissue incorporation, vascularisation, less adhesion formation and infection tolerance. Therefore, it is essential for the clinician to choose a material that produces the least amount of foreign-body reaction and also does not allow easy bacterial attachment (Albo *et al.*, 2006; Carbonell *et al.*, 2005).

AlloDerm (LifeCell Corp., New Jersey, USA) is an acellular dermal matrix derived from donated human skin and classified as banked human tissue. It is treated to remove both the epidermis and cellular components while maintaining an intact basement membrane and collagen. Bard CollaMend Implant (Davol Inc., Cranston, Rhode Island, USA) is a porous lyophilised acellular porcine dermal collagen dressing. It is processed to remove all non-collagenous cellular components and is cross-linked to increase strength and endurance.

The purpose of the study reported here was to compare and evaluate two biologic prosthetic biomaterials, commercially available and recommended for repair of abdominal wall defects, one cross-linked and the other noncross-linked and to compare them to Permacol®, for abdominal hernia repair in a rat model.

5.4.2 Hypothesis

AlloDerm and Bard CollaMend Implant are safe and clinically efficient matrices for use in ventral hernia repair, in a rodent model.

5.4.3 Aims and Objectives

- Assess AlloDerm and Bard CollaMend Implant biocompatibility in a rat model.
- Compare AlloDerm and Bard CollaMend Implant as regenerative tissue matrices in a ventral hernia repair model.
- Compare AlloDerm and Bard CollaMend Implant performances to Permacol® surgical implant, in a ventral hernia repair model.

5.4.4 Materials and Methods

The study was performed in compliance with the Good Laboratory Practice Regulations 1999 (S.I. No 3106), as described in Section 5.1.4.
AlloDerm was purchased from LifeCell Corporation as a 5cm x 10cm sheet; thickness 0.79 - 1.78mm. AlloDerm is supplied in a foil bag within a non-sterile inner peel-pouch.
Bard CollaMend Implant (hereafter nominated simply as CollaMend) was provided by TSL plc., as a 20.3cm x 25.4cm sheet; CollaMend was lyophilized and double-packed in a Tyvek® envelope within a peel-open aluminium foil pouch, which is impermeable to moisture and oxygen.

5.4.4.1 Study Design

Since there was limited availability of materials, the study was designed to include the largest possible number of items per group, *i.e.*, the area of each biomaterial was divided in order to yield the maximum number of grafts (with a constant area), which resulted in 18 grafts from AlloDerm and 27 grafts from CollaMend. Six treatment groups were constructed and divided between 3 time-points as in Table 5.12.

Table 5.12 – Study groups and time point design. A= AlloDerm, C= CollaMend.

Termination time point						
Months	**1**		**3**		**6**	
Group	**A-1**	**C-1**	**A-2**	**C-2**	**A-3**	**C-3**
Animals	**6**	**9**	**6**	**9**	**6**	**9**

Male Wistar-Han^{TM} rats were used with weights between 250 and 310g. Body weights were recorded in the day of surgery and at the termination day. Animals were randomly distributed within the 6 groups.

Both dermal matrices were pre-treated according to the manufacturer's instructions. AlloDerm was re-hydrated in a two-step bath. The tissue was submerged and soaked in 0.9% saline solution for a minimum of 5 minutes or until the backing separated from the AlloDerm. Using sterile non-toothed forceps the backing was discarded and the tissue aseptically transferred to a second bath of saline solution where it remained completely submerged for 30 minutes or until the tissue was fully re-hydrated. According to its manufacturers, complete re-hydration should be achieved in 10 to 40 minutes, depending on thickness of the tissue. AlloDerm must be used within 4 hours of re-hydration.

AlloDerm has a basement membrane and a dermal surface; when applied to the wound bed in a grafting procedure, or as an implant, the dermal surface must be placed against the wound bed or against the most vascular tissue. There was some difficulty in identifying the dermal side, therefore 3 animals per group were implanted with the "dermal side" facing the wound bed, and the other 3 implanted with the "dermal side" facing the skin.

CollaMend was completely hydrated before use by immersion in a 0.9% sterile saline solution for a minimum of 3 minutes.

After complete hydration both dermal materials were aseptically trimmed to the desired dimensions. Pieces of non-implanted material were fixed in a 10% NBF solution for histological analysis.

5.4.4.2 Surgical Procedure

1. Rats were induced and maintained under general anaesthesia according to the procedure described in Section 2.2.5.
2. A ventral midline incision was made from just below the level of the rib cage extending approximately 1.5cm distally.
3. Skin was elevated and retracted to allow access to a site at the mid lateral aspect of the caudal peritoneal wall.
4. Using a template, a 3cm x 0.5cm piece of peritoneal wall was excised to leave the peritoneum intact (Figure 5.105).
5. A piece of biomaterial, 5cm x 2.5cm, was placed to cover and overlap the excision equally at each aspect. This procedure was performed only in one side of the midline, the other side underwent creation of a ventral hernia defect without biomaterial implantation; therefore, was used as control.
6. The biomaterial was secured by absorbable sutures through test material into peritoneal wall.
7. The ventral midline incision was closed with interrupted sutures.
8. Once recovered from anaesthetic, animals were returned to the animal accommodation, singly housed.

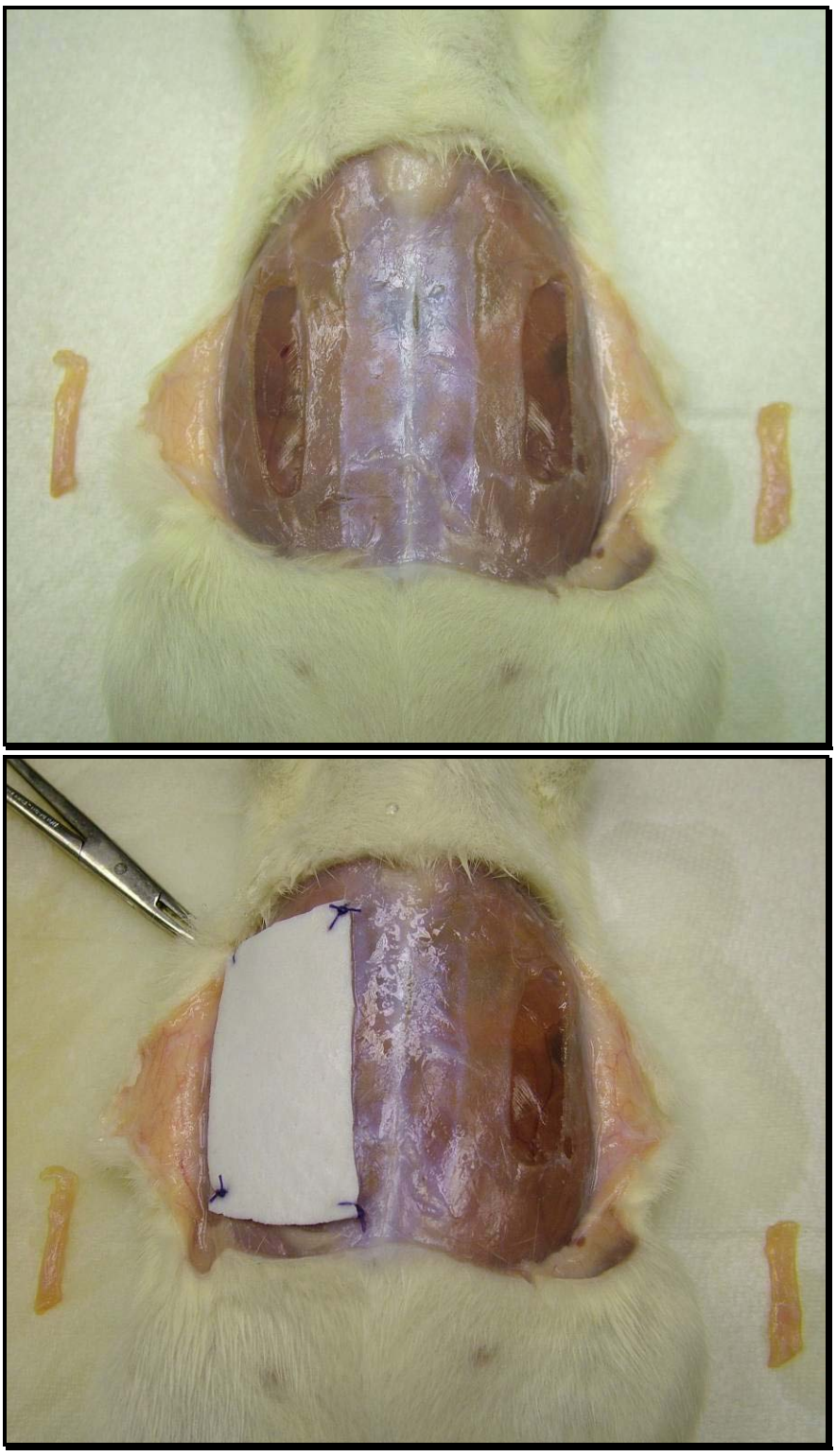

Figure 5.105 – Ventral hernia repair model. Two defects were created leaving the peritoneum intact, one defect was covered with the biomaterial tested and the second defect was left to heal naturally as control.

5.4.4.3 Necropsy

Animals were euthanased with an intra-peritoneal injection of sodium pentobarbitone and the operative sites identified and exposed. The complete operative site together with adjacent tissue was removed and one third (longitudinally) was resected to be used fresh for integration strength testing by way of a tensiometer, another third was frozen in liquid nitrogen and kept at -80^{o}C for possible later examination, and the remainder was fixed in 10% NBF for routine histology.
From the opposite, control side of the animal, a similar sized piece of peritoneal wall was excised and divided in two halves, one was fixed and the other stored at -80^{o}C.

5.4.5 Statistical Analysis

Histometric scores (integration, cellular density, cellular penetration, inflammatory cells and neo-vascularisation) were analysed per matrix type and over time using a two-way ANOVA to look for interaction between mesh type and time-point. These tests were performed in conjugation with Levene's test to check for homogeneity of variances; when variances were significantly different two separate one-way variance analysis were performed instead. One-way ANOVA was also used to analyse the tensiometry results over time. When the ANOVA (one-way and two-way) results were significant, least significant difference (LSD) and Bonferroni post hoc tests were used to identify differences within groups; when the variances were unequal Tamhanes's T2 post hoc test was used. $P<0.05$ was considered as statistically significant for all tests applied. Pearson correlation was used to find associations between parameters. Statistical analysis was performed using SPSS Statistics 16.0 (SPSS Inc. Chicago, USA). Graphical representation of data was performed using Graphpad Prism statistics software, version 4 (GraphPad Software, Inc., USA).

Results are presented individually per biomaterial tested and in the end compared and discussed collectively.

5.4.6 Results – AlloDerm

There were no situations which the NACWO or PPL License Holder were unable to deal with and therefore nothing was referred to the named Veterinary Physician.

5.4.6.1 Tensiometry

Tensiometry studied the resistance of the AlloDerm/surrounding tissue complex to a constant force applying a separation moment, measured as the maximum tension the material can withstand without integration failure. The individual materials within the complex may also fail.

Tensiometry results are displayed in Table 5.13 to Table 5.15. Two AlloDerm implants separated from the adjacent host tissue at 1 month post implantation, the remaining implants failed by splitting of the muscle or suture failure. Separation means separation between the implant and the surrounding tissue. The graft tension orientation was always the same; AlloDerm was sutured to the fixed end of the tensiometer.

Table 5.13 – Tensiometry results for AlloDerm implants at 1 month post implantation.

Animal number	Max Load (kg)	Ext at Max Load (mm)	Total Extension (mm)	Separation
$A_{1.1}$	0.669	41.79	69.27	No (suture snapped)
$A_{1.2}$	0.808	22.25	61.97	No (muscle split)
$A_{1.3}$	0.984	23.73	32.86	No (muscle split)
$A_{1.4}$	1.231	33.81	61.22	Yes
$A_{1.5}$	0.969	35.26	73.80	Yes
$A_{1.6}$	0.827	13.33	76.19	No
Mean	**0.915**	**28.362**	**62.552**	
SD	**0.194**	**10.415**	**15.757**	

Group A-2 showed a lower mean value for maximum load, but there was no significant difference between groups for all parameters analysed. Only one implant separated from the adjacent tissue in group A-2; the other implants remained attached to the surrounding tissue while the muscle tore. In one animal the travel limit of the tensiometer was exceeded, separation did not occur, stretching of AlloDerm was observed for all implants.

Table 5.14 – Tensiometry results for AlloDerm implants at 3 months post implantation.

Animal number	Max Load (kg)	Ext at Max Load (mm)	Total Extension (mm)	Separation
$A_{2.1}$	0.895	35.44	47.29	No (muscle split)
$A_{2.2}$	0.780	28.03	72.62	Yes
$A_{2.3}$	0.729	16.14	33.00	No (muscle split)
$A_{2.4}$	0.380	16.57	54.12	No (muscle split)
$A_{2.5}$	0.578	28.20	64.14	No (muscle split)
$A_{2.6}$	0.190	58.49	79.85	No (travel limit exceeded)
Mean	**0.592**	**30.478**	**58.503**	
SD	**0.266**	**15.617**	**17.217**	

During the tensiometry analysis it was difficult to identify the implant in 2 animals from group A-3. Since this was a potential area for sample variability which would lead to results which were not comparable, the tensiometry results for those samples were ignored. It was later confirmed by histological analysis that the implants in those animals were not present.

In group A-3 implants did not separate from the adjacent tissue; the travel limit was exceeded in two of the implants and in the other two implants AlloDerm was delaminated and tore.

Table 5.15 – Tensiometry results for AlloDerm implants at 6 months post implantation. *P<0.05.

Animal number	Max Load (kg)	Ext at Max Load (mm)	Total Extension (mm)	Separation
$A_{3.1}$	0.425	25.74	32.68	No (travel limit exceeded)
$A_{3.2}$	0.855	20.46	32.54	No (AlloDerm delaminated)
$A_{3.5}$	1.506	22.52	32.68	No (travel limit exceeded)
$A_{3.6}$	0.499	11.34	18.73	No (AlloDerm delaminated)
Mean	**0.821**	**20.015**	**29.158***	
SD	**0.494**	**6.178**	**6.952**	

Maximum load and extension at maximum load values were compared between the 3 groups and there was no evidence of a significant difference between time-points. Total extension was significantly different between the groups A-1 and A-3, and between A-2 and A-3.

5.4.6.2 Histopathology

Sections were examined for implant presence, acute inflammation, chronic inflammation, seroma, fibrosis, giant cells, tissue integration, cellular penetration, cellular density, neo-vascularisation and collagen degradation.

Strips from AlloDerm before implantation were taken and processed for comparison with the implanted AlloDerm. Histology of the pre-implanted AlloDerm showed good non-denatured collagen and no cells were visible in the matrix (Figure 5.106).

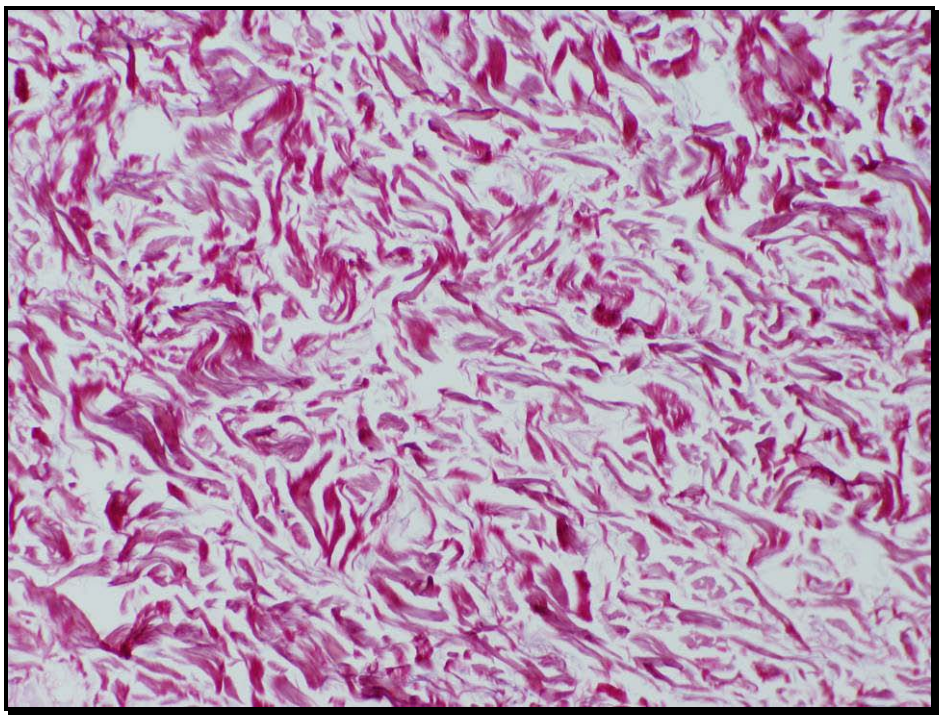

Figure 5.106 – AlloDerm (picro sirius red, 100X).

All animals lived until necropsy and biomaterial harvest. All animals were healthy with body weight values as expected.

Group A-1 – 1 month

Four animals developed seroma 8 days post implantation, which contributed to the inflammatory responses observed. Another animal developed a small open wound that did not affect his health and behaviour, but may have contributed to the absence of a seroma; the inflammatory response in this implant was severe. After necropsy a sub-clinical seroma was found in the remaining animal. In 3 of the animals that developed seroma the Alloderm was implanted with the dermal side facing the wound, in the other 2 animals the implant dermal side was facing the skin.

Two implants showed remains of a severe acute and chronic inflammatory responses (Figure 5.107). AlloDerm was heavily invaded by inflammatory cells but in places where the inflammatory response was absent the implant was cell free (Figure 5.108). In both implants the inflammatory response was between the AlloDerm and the

peritoneal wall. The remaining implants had moderate levels of acute and chronic inflammatory responses.

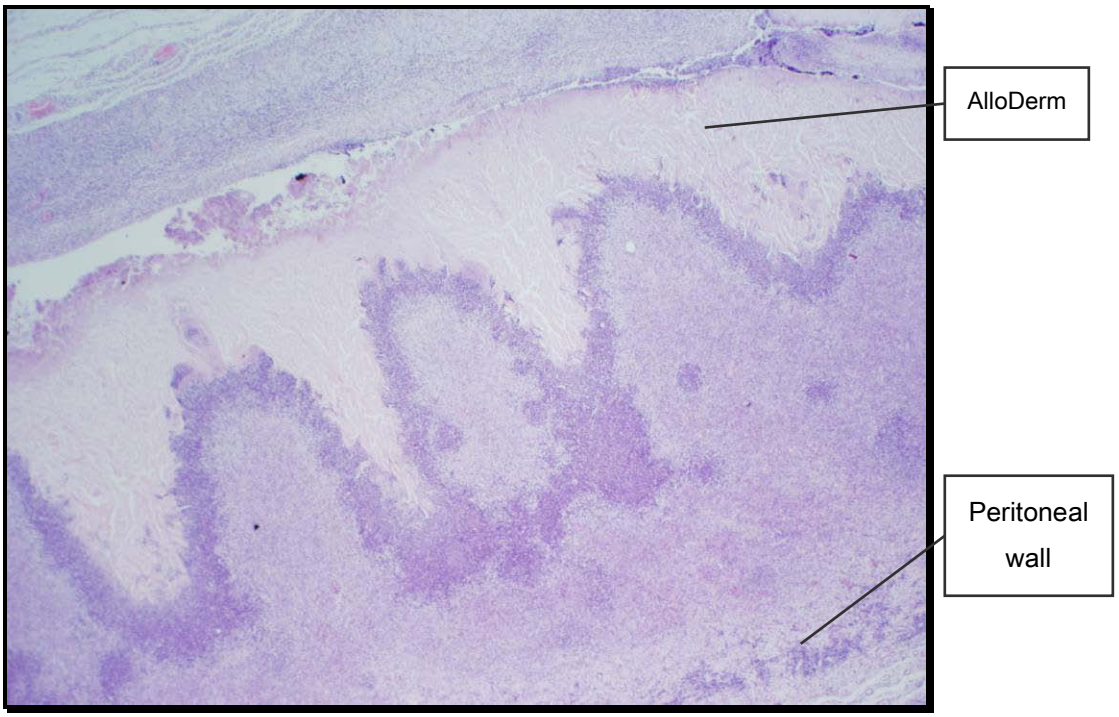

Figure 5.107 – AlloDerm implant, 1 month post implantation, showing severe acute and chronic inflammatory responses (H&E, 20X).

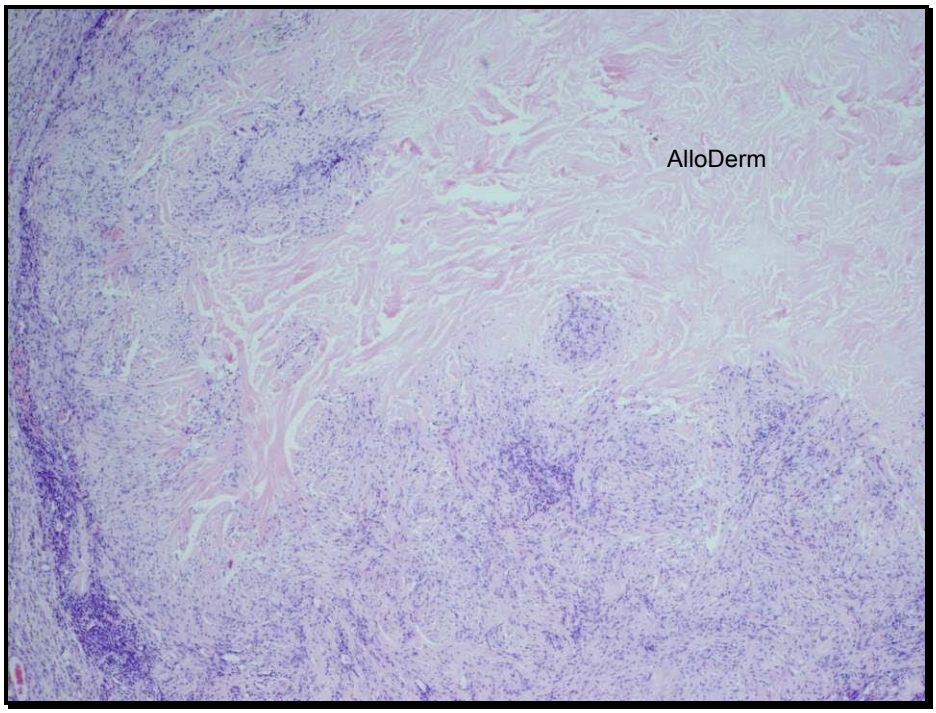

Figure 5.108 – AlloDerm implant 1 month post implantation, areas where the inflammatory response has not reached are cell free (H&E, 40X).

Lymphocytes, macrophages and polymorphs were present in all implants (Figure 5.109). Lymphocytes were present in a large number and active, which indicates some immune response. In 3 implants neutrophils were acting as a barrier, surrounding the implant and separating it from the adjacent tissue (Figure 5.110). Giant cells and fibrotic activity were present in 4 implants.

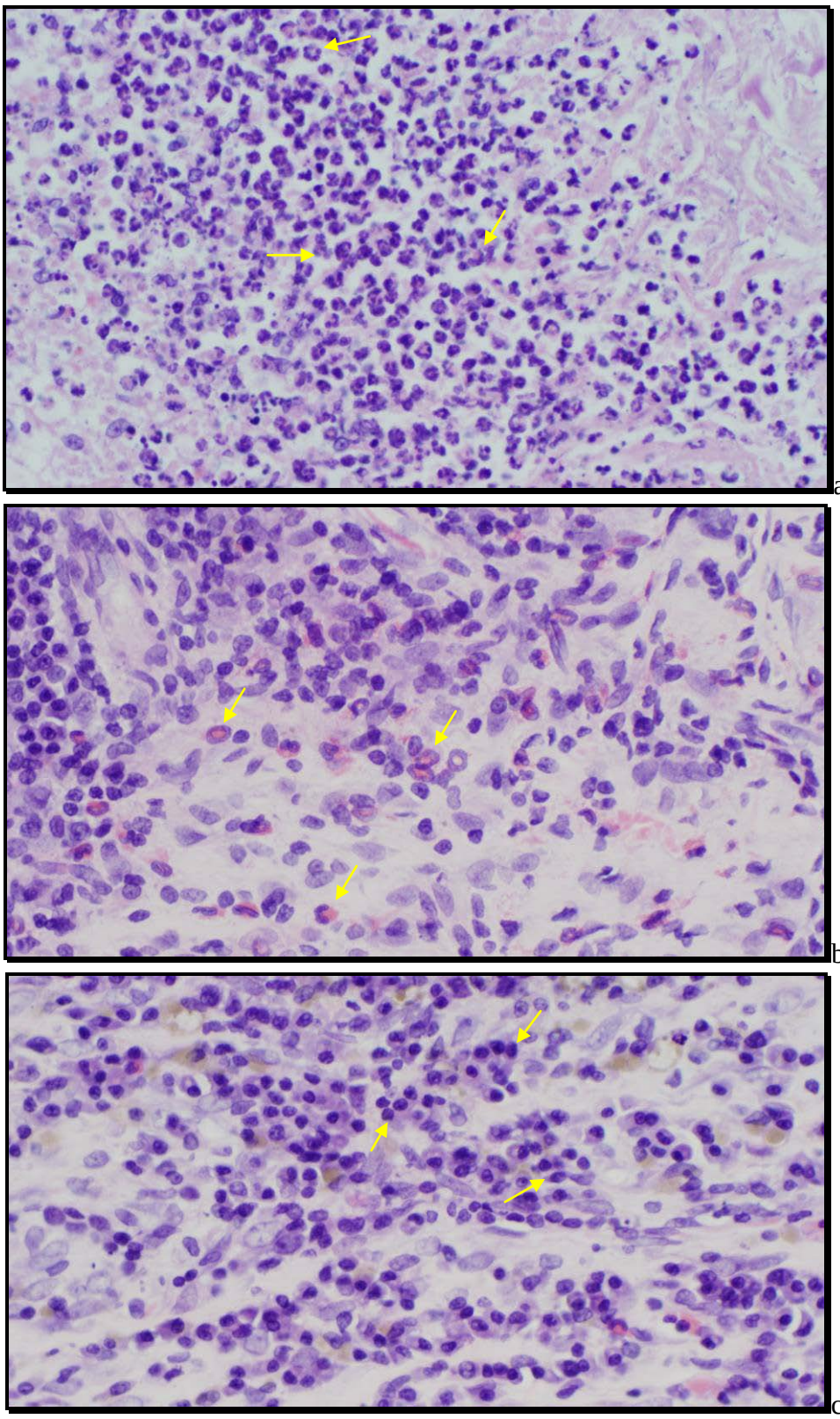

a)

b)

c)

Figure 5.109 – Polymorphs and lymphocytes in a 1 month post implantation AlloDerm implant: a) Neutrophils, b) Eosinophils, c) Lymphocytes, (H&E, 400X).

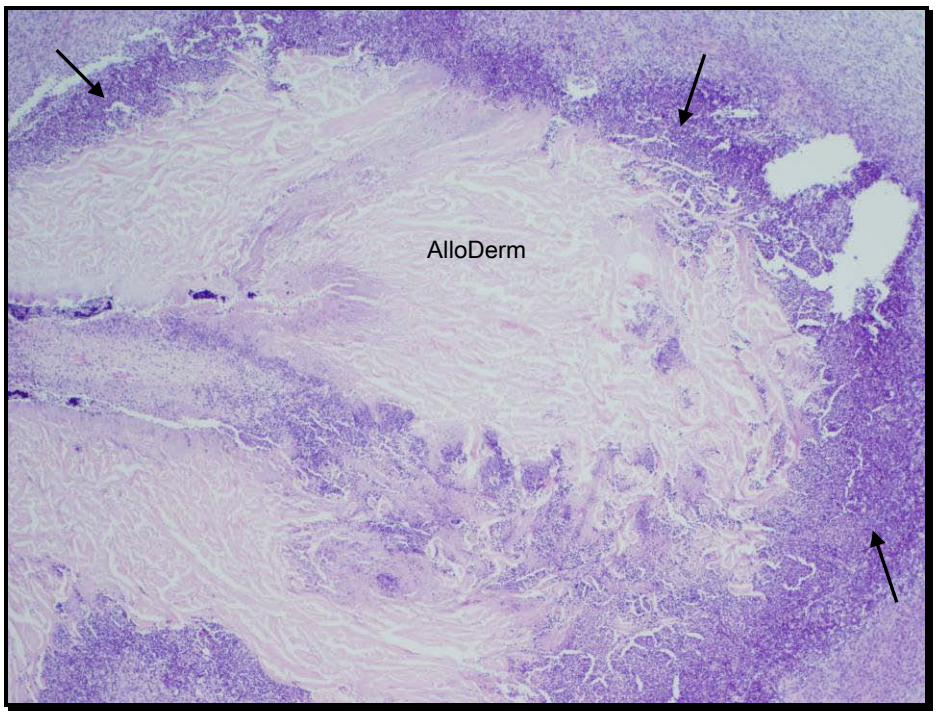

Figure 5.110 – Neutrophils barrier (arrows) separating an AlloDerm implant from the surrounding tissue, 1 month post implantation (H&E, 40X).

At 1 month post implantation, when cellular density was high, blood vessels were visible to support the inflammation. In these places AlloDerm lost its original configuration and was remodelled (Figure 5.111). Implant cell free areas kept the original structure (Figure 5.112).

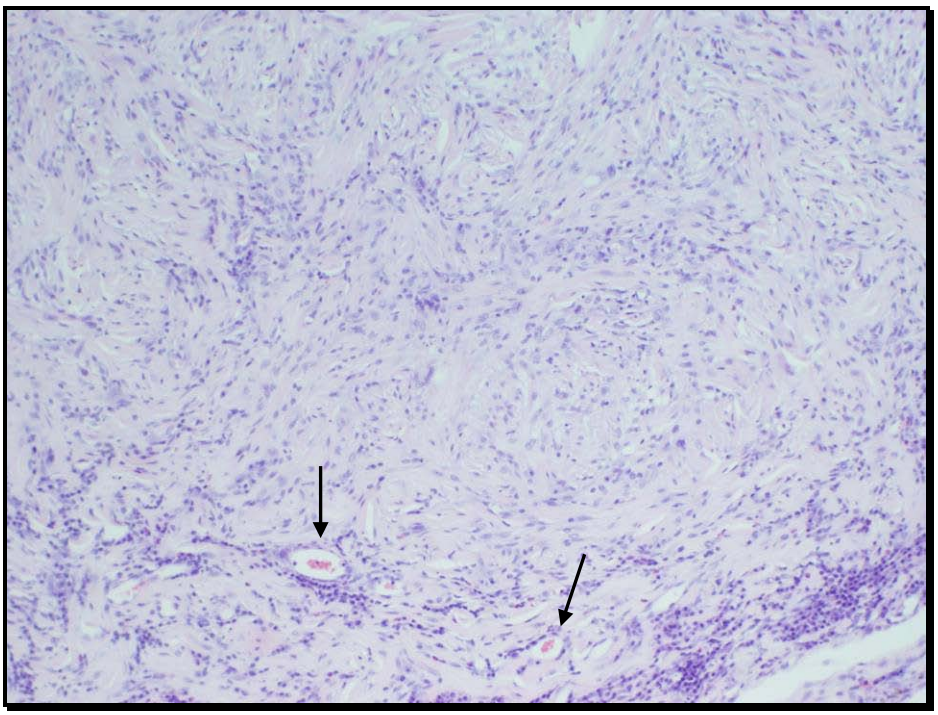

Figure 5.111 – Remodelled AlloDerm with formed vessels (arrows) at 1 month post implantation (H&E, 100X).

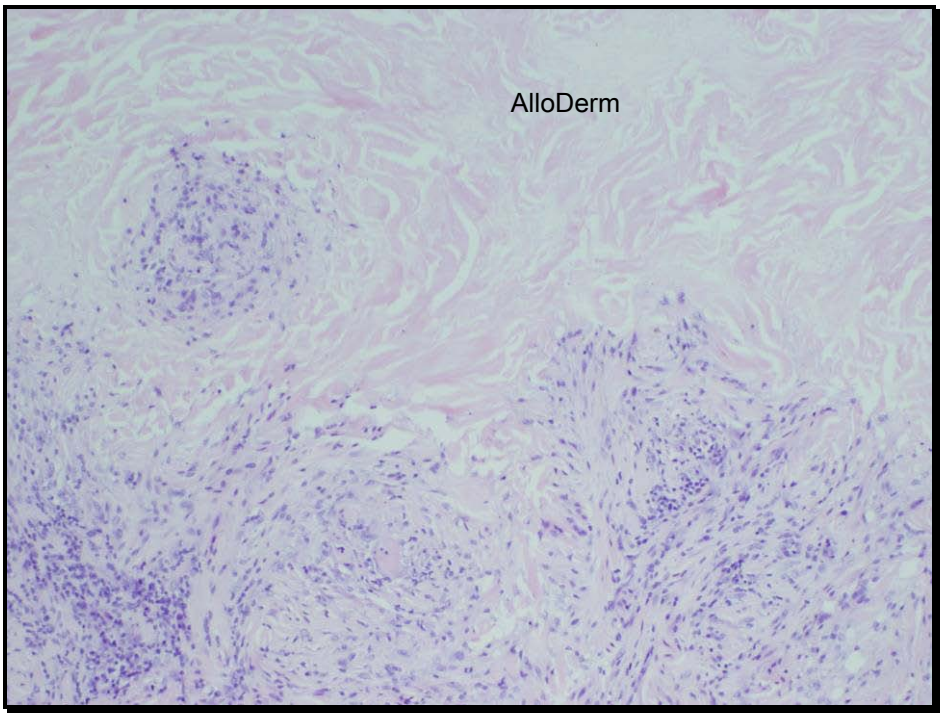

Figure 5.112 –AlloDerm with cell free areas maintaining its original configuration, cellular areas were remodelled, 1 month post implantation (H&E, 100X).

Control tissue showed no reactivity to the surgical procedure. On examination under polarized light, normal, non-denatured collagen patterning is demonstrated in the controls.

At 1 month post implantation the collagen from the AlloDerm implants was losing its natural birefringence especially at the edges which indicates collagen degradation (Figure 5.113). Collagen degradation was probably a consequence of the high cellular activity caused by the inflammatory response observed.

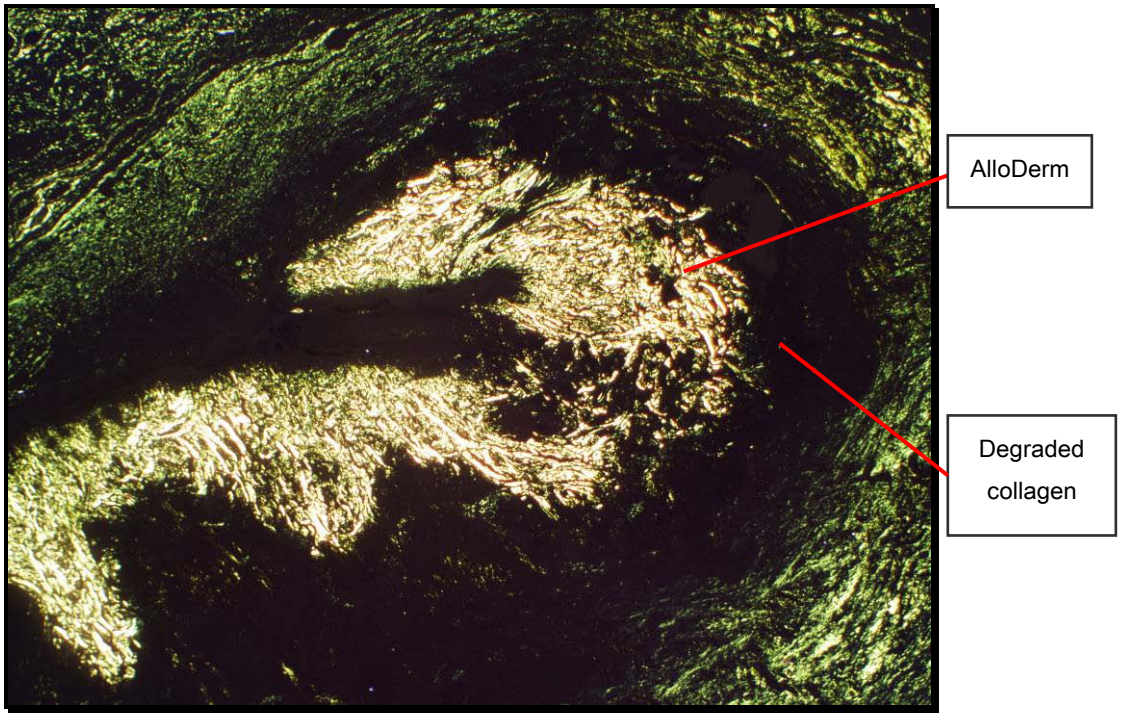

Figure 5.113 – Degraded collagen in an AlloDerm implant, under polarized light (picro sirius red, 20X).

The next figure shows a graphical representation of results for 1 month post implantation. At this time point implants that were not fully present were partially degraded as a result of a severe inflammatory response. Seroma refers to the number of animals that developed seroma during the study time, independently if the seroma was absorbed or not.

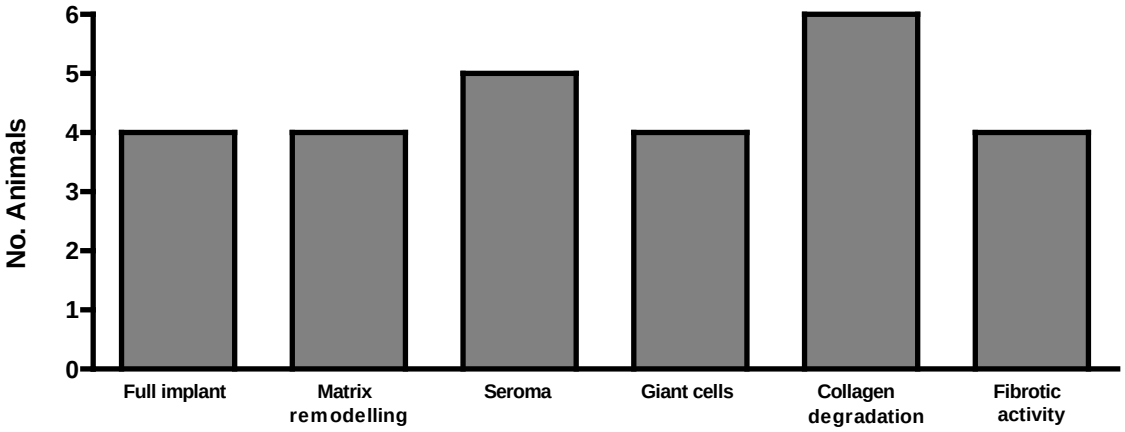

Figure 5.114 – AlloDerm results at 1 month post implantation.

Group A-2 – 3 months

At 3 months post implantation 3 of the implants were intact, whereas the others were only partially present (Figure 5.115 and Figure 5.116).

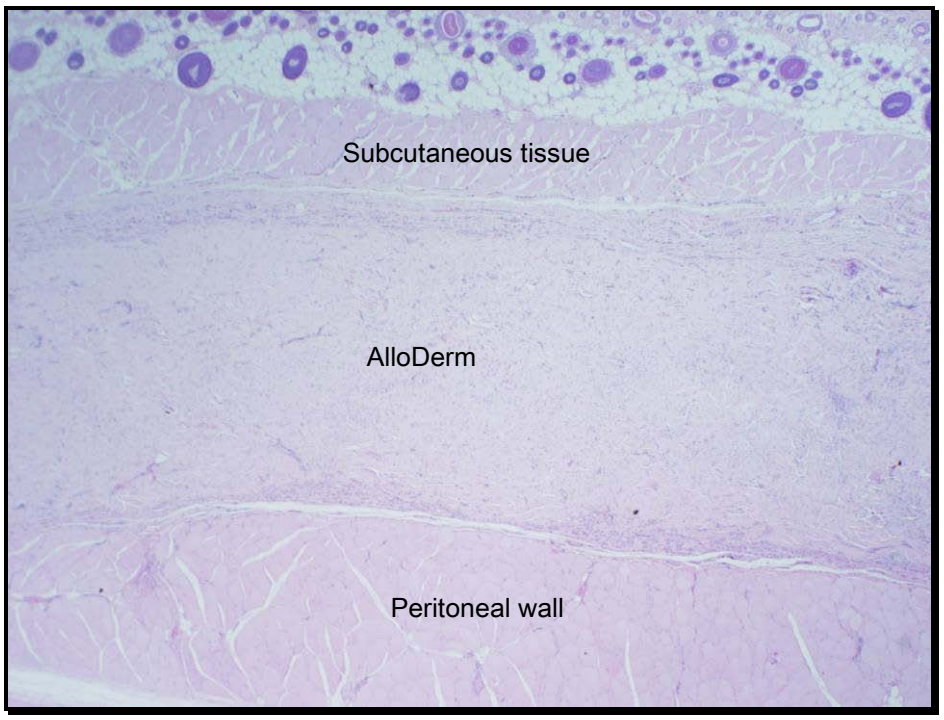

Figure 5.115 – AlloDerm implant fully present after 3 months implantation (H&E, 20X).

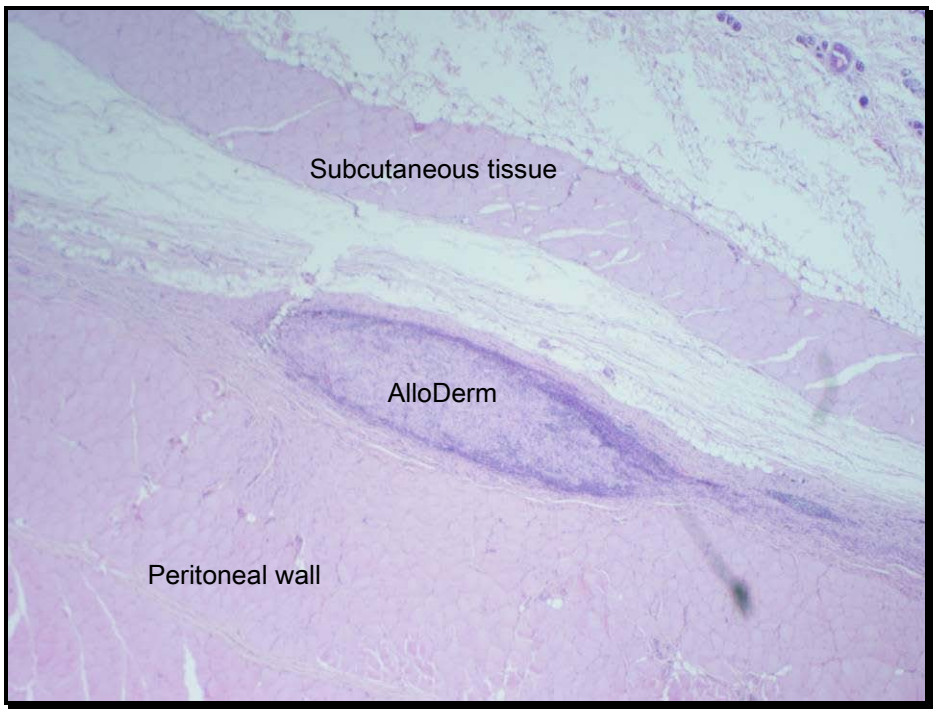

Figure 5.116 – Remains of an AlloDerm implant after 3 months implantation (H&E, 20X).

Three of the animals from this group developed seroma in the second week of the study, in one animal the dermal side of AlloDerm was facing the skin and in the other two was facing the wound. Most implants showed remains of marginal to moderate acute and chronic inflammatory response, these responses were significantly different from the values obtained at 1 month post implantation. Because of the inflammatory response, implants were heavily populated with cells and AlloDerm configuration changed when a high cellular density was observed but, as observed in the 1 month post implantation implants, areas where AlloDerm maintained its original configuration were cell free (Figure 5.117).

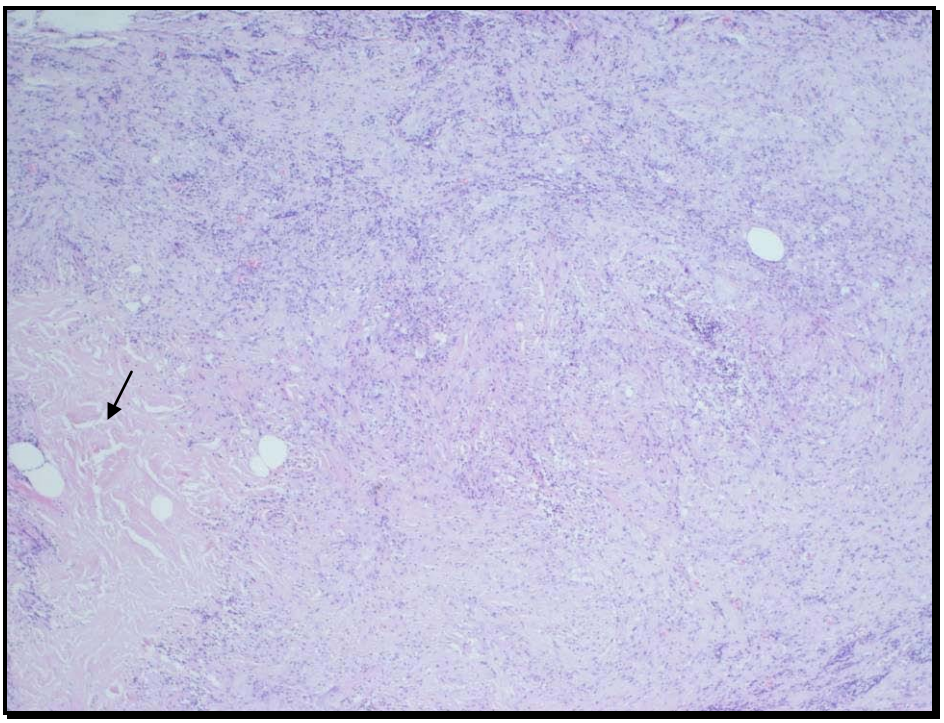

Figure 5.117 – AlloDerm implant at 3 months post implantation; the arrow indicates AlloDerm in its initial configuration (H&E, 40X).

Lymphocytes were visible in an excessive number and were active which indicates a significant immune response. A barrier, mainly constituted by lymphocytes, was visible surrounding the implants (Figure 5.118). Despite the lymphocyte barrier cellular penetration achieved 100% in all implants.

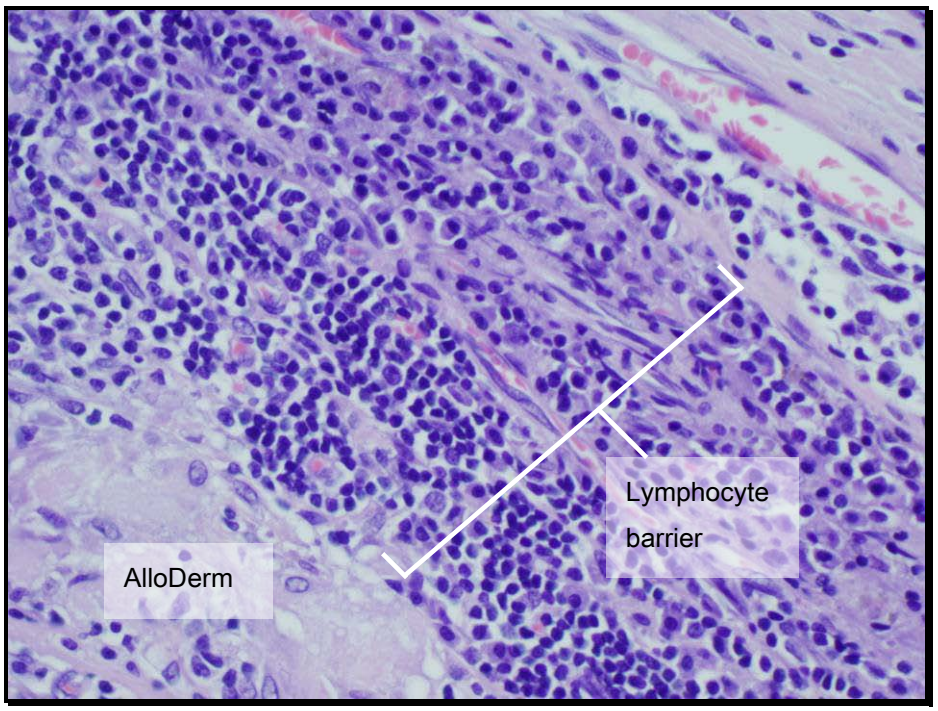

Figure 5.118 – Lymphocyte barrier between the implant and the surrounding tissue (H&E, 400X).

Macrophages were visible in a large number, especially in the edges of the implants; giant cells were present in 5 implants **(**Figure 5.119a). Giant cells formed around fragments of the implant as a result of a chronic inflammation. Mature vessels and vessel sprouts were present to support cells (Figure 5.119b). Integration with the surrounding tissue, at 3 months post implantation, was moderate to complete and after statistical analysis the integration increase was considered significantly different compared to results at 1 month post implantation.

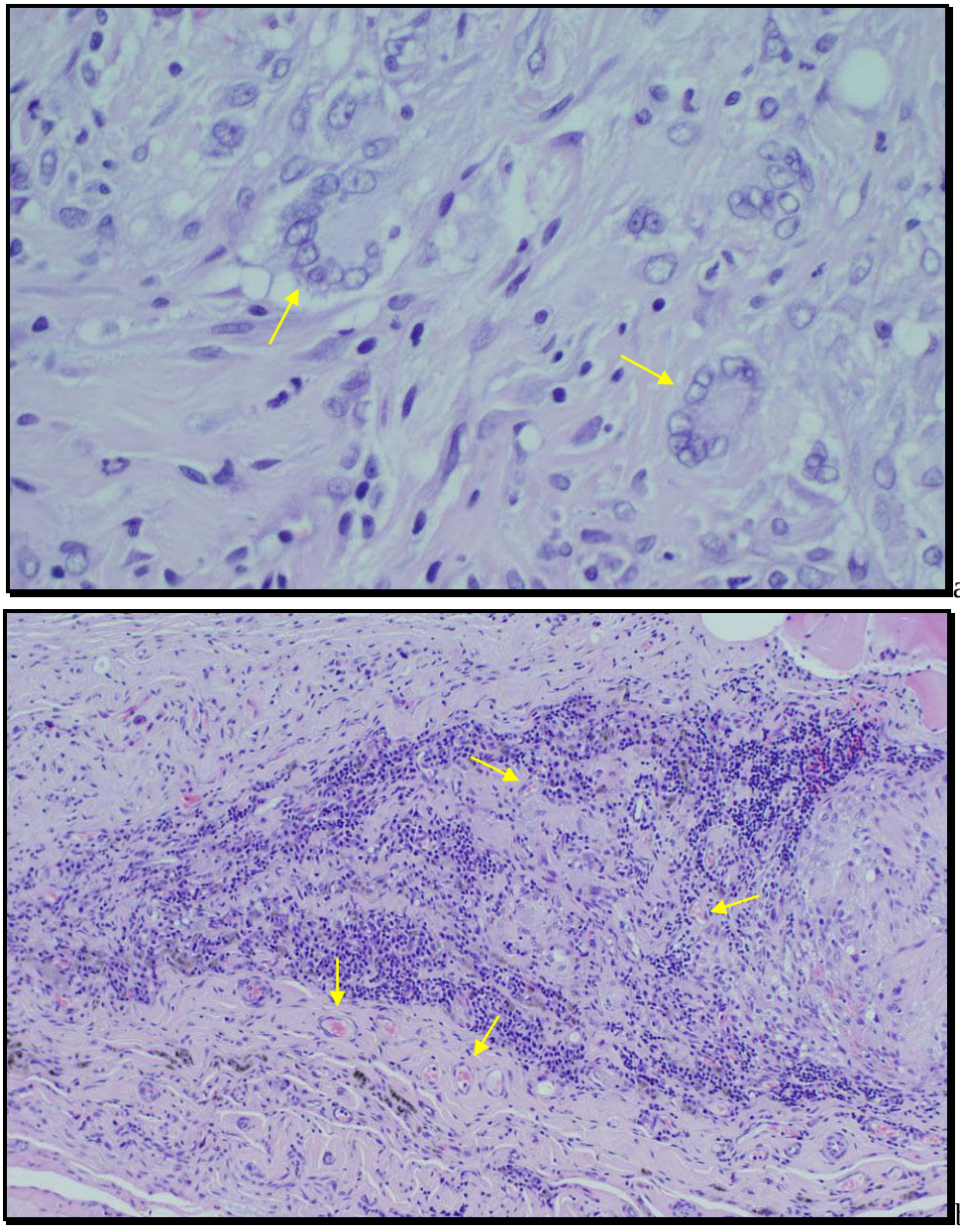

a)

b)

Figure 5.119 – AlloDerm implant 3 months post implantation: a) giant cells digesting the implant (H&E, 400X); b) vessels in the centre of the implant (H&E, 100X).

The AlloDerm implanted in animal $A_{2.4}$ had hair in one of the sides; this side was implanted facing the skin. After 3 months implantation, the implant was almost entirely present with visible hair follicles (Figure 5.120).

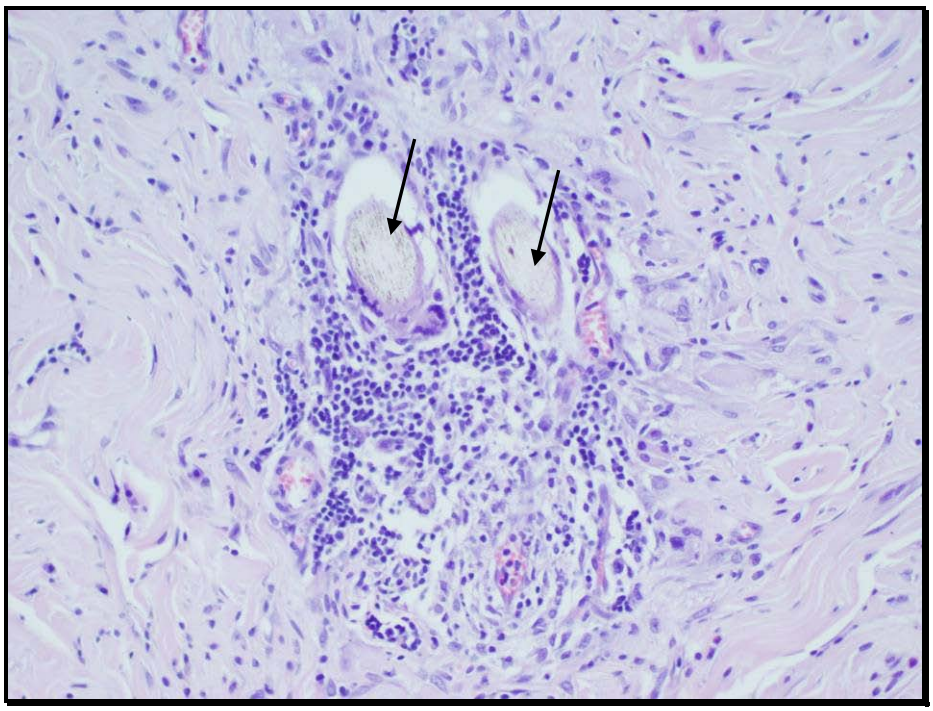

Figure 5.120 – Hair follicles present in an AlloDerm implant, 3 months post implantation (H&E, 200X).

At 3 months post implantation implants with moderate inflammatory response showed collagen degradation demonstrating implant breakdown (Figure 5.121).

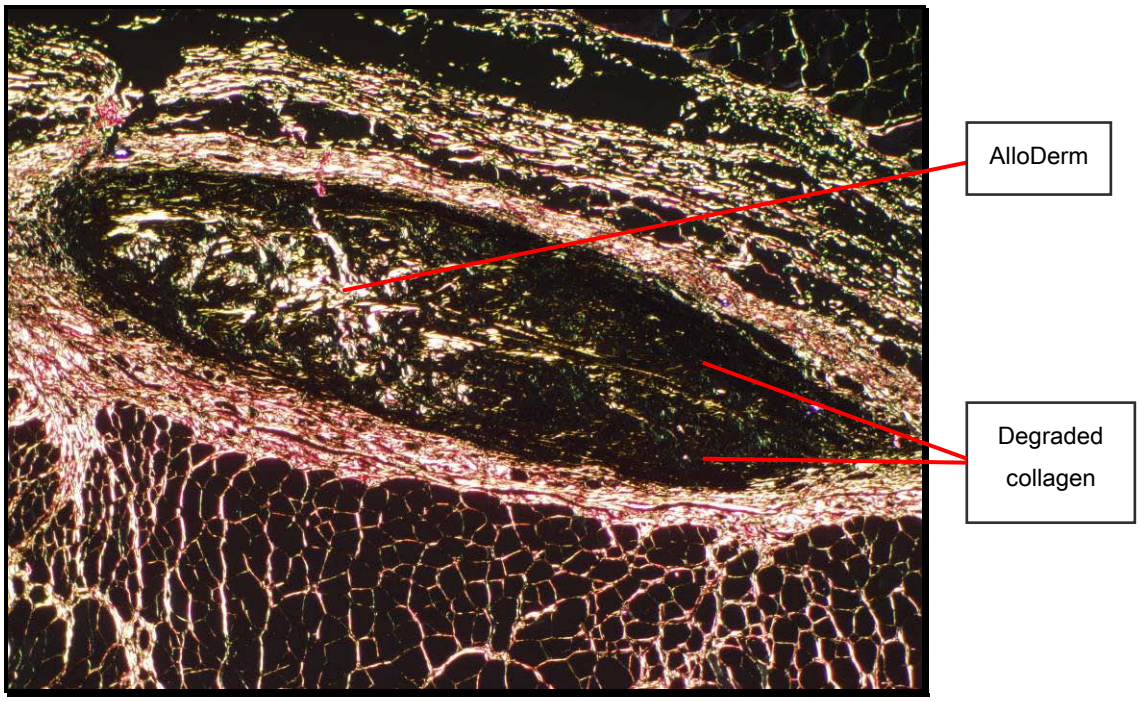

Figure 5.121 – Collagen degradation in an AlloDerm implant, 3 months post implantation (picro sirius red, 40X).

All tissue controls showed a healed wound, reactivity was not observed in these tissues.

Figure 5.122 shows the 3 months post implantation results. Histometric results for parameters: inflammation, integration, cellular density, cellular penetration and neo-vascularisation were scored as described in Section 5.1.6.

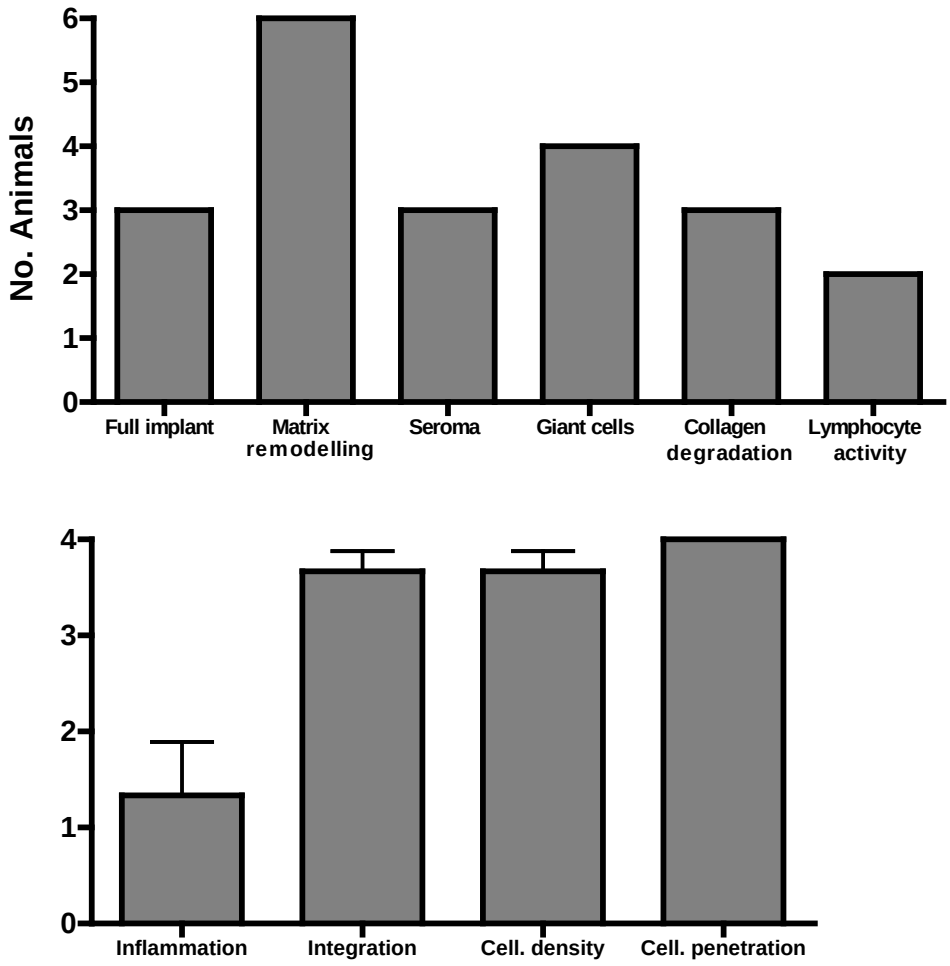

Figure 5.122 – AlloDerm results 3 months post implantation (error bars show standard deviation).

Group A-3 – 6 months

At 6 months post implantation it was difficult to identify the implants; in two animals AlloDerm was absent but remains of the sutures were visible identifying the implantation site (Figure 5.123).

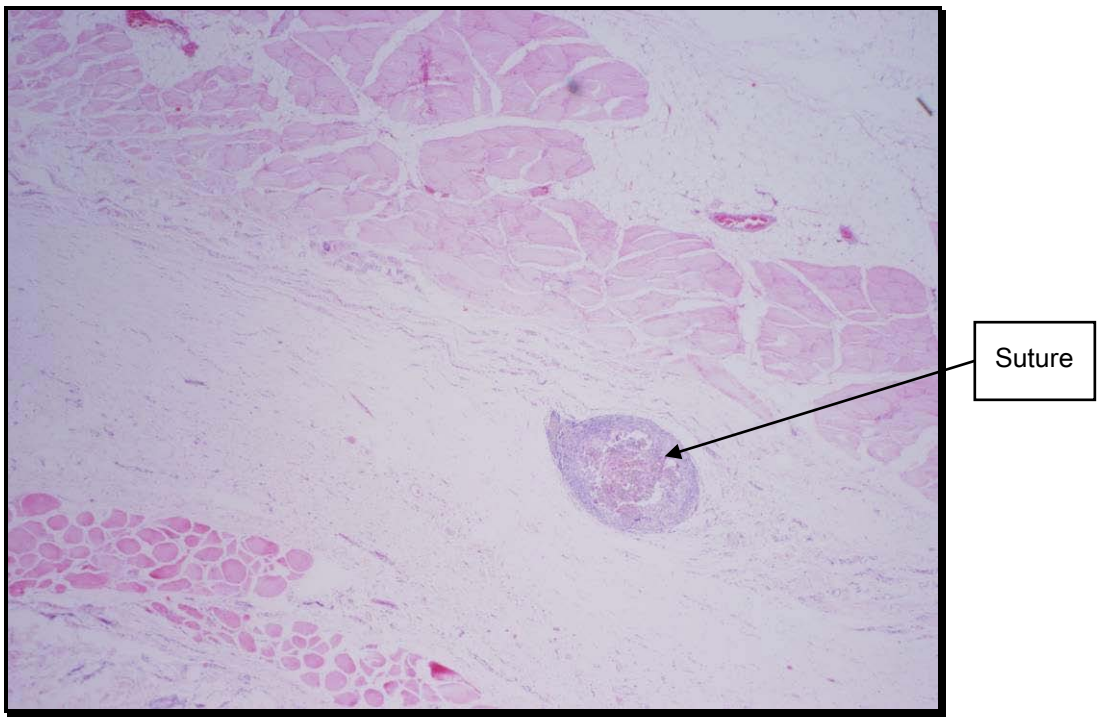

Figure 5.123 – No visible AlloDerm at 6 months post implantation (H&E, 20X).

Three animals from this group developed seroma, in one animal the seroma had to be drained because of its large size. From these animals 2 were implanted with the dermal side of AlloDerm facing the wound and one with the dermal side facing the skin. All further data refers to the 4 samples that still had the implant present at 6 months post implantation.

Implants showed complete integration in 3 samples and moderate integration in one (Figure 5.124). Although integration at 6 months implantation did not show a significant difference from the values obtained at 3 months post implantation, integration in group A-3 increased significantly when compared to group A-1.

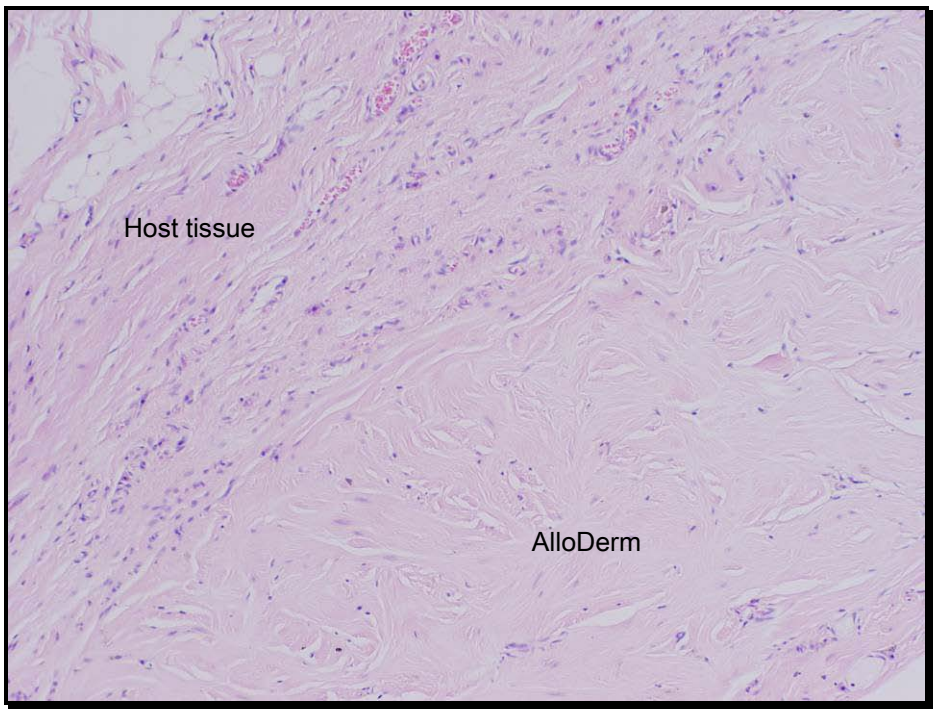

Figure 5.124 – AlloDerm implant, 6 months post implantation, well integrated with the surrounding tissue (H&E, 100X).

Cellular density reached moderate levels and cellular penetration was 100% in all AlloDerm implants (Figure 5.125). Cellular density in this group was significantly different from the 3 months group. Neo-vascularisation was present to support the cells.

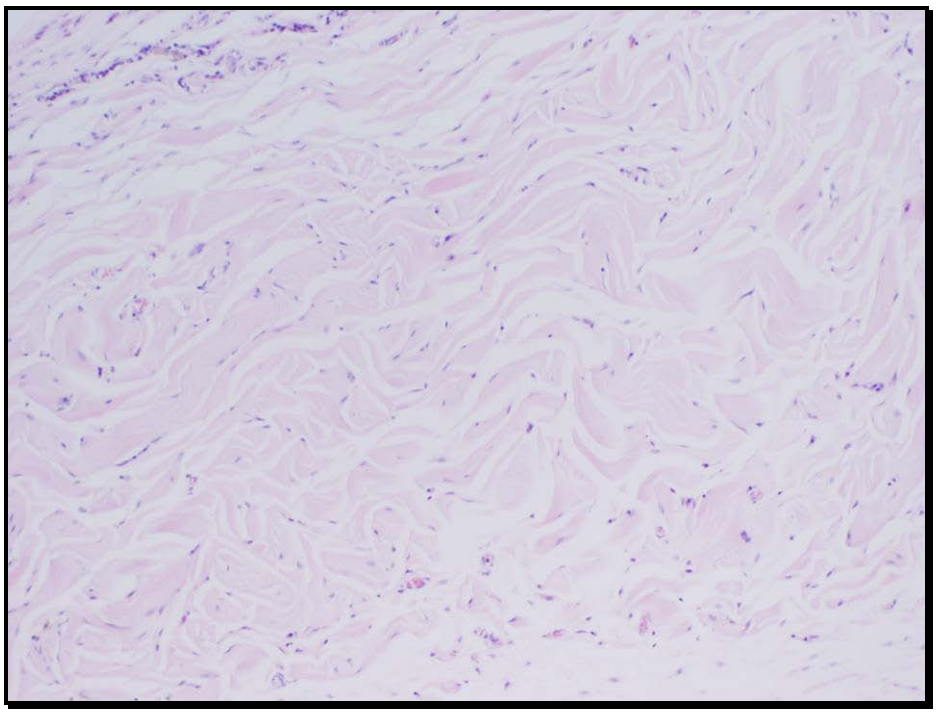

Figure 5.125 – Complete cellular penetration of an AlloDerm implant (H&E, 100X).

Macrophagic activity was present in 3 of the implants and 1 of these had giant cells. On examination under polarized light, normal, non-denatured collagen patterning was present (Figure 5.126). Given that at 1 and 3 months post implantation there was collagen degradation, the normal birefringent collagen patterning observed at 6 months is probably caused by deposition of new collagen, although implants show both mature (thick fibres) and new collagen (thin fibres).

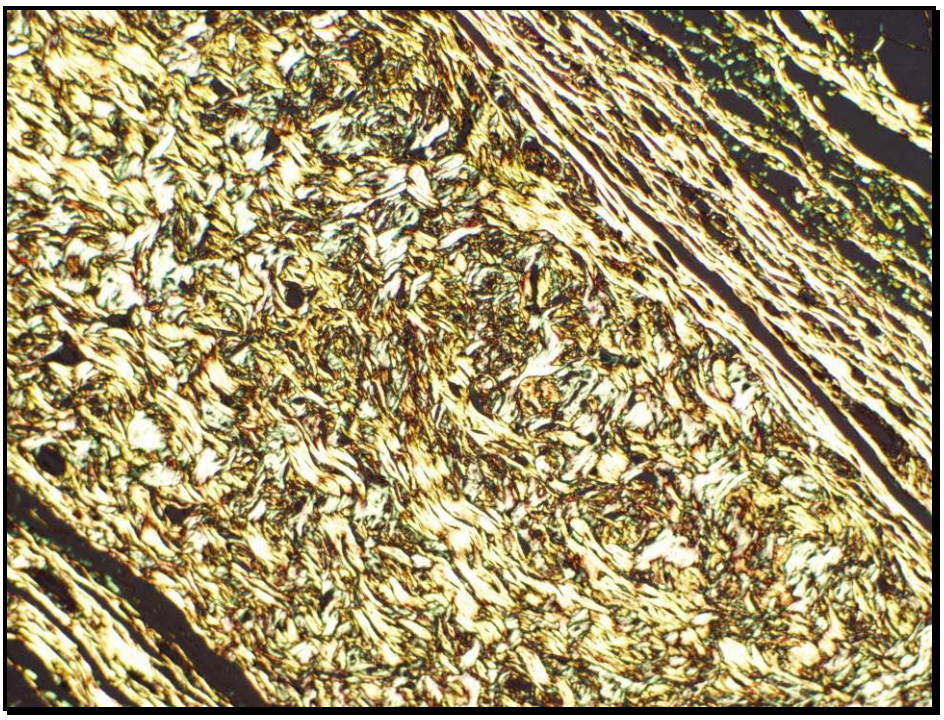

Figure 5.126 – AlloDerm implant stained with picro sirius red, 6 months post implantation (100X).

All tissue controls showed healed wounds, reactivity was not observed in these tissues.

Figure 5.127 shows the results for the 6 months post implantation group.

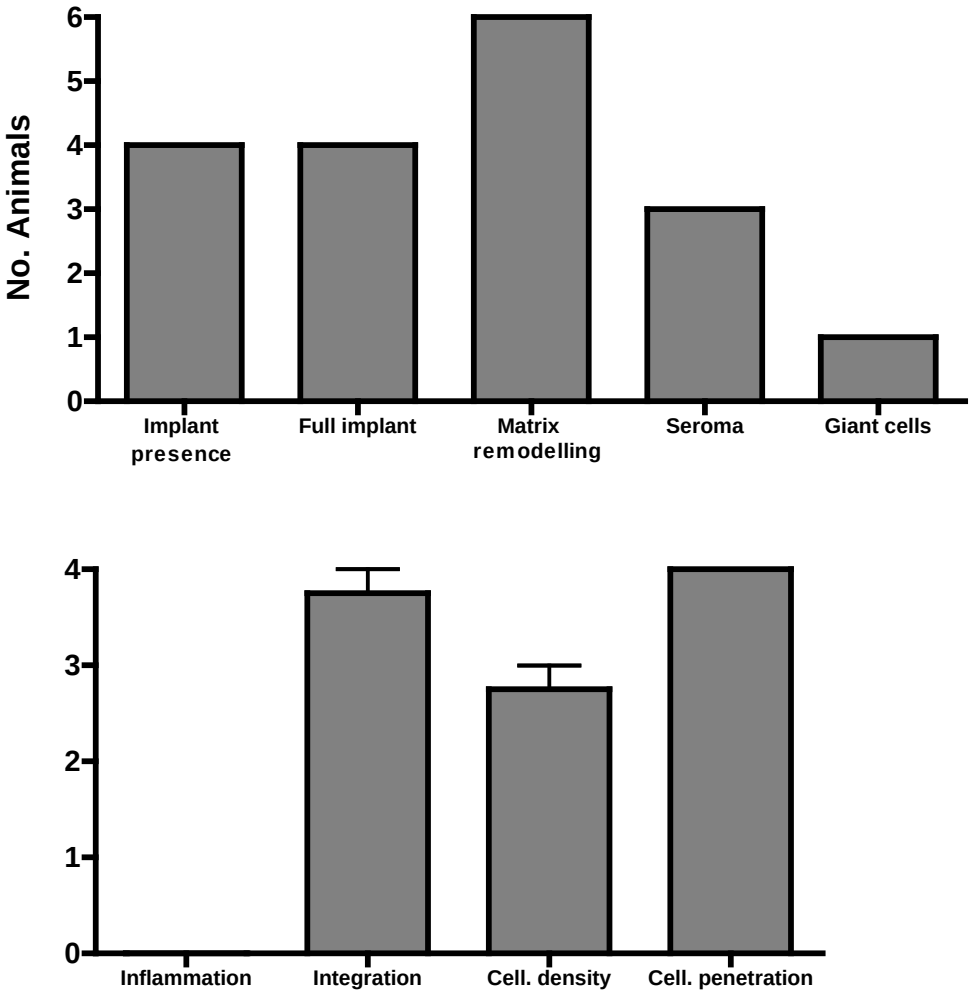

Figure 5.127 – AlloDerm results at 6 months post implantation. Histometric results were scored according to the system described in Table 5.2.

Figure 5.128 shows comparison between 1, 3 and 6 months results, mean values are used. Cellular density and cellular penetration were not quantified at 1 month post implantation because at this time-point cells were mainly present as a result of the inflammatory response.

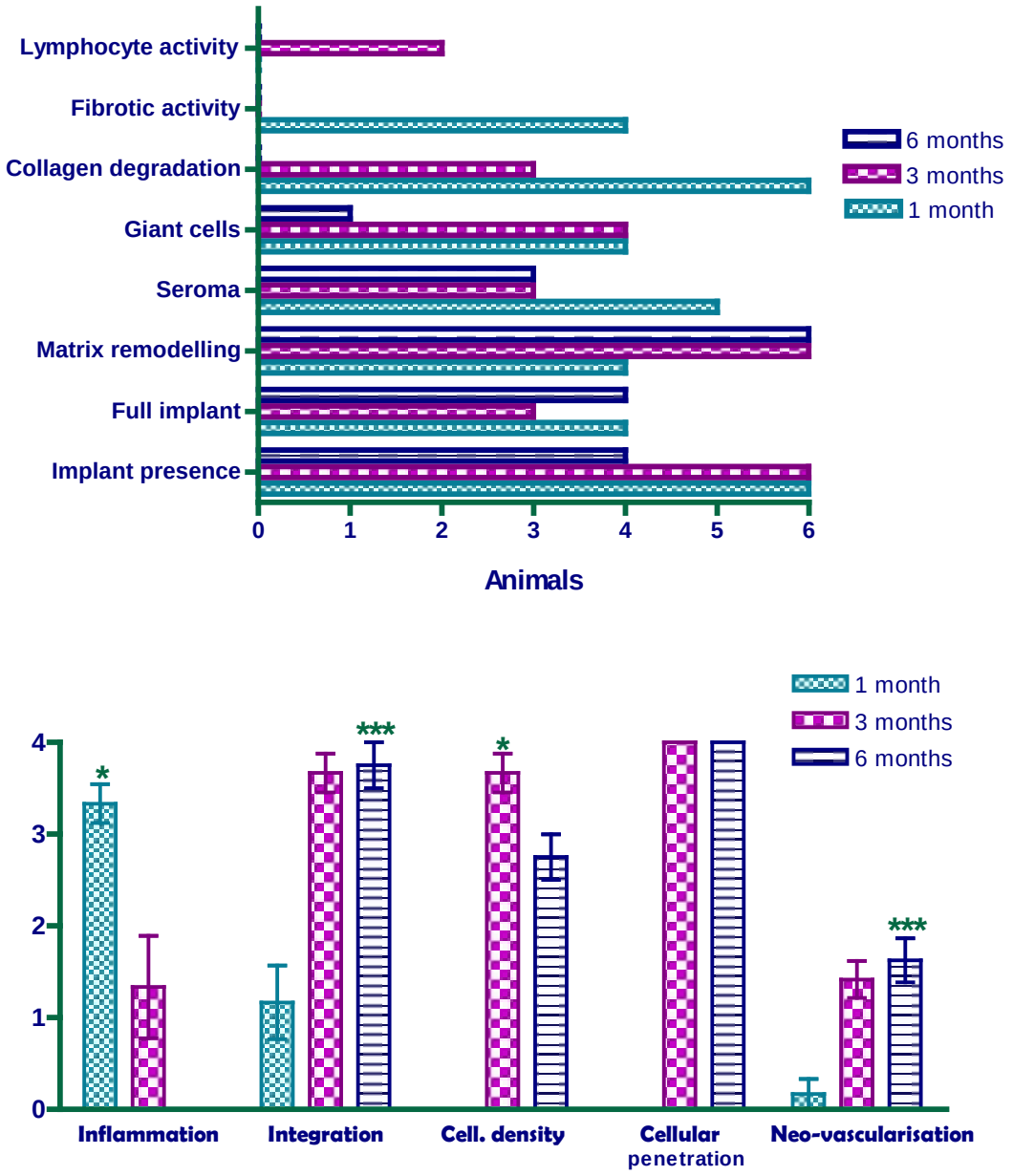

Figure 5.128 – AlloDerm results at 1, 3 and 6 months post implantation, P<0.05 = *, P<0.01 = ***. Histometric results were scored according to the system described in Table 5.2.

5.4.7 Results – CollaMend

One animal from group C-2 and one animal from group C-3 died post operatively. All other animals recovered well from surgery.

During the surgical procedure CollaMend was found to be an inflexible, stiff material which was difficult to suture into place.

Sixteen days post surgery one animal from group C-2 had an open wound lateral to the middle incision caused by the friction between the implant and the skin, there was evidence of implant extrusion and the animal had to be sacrificed. Since the implant was detached from the surrounding tissues tensiometry was not performed in this sample.

Approximately 4 weeks post-implantation 6 animals were noted to have folded implants which were visible externally. It is probable that natural body movements caused the implants to fold and implant physical properties did not allow return to its original orientation. As a result of which seroma developed between the implant and the peritoneal wall (Figure 5.129). Eventually animals with seroma chewed through the skin overlying the implants which were then exposed such that the animals had to be terminated prematurely (Table 5.16).

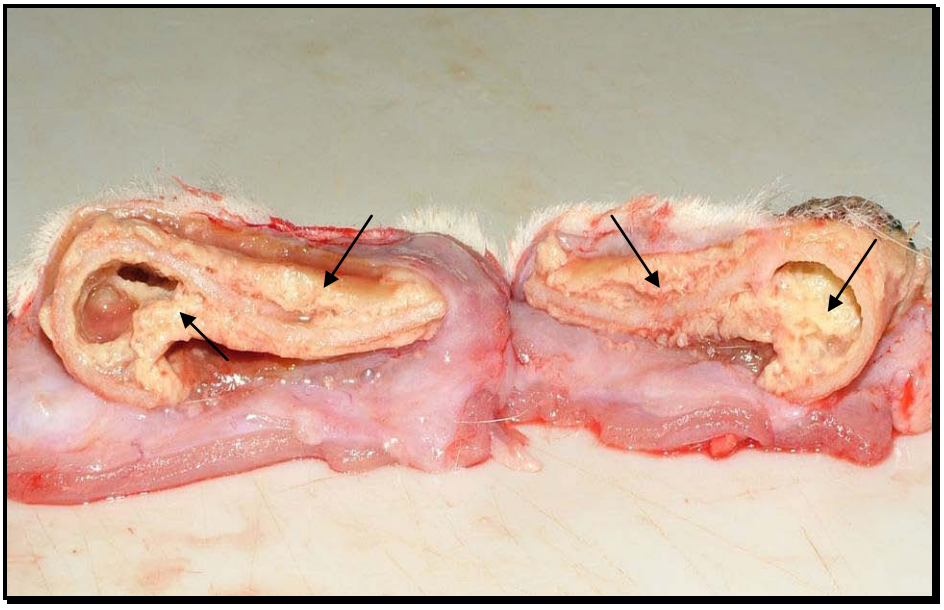

Figure 5.129 – CollaMend implant folded, the remains of seroma (arrows) are visible surrounding the implant and in the overlap region.

Table 5.16 – Animals with earlier termination time points.

Group	Termination day	Cause
C-2	16	Implant extrusion
C-1	19	Seroma/open wound
C-1	27	Seroma/open wound
C-2	35	Seroma/open wound
C-3	40	Seroma/open wound
C-2	49	Seroma/open wound
C-2	64	Seroma/open wound

5.4.7.1 Tensiometry

Although tensiometry was performed in all samples, data was analysed only from groups of animals with the same termination day; mean and standard deviation were calculated.

In group C-1 CollaMend was easily separated from the surrounding tissue (Figure 5.130).

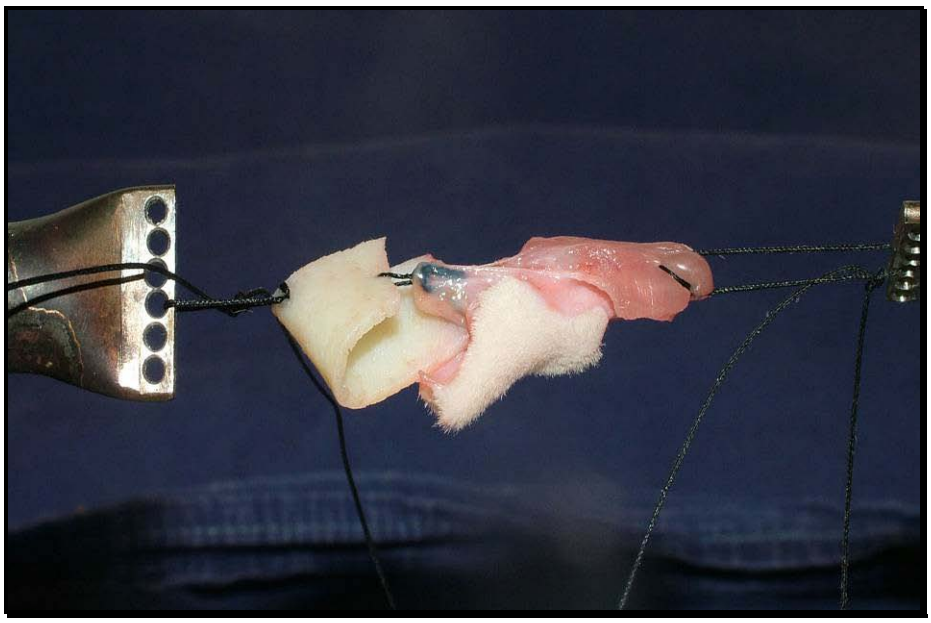

Figure 5.130 – Tensiometry of animal from group C-1.

Seven animals from group C-1 reached the protocol experimental end-time point; tensiometry was not performed in one sample since the implant detached from the host tissue while suturing it to the fixed end of the tensiometer. During tensiometry testing implant was separated from the host tissue in 5 of the 6 implants tested (Table 5.17). The remaining implant failed because sutures broke before separation occurred.

Table 5.17- Tensiometry results for CollaMend implants, 1 month group.

Animal	Max Load (kg)	Extension at Max. Load (mm)	Total Extension (mm)	Separation	Comments
$C_{1.1}$	0.293	42.12	64.48	Yes	Implant and tissue connected only by sutures
$C_{1.2}$	0.304	19.39	76.38	Yes	
$C_{1.4}$	0.280	37.85	38.44	Yes	
$C_{1.6}$	0.286	14.64	45.32	No	Sutures snapped
$C_{1.7}$	-	-	-	-	*
$C_{1.8}$	0.035	22.22	26.32	Yes	
$C_{1.9}$	0.212	39.71	42.83	Yes	
Mean	**0.235**	**29.322**	**48.962**		
SD	**0.103**	**11.909**	**18.258**		

* CollaMend separated from tissue while suturing it to the tensiometer.

In group C-2 CollaMend was easily separated from the surrounding tissue as observed at 1 month post implantation, integration with the host tissue was low. Only 4 animals from the initial 9 were sacrificed at 3 months post implantation.

The tensiometer results presented here may be biased since they include the sutures originally holding the CollaMend to the peritoneal wall, as well as or rather than integration of CollaMend with the surrounding host tissue alone. Separation was observed in 3animals.

Table 5.18 – Tensiometry results for CollaMend implants, 3 months group.

Animal	Max Load (kg)	Extension at Max Load (mm)	Total Extension (mm)	Separation	Comments
$C_{2.3}$	0.236	20.14	44.20	Yes	
$C_{2.6}$	1.120	22.54	50.09	Yes	Implant and tissue connected only by sutures
$C_{2.7}$	0.280	12.40	50.13	Yes	
$C_{2.9}$	0.267	15.52	48.26	No	Muscle split
Mean	**0.476**	**17.650**	**48.170**		
SD	**0.430**	**4.554**	**2.787**		

In group C-3 two of the CollaMend implants failed by tearing while performing tensiometry, one implant tore through the sutures and the other in the centre (Figure 5.131). The travel limit of the moving end of the tensiometer was exceeded in 3 of the 7 CollaMend implants tested (Table 5.19). Maximum load and extension at maximum load mean values were higher than at 1 and 3 months.

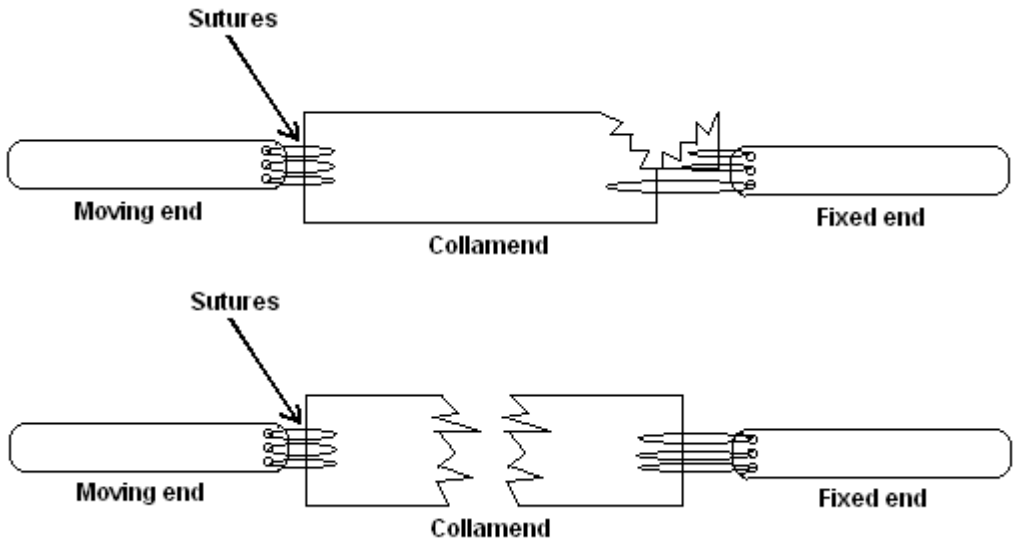

Figure 5.131 – Schematic representation of CollaMend mode of failure at 6 months post implantation.

Table 5.19- Tensiometry results for CollaMend implants, 6 months group.

Animal	Max Load (kg)	Extension at Max Load (mm)	Total Extension (mm)	Separation	Comments
$C_{3.1}$	0.744	19.14	33.76	No	
$C_{3.2}$	0.936	48.34	54.47	No	
$C_{3.3}$	0.808	10.75	25.00	Yes	
$C_{3.5}$	0.398	13.51	78.97	No[A]	Travel limit exceeded
$C_{3.6}$	1.318	49.95	78.97	No	
$C_{3.7}$	0.960	54.04	78.97	Yes[B]	
$C_{3.8}$	0.666	20.92	78.87	Yes	C
Mean	**0.833**	**30.950**	**61.287**		
SD	**0.285**	**18.925**	**23.693**		

[A] – CollaMend tore where sutured to the static end.

[B] – Only a few muscles fibres were attached to the sutures holding the CollaMend.

[C] – Although the implant failed, tearing in the centre, it was held only by the sutures to the surrounding tissue.

5.4.7.2 Histopathology

The semi-quantitative histometric grading system used was as described in Section 5.1.6.

Hydrated, non-implanted CollaMend was fixed and processed for histological analysis as control. Figure 5.132 shows the structure of CollaMend, which is acellular and, under polarised light, collagen shows its natural birefringence a characteristic of non-denatured collagen. CollaMend structure is similar to normal porcine dermal collagen structure, although CollaMend fibres look less compact and dense than porcine dermal collagen fibres, this may be explained by the manufacturers process. Space seen between fibres is probably a result of the decellularisation step.

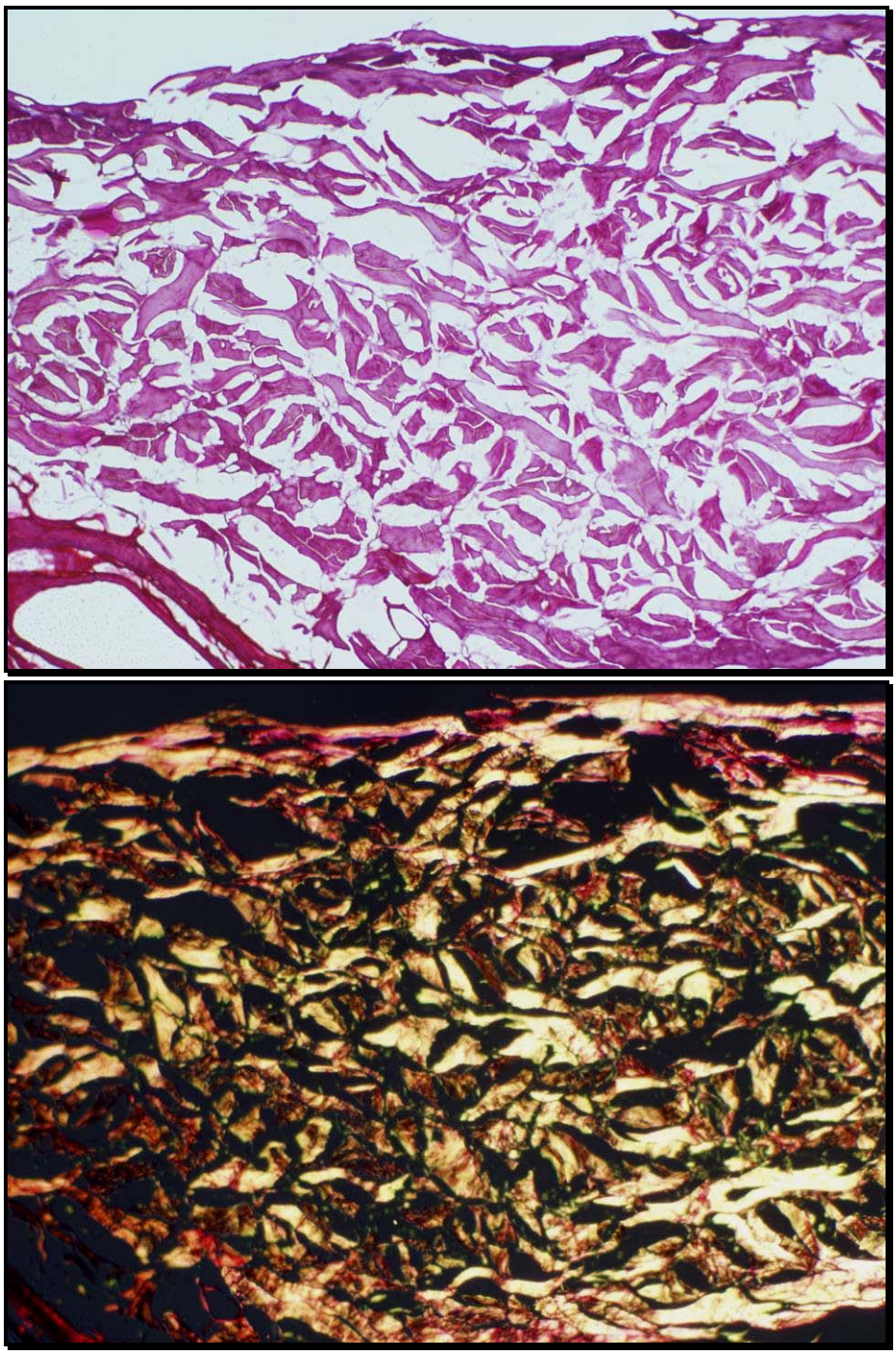

Figure 5.132 – CollaMend stained with picro sirius red, in the bottom image the section was visualised under polarised light (100X).

Group C-1 – 1 month

The implant retrieved from the animal sacrificed 19 days post implantation showed evidence of a marginal acute inflammatory response most probably due to the

exposure of the implant (Figure 5.133). It could be seen macroscopically that CollaMend implant was not integrated with the adjacent host tissue and histology showed a sub-clinical seroma separating implant from host tissues.

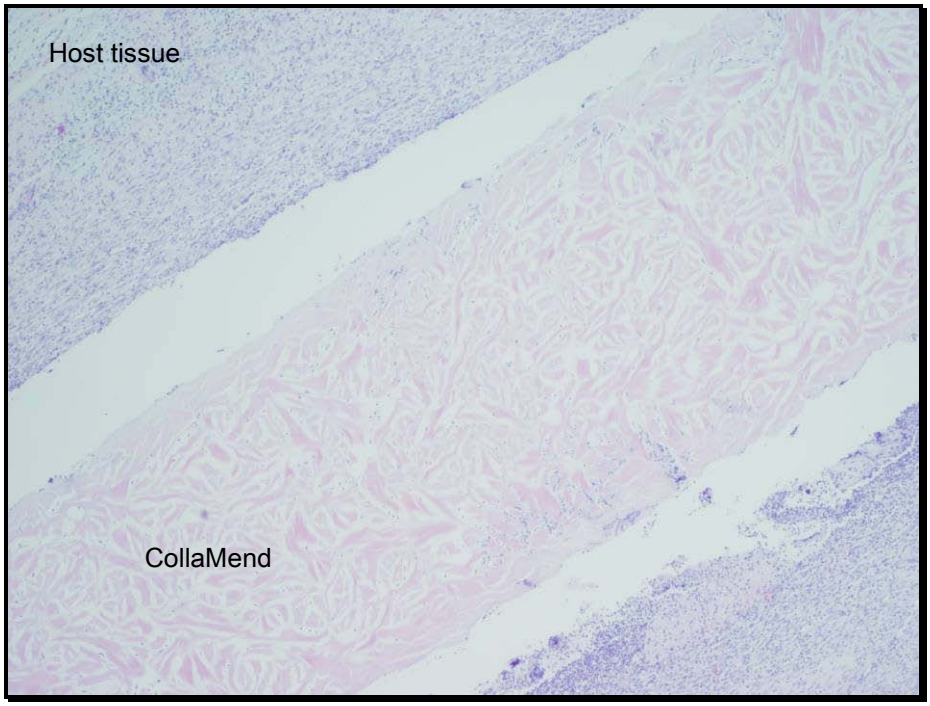

Figure 5.133 – Marginal acute inflammation 19 days post implantation (H&E, 40X).

Cellular density was minimal but that was not an impediment for cellular penetration, which was 100%. Neo-vascularisation was not present.

The animal sacrificed 27 days post implantation showed minimal acute and chronic inflammatory responses probably as a consequence of the open wound; macrophages, neutrophils and giant cells were present (Figure 5.134). Again, there was no integration between the implant and the surrounding tissue. Cellular density was marginal and some parts of the implant were completely cell free, cellular penetration varied from 0 to 100% (Figure 5.135). At this time point blood vessels and vessel sprouts were visible especially at the edges of the implant.

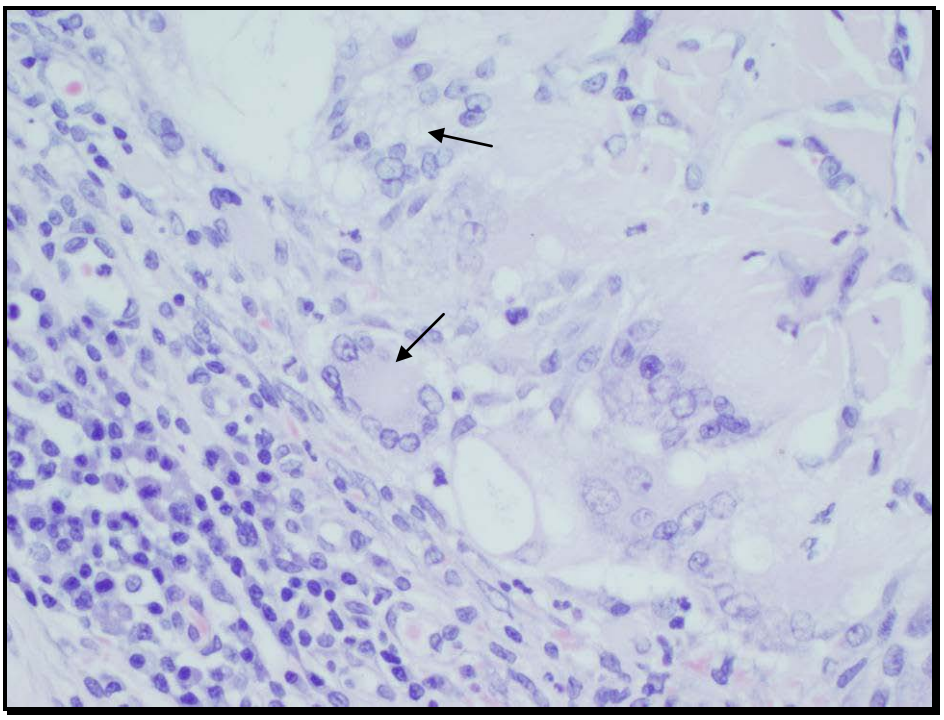

Figure 5.134 – Giant cells (arrows) and macrophages in a CollaMend implant after 27 days implantation (H&E, 400X).

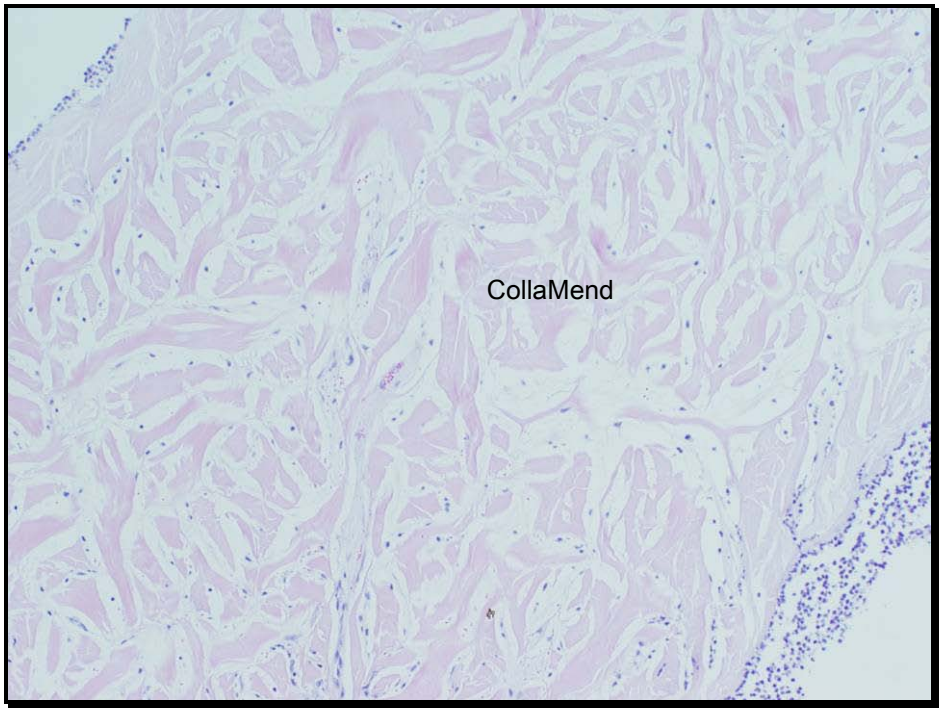

Figure 5.135 – Complete cellular penetration in a CollaMend implant 27 days post implantation (H&E, 100X).

After 1 month of surgery CollaMend was discernible subcutaneously and felt hard to the touch in all animals. Apart from the presence of macrophages, at low numbers, no inflammatory response was observed in any of the 7 animals (Figure 5.136).

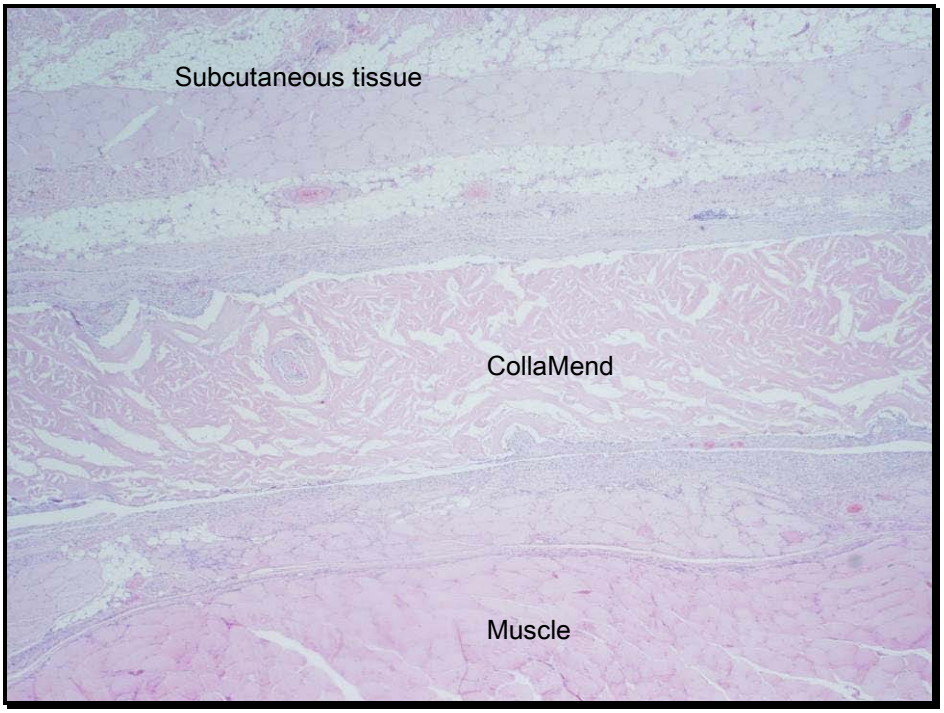

Figure 5.136 – CollaMend implant 1 month post implantation (H&E, 20X).

Integration with surrounding tissue was generally very low or absent; although, at one aspect, the beginning of micro-interdigitations between the edge of the implant and the immediately adjacent tissue was observed. Cellular density was marginal and in a few aspects of the implants cells were observed covering the surface without infiltrating the matrix (Figure 5.137).

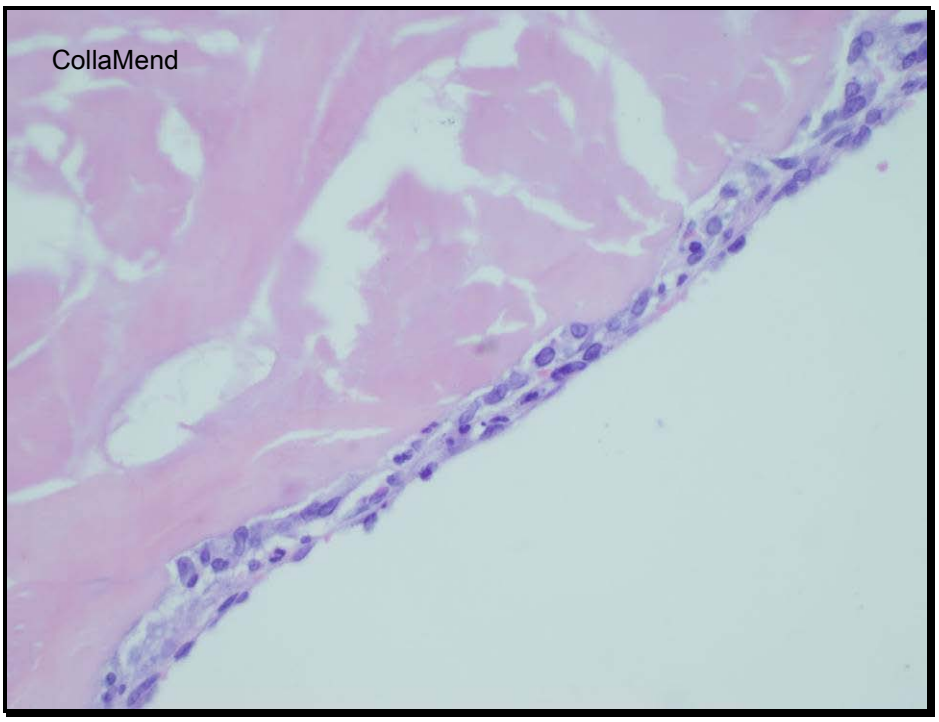

Figure 5.137 – Cells at the edge of a CollaMend implant, 1 month post implantation (H&E, 400X).

Although some areas of the implants were cell free, the remaining areas were populated even if at a low density (Figure 5.138). Cells were mostly observed in the spaces between fibres and not within the collagen.

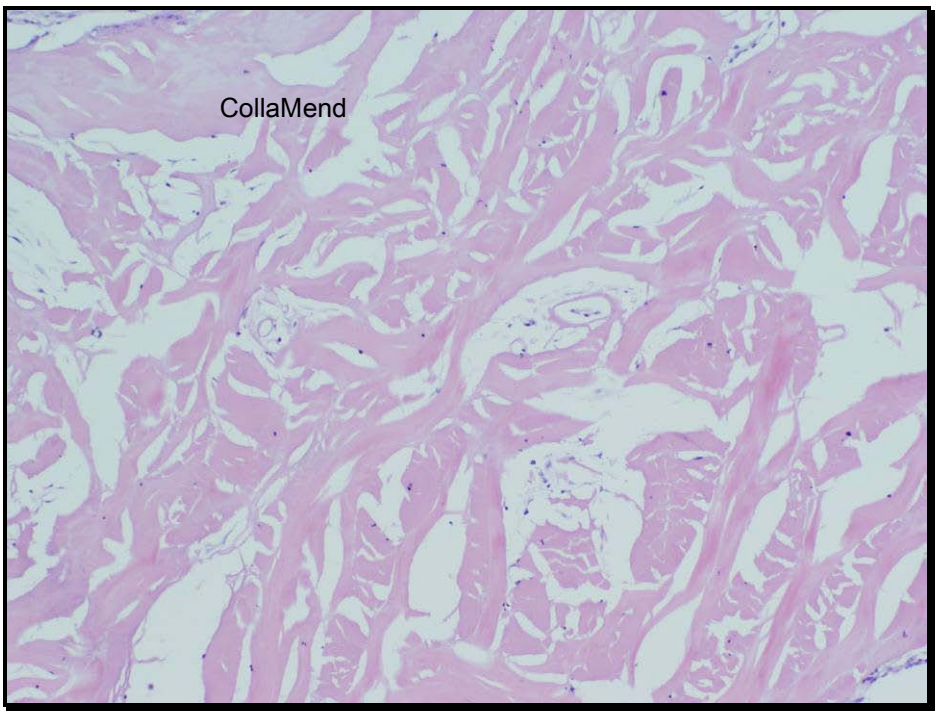

Figure 5.138 – Marginal cellular density in a CollaMend implant, 1 month post implantation (H&E, 100X).

Independent of cellular density, cellular penetration reached 100%. Residues were observed at the edges of one implant; those particles appeared to be degraded material but also seem to form a border between the implant and the surrounding tissue (Figure 5.139).

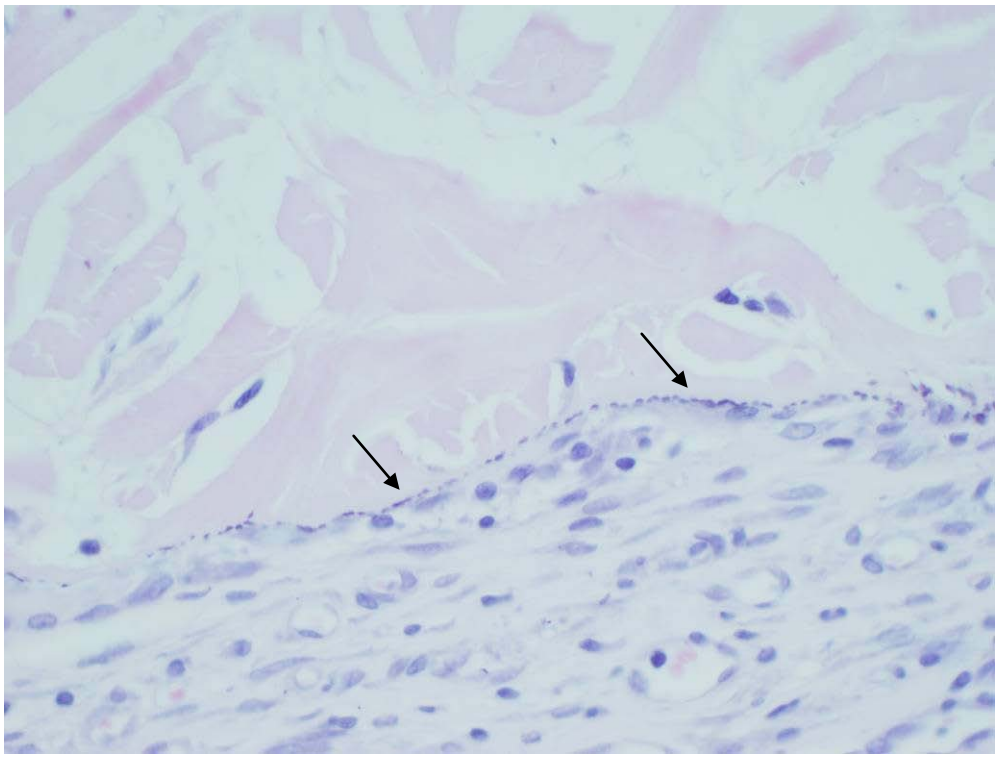

Figure 5.139 – Residues at one aspect of a CollaMend implant after 1 month implantation (H&E, 400X).

Control tissue (from the defect without mesh implantation) showed no tissue reactivity, which attests that the tissue reactivity observed in the implanted samples is not related to the surgical procedure and is implant specific.

Capillaries were observed in 2 implants; in one within the natural pores of the collagen matrix and in the other at one aspect of the implant particularly more populated (Figure 5.140). In the latter, a cell free hair follicle is present and, although usually these structures are cell populated and vascularised, in this case cells preferred to surround the natural pore and capillaries are present to support cells.

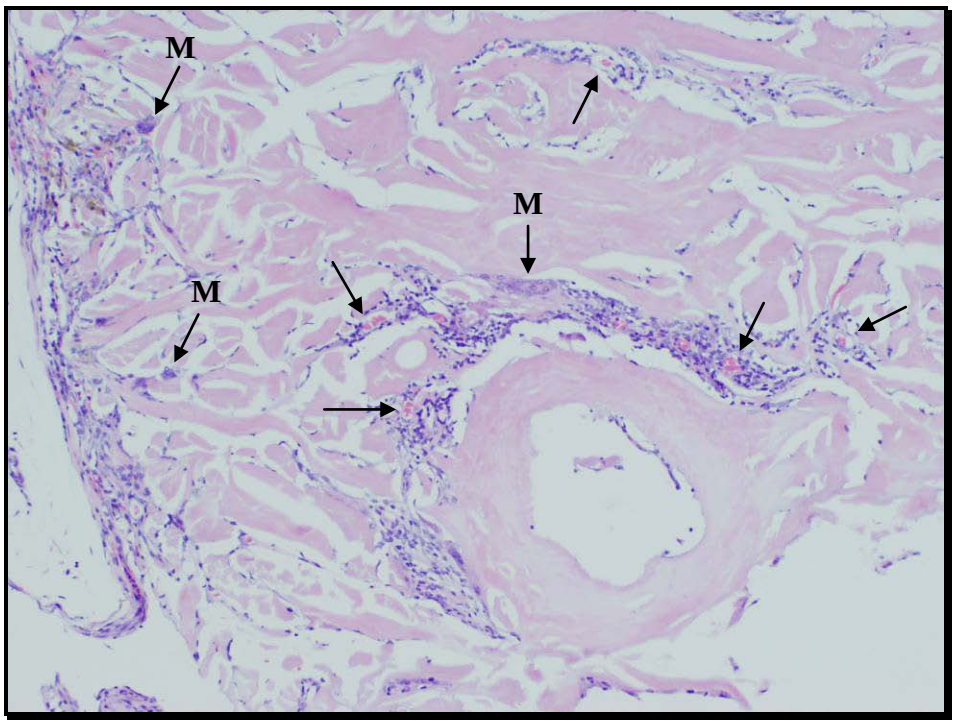

Figure 5.140 – Small capillaries (arrows) at one aspect of a CollaMend implant, macrophages are also present (M), 1 month post implantation (H&E, 100X).

A fibrous capsule was observed surrounding all implants, probably as an integration process rather than encapsulation (Figure 5.141).

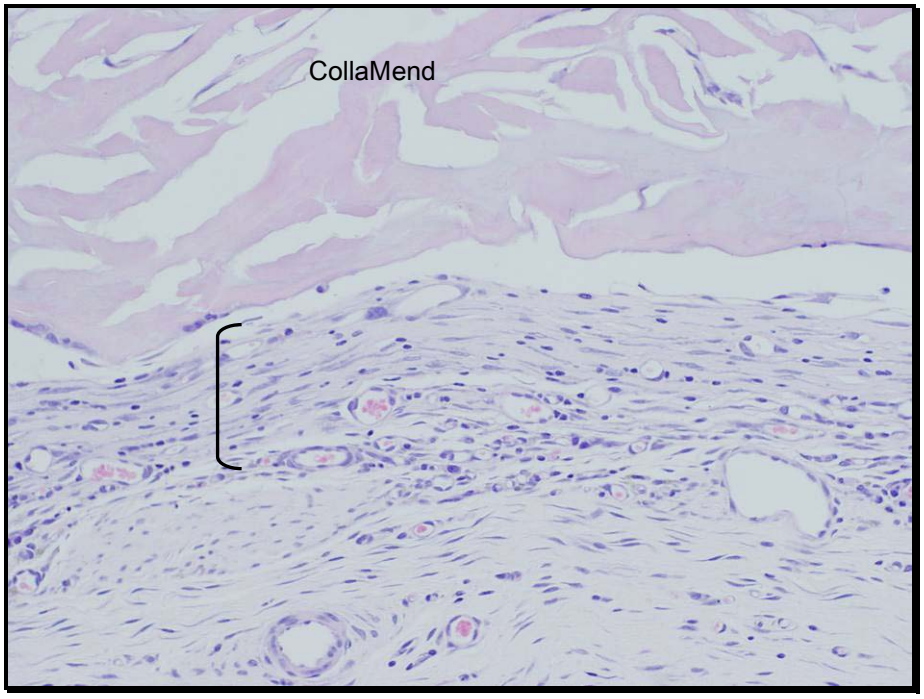

Figure 5.141 – Fibrin (bracket) surrounding a CollaMend implant (H&E, 200X).

An unexpected feature was the round-shape of cells, particularly when present in the centre of the implant, (Figure 5.142). Morphologically these cells did not looked like leukocytes, showing features of fibroblast-like cells, although the observed round-shape is in contrast to the usual needle-shape. Round-shape fibroblasts are usually observed when cells cannot adhere easily to a substrate.

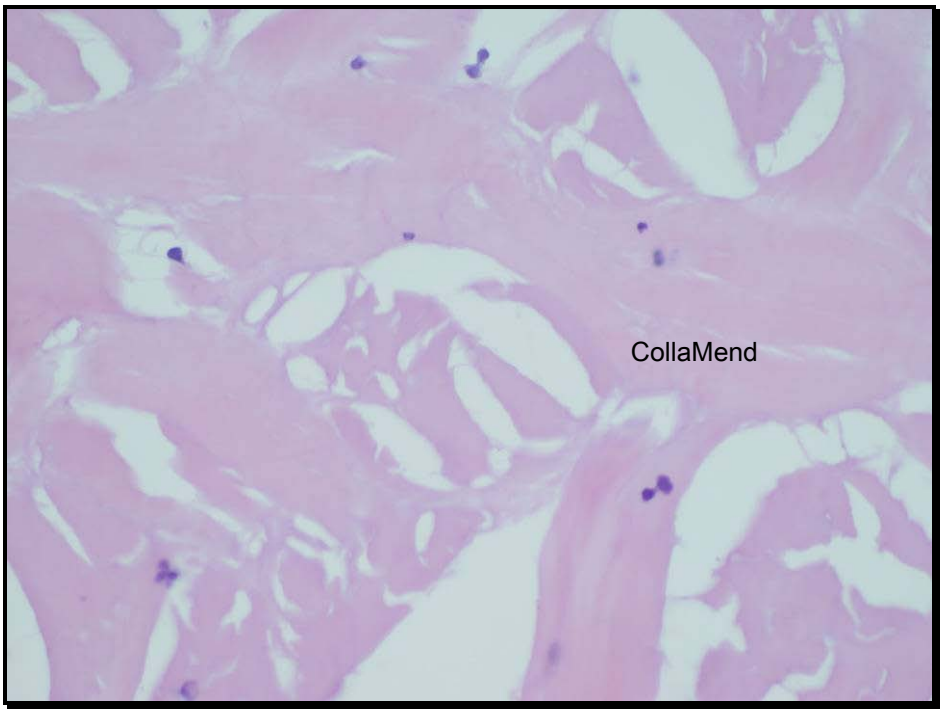

Figure 5.142 – Round-shape cells in the centre of an implant (H&E, 400X).

Under polarised light all implants showed natural birefringence and good quality collagen (Figure 5.143).

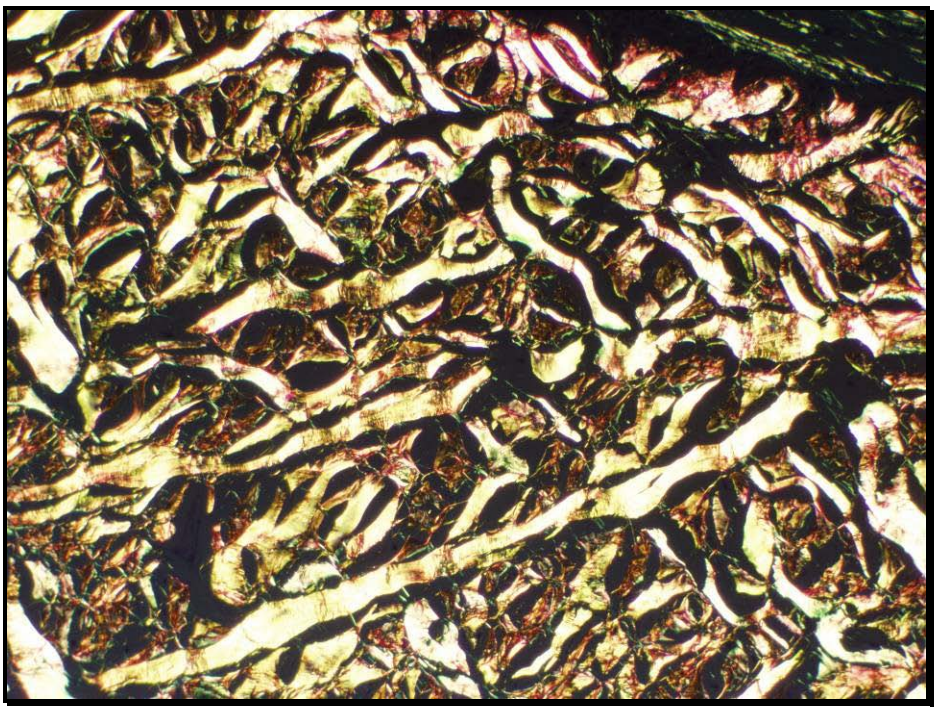

Figure 5.143 – Good quality, non-denatured collagen in a CollaMend implant, 1 month post implantation (picro sirius red, 100X).

Figure 5.144 shows results for CollaMend implant one month post implantation. Mean and standard deviations were calculated per each parameter analysed.

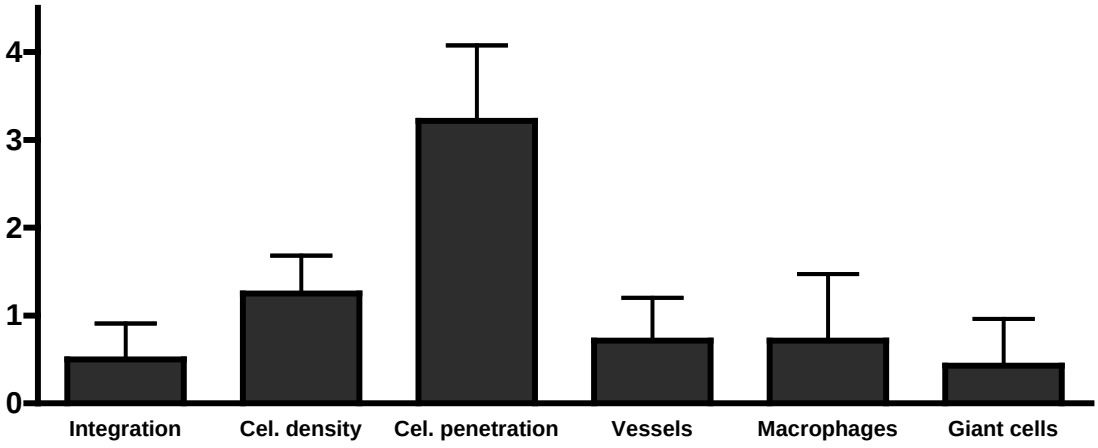

Figure 5.144 – Histometric score for CollaMend implant in animals sacrificed one month post implantation, according to the scoring system described in Table 5.2.

Group C-2 – 3 months

Although this group had originally 9 animals only 4 reached the protocol experimental end-time point; 1 animal died post-operatively and 4 animals were sacrificed earlier due to implant related complications. After 16 days of implantation one animal was sacrificed because of implant extrusion; the open wound probably contributed to the pus observed during the necropsy and to the moderate suppurative inflammatory response (purulent inflammation) present in this implant (Figure 5.145). The inflammatory exudate was particularly rich in neutrophils and was indicative of wound infection.

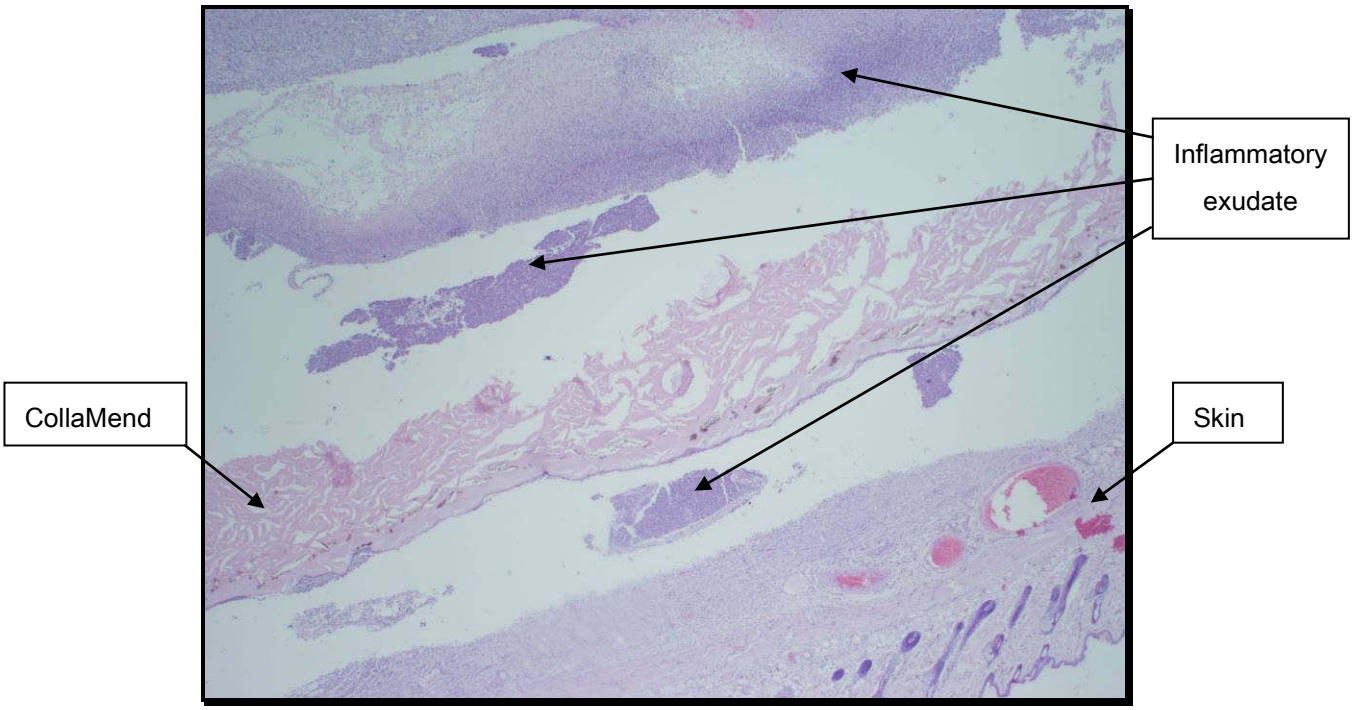

Figure 5.145 – Moderate acute inflammation 16 days post implantation (H&E, 40X).

It was easy to see macroscopically that the CollaMend implant was not integrated with the adjacent host tissue. Cellular density and cellular penetration were poor; neutrophils were mainly observed at the edges of the implant moving through the natural pores of CollaMend (Figure 5.146). Neo-vascularisation was not present.

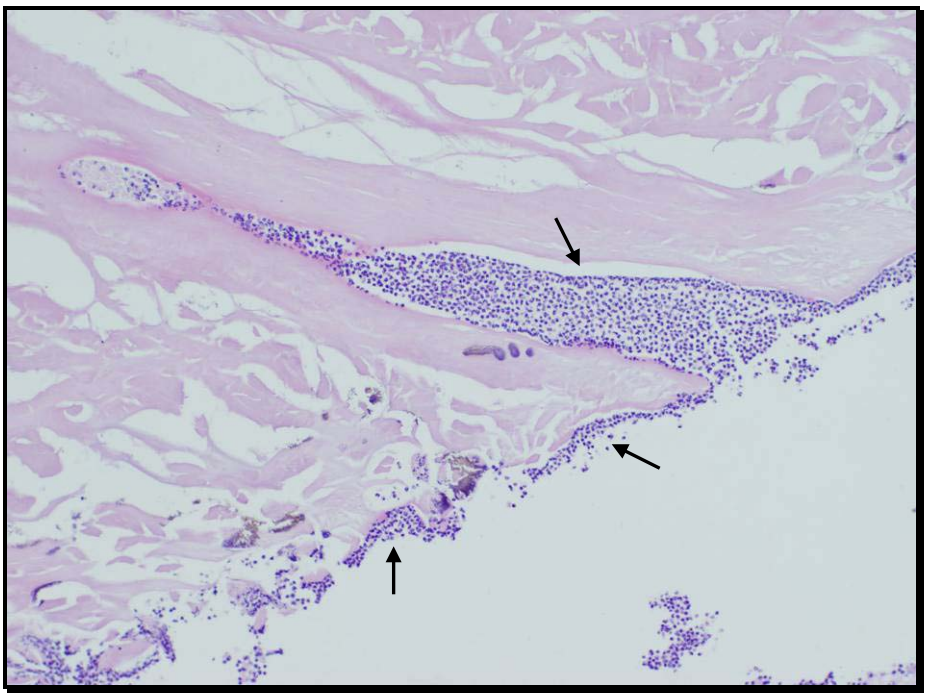

Figure 5.146 – Inflammatory cells (arrows) on the surface of the implant and penetrating through the natural pores of the collagen (H&E, 100X).

Bacteria were visible in some aspects of the implant; since this occurred on the surface facing the skin it was probably a consequence of the open wound. Interestingly, when bacteria are present CollaMend's configuration is different (Figure 5.147). The layer between the bacteria and the surface of the implant, *i.e.*, the area bacteria penetrated, looks remodelled and compact compared to the rest of the implant.

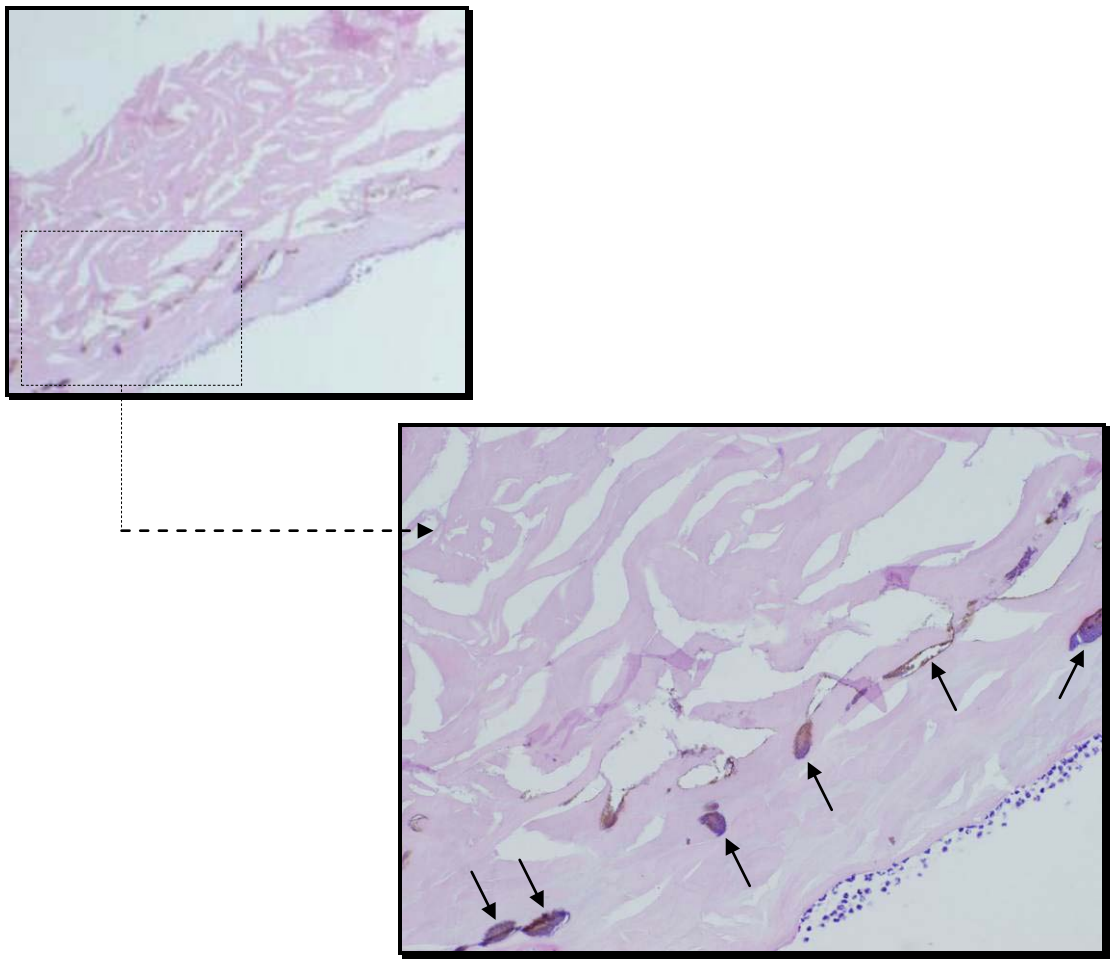

Figure 5.147– Bacteria (arrows) present in a CollaMend implant. Neutrophils present on the surface (H&E, 200X).

Between the skin and the implant an enlarged active lymph node was visible (Figure 5.148), this occurrence suggests an immune response and may be a consequence of the bacterial infection or the presence of the CollaMend xenogeny.

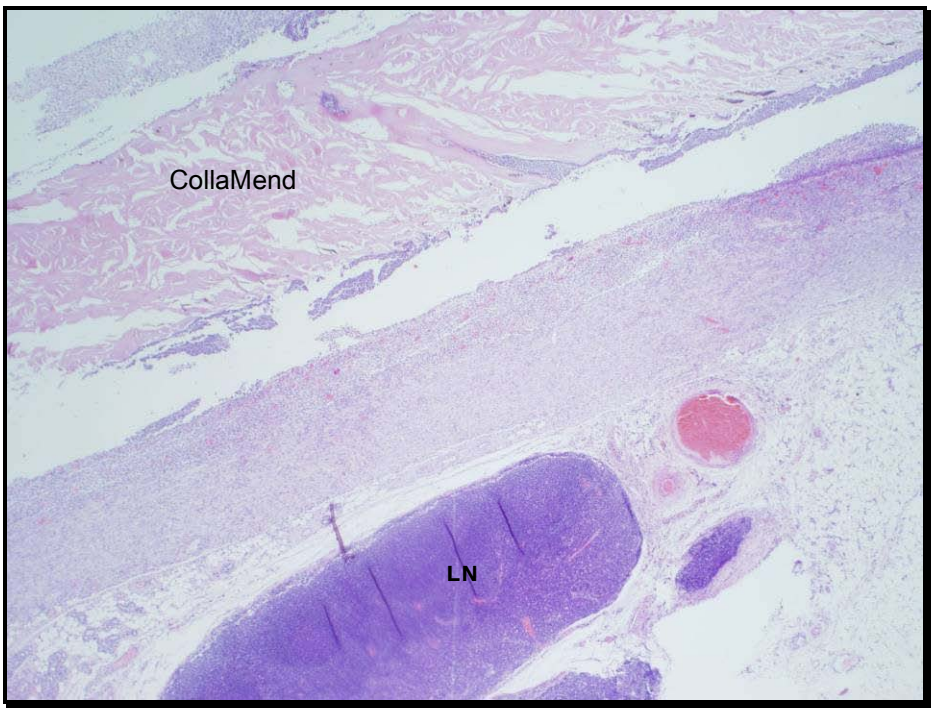

Figure 5.148 – Enlarged active lymph node (LN) between skin and a CollaMend implant (H&E, 20X).

In the control tissue of this animal no tissue reactivity was observed.

Three animals from this group developed seroma; after approximately 3 weeks the seroma was hard to touch and as a consequence open wounds occurred leading to the earlier termination of these animals.

As a consequence of the open wounds, samples from those animals showed moderate suppurative inflammation with high amounts of neutrophils in the exudate surrounding the implant and bacteria (Figure 5.149).

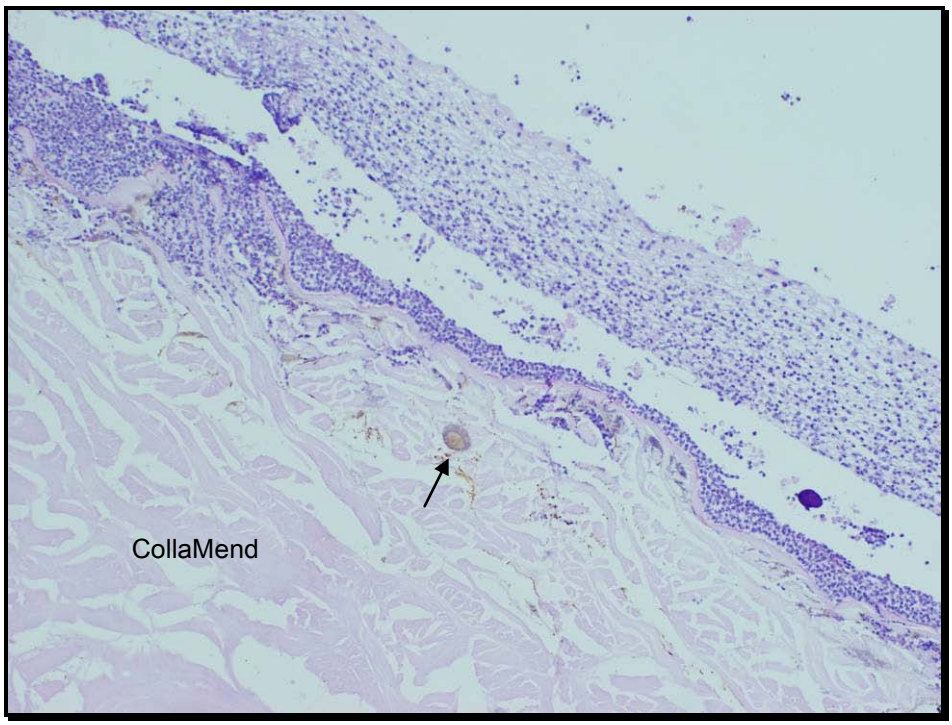

Figure 5.149 – Inflammatory cells and bacteria (arrow) present at the edges of the implant (H&E, 100X).

In the animal sacrificed 35 days post implantation a purulent inflammation was present between the implant and skin, and the implant and peritoneal wall. The only cells present in the implant were inflammatory cells and there was no integration with the surrounding tissue.

The animal sacrificed at day 49 presented an exteriorised implant; consequently the exposed area of the implant was dry, hard, had a yellow colour and was firmly attached to the surrounding superficial layers of the skin rather than being integrated with the deeper dermal tissue (Figure 5.150). After removing the implant together with surrounding tissue, pus was found between the implant and the peritoneal wall confirming the presence of infection. Histological analysis showed seroma remains and a moderate acute and chronic inflammatory response between the implant and the peritoneal wall. The presence of pus prevented the implant from integrating with the surrounding tissue.

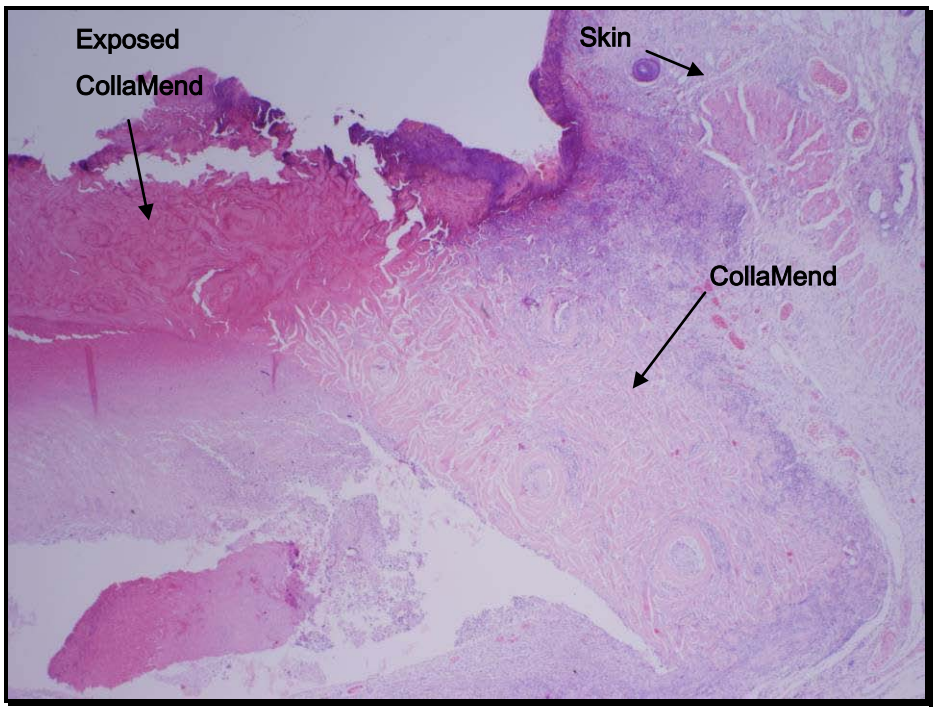

Figure 5.150 – CollaMend implant partially exposed (H&E, 20X).

The areas of the CollaMend implant that were not exposed were moist and with a white colour. These parts were well populated by cells that penetrated 100% of the implant and vessels were visible to support the high cellular density (Figure 5.151).

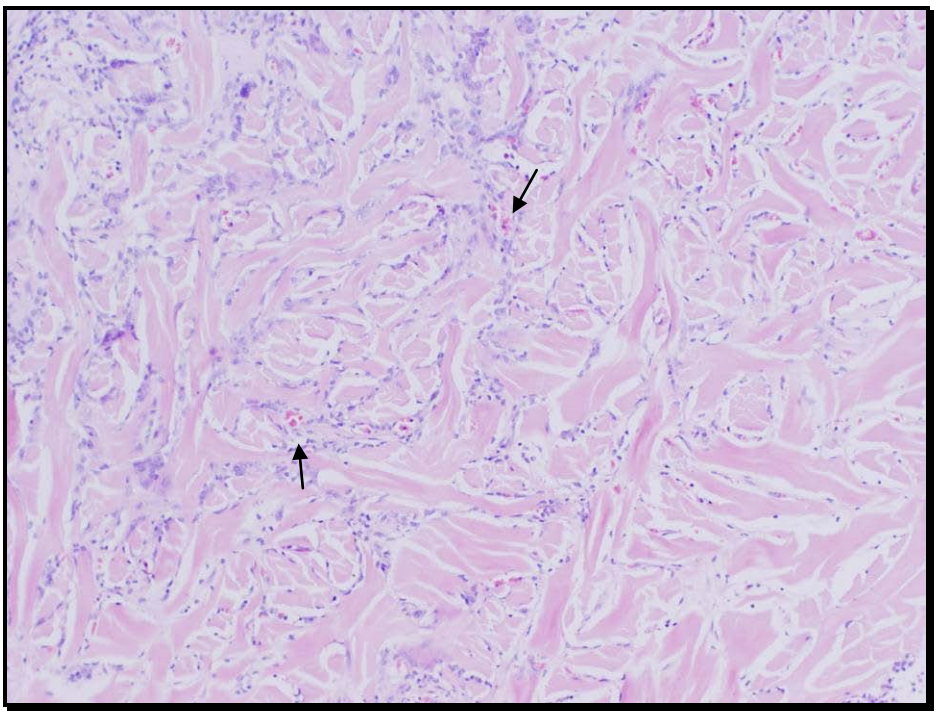

Figure 5.151 – Moderate cellular density and complete cellular penetration in a CollaMend implant 49 days post implantation. Vessel sprouts are identified by arrows (H&E, 100X).

Macrophages and giant cells were present, especially at the edges of the implant and were indicative of the moderate inflammatory response (Figure 5.152).

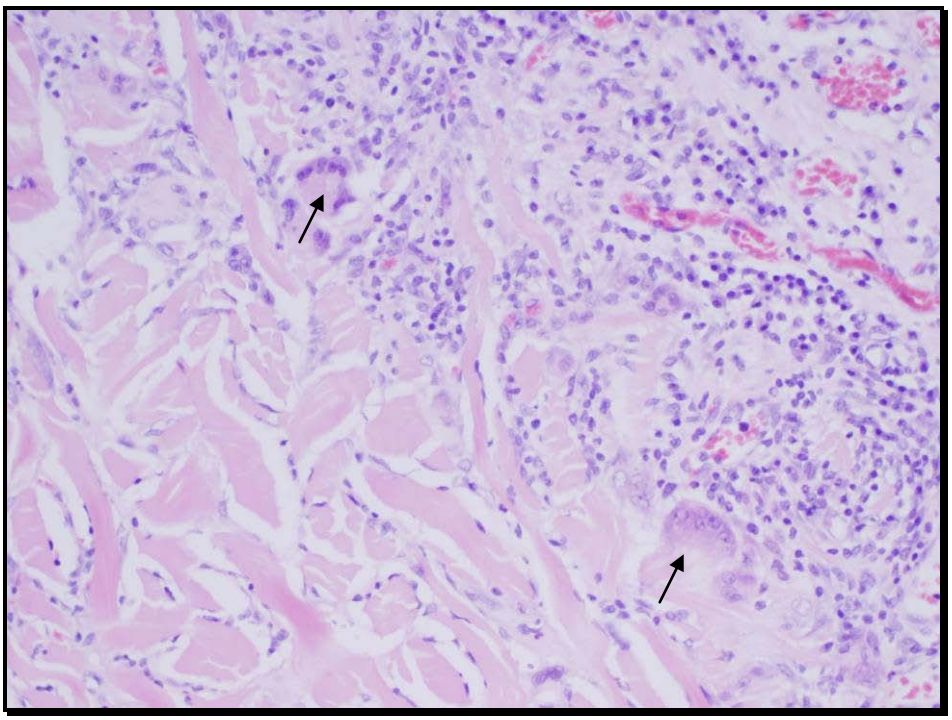

Figure 5.152 – Giant cells present at the edges of a CollaMend implant (H&E, 200X).

The implant from the animal sacrificed 64 days post surgery showed moderate integration with the surrounding tissue at the smaller surfaces (corner of implant) but no integration in the long surfaces (implant length and width) (Figure 5.153). In the areas where integration was minimal, cells penetrated the implant reaching 15% in depth. This implant showed evidence of a marginal chronic inflammatory response, with macrophages present in several aspects of the implant.

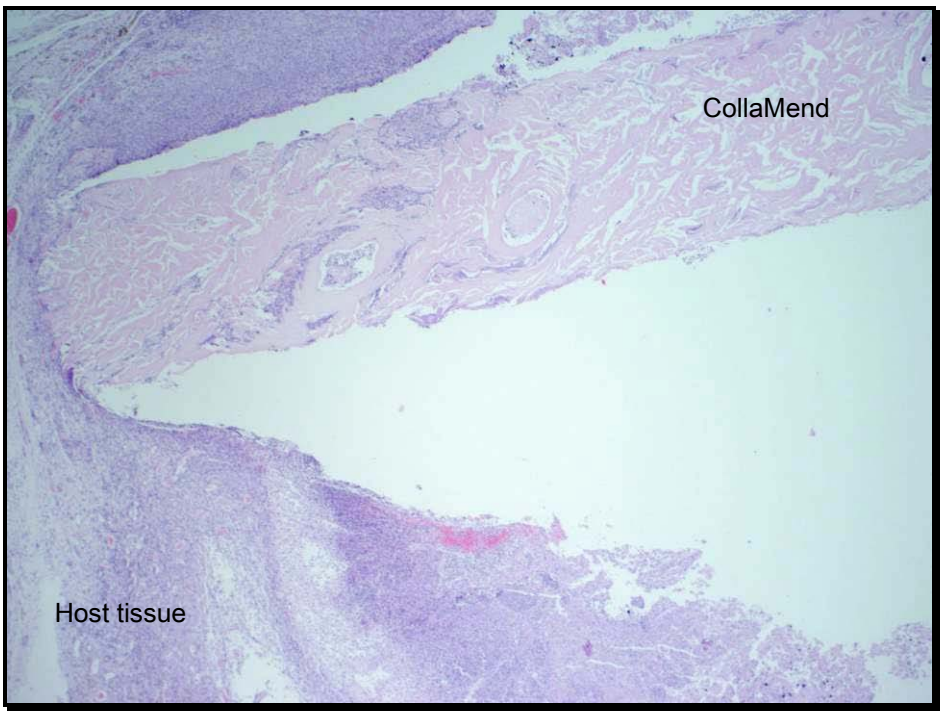

Figure 5.153 – No integration with surrounding tissue in the long surfaces (H&E, 20X).

The 4 implants recovered at 3 months post implantation showed no evidence of an inflammatory response and integration with the adjacent tissue was minimal, which was significantly different from 1 month post implantation (Figure 5.154). Cellular density was minimal and cells were observed fully penetrating the implant, mainly through natural fissures (Figure 5.155). Contrary to what was observed after 1 month implantation these cells had a needle-shape form and were elongated, this suggests that over time cells overcome the factor causing detrimental conditions for their maintenance and growth.

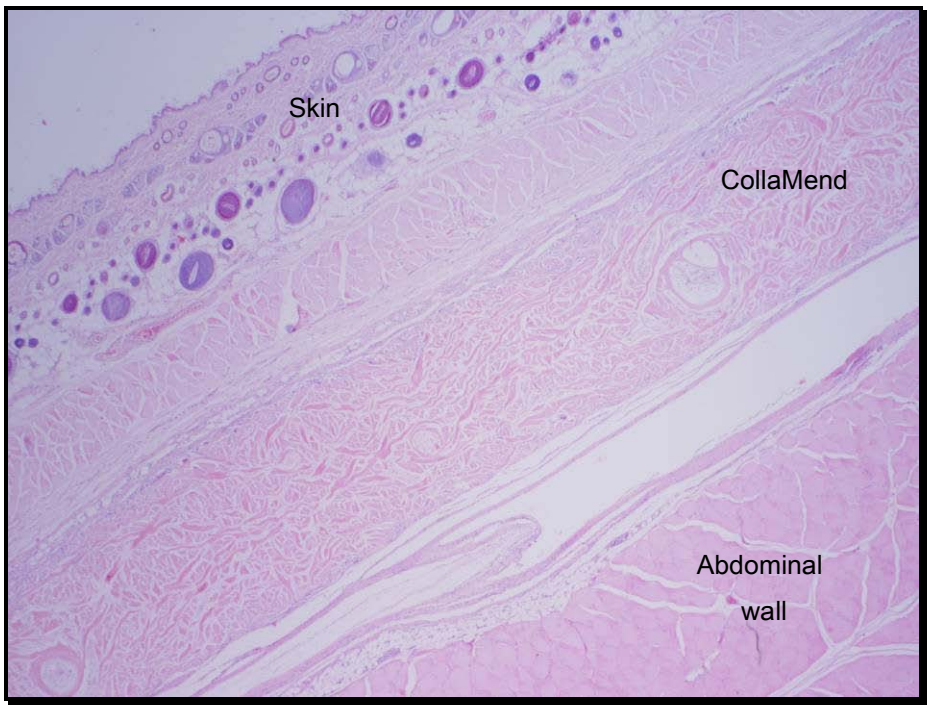

Figure 5.154 – CollaMend implant 3 months post implantation; minimal integration with surrounding tissue (H&E, 20X).

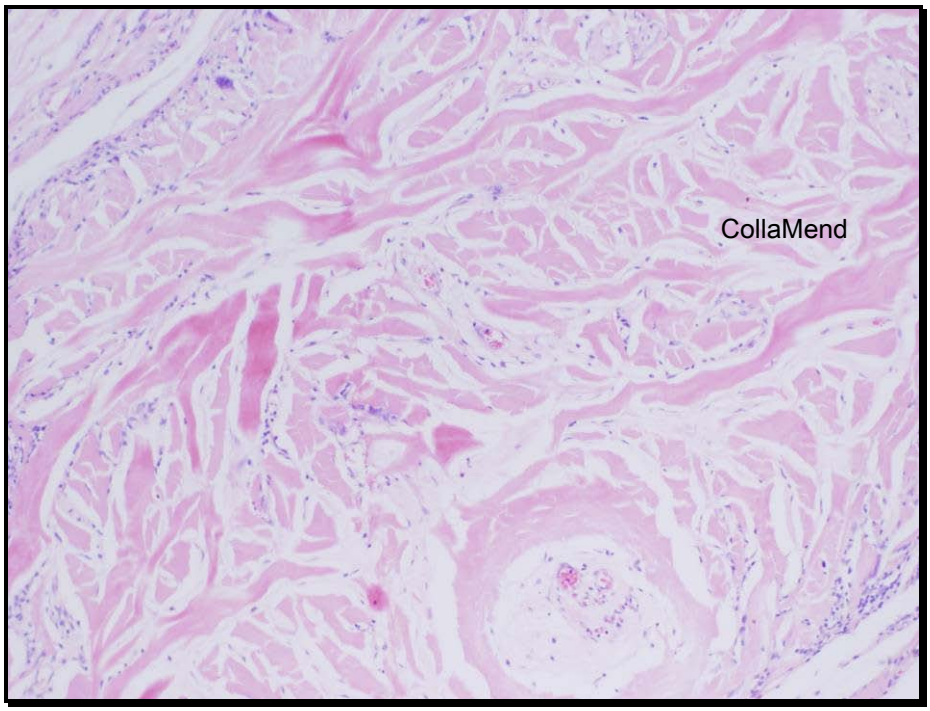

Figure 5.155 – Good cellular penetration with vessels to support the cellular activity, CollaMend implant 3 months post implantation (H&E, 100X).

Macrophages and giant cells were present in the edges of the implants, which is consistent with a foreign body reaction. Vessel sprouts and mature vessels were observed in the edges and centre of the implant, although at low levels (Figure 5.156).

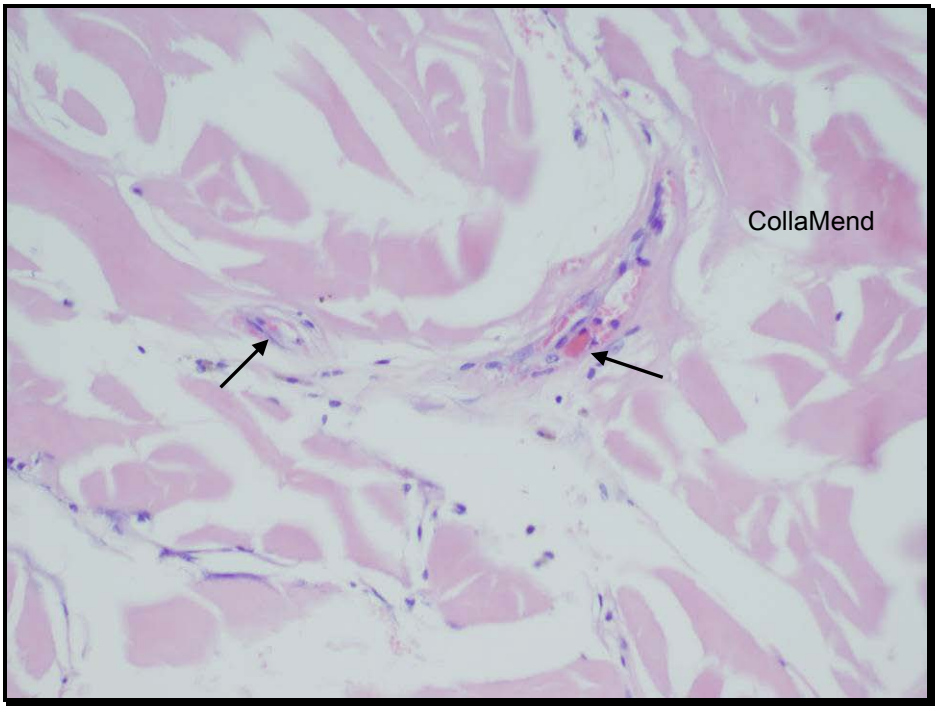

Figure 5.156 – Vessel sprouts and mature vessel in the centre of a CollaMend implant (H&E, 200X).

At 3 months post implantation CollaMend implant showed good quality collagen in all samples tested; no degradation was observed (Figure 5.157).

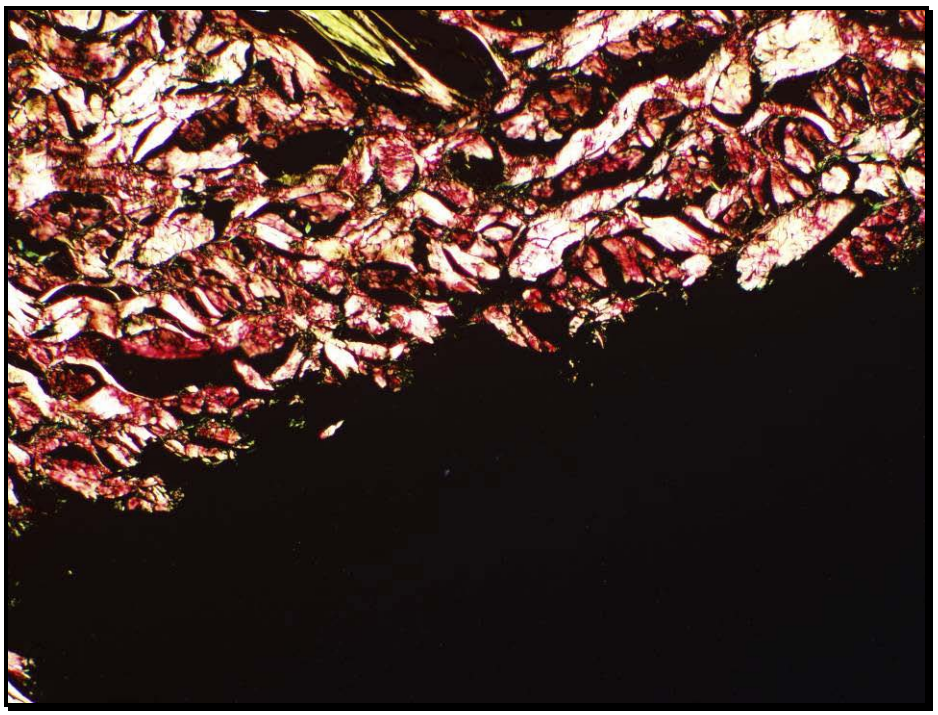

Figure 5.157 – Good quality collagen (picro sirius red, 100X).

Tissue controls taken from group C-2 did not show any tissue reactivity.

Figure 5.158 shows results for group C-2, means and standard deviations were calculated per each parameter analysed.

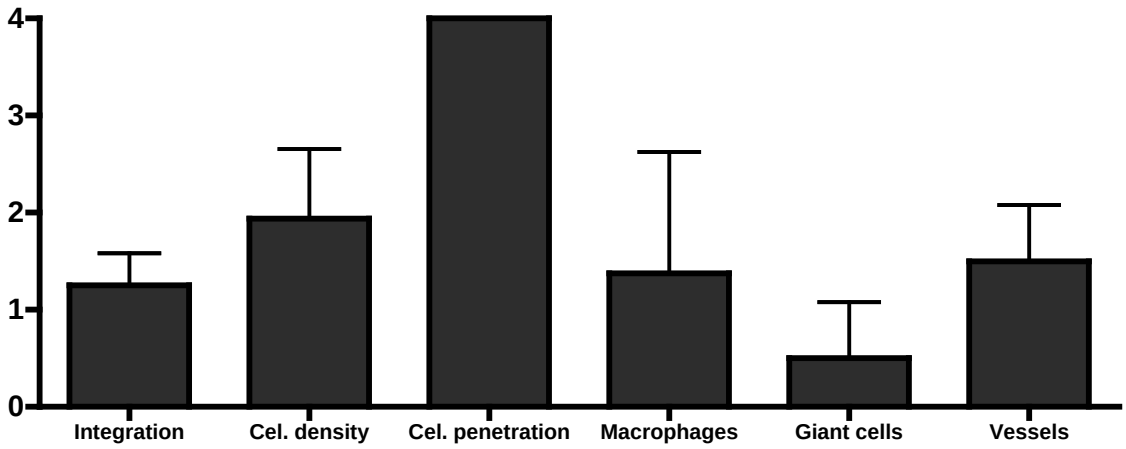

Figure 5.158 – Results for group C-2. Histometric analysis made according to the scoring system described in Table 5.2.

Group C-3 – 6 months

One animal from this group died post operatively and was not replaced. Another animal was sacrificed at day 40 due to exposure of the implant resulting from development of a seroma.

The animal terminated at day 40 had the implant surrounded by pus, the inflammatory reaction was severe and the implant was folded. Histology results showed the implant detached from the surrounding tissue (integration was absent), and two enlarged lymph nodes were in the proximity of the implant. A moderate suppurative inflammation was present with high amounts of leukocyte exudates (Figure 5.159).

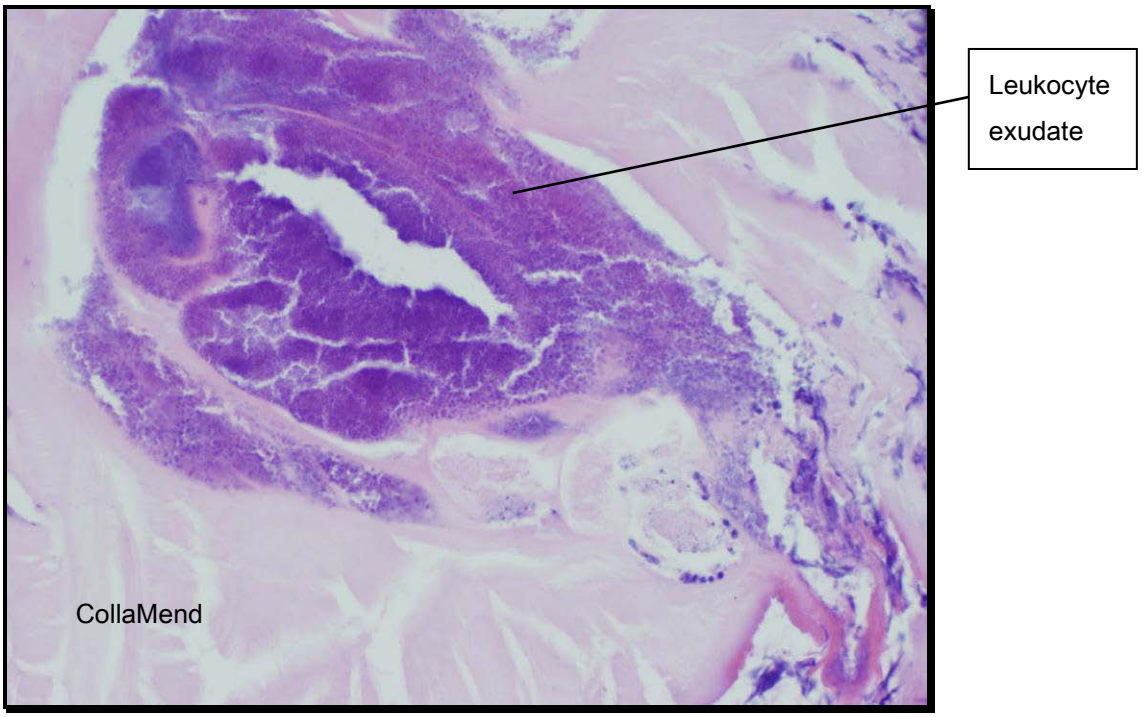

Figure 5.159 – Suppurative inflammation in a CollaMend implant (H&E, 400X).

Probably as a consequence of the open wound, bacteria were present in the implant and surrounding tissue. Except for the inflammatory cells present the implant was cell free. Macrophages and giant cells were present in one corner of the implant. Despite the bacteria and leukocytes collagen was not degraded or remodelled.

At 6 months post implantation 7 animals were sacrificed and implants macroscopically identified for tissue harvesting. Under polarised light implants showed good quality collagen, degradation was not observed and collagen was naturally birefringent (Figure 5.160).

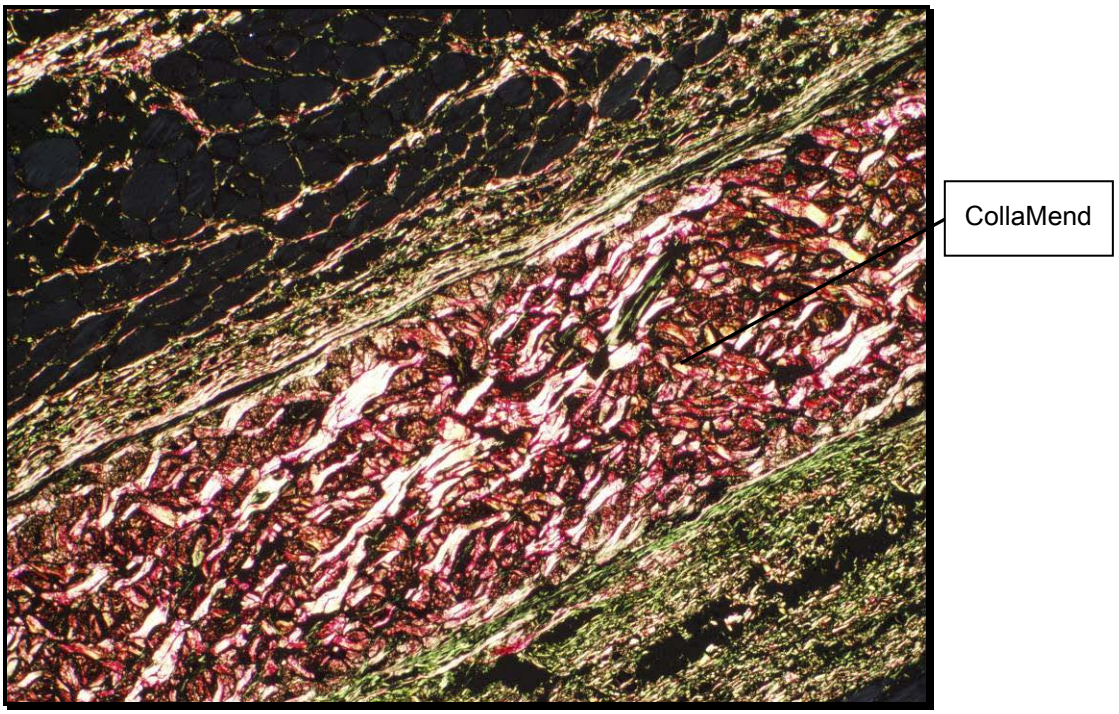

Figure 5.160 – CollaMend 6 months post implantation (picro sirius red, 40X).

Two animals showed a small lump externally, which autopsy proved to be CollaMend folded in one extremity, in the first animal (Figure 5.161). At 6 months post implantation the absorbable sutures used had been absorbed; at this time the implant was expected to be integrated with surrounding tissue. The folded extremity in this implant suggests that integration was low and since no sutures were present the implant folded having remained stiff for the duration of the study. A marginal inflammatory response was present where the implant was folded.

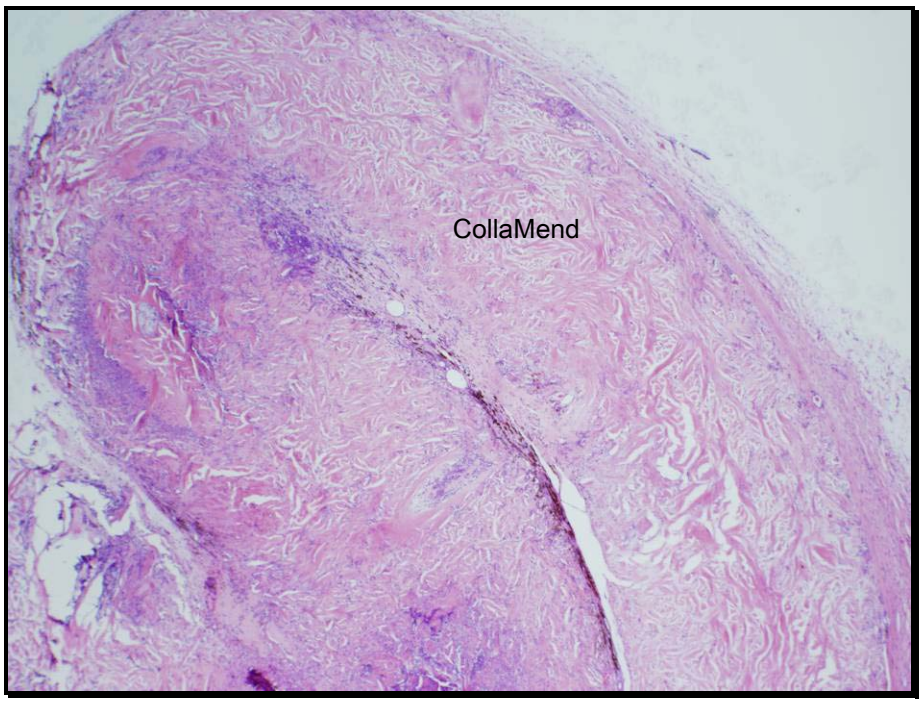

Figure 5.161 – Folded CollaMend 6 months post implantation (H&E, 20X).

In the second animal, after internal examination, a fibrotic mass was visible between the implant and the peritoneal wall demonstrating a marked tissue response to the implant (Figure 5.162).

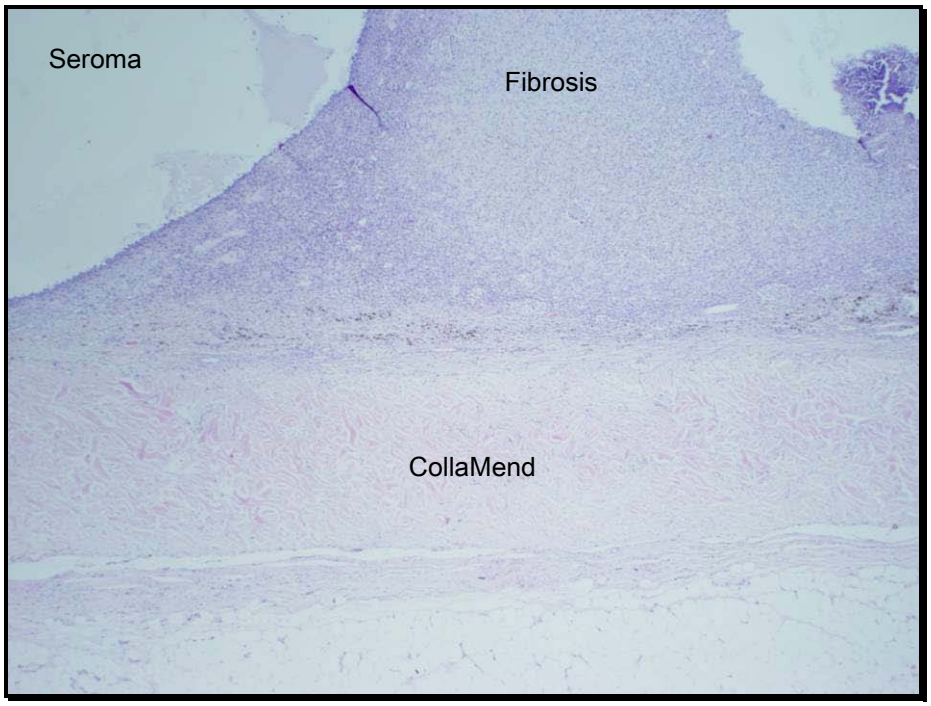

Figure 5.162 – Evidence of a seroma and fibrosis in a CollaMend implant after 6 months implantation (H&E, 20X).

In the same implant among the fibrotic tissue new collagen was forming and the initial stage of calcification was observed (Figure 5.163). Calcification was confirmed with von Kossa's staining.

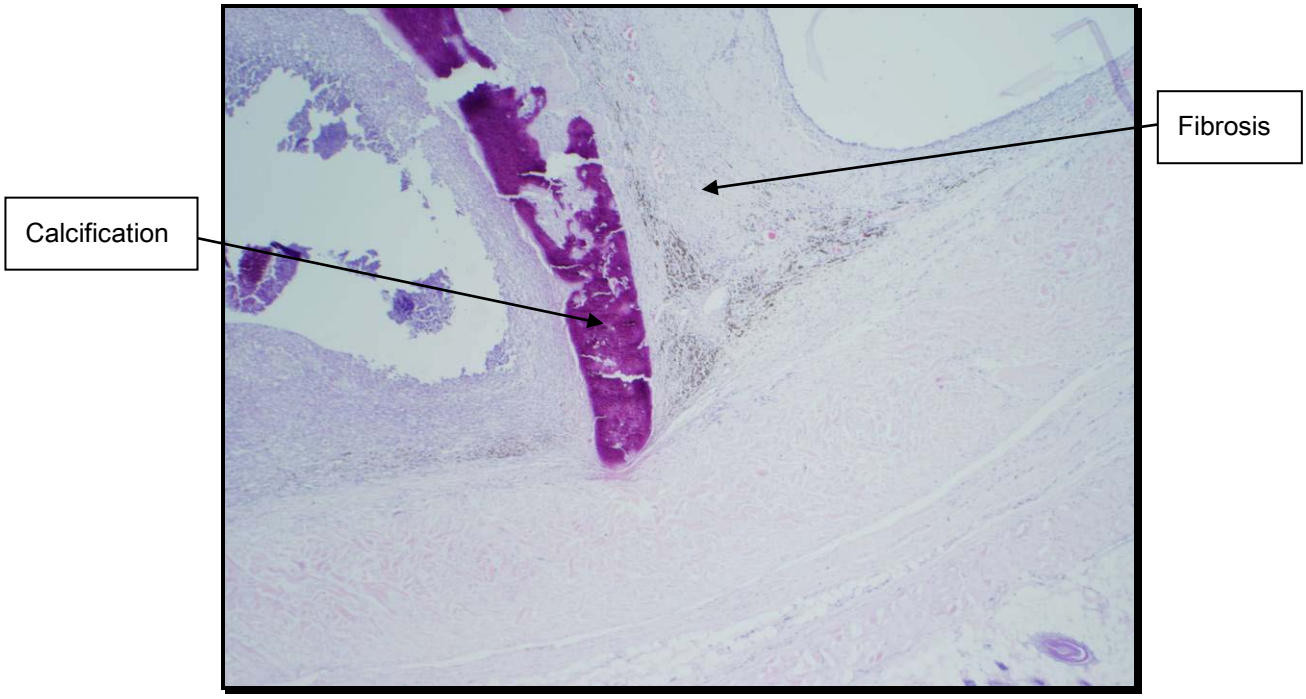

Figure 5.163 – Calcified tissue adjacent to a CollaMend implant after 6 months implantation (H&E, 20X).

After 6 months implantation histopathology showed CollaMend implants structurally similar to day 0; the biomaterial's collagen was not remodelled by the host cells. Integration with the surrounding tissue was mainly low, especially in the side in touch with the peritoneal wall, in some localized areas of the implant border facing the skin integration reached moderate levels (Figure 5.164 and Figure 5.165).

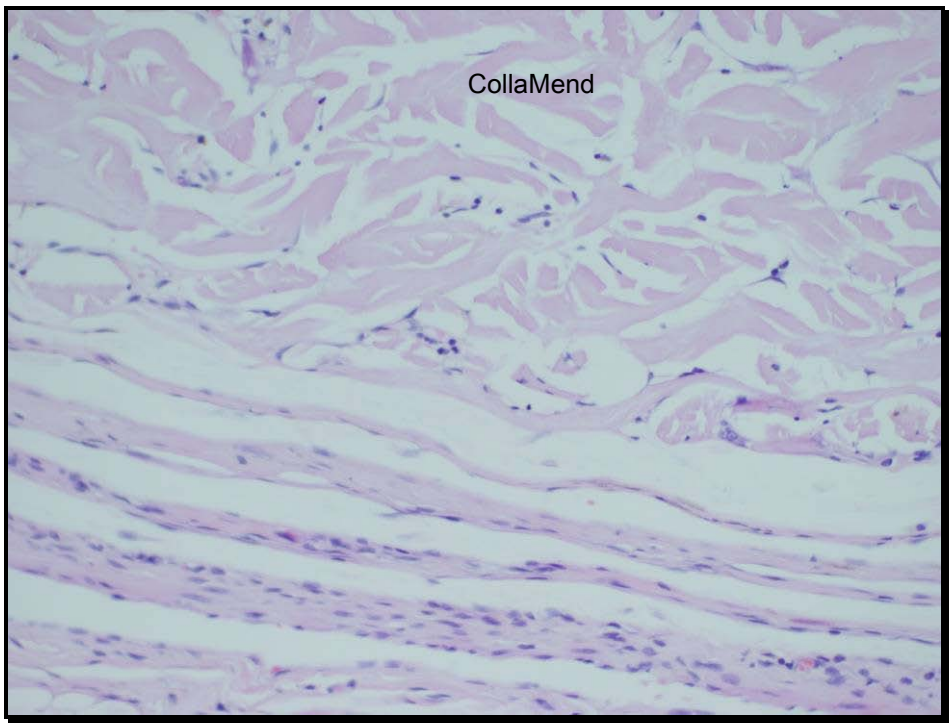

Figure 5.164 – Marginal integration with the surrounding tissue in a CollaMend implant, 6 months post implantation (H&E, 200X).

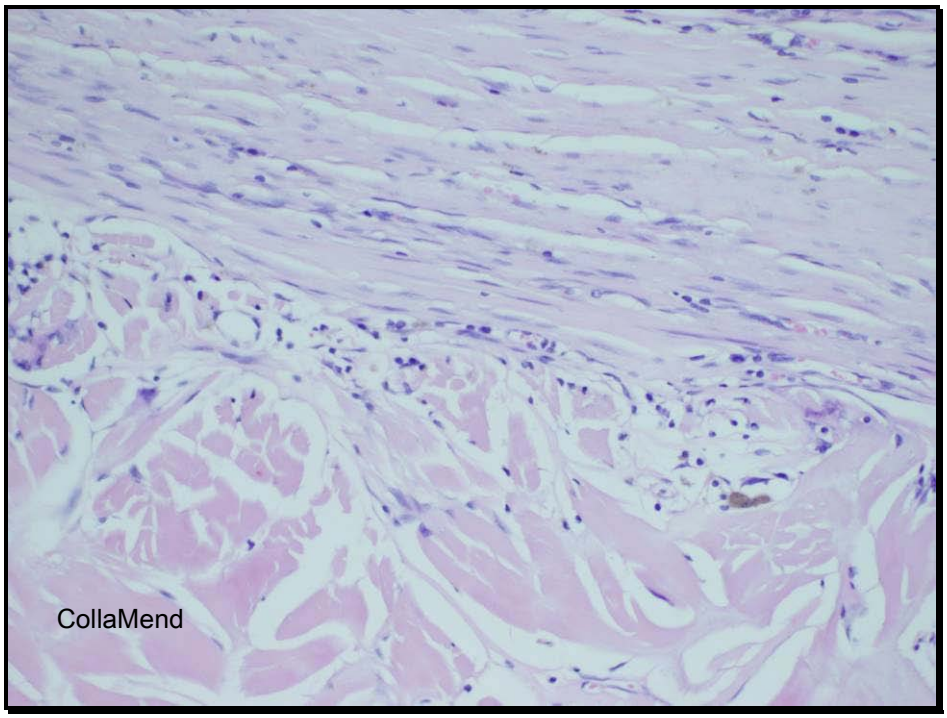

Figure 5.165 – Moderate integration with the surrounding tissue in a CollaMend implant, 6 months post implantation (H&E, 200X).

Cellular density varied from minimal to moderate at 6 months post implantation and cellular penetration reached 100% in all implants (Figure 5.166), cells showed an elongated-shape and were localized within the natural pores of the matrix. Interestingly where integration was higher cellular density was lower and the opposite was also observed.

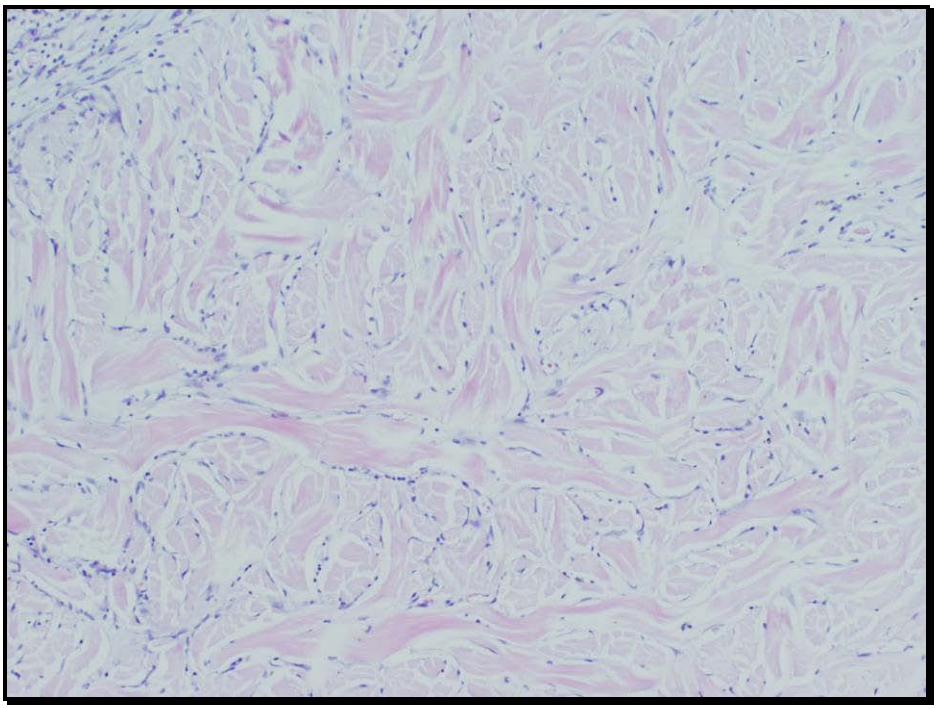

Figure 5.166 – Moderate cellular density in a CollaMend implant at 6 months post implantation (H&E, 100X).

Vessel sprouts and mature vessels were observed in high numbers both at the edges and in the centre of the implants (Figure 5.167).

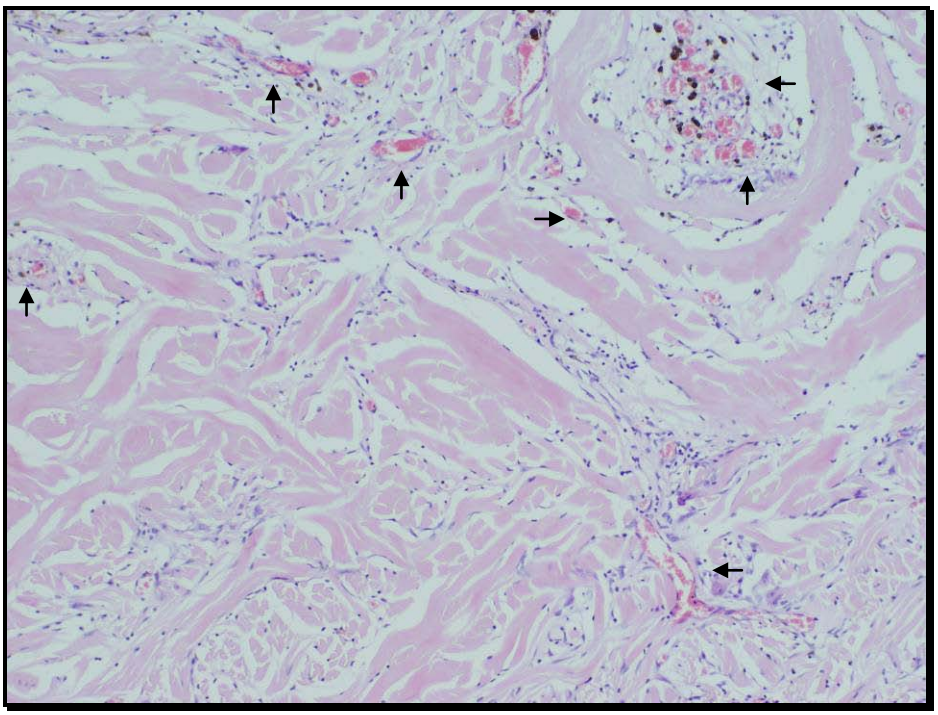

Figure 5.167 – Moderate cellular density with 100% cellular penetration in a CollaMend implant. Vessel sprouts and mature vessels (arrows) are present both in natural pores as within the matrix to support the cellular density (H&E, 100X).

Five implants showed minimal to moderate number of macrophages and giant cells, where giant cells were present collagen was degraded (Figure 5.168). This occurred more often in the middle of the implant than in the borders.

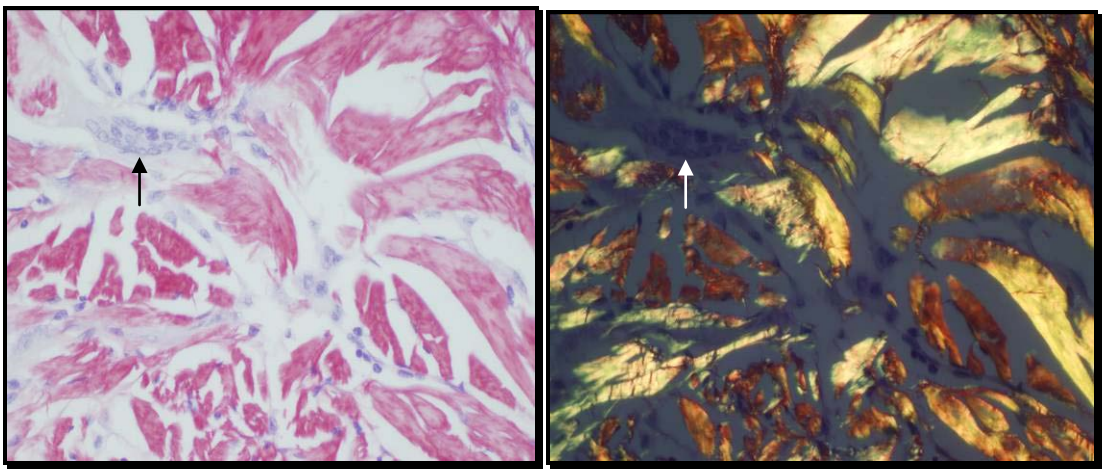

Figure 5.168 – Giant cell in a CollaMend implant. Left: picro sirius red stain; right: picro sirius red under polarized light showing collagen degradation (400X).

Lymphocytes and plasma cells were also observed suggesting an immune response. One implant showed a localized chronic inflammatory response, with high numbers of lymphocytes, giant cells and macrophages. In this area cellular density was complete and integration with surrounding tissue was absent (Figure 5.169).

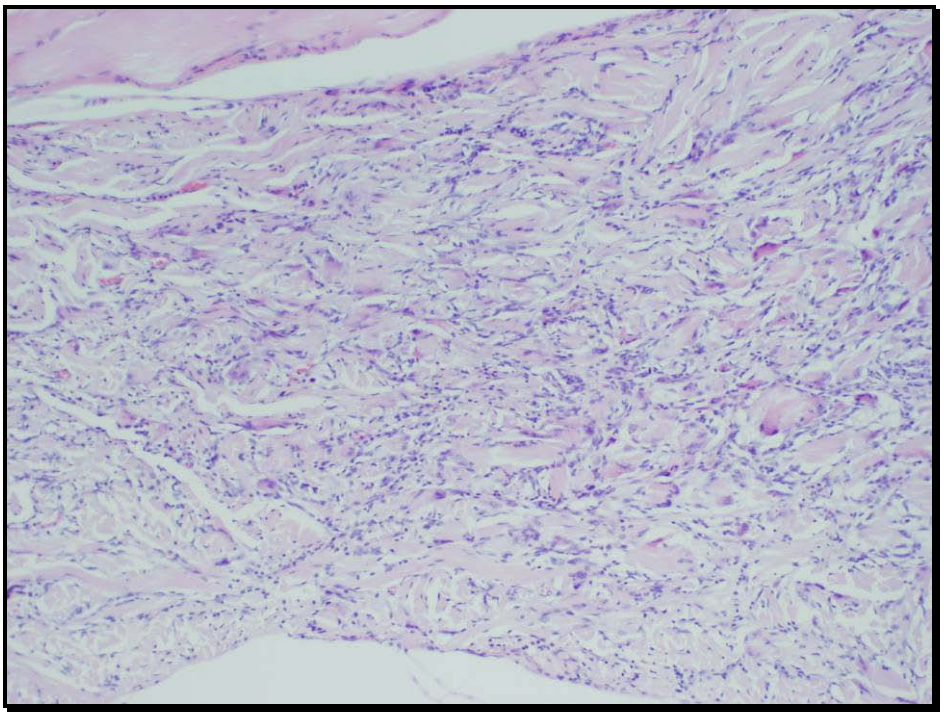

Figure 5.169 – Chronic inflammatory response in a CollaMend implant, 6 months post implantation (H&E, 100X).

Control tissue showed healed hernias in 6 animals; however, the surgical site of one animal was not completely healed showing a void between the peritoneal wall and the skin, probably from an early seroma, although this animal did not show external sign of seroma throughout the study (Figure 5.170).

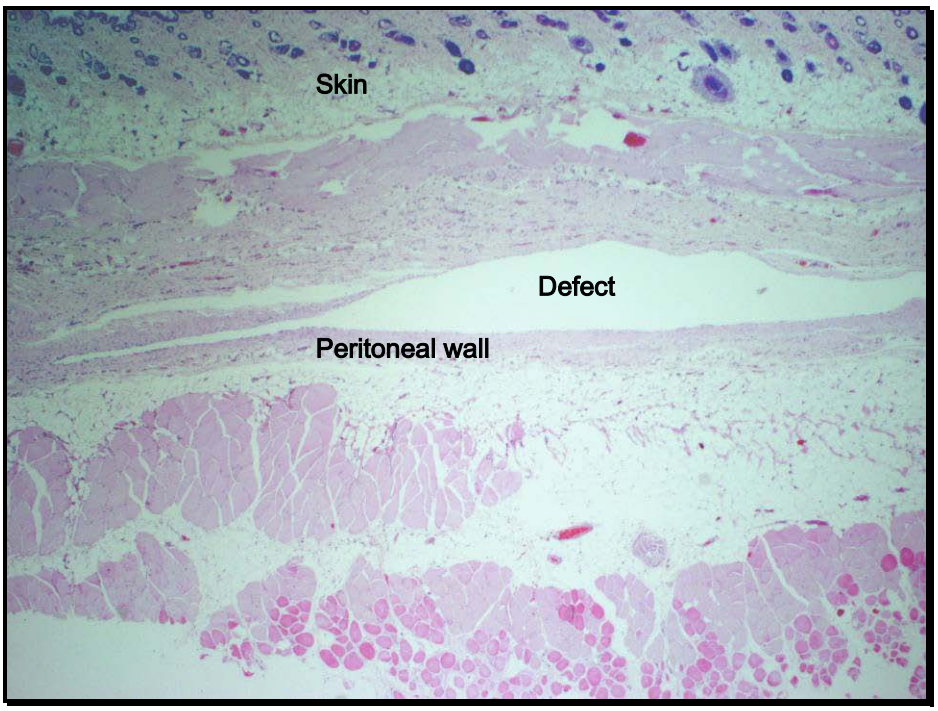

Figure 5.170 – Control tissue not completely healed (H&E, 40X).

Except for the areas where giant cells were present the rest of the collagen in the implants was not denatured and showed good quality.

Figure 5.171 shows the results for animals sacrificed at 6 months post implantation. Mean and standard deviations were used to represent results graphically.

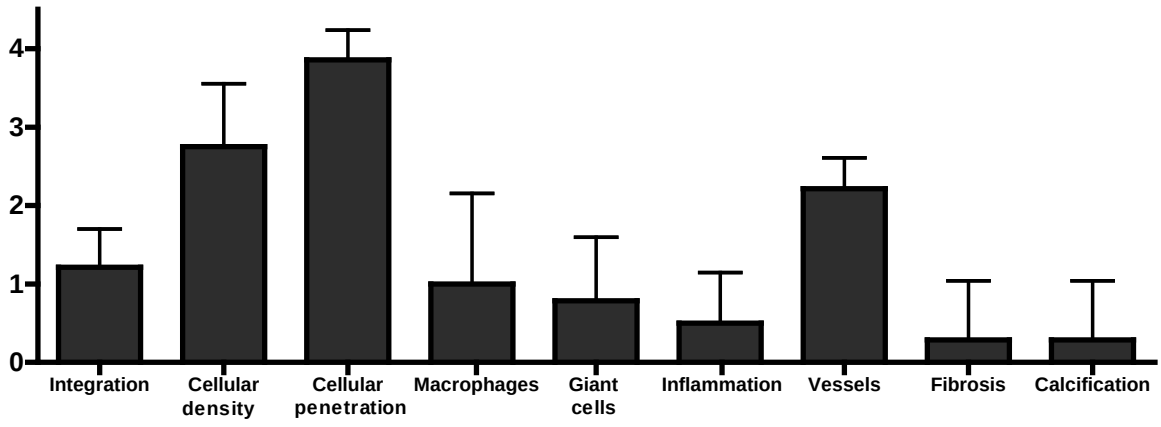

Figure 5.171 – CollaMend results of group C-3. Histometric analysis made according to the scoring system described in Table 5.2.

Next image shows comparison between the 3 groups for CollaMend implants.

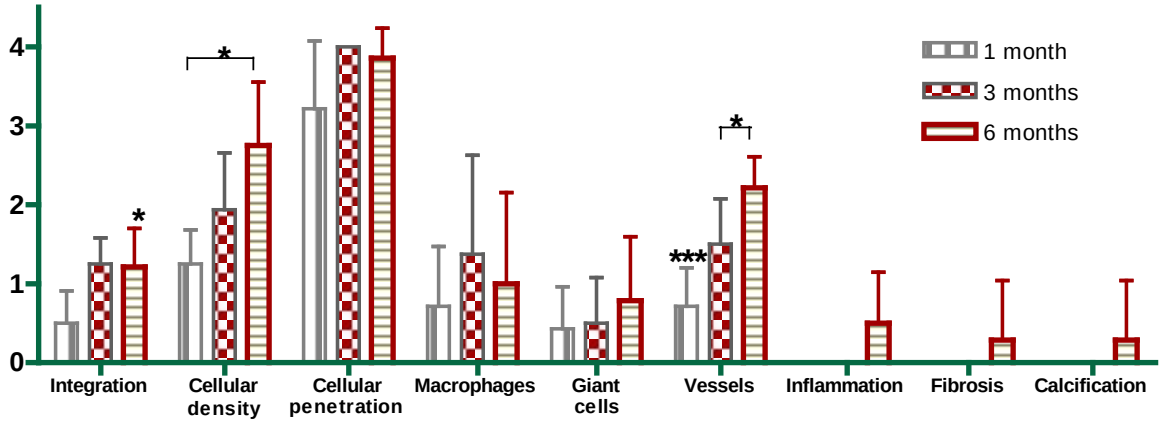

Figure 5.172 – CollaMend results of all groups. * P<0.05, *** P<0.01. Histometric analysis made according to the scoring system described in Table 5.2.

Table 5.20 shows the statistical results for this study. Integration was statistically significant for both factors – matrix type and time – and the interaction between factors was also significant, *i.e.*, mesh integration to surrounding tissue was different over time, depending on mesh type. Since AlloDerm implants had severe inflammatory responses at 1 month post implantation, cellular density and cellular penetration were not quantified in that group, therefore it was not possible to analyse the interaction between time points and mesh type for these 2 factors.

Table 5.20 – Statistical significance for each factor analysed and for the interaction between factors.

	Integration	**Inflammatory response**	**Macrophages**	**Vessels**
Mesh type	P<0.001	NS	NS	P<0.05
Time	P<0.001	NS	NS	P<0.001
Implantation site * Time	P<0.01	NS	NS	NS

Inflammatory response and macrophage presence were not significantly different per factor analysed and there was no evidence of an interaction between mesh type and time point.
Neo-vascularisation was significantly different for both meshes and for time-point, although there was no significant interaction between mesh type and time course.

5.4.8 Discussion

Implantation of a synthetic prosthetic mesh for hernia repair into a contaminated field leads to high rates of infection and consequently often hernia recurrence. Biologic prostheses are recommended in such cases. Their potential benefits include fewer tendencies toward infection, biocompatibility and low host foreign-body responses. There are several types of biologic prostheses clinically used for hernia repair and these are mainly characterised by their animal source and treatments applied. In common they have the fact of being acellular. This study investigated two commercially available biologic prostheses recommended by manufacturers as being effective in abdominal wall hernia repair; they were AlloDerm a noncross-linked human derived mesh and CollaMend a cross-linked porcine derived biological mesh.

Histology of pre-implanted meshes showed acellular matrices for both materials. AlloDerm collagen fibres are not structured in a particular orientation and are mostly constituted by low thickness fibres. CollaMend showed a highly porous collagen matrix with thicker fibres compared to AlloDerm; the percentage of porosity suggests that CollaMend is harvested from the most superficial dermis – dermal papilla.

Tensiometry results for AlloDerm showed high maximum load values at 1 month post implantation; these decreased with time although there was not a significant difference between the time-points tested. The inflammatory response may have affected the tensiometry results at 1 month, especially as it was reaching chronic levels. The increase in the maximum load value from 3 to 6 months suggests an increase in the level of integration, which is corroborated by the histological analysis. It is important to note that stretching of AlloDerm was observed in all implants

throughout tensiometry analysis; this is probably related to the amount of elastin present in human skin.

The tensiometry results for CollaMend were dubious, since most of the resistance observed was conferred by the sutures attaching implants to the host tissue and not by the material. Integration with the surrounding tissue was low as macroscopically observed whilst performing the tensiometry test; these findings were confirmed later by the histopathology analysis. Furthermore, tensiometer mode of failure – tear of implant – observed with two implants at 6 months post implantation does not support CollaMend as being biomechanically strong as claimed by the manufacturers.

Both the physical and mechanical properties of CollaMend interfered with the study model assessed. The folding of the implant caused discomfort to the animals and eventually exposure of the implant.

In the first case reported herein, the animal had to be sacrificed as a result of an open wound caused by the friction between the implant and the skin. This caused a moderate suppurative inflammation, an acute inflammatory response where the exudate was particularly rich in neutrophils. This type of inflammation is most commonly seen as a result of infection by bacteria where the mixture of neutrophils, necrotic tissue and tissue fluid in the acute inflammatory exudate forms pus. The bacteria seemed to have a remodelling effect in the CollaMend, though collagen was not degraded. This observation questions the durability of CollaMend, particularly in complex environments such as infected wounds.

Similar results were obtained from animals that were sacrificed earlier as a result of seroma development and subsequent open wound. Histology showed moderate suppurative inflammation, enlarged active lymph nodes and presence of bacteria. These results are probably caused by the exposure of CollaMend and not directly related to CollaMend biocompatibility.

All AlloDerm groups developed seroma and usually it took between 2 and 3 weeks for the liquid to be naturally absorbed. Seroma formation did not seem to be related to the orientation of the implant, seroma were developed when the dermal side was facing both the wound and the skin. Despite seroma formation these animals did not experience implant extrusion and folding of the implant was not observed.

The marketing literature for both devices claims host acceptance and strong repair of soft tissue defects. The host response in the present study showed that there were differences in the amount and temporal appearance of inflammatory cells and the morphologic structural integrity of the meshes over time.

AlloDerm presence was associated with moderate to severe suppurative acute and chronic inflammatory reactions at 1 month post implantation, consisting of an exudate rich in polymorphonucleocytes and lower numbers of mononucleocytes. Fibrotic activity was also observed at this time point with high concentration of fibrin surrounding the implants. Inflammation diminished over the study time, for the AlloDerm groups, associated with which integration with the surrounding tissue increased. After 3 months implantation the polymorphonucleocytes infiltration was resolved but macrophages and giant cells numbers were maintained, decreasing at 6 months. These results are in accordance with a study performed by Gaertner and co-workers where they tested AlloDerm for ventral hernia repair in a rat model and reported minimal inflammation at 3 months post implantation (Gaertner *et al.*, 2007). Cellular density was lower at 6 months when compared to the 3 months implants, suggesting that after the inflammatory response cells decrease in number leaving the implant only minimally populated; this is in keeping with normal wound healing. Independent of cell density, cells penetrated 100% of the implants, both at 3 and 6 months.

Both inflammatory response and lymphocyte activity (observed at low levels at 1 month but at high levels at 3 months) suggest the occurrence of an immune response, which questions the biocompatibility of AlloDerm. Biomaterials should be biocompatible and should not induce intense inflammatory reactions, since that may impair the function of local host tissue defences by reducing leukocyte ability to opsonise and phagocytise bacteria.

Literature review revealed contradictory outcomes when using AlloDerm for abdominal wall reconstruction. While some authors reported no complications others reported a wide range of mesh-associated problems. Buinewicz and Rosen used AlloDerm to repair ventral hernias in 44 patients (mean follow-up 20 months), 8 of whom had previous wound infections and reported no complications or postoperative wound infections (Buinewicz and Rosen, 2004). Patton and colleagues performed abdominal wall reconstruction with AlloDerm in 67 patients, with an average follow up of 10.6 months, and reported 18% recurrent hernias (12 patients), 11 patients had

wound infection, 2 patients needed mesh removal, 3 patients developed seroma and 3 patients developed fistulas (Patton *et al.*, 2007). Similarly, Gupta and colleagues reported a clinical study with 33 patients using AlloDerm to repair ventral hernias, with a follow up of 18 months; they observed 24% of hernia recurrence, 6% seroma development and 45% of diastasis or bulging of muscle (Gupta *et al.*, 2006).

Although there was no inflammatory response 1 month post implantation in the CollaMend implants, cellular density was marginal since implants were mostly cell free. When cells were present, cellular penetration could reach 100%. The presence of round-shaped fibroblasts-like cells suggests that this collagen matrix does not offer favourable conditions for the maintenance and growth of these cells in the earlier stages of implantation. The shape of fibroblasts determines quality of cell adhesion on the substrate. In normal conditions fibroblasts are elongated, a round shape indicates unsuccessful adhesion while a flat, non-elongated shape provides evidence of inadequate adhesion. However, at 3 and 6 months post implantation cells were needle-shaped suggesting that with time cells overcome the detrimental factors that impede their growth and proliferation in the early stages of implantation; cells may produce substances or induce other cells to produce substances that will change the chemistry and signalling of CollaMend matrix. Another possible explanation for this time-related change lays in the interaction between CollaMend and surrounding environment; with time CollaMend components may change chemically as a result of exposure to interstitial fluid and cell signalling, becoming more biologically friendly to the host cells; or the implant's surroundings adjust and adapt to CollaMend's presence.
Unfortunately, to the authors' best knowledge there are no published articles concerning the use of CollaMend for hernia repair, therefore, it is not possible to compare the results obtained in this study to others author's work.

Macrophages and multinucleated giant cells were present in higher numbers following an inflammatory response in the AlloDerm groups and at lower numbers at 1 and 3 months in CollaMend matrices; these type of cells are associated with a foreign body type reaction. When monocytes differentiate into tissue macrophages, they acquire the ability for the regulated production of MMPs as well as the counter-regulatory inhibitor TIMP (tissue inhibitor of metalloproteinases) (Senior *et al.*, 1982; Welgus *et*

al., 1990)**.** Macrophages control tissue degradation not only directly, by releasing MMPs and TIMP, but also indirectly, by stimulating the MMPs gene expression of resident tissue fibroblasts through the release of IL-1 and tumour necrosis factor (Dayer *et al.*, 1986; Lacraz *et al.*, 1994).

CollaMend implants did not show collagen degradation at 1 and 3 months but collagen degradation was observed at very low levels at 6 months post implantation when a localized chronic inflammatory response was present. This response was related to giant cell presence but implants were not remodelled or absorbed. The opposite was observed in AlloDerm implants. When inflammatory cells were present, AlloDerm was remodelled losing its initial structure and assuming a configuration where fibres were spatially orientated. AlloDerm implant presence decreased with time; at 1 month and 3 months post implantation all implants were present; however there was partial degradation of 2 and 3 implants at 1 and 3 months respectively. At 6 months post implantation, 2 implants were completely absent and the remaining showed highly birefringent collagen. This implies that although the AlloDerm collagen is degraded in the earlier stages of implantation, neo-collagenesis occurs and new collagen is formed when the implant is maintained. Observation of collagen pattern in the 6 months AlloDerm implants showed both mature fibres and new thin collagen fibres. Although new collagen is deposited within the AlloDerm matrix, implants maintain some of their original composition.

Such a difference between the morphologic structural integrity of the analysed prosthetic materials may derive from the fact that CollaMend is cross-linked which should increase its resistance to proteolytic activity.

At 3 and 6 months post implantation the inflammatory response was lower in the AlloDerm implants and fibroblastic ingrowth was observed. Cells easily penetrated the matrix reaching 100% cellular penetration at these time-points. Although extension of cellular penetration increased, cellular density diminished but integration with surrounding tissue was enhanced over time. Once more these results provide further evidence for the notion that consistent and continuous cellular infiltration and proliferation are not essential for tissue/implant integration. In conjunction with tissue/implant integration, neo-vascularisation also increased with time. These results suggest a relationship between integration and neo-vascularisation, both parameters increasing over time independent of cellular density and cellular penetration, although

correlation tests did not show a statistical correlation between integration and neo-vascularisation.

CollaMend cellular density increased through the study and reached mild levels at 6 months post implantation. Independent of cell number the extension of cellular infiltration reached 100% for all implants; cellular penetration was observed through spaces between collagen fibres and not within the collagen. Due to the high porosity of CollaMend implants tissue cells moved easily inside the prosthetic material but density levels were not high. With the increase of cellular density, neo-vascularisation levels were raised and significant differences were observed along the study period. While there was no evidence of an inflammatory reaction or immunogenic response in the early stages of this study, for CollaMend, a localized chronic inflammatory response consisting of high numbers of lymphocytes, giant cells and some plasma cells accompanied by fibrosis and calcification were observed in one implant after 6 months implantation. In this implant integration with surrounding tissue was low and that may be explained by the fibrotic mass found between the implant and the peritoneal wall, which decreased the contact area between the implant and the adjacent tissue.
It was observed in group C-3 that integration was always greater in the side implanted facing the skin, whereas the CollaMend side in touch with peritoneal wall had low integration. This result questions the efficiency of CollaMend when used as a hernia repair biomaterial, since lack of integration with the muscle will decrease the healing rate and will not provide tissue support for hernia healing.

One of the aims of this study was to compare AlloDerm and CollaMend performances in ventral hernia repair to Permacol® surgical implant performance (in-house study, data not published), in a rat model. When Permacol® was used as a regenerative tissue for repair of a ventral hernia it was associated, at 1 month post implantation, with a marginal acute and chronic inflammatory response that was resolved after 3 months of implantation. Integration with the host tissue was mild in the earlier stages (1 month), increasing to moderate to complete levels at 3 months post implantation. Marginal calcification was observed in the centre of implants at 6 months post implantation and, maybe as a consequence, integration with surrounding tissue decreased to minimal levels. When testing mechanical strength through tensiometry, maximum

load values increased over time but extension at maximum load and total extension decreased after 6 months implantation. Permacol® did not cause development of seroma or extrusion of implant and, as observed with CollaMend implants, was not degraded or remodelled. Furthermore, by 6 months the matrix showed the same configuration and morphologic structure as pre-implanted Permacol®. Hence, cross-linking is very likely the source of Permacol® and CollaMend permanence in long-term studies. Permacol® surgical implant has been used in abdominal wall reconstruction. Catena and co-workers where faced with complicated incisional hernias with contamination, used Permacol® for hernia repair in 7 patients and reported no recurrence or wound infection post surgery. The mean follow up was 11 months (Catena *et al.*, 2007). Shaikh and colleagues used Permacol® in 8 patients for reconstruction of acute abdominal wall defects and in 12 patients with chronic abdominal wall defects. Sixteen percent had an uneventful recovery while 2 patients developed seroma, there were 3 hernia recurrences, 2 patients developed wound infection, 1 patient had a wound hematoma, 1 patient had a wound dehiscence and one patient develop a wound sinus (Shaikh *et al.*, 2007).

During wound healing fibroblasts produce collagen type III which acts as a temporary scaffold for fibroblast attachment. Through a complex process of remodelling and maturation, collagen type III is replaced by collagen type I, which is related to long-term strength (Hammond *et al.*, 2008). Both recurrent and incisional hernias can be regarded as a consequence of a non healing wound. This implies that the ECM collagen ratio is favouring collagen type III resulting in loss of tensile strength and predisposing tissue to hernia formation. Therefore, it is sensible to use collagen type I based prostheses for hernia repair. Both human skin and porcine skin are constituted mainly by collagen type I and collagen type III. The ratio between these two collagen types may vary depending of the depth of skin analysed but commonly achieve ratios of 6:1 (type I/ type III) (Epstein and Munderloh, 1978).

There was no tissue reactivity observed in the controls and there was no evidence of long-lasting damage from the surgical procedure, although one control sample from a CollaMend group presented histological evidence of a seroma.

When faced with the decision to use a biological prosthetic material for abdominal wall repair the surgeon must choose between human, porcine or bovine sources. Patients should be informed of the type of prosthetic material they will be implanted with, particularly if the surgeons decide on a porcine derived biomaterial, which may raise religious concerns. Other important factors that may influence the choice of the surgeon are prosthesis availability and price. Availability of cadaveric allograft is dependent on organ donation banks; on the other hand, porcine/bovine dermis is much more abundant and structurally very similar to human dermis and this increases off-the-shelf accessibility. The cost of any implant material may be significant; it is difficult to compare prosthesis cost since they are provided in different sizes. In addition, costs should include theatre time and post-surgical treatments. As an example of the prosthesis analysed in this study, a 4cm x 16cm piece of CollaMend costs £900, an AlloDerm piece of the same size with 0.79 - 2.03mm thickness costs £1523.53 and the closest size available for Permacol® would be a 4cm x 18cm, 1mm thickness, costing £525. By comparison, Permacol® surgical implant is the least expensive option from these three biomaterials.

Other important features when choosing a dermal material include size, thickness, storage and rehydration (pre-treatment). Permacol® is available in large sizes, up to 18cm x 28cm, and different thicknesses, from 0.75 to 1.5mm, it is easy to store since it does not need to be kept refrigerated and can be used directly out of the package. Alloderm, is available in sizes from 3cm x 12cm up to 16cm x 20cm; however, larger sizes are available upon request; two thicknesses are available 0.79 - 2.03mm and 2.06 - 3.3mm. AlloDerm needs to be kept refrigerated and rehydration prior to use is necessary, rehydration may take from 10 to 40 minutes depending of size and thickness of implant. CollaMend is available in different sizes from 2cm x 4cm up to 6cm x 12cm in a rectangular shape or from 10.2cm x 15.2cm up to 20.3cm x 25.4cm in an elliptical shape. Thickness of all sizes is approximately 1mm. It does not need refrigeration but needs to be rehydrated at least for 3 minutes before use. Shelf time is approximately the same for these 3 biomaterials.

5.4.9 Conclusion

Experimental investigations in biologic prosthetic materials are important as adverse effects and unfavourable properties of products have been demonstrated in laboratory trials after their introduction to clinics and, occasionally, complications occur clinically due to the use of unsuitable materials.

In the rodent model reported here AlloDerm showed reactivity with the host tissue. Inflammatory response was not related to the surgical procedure, since control tissue showed no reactivity. Seroma developed in 11 of the 18 animals independently of the implant orientation, which suggests that the implant orientation does not affect the implant-host interaction. All implants showed moderate to severe inflammatory responses in the earlier stages of implantation, which decreased with time. At 3 months post implantation lymphocyte activity suggests an immune response; although AlloDerm is manufactured as an acellular product the presence of hair in one of the implants and the immune response suggests that the cell removing process used may not be 100% efficient at removing immunologically active DNA.

AlloDerm implants showed collagen degradation at different levels in the earlier stages of implantation, as well as matrix remodelling. After 6 months implants were partially remodelled and 2 implants were absent, the implants that were present showed new collagen deposition; this suggests that over time AlloDerm may be remodelled by neo-collagenesis or may completely disappear before the new collagen is formed depending on the rate of matrix degradation which is controlled by the host tissue response. In normal tissue collagen is a stable molecule with a long half-life; however, half-life is shortened as a result of tissue reactivity to the implant. In the clinical setting if a biologic prosthesis is absorbed before adequate collagen deposition and maturation, it may result in a weakened wound environment during the repair process ultimately compromising wound healing and strength of repair. The data presented here may support this theory in the case of AlloDerm.

The physical and mechanical properties of CollaMend caused discomfort in the animals and as a result there was formation of additional wounds and exposure of the implants. CollaMend seems to be easily populated by cells, although these do not remodel the matrix and implants maintain their original structure until 6 months.

However, when implants were exposed and a suppurative inflammation occurred bacteria remodelled the edges of CollaMend, which questions CollaMend longevity particularly in complex environments such as infected wounds. The fibrotic tissue observed in one of the implants after 6 months implantation, in conjunction with the seroma remains, calcification and the new collagen being formed as a response to the original inflammation, suggests that CollaMend causes tissue-specific reactivity.

The number of giant cells and macrophages present in the implants increased over time suggesting a delayed chronic inflammatory response. Although the level of collagen degradation observed was low this may increase with time, since this was not observed in the earlier stages of the study.

The CollaMend apparent inability to integrate with the peritoneal wall and therefore give tissue support for hernia repair is a problem not only for this type of clinical procedures but also in the clinical setting where degradation of a biological implant prior to neo-collagenesis may compromise wound healing and strength of repair; in addition its stiffness and limited malleability are an obvious difficulty for surgical procedures and physical comfort.

In the rat model reported here the results do not support Bard CollaMend Implant as a suitable material for hernia repair. The host response to AlloDerm suggest that this material causes an immune reaction and the rapid rate of remodelling and degradation of AlloDerm matrix may bring further problems in the clinical setting when the overall quality and strength of the new formed tissue is insufficient for abdominal wall repair.

6.0 GENERAL DISCUSSION

One of the main therapeutic and commercial needs in tissue repair and regeneration which is not yet fulfilled is for novel biomaterials designed to optimise cellular potential resulting in good quality repair of tissues or organs and, therefore, restoration of their function.

Several natural and synthetic materials have been used to construct extracellular matrices to be used as tissue substitutes or to assist in tissue regeneration. Synthetic meshes do not present epitopes recognisable by cellular adhesion receptors which would induce cell-matrix adhesions; for that reason, natural materials can be advantageous since their structural proteins will have surface topography and signalling suitable for cell-matrix interaction.

Collagen is the main structural constituent of connective tissues; hence, it has been extensively applied in biomaterials applications such as wound dressings, matrices for controlled release of active agents (drugs or growth factors) or as a tissue engineered scaffold (Duan and Sheardown, 2005). The design, development and application of collagen-based biomaterials in human clinical procedures continues to increase. Collagen-based biomaterials present numerous advantages such as biocompatibility, low toxicity, low antigenicity and well-documented physical, structural, chemical and immunological properties. Moreover, it is easily isolated and purified in large quantities and can be processed into several forms.

Collagen type I is the most abundant protein in the body, constituting approximately 95% of total collagen in bone, cornea, teeth and tendons, and more than 85% in dermis, gingiva and heart valves (Kafienah *et al.*, 1998). As a result, type I collagen-based biomaterials are often used for tissue regeneration, repair or replacement.

In order to ensure *in situ* biocompatibility, collagen-based biomaterials are subjected to cellular removal and are sterilized. Depending on the intended clinical application further treatments can be applied including removal of non-collagenous tissue, cross-linking, increase of porosity and addition of cells, to name just a few.

Natural collagen can have a high enzymatic turnover rate *in vivo* which makes stabilization of collagen-based biomaterials advantageous, particularly when a

collagen-based biomaterial has been pre-treated by removal of the cellular components. In addition, collagen bioprosthetic devices often contain non-collagenous proteins which some studies have shown to be the main immunogenic components of collagen-based biomaterials (Lynn *et al.*, 2004). The formation of covalent intermolecular cross-links between collagen molecules is an effective method to improve mechanical integrity, stability and to mask reactive epitopes, therefore, diminishing antigenicity.

Before commercialisation is permitted all biomaterials must be proven to be functional and suitable for clinical use, which demands compliance with the requirements established by FDA or CEN. However, even when a biomaterial fulfils all requirements and it is certified to be used in the clinical field the complexity of host responses can always originate an unexpected result. Continuous experimental analyses on biomaterials are of extreme importance as adverse effects of currently available products have been demonstrated in laboratory trials (Petter-Puchner *et al.*, 2008; Poulose *et al.*, 2005)

In the research described in this thesis an acellular cross-linked collagen-based biomaterial (Permacol® surgical implant) was studied and compared to acellular noncross-linked and cellular naturally cross-linked equivalents. Several studies were designed to evaluate and compare these dermal collagen porcine derived matrices. Permacol® surgical implant is claimed to be a non-resorbable, acellular, non-cytotoxic, substantially non-antigenic collagenous fibrous tissue which retains the natural structure and original architecture of dermal collagen and is suitable for soft tissue repair as a permanent biomaterial. Studies comprised: analysis of structure, composition and mechanical properties; cross-linking quantification; assessment of resistance to proteolytic enzymes; *in vitro* models to observe fibroblast interaction with the dermal matrices and analysis of Permacol® performance when in presence of putative pathogens; and *in vivo* studies designed to assess Permacol® biocompatibility and effectiveness as a repair material and as bulking tissue. Permacol® was compared to acellular noncross-linked collagen and to two other commercially available dermal collagen biomaterials – AlloDerm and CollaMend.

6.1 ANALYSIS OF METHODOLOGY

The work presented in this thesis does not follow a chronological order of completion; the several studies were grouped into chapters according to topic and objectives. The chapters therefore have been structured to best present each aspect of the overall project.

6.1.1 Methodology for Biophysical and Biochemical Characterisation

Several factors such as the type and the concentration of collagen used, treatment with cross-linking agents and preparation methods can affect the structural integrity of collagen-based biomaterials. Biomaterials must withstand physiological loads in both short and long term applications. The mechanical strength of a biomaterial decreases with time *in vivo*; therefore, when designing a biomaterial it is essential to consider if such a material will be used in non-load-bearing applications or in constant stress/load applications. Equally important is biomaterial's performance when sutured under tension; therefore, tensile strength tests were performed to characterise the mechanical strength of the biomaterials studied.

The standard method for measuring the **tensile strength** of a material is by applying an axial force and measuring the corresponding extension (Barber *et al.*, 2006; Derwin *et al.*, 2006; Figallo *et al.*, 2007; Liang *et al.*, 2004). Tensile strength was measured and recorded by tensiometry and maximum load, extension at maximum load and total extension. Values for load were plotted against extension and a stress graph obtained where the elastic limit of each matrix indicates the transition from linear behaviour to nonlinear behaviour, which leads to a peak representing the maximum load. Complete failure is further denoted by total extension.

Water uptake analysis is a common technique used to characterise physical and mechanical properties of materials (Wang and Hon, 2003). Through this technique the material behaviour in an aqueous environment can be predicted and, by measuring the absorption capacity of material fluid dynamics, exudate absorption and drug release

can be estimated. Fluid and exudate absorption capacities will directly influence nutrient supply, waste removal and proteolytic activity within a biomaterial, subsequentely affecting the viability of an implant. A high absorbance capacity is desired, for example, when an implant is used as a bridge or replacement of a tissue defect; in such a case, it is necessary to supply the implant and the resulting cellular response with good fluid flow. Conversely, occasionally a biomaterial may be designed to act as a barrier/membrane, as when implanted in regular contact with specific fluids (e.g. bowel, bladder). In such a case, it is expected that such a biomaterial will have low fluid absorbance capacity and/or have specific permeability. Since water uptake will vary depending on material composition and structure, it is possible to compare different materials by analysis of their degree of swelling.

Cross-linking quantification was performed using two colorimetric methods: TNBS and ninhydrin assays.

The TNBS assay is an indirect method to quantify level of cross-linking (Azarmi *et al.*, 2006). The primary amines of the proteins present in the sample react with TNBS originating a trinitrophenyl (TNP) derivative (Bullock *et al.*, 1997; Sarti *et al.*, 1995). The free terminal amino groups ($-NH_2$) of the peptide chains are considered to be the groups which will react with TNBS (Weber *et al.*, 2000). The extent of this reaction is determined spectrophotometrically. Some authors choose to read the absorbance of the un-reacted against a control which will indirectly give the value of TNP-derivative formed (Weber *et al.*, 2000), while others prefer to read the formation of the TNP-derivative directly (Sarti *et al.*, 1995).

Regardless of the high reproducibility of the TNBS method, discrepancies were found between published procedures. The differences found were related to incubation time (5 minutes to 2 hours) (Fields, 1971; Morçöl *et al.*, 1997), buffers (borate, sodium hydrogen carbonate) (Azarmi *et al.*, 2006; Cayot and Tainturier, 1997), incubation temperature (room temperature to 40^{o}C) (Morçöl *et al.*, 1997; Satake *et al.*, 1960), neutralisation of reaction before measuring the absorbance and the wavelength of the monochromatic light for the absorbance measurements. The latter includes ultra violet light (wavelength of 340 to 367nm) (Azarmi *et al.*, 2006; Bullock *et al.*, 1997; Satake *et al.*, 1960) and visible light (wavelength of 410 to 420nm) (Fager *et al.*, 1977; Morçöl *et al.*, 1997).

After careful analysis of published protocols, conditions suitable for quantification of free amino groups in insoluble collagen matrices were chosen. To ensure that all free amino acids had been trinitrophenylated the TNBS was allowed to react with the protein at 40^{o}C for 2 hours at a pH of 8.5. A side reaction leads to the formation of TNP-sulphonic acid which will react with hydroxyl ions increasing the blank extinction (Fields, 1971). To stop the side reaction from interfering with the results, the pH of the solution was decreased (by incubation with 6N HCl) after the amino groups have been trinitrophenylated. By this process only the non-sulfited form is present in solution therefore the absorbance measured is related to the TNP-protein derivatives. Several published studies described 420nm as the wavelength showing the highest sensitivity for TNP-protein derivatives (Cayot and Tainturier, 1997; Fields, 1971; Morçöl *et al.*, 1997; Sarti *et al.*, 1995); as a result, this was the wavelength chosen for the protocol used.

A ninhydrin method was introduced for quantitative determination of amino acids in the 1950s (Moore and Stein, 1954). This method has since been widely used to characterize amino acids and proteins (Fountoulakis and Lahm, 1998; Sun *et al.*, 2006). This reaction is unique among chromogenic reactions as ninhydrin hydrates with amino groups at pH 5.5 resulting in the formation of the same soluble chromophore, denominated Ruhemann's purple, by all primary amines (Friedman, 2004). Although this technique is extensively used, several features associated with it are inconsistent. Variations present in the ninhydrin protocols included buffers used (phosphate, sodium acetate, potassium acetate, lithium acetate), heating temperatures (from 85^{o}C to 100^{o}C), incubation time (from 5 to 45 minutes), pH values (from 5 to 8) and solvents (water, absolute alcohol, DMSO, ethylene glycol) (Friedman, 2004; Gaitonde, 1967; Moore and Stein, 1954; Starcher, 2001; Sun *et al.*, 2006). Sun and colleagues performed a study evaluating several experimental conditions and reported on the best and more convenient experimental conditions for the use of the ninhydrin method (Sun *et al.*, 2006), so their suggestions were followed in the current studies.

Literature review revealed considerable variations in experimental conditions of both methods used for cross-linking quantification. The presence of hydroxy ions may compromise the results from the TNBS assay by decreasing selectivity for primary amino groups (Adler-Nissen, 1979; Panasiuk *et al.*, 1998). Although this step was

avoided by decreasing the pH and therefore obtaining only the non-sulfited form of TNP in solution, some authors do not agree that decreasing the pH is enough to increase TNBS specificity (Cayot and Tainturier, 1997). Ninhydrin is considered to be more selective for alfa amino groups and derivatives but the amount of colour produced will vary with the product to be examined and is not always stoichiometric (Friedman, 2004). When Panasiuk and co-workers compared TNBS versus ninhydrin assay, they reported that the results from these methods were not correlated and they considered TNBS method more accurate than ninhydrin (Panasiuk *et al.*, 1998).

In general, both methods have advantages as the protocols are simple, convenient, reproducible and can be used routinely in a large number of samples. The major disadvantage seems to be specificity problems and lack of sensitivity for the TNBS and ninhydrin assays, respectively.

Other techniques that can be used to calculate the degree of cross-linking include high performance liquid chromatography (HPLC) (Kaga *et al.*, 2003), electrophoresis (Everaerts *et al.*, 2007), Raman spectroscopy (Gosselin *et al.*, 2007), mass spectrophotometry (Tang *et al.*, 2005), size-exclusion chromatography (Hartley *et al.*, 1993) and nuclear magnetic resonance (Banci *et al.*, 1990). Although these are more modern techniques for determining compounds containing amino groups, TNBS and ninhydrin assays are safe and there is no need for expensive equipment. In addition, numerous papers report the use of these methods to determine the level of cross-linking of proteins with satisfactory results.

Cellular composition of the collagen matrices was analysed by routine H&E staining. Haematoxylin stains basophilic structures such as nucleic acid which allows visualisation of cell nucleus or nucleic remnants. In addition, this stain allows visualisation of the basic **structure** of materials including fibre direction, thickness and morphology. SEM was used to further evaluate matrix structures and identify matrix components. DNA extraction and quantification can be used for analysis of cellular composition of materials, but since the materials analysed in this thesis were composed of non soluble collagen, collagenase would have to be used to disrupt the molecules and increase collagen solubility for total DNA extraction. Collagenase has been implicated in increased DNA synthesis (Liu *et al.*, 1994); therefore its use could affect the cellular fractions.

Tissue Science Laboratories describe Permacol® surgical implant as a biomaterial mainly constituted by collagen (approximately 97% collagen type I and 3% collagen type III) and comprising 1 to 5% elastin (US Patent no. 5,397,353). Therefore, a picro sirius red stain was combined with Miller elastin stain to identify collagen and elastin simultaneously.

Other methods used to characterize the structure, chemistry and composition of a biomaterial include mass spectrophotometry (Sosnik *et al.*, 2006), atomic force microscopy (Choudhary *et al.*, 2006), transmission electron microscopy (Zhao and Frost, 2008), energy dispersive X-ray (Verné *et al.*, 2008) and electron spectroscopy for chemical analysis (Choudhary *et al.*, 2006), to name just a few; such equipment was not available.

Studies have demonstrated that a high degree of porosity increases the surface area available for cell attachment and provides enough space for cell migration (Figallo *et al.*, 2007). **Pore size** is therefore an important feature of a biomaterial which will not only influence cell behaviour but also mediate the diffusion of nutrients and waste products and, in general, implant permeability. For example, the porosity of a biomaterial is of extreme importance when implanting cartilage or bone substitutes, since good fluid mechanics and joint lubrification are essential and can be enhanced by appropriate material porosity. Pore size was measured by software analysis (DPController software); H&E sections were used at an objective magnification of forty times and at least 10 fields of view were screened for pore size measurement. The range, mean and standard deviations were calculated per type of matrix. The use of a software analysis system is a common technique for pore measurement which can be applied to images obtained by light microscopy or SEM (Yang, 2008). Other methods for pore size measurement involve the use of digitized images where a linear interception program is used to provide a mean pore size (O'Brien *et al.*, 2005) or confocal reflection microscopy can be applied to acquire 3-D microstructural information and average pore size (O'Brien *et al.*, 2007).

Collagen-based biomaterials are degraded *in vivo* and the rate of such degradation will depend on the host response to the implanted material. Therefore, for long term retention the collagen structure must be reinforced so that the biomaterial will persist

in the body for the required period; this is usually achieved by cross-linking the proteins constituting the biomaterial. The efficiency of cross-linking and the level of **resistance to proteolytic enzymes**, of different dermal porcine collagen matrices, were assessed by collagenase and elastase assays to assess collagen and elastin stability respectively (Rault *et al.*, 1996; Trengove *et al.*, 1999).

To further analyse the collagen-based matrices resistance to specific enzymes produced during wound healing and particularly when in presence of inflammation, matrices were digested with human neutrophil elastase (HNE) and human neutrophil collagenase (MMP-8). In the clinical setting, the wound exudate can be collected and tested with anti-human Enzyme-Linked ImmunoSorbent Assay (ELISA) kits which can be used to perform specific or non-specific protease activity assays. In the studies reported here, enzyme concentrations reported to be found in chronic wound fluids were used for MMP-8 and HNE (Aiba-Kojima *et al.*, 2007; Trengove *et al.*, 1999). Enzymes were tested individually for optimization of the reaction conditions. However, *in vivo* a wound is exposed to a cocktail of enzymes which are synthesized as part of a healing cascade but many will overlap and the mechanisms regulating their degradative action are complex and not yet fully understood (Thomas *et al.*, 1999; von Lampe *et al.*, 2000). Therefore, these experiments can give the researcher an idea of how a particular material will behave when in presence of each of these enzymes, but the conditions tested do not represent an *in vivo* situation hence in such a case the results may be different.

To assess **fluid flow** dynamics through cross-linked and noncross-linked collagen matrices a modified Ussing chamber assay was designed and a further *in vivo* experiment was performed. The modified Ussing chamber allowed the studying of matrix resistance to fluid and the analysis of Permacol® permeability characteristics. Mineral deposition was not observed but since this was a short term study it is possible that to achieve saturation point the experiment would have to be performed for longer periods or the buffer solution should have a higher molarity.

To assess interstitial fluid flow dynamics *in situ*, in cross-linked and noncross-linked collagen matrices, a rat model was used. Evans blue dye was injected intradermally and interstitial fluid movements observed for a period of 3 days.

6.1.2 Cell Culture Methodology

Primary cultures of porcine fibroblasts were developed because cells were needed in early passages to avoid phenotypic changes and guarantee high cellular proliferation. Pigs were chosen as the cell source since Permacol® surgical implant is porcine derived and it was thought that porcine fibroblasts would interact naturally with a porcine matrix. Moreover, by using porcine cells cross-species related problems were avoided, including for example matrix surface signals recognition difficulties which would result in decreased cellular adherence.

The analysis of **cell viability** is frequently a controversial subject particularly when using merely one of the many methods available. Often what is measured is a factor which infers the overall health of the cells rather than a definitive measurement of viability. The MTT assay was chosen to analyse cell viability, a method which measures the activity of dehydrogenases in reducing MTT to formazan (Wang *et al.*, 2006). The reaction occurs mostly in the mitochondria and as such can be considered a measure of mitochondrial activity and by association of cell viability. However, many conditions can affect the metabolic activity which may increase or decrease the MTT reduction while the number of viable cells is constant. The assay, however, is quick, simple and inexpensive. The other indicator of cell health used was the Trypan blue exclusion assay. Cells that have had their cell membrane damaged allow the uptake of the Trypan blue dye, while intact cells do not. Hence, stained cells are considered non-viable cells, while a breached cell membrane indicates loss of viability this does not exclude apoptotic cell death. The assay is inexpensive, simple but time consuming and not wholly consistent. Each assay, therefore, has limitations in directly determining cell viability but their combination helps to determine the overall cell viability.

6.1.3 Surgical Procedures

The rat was chosen as the experimental species for all *in vivo* studies because of published and in-house knowledge of pathogeneses in this species. Furthermore, the

rat is the lowest evolutionary animal in which this work could reasonably be carried out.

Subcutaneous implantation was chosen in two studies (Chapters 5.1 and 5.2) since this location is easy to access in the rats, the surgical procedure is very simple, poses no clinical difficulties and, at this surgical location, implants are in full contact with host cells and tissues making it a good implantation site for biocompatibility tests.

Hypotheses related to cellular penetration in Permacol® surgical implant were tested and compared by analysis of Permacol® vascularisation and cellular ingrowth in different implantation sites. The primary objective of the study was to analyse if the level of neo-vascularisation and cellular density observed in Permacol® were influenced by the level of vascularisation of the immediately surrounding host tissue. Muscle and liver are highly vascularised tissues and therefore were chosen as implantation sites in Chapter 5.3.

Permacol® surgical implant is recommended for soft tissue repair and therefore has been clinically used for hernia repair due to its versatility and malleability. It is manufactured in several sizes, can be easily trimmed to the desired shape and it is easy to suture. Permacol® has been used in the repair of different types of hernia including abdominal (Liyanage *et al.*, 2006; Parker *et al.*, 2006; Saettele *et al.*, 2007), perineal (Abhinav *et al.*, 2008; Skipworth *et al.*, 2007), Littre's (Smart *et al.*, 2007) and parastomal (Inan *et al.*, 2007). The hernia repair model used in Chapter 5.4 was chosen to evaluate the biomaterial's biocompatibility and the healing rate of an abdominal wall defect by itself or in conjugation with the biomaterial. A model where the peritoneum was left intact was chosen since at the moment adhesion formation was not of interest. Additionally, this model was previously used in-house to test other commercially available biological prostheses recommended for hernia repair (data not published), including Permacol®.

6.2 THESIS DISCUSSION

The structure, composition and surface of a biomaterial must be suitably characterized to provide baseline information upon which the performance of an implant material can be related. Initial tests are used to define the general properties of a potential biomaterial and include determination of chemical composition, basic mechanical properties, such as tensile strength, level of porosity, structure and surface properties. The results from this initial characterization should be known and used in the preliminary selection of any biomaterial. A second level of characterization defines the features more closely related to the potential applications of the biomaterial which include cytotoxicity tests, cell-cell and cell-matrix interactions, function-related analysis and biocompatibility tests.

In the research reported in this thesis, several dermal collagen matrices were analysed and compared to each other. These matrices were characterized related to their physical and biochemical features. Tests used to define their properties included: evaluation through mechanical load by the means of a tensiometer; analysis of level of cross-linking by swelling ratios and spectrophotometric methods; microscopical analysis of structure, composition and porosity; and resistance to proteolytic activity. In addition, biological characterisation was performed through several studies designed to evaluate and compare biological responses and *in situ* biocompatibility.

Permacol® surgical implant manufacture is characterised by two main processes: cellular extraction by trypsinization and cross-linking with HMDI. Permacol® physical and biochemical characteristics were compared to those of the original (source) tissue, dermal porcine collagen, and to a process intermediate – acellular but not cross-linked porcine dermal collagen.

Surface and structural analysis of the collagen-based matrices showed distinctive features for each matrix. Porcine dermal collagen originally is composed of compact bundles of collagen fibres in a random orientation, forming an entangled structure. After decellularization the collagen fibres are more distinct following removal of interstitial tissues, therefore it was possible to visualize a well organized collagenous tissue composed of thick fibres. The cross-linked acellular matrix exhibited fibres in a

regular interweaving pattern with fibres showing higher resolution and organization than the noncross-linked acellular matrix. These results correlate with the analysis of pore size, where Permacol® showed the lowest pore size which can be explained by the increase in intra- and intermolecular bonds between the collagen molecules which decreases the size of the natural septae between collagen fibres and consequently decreases pore size.

Stabilization of collagen-based biomaterials either by physical or chemical methods is necessary in order to decrease the susceptibility to enzymatic degradation. Physical cross-linking, although circumventing the introduction of potentially cytotoxic chemical residues, generally does not result in a suitable high degree of cross-linking for tissue-engineering applications (Duan and Sheardown, 2005). Chemical cross-linking is an alternative procedure which is believed to result in a higher cross-linking density. Chemical cross-linking reagents include glutaraldehyde, diisocyanates such as HMDI, acyl azide and EDC. The first three cross-linkers are "bridge-forming", which means that the collagen molecules are linked by an intermediate molecule, while EDC forms "zero-length" bonds, *i.e.*, the collagen molecules are directly connected to one another since no additional chemical entities are introduced between the conjugating molecules (Duan and Sheardown, 2005; Everaerts *et al.*, 2007).
Permacol® surgical implant is cross-linked through a patented process using HMDI as the cross-linking reagent. Treatment of collagen-based biomaterials with HMDI mainly involves the formation of new bonds containing stable urea groups resulting from the reaction of isocyanate groups with amine groups (Olde Damink *et al.*, 1995).
In this thesis, the level of cross-linking of collagen-based matrices was analysed by water absorption properties and by quantifying the free-amino groups present within a collagen matrix, which relates to the number of molecules that are not chemically bound. The amount of free amino groups gives a quantitative analysis of level of cross-linking; on the other hand, by comparing the swelling ratios of cross-linked and noncross-linked materials a qualitative analysis of cross-linking level is obtained. Water uptake properties are important since these are related to exudate absorption; when a biomaterial is implanted in an infected site or/and when a severe inflammatory response is present, the exudate surrounding the implant will be rich in proteolytic

enzymes which may surround and infiltrate the matrix increasing substrate availability for enzyme digestion.

The evaluation of the cross-linking level by both the TNBS and ninhydrin assays, in conjugation with the results obtained from the water uptake analysis suggest that Permacol® surgical implant level of cross-linking is not much higher than that of normal porcine dermal collagen. Therefore, it is hypothesised that the main differences between Permacol® and porcine dermal collagen are a result of the decellularisation process and the amount of intra- and intermolecular bonds established by cross-linking is only slightly greater than the number of bonds existing in normal porcine dermal collagen.

The mechanical test performed corroborated these results. The three types of matrix showed some variation in tensile strength but differences were not significant. Dermal porcine collagen proved to be a resistant matrix and matrices did not fail under the force applied.

Since, to this point, the main differences observed between the collagen matrices tested were structure and collagen fibres orientation, further tests were designed to predict their performance when *in vivo* and to compare biological responses.

Enzymatic stability of the collagen matrices was tested *in vitro*. The efficiency of cross-linking was evaluated by collagenase and elastase digestions (Rault *et al.*, 1996). Furthermore, another cross-linker was used and compared to the reagent used to cross-link Permacol®. Once again Permacol® and dermal porcine collagen showed similar results for collagenase digestion. However, Permacol® was more resistant to pancreatic elastase, showing significantly less tissue digestion at all time points; this can perhaps be explained by the decreased amount of elastin in this type of matrix when compared to normal dermal porcine collagen (significant amounts of elastin were not observed histologicaly in Permacol®, outside of perivascular tissue). EDC-treated dermal collagen showed evidence of increased resistance to both enzymes, a result in accordance with other studies where collagen scaffolds cross-linked with EDC have been shown to exhibit decreased degradation rates (Olde Damink *et al.*, 1996; Zeeman *et al.*, 1999). Contrarily, noncross-linked collagen matrices were the most vulnerable to enzymatic digestion, a result which was expected since the

decellularization process cleaves natural cross-links and leaves collagen fibres more susceptible to proteolytic degradation.

It is important to understand and predict the behaviour of collagen-based biomaterials when in the presence of specific enzymes, not only because post implantation these materials can be infiltrated by inflammatory cells and therefore, be exposed to their enzymes, but also because collagen plays an important role in neo-vascularisation. As one of the ECM components, collagen supports blood vessels, not merely by acting as a scaffold but also by supplying biochemical signals for cell migration (Carmeliet, 2004). During neo-vascularisation extracellular proteinases break down collagen and other ECM components (Bhushan *et al.*, 2002) to allow access to migrating endothelial cells. While some degree of collagen degradation is necessary for neo-vascularisation to occur, uncontrolled ECM degradation can impede cell migration since cells require substrate with which to interact for migration and proliferation. Remodelling and restructuring of ECM is also necessary for cell adherence and deposition of basement membrane, which is important for tissue vascularisation (Han *et al.*, 2001).

Permacol®, acellular noncross-linked collagen and dermal porcine collagen were tested for resistance to human neutrophil elastase and MMP-8. Both enzymes are commonly found during an acute inflammatory reaction and in chronic wound exudate (Aiba-Kojima *et al.*, 2007; Edwards *et al.*, 2005; Hasty *et al.*, 1987; Mallya *et al.*, 1990b; Netzel-Arnett *et al.*, 1991; Nwomeh *et al.*, 1999; Zhu *et al.*, 2001). Only the noncross-linked matrix was digested by human neutrophil elastase, both Permacol® and dermal porcine collagen were unaffected by this enzyme and, although MMP-8 (human neutrophil collagenase) has been reported to cleave collagen type I (Aiba-Kojima *et al.*, 2007; Mallya *et al.*, 1990b; Netzel-Arnett *et al.*, 1991; Nwomeh *et al.*, 1999), the collagen matrices were not digested by this enzyme under the conditions tested. During an inflammatory response and in a chronic wound a wide range of cells are present producing enzymes and other proteins which may induce or inhibit further production of proteolytic enzymes. Therefore, it is possible that the enzymes tested can not easily digest dermal collagen individually but will do so when conjugated with other enzymes, as increased concentrations may be necessary for tissue digestion.

When testing for resistance to proteolytic enzymes, control samples (matrices incubated in buffer only) showed an increase in weight which diminished with longer incubation periods. The salts from the reaction buffer were probably incorporated into the collagen matrices and since these were immediately lyophilised after digestion, salts were not solubilised into an aqueous solution before weight measurements. Since the weight gain was more prominent in the Permacol® samples, the results suggested that Permacol® structure was more likely to retain substances in solution.

The permeability of biomaterials has great influence in their *in situ* performance related to nutrient transport and waste removal within the structure. Permeability of a material is dependent on its porosity: pore size, orientation, distribution and interconnectivity (Aiba-Kojima *et al.*, 2007; O'Brien *et al.*, 2007). These parameters will define how a fluid moves through the biomaterial. Scaffold permeability has also been shown to affect scaffold biodegradation rate (Agrawal *et al.*, 2000) and some authors believe that flow may have an important role in determining whether neovessels regress or persist (Carmeliet, 2003). Therefore, the fluid dynamics of a biomaterial will also affect the *in vivo* performance.

Permacol® and noncross-linked dermal collagen were tested for resistance to flow in a modified Ussing chamber. A calcium solution was used at 37^{o}C and the flow was kept constant for periods of 3 and 6 hours. There were no differences between matrices, suggesting that the cross-linking process does not promote resistance to fluid flow. Additionally, over the duration of these studies, samples did not show any evidence of calcium deposits within the collagen fibres. To further compare these two matrices, related to interstitial fluid flow patterns, a rodent model was designed where each matrix was subcutaneously implanted and an Evans blue dye solution injected intradermaly. This dye binds strongly with albumin and, as a result, the interstitial fluid can be macroscopically observed. Once again there was no difference between the collagenous matrices; both matrices were infiltrated by interstitial fluid and subsequent quantification of the Evans blue-albumin complex (EBA) within implants showed no significant difference between the amounts of EBA absorbed.

Although these experiments were short-term, results gave no evidence of differences between the permeability of the cross-linked and noncross-linked matrices tested.

The biophysical and mechanical properties of scaffolds influence the interactions between cells and the surrounding ECM and therefore those properties will influence and regulate cell migration. Furthermore, cell migration is also known to be mediated by biochemical stimuli and cellular interactions (Harley *et al.*, 2008) and these will be influenced by matrix surface signals and surface contact guidance.

The biological features of collagen-derived biomaterials were analysed by *in vitro* tests where cell-matrix interactions are evaluated. *In vitro* techniques involve compromises and deviations from *in vivo* conditions; for example the absence of a diffusion system affects metabolic rates *in vitro*, which are lower than observed *in vivo*. As discussed previously, the topography and nature of a substrate will influence the morphology and function of cells, lack of these environment factors may cause inactivation or dedifferentiation of cells. A further pertinent factor is the presence of other cell types *in vivo*; this interaction between cells may affect cell shape and function.

Despite the limitations of *in vitro* models, these also offer several advantages. From a practical, cost-effective and ethical point of view, *in vitro* models decrease the need for *in vivo* studies. The latter not only may arouse ethical concerns but also need specific facilities and working conditions with specialised staff and equipment. All these increase the cost of these analyses and can be time consuming. An appropriate and well-planned *in vitro* study can provide useful data regarding the material to be tested and predict *in situ* behaviour.

In these studies, primary cultures of porcine dermal fibroblasts were prepared and cultured in the presence of different porcine dermal collagen matrices in the form of sheets. This experiment was designed to provide data on cell-matrix interactions, including cell adhesion, proliferation and infiltration and, to compare the biological features of the different types of collagen matrices. Permacol® surgical implant, acellular noncross-linked collagen and porcine dermal collagen were incubated with porcine fibroblasts and with skin explants.

Porcine fibroblasts and porcine skin (explant) were chosen since the collagen tested also had a porcine origin. Furthermore, there are reports giving evidence of lack of cellular penetration into Permacol® *in vivo* both in rats (Boon *et al.*, 1995; Zheng *et*

al., 2004) and humans (Hammond *et al.*, 2008) and it was thought that this feature could be species-specific, consequently allogeneic cells were used.

Cell migration and proliferation have a critical role in several physiological and pathological processes as well as in the successful performance of scaffold-based tissue engineered biomaterials. If a biomaterial does not provide recognisable surface signals, cells will not adhere to the matrix which may impair further integration with the host tissue. Active cell motility is essential in physiological tissue development and homeostasis, being indispensable for appropriate wound healing. Fibroblast adherence, proliferation and migration were evaluated when using different collagen-derived matrices under 3 regimes: out of the package matrix (non-soaked), matrix soaked overnight in PBS and matrix soaked overnight in fibroblast medium.

When non-soaked matrices were incubated with fibroblasts, cells showed no preference for a particular type of matrix; all matrices performed similarly allowing cellular adherence and proliferation but cellular penetration was only observed focally into Permacol® and dermal porcine collagen. This was an interesting result, since the analysis of structure and measurement of pore size characterized acellular noncross-linked matrices as having the wider pores and the lack of interstitial tissues between collagen fibres suggested that this matrix would promote cell migration. Since this was not observed, it is likely that the cell extraction process changes the 3-D structure of the collagen matrix, affecting cell-matrix interactions. Cell adhesion and cell infiltration into matrices do not only depend on receptor-mediated biochemical signalling, the 3-D structure of the biomaterial is of major importance in cell function. Many authors defend the concept that cell-matrix interaction can control cellular phenotype, cell growth and behaviour (Friedl and Bröcker, 2004). The decellularization process does not seem to affect surface biochemical signalling, since NonXL matrices supported cell adherence, but the enzymatic process changes the matrix architecture which may result in a structure that alters cell movement.

When matrices were pre-treated with fibroblast medium, prior to fibroblast incubation, cells were observed forming a monolayer at the surface of the matrices. In this experiment cellular migration was observed only in the dermal porcine collagen matrix (Raw). For cells to migrate through a 3-D structure they have to overcome biophysical matrix resistance. Cells may overcome biophysical resistance through

shape change, contact-dependent matrix remodelling and cell-independent proteolysis by secreted proteases. During migration cells adapt morphologically to the ECM environment, finding and using the least resistant pathway most suitable for migration. That can be accomplished by proteolysis of ECM components by serine proteases, such as elastase, and MMPs, after which, through adhesion and de-adhesion occurrences, cells move within matrices.

In the *in vitro* tests, cell infiltration and migration were only observed in the cross-linked matrices (Permacol® and Raw collagen). This suggests that although the decellularization process changes the 3-D structure of the material, by cross-linking it with HMDI the collagen returns to the original structure or to a similar configuration.

The fact that fibroblasts did not easily migrate into the collagen matrices implies that the cells could not overcome the biophysical resistance. It is important to keep in mind that *in vitro* conditions are constant and controlled, while in an *in vivo* situation there are many factors influencing one outcome. Under the conditions tested fibroblasts may not produce the enzymes necessary or in enough concentrations to easily infiltrate the matrices. It is possible that for cell penetration to occur fibroblasts would have to be induced to synthesise the required enzymes.

Alternatively, cells can migrate through a biomaterial without structural matrix remodelling by overcoming the biophysical resistance through morphological adaptation. When pores and fissures within a matrix are wide enough, or if the substrate is flexible (elastic) enough, in relation to the size of a given cell body, cell-shape change may be adequate to overcome matrix physical barriers and allow migration (Friedl and Bröcker, 2004). Although Permacol® pore size was not significantly different from the original porcine dermal collagen, pores within these matrices may not be wide enough to allow cell migration without ECM enzymatic remodelling.

These results are in accordance to other studies reported, where Permacol® surgical implant was cultured with human fibroblasts (Jarman-Smith *et al.*, 2004), smooth muscle cells (Kimuli *et al.*, 2004), normal human urothelial cells (Kimuli *et al.*, 2004) and human peritoneal mesothelial cells (Wilshaw *et al.*, 2008). All those studies reported that Permacol® supports cell attachment and proliferation but cellular penetration was not easily observed.

It is still unclear what happen to the cells when matrices were pre-soaked in PBS. Cells were not attached to the matrices surface or to the plastic surface of the well plate; in addition, cells were not found, in significant quantities, in suspension throughout the experiment. The experiment was repeated 3 times; therefore, technical error has been eliminated as the cause of such an intriguing result.

When testing matrices for skin explant outgrowth, non-soaked matrices showed low efficiency and Permacol® was the only material that supported cell outgrowth under those conditions. However, when matrices were pre-treated with fibroblast medium fibroblasts were visible forming a monolayer at the surface of all matrix types tested, although cellular penetration was not observed.

Overall, the results obtained from culturing porcine fibroblasts with Permacol®, NonXL and Raw collagen give further evidence that the chemical treatments performed during the manufacture of Permacol® surgical implant do not impair or decrease cell attachment and proliferation since results were similar for all matrices tested. Nevertheless, fibroblasts did not easily penetrate the collagen-based biomaterial disproving the hypothesis stated earlier where it was suggested that the lack of cellular penetration was caused by species-specific factors. However, *in vitro* tests are limited and it was necessary to further evaluate cell-matrix interactions in an *in vivo* setting.

All implanted biomaterials are treated by the host tissues and cells as foreign bodies, independent of the biomaterial type of matrix and treatments performed. However, the severity of the reaction varies with the biocompatibility of the material; this may result in a marginal acute inflammatory reaction in the early stages of implantation, which may subsequently subside, or in severe acute and chronic inflammatory responses leading to rejection of the implanted material.
The use of porcine derived biomaterials, rather than bovine or human, avoids concerns regarding excessive immunoreactivity or prion transmission. Porcine dermal collagen shares approximately 97% similarity with human tissue (Skipworth *et al.*, 2007). Nevertheless, some reactivity is to be expected and the host reaction may

increase or decrease depending on the treatments used during the manufacturer of the biomaterial.

Permacol® surgical implant is commercialized for soft tissue repair, it has not only been used as repair tissue (Abhinav *et al.*, 2008; Catena *et al.*, 2007; Gaertner *et al.*, 2007; Inan *et al.*, 2007; Liyanage *et al.*, 2006; Parker *et al.*, 2006; Pentlow *et al.*, 2008; Richards *et al.*, 2005; Saettele *et al.*, 2007; Sarmah and Holl-Allen, 1984; Shabbir *et al.*, 2005) but also as bulking material (Saray, 2003) and for soft tissue augmentation (Benito-Ruiz *et al.*, 2006). Although there are many published papers reporting the use of Permacol® in the clinical field, the number of research papers characterizing and evaluating Permacol® performance is much lower.

As a biomaterial Permacol® needs to be efficient and functional. To successfully achieve such aims Permacol® requires certain characteristics commonly considered to be essential features of an ideal biomaterial. These characteristics include non-toxicity, biocompatibility, adequate defect correction, constant volume until host tissue regeneration, decreased scarring and good aesthetic results.

A study was designed where Permacol® biocompatibility, migration, remodelling and volume were evaluated, at short-, mid- and long-term, and compared to acellular noncross-linked porcine dermal collagen (NonXL). Permacol® and NonXL collagen were implanted subcutaneously into abdominal pockets in rats and, as each animal received both implants results were paired and directly comparable.

Throughout the study NonXL implants showed higher mean values of cellular penetration than Permacol®. This difference was statistically significant at 3 and 6 months but at 12 months post implantation there was no difference between the mean groups of both matrices. These results give further evidence of the limits of *in vitro* tests since, when cultured with fibroblasts, Permacol® showed focal cellular penetration but the same was not observed in the NonXL samples. *In vivo*, despite the low number of cells present within the matrix, cellular penetration increased over time in the Permacol® implants including when cellular density decreased from 3 to 6 months in this matrix.

Similarly to what was observed with cellular penetration, cellular density was also higher in the NonXL implants until 6 months post implantation. NonXL implants showed higher numbers of cells in the central portions of the matrix, within the

natural clefts between the denser collagen fibres and, as observed with Permacol®, this parameter decreased from 3 months to 6 months. At long-term, these two matrices performed differently, as cellular density increased significantly at 12 months for Permacol® whilst the NonXL implants showed a lower value for cellular density at this time point.

There are several factors that may cause or influence decreased cellular density: i) cross-linking of the matrix proteins, which may elicit a physical barrier by diminishing pore size so that cells are incapable of travelling freely though the matrix; ii) degradation of matrix over time and subsequent release of cross-linking sub-products, which may have toxic properties; iii) the cross-linking method may leave cell-detrimental residues within the matrix; iv) after cross-linking, matrices become more resistant to enzymatic digestion and some protein digestion may be necessary for cellular penetration to occur naturally; v) cells do not recognize the collagen-based biomaterials as ECM. Some authors have suggested that HMDI-treated porcine dermis did not allow tissue ingrowth (Gandhi *et al.*, 2005). This study suggests that tissue ingrowth into Permacol® is possible but limited, especially at the early stages. With time cellular density increased to minimal levels and cellular penetration was over 75%. At all time points, degradation of collagen was not observed; hence, it is improbable that detrimental products are formed due to matrix degradation. Furthermore, when fibroblasts were cultured for 28 days in the presence of Permacol®, if toxic residues from the cross-linking process had been present within the matrix these would have been solubilised into the medium causing cell toxicity, which would have been recorded during the performance of viability tests. Lastly, if cellular migration was impaired by the HMDI-treatment, high levels of cellular density and cellular penetration in the NonXL implants would be expected and this was not observed. The cellular response observed in this study suggests that the cross-linking process is not the cause for low cell ingrowth into Permacol®. However, both matrices tested underwent the same enzymatic decellularisation process. Trypsin has been characterized as a serine protease that predominantly cleaves peptide chains at the carboxyl side of the amino acids lysine and arginine, except when either is followed by proline. Consequently, this enzyme is known for not being able to digest collagen (Olsen *et al.*, 2004). However, more recent studies using mass spectroscopy have reported trypsin cleavage before proline; although not being a favoured pathway

it still happens (Rodriguez *et al.*, 2008). Canavan and co-workers reported that trypsinisation of cells is concurrent with damage to the extracellular matrix underlying the cells (Canavan *et al.*, 2005). Since the ECM is known to be vital to the adhesion, proliferation and differentiation of cells (Gospodarowicz *et al.*, 1978), this has important implications for the *in vivo* performance of biomaterials treated with trypsin. If the decellularisation process is changing the collagen structure and signalling, the surfaces of the matrices may change not only structurally but also chemically. The acellular collagen matrices may not then provide suitable signals for cell migration, which can affect the *in vivo* performance of a biomaterial by reducing the initial level of cellular density and consequentely affecting integration with the surrounding tissue and vascularisation of the implant.

A further explanation for the lack of cellular density in the implants may be that, after wound healing, fibroblasts are eliminated by apoptosis, resulting in a decrease in tissue cellularity (Kuhn and McDonald, 1991; Kuhn *et al.*, 1989; Nho *et al.*, 2006). If the presence of the implants and the surgery performed caused tissue injury a wound healing process may have been induced and, therefore, the earlier proliferative phase subsides with time and cell presence decreases.

When analysing all parameters measured it was observed that cellular density and neo-vascularisation followed the same trends over time. Vessels were observed in the central portions of the matrices, within the natural clefts between the denser collagen fibres, at mid- and long-term.

Although vessel presence increased in the Permacol® implants, it decreased over time in the NonXL implants. Vessel regression and devascularisation are processes which are still not completely understood, some studies have reported that vascular regression is a regulated process with endothelial cells undergoing apoptosis (Desmouliere *et al.*, 1995; Greenhalgh, 1998). Others were unable to show the presence of apoptotic endothelial cells during the devascularisation phase in bovine ovaries (Augustin *et al.*, 1995). These results are consistent with the results reported herein where apoptotic cells were not observed at the time points analysed. Thus there appears to be conflicting evidence regarding the mechanisms of vascular remodelling and so far it is not known if this mechanism is species-specific.

Some authors support the notion that breakdown products resulting from ECM degradation can act as angiogenic factors (Arnold and West, 1991). In this case, cross-linked matrices with increased resistance to proteolytic digestion would be less vascularised, which was not observed.

Integration with the surrounding tissue was higher at all time points in the Permacol® implants and increased over time. Similarly, the implant-host tissue interface showed increased tensile strength over time for the cross-linked implants. NonXL samples showed lower deposition of collagen in the implant-host tissue interface and therefore, integration was lower.

At 3 months post implantation there was no evidence of acute inflammation, but macrophages were present in both matrix types which may be related to a late chronic inflammatory response. By 6 months this subsided although giant cells were observed at low numbers in the Permacol® implants only. Cellular extraction removes immunogenic proteins but may also expose ECM proteins that were previously masked; therefore, higher levels of immune response were expected in NonXL samples. Additionally, during the *in vitro* experiments, NonXL collagen showed less resistance to enzymatic digestion which makes it more susceptible to enzymatic remodelling. Although inflammatory cells were present in low numbers in the NonXL implants, collagen remodelling was not observed; in addition, fibroblast ingrowth was observed throughout the study at minimal levels of density and these cells produce MMP-1 (fibroblast collagenase) which mediates ECM degradation and remodelling during wound healing (Abraham *et al.*, 2007). Both matrices tested seemed resistant to *in vivo* remodelling during a 12 month period.
Although collagen remodelling was not observed, one NonXL implant showed some level of degradation and the decrease in implant thickness at 12 months, in conjunction with the changes observed in the shape of the implant borders, suggest that the NonXL implants are being slowly absorbed.

Focal points of mineralisation were present in 4 of 6 Permacol® implants and in 1 of 5 Permacol® implants at 6 and 12 months post implantation, respectively. The minerals were identified as being hydroxyapatite by histological techniques and SEM analysis.

Hydroxyapatite crystals, which contain calcium and inorganic phosphate ions, are deposited both within and between collagen fibrils in bone (Murshed *et al.*, 2005). Extracellular mineralisation occurs naturally and exclusively in bone, teeth and in growth plate cartilage (Murshed *et al.*, 2005); if present in other body sites it is considered ectopic (*i.e.*, a pathological process). Permacol® calcification has been reported before by Kelley and colleagues during a 12 months study in mice (Kelley *et al.*, 2005) and was also previously observed in other in-house studies (data not published). The results reported from those studies are in agreement with the results obtained in this thesis; there was no evidence of a cellular host response directed towards the mineralised tissue. While such calcification is not toxic to the animal, if there is associated loss of flexibility in the implant this would be a disadvantage and would reduce its value as a replacement or repair tissue implant.

It is not clear why calcification occurred only in the cross-linked implants, the fact that the NonXL matrices were mineral-free suggests that mineral deposition is related to cross-linking. Murshed and colleagues showed that removal of pyrophosphate (an inhibitor of inorganic phosphate) and the presence of fibrillar collagen-rich scaffold were necessary and sufficient conditions to induce ectopic ECM mineralisation (Murshed *et al.*, 2005). Furthermore, collagen has been implicated as a nucleator of apatite in vascular prostheses (Kim *et al.*, 1999). Two different collagen-based scaffolds were tested in this study but for a depletion of pyrophosphate to occur the implantation would have to induce cellular responses.

Calcification may be associated with several conditions: 1) HMDI-treatment; 2) organic matrix composition; 3) mechanical stress and 4) cell injury. Condition number 1 includes direct and indirect effects; the first refers to toxicity products resulting from the bifunctional reagent, while the latter is associated with the structural changes resulting from cross-linking the collagen matrix. HMDI has been studied extensively as a cross-linking reagent and the literature defends HMDI as not promoting calcification (Vasudev *et al.*, 2000). The structural changes may influence mineral deposition since, as has previously been shown, the collagen matrices show a tendency to retain salts from the surrounding medium. Conditions numbers 2 and 3 are both related to implantation site; depending on the surrounding tissue, different proteins may be deposited within the biomaterial and the implantation site also affects the mechanical load upon the implant. The fourth condition considers cell injury as a

probable cause of implant calcification. Cell injury results in an influx of Ca^{2+} into the cell and in an increase of cytosolic phosphate (Pi) (Kim *et al.*, 1999); concomittant increases in intracellular Ca^{2+} and Pi have been associated with calcification.

Given that the lack of cell migration into Permacol® implants does not seem caused by the cross-linking process, a second *in vivo* study was designed to evaluate the influence of implantation site in cellular response and in matrix calcification. In the model Permacol® implants were implanted either intramuscularly or into pockets made in the liver. In both sites implants were readily exposed to the immune system because of the highly vascularised nature of the muscle and liver tissues.

Host reactions following implantation of biomaterials can include tissue injury, blood–material interactions, provisional matrix formation, acute inflammation, chronic inflammation, granulation tissue development and foreign body reaction (Anderson, 2001). The first termination point of this study was 3 months post implantation, at this time there was no evidence of an inflammatory response, a few macrophages and Kupffer cells were present at the edges of the implants in the muscle and liver, respectively, but at low numbers. The number of macrophages in the intramuscular implants diminished with time, Kupffer cell numbers increased at 6 months in the liver implants but by 12 months there was no evidence of inflammatory cells in the implants.

As observed previously, when Permacol® was implanted subcutaneously, integration with the host surrounding tissue reached minimal to moderate levels both in the liver and muscle and integration increased with time. However, even though host tissue accepted and integrated with the implants, these were not remodelled and maintained the same structure and appearance throughout the study. In addition, collagen was not degraded and highly birefringent fibres were observed at all time points.

Again, Permacol® was infiltrated by higher numbers of cells at 3 months post implantation after which cellular density decreased at 6 months but increased once more at 12 months post implantation. Therefore, independent of the implantation site, cells seem to have a temporal behaviour pattern, in the earlier stages of implantation Permacol® implants are infiltrated by cells which disappear at mid-term, but cell numbers increase again long-term. The high density of cells earlier on is followed by

a period of cell absence and this is in keeping with a natural wound healing process (Braddock *et al.*, 1999; Broughton *et al.*, 2006; Laurens *et al.*, 2006).

Cellular density and cellular penetration were always at low levels in the implants placed inside the liver; as a result matrix neo-vascularisation was only observed after 6 months implantation and was limited to the edges. These results are not surprising since liver is a highly specialized tissue with a low percentage of collagen that is mostly restricted to the portal tracts and Glisson's capsule (Chapman and Eagles, 2007). Therefore the specialized cells present within the liver probably do not recognize collagen as a suitable extracellular matrix.

Neo-vascularisation was observed at all time points in the intramuscular implants. Initially vessels were observed mainly at the edges but at 6 months post implantation the vessel numbers increased and vessels were observed both at the edges and centre. Contrary to what was observed subcutaneously, herein there was a decrease in neo-vascularisation at long-term. It is not know if this factor is related to the amount of mineralisation observed in the intramuscular implants at 12 months post implantation. Permacol® calcification was again observed but this time it started as early as 3 months post implantation. Two out of 6 implants showed focal points of mineralisation after 3 months (average area mineralised = 35%/implant), 4 of 6 implants were calcified at 6 months (average area mineralised = 25%/implant) and all 4 implants recovered at 12 months were mineralised (average area mineralised = 54%/implant). Mineralisation was not observed in the implants placed in the liver; moreover, the temporal difference (first occurrence of mineral deposition) observed between the Permacol® implanted subcutaneously and intramuscularly suggests that the location of the implant influences the implant performance. The site of implantation has been previously reported to influence the implant-host interactions and implant outcome (Wlodarski *et al.*, 1973). These results give further evidence that the implantation site influences implant-host interactions in particular deposition of minerals within the implant matrix.

Permacol® was found at the surface of the liver lobe where it had been inserted. Mammals retain a constant liver-body volume ratio and when injury occurs the liver is capable of generating a proliferative response which will heal the tissue by mitosis and DNA synthesis (Khan and Mudan, 2007). The migration of the implants towards

the surface of the lobe may be explained by cell proliferation, in which the tissue regeneration may have pushed the implant through the pocket towards the surface. Implants were still partially inserted in the hepatic tissue and were surrounded by Glisson's capsule material.

During implantation of a biomaterial, disruption of the normal vascular supply to surrounding tissues occurs. This results in reduction in the supply of oxygen and nutrients to post-surgical sites as well as accumulation of metabolic products (Diamond *et al.*, 2005). Ultimately adhesions develop post-surgery, therefore it is crucial to use a biomaterial that will not induce adhesions and if possible will decrease the rate of adhesion formation. Omental adhesions were observed in the Glisson's capsule material covering the implants but, since the adhesions were not directly in contact with the implant, it is probable that they are a result of the surgical procedure and not of the biomaterial itself.

Implants were not degraded, broken down or remodelled when implanted either intramuscularly or in the liver, suggesting that the implant was accepted as benign material and did not promote an inflammatory response or rejection; additionally, encapsulation of the implants was not observed.

Overall, the implantation site does seem to influence the level and temporal occurrence of mineral deposition into Permacol® surgical implants. Cellular response was different depending on the implantation site: when implanted subcutaneously and intramuscularly Permacol® cellular density was significantly higher than when implanted into the liver; the levels of cellular penetration were higher subcutaneously, followed by the intramuscular implants and the liver promoted the lowest percentage of cellular infiltration. Neo-vascularisation varied in the 3 implantation sites and intramuscular implantation provided the highest numbers of new vessels, while implantation into liver yielded low levels of neo-vascularisation. In common, the implantation sites showed the same levels and pattern of integration with the surrounding tissue, implant integration increased over time varying from minimal to moderate levels independent of the implantation position.

Subsequent to studying Permacol® surgical implant biocompatibility and performance *in situ,* further *in vitro* and *in vivo* tests were designed to test for function efficiency and possible clinical applications.

Over time an increasing number of microorganisms, many of which are putative human pathogens, have been reported to produce enzymes that can degrade collagen and therefore extracellular matrix (Bergin and Wraight, 2007; Brook and Frazier, 1998; Daeschlein *et al.*, 2007; Davies *et al.*, 2007; Edwards and Harding, 2004; Hill *et al.*, 2003; Kingsley, 2003; Sapico *et al.*, 1980; Valencia *et al.*, 2004). The precise contribution of bacterial proteases to the damage of tissue in non-healing wounds is not known. Inflammatory cells present at the wound, which are elicited as an immune response to the bacterial infection or to the tissue damage, can also produce collagenases capable of degrading the ECM (Edwards *et al.*, 2005; Hasty *et al.*, 1987; Nwomeh *et al.*, 1999; Sun *et al.*, 2000). Consequently, it is the conjunction of these two factors (bacteria and leukocytes) that most likely contributes to impaired healing.
If a biomaterial, clinically used in a contaminated field, offers no resistance to bacterial degradation and, in addition, acts as a substrate for bacterial proliferation, the increased production of digestive enzymes may result in further necrosis of host tissue allowing the bacteria to gain access to deeper tissues thus deteriorating the healing rate. The ability of Permacol® surgical implant to resist or tolerate infection was assessed in vitro by culturing it with pathogens commonly found in chronic wounds (*Staph. aureus, E. coli, Pseudomonas aeruginosa* and *Candida albicans*), individually and in a poly-microbial culture.
Under the conditions tested, Permacol® surgical implant did not show evidence of a bactericidal or bacteriostatic effect. In addition, the bacteria and yeast tested were not able to easily infiltrate the matrix independent of bacterial load and the collagenous matrix was not degraded or remodelled by the microorganisms. It is probable that when cultured *in vitro* the microorganisms tested do not produce the required enzymes to degrade Permacol®, or the required enzymes are produced but not in enough quantity to effect matrix degradation; another explanation is that the particular strains tested may not produce collagenolytic enzymes or simply, Permacol® is resistant to degradation by these microorganisms under the conditions tested.

The fact that Permacol® offered some resistance to bacterial infiltration, allowing the test microorganisms to proliferate only on the surface, suggests that dermal porcine collagen-based biomaterials may be a good option as a soft tissue repair material in contaminated fields. Additionally, since bacteria do not easily infiltrate Permacol® the latter can be used as a protective barrier between the wound bed and external contaminants.

The use of a wound dressing that does not promote bacterial proliferation is not sufficient in all cases. Antimicrobial agents are also needed and dressings that will restore infection to acceptable levels are required. Silver-coated materials are commonly used dressings (in for example burns) and these are available in a variety of forms and have different delivery systems (Klasen, 2000a). In the 1960s Moyer introduced the use of 0.5% silver nitrate for the treatment of burns (Moyer *et al.*, 1965). He reported that such solution does not interfere with epidermal proliferation and has an antibacterial effect against *Staph. aureus, Pseudomonas aeruginosa* and *E. coli* (Bellinger and Conway, 1970; Moyer *et al.*, 1965). His discovery directed further research and silver combined with other substances originated many compounds used as anti-microbials (Rai *et al.,* 2008). Because of the growing microbial resistance against metal ions and antibiotics and the development of resistant strains, silver dressings are of current interest (Gong *et al.*, 2007). Silver ions have been delivered through many forms; currently, nanocrystalline silver particles are most promising since nanoparticles show good antibacterial properties due to their large surface area to volume ratio (Durán *et al.*, 2007).

Permacol® apparent resistance to pathogen degradation was promising, showing Permacol® as a prospective biomaterial to be used in contaminated clinical fields. Therefore, nanocrystalline silver-coated Permacol® biocompatibility was tested in a rat model to assess *in vivo* characteristics and performance of silver-coated Permacol®.

Although a coating of silver particles was observed histologically covering the surface of the Permacol® prior to implantation, after 2 weeks the silver particles were mostly absent and those remaining were being ingested by macrophages suggesting that the nanocrystalline silver particles induced a cellular response. Although silver nanoparticles in most reported studies are suggested to be non-toxic, Hussain and

colleagues studied the toxicity of different sizes of silver nanoparticles on a rat liver cell line and found that, after being exposed for 24 hours, mitochondrial cells displayed abnormal size, cellular shrinkage and irregular shape (Hussain *et al.*, 2005). When Burd and co-workers tested five commercially available silver-dressings for cytotoxicity effects in keratinocytes and fibroblast cultures, they found that three of the silver dressings showed cytotoxicity. Furthermore, when they tested the same dressings in a full-thickness excision skin murine model the dressings were associated with delayed reepithelialisation (Burd *et al.*, 2007).

Despite the initial cellular reaction, the inflammatory response subsided and at 4 weeks post implantation the silver particles present at the edges of the implants, although in low number, were not being phagocytised. Furthermore, integration with the surrounding tissue increased with time and the *in vivo* performance of Permacol® did not seem to be affected when coated with nanocrystalline silver, independent of the concentration used. The above results suggest that silver particles show some cytotoxicity initially and as a consequence were mostly removed by the host cells; however, with time the toxicity levels decrease or cells and tissue adjust to the presence of silver. In the presence of an infection it is not clear if the inflammatory cells will target the silver particles or the pathogens. If silver is removed before exerting its anti-microbial effect such a dressing would be ineffective in that particular situation but if the host cellular response focuses on the microorganisms, the nanoparticles will attach to the pathogen cell membrane attacking the respiratory chain and cell division processes leading to cell death (Feng *et al.*, 2000) and assisting wound healing by decreasing the bacterial load.

Nanoparticles of silver are currently of interest as they have defined chemical, optical and mechanical properties (Rai *et al.*, 2008) and show good antibacterial properties. Regardless of their advantageous properties, the delivery system used is of extreme importance. Silver has to be delivered efficiently which includes appropriate concentration and treatment length. In the study reported here within 2 weeks post implantation the nanoparticles were reduced to a tenth of the original concentration. Clearly, if silver coating is to be maintained for prolonged periods of time the coating process must be revised.

The use of silver-coated Permacol® in biomedical and therapeutic applications may be a suitable choice to assist healing in complicated wounds particularly if the tissues are

infected. However, further detailed studies need to be carried out – it would be especially useful to assess silver-coated Permacol® performance in an *in vivo* model of a chronic wound or in an infected area.

One clinical setting many times associated with infection is abdominal wall defects, particularly hernias. Abdominal wall hernias are a common condition treated by surgeons but recurrences and complications remain a difficult problem (Burger *et al.*, 2004; Matthews *et al.*, 2003; Vrijland *et al.*, 2002). Abdominal wall defects and hernias can be repaired by primary closure, though when the defect is large, as with pre-existing loss of abdominal wall layers or in paediatric patients, adequate tissue for direct closure is often not available (Chang *et al.*, 2007; Hirsch, 2004; Kolker *et al.*, 2005). In these situations, primary closure generally leads to excessive tension at the suture site resulting in hernia recurrence (Saettele *et al.*, 2007). Closure procedures for large defects include the use of implantable biomaterials such as collagen-based materials, the use of such materials aims to reduce tension and therefore recurrence. In addition, biological materials reduce the occurrence of postsurgical intra-abdominal adhesions which are a major complication associated with abdominal surgery and can be aggravated if synthetic prostheses are used (Wilshaw *et al.*, 2008).

The efficiency and performance of Permacol® surgical implant as repair tissue was compared to two commercially available biomaterials, in a rodent model of abdominal wall hernia repair. The chosen biomaterials were CollaMend and AlloDerm, the first is a porcine-derived collagen based cross-linked biomaterial and the latter a noncross-linked human-derived dermal collagen. Both materials are commercialised as acellular and recommended for abdominal hernia repair by the manufacturers.

The severe acute and chronic inflammatory reactions and immune response observed with AlloDerm, and the presence of hair in one of the implants, suggest that the decellularisation process is not completely effective. Although the analysis of pre-implanted AlloDerm showed no evidence of cells in this study, Wilshaw and colleagues tested mesothelial cell adhesion, *in vitro*, to AlloDerm and reported evidence of cellular remnants on the surface of the material (Wilshaw *et al.*, 2008).

The occasional presence of cellular residues within AlloDerm matrix may be a batch problem, maybe the cell extraction process is not completely efficient or it may not be always reproducible. Either way, this results in a reduction of the biocompatibility of

the biomaterial which may explain partially the contradictory data published related to AlloDerm. While some authors have reported the use of AlloDerm for hernia repair as successful (Buinewicz and Rosen, 2004) others encountered a range of mesh-related complications including recurrence of hernias (Alaedeen *et al.*, 2007; Espinosa-de-los-Monteros *et al.*, 2007; Gupta *et al.*, 2006; Patton *et al.*, 2007; Schuster *et al.*, 2006), wound infection (Bellows *et al.*, 2007; Espinosa-de-los-Monteros *et al.*, 2007; Patton *et al.*, 2007), biomaterial removal (Patton *et al.*, 2007), seroma (Butler *et al.*, 2005; Gupta *et al.*, 2006; Patton *et al.*, 2007), fistulas (Butler *et al.*, 2005; Patton *et al.*, 2007), wound dehiscence (Bellows *et al.*, 2007; Butler *et al.*, 2005) and diastasis or bulging of muscle (Gupta *et al.*, 2006).

During tensile strength assessment of the AlloDerm-host complex AlloDerm stretched at all times which may be explained by the levels of elastin in human skin. This feature is of importance and surgeons should be aware of such a phenomenon when choosing the most suitable biomaterial for hernia repair. In a clinical setting where high tension is expected AlloDerm may not be the ideal biomaterial since it will easily stretch influencing the healing rate and may lead to hernia recurrence. This characteristic of the AlloDerm *in situ* has been reported by others (Gaertner *et al.*, 2007; Gupta *et al.*, 2006).

As observed in the Permacol® implants, cellular density also decreased at 6 months post implantation suggesting that the decrease of cell numbers from 3 to 6 months is not caused by the type of matrix but it may be part of implant integration and wound healing processes.

AlloDerm was remodelled by inflammatory cells present during the inflammatory response and besides losing the original structure, the volume of AlloDerm present decreased with time. Degradation of collagen was observed in all implants at 1 month post implantation; this was likely due to the proteolytic activity of enzymes synthesized by inflammatory cells since degradation was higher when a severe inflammation was observed. The levels of inflammation decreased at 3 months post implantation related to which collagen degradation also decreased; nevertheless the volume of implant present was lower which is probably a consequence of the earlier higher levels of inflammation. At 6 months post implantation 2 of the 6 implants were completely absent and new thin collagen fibres were visible in the implantation site. By picro-sirius red staining and polarised light optics, newly deposited collagen

matrix was evident. The birefringent pattern was green, which is usually indicative of fine, immature, minimally organised collagen fibres (Cuttle *et al.*, 2005; Junqueira *et al.*, 1982; Junqueira *et al.*, 1979).

These results suggest that AlloDerm can be degraded by the host cells as early as 1 month post implantation and with time the matrix is completely replaced by neocollagen. The rate of collagen turnover will depend on the rate of healing which is directly associated with the host response towards the implant. Such features will influence greatly the success of the hernia repair since, if the deposition of new collagen and maturation of fibres does not occur concurrently to matrix degradation, the new tissue may be too weak and liable to hernia recurrence.

The use of CollaMend for hernia repair in the model study herein gave unsatisfactory results. CollaMend's stiffness caused great problems throughout the study resulting in the early sacrifice of several animals due to extrusion of the implants. Furthermore, during surgery CollaMend was difficult to handle. Although CollaMend and Permacol® are derived from porcine dermal collagen, CollaMend's structure suggests that the collagen is harvested from the dermal papilla, while Permacol® originates from the reticular dermis. In addition, Permacol® is cross-linked by HMDI-treatment and CollaMend by EDC-treatment. Even though both biomaterials share the same tissue source there are important differences in the manufacturers process which results in different characteristics and different *in vivo* performances. The rigidity observed in CollaMend may result from the manufacturers' processes or from the original tissue itself. Papillary dermis is intradigitated with thin elastic fibres whereas reticular dermis has thick elastic fibres; as a result the deeper layer of dermis (reticular) is more elastic and less rigid than the dermis papilla (Montagna and Parakka, 1974).

While AlloDerm and Permacol® integration with the surrounding tissue increased with time, CollaMend did not easily integrate with host tissues, particularly the implant side facing the abdominal defect. This result questions CollaMend's efficiency in such a clinical setting since integration is essential for tissue regeneration and repair of the hernia. Additional to the lack of integration, round-shaped fibroblast-like cells were present at 1 month post implantation which suggests that CollaMend's surface may not provide adequate signalling for cell-matrix interactions. Cells were not present at high densities but even when at low density they easily infiltrated the

matrix, it is possible that the high levels of cellular penetration are a result of the high level of matrix porosity. This may explain the difference between the levels of cellular density and cellular penetration between this matrix and Permacol®. It might be useful to increase Permacol®'s percentage of porosity or pore size and assess cellular ingrowth and vascularisation. MacLeod and colleagues used CO_2 laser to increase Permacol® porosity and reported that more cells were observed through the new pores but the residual areas remained relatively cell free (MacLeod *et al.*, 2004c).

The inflammatory responses observed were different for the 3 biomaterials analysed. While AlloDerm induced severe inflammatory reactions which subsided with time, Permacol® was associated with a marginal acute and chronic inflammatory response at 1 month post implantation that was resolved at 3 months and CollaMend did not show evidence of inflammatory reactions except when animals had open wounds. In such cases, severe suppurative acute inflammation was observed and bacteria were present, in this situation the superficial layers of CollaMend in contact with bacteria were remodelled and this questions its durability when used in a contaminated field. The host response to an implant depends on the biocompatibility of the implant, which will depend on the structure, composition, signals and immunogenicity of the matrix. In the hernia repair model studied in this thesis the cross-linked materials induced lower inflammatory responses than the noncross-linked matrix, the cross-linking may have reduced the antigenicity of the biomaterials. Protein cross-linking has been reported by many as an efficient way of reducing the amount of protein epitopes which can be recognised by the host antibodies inducing an immune response (Schmidt and Baier, 2000; Yu *et al.*, 2008). In this case the matrix cross-linking can not be reported as the only or main factor responsible for lower inflammatory reactions. Several other factors may have influenced the *in vivo* performance including tissue source, decellularisation process, sterilization methods and matrix properties. Both cross-linked matrices tested are porcine derived while AlloDerm originates from human dermis, the latter may react more easily or at higher levels with rat tissue.

All *in vivo* studies assessed for this thesis showed a common result, a conclusion that the level of implant-host tissue integration was independent of the level of cellular density observed within the implants. CollaMend's performance gives further

evidence that high cellular density and vascularisation of an implant is not necessary for good integration to occur. In this case, CollaMend was readily infiltrated by host cells and the number of new vessels present within the implant increased with time but the implant was not integrated with the immediately adjacent tissue.
Although macro- and microscopically CollaMend seemed intact, in which histology analysis did not show remodelling of the matrix and collagen was not degraded, two implants failed by tearing during the tensile strength test 6 months post implantation. Therefore, CollaMend implants are not mechanically strong and are not elastic. According to the results described above, CollaMend does not seem suitable for abdominal hernia repair.

AlloDerm and CollaMend manufacturers claim that these biomaterials are biocompatible and provide strong repair of soft tissue defects, but the results reported in this thesis do not confirm such recomendations. Since a rodent model was used it is not possible to state that AlloDerm and CollaMend are not biocompatible and that these biomaterials are inappropriate for human abdominal hernia repair. Nevertheless, the results suggest caution when using either material in such a clinical setting. Animal models do not ideally mimic the human situation and there is a social effort to find alternatives to animal models in research. Regardless of the ethical concerns that animal models may invoke, currently there are no other methods considered to be appropriate and sufficient to guarantee the safety and functionality of a biomaterial before clinical use. It is the conjugation of various tests that allow meticulous characterization of a biomaterial and provide information to predict its performance *in vivo*, although *in situ* responses will always depend on the patient and, therefore, unexpected results may occur.

6.3 CONSIDERATIONS

When a biomaterial is used to replace or repair damaged tissue or organs, the patient is benefitting from over 50 years of research. Although the results of implantation of

foreign tissue, organs and prosthetic materials have improved markedly in the last years, immunosuppressant drugs are still widely used and many times their use is indispensable. A clinical setting where successful implantation was independent of the use of long-term immunosuppressant drugs would be the ultimate aim of researchers.

New approaches such as the use of biocompatible materials (with or without cells) and stem cell technology are currently the main focus of researchers working in tissue engineering. While autologous cells have many potential advantages, availability is constrained; increasing patient morbidity and the required culturing time necessarily increases procedure duration. In addition autologous cells cannot be used easily in large scale treatments. Sources of autologous cells are limited and can be further reduced depending on the type of cell; furthermore, cells require a harvesting operation with enrichment and control of phenotype. In contrast, xenogenic cells are easily available but the use of xenogenic or allogenic cells requires selective elimination of the immunological barrier in transplantation. Even when implantation is successful and the tissue/material is not rejected by the host, transplanted cells, tissues and materials need to stay viable which implies nourishment through the host vasculature. If neo-vascularisation does not happen quickly the transplanted cells will die. Additionally waste removal is equally important, otherwise, high level of toxins will cause cell death. Therefore, there remains great interest and potential for developing and using acellular biomaterials.

Because of its many favourable characteristics, collagen has been used as the base protein for the extracellular matrix of many materials, collagen is useful alone or in combination with other components, it can also be easily modified for promoting organ and tissue regeneration. Acellular collagen-based biomaterials can be prepared in several forms: solid, gel, foams or paste and therefore, can be used in a wide range of treatments.

This thesis mainly reports on Permacol® surgical implant characteristics and *in vivo* performance in different settings. Although the results provided a great deal of new information related to this biomaterial, many new questions have been raised that will need an answer. This includes how calcification of the matrix occurs and how it affects Permacol® performance *in vivo* and if calcification is species-specific and whether the lack of collagen remodelling and replacement affects permanent healing,

cell-matrix interaction and Permacol® performance in contaminated fields. To understand mineral deposition with time, several studies would have to be designed. Initially, Permacol® structure would have to be thoroughly analysed and, for a better understanding of the cross-linking effect, Permacol® structure should be compared to normal porcine collagen and to Permacol® with lower and higher levels of cross-linking. Following this, *in vitro* tests where several solutions with different concentrations of calcium and inorganic phosphate could be used static or with movement to assess salt deposition. Similarly, the culture of fibroblasts in the presence of Permacol® could be manipulated by increasing the external concentrations of calcium and inorganic phosphate; if calcification was observed it could be useful to impregnate Permacol® with pyrophosphate (inhibitor of mineral nucleation) and see if calcification still occurs. Finally, *in vivo* models would have to be used for long term studies, in species rather than rat and results compared to confirm if calcification is species-dependent.

To study collagen remodelling of Permacol®, the collagen from the biomaterial would have to be labelled before implantation and the fluorescence or radioactivity measured before and after implantation. This technique could also be useful when enzymatic degradation tests are performed.

Permacol® surface signalling should be studied in detail to understand cell-matrix interactions and cell-cell interactions. Normal porcine collagen should be used as control and differences explored.

Lastly, it would be useful to study Permacol® performance in an *in vivo* model of chronic wound both in the presence and absence of infection. Such a study would provide useful information for both scientists and clinicians. Additionally, the same model could be used to assess the performance of other commercially available biomaterials that are recommended for repair of wounds in complicated settings.

Permacol® surgical implant gave evidence of being an efficient and appropriate biomaterial when used as bulking tissue and for soft tissue repair, additionally its tolerance to enzymatic digestion suggests it could be used in infected areas. Overall it is concluded that Permacol® surgical implant is a versatile biomaterial which can be used in a range of settings.

7.0 REFERENCES

1. Abhinav, K.; Shaaban, M.; Raymond, T.; Oke, T.; Gullan, R. and Montgomery, A. C. (2008) Primary reconstruction of pelvic floor defects following sacrectomy using Permacol graft. European Journal of Surgical Oncology 35(4):439-443.

2. Abraham, C. S.; Deli, M. A.; Joo, F.; Megyeri, P. and Torpier, G. (1996) Intracarotid tumor necrosis factor-alpha administration increases the blood-brain barrier permeability in cerebral cortex of the newborn pig: quantitative aspects of double-labelling studies and confocal laser scanning analysis. Neuroscience Letters 208(2):85-88.

3. Abraham, G. A.; Murray, J.; Billiar, K. and Sullivan, S. J. (2000) Evaluation of the porcine intestinal collagen layer as a biomaterial. Journal of Biomedical Materials Research 51(3):442-452.

4. Abraham, L. C.; Dice, J. F.; Lee, K. and Kaplan, D. L. (2007) Phagocytosis and remodeling of collagen matrices. Experimental Cell Research 313(5):1045-1055.

5. Adler-Nissen, J. (1979) Determination of the degree of hydrolysis of food protein hydrolysates by trinitrobenzenesulfonic acid. Journal of Agricultural and Food Chemistry 27(6):1256-1262.

6. Agrawal, C. M.; McKinney, J. S.; Lanctot, D. and Athanasiou, K. A. (2000) Effects of fluid flow on the in vitro degradation kinetics of biodegradable scaffolds for tissue engineering. Biomaterials 21(23):2443-2452.

7. Aiba-Kojima, E.; Tsuno, N. H.; Inoue, K.; Matsumoto, D.; Shigeura, T.; Sato, T.; Suga, H.; Kato, H.; Nagase, T.; Gonda, K.; Koshima, I.; Takahashi, K. and Yoshimura, K. (2007) Characterization of wound drainage fluids as a source of soluble factors associated with wound healing: comparison with platelet-rich plasma and potential use in cell culture. Wound Repair and Regeneration 15(4):511-520.

8. Alaedeen, D.; Lipman, J.; Medalie, D. and Rosen, M. (2007) The single-staged approach to the surgical management of abdominall wall hernias in contaminated fields. Hernia 11:41-45.

9. Albo, D.; Awad, S.; Berger, D. and Bellows, C. (2006) Decellularized human cadaveric dermis provides a safe alternative for primary inguinal hernia repair in contaminated surgical fields. The American Journal of Surgery 192:e12-e17.

10. Anderson, J. (2001) Biological responses to biomaterials. Annual Review of Materials Research 31:81-110.

11. Arnold, F. and West, D. (1991) Angiogenesis in wound healing. Pharmac.Ther. 52:407-422.

12. Augustin, H. G.; Braun, K.; Telemenakis, I.; Modlich, U. and Kuhn, W. (1995) Ovarian angiogenesis. Phenotypic characterization of endothelial cells in a physiological model of blood vessel growth and regression. American Journal of Patholology 147(2):339-351.

13. Azarmi, S.; Huang, Y.; Chen, H.; McQuarrie, S.; Abrams, D.; Roa, W.; Finlay, W. H.; Miller, G. G. and Lobenberg, R. (2006) Optimization of a two-step desolvation method for preparing gelatin nanoparticles and cell uptake studies in 143B osteosarcoma cancer cells. Journal of Pharmacy & Pharmaceutical Sciences 9(1):124-132.

14. Badylak, S. (2007) The extracellular matrix as a biologic scaffold material. Biomaterials 28:3587-3593.

15. Banci, L.; Bertini, I.; Caliceti, P.; Monsu, S. L.; Schiavon, O. and Veronese, F. M. (1990) Spectroscopic characterization of polyethyleneglycol modified superoxide dismutase: 1H NMR studies on its Cu2Co2 derivative. Journal of Inorganic Biochemistry 39(2):149-159.

16. Barber, F. A.; Herbert, M. A. and Coons, D. A. (2006) Tendon augmentation grafts: biomechanical failure loads and failure patterns. Arthroscopy 22(5):534-538.

17. Batchelor, A. and Chandrasekaran, M. (Eds.); Service Characteristics of Biomedical Materials and Implants. 1st Edition. London: Imperial College Press, 2004.

18. Bell, E.; Ivarsson, B. and Merril, C. (1979) Production of a tissue-like structure by contraction of collagen lattices by human fibroblasts of different proliferative potential in vitro. Proceedings of the National Academy of Sciences 76(3):1274-1278.

19. Bellinger, C. G. and Conway, H. (1970) Effects of silver nitrate and sulfamylon on epithelial regeneration. Plastic Reconstruction Surgery 45(6):582-585.

20. Bellows, C.; Albo, D.; Berger, D. and Awad, S. (2007) Abdominal wall repair using human acellular dermis. The American Journal of Surgery 194:192-198.

21. Benbow, U.; Schoenermark, M.; Mitchell, T.; Rutter, J.; Shimokawa, K.; Nagase, H. and Brinckerhoff, E. (1999) A Novel Host/Tumor Cell Interaction Activates Matrix Metalloproteinase 1 and Mediates Invasion through Type I Collagen. The Journal of Biological Chemistry 274(36):25371-25378.

22. Benito-Ruiz, J.; Guisantes, E. and Serra-Renom, J. M. (2006) Porcine dermal collagen: a new option for soft-tissue reconstruction of the lip. Plastic Reconstructive Surgery 117(7):2517-2519.

23. Bergin, S. and Wraight, P. (2007) Silver based wound dressings and topical agents for treating diabetic foot ulcers (review). The Cochrane Collaboration :1-10.

24. Bhol, K. and Schechter, P. (2005) Topical nanocrystalline silver cream suppresses inflammatory cytokines and induces apopotosis of inflammatory cells in a murine model of allergic contact dermatitis. British Journal of Dermatology 152:1235-1242.

25. Bhushan, M.; Young, H.; Brenchley, P. and Griffiths, C. (2002) Topical Review: Recent advantages in cutaneous angiogenesis. British Journal of Dermatology 147:418-425.

26. Black, J. (Eds.); Biological Performance of Materials - Fundamentals of Biocompatibility. 4th Edition. Boca Raton: CRC Press, 2006.

27. Boon, M.; Ruijgrok, J. and Vardaxis, M. (1995) Collagen implants remain supple not allowing fibroblast ingrowth. Biomaterials 16:1089-1093.

28. Bottano, D. and Heidaran, M. (2001) Engineered extracellular matrices: a biological solution for tissue repair, regeneration and replacement. e-biomed 2:9-12.

29. Bowler, P. G. (2003) The 10(5) bacterial growth guideline: reassessing its clinical relevance in wound healing. Ostomy Wound Management 49(1):44-53.

30. Bowler, P. G.; Duerden, B. I. and Armstrong, D. G. (2001) Wound microbiology and associated approaches to wound management. Clinical Microbiology Reviews 14(2):244-269.

31. Braddock, M.; Campbell, C. J. and Zuder, D. (1999) Current therapies for wound healing: electrical stimulation, biological therapeutics, and the potential for gene therapy. International Journal of Dermatology 38(11):808-817.

32. Brandner, J.; Zacheja, S.; Houdek, P.; Moll, I. and Lobmann, R. (2007) Molecular factors of keratinocytes in diabetic wounds. Diabetes Care

33. Braybrook, J. E. (Eds.); Biocompatibility Assessment of Medical Devices and Materials. 1st Edition. Chichester: John Wiley & Sons, 1997.

34. Brook, I. and Frazier, E. H. (1998) Aerobic and anaerobic microbiology of chronic venous ulcers. International Journal of Dermatology 37(6):426-428.

35. Broughton, G.; Janis, J. and Attinger, C. (2006) The basic science of wound healing. Plastic and Reconstructive Surgery June supplement:12S-34S.

36. Brown, N.; Smyh, E.; Cross, S. and Reed, M. (2002) Angiogenesis induction and regression in human surgical wounds. Wound Repair and Regeneration 10(4):245-251.

37. Brown, R.; Prajapati, R.; McGrouther, D.; Yannas, I. and Eastwood, M. (1998) Tensional homeostasis in dermal fibroblasts: mechanical responses to mechanical loading in three-dimensional substrates. Journal of Cellular Physiology 175(3):323-332.

38. Brussee, V.; Tardif, F. and Tremblay, J. P. (1997) Muscle fibers of mdx mice are more vulnerable to exercise than those of normal mice. Neuromuscular Disorders 7(8):487-492.

39. Buinewicz, B. and Rosen, B. (2004) Acellular cadaveric dermis (AlloDerm): a new alternative for abdominal hernia repair. Annals of Plastic Surgery 52(2):188-194.

40. Bullock, J.; Chowdhury, S.; Severdia, A.; Sweeney, J.; Johnston, D. and Pachla, L. (1997) Comparison of results of various methods used to determine the extent of modification of methoxy polyethylene glycol 5000-modified bovine cupri-zinc superoxide dismutase. Analytical Biochemistry 254(2):254-262.

41. Burd, A.; Kwok, C.; Hung, S.; Chan, H.; Gu, H.; Lam, W. and Huang, L. (2007) A comparative study of the cytotoxicity of silver-based dressings in monolayer cell, tissue explants, and animal models. Wound Repair and Regeneration 15:94-104.

42. Burger, J. W.; Luijendijk, R. W.; Hop, W. C.; Halm, J. A.; Verdaasdonk, E. G. and Jeekel, J. (2004) Long-term follow-up of a randomized controlled trial of suture versus mesh repair of incisional hernia. Annals of Surgery 240(4):578-583.

43. Butler, C.; Langstein, H. and Kronowitz, S. (2005) Pelvic, abdominal, and chest wall reconstruction with AlloDerm in patients at increased risk for mesh-related complications. Plastic and Reconstructive Surgery 116:1263-1275.

44. Canavan, H. E.; Cheng, X.; Graham, D. J.; Ratner, B. D. and Castner, D. G. (2005) Cell sheet detachment affects the extracellular matrix: a surface science study comparing thermal liftoff, enzymatic, and mechanical methods. Journal of Biomedical Materials Research A 75(1):1-13.

45. Carbonell, A.; Matthews, B.; Dréau, D.; Foster, M.; Austin, C.; Kercher, K.; Sing, R. and Heniford, B. (2005) The susceptibility of prosthetic biomaterials to infection. Surgical Endoscopy 19:430-435.

46. Carmeliet, P. (2004) Review: Manipulating angiogenesis in medicine. Journal of Internal Medicine 255:538-561.

47. Carmeliet, P. (2003) Angiogenesis in health and disease. Nature Medicine 9(6):653-660.

48. Catena, F.; Ansaloni, L.; Gazzotti, F.; Gagliardi, S.; Di, S. S.; D'Alessandro, L. and Pinna, A. D. (2007) Use of porcine dermal collagen graft (Permacol) for hernia repair in contaminated fields. Hernia 11(1):57-60.

49. Cavallini, M. (2007) Autologous fibroblasts to treat deep and complicated leg ulcers in diabetic patients. Wound Repair and Regeneration 15:35-38.

50. Cayot, P. and Tainturier, G. (1997) The quantification of protein amino groups by the trinitrobenzenesulfonic acid method: a reexamination. Analytical Biochemistry 249(2):184-200.

51. Cen, L.; Liu, W.; Cui, L.; Zhang, W. and Cao, Y. (2008) Collagen tissue engineering: development of novel biomaterials and applications. Pediatric Research 63(5):492-496.

52. Chang, E. I.; Foster, R. D.; Hansen, S. L.; Jazayeri, L. and Patti, M. G. (2007) Autologous tissue reconstruction of ventral hernias in morbidly obese patients. Archives of Surgery 142(8):746-749.

53. Chapman, G. B. and Eagles, D. A. (2007) Ultrastructural features of Glisson's capsule and the overlying mesothelium in rat, monkey and pike liver. Tissue Cell 39(5):343-351.

54. Chaudhry, A.; Griffiths, E. A.; Shah, N. and Ravi, S. (2008) Surgical excision of an abdominal wall granular cell tumour with Permacol(R) mesh reconstruction: a case report. International Seminars in Surgical Oncology 5:1-4.

55. Choudhary, S.; Berhe, M.; Haberstroh, K. M. and Webster, T. J. (2006) Increased endothelial and vascular smooth muscle cell adhesion on nanostructured titanium and CoCrMo. International Journal of Nanomedicine 1(1):41-49.

56. Chung, H. J. and Park, T. G. (2007) Surface engineered and drug releasing pre-fabricated scaffolds for tissue engineering. Advanced Drug Delivery Reviews 59(4-5):249-262.

57. Cillo, J. E. Jr.; Caloss, R.; Miles, B. A. and Ellis, E., III (2007) An unusual response associated with cross-linked porcine dermal collagen (ENDURAGen) used for reconstruction of a post-traumatic lateral nasal wall deformity. Journal of Oral Maxillofacial Surgery 65(5):1017-1022.

58. Coons, D. A. and Barber, F. A. (2006) Tendon graft substitutes - rotator cuff patches. Sports Medicine and Arthroscopy Review 14(3):185-190.

59. Cooper, R. (2004) A review of the evidence for the use or topical antimicrobial agents in wound care. World Wide Wounds

60. Courtman, D. W.; Errett, B. F. and Wilson, G. J. (2001) The role of crosslinking in modification of the immune response elicited against xenogenic vascular acellular matrices. Journal of Biomedical Materials Research 55(4):576-586.

61. Courtman, D. W.; Pereira, C. A.; Kashef, V.; McComb, D.; Lee, J. M. and Wilson, G. J. (1994) Development of a pericardial acellular matrix

biomaterial: biochemical and mechanical effects of cell extraction. Journal of Biomedical Materials Research 28(6):655-666.

62. Cuttle, L.; Nataatmadja, M.; Fraser, J. F.; Kempf, M.; Kimble, R. M. and Hayes, M. T. (2005) Collagen in the scarless fetal skin wound: detection with picrosirius-polarization. Wound Repair Regeneration 13(2):198-204.

63. Daeschlein, G.; Assadian, O.; Kloth, L.; Meinl, C.; Ney, F. and Kramer, A. (2007) Antibacterial activity of positive and negative polarity low-voltage pulsed current (LVPC) on six typical Gram-positive and Gram-negative bacterial pathogens of chronic wounds. Wound Repair and Regeneration 15:399-403.

64. Darland, D. and D'Amore, P. (1999) Commentary: Blood vessel maturation: vascular development comes of age. The Journal of Clinical Investigation 103(2):157-158.

65. Davies, C. E.; Wilson, M. J.; Hill, K. E.; Stephens, P.; Hill, C. M.; Harding, K. G. and Thomas, D. W. (2001) Use of molecular techniques to study microbial diversity in the skin: chronic wounds reevaluated. Wound Repair and Regeneration 9(5):332-340.

66. Davies, C.; Hill, K.; Newcombe, R.; Stephens, P.; Wilson, M.; Harding, K. and Thomas, D. (2007) A prospective study of the microbiology of chronic venous leg ulcers to reevaluate the clinical predictive value of tissue biopsies and swabs. Wound Repair and Regeneration 15:17-22.

67. Davis, G. and Senger, D. (2005) Endothelial Extracellular Matrix: biosynthesis, remodeling, and functions during vascular morphogenesis and neovessel stabilization. Circulation Research 97:1093-1107.

68. Dayer, J. M.; de, R. B.; Burrus, B.; Demczuk, S. and Dinarello, C. A. (1986) Human recombinant interleukin 1 stimulates collagenase and prostaglandin E2 production by human synovial cells. Journal of Clinical Investigation 77(2):645-648.

69. den Braber, E. T.; de Ruijter, J. E.; Ginsel, L. A.; von Recum, A. F. and Jansen, J. A. (1996) Quantitative analysis of fibroblast morphology on microgrooved surfaces with various groove and ridge dimensions. Biomaterials 17(21):2037-2044.

70. Dench, J. E.; Scott, S. M.; Lunniss, P. J.; Dvorkin, L. S. and Williams, N. S. (2006) Multimedia article. External pelvic rectal suspension (the express procedure) for internal rectal prolapse, with or without concomitant rectocele repair: a video demonstration. Diseases of the Colon & Rectum 49(12):1922-1926.

71. Deodhar, A. and Rana, R. (1997) Surgical physiology of wound healing: a review. Journal of Postgraduate Medicine 43(2):52-56.

72. Derwin, K. A.; Baker, A. R.; Spragg, R. K.; Leigh, D. R. and Iannotti, J. P. (2006) Commercial extracellular matrix scaffolds for rotator cuff tendon

repair. Biomechanical, biochemical, and cellular properties. The Journal of Bone and Joint Surgery 88(12):2665-2672.

73. Desai, T. A. (2000) Micro- and nanoscale structures for tissue engineering constructs. Medical Engineering Physics 22(9):595-606.

74. Desmouliere, A.; Redard, M.; Darby, I. and Gabbiani, G. (1995) Apoptosis mediates the decrease in cellularity during the transition between granulation tissue and scar. American Journal of Pathology 146(1):56-66.

75. Di Vita, G.; Patti, R.; D'Agostino, P.; Caruso, G.; Arcara, M.; Buscemi, S.; Bonventre, S.; Ferlazzo, V.; Arcoleo, F. and Cillari, E. (2006) Cytokines and growth factors in wound drainage fluid from patients undergoing incisional hernia repair. Wound Repair and Regeneration 14:259-264.

76. Diamond, M.; El-Hammady, E.; Munkarah, A.; Bieber, E. and Saed, G. (2005) Modulation of the expression of vascular endothelial growth factor in human fibroblasts. Fertility and Sterility 83(2):405-409.

77. Diem, K. and Lentner, C. E. (Eds.); Scientific Tables. 7th Edition. Basle: Documenta Geigy, 1970.

78. Duan, X. and Sheardown, H. (2005) Crosslinking of collagen with dendrimers. Journal of Biomedical Materials Research 75A:510-518.

79. Durán, N.; Marcato, P.; De Souza, G.; Alves, O. and Esposito, E. (2007) Antibacterial effect of silver nanoparticles produced by fungal process on textile fabrics and their effluent treatment. Journal of Biomedical Nanotechnology 3(2):203-208.

80. Eckes, B.; Kessler, D.; Aumailley, M. and Krieg, T. (2000) Interactions of fibroblasts with the extracellular matrix: implications for the understanding of fibrosis. Springer Seminars in Immunopathology 21:415-429.

81. Edwards, J. V.; Caston-Pierre, S.; Bopp, A. F. and Goynes, W. (2005) Detection of human neutrophil elastase with peptide-bound cross-linked ethoxylate acrylate resin analogs. Journal of Peptide Research 66(4):160-168.

82. Edwards, R. and Harding, K. G. (2004) Bacteria and wound healing. Current Opinion in Infectious Diseases 17(2):91-96.

83. Ehrlich, H. and Krummel, T. (1996) Regulation of wound healing from a connective tissue perspective. Wound Repair and Regeneration 4:203-210.

84. Epstein, E. H. Jr. and Munderloh, N. H. (1978) Human skin collagen. Presence of type I and type III at all levels of the dermis. The Journal of Biological Chemistry 253(5):1336-1337.

85. Espinosa-de-los-Monteros, A.; de la Torre, J. I.; Marrero, I.; Andrades, P.; Davis, M. R. and Vasconez, L. O. (2007) Utilization of human cadaveric acellular dermis for abdominal hernia reconstruction. Annals of Plastic Surgery 58(3):264-267.

86. Everaerts, F.; Torrianni, M.; Hendriks, M. and Feijen, J. (2007) Quantification of carboxyl groups in carbodiimide cross-linked collagen sponges. Journal of Biomedical Materials Research Part A 83(4):1176-1183.

87. Fager, R. S.; Shapiro, S. and Litman, B. J. (1977) A large-scale purification of phosphatidylethanolamine, lysophosphatidylethanolamine, and phosphatidylethanolamine, and phosphatidylcholine by high performance liquid chromatography: a partial resolution of molecular species. Journal of Lipid Research 18(6):704-709.

88. Falanga, V. (1993) Chronic wounds: pathophysiologic and experimental considerations. The Journal of Investigative Dermatology 100(5):721-725.

89. Falanga, V. (2002) Wound bed preparation and the role of enzymes: a case for multiple actions of therapeutic agents. Wounds 14(2):47-57.

90. Feng, Q. L.; Wu, J.; Chen, G. Q.; Cui, F. Z.; Kim, T. N. and Kim, J. O. (2000) A mechanistic study of the antibacterial effect of silver ions on Escherichia coli and Staphylococcus aureus. Journal of Biomedical Materials Research 52(4):662-668.

91. Fields, R. (1971) The measurement of amino groups in proteins and peptides. Biochemical Journal 124:581-590.

92. Figallo, E.; Flaibani, M.; Zavan, B.; Abatangelo, G. and Elvassore, N. (2007) Micropatterned biopolymer 3D scaffold for static and dynamic culture of human fibroblasts. Biotechnology Progress 23(1):210-216.

93. Flecknell, P. (Eds.); Laboratory Animal Anaesthesia - A Practical Introduction for Research Workers and Technicians. 2nd Edition. London: Academic Press Limited, 1996.

94. Folkman, J. (1997) Angiogenesis and angiogenesis inhibition: An overview. (1):1-8.

95. Folkman, J. and Shing, Y. (1992) Angiogenesis - Minireview. The Journal of Biological Chemistry 267(16):10931-10934.

96. Fountoulakis, M. and Lahm, H. W. (1998) Hydrolysis and amino acid composition of proteins. Journal of Chromatography A 826(2):109-134.

97. Friedl, P. and Bröcker, E.-B. (2000) The biology of cell locomotion within three-dimensional extracellular matrix. Cellular and Molecular Life Sciences 57:41-64.

98. Friedl, P. and Bröcker, E.-B. (2004) The biology of cell locomotion within three-dimensional extracellular matrix. Cellular and Molecular Life Sciences 57:41-64.

99. Friedman, M. (2004) Applications of the ninhydrin reaction for analysis of amino acids, peptides, and proteins to agricultural and biomedical sciences. Journal of Agricultural and Food Chemistry 52:385-406.

100. Friess, W. (1998) Collagen - biomaterial for drug delivery. European Journal of Pharmaceutics and Biopharmaceutics 45:113-136.

101. Fry, D. L. (1977) Aortic Evans blue dye accumulation: its measurement and interpretation. American Journal of Physiology 232(2):H204-H222.

102. Gaertner, W.; Bonsak, M. and Delaney, J. (2007) Experimental evaluation of four biologic prostheses for ventral hernia repair. Journal of Gastrointestinal Surgery 11(10):1275-1285.

103. Gaitonde, M. K. (1967) A spectrophotometric method for the direct determination of cysteine in the presence of other naturally occurring amino acids. Biochemistry Journal 104(2):627-633.

104. Gandhi, S.; Kubba, L. M.; Abramov, Y.; Botros, S. M.; Goldberg, R. P.; Victor, T. A. and Sand, P. K. (2005) Histopathologic changes of porcine dermis xenografts for transvaginal suburethral slings. American Journal of Obstetrics and Gynecology 192(5):1643-1648.

105. Garcia, Y.; Collighan, R.; Griffin, M. and Pandit, A. (2006) Assessment of cell viability in a three-dimensional enzymatically cross-linked collagen scaffold. Journal of Materials Science: Materials in Medicine 18(10):1991-2001.

106. Glowacki, J. and Mizuno, S. (2008) Collagen scaffolds for tissue engineering. Biopolymers 89(5):338-344.

107. Gong, P.; Li, H.; He, X.; Wang, K.; Hu, J.; Tan, W.; Zhang, S. and Yang, X. (2007) Preparation and antibacterial activity of Fe3O4@Ag nanoparticles. Nanotechnology 18(28):604-611.

108. Gospodarowicz, D.; Greenburg, G. and Birdwell, C. R. (1978) Determination of cellular shape by the extracellular matrix and its correlation with the control of cellular growth. Cancer Research 38(11 Pt 2):4155-4171.

109. Gosselin, M. E.; Kapustij, C. J.; Venkateswaran, U. D.; Leverenz, V. R. and Giblin, F. J. (2007) Raman spectroscopic evidence for nuclear disulfide in isolated lenses of hyperbaric oxygen-treated guinea pigs. Experimental Eye Research 84(3):493-499.

110. Green, C. (Eds.); Animal Anaesthesia. 2nd Edition. London: Laboratory Animals Ltd, 1982.

111. Greenhalgh, D. G. (1998) The role of apoptosis in wound healing. International Journal of .Biochemistry and Cell Biology 30(9):1019-1030.

112. Grinnell, F. (1994) Mini-review on the cellular mechanisms of disease - Fibroblasts, myofibroblasts, and wound contraction. The Journal of Cell Biology 124(4):401-404.

113. Grinnell, F. (2000) Fibroblast-collagen matrix contraction: growth factor signalling and mechanical loading. Trends in Cell Biology 10:362-365.

114. Grinnell, F. (2003) Fibroblast biology in three-dimensional collagen matrices. Trends in Cell Biology 13(5):264-269.

115. Grinnell, F. and Lamke, C. (1984) Reorganization of hydrated collagen lattices by human skin fibroblasts. Journal of Cell Science 66:51-62.

116. Grinnell, F.; Zhu, M.; Carlson, M. and Abrams, J. (1999) Release of mechanical tension triggers apoptosis of human fibroblasts in a model of regressing granulation tissue. Experimental Cell Research 248:608-619.

117. Gupta, A.; Zahriya, K.; Mullens, P.; Salmassi, S. and Keshishian, A. (2006) Ventral herniorrhaphy: experience with two different biosynthetic mesh materials, Surgisis and AlloDerm. Hernia 10:419-425.

118. Hamer, P.; McGeachie, M.; Davies, M. and Grounds, M. (2002) Evans Blue Dye as an iv vivo marker of myifibre damage: optimising parameters for detecting initial myofibre membrane permeability. Journal of Anatomy 200:69-79.

119. Hammond, T. M.; Chin-Aleong, J.; Navsaria, H. and Williams, N. S. (2008) Human in vivo cellular response to a cross-linked acellular collagen implant. British Journal of Surgery 95(4):438-446.

120. Han, Y. P.; Tuan, T. L.; Wu, H.; Hughes, M. and Garner, W. L. (2001) TNF-alpha stimulates activation of pro-MMP2 in human skin through NF-(kappa)B mediated induction of MT1-MMP. Journal of Cell Science 114(Pt 1):131-139.

121. Harada, S.; Nakada, Y.; Yamashita, F. and Hashida, M. (2005) Biopharmaceutical considerations on antihistamine effects of topically administered emedastine. Journal of Pharmaceutical Science 94(1):17-24.

122. Harley, B. A.; Kim, H. D.; Zaman, M. H.; Yannas, I. V.; Lauffenburger, D. A. and Gibson, L. J. (2008) Microarchitecture of three-dimensional scaffolds influences cell migration behavior via junction interactions. Biophysical Journal 95(8):4013-4024.

123. Harper, C. (2001) Permacol: clinical experience with a new biomaterial. Hospital Medicine 62(2)

124. Harrington, D. J. (1996) Bacterial collagenases and collagen-degrading enzymes and their potential role in human disease. Infection and Immunity 64(6):1885-1891.

125. Harris, A. K.; Stopak, D. and Wild, P. (1981) Fibroblast traction as a mechanism for collagen morphogenesis. Nature 290(5803):249-251.

126. Hartley, J. A.; Souhami, R. L. and Berardini, M. D. (1993) Electrophoretic and chromatographic separation methods used to reveal interstrand crosslinking of nucleic acids. Journal of Chromatography 618(1-2):277-288.

127. Hasty, K. A.; Jeffrey, J. J.; Hibbs, M. S. and Welgus, H. G. (1987) The collagen substrate specificity of human neutrophil collagenase. Journal of Biological Chemistry 262(21):10048-10052.

128. Hata, S.; Namae, M. and Nishina, H. (2007) Liver development and regeneration: from laboratory study to clinical therapy. Development, Growth & Differentiation 49(2):163-170.

129. Hawkins, B. T. and Egleton, R. D. (2006) Fluorescence imaging of blood-brain barrier disruption. Journal of Neuroscience Methods 151(2):262-267.

130. Haynes, C. and Norde, W. (1994) Globular proteins at solid/liquid interfaces. Colloids and Surfaces B.Biointerfaces 2:517-566.

131. Higgins, G. and Anderson, R. (1931) Experimental pathology of liver: Restoration of liver of white rats following partial surgical removal. Archives of Pathology 12:186-202.

132. Hill, K. E.; Davies, C. E.; Wilson, M. J.; Stephens, P.; Harding, K. G. and Thomas, D. W. (2003) Molecular analysis of the microflora in chronic venous leg ulceration. Journal of Medical Microbiology 52(Pt 4):365-369.

133. Hin, T. E. (Eds.); Engineering Materials for Biomedical Applications. 1st Edition. Singapore: World Scientific Publishing Co., 2004.

134. Hirsch, E. (2004) Repair of an abdominal wall defect after a salvage laparotomy for sepsis. Journal The American College of Surgeons 198(2):324-328.

135. Hussain, S. M.; Hess, K. L.; Gearhart, J. M.; Geiss, K. T. and Schlager, J. J. (2005) In vitro toxicity of nanoparticles in BRL 3A rat liver cells. Toxicology In Vitro 19(7):975-983.

136. Inan, I.; Gervaz, P.; Hagen, M. and Morel, P. (2007) Multimedia article. Laparoscopic repair of parastomal hernia using a porcine dermal collagen (Permacol) implant. Diseases of the Colon & Rectum 50(9):1465-1465.

137. Isenburg, J.; Simionescu, D. and Vyavahare, N. (2005) Tannic acid treatment enhances biostability and reduces calcification of glutaraldehyde fixed aortic wall. Biomaterials 26:1237-1245.

138. Jackson, C.; Xue, M.; Thompson, P.; Davey, R.; Whitmont, K.; Smith, S.; Buisson-Legendre, N.; Sztynda, T.; Furphy, L.; Cooper, A.; Sambrook, P. and March, L. (2005) Activated protein C prevents inflammation yet stimulates angiogenesis to promote cutaneous wound healing. Wound Repair and Regeneration 13:284-294.

139. Jarman-Smith, M.; Bodamyali, T.; Stevens, C.; Howell, J.; Horrocks, M. and Chaudhuri, J. (2004) Porcine collagen crosslinking, degradation and its capability for fibroblast adhesion and proliferation. Journal of Materials Science: Materials in Medicine 15:925-932.

140. Jiang, H. and Grinnell, F. (2005) Cell-matrix entanglement and mechanical anchorage of fibroblasts in three-dimensional collagen matrices. Molecular Biology of the Cell 16:5070-5076.

141. Junqueira, L.; Bignolas, G. and Brentani, R. (1979) Picrosirius staining plus polarization microscop, a specific method for collagen detection in tissue sections. Histochemical Journal 11:447-455.

142. Junqueira, L.; Montes, G. and Sanchez, E. (1982) The influence of tissue section thickness on the study of collagen by the picrosirius-polarization method. Histochemistry 74:153-156.

143. Kafienah, W.; Buttle, D. J.; Burnett, D. and Hollander, A. P. (1998) Cleavage of native type I collagen by human neutrophil elastase. Biochemical Journal 330 (Pt 2):897-902.

144. Kaga, N.; Soma, S.; Fujimura, T.; Seyama, K.; Fukuchi, Y. and Murayama, K. (2003) Quantification of elastin cross-linking amino acids, desmosine and isodesmosine, in hydrolysates of rat lung by ion-pair liquid chromatography-mass spectrometry. Analytical Biochemistry 318(1):25-29.

145. Kavitha, O. and Thampan, R. V. (2008) Factors influencing collagen biosynthesis. Journal of Cellular Biochemistry 104(4):1150-1160.

146. Kelley, P.; Gordley, K.; Higuera, S.; Hicks, J. and Hollier, L. (2005) Assessing the long-term retention and permanency of acellular cross-linked porcine dermal collagen as a soft-tissue substitute. Plastic and Reconstructive Surgery 116(6):1780-1784.

147. Khan, A. Z. and Mudan, S. S. (2007) Liver regeneration: mechanisms, mysteries and more. ANZ Journal of Surgery 77(1-2):9-14.

148. Khor, E. (1997) Methods for the treatment of collagenous tissues for bioprostheses - Review. Biomaterials 18:95-105.

149. Kim, K.; Herrera, G. and Battarbee, H. (1999) Role of glutaraldehyde in calcification of porcine aortic valve fibroblasts. American Journal of Pathology 154(3):843-852.

150. Kimuli, M.; Eardley, I. and Southgate, J. (2004) In vitro assessment of decellularized porcine dermis as a matrix for urinary tract reconstruction. British Journal of Urology International 94:859-866.

151. Kingsley, A. (2003) The wound infection continuum and its application to clinical practice. Ostomy Wound Management 49(7A Suppl):1-7.

152. Klasen, H. J. (2000b) A historical review of the use of silver in the treatment of burns. II. Renewed interest for silver. Burns 26(2):131-138.

153. Klasen, H. J. (2000a) Historical review of the use of silver in the treatment of burns. I. Early uses. Burns 26(2):117-130.

154. Kolker, A. R.; Brown, D. J.; Redstone, J. S.; Scarpinato, V. M. and Wallack, M. K. (2005) Multilayer reconstruction of abdominal wall defects with acellular dermal allograft (AlloDerm) and component separation. Annals of Plastic Surgery 55(1):36-41.

155. Konttinen, Y.; Ainola, M.; Valleala, H.; Ma, J.; Ida, H.; Mandelin, J.; Kinne, R.; Santavirta, s.; Sorsa, T.; López-Otín, C. and Takagi, M. (1999) Analysis of 16 different matrix metalloproteinases (MMP-1 to MMP-20) in the synovial membrane: different profiles in trauma and rheumatoid arthritis. Annals of the Rheumatic Diseases 58:691-697.

156. Krampert, M.; Kuenzle, S.; Thai, S. N.-M.; Lee, N.; Iruela-Arispes, M. and Werner, S. (2005) ADAMTS1 Proteinase is up-regulated in wounded skin and regulates migration of fibroblasts and endothelial cells. The Journal of Biological Chemistry 280(25):23844-23852.

157. Kuhn, C. and McDonald, J. A. (1991) The roles of the myofibroblast in idiopathic pulmonary fibrosis. Ultrastructural and immunohistochemical features of sites of active extracellular matrix synthesis. The American Journal of Pathology 138(5):1257-1265.

158. Kuhn, C. 3.; Boldt, J.; King, T. E., Jr.; Crouch, E.; Vartio, T. and McDonald, J. A. (1989) An immunohistochemical study of architectural remodeling and connective tissue synthesis in pulmonary fibrosis. The American Review of Respiratory Diseases 140(6):1693-1703.

159. Kuhn, M.; Smith, P.; Hill, D.; Ko, F.; Meltzer, D.; Vande Berg, J. and Robson, M. (2000) In vitro fibroblast populated collagen lattices are not good model of in vivo clinical wound healing. Wound Repair and Regeneration 8(4):270-276.

160. Lacraz, S.; Dayer, J. M.; Nicod, L. and Welgus, H. G. (1994) 1,25-dihydroxyvitamin D3 dissociates production of interstitial collagenase and 92-kDa gelatinase in human mononuclear phagocytes. The Journal of Biological Chemistry 269(9):6485-6490.

161. Laurens, N.; Koolwijk, P. and de Maat, M. P. (2006) Fibrin structure and wound healing. Journal of Trombosis and Haemostasi 4(5):932-939.

162. Lavery, W. L. (2000) How relevant are animal models to human ageing? Journal of the Royal Society of Medicine 93(6):296-298.

163. Lee, T.; Midura, R.; Hascall, V. and Vesely, I. (2001a) The effect of elastin damage on the mechanics of the aortic valve. Journal of Biomechanics 34:203-210.

164. Lee, W. K.; Park, K. D.; Kim, Y. H.; Suh, H.; Park, J. C.; Lee, J. E.; Sun, K.; Baek, M. J.; Kim, H. M. and Kim, S. H. (2001b) Improved calcification resistance and biocompatibility of tissue patch grafted with sulfonated PEO or heparin after glutaraldehyde fixation. Journal of Biomedical Materials Research - Applied Biomaterials 58(1):27-35.

165. Leong, K. F.; Cheah, C. M. and Chua, C. K. (2003) Solid freeform fabrication of three-dimensional scaffolds for engineering replacement tissues and organs. Biomaterials 24(13):2363-2378.

166. Liang, H. C.; Chang, Y.; Hsu, C. K.; Lee, M. H. and Sung, H. W. (2004) Effects of crosslinking degree of an acellular biological tissue on its tissue regeneration pattern. Biomaterials 25(17):3541-3552.

167. Lingen, M. W. (2001) Role of leukocytes and endothelial cells in the development of angiogenesis in inflammation and wound healing. Archives of Pathology and Laboratory Medicine 125(1):67-71.

168. Liu, M. L.; Mars, W. M.; Zarnegar, R. and Michalopoulos, G. K. (1994) Collagenase pretreatment and the mitogenic effects of hepatocyte growth factor and transforming growth factor-alpha in adult rat liver. Hepatology 19(6):1521-1527.

169. Liyanage, S.; Purohit, G.; Frye, J. and Giordano, P. (2006) Anterior abdominal wall reconstruction with a Permacol implant. Journal of Plastic, Reconstructive et Aesthetic Surgery 59:553-555.

170. Lu, S.; Gao, W. and Gu, H. Y. (2008) Construction, application and biosafety of silver nanocrystalline chitosan wound dressing. Burns 34(5):623-628.

171. Lynn, A.; Yannas, I. and Bonfield, W. (2004) Antigenicity and Immunogenicity of Collagen. Journal of Biomedical Materials Research Part B: Applied Biomaterials 71B:343-354.

172. MacLeod, T.; Sarathchandra, P.; Williams, G.; Sanders, R. and Green, C. (2004a) Evaluation of a porcine origin acellular dermal matrix and small intestinal submucosa as dermal replacements in preventing secondary skin graft contraction. Burns 30:431-437.

173. MacLeod, T.; Sarathchandra, P.; Williams, G.; Sanders, R. and Green, C. (2004b) The diamond CO_2 laser as a method of improving the vascularisation of a permanent collagen implant. Burns 30:704-712.

174. MacLeod, T.; Sarathchandra, P.; Williams, G.; Sanders, R. and Green, C. (2004c) The diamond CO_2 laser as a method of improving the vascularisation of a permanent collagen implant. Burns 30:704-712.

175. MacLeod, T.; Williams, G.; Sanders, R. and Green, C. (2005) Histological evaluation of Permacol as a subcutaneous implant over a 20-week period in the rat model. British Journal of Plastic Surgery 58:518-532.

176. Mallya, S. K.; Mookhtiar, K. A.; Gao, Y.; Brew, K.; Dioszegi, M.; Birkedal-Hansen, H. and Van Wart, H. E. (1990b) Characterization of 58-kilodalton human neutrophil collagenase: comparison with human fibroblast collagenase. Biochemistry 29(47):10628-10634.

177. Mallya, S. K.; Mookhtiar, K. A.; Gao, Y.; Brew, K.; Dioszegi, M.; Birkedal-Hansen, H. and Van Wart, H. E. (1990a) Characterization of 58-kilodalton

human neutrophil collagenase: comparison with human fibroblast collagenase. Biochemistry 29(47):10628-10634.

178. Masyuk, T. V.; Ritman, E. L. and LaRusso, N. F. (2003) Hepatic artery and portal vein remodeling in rat liver: vascular response to selective cholangiocyte proliferation. Am.J.Pathol. 162(4):1175-1182.

179. Matsuda, R.; Nishikawa, A. and Tanaka, H. (1995) Visualization of dystrophic muscle fibers in mdx mouse by vital staining with Evans blue: evidence of apoptosis in dystrophin-deficient muscle. Journal of Biochemistry 118(5):959-964.

180. Matthews, B. D.; Pratt, B. L.; Pollinger, H. S.; Backus, C. L.; Kercher, K. W.; Sing, R. F. and Heniford, B. T. (2003) Assessment of adhesion formation to intra-abdominal polypropylene mesh and polytetrafluoroethylene mesh. Journal of Surgical Research 114(2):126-132.

181. Metcalfe, A. D. and Ferguson, M. W. (2007) Tissue engineering of replacement skin: the crossroads of biomaterials, wound healing, embryonic development, stem cells and regeneration. Journal of the Royal Society Interface 4(14):413-437.

182. Metcalfe, D. D.; Baram, D. and Mekori, Y. A. (1997) Mast cells. Physiological Reviews 77(4):1033-1079.

183. Montagna, W. and Parakka, P. (Eds.); The structure and function of skin. 3rd. New York: Academic Press, 1974.

184. Moore, S. and Stein, W. (1954) A modified ninhydrin reagent for the photometric determination of amino acids and related compounds. The Journal of Biological Chemistry 211(2):907-913.

185. Morçöl, T.; Subramanian, A. and Velander, W. H. (1997) Dot-blot analysis of the degree of covalent modification of proteins and antibodies at amino groups. Journal of Immunological Methods 203(1):45-53.

186. Moyer, C. A.; Brentano, L.; Gravens, D. L.; MARGRAF, H. W. and Monafo, W. W., Jr. (1965) Treatment of large human burns with 0.5% silver nitrate solution. Archives of Surgery 90:812-867.

187. Murshed, M.; Harmey, D.; Millan, J. L.; McKee, M. D. and Karsenty, G. (2005) Unique coexpression in osteoblasts of broadly expressed genes accounts for the spatial restriction of ECM mineralization to bone. Genes and Development 19(9):1093-1104.

188. Mustoe, T. (2004) Understanding chronic wounds: a unifying hypothesis on their pathogenesis and implications for therapy. The American Journal of Surgery 187:65S-70S.

189. Netzel-Arnett, S.; Mallya, S. K.; Nagase, H.; Birkedal-Hansen, H. and Van Wart, H. E. (1991) Continuously recording fluorescent assays optimized for five human matrix metalloproteinases. Analytical Biochemistry 195(1):86-92.

190. Ng, C. P. and Swartz, M. A. (2003) Fibroblast alignment under interstitial fluid flow using a novel 3-D tissue culture model. American Journal of Physiological and Heart Circulation Physiology 284(5):H1771-H1777.

191. Ng, C.; Hinz, B. and Swartz, M. (2005) Interstitial fluid flow induces myofibroblast differentiation and collagen alignment in vitro. Journal of Cell Science 118:4731-4739.

192. Nho, R.; Xia, H.; Diebold, D.; Kahm, J.; Kleidon, J.; White, E. and Henke, C. (2006) PTEN regulates fibroblast elimination during collagen matrix contraction. The Journal of Biological Chemistry 281(44):33291-33301.

193. Nwomeh, B. C.; Liang, H. X.; Cohen, I. K. and Yager, D. R. (1999) MMP-8 is the predominant collagenase in healing wounds and nonhealing ulcers. Journal of Surgical Research 81(2):189-195.

194. O'Brien, F. J.; Harley, B. A.; Waller, M. A.; Yannas, I. V.; Gibson, L. J. and Prendergast, P. J. (2007) The effect of pore size on permeability and cell attachment in collagen scaffolds for tissue engineering. Technology and Health Care 15(1):3-17.

195. O'Brien, F. J.; Harley, B. A.; Yannas, I. V. and Gibson, L. J. (2005) The effect of pore size on cell adhesion in collagen-GAG scaffolds. Biomaterials 26(4):433-441.

196. Ojeh, N.; Frame, J. and Navsaria, H. (2001) In vitro characterization of an artificial dermal scaffold. Tissue Engineering 7(4):457-472.

197. Okuyama, T. and Satake, K. (1960) On the preparation and properties of 2, 4, 6- trinitrophenyl- amino acidas and peptides. Journal of Biochemistry 47:454-

198. Olde Damink, L. H.; Dijkstra, P. J.; van Luyn, M. J.; van Wachem, P. B.; Nieuwenhuis, P. and Feijen, J. (1995) Cross-linking of dermal sheep collagen using hexamethylene diisocyanate. Journal of Materials Science: Materials in Medicine 6:429-434.

199. Olde Damink, L.; Dijkstra, P.; van Luyn, M.; van Wachem, P.; Nieuwenhuis, P. and Feijen, J. (1996) In vitro degradation of dermal sheep collagen cross-linked using a water-soluble carbodiimide. Biomaterials 17:679-684.

200. Oliver, R. and Grant, R. (1995) Implant tissue. U.S. Patent 5,397,353.

201. Oliver, R.; Grant, R.; Cox, R. and Cooke, A. (1980) Effect of aldehyde cross-linking on human dermal collagen implants in the rat. British Journal of Experimental Pathology 61:544-549.

202. Oliver, R.; Grant, R. and Kent, C. (1972) The fate of cutaneously and subcutaneously implanted trypsin purified dermal collagen in the pig. British Journal of Experimental Pathology 53:540-549.

203. Oliver, R.; Hulme, M. and Mudie, A. (1975) Skin collagen allografts in the rat. Nature 258:537-539.

204. Olsen, J. V.; Ong, S. E. and Mann, M. (2004) Trypsin cleaves exclusively C-terminal to arginine and lysine residues. Molecular and Cellular Proteomics 3(6):608-614.

205. Panasiuk, R.; Amarowicz, R.; Kostyra, H. and Sijtsma, L. (1998) Determination of a-amino nitrogen in pea protein hydrolysates: a comparison of three analytical methods. Food Chemistry 62(3):363-367.

206. Parker, D.; Armstrong, P.; Frizzi, J. and North Jr, J. (2006) Porcine dermal collagen (Permacol) for abdominal wall reconstruction. Current Surgery 63(4):255-258.

207. Patton, J.; Berry, S. and Kralovich, K. (2007) Use of human acellular dermal matrix in complex and contaminated abdominal wall reconstruction. The American Journal of Surgery 193:360-363.

208. Pentlow, A.; Smart, N. J.; Richards, S. K.; Inward, C. D. and Morgan, J. D. (2008) The use of porcine dermal collagen implants in assisting abdominal wall closure of pediatric renal transplant recipients with donor size discrepancy. Pediatric Transplantation 12(1):20-23.

209. Petter-Puchner, A.; Fortelny, R.; Walder, N.; Mittermayr, R.; Ohlinger, W.; van Griensven, M. and Redl, H. (2008) Adverse effects associated with the use of porcine cross-linked collagen implants in an experimental model of incisional hernia repair. Journal of Surgical Research 145:105-110.

210. Pichova, I.; Pavlickova, L.; Dostal, J.; Dolejsi, E.; Hruskova-Heidingsfeldova, O.; Weber, J.; Ruml, T. and Soucek, M. (2001) Secreted aspartic proteases of Candida albicans, Candida tropicalis, Candida parapsilosis and Candida lusitaniae. Inhibition with peptidomimetic inhibitors. European Journal of Biochemistry 268(9):2669-2677.

211. Poulose, B. K.; Scholz, S.; Moore, D. E.; Schmidt, C. R.; Grogan, E. L.; Lao, O. B.; Nanney, L.; Davidson, J. and Holzman, M. D. (2005) Physiologic properties of small intestine submucosa. Journal of Surgical Research 123(2):262-267.

212. Prior, B. M.; Yang, H. T. and Terjung, R. L. (2004) What makes vessels grow with exercise training? Journal of Applied Physiology 97(3):1119-1128.

213. Prussin, C. and Metcalfe, D. D. (2003) 4. IgE, mast cells, basophils, and eosinophils. Journal of Allergy and Clinical Immunology 111(2 Suppl):S486-S494.

214. Rai, M.; Yadav, A. and Gade, A. (2008) Silver nanoparticles as a new generation of antimicrobials. Biotechnology Advances

215. Rault, I.; Frei, V. and Herbage, D. (1996) Evaluation of different chemical methods for cross-linking collagen gel, films and sponges. Journal of Materials Science: Materials in Medicine 7:215-221.

216. Rayment, E. A.; Upton, Z. and Shooter, G. K. (2008) Increased matrix metalloproteinase-9 (MMP-9) activity observed in chronic wound fluid is related to the clinical severity of the ulcer. British Journal of Dermatology 158(5):951-961.

217. Reiser, K.; McCormick, R. J. and Rucker, R. B. (1992) Enzymatic and nonenzymatic cross-linking of collagen and elastin. FASEB Journal 6(7):2439-2449.

218. Resau, J. H.; Sakamoto, K.; Cottrell, J. R.; Hudson, E. A. and Meltzer, S. J. (1991) Explant organ culture: a review. Cytotechnology 7(3):137-149.

219. Rhee, S. and Grinnell, F. (2007) Fibroblast mechanics in 3D collagen matrices. Advanced Drug Delivery Reviews 59(13):1299-1305.

220. Richards, S. K.; Lear, P. A.; Huskisson, L.; Saleem, M. A. and Morgan, J. D. (2005) Porcine dermal collagen graft in pediatric renal transplantation. Pediatric Transplantation 9(5):627-629.

221. Rodriguez, J.; Gupta, N.; Smith, R. D. and Pevzner, P. A. (2008) Does trypsin cut before proline? Journal of Proteome Research 7(1):300-305.

222. Roy, P.; Petroll, W.; Chuong, C.; Cavanagh, H. and Jester, J. (1999) Effect of cell migration on the maintenance of tension on a collagen matrix. Annals of Biomedical Engineering 27:721-730.

223. Rundhaug, J. (2005) Matrix metalloproteinases and angiogenesis. Journal of Cellular and Molecular Medicine 9(2):267-285.

224. Saettele, T. M.; Bachman, S. L.; Costello, C. R.; Grant, S. A.; Cleveland, D. S.; Loy, T. S.; Kolder, D. G. and Ramshaw, B. J. (2007) Use of porcine dermal collagen as a prosthetic mesh in a contaminated field for ventral hernia repair: a case report. Hernia 11(3):279-285.

225. Sapico, F. L.; Canawati, H. N.; Witte, J. L.; Montgomerie, J. Z.; Wagner, F. W., Jr. and Bessman, A. N. (1980) Quantitative aerobic and anaerobic bacteriology of infected diabetic feet. J.Clin.Microbiol. 12(3):413-420.

226. Saray, A. (2003) Porcine dermal collagen (Permacol) for facial contour augmentation: preliminary report. Aesthetic Plastic Surgery 27:368-375.

227. Sarmah, B. and Holl-Allen, R. (1984) Porcine dermal collagen repair of incisional herniae. British Journal of Surgery 71(7):524-525.

228. Sarti, P.; Molinari, A.; Arancia, G.; Meloni, A. and Citro, G. (1995) A modified spectroscopic method for the determination of the transbilayer distribution of phosphatidylethanolamine in soya-bean asolectin small unilamellar vesicles. Biochemical Journal 312 (Pt 2):643-648.

229. Satake, K.; Okuyama, T.; Ohashi, M. and Shinoda, T. (1960) The spectrophotometric determination of amine, amino acid and peptide with 2, 4, 6- trinitrobenzene 1-sulfonic acid. The Journal of Biochemistry 47(5):654-660.

230. Schmidt, C. E. and Baier, J. M. (2000) Acellular vascular tissues: natural biomaterials for tissue repair and tissue engineering. Biomaterials 21(22):2215-2231.

231. Schuster, R.; Singh, J.; Safadi, B. Y. and Wren, S. M. (2006) The use of acellular dermal matrix for contaminated abdominal wall defects: wound status predicts success. The American Journal of Surgery 192(5):594-597.

232. Segal, S. S. (2005) Regulation of blood flow in the microcirculation. Microcirculation 12(1):33-45.

233. Sempowski, G.; Borrello, M.; Blieden, T.; Barth, R. and Phipps, R. (1995) Fibroblast heterogeneity in the healing wound. Wound Repair and Regeneration 3:120-131.

234. Senior, R. M.; Campbell, E. J.; Landis, J. A.; Cox, F. R.; Kuhn, C. and Koren, H. S. (1982) Elastase of U-937 monocytelike cells. Comparisons with elastases derived from human monocytes and neutrophils and murine macrophagelike cells. Journal of Clinical Investigation 69(2):384-393.

235. Sethi, K.; Yannas, I.; Mudera, V.; Eastwood, M.; McFarland, C. and Brown, R. (2002) Evidence for sequential utilization of fibronectin, vitronectin, and collagen during fibroblast-mediated collagen contraction. Wound Repair and Regeneration 10:397-408.

236. Shabbir, J.; Baillor, D. and Widdison, A. (2005) Treatment of anastomotic-vaginal fistula complicating colorectal resection using Permacol interposition in lieu of omentum. International Journal of Colorectal Disease

237. Shaikh, F. M.; Giri, S. K.; Durrani, S.; Waldron, D. and Grace, P. A. (2007) Experience with porcine acellular dermal collagen implant in one-stage tension-free reconstruction of acute and chronic abdominal wall defects. World Journal of Surgery 31(10):1966-1972.

238. Siedle, B.; Cisielski, S.; Murillo, R.; Löser, B.; Castro, V.; Klaas, C.; Hucke, O.; Labahn, A.; Melzig, M. and Merfort, I. (2002) Sesquiterpene lactones as inhibitors of human neutrophil elastase. Bioorganic & Medicinal Chemistry 10:2855-2861.

239. Silver, F. and Christiansen, D. (Eds.); Biomaterials, Science and Biocompatibility. 1st Edition. New York: Springer, 1999.

240. Singer, A. and Clark, R. (1999) Cutaneous wound healing. The New England Journal of Medicine :738-746.

241. Skipworth, R. J.; Smith, G. H. and Anderson, D. N. (2007) Secondary perineal hernia following open abdominoperineal excision of the rectum: report of a case and review of the literature. Hernia 11(6):541-545.

242. Smart, N.; Immanuel, A. and Mercer-Jones, M. (2007) Laparoscopic repair of a Littre's hernia with porcine dermal collagen implant (Permacol). Hernia 11(4):373-376.

243. Smetana, A. B.; Klabunde, K. J.; Marchin, G. R. and Sorensen, C. M. (2008) Biocidal activity of nanocrystalline silver powders and particles. Langmuir 24(14):7457-7464.

244. Smith, G. H.; Skipworth, R. J.; Terrace, J. D.; Helal, B.; Stewart, K. J. and Anderson, D. N. (2007) Paraileostomy recontouring by collagen sealant injection: a novel approach to one aspect of ileostomy morbidity. Report of a case. Diseases of the Colon & Rectum 50(10):1719-1723.

245. Sosnik, A.; Sodhi, R. N.; Brodersen, P. M. and Sefton, M. V. (2006) Surface study of collagen/poloxamine hydrogels by a 'deep freezing' ToF-SIMS approach. Biomaterials 27(11):2340-2348.

246. Speer, D.; Ulreich, J.; Young, N.; Yuen, D. and Li, S.-T. (2006) Directionally guided angiogenesis within extruded type I collagen filaments in vivo. The Journal of Histotechnology (29):267-276.

247. Starcher, B. (2001) A ninhydrin-based assay to quantitate the total protein content of tissue samples. Analytical Biochemistry 292(1):125-129.

248. Stevens, A.; Lowe, J. and Young, B. (Eds.); Wheater's Basic Histopathology - A colour atlas and text. 4th Edition. London: Churchill Livingstone, 2002.

249. Sun, H. B.; Smith, G. N., Jr.; Hasty, K. A. and Yokota, H. (2000) Atomic force microscopy-based detection of binding and cleavage site of matrix metalloproteinase on individual type II collagen helices5. Analytic Biochemistry 283(2):153-158.

250. Sun, S.-W.; Lin, Y.-C.; Weng, Y.-M. and Chen, M.-J. (2006) Efficiency improvements on ninhydrin method for amino acid quantification. Journal of Food Composition and Analysis 19:112-117.

251. Sung, H.-W.; Hsu, C.-S.; Wang, S.-P. and Hsu, H.-L. (1997) Degradation potential of biological tissues fixed with various fixatives: an in vitro study. Journal of Biomedical Materials Research 35:147-155.

252. Tang, Y.; Chen, Y.; Lichti, C. F.; Hall, R. A.; Raney, K. D. and Jennings, S. F. (2005) CLPM: a cross-linked peptide mapping algorithm for mass spectrometric analysis. BMC Bioinformatics 6 Suppl 2:S9-

253. Thomas, D. W. and Harding, K. G. (2002) Wound healing. British Journal of Surgery 89(10):1203-1205.

254. Thomas, G. T.; Lewis, M. P. and Speight, P. M. (1999) Matrix metalloproteinases and oral cancer. Oral Oncology 35(3):227-233.

255. Tomasek, J.; Gabbiani, G.; Hinz, B.; Chaponnier, C. and Brown, R. (2002) Review: Myofibroblasts and mechano-regulation of connective tissue remodelling. Nature Reviews - Molecular Cell Biology 3:349-363.

256. Tomasek, J.; Haaksma, C.; Eddy, R. and Vaughan, M. (1992) Fibroblast contraction occurs on release of tension in attached collagen lattices:

dependency on an organized actin cytoskeleton and serum. The Anatomical Record 232:359-368.

257. Trengove, N. J.; Stacey, M. C.; MacAuley, S.; Bennett, N.; Gibson, J.; Burslem, F.; Murphy, G. and Schultz, G. (1999) Analysis of the acute and chronic wound environments: the role of proteases and their inhibitors. Wound Repair and Regeneration 7(6):442-452.

258. Tyagi, S. and Simon, S. (1993) Regulation of neutrophil elastase activity by elastin-derived peptide. The Journal of Biological Chemistry 268(22):16513-16518.

259. Valencia, I.; Kirsner, R. and Kerdel, F. (2004) Microbilogic evaluation of skin wounds: alarming trend toward antibiotic resistance in an inpatient dermatology service during a 10-year period. Journal of the American Academy of Dermatology 50:845-849.

260. Valentin, J. E.; Badylak, J. S.; McCabe, G. P. and Badylak, S. F. (2006) Extracellular matrix bioscaffolds for orthopaedic applications. A comparative histologic study. The Journal of Bone and Joint Surgery 88(12):2673-2686.

261. Varani, J.; Hattori, Y.; Chi, Y.; Schmidt, T.; Perone, P.; Zeigler, M. E.; Fader, D. J. and Johnson, T. M. (2000) Collagenolytic and gelatinolytic matrix metalloproteinases and their inhibitors in basal cell carcinoma of skin: comparison with normal skin. British Journal of Cancer 82(3):657-665.

262. Vasudev, S. C.; Chandy, T. and Sharma, C. P. (2000) The anticalcification effect of polyethylene glycol-immobilized on hexamethylene diisocyanate treated pericardium. Artificial Cells, Blood Substitutes, and Immobilization Biotechnology 28(1):79-94.

263. Verné, E.; Bretcanu, O.; Balagna, C.; Bianchi, C. L.; Cannas, M.; Gatti, S. and Vitale-Brovarone, C. (2008) Early stage reactivity and in vitro behavior of silica-based bioactive glasses and glass-ceramics. Journal of Materials Science - Materials in Medicine

264. Vidaurre, A.; Castilla Cortázar, I. and Gómex Ribelles, J. (2007) Polymeric scaffolds with a double pore structure. Jounal of Non-Crystalline Solids 353:1095-1100.

265. Vlachou, E.; Chipp, E.; Shale, E.; Wilson, Y. T.; Papini, R. and Moiemen, N. S. (2007) The safety of nanocrystalline silver dressings on burns: a study of systemic silver absorption. Burns 33(8):979-985.

266. von Lampe, B.; Barthel, B.; Coupland, S. E.; Riecken, E. O. and Rosewicz, S. (2000) Differential expression of matrix metalloproteinases and their tissue inhibitors in colon mucosa of patients with inflammatory bowel disease. Gut 47(1):63-73.

267. Vrijland, W. W.; van den Tol, M. P.; Luijendijk, R. W.; Hop, W. C.; Busschbach, J. J.; de, L.; van, G. D.; Rottier, A. B.; Vegt, P. A.; IJzermans, J.

N. and Jeekel, J. (2002) Randomized clinical trial of non-mesh versus mesh repair of primary inguinal hernia. British Journal of Surgery 89(3):293-297.

268. Wadman, M. (2005) Scar prevention: the healing touch. Nature 436(7054):1079-1080.

269. Waldvogel, F. and Swartz, M. (1969) Collagenotytic activity of bacteria. Journal of Bacteriology 98(2):662-667.

270. Wang, J. W. and Hon, M. H. (2003) Sugar-mediated chitosan/poly(ethylene glycol)-beta-dicalcium pyrophosphate composite: mechanical and microstructural properties. Journal of Biomedical Materials Research 64(2):262-272.

271. Wang, X.; Ge, J.; Wang, K.; Qian, J. and Zou, Y. (2006) Evaluation of MTT assay for measurement of emodin-induced cytotoxicity. Assay and Drug Development Technologies 4(2):203-207.

272. Watanabe, K. (2004) Collagenolytic proteases from bacteria. Applicable Microbiology and Biotechnology 63(5):520-526.

273. Weber, C.; Kreuter, J. and Langer, K. (2000) Desolvation process and surface characteristics of HSA-nanoparticles. International Journal of Pharmaceutics 196(2):197-200.

274. Welgus, H. G.; Campbell, E. J.; Cury, J. D.; Eisen, A. Z.; Senior, R. M.; Wilhelm, S. M. and Goldberg, G. I. (1990) Neutral metalloproteinases produced by human mononuclear phagocytes. Enzyme profile, regulation, and expression during cellular development. Journal of Clinical Investigation 86(5):1496-1502.

275. Wilshaw, S. P.; Burke, D.; Fisher, J. and Ingham, E. (2008) Investigation of the antiadhesive properties of human mesothelial cells cultured in vitro on implantable surgical materials. Journal of Biomedical .Materials Research Part B: Applied Biomaterials

276. Wilson, C. J.; Clegg, R. E.; Leavesley, D. I. and Pearcy, M. J. (2005) Mediation of biomaterial-cell interactions by adsorbed proteins: a review. Tissue Engineering 11(1-2):1-18.

277. Wlodarski, K.; Hancox, N. M. and Brooks, B. (1973) The influence of cortisone and implantation site on bone and cartilage induction in various animals. The Journal of Bone and Joint Surgery 55(3):595-603.

278. Xu, J.; Zutter, M.; Santoro, S. and Clark, R. (1998) A three-dimensional collagen lattice activates NF-kB in human fibroblasts: role in integrin alfa2 gene expression and tissue remodeling. The Journal of Cell Biology 140(3):709-719.

279. Xu, L.; McLennan, S. V.; Lo, L.; Natfaji, A.; Bolton, T.; Liu, Y.; Twigg, S. M. and Yue, D. K. (2007) Bacterial load predicts healing rate in neuropathic diabetic foot ulcers. Diabetes Care 30(2):378-380.

280. Yang, C. H. (2008) Evaluation of the release rate of bioactive recombinant human epidermal growth factor from crosslinking collagen sponges. Journal of Materials Science: Materials in Medicine 19(3):1433-1440.

281. Young, B.; Lowe, J.; Stevens, A. and Heath, J. (Eds.); Wheater's Functional Histology - A Text and Color Atlas. 5th Edition.Elsevier Limited, 2006.

282. Yu, X. X.; Wan, C. X. and Chen, H. Q. (2008) Preparation and endothelialization of decellularised vascular scaffold for tissue-engineered blood vessel. Journal of Materials Science: Materials in Medicine 19(1):319-326.

283. Zeeman, R.; Dijkstra, P. J.; van Wachem, P. B.; van Luyn, M. J.; Hendriks, M.; Cahalan, P. T. and Feijen, J. (1999) Successive epoxy and carbodiimide cross-linking of dermal sheep collagen. Biomaterials 20(10):921-931.

284. Zhao, Y. and Frost, R. L. (2008) Synthesis and surface characterization of yttrium doped boehmite nanofibers. Journal of Colloid and Interface Science 326(1):289-299.

285. Zheng, F.; Lin, Y.; Verbeken, E.; Claerhout, F.; Fastrez, M.; De, R. D. and Deprest, J. (2004) Host response after reconstruction of abdominal wall defects with porcine dermal collagen in a rat model. Ameriacan Journal of Obstetrics and Gynecology 191(6):1961-1970.

286. Zhu, Y. K.; Liu, X. D.; Skold, C. M.; Umino, T.; Wang, H. J.; Spurzem, J. R.; Kohyama, T.; Ertl, R. F. and Rennard, S. I. (2001) Synergistic neutrophil elastase-cytokine interaction degrades collagen in three-dimensional culture. American Journal of Physiology - Lung Cellular and Molecular Physiology 281(4):L868-L878.